Vol. 108 July 1, 1979
Complete in one issue

ISSN 0003-2670

ANALYTICA CHIMICA ACTA

International journal devoted to all branches of analytical chemistry

EDITORS

A. M. G. MACDONALD (Birmingham, Great Britain)
D. M. W. ANDERSON (Edinburgh, Great Britain)

Editorial Advisers

F. C. Adams, Antwerp
R. P. Buck, Chapel Hill, N.C.
E. A. M. F. Dahmen, Enschede
G. den Boef, Amsterdam
G. Duyckaerts, Liège
D. Dyrssen, Göteborg
W. Haerdi, Geneva
G. M. Hieftje, Bloomington, Ind.
J. Hoste, Ghent
A. Hulanicki, Warsaw
E. Jackwerth, Bochum
G. Johansson, Lund
D. C. Johnson, Ames, Iowa
J. H. Knox, Edinburgh
P. D. LaFleur, Washington, D.C.
D. E. Leyden, Denver, Colo.
H. Malissa, Vienna
A. Mizuike, Nagoya
G. H. Morrison, Ithaca, N.Y.
E. Pungor, Budapest
J. P. Riley, Liverpool
J. W. Robinson, Baton Rouge, La.
J. Růžička, Copenhagen
D. E. Ryan, Halifax, N.S.
W. Simon, Zürich
R. K. Skogerboe, Fort Collins, Colo.
W. I. Stephen, Birmingham
G. Tölg, Schwäbisch Gmünd, B.R.D.
A. Townshend, Birmingham
B. Trémillon, Paris
A. Walsh, Melbourne
H. Weisz, Freiburg i Br.
P. W. West, Baton Rouge, La.
T. S. West, Aberdeen
J. R. Willis, Melbourne
Yu. A. Zolotov, Moscow
P. Zuman, Potsdam, N.Y.

ELSEVIER SCIENTIFIC PUBLISHING COMPANY

ANALYTICA CHIMICA ACTA

International journal devoted to all branches of analytical chemistry
Revue internationale consacrée à tous les domaines de la chimie analytique
Internationale Zeitschrift für alle Gebiete der analytischen Chemie

PUBLICATION SCHEDULE FOR 1979 (incorporating the section on Computer Techniques and Optimization).

	J	F	M	A	M	J	J	A	S	O	N	D
Analytica Chimica Acta	104/1	104/2	105	106/1	106/2	107	108	109/1	109/2	110/1	110/2	111
Section on Computer Techniques and Optimization			112/1			112/2			112/3			112/4

Scope. *Analytica Chimica Acta* publishes original papers, short communications, and reviews dealing with every aspect of modern chemical analysis, both fundamental and applied. The section on *Computer Techniques and Optimization* is devoted to new developments in chemical analysis by the application of computer techniques and by interdisciplinary approaches, including statistics, systems theory and operation research. The section deals with the following topics: Computerized acquisition, processing and evaluation of data. Computerized methods for the interpretation of analytical data including chemometrics, cluster analysis, and pattern recognition. Storage and retrieval systems. Optimization procedures and their application. Automated analysis for industrial processes and quality control. Organizational problems.

Submission of Papers. Manuscripts (three copies) should be submitted to:
for *Analytica Chimica Acta:* Dr. A. M. G. Macdonald, Department of Chemistry, The University, P.O. Box 363, Birmingham B15 2TT, England;
for the section on *Computer Techniques and Optimization:* Dr. J. T. Clerc, Universität Bern, Pharmazeutisches Institut, Sahlistrasse 10, CH-3012 Bern, Switzerland.

Information for Authors. Papers in English, French and German are published. There are no page charges. Manuscripts should conform in layout and style to the papers published in this Volume. Authors should consult Vol. 102, p. 253 for detailed information. Reprints of this information are available from the Editors or from: Elsevier Editorial Services Ltd., Mayfield House, 256 Banbury Road, Oxford OX2 7DE (Great Britain).

Reprints. Fifty reprints will be supplied free of charge. Additional reprints (minimum 100) can be ordered. An order form containing price quotations will be sent to the authors together with the proofs of their article.

Advertisements. Advertisement rates are available from the publisher.

Subscriptions. Subscriptions should be sent to: Elsevier Scientific Publishing Company, P.O. Box 211, 1000 AE Amsterdam, The Netherlands. The section on *Computer Techniques and Optimization* can be subscribed to separately.

Publication. *Analytica Chimica Acta* (including the section on *Computer Techniques and Optimization*) appears in 9 volumes in 1979. The subscription for 1979 (Vols. 104–112) is Dfl. 1179.00 plus Dfl. 135.00 (postage) (total approx. U.S. $641.00). The subscription for the *Computer Techniques and Optimization* section only (Vol. 112) is Dfl. 131.00 plus Dfl. 15.00 (postage) (total approx. U.S. $71.00). Journals are sent automatically by air mail to the U.S.A. and Canada at no extra cost and to Japan, Australia and New Zealand for a small additional postal charge. All earlier volumes (Vols. 1–95) except Vols. 23 and 28 are available at Dfl. 144.00 (U.S. $70.00), plus Dfl. 10.00 (U.S. $5.00) postage and handling, per volume.

Claims for issues not received should be made within three months of publication of the issue, otherwise they cannot be honoured free of charge.

Customers in the U.S.A. and Canada who wish to obtain additional bibliographic information on this and other Elsevier journals should contact Elsevier/North Holland Inc., Journal Information Center, 52, Vanderbilt Avenue, New York, NY 10017. Tel: (212) 867-9040.

AL OF

HROMATOGRAPHY

NATIONAL JOURNAL ON CHROMATOGRAPHY, ELECTROPHORESIS AND RELATED METHO

EDITOR, Michael Lederer (Rome)

ASSOCIATE EDITOR, K. Macek (Prague)

EDITORIAL BOARD
W. A. Aue (Halifax)
V. G. Berezkin (Moscow)
V. Betina (Bratislava)
A. Bevenue (Honolulu, Hawaii)
P. Boulanger (Lille)
A. A. Boulton (Saskatoon)
G. P. Cartoni (Rome)
K. V. Chmutov (Moscow)
G. Duyckaerts (Liège)
L. Fishbein (Jefferson, Ark.)
A. Frigerio (Milan)
C. W. Gehrke (Columbia, Mo.)
E. Gil-Av (Rehovot)
G. Guiochon (Palaiseau)
I. M. Hais (Hradec Králové)
E. Heftmann (Berkeley, Calif.)
S. Hjertén (Uppsala)
E. C. Horning (Houston, Texas)
C. Horváth (New Haven, Conn.)
J. F. K. Huber (Vienna)
A. T. James (Sharnbrook)
J. Janák (Brno)
E.sz. Kováts (Lausanne)
K. A. Kraus (Oak Ridge, Tenn.)
E. Lederer (Gif-sur-Yvette)
A. Liberti (Rome)
H. M. McNair (Blacksburg, Va.)
Y. Marcus (Jerusalem)
G. B. Marini-Bettòlo (Rome)
Č. Michalec (Prague)
R. Neher (Basel)
G. Nickless (Bristol)
J. Novák (Brno)
N. A. Parris (Wilmington, Del.)
P. G. Righetti (Milan)
O. Samuelson (Göteborg)
G.-M. Schwab (Munich)
G. Semenza (Zürich)
L. R. Snyder (Tarrytown, N.Y.)
A. Zlatkis (Houston, Texas)

EDITORS, BIBLIOGRAPHY SECTION
K. Macek (Prague), J. Janák (Brno), Z. Deyl (Prague)

EDITOR, BOOK REVIEW SECTION
R. Amos (Abingdon)

EDITOR, NEWS SECTION
J. F. K. Huber (Vienna)

COORD. EDITOR, DATA SECTION
J. Gasparič (Hradec Králové)

ELSEVIER SCIENTIFIC PUBLISHING COMPANY
AMSTERDAM



including
CHROMATOGRAPHIC
REVIEWS
and
BIOMEDICAL
APPLICATIONS

Established in 1958, the JOURNAL OF CHROI
TOGRAPHY is now recognized as the authorita
journal in the field. It publishes papers on all asp
of chromatography, electrophoresis and rel
methods. Contributions consist mainly of rese
papers dealing with chromatographic theory, ins
mental development and their applications.

The JOURNAL OF CHROMATOGRAPHY inco
rates CHROMATOGRAPHIC REVIEWS which p
lishes reviews on all aspects of chromatogra
electrophoresis and related methods.

The JOURNAL OF CHROMATOGRAPHY has gained its position and r
tation by:

- **Publishing over 800 original papers on chromatography and related t**
  niques each year. It is thus the journal with more papers on chromatogr
  than all other analytical journals put together.
- **Publishing quarterly bibliographies covering all forms of chromatogr**
  and electrophoresis.
- **Publishing reviews both on chromatographic principles and on the f**
  of application of chromatographic and electrophoretic techniques.
- **Publishing collected chromatographic data especially from inacces**
  journals, as well as hitherto unpublished data.
- **Publishing each year the papers presented at several symposia.**

JOURNAL OF CHROMATOGRAPHY
BIOMEDICAL APPLICATIONS

OR, K. Macek (Prague)

ISULTING EDITOR,
ıderer (Rome)

ORIAL BOARD
ıdams (North Ryde)
Belenkii (Leningrad)
Bergelson (Moscow)
Boulton (Saskatoon)
V. Brooks (Glasgow)
. Curtius (Zürich)
. de Silva (Nutley, N.J.)
yl (Prague)
le Zeeuw (Groningen)
Drysdale (Boston, Mass.)
Horning (Houston, Texas)
ım (Oslo)
ksis (Toronto)
Liebich (Tübingen)
votný (Bloomington, Ind.)
ieu (Dijon)
ler (Strasbourg)
nyder (Tarrytown, N.Y.)
V. VandenHeuvel (Rahway, N.J.)
ıman (Mölndal)
ner (Leipzig)

OR, NEWS SECTION
. Huber (Vienna)

This section, established in 1977, forms an integral part of the JOURNAL OF CHROMATOGRAPHY. However, it may also be subscribed to separately.

BIOMEDICAL APPLICATIONS publishes papers dealing with the following aspects: developments in and applications of chromatographic and electrophoretic techniques related to clinical diagnosis (including the publication of normal values); screening and profiling procedures with special reference to metabolic disorders; results from basic medical research with direct consequences in clinical practice; combinations of chromatographic and electrophoretic methods with other physico-chemical techniques such as mass spectrometry.

ıdership:

omatographic techniques are now employed in most analytical problems, hat the journal is read by inorganic chemists, organic chemists, pharmaıgists, clinical researchers, industrial research and control laboratories, specting analysts and geologists, to mention but a few. It publishes papers n and is read in about 100 countries, principally the U.S.A., the U.K., nce, Germany, Czechoslovakia, Japan, and Canada.

ıxed and Abstracted in:

mical Abstracts, Biological Abstracts, Index Medicus, Environmental odicals Bibliography, Current Contents: Physical, Chemical & Earth ences Section and Life Sciences Section.

Publication Schedule and Subscription Information for 1979:

Journal of Chromatography, Volumes 162-180 (including **Chromatographic Reviews** and **Biomedical Applications** and cumulative indexes for volumes 161-180), 19 volumes in 39 issues - US $1288.25/Dfl. 2641.00 including postage.

Journal of Chromatography - Biomedical Applications, Volumes 162-164, 3 volumes in 12 issues - US $209.25/Dfl. 429.00 including postage.

Journal of Chromatography, Volumes 165-180 (including **Chromatographic Reviews** and cumulative indexes for volumes 161-180, excluding **Biomedical Applications**), 16 volumes in 27 issues - US $1116.00/Dfl. 2288.00 including postage.

A free sample copy is available on request.

The Dutch guilder price is definitive. US $ prices are subject to exchange rate fluctuations.

Orders should be sent to your usual supplier or to:
ELSEVIER SCIENTIFIC PUBLISHING COMPANY,
P.O. Box 211, 1000 AE Amsterdam, The Netherlands

Information for Authors:

Submission of Papers.

Papers in English, French and German may be submitted, if possible in three copies. Manuscripts should be submitted to:
The Editor of *Journal of Chromatography,* P.O. Box 681, 1000 AR Amsterdam, The Netherlands, or to:
The Editor of *Journal of Chromatography - Biomedical Applications,* P.O. Box 681, 1000 AR Amsterdam, The Netherlands.
Reviews are invited or proposed by letter to the Editors and will appear in *Chromatographic Reviews* or *Biomedical Applications.* An outline of the proposed review should first be forwarded to the Editors for preliminary discussion prior to preparation.

Types of Contributions.

The following types of papers are published in the *Journal of Chromatography* and in the section *Biomedical Applications:* Regular research papers (full-length papers), short communications and notes. Short communications are preliminary announcements of important new developments and will, whenever possible, be published with maximum speed. Notes are usually descriptions of short investigations and reflect the same quality of research as full-length papers, but should preferably not exceed four printed pages.

Reprints.

Fifty reprints will be supplied free of charge. Additional reprints may be ordered by the authors.

News.

News releases of new products and developments, and information leaflets of meetings should be addressed to: The Editor of the News Section, *Journal of Chromatography/Journal of Chromatography, Biomedical Applications,* Elsevier Scientific Publishing Company, P.O. Box 330, 1000 AH Amsterdam, The Netherlands.

A leaflet providing detailed "Instructions to Authors" is available from the publisher on request.

ANALYTICA CHIMICA ACTA
VOL. 108 (1979)

ANALYTICA CHIMICA ACTA

International journal devoted to all branches of analytical chemistry

EDITORS

A. M. G. MACDONALD (Birmingham, Great Britain)

D. M. W. ANDERSON (Edinburgh, Great Britain)

Editorial Advisers

F. C. Adams, Antwerp
R. P. Buck, Chapel Hill, N.C.
E. A. M. F. Dahmen, Enschede
G. den Boef, Amsterdam
G. Duyckaerts, Liège
D. Dyrssen, Göteborg
W. Haerdi, Geneva
G. M. Hieftje, Bloomington, Ind.
J. Hoste, Ghent
A. Hulanicki, Warsaw
E. Jackwerth, Bochum
G. Johansson, Lund
D. C. Johnson, Ames, Iowa
J. H. Knox, Edinburgh
P. D. LaFleur, Washington, D.C.
D. E. Leyden, Denver, Colo.
H. Malissa, Vienna
A. Mizuike, Nagoya
G. H. Morrison, Ithaca, N.Y.
E. Pungor, Budapest
J. P. Riley, Liverpool
J. W. Robinson, Baton Rouge, La.
J. Růžička, Copenhagen
D. E. Ryan, Halifax, N.S.
W. Simon, Zürich
R. K. Skogerboe, Fort Collins, Colo.
W. I. Stephen, Birmingham
G. Tölg, Schwäbisch Gmünd, B.R.D.
A. Townshend, Birmingham
B. Trémillon, Paris
A. Walsh, Melbourne
H. Weisz, Freiburg i Br.
P. W. West, Baton Rouge, La.
T. S. West, Aberdeen
J. B. Willis, Melbourne
Yu. A. Zolotov, Moscow
P. Zuman, Potsdam, N.Y.



ELSEVIER SCIENTIFIC PUBLISHING COMPANY

Anal. Chim. Acta, Vol. 108 (1979)

13.11.81.2522

© Elsevier Scientific Publishing Company, 1979.
All rights reserved. No part of this publication may be reproduced, stored in a retrieval system or transmitted in any form or by any means, electronic, mechanical, photocopying, recording or otherwise, without the prior written permission of the publisher, Elsevier Scientific Publishing Company, P.O. Box 330, 1000 AH Amsterdam, The Netherlands.

Submission of a paper to this journal entails the author's irrevocable and exclusive authorization of the publisher to collect any sums or considerations for copying or reproduction payable by third parties (as mentioned in article 17 paragraph 2 of the Dutch Copyright Act of 1912 and in the Royal Decree of June 20, 1974 (S. 351) pursuant to article 16 b of the Dutch Copyright Act of 1912) and/or to act in or out of Court in connection therewith.

Submission of an article for publication implies the transfer of the copyright from the author to the publisher and is also understood to imply that the article is not being considered for publication elsewhere.

Printed in The Netherlands

Analytica Chimica Acta, 108 (1979) 1—11
© Elsevier Scientific Publishing Company, Amsterdam — Printed in The Netherlands

STANDARDIZATION OF METHODS FOR THE DETERMINATION OF TRACES OF MERCURY
Part 4. Determination of Total Mercury in Gases by Atomic Absorption Spectrometry*

A REPORT PREPARED BY THE MERCURY ANALYSIS WORKING PARTY OF THE BUREAU INTERNATIONAL TECHNIQUE DU CHLORE**

BITC, 250 Avenue Louise, Bte 72, B-1050 Bruxelles (Belgium)

(Received 15th January 1979)

SUMMARY

Two procedures are given for the determination of total mercury in gases. Mercury and mercury compounds are captured on manganese dioxide or on a combination of activated charcoal and cellulose powder. After chemical treatment the mercury is determined by cold-vapour atomic absorption spectrometry. These procedures were accepted as reference methods by the member companies of the Bureau International Technique du Chlore. The procedures are applicable to a great variety of sample types, e.g. air, hydrogen, chlorine. The limit of detection is 0.01—0.02 μg of mercury per sample taken.

ZUSAMMENFASSUNG

Es werden 2 Verfahren für die Bestimmung des Gesamtquecksilber in Gasen beschrieben. Quecksilber und Quecksilberverbindungen werden an Mangandioxid oder einer Kombination von Zellulosepulver—Aktivkohle adsorbiert. Nach entsprechender chemischer Umsetzung wird das Quecksilber durch flammenlose Atomabsorptionsspektrometrie bestimmt. Die beiden Verfahren wurden als Standardmethode von den Mitgliedfirmen des Bureau International Technique du Chlore anerkannt. Die Analysenverfahren sind auf eine Vielzahl von Gasen anwendbar (z.B. Luft, Wasserstoff, Chlor). Die Nachweisgrenze liegt im Bereich von 0,01—0,02 μg Quecksilber absolut pro Probe.

RÉSUMÉ

On décrit deux méthodes de dosage du mercure total dans les gaz. Le mercure et ses composés sont retenus sur du bioxyde de manganèse ou sur de la poudre de cellulose—charbon actif. Après traitement chimique de la charge, le mercure est dosé par spectrophotométrie d'absorption atomique sans flamme. Ces méthodes ont été retenues à titre de méthodes de référence par les Sociétés membres du Bureau International Technique du Chlore. Elles sont applicables à une grande variété de types d'échantillons tels que l'air, l'hydrogène, le chlore. La limite de détection est de 0,01—0,02 μg de mercure dans la totalité de l'échantillon prélevé.

*Part 3, Anal. Chim. Acta, 87 (1976) 273.

**The members of the Working Party responsible for the preparation of this report were: J. A. Aliseda, R. Ankersmit, J. Barjhoux, R. Bult, W. T. Carter, W. Dürr, J. Garbayo, M. Garcia, Ch. Killens, L. Mariani, S. A. Norberg, F. Nouyrigat, M. Olivier, H. Romeis and A. de Yllana. This report has been approved by the General Technical Committee of the BITC, which also authorized its publication.

During their work, the BITC Working Party on Mercury Analysis have already standardized a reference method for the determination of total mercury in gases [1]. In the study of the emission of mercury to the air in cell rooms of chlor-alkali electrolysis plants, it became obvious that this reference method which is based on an evacuated bulb procedure so that aerosols containing mercury are also measured, is not suitable for routine determinations and for long sampling periods. Therefore, new methods had to be developed that would be simpler, faster (in the determination of mercury) and suitable for routine work. From this work, two procedures were chosen which were thoroughly evaluated and a programme of work was carried out to compare them with each other.

The methods proved to be applicable for mercury in other gaseous systems, such as wet air above brine saturation, hydrogen, nitrogen and chlorine, and for studying the exposure of workers to mercury. Because it is possible that the methods may be used for immission measurements in the vicinity of mercury cell chlor-alkali electrolysis plants where organo-mercury compounds may be present from other sources, the adsorption efficiency for these compounds was also investigated.

It should be emphasized that when the gas to be sampled is known to contain only free, elemental mercury, much simpler procedures based on u.v. absorption can be used for the mercury determination, and apparatus may be bought for this measurement. It is not the intention of this paper to give methods for this simple determination.

CHOICE OF SAMPLING PROCEDURE

In gases, mercury may be present in three forms: free, elemental mercury, mercury bound in inorganic and/or organic compounds, and mercury and/or mercury compounds, as aerosols or adsorbed on particulates. When gas samples are taken for mercury determinations, the sampling procedure has to be able to deal with all these forms.

Many methods have been described in the literature, for example, in the reviews of Ure [2] and Chilov [3]. These sampling procedures can be grouped as follows: (a) direct reading methods based on portable detectors (gas vapour meters), that measure only elemental mercury; (b) absorption in a solution, e.g. acidic permanganate in washing bottles [1]; (c) adsorption and/or filtration on solids, e.g. on glass fibre paper [4], activated charcoal [5—8] with or without impregnation with iodine, manganese dioxide [9], silver wool [10], carbon-loaded paper [11] and Chromosorb [12]. Because the direct reading methods measure only elemental mercury and because overestimation may arise from molecular absorption by organic and inorganic compounds or from light scattering by particulates, this procedure will not be discussed here.

It was considered necessary to replace the gas scrubbing techniques involving acidic permanganate solution because they are cumbersome to use, they easily give high results from contamination, and they do not quantitatively

recover mercury in aerosols. These disadvantages can be overcome by taking the gas sample in an evacuated bulb but it then becomes difficult to sample over extended periods. The limit of detection also becomes higher and it is not possible to correct for this immediately by increasing the sample volume. Therefore, methods based on combined solid filtration and solid adsorption were considered. Of the many possible methods, the following were chosen because of the ease with which the mercury can be determined.

Adsorption on manganese dioxide [13] is effective. After adsorption, the sampling material is completely dissolved in hydrochloric and nitric acids. Organo-mercury compounds are also adsorbed on manganese dioxide and many are destroyed by the free chlorine which is liberated when the sampling material is dissolved.

Adsorption on cellulose powder and activated charcoal [8] is also efficient. The sampling material and the adsorbed compounds can be burned in an oxy—hydrogen flame as described earlier [14]. In this way, the solution prepared contains all the mercury as mercury(II) chloride. This procedure has the advantage over the thermal desorption/silver amalgamation method [7] that a wider range of mercury concentrations can be covered by analyzing a suitable aliquot of the final mineralized solution. Because of the combustion step, all organic compounds will be destroyed effectively, so that the method is also applicable to air containing organic mercurials. No activated charcoal is necessary for chlorine gas, because there is no free, elemental mercury present in chlorine gas.

For both methods, the sampling material is packed in sampling tubes. Sampling is done with personal air-sampling (PAS) pumps (Sipin, Kratel, SKC, etc.) or vacuum pressure pumps (Millipore, etc.). The amount of air sampled is measured with a wet gas meter or by counting the number of strokes of the PAS pump.

During the development of both methods, a third method was also evaluated. This is based on adsorption on carbon-loaded paper [11], and proved to be very good when the mercury can be determined by x-ray fluorescence. It is advisable, however, to impregnate the paper with iodine and this interferes during the measurement by atomic absorption spectrometry [1].

The manganese dioxide method and the cellulose powder/activated charcoal method are described separately below.*

COLLECTION ON MANGANESE DIOXIDE

Scope and field of application

This method is suitable for the determination of total mercury in non-aggressive gases (e.g., air, hydrogen, see Note 5) or in chlorine gas. The procedure can be applied if mercury is present as a vapour (Hg^0, $HgCl_2$) as well as an

* For technical reasons, the text of the original methods has been modified and shortened in certain places; those interested in the original text can obtain it in French, German or English on application to the BITC.

aerosol (particulates or adsorbed on dust) or organic mercurials. The lower limit of detection is 0.02 μg Hg per determination (see Note 3).

Principle

The gas is drawn through an adsorption tube, containing manganese dioxide, to collect mercury and mercury compounds. The suction rate is variable, allowing isokinetic sampling if required. After sampling, the manganese dioxide is dissolved in a mixture of hydrochloric acid and nitric acid. In this solution the ionic mercury obtained is determined by cold-vapour atomic absorption spectrometry as described earlier [1].

Apparatus and reagents

An atomic absorption spectrophotometer and accessories as described previously [1] are required. Also required are a vacuum-pressure pump (e.g. Millipore XX 60.220.50), a wet gas meter and adsorption tubes (see [13]). These adsorption tubes are 150 mm long (5 mm i.d.).

Common reagents are not listed here (see Note 1). For all reagents necessary for the mercury determination, see [1] and Note 4.

Manganese dioxide. Suitable qualities are available commercially (10—25 mesh B.S., micro-analytical grade, e.g. Hopkin & Williams no. 548050 or BDH no. 11015, see Note 5).

Glass or quartz wool (e.g. Heraeus GmbH, nr. Mikro RZ 112). Treat with hot nitric acid, wash thoroughly with water, dry in a dust-free atmosphere and store in a box until required.

Hydrochloric acid (ca. 6 M). Distil to remove mercury contamination.

Procedures

Preparation of the adsorption tube for sampling. Carefully clean the tube with concentrated nitric acid, rinse with water and dry. Insert a quartz wool plug into the tube by means of a glass rod, followed by 1 g of manganese dioxide, and tamp well. Insert another quartz wool plug, followed by 1 g of manganese dioxide, tamp and insert a third quartz wool plug (see Note 6). Seal the tube with short pieces of PVC tube, stoppered at one end.

For mercury determinations near the lower limit of detection of the method, special precautions are necessary (see Note 2).

Sampling. Connect the adsorption tube to the vacuum pressure pump (the connecting tube may be of any length). Connect the wet gas meter to the outlet of the pump. Sample the air at a flow rate of about 3 l min^{-1} (max. 4 l min^{-1}). After sampling, seal the adsorption tube with the stoppered PVC tubes. Read the amount of air sampled from the wet gas meter.

Sample pretreatment. Clean the outside of the adsorption tube with water and dry with paper tissue. Break the adsorption tube with the help of the glass cutter at the point where the central quartz wool plug is situated. Transfer the first part of the manganese dioxide and the two quartz wool plugs (part I) into a 200-ml conical flask. Rinse the inside walls of the emptied part of the

tube with 20 ml of hydrochloric acid (ca. 6 M), 2 ml of concentrated nitric acid and a little water successively, and add these to the conical flask. Cover the conical flask with a watch glass, heat to boiling and boil until the manganese dioxide has completely dissolved (if the manganese dioxide does not completely dissolve within 10 min, cool, add a few drops of hydrogen peroxide (30%), and boil again). Cool, transfer the solution to a 50-ml volumetric flask, dilute to volume with water and mix.

Treat the second part of the manganese dioxide and the quartz wool plug (part II) in the same way as part I, to check the efficiency of the mercury adsorption (see Note 6).

Blank determinations. Carry out a daily blank by treating 1 g of manganese dioxide as given for part I under *Sample pretreatment.* The blank should not significantly exceed the upper limit of the confidence interval as given in Note 3. If it is significantly higher, check the adsorption material and the reagents used and replace any with high mercury levels. If the blank still exceeds the upper limit or if it is significantly lower than the lower limit of the confidence interval, redetermine the confidence interval and recalculate the limit of detection.

Determination of mercury content. Determine the amount of mercury, taking a maximum aliquot of 25 ml, both in the sample solution and in the blank solution according to the earlier recommended procedure [1], starting with: *Sample preparation for liquids and suspensions; brine and water samples.* For calibration, the method of standard additions must be used for both solutions to correct for any matrix effects, unless it has been proved that there are no matrix effects.

Calculation

The gas sampled contains:

$$\left[\frac{A_1 \times C_1}{A_2 - A_1} \times \frac{50}{V_1} - \frac{A_3 \times C_2}{A_4 - A_3} \times \frac{50}{V_2}\right] \times \frac{1}{V_3} \ \mu g \text{ Hg } m^{-3}$$

where A_1 = absorbance of sample solution without addition; A_2 = absorbance of sample solution with addition; A_3 = absorbance of blank solution without addition; A_4 = absorbance of blank solution with addition; C_1 = μg Hg in the addition to the sample solution; C_2 = μg Hg in the addition to the blank solution; V_1 = volume of the sample solution aliquot (ml); V_2 = volume of the blank solution aliquot (ml); V_3 = volume of the gas sampled (m^3).

COLLECTION ON CELLULOSE POWDER AND ACTIVATED CHARCOAL

Scope and field of application

This method is suitable for the determination of total mercury in non-aggressive gases (such as air, hydrogen); with a slight modification, the method is also applicable for the determination in chlorine gas. The procedure can be

applied if mercury is present as a vapour (Hg^0, $HgCl_2$) as well as an aerosol (particulates or adsorbed on dust) or organic mercurials. The lower limit of detection is 0.01 μg Hg per sampler assembly (see Note 3).

Principle

The gas sample is drawn by means of a pump through an adsorption tube containing cellulose powder and activated charcoal. For chlorine, only cellulose powder is used. The suction rate is variable, allowing isokinetic sampling if required. After sampling, all the adsorption material is burned in an oxy—hydrogen flame (Wickbold apparatus) according to the BITC procedure [14]. The mercury(II) obtained is condensed and finally determined by cold-vapour atomic absorption spectrometry [1].

Apparatus and reagents

An atomic absorption spectrophotometer and accessories as described previously [1] are required. Also required are a Wickbold combustion apparatus, fully described in [14] and now supplied by Heraeus as Type 4; a sampling pump (Personal Air Sampler, manufactured by Sipin, Kratel, SKC, etc.; flow rate of 50—200 ml min^{-1}, calibrated); a vacuum pump, capable of flow rates up to 200 l h^{-1}; a wet gas meter; soap flow meters (ranges 0—60 and 0—6 ml). For the adsorption tubes, two glass tubes having an outside diameter of 15 mm and threads on one end (such as manufactured by Sovirel, part numbers 4.703.01; 4.701.41; 4.701.23) are fused together to give a tube 190 mm long. Both ends are supplied with screw caps and washers to hold the connection tubes in position. It is advisable to keep the empty glass tubes in a bath of nitric acid (1 + 1) until required.

Common reagents are not listed here (see Note 1). For all reagents necessary for the Wickbold combustion and the mercury determination see [14] and Note 3.

Activated charcoal. Use a granular (particle size 1.5 mm) iodine-free material (E. Merck, Cat. no. 2514 or similar).

Cellulose powder. Schleicher & Schüll (Cat. no. 352005) powder is suitable.

Quartz wool (e.g. Heraeus GmbH, Hanau, nr. Mikro RZ 112). Treat with hot nitric acid, wash thoroughly with water, dry in a dust-free atmosphere, and store in a box until required.

Procedures

Preparation of the adsorption tube for sampling. Rinse the tube and the connections with water and dry in a mercury-free atmosphere. Attach the connection to one end of the tube. Insert a quartz wool plug into the tube, followed by 3.5 g of activated charcoal. Gently tap the tube using a glass rod. Insert the second quartz wool plug, followed by 1 g of cellulose powder and a third quartz wool plug. Tap again, press the plug tightly to the filling, and attach the second connection. Stopper the tube ends and store the tubes in the storage box until required. Keep a blank reference tube for each sampling series.

For the determination of mercury in chlorine gas, follow the same procedure, but fill the tube with a quartz wool plug, 2 g of cellulose powder, and a second quartz wool plug.

Sampling. Insert the adsorption tube directly in the gas stream with the cellulose powder layer at the inlet end and the activated carbon downstream. Connect the adsorption tube to the pump system, using plastic tubing of any required length. In the case of moist gases, it is advisable to put a small water trap between the adsorption tube and the pump. Pass the sample at a flow rate of 3 l min^{-1} (maximum).

If particulate matter is expected in the gas to be analyzed, the flow rate of the sampling system should be adjusted to give isokinetic conditions at the adsorption tube inlet.

If personal samplers are used, it is advisable to measure the flow rate with the soap flow meter before and after sampling, and to use these measurements to calculate the sample volume if it differs from the result obtained from the gas stroke counter of the sampling device.

For mercury determinations near the lower limit of detection of the method, special precautions have to be taken (see Note 2).

Combustion method. A detailed description of the operation of the Wickbold apparatus for this special application is given in [14] under *Combustion of solid samples.* Clean the apparatus with nitric acid and water. Heat the quartz boats in an electric furnace to about 1000°C for 1 h, cool, and finally store them. Assemble the apparatus, ignite the oxy-hydrogen flame and the Bunsen burner and heat the system for about 30 min.

Blank determination. Place 20 ml of water, 5 ml of sulphuric acid (1 + 4) and 0.5 ml of potassium permanganate solution (40 g l^{-1}) into the absorption vessel of the Wickbold apparatus. Carry out a 10-min combustion without sample. Analyze the complete absorber contents for mercury by cold-vapour atomic absorption to confirm that the apparatus is clean. It is satisfactory if less than 30 ng of mercury is found.

Carry out a daily blank using 1 g of cellulose powder and 3.5 g of activated charcoal. The blank should not significantly exceed the upper limit of the confidence interval as given in Note 3. If it is significantly higher, check the adsorption material and the reagents used, and replace any with high mercury levels. If the blank still exceeds the upper limit or if it is significantly lower than the lower limit of the confidence interval, redetermine the confidence interval and recalculate the limit of detection.

Combustion of the sample and mercury determination. Transfer the adsorbent into the quartz boat and burn as described for the blank determination. (A combustion time of 10 min is sufficient to remove the mercury quantitatively from the adsorbent and it is not necessary to continue the heating to complete the combustion of the charcoal.)

Wash the condensate into the 100-ml standard flask, dilute to volume with water and mix. Analyze this solution by atomic absorption spectrometry [14], using a calibration graph established for the range 0—2 μg of mercury per

60 ml. No matrix interferences have been observed and it will not normally be necessary to use the standard additions procedure.

Calculation

The gas sampled contains $(C—C_0) / V$ μg Hg m^{-3}, where C = μg Hg found in 100 ml of sample solution; C_0 = μg Hg found in the blank solution; V = volume of gas sampled (m^3)

General notes

1. Reagents. All reagents must be of analytical-reagent grade and must contain only a very low amount of mercury (E. Merck, Darmstadt, Germany, for example, markets reagents with guaranteed low mercury contents).

Because of the low levels of mercury concerned, extreme care must be taken in the preparation of all the reagents, especially the potassium permanganate solution; the container for this reagent must never be left unstoppered because it rapidly absorbs mercury from the atmosphere. In order to minimize contamination still further, it is advisable to fit as many of the reagent bottles as possible with dispensers. This arrangement, if used permanently, also minimizes the need for clean pipettes and measuring cylinders. A blank determination must always be done.

2. Determinations of very low amounts of mercury. Special precautions have to be taken for mercury determinations near the lower limit of detection of the methods. The tubes, connections, reagents and glass or quartz wool must be stored in a dust-free box in a mercury-free atmosphere. Filling of the tubes has to be done by an experienced laboratory technician, who is familiar with the problems involved in trace analysis. The following procedures are recommended.

Before preparing the adsorption tubes, carry out some blank determinations to check the mercury content of the reagents to be used. After filling, store the tubes vertically in the dust-free box. Fill at least an extra 3 tubes and for large series about 10% more; use these as blanks, and store them in the dust-free box during sampling with the other tubes.

Test the connections for leaks and then seal the tubes into polyethylene bags. After sampling, wash the tubes with diluted nitric acid, rinse them with water and dry.

Before starting the analysis, clean all glassware to be used with hot nitric acid. Check by analyzing the nitric acid used. When a Wickbold combustion apparatus is used, ensure that it gives a low blank; after all the samples have been burned, rinse the glassware again with nitric acid. Remove the solids burner, stopper it and store in the dust-free box; stopper the combustion chamber and condenser and cover the apparatus with polyethylene foil. Use the glassware (and the Wickbold apparatus) only for trace mercury analysis. Do not send the glassware to the general glass-cleaning department of the laboratory for cleaning. Store all glassware in dust-free boxes.

3. Blank monitoring; determination of the limit of detection. It is essential for correct operation of procedures with high sensitivity at concentration levels close to the limit of detection, to monitor and control the blank values in order to ensure that the results obtained are meaningful and that a realistic value for the limit of detection is quoted depending on the blank values which each individual laboratory can achieve.

For the method of analysis in use, carry out a series of ten blank determinations following the appropriate procedure given. Calculate the standard deviation of a single blank and use it to calculate the confidence interval (*CI*) from the expression: $CI = \bar{x} \pm st_{(P,f)}$, where $\bar{x}$ = mean of the blank values; s = standard deviation; t = Student's confidence coefficient (here 2.26); P = probability (here 95%, two-sided); f = degree of freedom (here, for 10 measurements, 9).

The limit of detection (*LD*) is given by the expression $LD = s\, t_{(P,f)}$, where s = standard deviation; t = Student's confidence coefficient (here 3.25); P = probability (here 99.5%, one-sided); f = degree of freedom (here, for 10 measurements, 9).

4. Preservation of mercury-containing solutions. More recent knowledge [15] about the preservation of mercury-containing solutions makes it advisable to stabilize the standard mercury solutions in [1] and [14] with acid dichromate. For this purpose, add 50 ml of dichromate solution [containing 4 g of potassium dichromate per litre of (1 + 1) nitric or sulphuric acid] before the standard mercury solution is diluted to 1 l.

5. Manganese dioxide. At the moment, manganese dioxide cannot be obtained with a specified low mercury content. Different batches may contain mercury in varying quantities; values between 70 ng Hg g^{-1} and 36000 ng Hg g^{-1} of MnO_2 have been found, but values between 100 and 300 ng Hg g^{-1} of MnO_2 are normal. Although the limit of detection is not directly related to the blank value, a high blank usually gives a higher standard deviation for the blank and therefore a higher limit of detection. The detection limit of 0.02 μg Hg (given in the Scope) was found with batches containing about 150 ng Hg g^{-1} of manganese dioxide.

If the maximum flow rate obtainable through the adsorption tubes is less than 3 l min^{-1}, the flow rate can be increased by sieving the manganese dioxide through a 22-mesh (B.S.) sieve (ca. 710 μm) and rejecting the fraction passed.

At ordinary temperatures and pressures, there is no appreciable reaction between manganese dioxide and hydrogen [16], so that there is no hazard in using the method for the determination of mercury in hydrogen.

6. Adsorption tubes with manganese dioxide. The contents of the second part of the adsorption tube are used only to check the efficiency of mercury adsorption. This check should be done at least when a new bottle of manganese dioxide is used or when an unknown gas stream is examined.

TESTING THE METHODS

The methods had been tested individually during development. Detailed results have been given in earlier papers [8, 13]. These tests were done with inert gases. The methods were compared by taking samples at the same place and time in two different cell rooms of chlor-alkali electrolysis plants with mercury cells, and with a wet gas stream with a high mercury and chlorine content. The results for cell room air agreed within ± 20% at levels of <100 μg Hg m^{-3}. For the wet gas, the methods were compared without a drying agent and by using a low sampling speed of 5 l h^{-1} (personal air sampler). The results agreed within ± 2% at the level of 500 μg Hg m^{-3}.

Later, the methods were tested for the determination of mercury in chlorine gas. The manganese dioxide method can be used for this determination without any modifications, but the cellulose powder—activated charcoal method needed some modification, because of the adsorption heat in the charcoal column. To avoid this, the adsorption capacity of cellulose powder alone was tested in the laboratory. By means of a permeation apparatus [17], gaseous chlorine from a steel cylinder was spiked with mercury. The insensitive evacuated-bulb method, which was to be used as an independent control procedure, required mercury concentrations in the range of 1—2 mg Hg m^{-3} to give reliable and statistically significant answers. Further evidence for the mercury recovery of the adsorption system to be tested was obtained by inserting four separate layers of cellulose powder in the adsorption tube, which subsequently could be analyzed separately for mercury by combustion in the oxy-hydrogen flame of the Wickbold apparatus; 1 g of cellulose powder was used for each layer, separated by quartz wool.

In order to obtain a mercury concentration which is constant with time, in the off-stream of the permeation apparatus, it is essential to equilibrate this device by passing chlorine through it under suitable test conditions for at least 4 h, prior to the start of the investigation. The test conditions selected were a chlorine gas flow of 50 l h^{-1} ± 5 l h^{-1}, and an integration time of 60 min. During the integration period, samples were taken in front of and after the adsorption tube with a 1000-ml evacuated bulb. After termination of the test, the separate layers of the adsorption tube were burned and the inorganic mercury in the condensate was determined according to the recommended method. The results are given in Table 1.

CONCLUSIONS

In many experiments and measurements, it has been proved that both methods give good results and are generally applicable. The sampling speed is not important for either method as long as the upper limits given are not exceeded. Both methods can be used for dry or wet air.

There are circumstances in which one method is more suitable than the other, however. The manganese dioxide method is easy to operate and cheap.

TABLE 1

Determination of mercury in chlorine gas

Mercury found in the cellulose powder layers			Evacuated bulb control measurements at system inlet[a]	
Layer	μg Hg	μg Hg m^{-3} Cl_2[b]	Measurement	μg Hg m^{-3} Cl_2
1	221	4420	1	4200
2	0.03	0.6	2	4900
3	0.03	0.6	3	4500
4	0.04	0.8	4	3900
			Mean c	4375
			Standard deviation	427

[a]Measurements in front of the adsorption tube. All evacuated bulb control measurements at system outlet (behind the adsorption tube) were less than 50 μg Hg m^{-3}.
[b]Total blank of the system: (cellulose powder + combustion gases + reagents) = 40 ng of mercury per combustion.

The adsorption material is completely dissolved, but possibly not all organic compounds will be completely mineralized. The charcoal—cellulose powder method allows efficient mineralization of all mercury compounds (also organics), and there is no interference from non-atomic absorption. It is, therefore, suitable when the gas composition is not known. However, the Wickbold combustion equipment is comparatively expensive, and an experienced specialized operator is essential.

REFERENCES

1 BITC Working Group Mercury Analysis, Anal. Chim. Acta, 72 (1974) 37. (Part 1).
2 A. M. Ure, Anal. Chim. Acta, 76 (1975) 1.
3 S. Chilov, Talanta, 22 (1975) 205.
4 W. Wiedner, H. Nathansen, G. Thümmler and H. Litke, Z. Ges. Hygiene, 20 (1974) 4.
5 A. E. Moffitt and R. E. Kupel, At. Absorpt. Newsl., 9 (1970) 113.
6 H. A. van der Sloot and H. A. Das, Anal. Chim. Acta, 70 (1974) 439.
7 F. P. Scaringelli, J. C. Puzak, B. J. Bennett and R. Denny, Anal. Chem., 46 (1974) 278.
8 W. Dürr and K. Hausmann, Fresenius Z. Anal. Chem., 283 (1976) 337.
9 M. K. Pakter, Gig. Sanit., 34 (1969) 401.
10 S. J. Long, D. R. Scott and R. J. Thompson, Anal. Chem., 45 (1973) 2227.
11 J. H. Janssen, J. E. van den Enk, R. Bult and D. C. de Groot, Anal. Chim. Acta, 84 (1976) 319.
12 R. S. Braman and D. L. Johnson, Environ. Sci. Technol., 8 (1974) 996.
13 J. H. Janssen, J. E. van den Enk, R. Bult and D. C. de Groot, Anal. Chim. Acta, 92 (1977) 71.
14 BITC Working Group Mercury Analysis, Anal. Chim. Acta, 84 (1976) 231 (Part 2).
15 C. Feldman, Anal. Chem., 46 (1974) 99.
16 J. W. Mellor (Ed.), A Comprehensive Treatise on Inorganic and Theoretical Chemistry, Vol. XII, Longmans, London, 1961, p. 252.
17 A. Cedergren, A. Wickby and K. Berger, Anal. Chem., 47 (1975) 100.

Analytica Chimica Acta, 108 (1979) 13—20
© Elsevier Scientific Publishing Company, Amsterdam — Printed in The Netherlands

A RAPID, SIMPLE METHOD FOR THE DETERMINATION OF TOTAL MERCURY IN FISH AND HAIR BY COLD-VAPOUR ATOMIC ABSORPTION SPECTROMETRY

D. GARDNER* and G. DAL PONT

CSIRO Division of Fisheries and Oceanography, P.O. Box 21, Cronulla, 2230 (Australia)

(Received 15th January 1979)

SUMMARY

Fuming nitric acid and acidified potassium permanganate are used to pre-digest fish or hair samples in Pyrex culture tubes. Cold-vapour atomic absorption spectrometry is used to detect the elemental mercury which is generated by reduction in a syringe. The absolute detection limit of the method is 0.66 ng Hg, and at levels of 0.14 and 0.60 parts per million (ppm) the standard deviations are ±0.009 and ±0.008 ppm, respectively. One person can handle batches of 50—100 samples per day including standards and blanks.

In most countries, in order to have health controls on mercury ingestion, limits are set on the mercury content of fish, the main source of dietary mercury. Human tissues store ingested mercury, and hair is usually chosen for monitoring mercury intake in persons at risk [1]. To determine these mercury concentrations, health authorities ideally need an analytical technique which is able to produce quickly and in large numbers results which are accurate and precise.

In a recent interlaboratory calibration exercise [2] the mercury concentration in a shark sample was determined by 21 laboratories and gave a spread in mean mercury concentrations from 0.39 to 1.00 ppm. Such a spread is not uncommon for interlaboratory exercises and health authorities have to be cautious about the levels reported for mercury in fish if decisions on generally acceptable limits are to be made from them.

The method reported here incorporates and improves on some of the better points of three other methods for the determination of total Hg [3—5]. The procedure is simple, can be carried out in moderately contaminated laboratories, and gives precise and accurate results for as many as 100 pre-weighed samples per day.

EXPERIMENTAL

Reagents

All reagents were analytical grade and were prepared in mercury-free water. These comprise: fuming nitric acid, (*d*, 1.52; Merck 455); 10% sulphuric acid

(*d*, 1.84; Merck 732 or M and B Proanalysis); a 6% (w/v) solution of potassium permanganate made up in mercury-free water (oxidizing solution); a reducing solution containing 0.5 g of NaCl, 1.0 g of hydroxylammonium sulphate and 2.0 g of tin(II) sulphate dissolved in 100 ml of 10% (v/v) H_2SO_4; magnesium perchlorate, which was renewed daily and more often if it became moist during use.

Standard mercury solutions

For the stock standard (1 mg Hg^{2+} ml^{-1}) 0.1354 g of $HgCl_2$ was dissolved in 5% HNO_3 to which 0.05% (w/v) $K_2Cr_2O_7$ had been added as a preservative; this solution is stable for years.

Working standards (1 μg Hg ml^{-1}) were prepared by diluting 1 ml of the stock solution to 1 l with 5% HNO_3 which contained 0.05% (w/v) $K_2Cr_2O_7$. Larger volumes can be prepared and stored by dispensing 5-ml aliquots into pre-combusted 10-ml glass ampoules which are sealed immediately. One ampoule can then be opened each day, allowing many months of work to be done from the same batch of standards.

Equipment

All glassware was stored in chromic acid. Before use it was rinsed well with mercury-free distilled water and drained until dry at room temperature. The apparatus comprised 50-ml Pyrex culture tubes with screw caps which had Teflon liners, a "Vortex Genie" tube mixer, 5- and 10-ml graduated pipettes, and micro dispensers with disposable tips able to inject 10—1000 μl.

Mercury absorption was measured at 253.7 nm (slit width 1.0 nm) on a Varian-Techtron AA6 atomic absorption spectrometer fitted with a Varian mercury vapour discharge tube operated at 3mA, and a Varian A25 recorder operated at a 5-mV span and a chart speed of 8 mm min^{-1}. The spectrometer was warmed for 30 min or until the digital display was steady at an absorbance of ±0.001.

Figure 1 shows the manifold designed to inject and flush the mercury vapour into the light patch of the spectrometer. The sample and air are drawn in through Teflon needle (a) and the mercury vapour is generated, as described later, in a 20-ml all-glass syringe (b). The syringe is connected to a luer-lock Teflon needle (c) which is, in turn, connected by a thin tube (4 mm × 60 mm) to the main gas flow tube (d). Once the vapour has been injected, the syringe is removed and a small stopper (m) is inserted into (c). High-purity nitrogen at 150 ml min^{-1} passes into a perspex valve (e). From there it can be passed through tube (d) and the magnesium perchlorate drying tube (f) which is attached by Tygon tubing (h) to a quartz-windowed absorption cell (g) (170 mm long with a volume of 29 ml) and finally through to the waste gas receptacle which contains acidified $KMnO_4$ (i). This nitrogen either flushes the mercury vapour to be determined into the light path or purges the cell clear of the last sample determined. By altering the position of the plunger (l), it can also be vented through (j) into the laboratory while mercury vapour from the next sample is being injected.

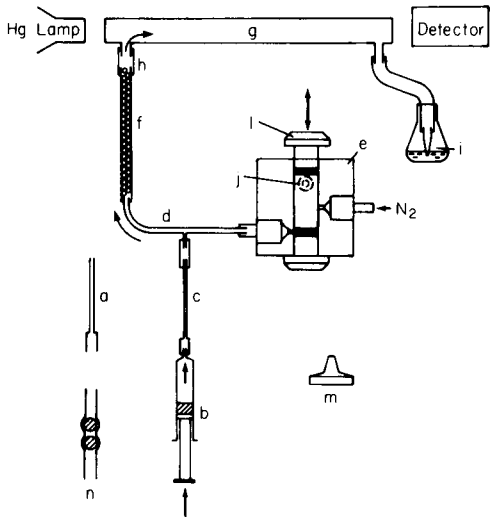


Fig. 1. The injection manifold used with the atomic absorption spectrometer. For identification of the components, see text.

Sample preparation

Fish. A sample (50 g) of muscle from fresh fish (gemfish, *Rexea solandri*) and New Zealand whiptail (blue genadier, *Macrurorus novaezelandiae*) from various trawls were placed into numbered Nasco Whirl-pak (100 × 200 mm) sterilized plastic bags. The bags were flash-frozen and stored for analysis. The surface layer of the frozen sample was scraped off and discarded, 0.4—0.5 g of thin slices was cut off with a sharp knife or a pellet was stamped out and the sample was put into a pre-weighed dry 50-ml Pyrex culture tube.

Samples (0.08—0.11 g) equivalent to a 0.4 g sample (wet weight) of freeze-dried shark [2, 6] and NBS albacore tuna reference material [7] were weighed dry, and then reconstituted by adding four parts by weight of mercury-free water for each part of fish weighed out.

Hair. Locks of hair (ca. 0.08 g) were placed in Teflon beakers, washed in 5% Teepol in an ultrasonic bath, and rinsed thoroughly with distilled water. Before weighing, samples were left in dust-free, mercury-free air to dry and to equilibrate with atmospheric moisture.

Blanks and standards. Between 100 and 500 μl of a working standard (1 μg Hg ml^{-1}) were dispensed into dry culture tubes. The volumes were made up to 500 μl with mercury-free distilled water. Several blanks with 500 μl of water were also prepared, one for calibration and the remainder for samples which would require dilution during the determination.

Procedure

After the culture tubes had been cleaned, dried and weighed, the sample was placed in the tubes which were then reweighed. Blanks and standards

were prepared, as described above. Fuming nitric acid (1 ml) was added to each tube and the screw caps replaced. The tubes were placed in a water bath at 60°C for 15 min and agitated intermittently. The tubes were cooled (preferably in an ice bath) and 2.5 ml of 10% sulphuric acid added. Still cooling the tubes, 10 ml of the oxidizing solution was added dropwise. A vortex mixer was used to mix the contents of the capped tubes. The oxidation was allowed to proceed for at least 30 min, before cooling the tubes in a water bath. A few crystals of hydroxylammonium sulphate were added and each tube was mixed to clear the suspension of manganese oxides. When the solution in each tube was clear, 0.1 g of sodium chloride was added. The tubes were mixed once more and allowed to come to room temperature before analysis.

The spectrometer was set up as described above, with the nitrogen flowing through the cell. The digest (2 ml), followed by 2 ml of reducing solution, were drawn through a Teflon needle into the syringe. The syringe was held vertically and 16 ml of air drawn in. The needle was replaced by a sealing cap (n) and the syringe shaken for 15 s. The nitrogen flow was vented through (j), then, with the syringe nozzle upright, the luer stopper (m) was removed, the syringe was immediately connected to (c), and the 16 ml of mercury vapour was injected into the cell. Once a small drop of the liquid entered (c), the syringe was removed and the luer stopper replaced. (This drop prevents any gas loss during the transfer; if excess of liquid is allowed to moisten the magnesium perchlorate, the drying tube must be dried, repacked and replaced, and 5 min allowed for the system to equilibrate before proceeding.) The nitrogen was redirected through the cell, and the maximum digital absorption value read or the peak height of the recorder signal measured.

The liquid remaining in the syringe can then be discarded and the syringe and needle rinsed with distilled water. The injection port is opened and cleared with the nitrogen flow. The whole determination takes 1 min to complete.

Various volumes of sample can be taken, if the same volume of standards and blanks is used for calibration. For preliminary determinations, the use of 2 ml of digest solution is recommended. Samples that are off-scale should be diluted with some of the blank solution.

If a result must be checked and there is no digest solution left except that remaining in the syringe after the first extraction, a further 16 ml of air can be introduced into the syringe. If the contents are shaken and injected as before, a second mercury determination can be made. Similar treatment of standards and blanks will give a second calibration curve. Depending on the initial mercury concentration of the digest, 5—7 extractions are possible before all the mercury (to below the detection limit) has been removed from that sample.

RESULTS

The mercury concentration (ppm) in the sample is given by:
K (sample absorption − blank absorption)/weight of sample (g),

where K is the mean of the ratios of mercury amounts in the standards (in μg) and their corrected absorption. On the instrument used, for the volumes of sample, reagent and air described in the procedure, the day-to-day value of K varied between 0.85 and 0.90.

The absorbance given by 2 ml of digest spiked with 80 ng of Hg was 0.100. The standard deviations for replicate dried samples of fish ranged from ±0.004 to ±0.009 ppm for levels of 0.240—0.930 ppm. For wet fish samples analyzed in batches, the standard deviation was ±0.008 ppm at a level of 0.140 ppm.

The absolute detection limit at the 95% confidence level, calculated as twice the standard deviation of the mean of the mercury concentrations in 2-ml aliquots from ten separate reagent blanks, was 0.66 ng when the spectrometer was operated in the clean room and 0.92 ng in a general laboratory.

DISCUSSION

Several methods [3, 5, 8] for the determination of mercury in organic matter and fish were examined. All included the classical reduction to elemental mercury by a tin(II) solution [9]. For rapid analysis of large numbers of samples, the chromic acid oxidation method [5] was found to have the greatest potential. However, the use of chromic acid has many disadvantages. These drawbacks include simple problems like the time required to make up the oxidizing solutions; the need to add water to the chromate in concentrated sulphuric acid; the brown appearance of the digest and its dark green colour after hydroxylammonium sulphate had been added, both of which prevent examination to see if all material has been oxidized fully; the heat of mixing 40% H_2SO_4 with reductant which changes the amount of mercury vapour in the vapour phase in the syringe; and the high blank (100 ng of Hg), which is four times greater than that for the permanganate digestion method. Acid permanganate was chosen as a suitable alternative oxidant.

A comparison of the chromic acid digestion method with the permanganate method described here showed that lower and more scattered mercury values are obtained by the former technique. Table 1 shows this difference for shark sample number 16—77 and Table 2 shows it for several New Zealand whiptails which were analyzed by both methods.

The technique described here differs from the permanganate method described by Uthe et al. [3] in that an initial digestion with fuming nitric acid is included. The total digestion time is only 45 min compared to 4 h if acidic permanganate is not used [10]. The digest is colourless and, as the concentration of the sulphuric acid present in the final digest is close to that in the reductant (10%), very little heat is evolved when the two are mixed. The results obtained for NBS tuna showed no significant trend with increasing sample weights up to 0.12 g (Table 1). More than 0.12 g of dry matter could not be completely digested by the oxidizing agents present, as indicated by turbidity in the final digest and resultant low mercury concentrations.

TABLE 1

Mean mercury levels (ppm) and standard deviations (s) in replicate (N) samples of freeze-dried NBS tuna standard samples, shark reference materials and frozen gemfish

	NBS Tuna[a]	Shark 16-77		Shark 101-78	Shark 102-78	Shark 103-78	Gemfish A	B
	$KMnO_4$	$KMnO_4$	Chromic	$KMnO_4$	$KMnO_4$	$KMnO_4$	$KMnO_4$	
N	9	8	11	6	6	6	6	6
Mean	0.93	0.60	0.55	0.24	0.36	0.69	0.13	0.14
s	0.02	0.009	0.02	0.011	0.004	0.014	0.008	0.008
Mean of all previous analyses	0.95	0.62	—	0.256	0.379	0.686	—	—
s of these means	0.10	0.143	—	0.045	0.051	0.108	—	—
No. of samples	—	259	—	92	113	120	—	—

[a]Sample weights were in the range 0.0884—0.1175 g and there was no significant trend in the results with increasing sample weight. However, other samples weighing 0.125—0.150 g gave lower results (0.86—0.90 ppm) and were turbid, indicating incomplete digestion.

TABLE 2

Mercury levels (ppm) in several New Zealand whiptails by the $KMnO_4$ method and a chromic acid digestion method [5]

Sample No.	$KMnO_4$	Chromic acid	Sample No.	$KMnO_4$	Chromic acid
1	0.14	0.14	6	0.37	0.36
2	0.52	0.47	7	0.5	0.4
3	0.12	0.11	8	0.22	0.19
4	1.65	1.45	9	1.49	1.30
5	0.24	0.23	10	0.58	0.55

The addition of sodium chloride to the clear digest after the hydroxylamine prevented foaming in the syringe, increased the amount of mercury in the vapour phase by 15%, and preserved the mercury in the digest if analysis could not be done immediately. In two weeks no change was found in digests preserved in this manner. Digests without sodium chloride lost 10—30% in the same period. The use of sodium chloride to preserve solutions containing mercury has been reported by Amke and Suwabe [11].

The apparatus used to inject the mercury vapour into the absorption cell was designed to minimize mercury losses in the lines by making them as short and narrow as possible and prevent mercury losses when the syringe was

replaced by the stopper. This was achieved through surface tension; the liquid in the permanganate trap (i) and the drop of digest injected into (c) trapped the mercury vapour in the manifold.

Figure 2 shows the difference in the baseline readings of analyses before and after the atomic absorption spectrometer was installed in a Class 100 clean air room. The decrease in the baseline noise lowered the absolute detection limit from 0.92 ng to 0.66 ng. The noise was due to particles in the air passing between the mercury lamp and the absorption cell. This effect was particularly bad on humid days, but was eliminated completely in the clean room.

The method was tested on NBS albacore tuna [7]. Table 1 shows the mercury concentrations found, the mean and standard deviation calculated, and the recommended mean and standard deviation supplied with the standard. Similarly, Table 1 shows the results of replicate analyses of shark reference material and an overall mean determined by averaging the mean mercury concentrations found by each laboratory participating in an Australian inter-laboratory calibration exercise [2, 6]. The results for replicate samples of frozen gemfish are also shown. The precision and accuracy are excellent. In fact, the mean concentrations for the shark samples, when compared to those of all the other participating laboratories, were always amongst the closest to the overall means and always had the smallest standard deviations.

In order to prove that the method will consistently give reproducible results, samples cut from frozen wet gemfish were analyzed periodically over a period of more than a year (Table 3). There was no trend in the mercury concentrations measured. The deviations from the means varied from ±0.02 to ±0.08 ppm for levels of 0.46—1.48 ppm. The increase in these standard deviations, over those calculated from replicate analyses of gemfish measured all on the same day, could be caused by slight variability in the time the fish was out of the freezer before samples were sliced off. This would affect the water content of the samples.

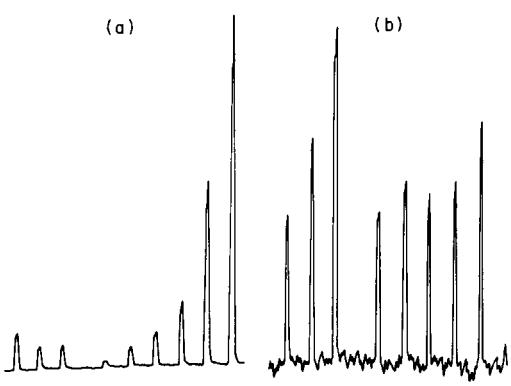


Fig. 2. Comparison between a series of mercury determinations measured in a clean room (a) and in a general laboratory on a humid day (b).

Hair was also successfully digested and analyzed at mercury levels from 0.05 to 32.40 ppm. As mercury levels often fluctuate dramatically along very short lengths of hair [12] a homogeneous sample could not be prepared and so a reproducibility test could not be done. Routine standard addition techniques showed that hair digests behaved in the same manner as those of the fish. These results will be reported in detail elsewhere. The method cannot be used to digest cereal products for mercury analysis as the levels contained are below the detection limit; nor can it be used for seaweeds as some dissolved organic material present prevents the reduction and release of mercury.

This method is recommended to laboratories that handle large numbers of samples and to those that require a technique which consistently gives precise and accurate results.

TABLE 3

Effect of storage on mercury content (ppm) of several gemfish preserved by freezing

Sample no.	April 18 1977	July 21 1977	July 14 1978	Mean	*s*
1	0.51	0.46	0.57	0.51	0.06
2	0.87	0.84	0.98	0.89	0.07
3	0.73	0.68	0.66	0.69	0.04
4	0.73	0.69	0.80	0.74	0.06
5	1.45	1.42	1.57	1.48	0.08
6	0.45	0.48	0.45	0.46	0.02

REFERENCES

1 T. W. Clarkson, in S. S. Brown (Ed.), Clinical Chemistry and Chemical Toxicology of Metals, Elsevier, New York, 1977.
2 Analytical Workshop of Mercury in Fish, Report on Australian Interlaboratory Survey by Australian Environment Council/Australian Fisheries Council Joint Technical Working Group on Marine Pollution, July 1977 (in preparation).
3 J. F. Uthe, F. A. J. Armstrong and M. P. Stainton, J. Fish Res. Board Can., 27 (1970) 805.
4 M. P. Stainton, Anal. Chem., 43 (1971) 625.
5 A. Bouchard, At. Absorpt. Newsl., 12 (1973) 115.
6 Analysis of total and organic mercury in fish, Report on Australian Interlaboratory Survey by Australian Environment Council/Australian Fisheries Council Joint Technical Working Group on Marine Pollution, October 1978 (in preparation).
7 P. D. LaFleur and W. P. Reed, Research Material 50, National Bureau of Standards, Washington, D.C., 1977.
8 D. Gardner, Anal. Chim. Acta, 93 (1977) 291.
9 W. R. Hatch and W. L. Ott, Anal. Chem., 40 (1968) 2085.
10 M. R. Hendzel and D. M. Jamieson, Anal. Chem., 48 (1976) 926.
11 M. Amke and K. Suwabe, Anal. Chim. Acta, 92 (1977) 55.
12 T. Giovanoli-Jakubczak, Arch. Environ. Health, 28 (1974) 139.

Analytica Chimica Acta, 108 (1979) 21—30
© Elsevier Scientific Publishing Company, Amsterdam — Printed in The Netherlands

THE DETERMINATION OF ORGANIC AND INORGANIC LEAD COMPOUNDS IN URBAN AIR BY ATOMIC-ABSORPTION SPECTROMETRY WITH ELECTROTHERMAL ATOMIZATION

W. DE JONGHE and F. ADAMS*

Department of Chemistry, University of Antwerp (U.I.A.), B-2610 Wilrijk (Belgium)

(Received 25th January 1979)

SUMMARY

A method for the simultaneous determination of inorganic and organic lead compounds in air is described, together with some results from its application at different sampling sites. Air-borne particulate lead is collected on a cellulose filter. Organic lead vapours are trapped in an iodine monochloride solution, placed behind the filter. A fraction of the cellulose filter is subjected to low-temperature ashing, after which the lead content in the residue is measured by electrothermal atomic-absorption spectrometry. The organolead material absorbed in the iodine monochloride solution, is determined by solvent extraction and electrothermal atomic-absorption spectrometry. For a 6-h sampling period, detection limits of the order of 10 ng m^{-3} for inorganic and 8 ng m^{-3} for organic lead materials may be obtained.

Organolead compounds are usually assumed to contribute only a negligible part to the total lead hazard in polluted areas, and in most air pollution measurements, sampling and analysis are focused on inorganic particulate lead. Yet, the brain tissues of individuals residing in the lower floors of urban buildings show significantly higher organic lead contents than those of residents in suburban or village areas [1]. In view of the great toxicity of organolead compounds, monitoring of their concentrations is therefore desirable.

Air-borne particulate lead is usually collected on a membrane or glass fibre filter. For the tetraalkyllead compounds, Moss and Browett [2] used an ICl/HCl solution, placed behind a filter. The organolead collected in this way was determined colorimetrically by the dithizone method. Extraction of the organic lead into methyl isobutyl ketone as the ammonium pyrrolidinedithiocarbamate [3] or the dithizonate [4], followed by atomic-absorption spectrometry has also been used. For a detection limit of 200 ng m^{-3}, sampling for 24 h is required. Lead particulates passing the filter are collected and determined as if they were organic lead, which may result in considerable positive errors.

Another way of collecting the organic lead compounds is by adsorption on activated carbon. After sampling, the adsorbed lead is removed from the carbon by treatment with oxidizing acids. The extracted lead can then be

determined colorimetrically by dithizone [5]. Here too, lengthy sampling periods of 2—4 days are required. Harrison et al. [6] described a more sensitive determination, by using a g.c. column for the adsorption and completing the analysis by atomic-absorption spectrometry.

Other, more elaborate procedures are based on gas chromatography ccupled with a specific detector like mass spectrometry [7], atomic-absorption spectrometry [8, 9] or a microwave plasma detector [10].

In this paper, the procedure for organic lead compounds as proposed by Hancock and Slater [11] is further tested and developed. A sensitive method for the determination of inorganic, particulate lead compounds is incorporated. Both analytical methods were thoroughly tested in practical circumstances at a great diversity of sampling sites.

EXPERIMENTAL

Apparatus

Amber-glass separating funnels provided with Teflon stopcocks and stoppers were used for extractions. Atomic-absorption analyses were done with a Perkin-Elmer 503 atomic-absorption spectrometer in combination with a PE HGA-74 graphite furnace atomizer. The source was a PE 303-6039 lead hollow-cathode lamp. Absorbances were read as peak heights from the built-in peak-read device of the spectrometer. A fast-response strip-chart recorder (Hitachi-PE 56) was used for recording the signals. The furnace was flushed with argon (l'Air Liquide N 46) at a flow rate of 300 ml min^{-1} internally and 900 ml min^{-1} externally. The gas flow could be changed during the atomization stage to vary the sensitivity, by means of the stopped (gas-stop), reduced (mini-flow) and continuous (gas-flow) flow settings. Aliquots were injected with Eppendorf micropipettes with disposable polypropylene tips.

Reagents

The preparations of the iodine monochloride solution (0.1 M), ammonium citrate—ammonia buffer (pH 11.1), EDTA solution (0.1 M) and dithizone solution (8×10^{-5} M) were analogous to those described by Hancock and Slater [11]. The oxidizing acid solution was prepared by diluting 1 ml of concentrated nitric acid and 3.4 ml of 30% (100 vol.) hydrogen peroxide to 100 ml with doubly-distilled water. Standard solutions were made with lead nitrate (Merck 9969) and with diethyllead dichloride (Pierce Inorganics P 10938). The water used was doubly distilled in a quartz apparatus after mixed-bed deionization.

Sampling procedure

The sampling technique used allows collection of both particulate lead and gaseous organic lead compounds. Figure 1 schematically shows the experimental setup. Air-borne particulate lead is collected on a Whatman-41 cellulose filter mounted in a Schleicher and Schüll FP 050/2 filter holder (50-mm diameter).

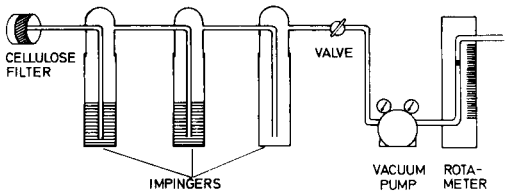


Fig. 1. Experimental sampling apparatus.

After passing the filter, the filtered air is led through an ICl/HCl solution, where the tetraalkyllead compounds are collected quantitatively by conversion to the corresponding dialkyllead dichlorides [2]: two amber-glass midget impingers, each containing 15 ml of a 0.1 M iodine monochloride reagent, are connected in series with Teflon pieces. These are connected to an empty impinger for protection of the pump. Air is drawn through the sampling train with a Millipore XX-60-220-50 vacuum pump. The flow rate, adjustable by means of a valve, is regulated to approximately 31 min^{-1} [11]. The sampled air volume is calculated from readings of a GC-Elliot 1100 rotameter.

Analysis for inorganic lead

About 7 cm^2 of the aerosol-loaded filter paper is cut into small pieces. These are transferred to a Teflon vessel of 3-ml capacity. This vessel is placed in a low-temperature ashing device (Tracerlab LTA 302) for 1 h; the working conditions are: 1.5 mm Hg pressure, oxygen flow of 25 ml min^{-1}, 100 W r.f. power. The residue is dissolved in 1 ml of 0.5 M nitric acid, by placing the Teflon vessel under an infrared lamp for a maximum of 10 min; the temperature should be kept below 50°C to prevent solvent losses. Figure 2 shows the increase in concentration as a function of time at several temperatures. An aliquot is taken from the 1 ml of solution and injected into the graphite-tube furnace of an atomic-absorption spectrometer.

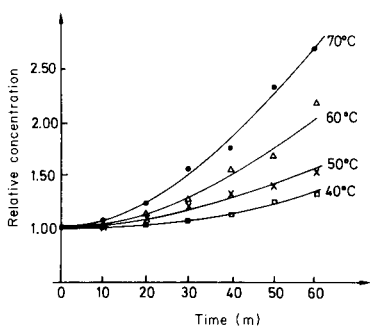


Fig. 2. Solvent losses caused by infrared irradiation.

Analysis for organic lead

After sampling, the iodine monochloride solutions are transferred from the impingers to 100-ml separating funnels, and the empty impingers are rinsed with 5 ml of doubly-distilled water, which is also transferred to the funnels. Then 20 ml of an ammonium citrate—ammonia buffer (pH 11.1) is added. The black precipitate of iodine that is formed disappears immediately on shaking. Then 40 μl of a 0.1 M EDTA solution is added and the separating funnel is shaken for 1 min; the EDTA masks any free lead ions present. The dialkyl lead is then selectively extracted with dithizone, by shaking for 1 min with 5 ml of a 8×10^{-5} M solution of dithizone in carbon tetrachloride. After phase separation, the organic layer is run off into a second separating funnel. The extraction is repeated with a fresh portion of dithizone, and the combined organic phases are then shaken for 1 min with 2 ml of the oxidizing acid solution. This converts the initially organic lead material to lead nitrate, which dissolves in the aqueous layer. The organic layer is run off, and the middle portion of the aqueous solution is collected in a polypropylene microtube.

The lead content of the aqueous solution is measured by electrothermal atomic absorption spectrometry. The optimal furnace program was established after an investigation of the ashing and atomization characteristics for an oxidizing acid solution of the following composition: 0.14 M nitric acid, 1% hydrogen peroxide, and 0.1 ppm Pb as lead nitrate. Measurements of the absorbances for increasing ashing temperature with constant atomization temperature, and for increasing atomization temperature with constant ashing temperature, resulted in a typical "double curve" (Fig. 3). The optimal ashing and atomization temperatures are therefore about 500°C and 2500°C. A study of ashing losses as a function of the ashing time for different ashing temperatures (Fig. 4) showed that there are no ashing losses at 500°C. The most important instrumental parameters are: wavelength, 283.3 nm; slit width, 1 mm; spectral bandwidth, 0.7 nm; lamp intensity, 10 mA; gas flow, variable; volume injected, 20 μl; drying cycle, 100°C/25 s; ashing cycle, 500°C/20 s; atomization cycle, 2500°C/10 s; cleaning cycle, 2700°C/10 s.

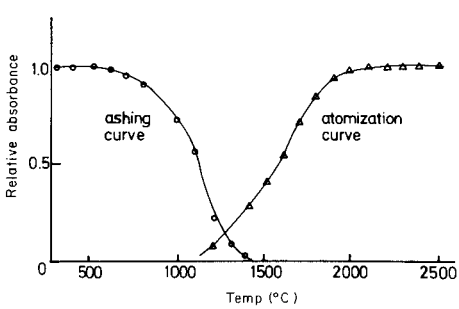


Fig. 3 (left). "Double curve" for an oxidizing acid solution containing 0.1 ppm Pb.

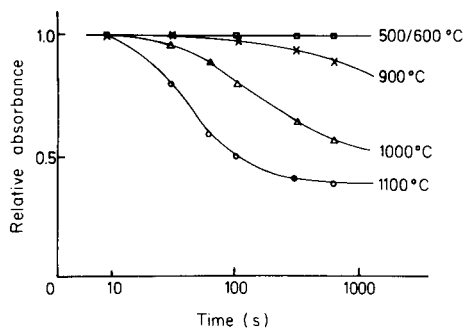


Fig. 4 (right). Ashing losses for different ashing temperatures.

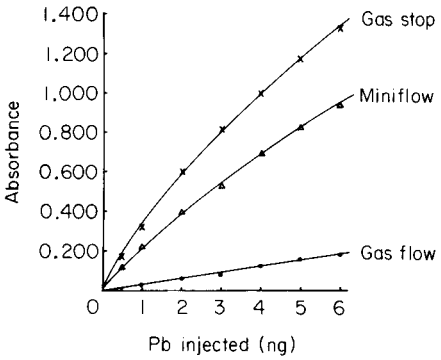


Fig. 5. Typical calibration curves for the 283.3-nm lead line.

Typical calibration curves for the gas-flow, mini-flow and gas-stop modes are shown in Fig. 5.

RESULTS AND DISCUSSION

Blank values

The blank value of the procedure, and thus the detection limit, results from impurities in the reagents and materials used. Free lead ions are probably the main source of blanks in the extraction procedure for the determination of organic lead compounds. Since all the free lead ions present in the iodine monochloride, buffer and EDTA solutions become masked, the blank contribution from these reagents can be neglected. To determine the lead content of the other reagents, a procedure analogous to that of Geladi and Adams [12] was used: 50-ml portions of the water and 25-ml portions of the CCl_4, HNO_3 and H_2O_2 were concentrated by boiling. The dry residue was redissolved in 0.1 M nitric acid of previously determined purity. In the case of dithizone, 40 mg was weighed in a Teflon vessel and subjected to low-temperature ashing. Then 2 ml of concentrated nitric acid was added, the mixture was evaporated to dryness, and the residue was redissolved in 0.1 M nitric acid. Corrections for the nitric acid were made after separate blank determinations.

Impurities from the separating funnels and microtubes were determined by shaking a portion of the oxidizing acid solution in the funnel or tube for 1 min. The blank is defined as the contribution of lead in 1 ml of oxidizing acid solution. The results are summarized in Table 1. The materials actually used are noted with asterisks.

From these data, the theoretical blank value of the whole procedure was calculated as 3.5 ng in the final aqueous solution. Experimental values, however, were significantly higher. A preliminary extraction of the dithizone solution lowered the blank considerably (Table 2). Apparently the dithizone solution becomes contaminated when exposed to the laboratory air. Without the preliminary extraction, the average blank for the re-extraction was 17.6 ng

TABLE 1

Blank value from the reagents and equipment
(*Indicates reagents and materials actually used.)

Reagent or material	Grade (manufacturer)	Pb concentration (ng g^{-1})	
H_2O	Distilled	0.16	
	Twice-distilled*	0.08	
HNO_3	Pro analysi (Merck 454)	2.4	
	Suprapure* (Merck 441)	2.1	
H_2O_2 (30%)	Pro analysi* (Merck 7210)	1.4	
CCl_4	Pro analysi* (Merck 2222)	0.2	
	Extra pure (Merck 2221)	0.4	
H_2Dz	Pro analysi* (U.C.B. 1332)	1100	
		after 1 h	after 24 h
Microtube, glass		2.7[a]	2.9[a]
polypropylene*		0.3[a]	0.6[a]
Separating funnel*		0.2[a]	n.d.

[a]Blank Pb concentration (ng g^{-1}) as defined in text.

TABLE 2

Relative contributions of the two dithizone extractions, and final recovery and precision from an iodine monochloride solution containing 288 ng of organolead

No.	Organolead found[a] in 1st extract		Organolead found[a] in 2nd extract		Total organolead[a] found	Recovery (%)
	(ng)	(% of total)	(ng)	(% of total)	(ng)	
1	240.3	83.0	49.3	17.0	289.6	100.6
2	178.5	63.5	102.8	36.5	281.3	97.7
3	166.3	61.8	102.8	38.4	269.1	93.4
4	285.0	98.3	4.9	1.7	289.9	100.7
5	171.2	57.3	127.4	42.7	298.6	103.7
Av.	208.3	72.9	77.4	27.1	285.7	99.2[b]

[a]Corrected for blanks. [b]R.s.d. = 3.9%.

(range 14—19 ng; n = 10), whereas with the preliminary extraction, the mean overall blank was 2.4 ng, with a mean standard deviation of 2.6 ng (n = 20).

To establish the mean overall blank value of the procedure for inorganic lead compounds in the particulate matter, 20 blank determinations were done with 2.75 × 2.75 cm^2 filter papers. A mean value of 7.9 ng was obtained, with a standard deviation of 2.3 ng. Thus the apparent lead concentration in the Whatman-41 filter was estimated, after correction for acid and water impuritie as 0.9 ng cm^{-2}.

Detection limits

Although there are several definitions of the detection limit of an analytical procedure [13], a frequently used criterion is that the minimum detectable amount is equal to three times the standard deviation of the blank. Hence for a 6-h sample at a flow rate of 3 l min^{-1}, the detection limits obtained are 10 ng m^{-3} for inorganic lead and 8 ng m^{-3} for organic lead.

Recovery and precision

The recovery and the precision of the two analytical methods were determined with samples made in the laboratory. For inorganic lead, known amounts of lead nitrate solutions were spotted on Whatman-41 filters. Typical values for recovery ranged between 98.3% and 103.9%, with standard deviations of approximately 6% for six replicate determinations. In the case of organic lead, known amounts of $Pb(C_2H_5)_2Cl_2$ were added to the iodine monochloride solution, and the procedure described above was applied. It should be noted that erroneous results will be obtained if traces of the sodium sulphite present in the buffer solution enter the second separating funnel. Absorbance signals with triple peaks are then recorded (Fig. 6). Accordingly, the separation of the organic layer into the second funnel should not be done precisely at the phase boundary but approximately 0.5 ml less. Consequently, a second extraction with the dithizone solution is required to extract all the organic lead present. In this way, very reproducible and quantitative measurements are possible (Table 2). Even for very low organic lead levels, the results are good (Table 3).

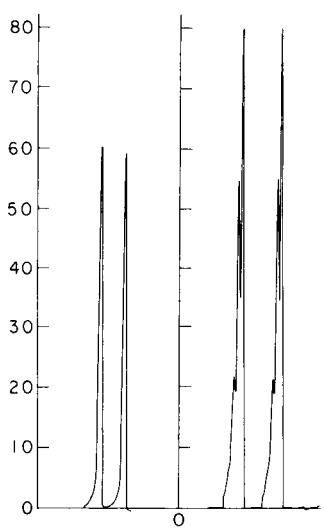


Fig. 6. Absorbance signals with (right) and without (left) the presence of sodium sulphite.

TABLE 3

Recovery and precision for very small amounts of organic lead compound in the iodine monochloride solution

Organolead added (ng)	Found (ng)[a]	Recovery (%)	R.s.d. (%)
21.6	21.1	97.7	10.2
43.2	43.7	101.1	6.9
64.8	64.3	99.2	5.4

[a]Average of 3 determinations.

TABLE 4

Influence of diverse ions on the procedure for organic lead compounds

Diverse ion[a]	Total blank[b] (ng)	Organolead recovered (ng)[c]				Mean recovery (%)
		1	2	3	Av.	
—	0.5	83.5	94.1	86.8	88.1	102.0
Al	0	94.9	80.8	87.5	87.7	101.5
Ca	3.7	79.5	94.1	89.6	87.7	101.5
Fe	1.6	88.1	85.1	81.6	84.9	98.3
Mg	1.6	87.7	83.5	81.7	84.3	97.6

[a]600 μg added. [b]Average of 3 determinations. [c]Recoveries of 86.4 ng of organolead from an ICl solution.

Interferences

Because of the great abundance of Mg, Al, Fe, Ca and inorganic lead in urban aerosols [14], the interference of these species with the organolead determination was examined. The results from solvent extractions in the presence of relatively large amounts of Mg, Al, Fe and Ca ions (Table 4) showe that there are no interferences. The influence of variable amounts of inorganic lead material on the blank of the procedure and on the recovery of organic lead can be seen in Fig. 7. In both cases straight lines are obtained. Hancock and Slater [11] found a similar linear dependence for the interference of inorganic lead on the blank value, but the present work indicates a lesser dependence of the blank on inorganic lead additions, with 5 ng of organolead being detected per 100 μg of inorganic lead present compared to 10 ng/100 μg For ambient inorganic lead concentrations, it can be concluded that the interference is negligible. Since the interferences on the inorganic lead determi nation have been described [12], they were not further investigated.

APPLICATION

The analytical methods outlined above were applied at various sampling site

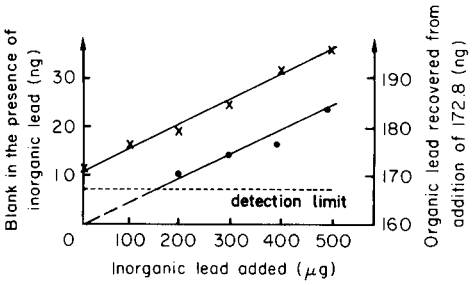


Fig. 7. Interference of inorganic lead on the determination of organic lead: (•) interference on blank value; (×) interference on recovery.

in Antwerp city during the period September—November, 1978. To obtain maximal sensitivity, samplings were done for 6 h from 11 a.m. to 5 p.m. Longer sampling periods are impractical because permanent attendance is required. The reproducibility of the analytical methods was checked by using two identical sampling units in parallel. The inorganic lead concentrations obtained with this method were compared with the results from x.r.f analyses as described by Van Espen and Adams [15]. The results of typical samplings are shown in Table 5.

During hot summer days, the sampling of organolead compounds was done in larger impingers loaded with 30 ml of the iodine monochloride solution, because of evaporation of the sampling solution. Analyses in those cases were

TABLE 5

Results from parallel measurements in the environment of Antwerp city. Results by x-ray fluorescence are shown between parentheses.

Sampling site (height)	Organolead (ng m^{-3})			Inorganic lead (ng m^{-3})			Total lead (ng m^{-3})	Organic—total lead ratio (%)
	1	2	Av.	1	2	Av.		
Rural (1.5 m)	⩽8	⩽8	⩽8	88 (⩽109)	103 (⩽121)	96	⩽104	—
Residential (5 m)	20	14	17	140 (⩽122)	128 (⩽137)	134	151	11.3
Downtown (1.5 m)	247	276	262	1040 (748)	959 (787)	1000	1262	20.8
Downtown (20 m)	115	108	112	598	585	592	704	15.9
Gasoline station (1.5 m)	171	214	192	596 (594)	598 (624)	597	789	24.3
Tunnel for road traffic (0.5 m)	105	118	112	6809 (4448)	6345 (6775)	6577	6689	1.7
Residential, near an emission source of inorg. lead (0.5 m)	13	11	12	218 (331)	226 (260)	222	234	5.1

done with twice the normal amounts described above. Tests have shown that this modification affects neither the reproducibility nor the recovery.

Except for the downtown samples, none of the analyses of the second impingers showed organolead contents above the detection limit. Nevertheless, for places where high organolead concentrations are expected, two impingers filled with iodine monochloride solution should be employed. Comparison of the results obtained with the two identical sampling units shows that the agreement for both lead species is satisfactory. For organolead concentrations above 20 ng m^{-3}, a mean relative standard deviation of 13% was obtained for 10 paired determinations, whereas for the inorganic lead this value was 9% for 15 paired determinations. The discrepancies between the results obtained by a.a.s. and x.r.f. analysis in Table 5 are somewhat larger than the differences that have been previously found [12]. This is caused by the rather low loading of the filters with the short sampling times used, so that only small lead fluorescence peaks are obtained. The precision of the x.r.f. determinations is therefore rather low, being of the order of 20%.

Although the data summarized in Table 5 reflect only the situation on a particular sampling day, the great diversity of the lead concentrations is striking. Moreover, it is clear that the combined method described is capable of monitoring a wide range of lead levels in environmental air.

This research was carried out within the framework of the National Research and Development Program on Environment of the Interministerial Commission for Science Policy. The x.r.f. analyses were performed by Patrick Verbeke. Stimulating discussions with Paul Geladi and Willy Van Mol are gratefully acknowledged.

REFERENCES

1 T. Nielsen and P. Grandjean, Nature, 274 (1978) 602.
2 R. Moss and E. V. Browett, Analyst, 91 (1966) 428.
3 L. J. Purdue, R. E. Enrione, R. J. Thompson and B. A. Bonfield, Anal. Chem., 45 (1973) 527.
4 D. M. Colwill and A. J. Hickman, Transport and Road Research Laboratory Report LR 545, Department of the Environment, 1973.
5 L. J. Snyder, Anal. Chem., 39 (1967) 549.
6 R. M. Harrison, R. Perry and D. H. Slater, Atoms. Environ., 8 (1974) 1187.
7 A. Laveskog, Proceedings of the Second International Clean Air Congress, Washington D.C. (1970) 549.
8 Y. K. Chau, P. T. S. Wong and P. D. Goulden, Anal. Chim. Acta, 85 (1976) 421.
9 D. A. Segar, Anal. Lett., 7 (1974) 89.
10 D. C. Reamer, W. H. Zoller and T. C. O'Haver, Anal. Chem., 50 (1978) 1449.
11 S. Hancock and H. Slater, Analyst, 100 (1975) 422.
12 P. Geladi and F. Adams, Anal. Chim. Acta, 96 (1978) 229.
13 K. Eckschlager, Errors, Measurement and Results in Chemical Analysis, Van Nostrand—Reinhold, New York, 1969.
14 R. Dams, Studie van de Samenstelling van atmosferische Aerosolen, University of Ghent, Belgium, 1974.
15 P. Van Espen and F. Adams, Anal. Chim. Acta, 75 (1974) 61.

Analytica Chimica Acta, 108 (1979) 31—38
© Elsevier Scientific Publishing Company, Amsterdam — Printed in The Netherlands

A STUDY OF ATOMIC ABSORPTION AND ATOMIC FLUORESCENCE ATOMIZATION SYSTEMS AS DETECTORS IN THE GAS CHROMATOGRAPHIC DETERMINATION OF LEAD

B. RADZIUK, Y. THOMASSEN[a], L. R. P. BUTLER[b] and J. C. VAN LOON*

Departments of Geology and Chemistry and The Institute for Environmental Studies University of Toronto, Toronto M5S 1A1 (Canada)

Y. K. CHAU

Canada Center for Inland Waters, P.O. Box 5050, Burlington L7R 4A6 Ontario (Canada)

(Received 30th November 1978)

SUMMARY

The suitability of various atomic absorption and atomic fluorescence atomizing systems connected to a gas chromatograph is compared for the determination of alkyl lead compounds. An electrothermally heated graphite tube gives the highest sensitivity but quartz tubes heated either in an air—acetylene flame or by electrical resistance wire provide adequate sensitivity for most applications. A "solvent peak" absorption thought earlier to be due to organic molecular absorption of radiation at the lead wavelength was shown to be due to deposition and remobilization of lead.

It is generally recognised by environmental analysts that the determination of the total concentration of metals in environmental samples may not be sufficient to ascertain the nature of pollution. Many metals (e.g. lead and mercury) are known to be more toxic as metallo—organic compounds than as inorganic compounds. Results based only on the total metal concentrations could thus lead to erroneous conclusions and be of less interest. Gas chromatographic techniques allow the separation of volatile compounds with relative simplicity and ease. However, conventional detectors show poor selectivity.

Kolb et al. [1] described a method in which an atomic absorption spectrometer was coupled to a gas chromatograph for the detection of alkyllead compounds. Atomic absorption measurements are highly selective and when an atomic absorption system is used, not only can the various compounds be identified but their relative concentrations measured. Recently, Van Loon et al. [2] described the use of non-dispersive atomic fluorescence spectrometry as a detector for chromatography. As with atomic absorption, this method is highly selective but has two additional advantages: the ability to

---

[a]On leave from Institute of Occupational Health, Oslo, Norway.
[b]On leave from National Physical Research Laboratory, CSIR, Pretoria, South Africa.

determine several elements simultaneously, and the possibility of obtaining better detection limits for some metals, especially if high-intensity spectral sources are employed.

Gas chromatographs are easily connected to atomic absorption or atomic fluorescence atomizing systems. This is done simply by connecting the end of the column via a transfer tube to the burner, furnace or tube atomizer. Atomic absorption furnaces and flame atomizers enable relatively large gas flows to be used in conjunction with large gaseous sample volumes (up to 10 cm^3). While several different configurations of g.c.—a.a.s. systems have been described in the past, these do not appear to have been compared and optimized before. In this paper, several atomizing systems are studied which include some configurations not previously reported. Atomic absorption and both dispersive and non-dispersive atomic fluorescence detection systems were used. Lead was selected as the element to be studied because of the widespread biological and environmental interest in the metal and its organo-metallic compounds.

EXPERIMENTAL

Apparatus

A Pye-Unicam Series 104 gas chromatograph was interfaced with the various detecting systems. The glass chromatographic column (150 cm long, 6 mm diameter) was packed with 3% OV-101 on Chromosorb W (80-100 mesh).

Atomic absorption and dispersive atomic fluorescence measurements were made with a Perkin-Elmer 603 spectrometer and a Perkin-Elmer Model 56 recorder. The radiation source was a Perkin-Elmer electrodeless discharge lead lamp operated from a Westinghouse Model 185 E EDL power supply. An R166 solar-blind photomultiplier was used as detector for the non-dispersive atomic fluorescence measurements. The source and amplifier were synchronized by using a Wavetek Model 180 sweep/function generator to trigger both units with a 285-Hz square-wave signal.

The systems used were as follows.

Flame system. A Perkin-Elmer 10-cm single-slot acetylene—air burner head was used. Effluent from the column was introduced into the burner through 1.6-mm (Type 316) stainless steel tubing to enter the volume immediately below the burner slot in the centre of the burner head. The tube was bent at right angles inside the burner to point upwards towards the burner slot so that the effluent entered the gas stream and mixed with it.

The fluorescence burner, which was similar to that described by Larkins [3], was connected with identical tubing. The flame which emerged from the circular burner head was separated by means of a laminar nitrogen flow. The sample effluent was introduced in a similar way to the atomic absorption flame.

Quartz tube in flame. The quartz tube was mounted on a Perkin-Elmer 10-cm triple-slot (Boling) burner head as shown in Fig. 1.

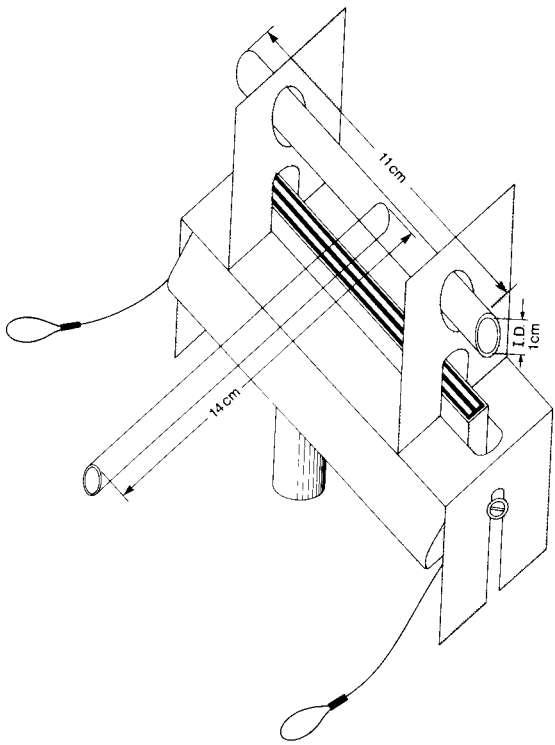
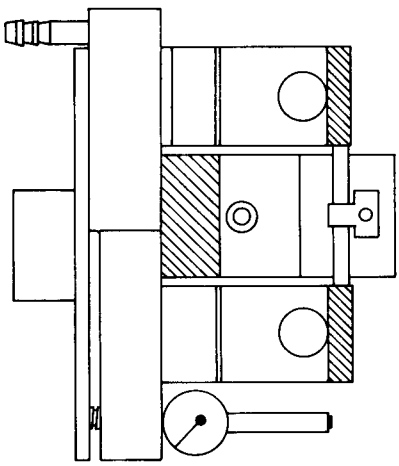


Fig. 1. Arrangement of quartz tube in flame. The tube was positioned 2 cm above the burner.

Perkin-Elmer HGA 2100 graphite furnace. This system, described elsewhere [4], has a tantalum transfer tube connected to the end of the chromatographic column. The HGA 2100 was flushed with argon.

Varian-Techtron CRA 63 carbon rod atomizer. The power supply was modified to provide up to 10 min of continuous operation at the ashing stage by replacing the 10-μF capacitor (C-11) in the control unit with a 100-μF capacitor. The standard CRA 63 working head is unsuitable for atomic fluorescence measurements because the atomization cell is located below the plane of the terminals, making detection at a convenient angle to the incident beam impossible. The electrodes were therefore relocated at the top of the terminals as shown in Fig. 2. The head was aligned horizontally in the light beam (both in cup and tube operation) by replacing the foot-adaptor with a piece of aluminium rod 25 mm in diameter. Redesigned masking plates were used to minimize stray light effects. The 1.6-mm stainless steel tubing was inserted into a hole bored through one of the electrodes and the side of the cup (or tube).

Quartz furnaces. A wire-wound, asbestos-covered quartz furnace as described



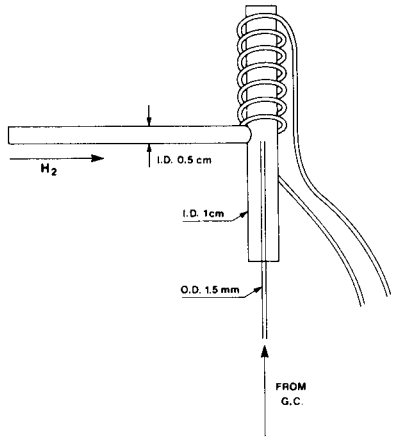


Fig. 2. Modified CRA 63 head showing relocation of the cup.

Fig. 3. Diagram of the quartz furnace used for fluorescence measurements.

by Chau et al. [5] was used for atomic absorption determinations. Figure 3 illustrates the furnace used for non-dispersive atomic fluorescence measurements. This furnace was also wrapped with resistance wire and asbestos. Both furnaces could be heated to 1000°C. Hydrogen was introduced by side arms. An inert gas sheath was used with the furnace for fluorescence measurements.

Reagents

Trimethylethyllead standards were obtained from the Ethyl Corporation. Freshly diluted secondary lead standards to cover the concentration range 0.15—1.5 μg Pb ml^{-1} of solvent were prepared daily in analytical-grade methanol or benzene. The analytical range was in fact about 0.15—15 μg Pb ml^{-1} but it was preferred to work in a lower range. Purified dry nitrogen was used as the carrier gas for gas chromatography and for flame shielding.

Procedures. The gas chromatograph oven was programmed from 50 to 200°C with a heating rate of 40°C min^{-1}. Trimethylethyllead standards were injected in 1—5 μl volumes. The carrier gas flow was set at 140 ml min^{-1}. The atomic absorption spectrometers were operated at the 283.3-nm lead resonance line with a spectral bandwidth of 0.7 nm. The electrodeless discharge lamp was operated at 10 W with all instrumentation.

Table 1 gives the operating conditions found to be most suitable for the various atomizers.

RESULTS AND DISCUSSION

The amount of lead as trimethylethyllead which gave a peak-to-background signal equal to twice the average noise level (S/N = 2) was taken as the

TABLE 1

Operating conditions for the atomization systems

Atomizing System	A.a.s.	A.f.s.
Flame	Air, 11 l min^{-1}. C_2H_2, 2 l min^{-1} Burner adjusted for optimum sensitivity while aspirating solution.	Air, 12 l min^{-1}. C_2H_2, 2 l min^{-1} Burner adjusted as for a.a.s.
Quartz tube in flame	Air, 11 l min^{-1}. C_2H_2, 5.5 l min^{-1}	—
HGA 2100	Continuous heating at 1500°C (indicated) for 20-min periods with charring stage.	—
CRA 63 tube	Continuous heating at setting 9 for 10-min periods with charring stage.	—
CRA 63 cup	Continuous heating at setting 9 for 10-min periods with charring stage.	Continuous heating at setting 7 for 10-min periods with charring stage.
	Nitrogen, 6 l min^{-1}	Nitrogen 6 l min^{-1}
Quartz furnace	—	Continuously heated at ca.1000°C Hydrogen, 0.6 1 min^{-1} Nitrogen 15 l min^{-1}

TABLE 2

Detectable amounts (S/N = 2) by atomic absorption and atomic fluorescence for trimethyllead with different atomization techniques

Atomizer	Atomization Temp. (°C)	Detectable amount (ng)	
		A.a.s.	A.f.s. (non-disp.)
Flame (C_2H_2—air)	2400	1.5	0.3[a]
Quartz tube in flame	970	0.09	
HGA 2100	1500	0.03	
CRA 63 tube	1500	0.07	
CRA 63 cup	1500[b]	0.15	0.2
Quartz furnace	1000	0.1	0.1

[a] Dispersive measurements gave the same result.
[b] 1000°C for fluorescence.

"detectable amount" and used as a measure of sensitivity to compare the atomizing systems. The results are shown in Table 2. It should be stressed that the results are relative and valid only for the chromatographic conditions used in this study. Whereas a change in chromatographic parameters could result in higher or lower values, there would be no relative change in the sensitivities of the atomizing systems under the conditions used. The gas chromatographic conditions selected were those most suitable for the separation of the alkylated lead compounds[4].

The most sensitive of the systems tested proved to be atomic absorption detection with the HGA 2100 furnace. However, it is likely that the CRA 63 tube detector would show an improvement in the detectable amount, probably similar to that for the HGA 2100 furnace, if the tube design had been such that the light beam could be better utilized. With the atomic absorption equipment employed, part of the incident radiation was blocked by the rim of the CRA 63 tube.

The detectable amounts obtained by non-dispersive atomic fluorescence are much poorer than expected compared to those obtained by the atomic absorption measurements with furnace and rod. This is somewhat unexpected, as when flame atomizers are used, atomic fluorescence signals are usually enhanced by a factor of 5 compared to atomic absorption signals. The reason may be the relatively short residence time of the atoms in the optical beam with the open cup compared to the partially closed furnace and tube systems.

Although there was little difference in the detectable amounts for dispersive and non-dispersive fluorescence, it should be noted that Neumann and Kreise [6] obtained very low detection limits for lead solution by using direct-line fluorescence. The atomizer was irradiated at 283.4 nm and a dispersive fluorescence detector permitted measurement at 405.9 nm. During the present work, no advantage could be found in measuring at 405.9 nm with the dispersive system.

As demonstrated previously [4], the detector response for alkylated lead compounds depends on the atomizing temperature. The optimal atomizing temperature varied to some extent among the systems studied here. However, the relationship obtained should hold for the non-flame systems. Where possible, the atomizing temperatures were set at 1500°C; in other cases the highest practical temperatures which could be obtained were employed. In the case of the CRA 63 cup atomizer, the temperature setting (1500°C) was a compromise between maximum atomization efficiency and minimum emission from the carbon cup.

Non-specific absorption

Atomic absorption spectrometry and atomic fluorescence spectrometry are element-specific, hence only compounds of the analyte element will be detected. This statement is true only if molecular absorption and/or light-scattering background interferences can be eliminated. When flame atomizers are used, these factors are seldom a serious problem, but both phenomena are frequently encountered with electrothermal atomizers. The deuterium background

corrector used in atomic absorption spectrometry will compensate adequately for broad-band light losses of a reasonable magnitude which are relatively constant over the bandpass of the monochromator. Light scattering generally behaves in this manner. In contrast, molecular absorption commonly consists of a continuum onto which is superimposed a fine structure arising from rotational molecular transitions. If a component of the fine structure overlaps the absorption line being employed, then deuterium background correction may compensate only partially.

In non-dispersive atomic fluorescence spectrometry correction for light scatter has not been demonstrated to be completely effective by any system proposed to date. This type of interference can be a serious source of error with these measurements.

Remobilization of lead

During this study, several cases of what was thought to be uncorrectable background absorption, viz. uncorrectable solvent signals, were encountered. It was found that many common methyl-containing and ethyl-containing compounds (e.g., methanol, ethanol, acetone, etc.) gave signals during elution of the compound. These signals were observed at both the 283.3-nm and 217.0-nm lead resonance lines. This phenomenon disappeared when a platinum hollow-cathode lamp was used (Pt-resonance line 283.03 nm) as the source at the same monochromator setting as for the lead determination (283.3 nm). This showed that the signals were *not* non-specific background signals but were due to lead absorption.

The effect was only observed when the effluent passed through a part of the apparatus (the transfer tube) which was at an elevated temperature (>300°C) before entering the atomizer. After several experiments, where it was found that the "solvent peak" disappeared after careful acid cleaning of the transfer tube, it was concluded that the peak was due to remobilization of lead deposited during previous runs. This was confirmed by passing inorganic lead as lead vapour through a clean tube. The peaks then reappeared when clean solvents were passed through the column.

The magnitude of the effect varied with the material used in the hot part of the transfer tube. It decreased with the type of material in the following order: silica, alumina $\gg$ stainless steel, carbon and tantalum.

While there appeared to be a negligible amount of lead deposited by decomposition of alkyllead compounds during a "normal" concentration run, contamination of the transfer tube resulted if a concentration above the analytical range were injected (i.e. >15 μg ml^{-1} depending on the atomizer type used).

The remobilization of lead is a well known effect and one wonders if this was the cause of the uncorrectable, non-specific absorption signals reported by Robinson et al. [7] for several other solvents; these signals were described as being "organic in nature" since they occurred when background correction was used. These authors observed that, when the temperature of the atomizer was increased, the non-specific absorption increased, and concluded that the

absorption was due to a combustion product rather than to incomplete combustion of the solvent molecules.

It is well documented that lead reacts easily with free radicals to form volatile alkyllead compounds [8]. This is believed to explain the presence of the "solvent peak".

Conclusions

The HGA 2100 electrothermal atomizer used in the atomic absorption system gave the highest sensitivity for the determination of lead compounds separated in the gas chromatograph. Atomic absorption measurements detected lower amounts of lead than the fluorescence detectors used. The quartz tube gave sensitivities which were adequate for many purposes and in the case of the quartz tube in flame, the detectable amount was only 3 times poorer than that with the electrothermal atomizers. Remobilization of inorganic lead by solvents, particularly those with methyl groups, usually takes place.

The simplicity of coupling atomic absorption atomizers to gas chromatographs may encourage more analysts to determine the species of the various metal compounds which could be of great value in analytical studies.

This work was supported by grants from The Ontario Ministry of the Environment under the Research Grants Programme of the Air Resources Branch and The Royal Norwegian Council for Scientific and Industrial Research and by the University of Toronto. Perkin-Elmer Corporation, Norwalk, Connecticut, kindly lent the atomic absorption equipment. The authors thank I. Davies for technical assistance.

REFERENCES

1 B. Kolb, G. Kemmner, F. H. Schleser and E. Wiedeking, Fresenius Z. Anal. Chem., 221 (1966) 166.
2 J. C. Van Loon, J. Lichwa and B. Radziuk, J. Chromatogr., 136 (1977) 301.
3 P. L. Larkins, Spectrochim. Acta, Part B, 26 (1971) 477.
4 B. Radziuk. Y. Thomassen, J. C. Van Loon and Y. K. Chau Anal. Chim. Acta, 105 (1979) 255.
5 Y. K. Chau, P. T. S. Wong and P. D. Goulden, Anal. Chim. Acta, 85 (1976) 421.
6 S. Neumann and M. Kreise, Spectrochim. Acta, Part B, 29 (1974) 127.
7 J. W. Robinson, E. L. Kiesel, J. P. Goodbread, R. Bliss and R. Marshall, Anal. Chim. Acta, 92 (1977) 321.
8 H. Shapiro and F. W. Frey, The Organic Compounds of Lead, J. Wiley, New York, 1975, pp. 63—97.

Analytica Chimica Acta, 108 (1979) 39—44
© Elsevier Scientific Publishing Company, Amsterdam — Printed in The Netherlands

ANALYTICAL APPLICATIONS OF EMULSIONS. DETERMINATION OF LEAD IN LUBRICATING OILS BY ATOMIC ABSORPTION SPECTROMETRY

J. HERNÁNDEZ-MÉNDEZ, L. POLO-DIEZ* and A. BERNAL-MELCHOR

Department of Analytical Chemistry, Faculty of Sciences, University of Salamanca, Salamanca (Spain)

(Received 2nd January 1979)

SUMMARY

Lead used in lubricating oils (ca. 0.2%) is determined by direct nebulization of oil—water emulsions into the flame of an atomic absorption spectrometer. The method is as accurate and precise as a similar method involving mineralization of the oil, and has the advantage of simplicity, speed and the use of aqueous standards for calibration.

The determination of metal in liquid organic samples is a classical problem in chemical analysis, because of the large variety of these samples. Most of the methods described in the literature involve time-consuming mineralization steps. With regard to atomic absorption spectrometry, attempts have been made to overcome these inconveniences by dilution of samples with suitable organic solvents, which allows direct aspiration of the sample into the flame, but this technique often has several inconveniences such as fluctuations of the instrumental signal, high noise levels and the necessity of using organometallic standards.

The method described here overcomes these problems by producing an emulsion of the organic sample which can be introduced directly into the flame. The formation and stabilization of emulsions usually requires the presence of a surfactant, a small amount of the organic sample being emulsified with a larger amount of water. In this way, an oil—water emulsion is obtained which is essentially aqueous. The system is strictly heterogeneous, but homogeneous enough to be introduced directly into the flame via a conventional nebulizer, so that the characteristic advantages of spraying aqueous solutions may be expected.

This principle has been applied to the determination of zinc in lubricating oils [1] and of metal ions (Fe, Cu) as oxinates after extraction into organic solvents (benzene, ethyl acetate) [2]. In addition, promising results have been obtained for the determination of lead in gasoline [3]. This paper shows the general way in which such emulsions can be prepared; the principle is applied to a particular oil—water system, for the determination of lead in used lubricating oils from cars.

EXPERIMENTAL

Apparatus, reagents and samples

A Pye-Unicam SP90 atomic absorption spectrometer equipped with a Pye-Unicam hollow-cathode lamp was used, measuring the lead line at 283.3 nm. The instrumental parameters, including the acetylene and air flows, were adjusted to give maximum sensitivity for lead. A Pulsatron Kerry 250 ultrasonic bath with an oscillating frequency of 50 kHz was used to produce the emulsions.

A standard lead nitrate solution (100 ppm lead in 1% nitric acid) was prepared by diluting a solution standardized gravimetrically as lead chromate. This and the other common reagents used were analytical-grade chemicals. MS-12 lipophilic surfactant (Hoechst) was used as a 10% benzene solution; the hydrophilic—lipophilic balance, h.l.b., evaluated experimentally was in the range 6—8. The following hydrophilic surfactants were prepared as aqueous 4% solution: Tween 20 (polyoxyethylene sorbitan monolaurate; h.l.b. = 16.7); Tween 80 (polyoxyethylene sorbitan monooleate; h.l.b. = 15.0) and Brij 35 (polyoxyethylene lauryl ether; h.l.b. = 16.9).

The samples were commercial unused and used "Calvo Sotelo" Company lubricating oils. Used samples were taken from cars.

Standard method for lead determination in lubricating oils [4]

In a small porcelain capsule, about 0.25 g of the used oil is accurately weighed and heated gently on a hot plate until white fumes disappear. The oil is then calcined at 550—600°C for about 1 h. The residue obtained is dissolved in a few drops of concentrated hydrochloric acid, and the solution is diluted to 100 ml in a volumetric flask with distilled water and aspirated into the flame. Calibration is done with aqueous lead standards.

Emulsion method

In a 50-ml volumetric flask, about 0.1 g of the used oil (previously filtered after heating at 50—60°C) is weighed accurately. Then, 2 ml of the MS-12 solution plus 5 ml of the Tween 20 solution and about 25 ml of distilled water are added. The flask is placed in the ultrasonic device for 3 min and the volume made up with distilled water. The emulsion is aspirated directly into the flame. Calibration is done by applying this procedure to emulsions containing 0.1 g of unused lubricating oil free of lead and suitable volumes of the standard lead nitrate solution.

RESULTS AND DISCUSSION

Emulsions obtained by the above procedure from used lubricating oils produce flame absorptions at the wavelengths of the lead resonance lines (217 and 283 nm); the line at 283.3 nm was chosen for study. The absorption increases in proportion to the amount of sample as well as that of the aqueous lead nitrate added. A blank prepared from an unused oil gave no significant absor-

bance. In order to use this signal for analytical purposes, the conditions for obtaining and stabilizing the emulsions were determined.

Choice of surfactant

The formation of stable emulsions requires the presence of a surfactant which must have particular properties for each oil—water system. The emulsifying ability of a surfactant, especially non-ionic ones, is shown by the hydrophilic—lipophilic balance (h.l.b.) which is expressed by an empirical value. The hydrophilic character increases with this value. Usually, there is a large variety of commercial surfactants with a suitable h.l.b for a particular system; however, it is rare for a single surfactant to have the optimum functional properties to form and stabilize an emulsion; thus, industry normally makes use of mixtures of surfactants for emulsification purposes, and this principle seems applicable for producing analytical emulsions. In this case, the h.l.b. of the mixture will be the weighted average of the individual h.l.b. values. The amount of surfactants necessary is usually small, so that these compounds are used in dilute solutions.

In order to obtain oil—water emulsions from lubricating oils, the literature recommends a h.l.b. in the 8—18 range. In the present investigation, attempts were made to obtain the optimum h.l.b. by mixing the MS-12 lipophilic surfactant dissolved in benzene and the hydrophilic one (Tween 80, Tween 20 or Brij 35). Mixtures of each of these surfactants with the lipophilic one are expected to be within the suitable h.l.b. range. The stability of the emulsion is the most important factor from the analytical point of view. The emulsion is considered stable when the absorbances obtained from samples from different locations in the flask do not show significant differences.

Results obtained show that the Tween 20 and Brij 35 produce emulsions stable for at least 6 h; however, Tween 20 is more suitable because foams are not observed (foaming must be avoided because it is difficult to make up the volume and adsorption onto bubbles is possible, thus disturbing the homogeneity of the sample). As the relative amounts of MS-12 and Tween 20 affect the h.l.b. value of the mixture, the effect of h.l.b. was studied. The results are shown in Table 1. Stable emulsions were obtained for h.l.b. values of 12 and 14, but in the latter case some foaming was observed, and thus a h.l.b. of 12 was preferred.

Another factor which must be taken into account is the total amount of surfactant added. As is shown in Fig. 1, increasing the concentration of surfactant increases the absorbance. Emulsions stable for at least 6 h are obtained for 0.4—0.8% surfactant. The instability of emulsions containing less than 0.4% surfactant may be due to the fact that a minimum amount of surfactant is necessary to cover the droplets which form the dispersed phase. For 0.8% surfactant the instability of the emulsions must be due to the large amount of benzene introduced as solvent for the lipophilic surfactant.

TABLE 1

Effect of the relative concentrations of surfactants (h.l.b.) on lead absorbance (A) and emulsion stability

Surfactant (%)		H.l.b.	Weight of sample (g)	A	A/g	Emulsion stability
MS-12	Tween 20					
			0.1023	0.105	1.03	
0.20	0.48	14	0.1022	0.105	1.03	⩾6 h
			0.1042	0.105	1.01	
			0.1009	0.108	1.07	
0.40	0.40	12	0.1078	0.115	1.07	⩾6 h
			0.1063	0.115	1.08	
			0.1028	0.130	1.26	
0.60	0.32	10	0.0981	0.123	1.25	Unstable
			0.1019	0.175	1.72	
			0.1056	0.123	1.16	
0.80	0.24	9	0.0988	0.163	1.65	Unstable
			0.1035	0.170	1.64	

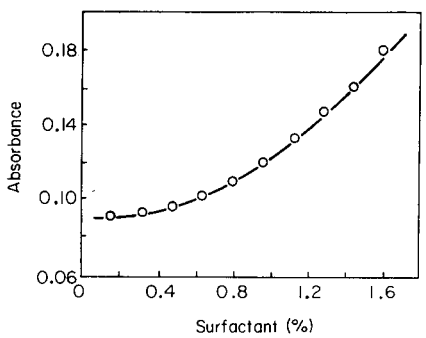


Fig. 1. Effect of the amount of surfactant on lead absorbance (corresponding to 0.1 g of sample).

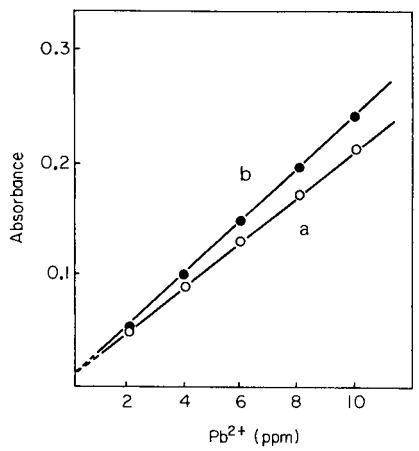


Fig. 2. Calibrations for lead with (a) aqueous solutions; (b) emulsions.

Selection of dilution ratio and emulsification time

The optimum oil—water ratio is conditioned by the sensitivity of the atomic absorption measurements and the stability of the emulsions obtained. About 0.1 g of oil, in a total volume of 50 ml, is suitable.

The formation of stable emulsions requires certain amounts of energy. Dif-

ferent techniques can be used for this purpose, mechanical ones being the most often used. However, more reproducible results are obtained by using an ultrasonic instrument which also allows the emulsions to be handled easily. The absorbance increases with emulsification time up to 3 min, above which the absorbance remains constant.

Calibration

Emulsions for calibration were prepared from aqueous lead nitrate solutions to which the same amounts of lead-free oil and surfactants were added as for preparing the sample emulsions. The concentration of lead in the final emulsions was 1—10 ppm. The calibration graph is linear over this range (Fig. 2), with a slightly (17%) higher sensitivity than that obtained from aqueous standards. Calibration in the absence of oil could be employed by using an empirical factor but emulsion calibration is to be preferred.

Characteristics of the method

The reproducibility and accuracy were evaluated by applying the specified procedure ten times to each of two samples of used lubricating oil; sample weights were close to 0.1 g. The results are shown in Table. 2. A *t*-test showed that there is no significant difference between the two methods at the 99% probability level. When the standard method was applied to unfiltered samples, the lead contents found were high because of the presence of large solid particles in the oil which must contain lead. In the emulsion method, filtering is necessary to avoid clogging of the aspiration system.

Conclusions

The method based on the formation of oil—water emulsions from the sample and further aspiration directly into the flame is applicable to the determination of lead in lubricating oils after removing large solid particles. The method is as precise and accurate as the standard method, and can be very useful. It does not require a mineralization step, thus offering the important

TABLE 2

Comparative study of the standard and emulsion methods for two samples (1 and 2)

	Standard [4]		Emulsion	
	1	2	1	2
Pb in oil[a] ($mg\ g^{-1}$)	1.76	2.99	1.73	2.95
Standard deviation	0.019	0.023	0.033	0.033
s_r (%)	1.1	0.8	1.9	1.1

[a]Mean of 10 determinations.

advantages of simplicity and speed. Moreover, aqueous lead nitrate calibration solutions are used which avoids the use of organometallic standards.

The principle on which the method is based seems to have general applicability and might be used for the determination of metal components in other organic solvents by using a suitable surfactant and controlling the other parameters involved in obtaining and stabilizing emulsions.

REFERENCES

1 V. Berenguer-Navarro and J. Hernández-Méndez, Quim. Anal., 31 (1977) 81.
2 V. Berenguer-Navarro, M. Espla-Moncho and J. Hernández-Méndez, Quim. Anal., 31 (1977) 329.
3 L. Polo-Diez, J. Hernández-Méndez and F. Pedraz-Penalva, paper presented at Euroanalysis III, Dublin 1978.
4 J. A. Burrows and J. C. Heerdt, Anal. Chem., 37 (1965) 579.

Analytica Chimica Acta, 108 (1979) 45—52
© Elsevier Scientific Publishing Company, Amsterdam — Printed in The Netherlands

ATOMIC ABSORPTION SPECTROMETRIC METHODS FOR ANALYSIS OF HIGH-PURITY GALLIUM AND RHENIUM AND LAYERS OF DOPED SILICON

I. G. YUDELEVICH, L. V. ZELENTSOVA, N. F. BEISEL and T. A. CHANYSHEVA

Institute of Inorganic Chemistry, Siberian Branch of the U.S.S.R. Academy of Sciences, Novosibirsk (U.S.S.R.)

L. VECHERNISH

Research Institute for Telecommunication, Budapest (Hungary)

(Received 24th November 1978)

SUMMARY

Atomic absorption spectrometry with electrothermal atomization is used to determine 13 and 15 elements in high-purity rhenium and gallium, respectively. Flame emission is used for K, Na and Li. Improved detection limits are achieved by extraction of the matrix. Thin films (0.01—1 μm) of doped silicon are analyzed for As, Sb, In and Tl by a similar atomic absorption method, after chemical or electrochemical stripping of the layers.

Because of its high precision and low detection limits, atomic absorption spectrometry can be successfully used to analyze high-purity materials. The present paper reports atomic absorption and flame atomic emission methods developed for the determination of trace impurities in high-purity gallium and rhenium as well as methods for layer-by-layer analysis of semiconductor silicon films for doping impurities (As, In, Sb, Tl).

ANALYSIS OF GALLIUM AND RHENIUM

Experimental

Apparatus. A Perkin-Elmer model 303 atomic absorption spectrometer supplied with burners for air—acetylene and nitrous oxide—acetylene flames and a HGA-74 graphite furnace atomizer was employed for atomic absorption determinations. Non-selective absorption was compensated with a deuterium background corrector. The flame emission measurements were made with a laboratory-built flame photometer based on a prism spectrograph ISP-51. PTFE vessels were used for the decomposition and evaporation of metal samples and for the preparation of standards.

Reagents. Perrhenic acid was prepared by passing a 7% solution of ammonium perrhenate in deionized water through a KU-2 cation-exchange resin in the H^+-form. High-purity hydrogen peroxide was further purified by ion-

exchange. Hydrochloric acid (12 M) was prepared by saturation with hydrogen chloride of hydrochloric acid tri-distilled in a quartz apparatus.

High purity nitric acid was tri-distilled in a quartz apparatus. Water was purified by ion-exchange on a column of KU-2 and AB-17 cation- and anion-exchange resins. Tri-n-octylamine oxide was used as a 0.3 M solution in toluene

Sample pretreatment. Metallic rhenium (50 mg) was dissolved in 1 ml of concentrated nitric acid and diluted with deionized water to 5 ml. This solution was analyzed directly.

When extractive separation of the matrix was required 1 g of the sample was dissolved in hydrogen peroxide. Rhenium was isolated by two extractions with the tri-n-octylamine oxide solution in toluene. The aqueous phase was evaporated to a drop, washed out with 0.2 ml of concentrated nitric acid and diluted to 2 ml with deionized water.

Metallic gallium (50 mg) was dissolved in a mixture of 0.3 ml of 5 M hydrochloric acid and 0.1 ml of concentrated nitric acid by heating at 95°C for 2 h. After dissolution, deionized water was added to bring the volume to 5 ml. This solution was analyzed for potassium, sodium and calcium. Other elements were determined after further appropriate dilution.

If separation of the matrix with β,β'-dichlorodiethyl ester (chlorex) was required, gallium (1 g) was dissolved in a mixture of 3 ml of 12 M hydrochloric acid and 1 ml of concentrated nitric acid with suitable heating. The solution was evaporated to a syrup and treated with 1 ml of 12 M hydrochloric acid for more complete removal of nitric acid, which inhibits the extraction. After this treatment, 10 ml of 12 M hydrochloric acid was added and the matrix was extracted three times with chlorex. The aqueous phase was evaporated under an i.r. lamp and the residue dissolved in 1 ml of 0.3 M hydrochloric acid. Temperature control during the dissolution and the use of minimum volumes of acids minimize the blanks.

Analytical measurements. These were carried out as described below.

Results and discussion

In the atomic absorption determination of trace impurities in high-purity rhenium, electrothermal atomization was used to achieve fractional evaporation of impurities from the very involatile rhenium matrix (rhenium melts at 3167°C and boils at 5370°C). Reduction of the perrhenic acid obtained by dissolution of rhenium in hydrogen peroxide or nitric acid occurs during thermal decomposition of samples and standards in the graphite furnace and yields rhenium metal. To improve the detection limits the kinetics of trace-impurity evaporation was studied under different conditions of furnace heating; optimum conditions were thus established. These are summarized in Table 1. Such a procedure ensures negligible evaporation of rhenium.

For the determination of Na, K and Li, a flame emission method was used, involving aspiration of the solutions into an air—acetylene flame at 4 ml min^{-1}.

The influence of rhenium on the atomic absorption or emission of the analyte elements was examined. Rhenium affects considerably only the analytical signals for bismuth and potassium (Fig. 1).

TABLE 1

Conditions for determination of impurities in rhenium by graphite furnace atomic absorption spectrometry

Element	Wavelength (nm)	Ashing step[a]		Atomization temp. (°C)
		Time of temp. increase(s)	Final temp. (°C)	
Ag	328.1	70	600	2500
Al	309.3	60	1450	2700
Bi	223.0	70	600	1900
Ca	422.7	60	1400	2340
Cd	228.8	70	600	1900
Cr	357.9	45	1200	2700
Cu	324.7	75	1000	2550
Fe	248.3	35	1150	2530
Mg	285.2	80	1150	2500
Mn	279.5	75	1000	2600
Ni	232.0	35	1150	2560
Pb	283.3	85	700	2100
Zn	213.8	85	700	1900

[a]Drying for 20—60 s at 100°C for different sample volumes.

On the basis of these investigations atomic absorption methods were developed for the determination of Ag, Al, Bi, Ca, Cd, Cr, Cu, Fe, Mg, Mn, Ni, Pb and Zn and atomic emission methods for the determination of K, Na and Li in high-purity rhenium [1]. These elements were chosen in accord with technical requirements imposed on special-purity rhenium, but may be extended

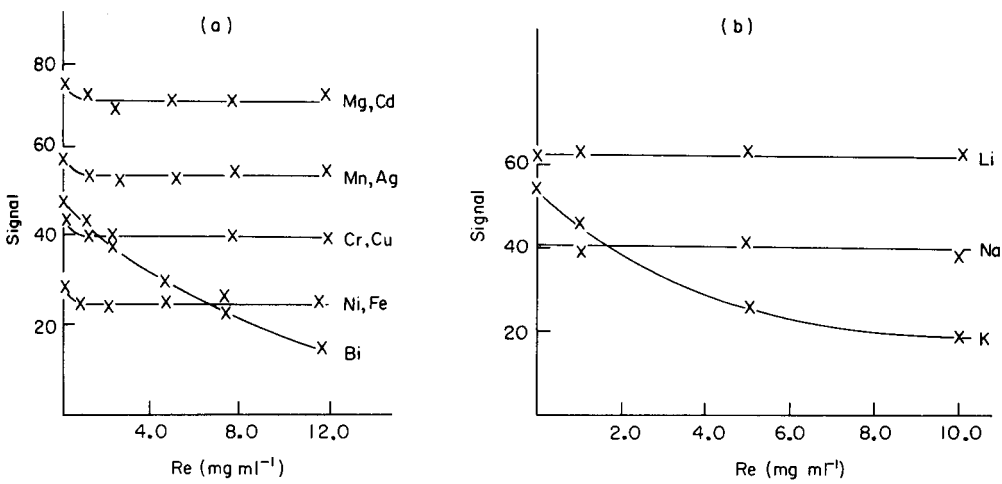


Fig. 1. Influence of rhenium on the analytical signal for some impurities obtained by (a) atomic absorption analysis in the graphite furnace; (b) flame emission analysis.

TABLE 2

Detection limits[a] for trace impurities in high-purity rhenium (%)

Impurity	Direct method analysis	Extractive method	Impurity	Direct method analysis	Extractive method
Ag	9×10^{-7}	—	K	9×10^{-5}	—
Al	2×10^{-5}	$1—2 \times 10^{-5}$	Li	8×10^{-6}	—
Bi	2×10^{-4}	2×10^{-7}	Mg	6×10^{-7}	$1—3 \times 10^{-5}$
Ca	2×10^{-5}	$0.5—2 \times 10^{-4}$	Mn	6×10^{-7}	$0.2—1 \times 10^{-6}$
Cd	5×10^{-7}	4×10^{-8}	Na	8×10^{-6}	—
Cr	9×10^{-6}	3×10^{-7}	Ni	1×10^{-4}	1×10^{-6}
Cu	7×10^{-6}	—	Pb	1×10^{-5}	$0.8—2 \times 10^{-6}$
Fe	8×10^{-6}	$0.3—1 \times 10^{-5}$	Zn	6×10^{-7}	$0.2—3 \times 10^{-6}$

[a] 4σ values.

if necessary. For the determination of molybdenum and tungsten which hardly atomize in the graphite furnace because of the formation of refractory carbides, an atomic absorption method with an air—acetylene flame [2] may be used.

To eliminate the influence of the matrix and to evaluate possibilities for improving the detection limits of some of the trace impurities, an extractive separation of the matrix with a solution of tri-n-octylamine oxide in toluene [2, 3] was used. The detection limits obtained with and without extraction are listed in Table 2. The accuracy of the extractive atomic absorption method was checked by addition of known amounts of analyte. There was no significant systematic error. The relative standard deviation was 0.03—0.07 for the flame emission determination and 0.13—0.30 for the graphite furnace measurement.

The electrothermal atomic absorption method was used also for the determination of some impurities in high-purity gallium. Investigations of the effect of ashing and atomization conditions enabled optimal heating conditions for the graphite furnace to be established for the determination of fifteen trace elements in gallium (Table 3). Drying was carried out at 100°C for 20—60 s, depending on the volume of sample taken. Potassium and sodium were again determined by flame atomic emission spectrometry.

The influence of hydrochloric acid (0.1—10 M) and gallium on the absorbance of the analyte elements was studied.

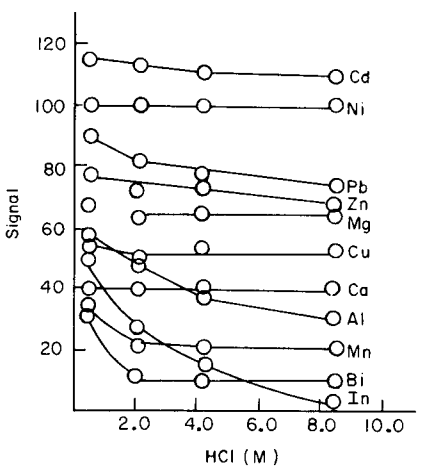
The presence of hydrochloric acid decreased the analytical signals, particularly for bismuth, indium and aluminium (Fig. 2). No influence of gallium was detected if its concentration did not exceed 0.5 mg ml^{-1} (Fig. 3); larger amounts led to decreased absorbance of many impurities, especially Bi, Fe, Cd and Zn. Therefore, a direct atomic absorption method was employed only for the determination of Cu, Ca, Mg, Mn and Al in gallium; K and Na were determined by flame emission. The detection limits are given in Table 4. To elim-

TABLE 3

Recommended furnace condition for the determination of impurities in gallium

Element	Ashing		Atomization[a]	
	Temp. (°C)	Time (s)	Temp. (°C)	Argon flow (ml min^{-1})
Ag	380	20	2150	0
Al	1500	20	2700	50
As	195	20	2400	0
Bi	340	15	1900	0
Ca	1500	15	2610	50
Cd	300	15	1900	0
Cr	1200	25	2700	0
Co	1100	15	2600	0
Cu	580	15	2470	0
In	640	20	2130	0
Mg	1020	15	2610	350
Mn	760	15	2600	0
Ni	1020	10	2620	0
Pb	490	15	2090	0
Zn	400	15	1900	350

[a]Atomization takes 8 s for all elements.



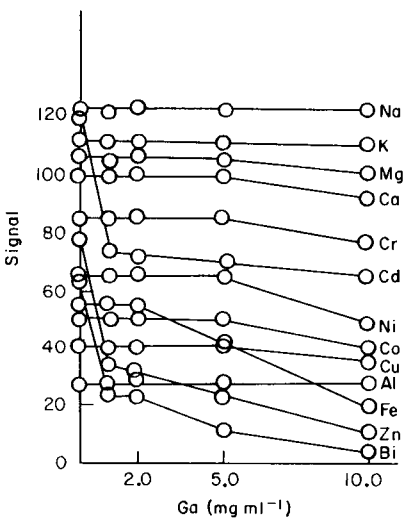


Fig. 2. Influence of hydrochloric acid on the maximum absorbance of some analyte elements.

Fig. 3. Influence of gallium on the absorbance of some analyte elements.

TABLE 4

Detection limits[a] for trace impurities in high-purity gallium (%)

Impurity	Direct method	Extractive method	
		Possible detection limit	Value restricted by blank
Ag	—	1×10^{-9}	2×10^{-8}
Al	$2\text{—}9 \times 10^{-6}$[b]	5×10^{-7}	2×10^{-6}
As	—	5×10^{-7}	5×10^{-7}
Bi	—	2×10^{-8}	2×10^{-7}
Ca	$4 \times 10^{-5}\text{—}1 \times 10^{-4}$[b]	1×10^{-5}	4×10^{-5}
Cd	—	5×10^{-10}	2×10^{-8}
Co	—	2×10^{-7}	2×10^{-7}
Cr	—	2×10^{-8}	4×10^{-8}
Cu	8×10^{-6}	5×10^{-8}	1×10^{-7}
In	—	1×10^{-7}	1×10^{-7}
Mg	$4\text{—}9 \times 10^{-6}$[b]	1×10^{-9}	4×10^{-6}
Mn	6×10^{-6}	1×10^{-9}	1×10^{-7}
Ni	—	5×10^{-7}	4×10^{-6}
Pb	—	3×10^{-8}	1×10^{-7}
Zn	—	1×10^{-9}	9×10^{-6}

[a] 4σ values. [b] Restricted by blank.

inate the influence of hydrochloric acid, appropriate quantities were added to standards and samples. A check of the accuracy of the method by a *t*-test indicated no systematic errors. The relative standard deviation is 0.08—0.20 for the graphite furnace and 0.06 for the flame emission determinations.

To improve detection limits, an extractive separation of the matrix was employed. The detection limits of the extractive atomic absorption method are given in Table 4. They are restricted by blank values, but can be reduced further by providing purer experimental conditions.

ANALYSIS OF SILICON FILMS

Experimental

Reagents. High-purity nitric acid was triple-distilled in a quartz apparatus and high-purity hydrofluoric acid was distilled in PTFE apparatus.

Procedure. In layer-by-layer determinations of As, In, Sb, Tl in silicon, chemical etching with a mixture of hydrofluoric and nitric acids (1:250 to 1:50) was employed to remove 0.1—1.0 μm layers. To remove 0.01—0.1 μm layers, anodic oxidation was used followed by chemical etching of the oxide layer with diluted hydrofluoric acid (1:100) [4]. After chemical etching, solutions (0.5—0.8 ml) were evaporated under an i.r. lamp in conical PTFE vessels. The dry residue was twice treated with 0.1 ml of concentrated nitric acid, and each time the solution was evaporated completely. For the deter-

mination of As and Sb, the dry residue was dissolved in 0.5—1.0 ml of deionized water; for determining In and Tl, it was dissolved in 0.5—1.0 ml of 0.3% and 1% nitric acid, respectively. Aliquots of 20 μl were used for analysis in the graphite furnace, the conditions for which are given in the text below.

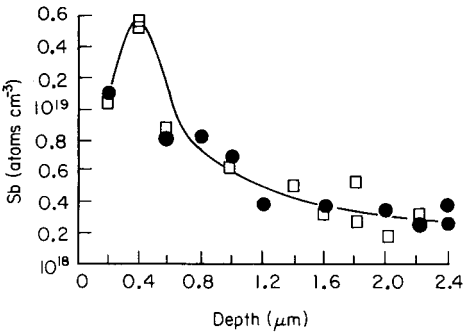
Results and discussion

A three-stage temperature program was employed for the determination of As, In, Sb and Tl in the graphite furnace: drying at 100°C for 20—30 s, ashing and atomization. To choose temperatures for the second and third stages, the dependence of analyte absorbance on the ashing temperature at the maximum atomization temperature and the dependence of the absorbance on the atomization temperature at constant ashing temperature were evaluated for each element. For the latter experiments, the ashing temperature chosen was that which gave the maximum analytical signal for a given element. The optimal ashing and atomization temperatures obtained in this way were: 420°C and 2420°C for As; 900°C and 2100°C for In; 300°C and 2050°C for Sb; and 100°C and 2400°C for Tl. In each case the ashing time was 15 s and the atomization time was 8 s.

For analysis, etching solutions were usually diluted with deionized water (1 + 4) and analyzed with respect to standards containing appropriate amounts of pure etching acid (silicon up to a 10^4 fold excess does not influence the analytical signal). The presence of the matrix degrades the detection limit. Thus, to improve detection limits, the matrix can be removed by evaporation accompanied by treatment with concentrated nitric acid [5]. Solutions prepared by this method contain small amounts of nitric acid which may influence the results if aqueous standards are used. The influence of 0.01—10% of nitric acid was examined. It enhanced the absorbance of In and Tl. To ensure accuracy, as well as to improve the detection limits, In and Tl standards were prepared in 0.3—1% HNO_3 and residues after sample evaporation were dissolved in the same solutions. As and Sb were analyzed against aqueous standards.

There were no impurity losses in etching and during the treatment of samples, and there were no "memory" effects when passing from layer to layer. Application of *t*-tests showed that there were no systematic errors. The method makes it possible to determine down to 1×10^{-10} g of As, 3×10^{-11} g of Sb and 2×10^{-11} g of In and Tl with coefficients of variation of 30%, 13%, 13% and 8%, respectively, in thin silicon layers. When impurities are determined in silicon layers thinner than 0.1 μm obtained by anodic oxidation, further sample treatment is unnecessary. Etching solutions can be analyzed with standards containing the same amount of hydrofluoric acid as the samples.

The methods developed were employed for constructing concentration profiles of doping impurities in epitaxial silicon layers. Figures 4 and 5 demonstrate typical antimony profiles found by chemical etching and arsenic profiles found by electrochemical etching. The results compare well with those obtained by polarography and neutron activation analysis, which are also shown in Figs. 4 and 5.



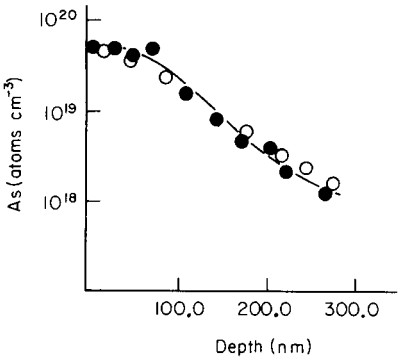


Fig. 4. Comparison of antimony distribution profiles in silicon obtained by (•) inverse voltammetric and (□) atomic absorption methods.

Fig. 5. Concentration profiles of arsenic distribution in epitaxial layers of silicon obtained by (•) atomic absorption and (□) atomic absorption methods.

REFERENCES

1 L. V. Zelentsova, I. G. Yudelevich and V. P. Shaburova, Zh. Anal. Khim., 32 (6) (1977) 1166.
2 V. P. Shaburova and I. G. Yudelevich, Chem. Anal., 19 (1974) 941.
3 I. G. Yudelevich, V. P. Shaburova, V. G. Torgov, O. I. Scherbakova and V. A. Usova, Zh. Anal. Khim., 28 (1973) 1049.
4 I. R. Shelpakova, I. G. Yudelevich, T. A. Chanysheva, O. I. Scherbakova and V. A. Usova, Zh. Anal. Khim., 30 (7) (1975) 1310.
5 I. G. Yudelevich, L. M. Buyanova, N. F. Bakhturova and T. M. Korda, Izv. SO AN SSSR, Ser. Khim. Nauk. N12, vyp. 5, 1976, p. 52.

Analytica Chimica Acta, 108 (1979) 53—61
© Elsevier Scientific Publishing Company, Amsterdam — Printed in The Netherlands

SIGNAL ENHANCEMENT IN CARBON-FILAMENT ATOMIC ABSORPTION SPECTROMETRY BY METAL—OXYGEN REACTIONS

R. H. EKLUND and J. A. HOLCOMBE*

Department of Chemistry, University of Texas at Austin, Austin, Texas 78712 (U.S.A.)

(Received 15th November 1978)

SUMMARY

Investigations of signal enhancement in carbon-filament atomic absorption spectrometry are described. Several enhancements are shown to be due to preferential binding of the oxygen by the added interferent in the gas phase. This prevents the analyte atoms from reacting with the oxygen, thereby preserving or enhancing the atom concentration and thus the absorbance signal.

Over the past few years, atomic absorption spectrometry with a carbon filament or tube (f.a.a.s.) has attained widespread use for trace metal analysis. While f.a.a.s. has the advantages of small sample size, high sensitivity and ease of application, it is very prone to matrix or interference effects. Little progress has been made in elucidating the fundamental causes for most of these interferences.

Before these interferences can be fully understood, the atomization process of simple metal salts must be examined. Campbell and Ottaway [1] and Aggett and Sprott [2] have examined the thermodynamics of metal-oxide (MO) reduction by graphite. A correlation between the temperature at which the reduction became favorable and the appearance temperature of the element was attempted. Sturgeon et al. [3] have extended this to form a combined kinetic/thermodynamic model of the vaporization process. For many metal salts, the atomization—vaporization processes involve the following reactions:

$$MX(s) \rightarrow MO(s) \qquad (X = NO_3^-, SO_4^{2-}) \qquad (1)$$

$$MO(s) + C(s) \rightarrow M(s) + CO(g) \qquad (2)$$

$$M(s) \rightarrow M(l) \rightarrow M(g) \qquad (3)$$

Sturgeon et al. showed that for the metal salt MX, thermal dissociation of MO may also be important in the production of gaseous free atoms. After the sample has been atomized and vaporized, there are three primary ways for the atomic density to be depleted: diffusion out of the observation zone, condensation reactions, and oxidative or other recombination reactions.

Aggett and West [4] have shown through the use of a double filament atomizer that interferences do occur in the gas phase and that the extent of the interference increases with increasing height above the atomizer surface. Other studies in which hydrogen was added to the sheath gas [5—7] also have alluded to the existence of gas-phase reactions as the cause of interferences. While recombination and condensation processes can account for depression of the analyte signal, they cannot adequately explain signal enhancements.

Owing to the strength of the MO bond and the usual presence of oxygen-containing species in the sample, some interferences are believed to be due to reactions of the metal with oxygen or oxygen-containing species [2, 8]. For example, recent work in this laboratory has shown that the presence of traces of oxygen in the sheath gas causes the atomic population of germanium to disappear above the surface of a carbon filament atomizer significantly faster than in the absence of oxygen and that the introduction of 5—10% of hydrogen into the sheath gas preserves or enhances the atomic signal at elevated heights. Preservation of the free atom density may be a consequence of the direct reduction of the metal oxide by hydrogen or of oxygen removal by reactions with hydrogen, so as to minimize oxide formation [9]. Since both pathways give the same result, reaction kinetics rather than equilibrium consideration will determine the mechanism by which hydrogen preserves the free atom density. In this paper, therefore, the term oxygen scrubbing will be used to describe the process of increasing the free atom concentration by preferentially binding any oxygen present in the system, irrespective of which of the pathways is involved. Extension of oxygen scrubbing by hydrogen to include competitive reactions of various metals for oxygen has led to a mechanism that explains many of the signal enhancements previously reported in the literature.

Given a gas-phase environment consisting of oxygen and two metals, thermodynamics predicts that the metal with the higher affinity for oxygen preferentially forms the oxide if oxygen is the limiting reactant and local chemical equilibrium exists in the vapor. It has been shown that when considering gas-phase reactions above the atomizer surface, thermodynamics may not fully characterize the extent of reaction, and reaction kinetics may be a significant factor in determining the extent of free atom depletion [10]. For the metal—oxygen reaction $M(g) + O_2(g) \rightarrow MO(g) + O(g)$, the rate is given by $-\partial M/\partial t = k[M][O_2]$. Thus the concentration of the metal will play a major role in determining the rate of the reaction. Since most interference effects are considered when the concomitant element is present in a large excess, the rate of the reaction will be relatively fast and thermodynamics should adequately describe the extent of the reaction in most cases.

On the assumption that the extents of diffusion and condensation are constant for a given analyte, it should be possible to add sufficient metal to react preferentially with the oxygen in the system. This should preserve the atomic population of the metal of interest and thus apparently enhance its

signal relative to that observed without any added concomitants. The following studies explore these metal—oxygen competition reactions as a means of explaining signal enhancements above a carbon-filament atomizer.

EXPERIMENTAL

The carbon-filament atomizer was of the basic design of Alder and West [11] with a minor modification made to enclose the sides of the atomizer to minimize air entrainment in the sheath gas. The atomizer power supply and temperature control unit [12] were capable of stepping to a reproducible final preset temperature at 3000 K s^{-1}. The filaments (2.5 mm wide, 18 mm long) were machined from 4.6-mm diameter spectroscopic-grade graphite rods. A pyrolytic coating was deposited on the rod by the procedure of Szydlowski et al. [13].

Nitrogen sheath gas was introduced through a gas box below the filament which was designed to insure laminar flow at the flow rates used. Its flow was controlled by rotameters at 2.7 l min^{-1} which yielded a linear velocity of 10 cm s^{-1}. The nitrogen was passed over hot copper turnings to remove any residual oxygen before entering the gas box.

The image of the rod was rotated by 90° by using a two-mirror configuration [14] and was focused on the monochromator entrance slit. In this manner a spatial region above the atomizer equal to the width of the monochromator entrance slit was isolated. Vertical translation of the atomizer using micrometer drives permitted selected spatial viewing at different heights.

A 1.5-m Two-Mirror Fastie (Jarrell-Ash) spectrograph equipped with a polychromator head and an R106 photomultiplier (Hamamatsu TV Co.) was used to carry out the absorption studies. The entrance slit was 1 mm tall and 200 μm wide and resulted in a spectral bandpass of slightly more than 0.1 nm.

Reagent-grade chemicals and triply distilled water were employed in all studies. Metals were dissolved as the nitrates with the exception of lanthanum and vanadium which were dissolved as oxides in dilute nitric acid. For the transient studies, a 2.0-μl sample of either a 650-ppb lead solution or a 250-ppb chromium solution was used. By pipetting appropriate amounts of a 500-ppm stock solution, 10- and 100-fold excesses of lanthanum or vanadium relative to the analyte were obtained.

By drilling two wells in the rod (2.0 mm diam., 1.5 mm deep) and placing milligram amounts of the pure metal in these holes, steady-state studies were conducted above the atomizer surface. Separation of these wells on the surface by 1 mm insured that any observed signal changes resulted from gas-phase reactions and not from possible solid state or surface reactions. For these steady-state experiments, the output from the photomultiplier was recorded directly on a strip-chart recorder. In the transient studies, the output signal was digitized with a Biomation (Model 805) transient recorder and the digitized information transferred to a computer for data reduction and analysis.

RESULTS AND DISCUSSION

Before any examination of the competitive metal—oxygen reactions can be made, a means of examining the favorability of any such reaction must be established. If it is assumed that these reactions are fast and that equilibrium control predominates, thermodynamic data could be used to calculate the equilibrium constants and the degree of metal oxide formation. Unfortunately, thermodynamic data are not available for a large number of elements. In order to make semi-quantitative predictions on the relative favorability of most metal—oxygen reactions, the MO bond energy can be used. This is reasonable because the main difference between the bond energy and the free energy ΔG of a homogeneous gas-phase reaction is the $T\Delta S$ term. At the elevated vapor temperatures encountered, the value of this term should be of the same order of magnitude for most metal vapors. Calculations based on 17 metals for which thermodynamic data are available [15] reveals a linear relationship between the MO bond energy and ΔG for the metal—oxygen reaction (Fig. 1).

Steady-state studies

For these studies, metal pairs were chosen so that their vapor pressures were approximately the same at an atomizer temperature giving an absorbance signal of 0.2—0.6 from the analyte. Additionally, metal pairs were selected such that their MO bond energies differed by at least 50 kcal mol^{-1}. Table 1 lists the boiling points and MO bond energies for the metals used.

Figure 2 shows the steady-state absorbance—height profile for chromium alone and with germanium metal present in the second hole in the rod. The addition of germanium causes an enhancement in the chromium absorbance above the rod up to heights approaching 2 mm, with the largest enhancement

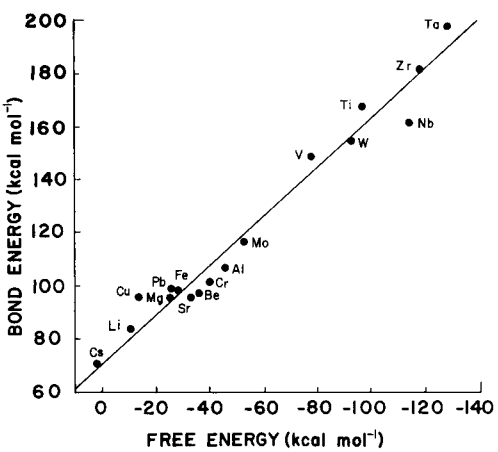


Fig. 1. Plot of MO bond energy versus the free energy ΔG of the reaction M(g) + $1/2O_2$(g → MO(g) at 1000 K.

TABLE 1

Metal oxide bond energies and boiling points of selected elements

Element	Bond energy (kcal mol^{-1}) [16]	B.p. (K) [17]
Ag	47	2436
Cr	102	2945
Ge	157	3107
La	194	3730
Mn	97	2335
Pb	99	2023
V	149	3682

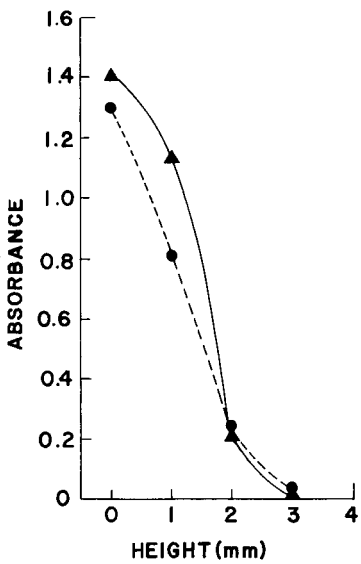


Fig. 2. Chromium atomic absorbance—height profile for Cr metal only (•) and Cr metal with Ge metal (▲) present. Height refers to the height above the filament.

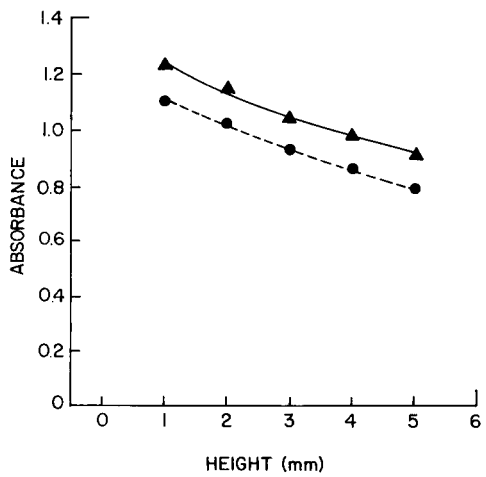


Fig. 3. Silver atomic absorbance—height profile for Ag metal only (•) and Ag metal with Mn metal (▲) present.

being 60% at 1 mm. The fact that this signal enhancement is not observed at 2 mm above the filament is believed to be due to condensation of the chromium in the gas phase as the vapor temperature decreases and the partial pressure of chromium exceeds its saturation vapor pressure. When the gallium two-line absorbance method [18] was used, the vapor temperature was found to decrease by several hundred Kelvin over the spatial zone of interest. Therefore, the conditions necessary for supersaturation and for condensation are available at elevated heights. It has been shown that metal vapor conden-

sation does occur on a time scale which is short relative to the movement of the atomic species above the atomizer [19]. The idea of signal depression resulting from condensation and occlusion of the analyte in the condensate has been previously considered by other workers [4, 11, 20].

In Fig. 3, the steady-state absorbance—height profiles for silver with and without manganese are presented. Because silver forms such a weak bond with oxygen, these studies were conducted with air (0.01 l min^{-1}) being introduced in the sheath gas to favor the formation of silver oxide. As before, a 10—20% enhancement of the silver signal is observed. Unlike the Cr—Ge couple, the silver absorbance signal persists up to 5 mm above the atomizer surface. This may be explained by the fact that silver has an oscillator strength which is 32% larger than that for chromium [21] which in turn dictates that a reduced atomic concentration is necessary to produce an absorbance signal of the same magnitude. This will make condensation less likely until the cooler temperatures at greater heights above the atomizer are reached.

Transient studies

A series of transient studies was undertaken to verify that the results of the steady-state experiments could be extended to the transient systems encountered in f.a.a.s. where the metals are not present initially in their elemental state and may exhibit greatly dissimilar vapor pressures. All of these experiments were done with the rod heated to a final temperature of 2300 K. Studies of the chromium absorbance with and without germanium present showed similar results to those already presented in Fig. 2. In these studies, the chromium sample was pipetted onto the atomizer surface between the two wells which contained germanium metal. Germanium metal was used instead of a solution of germanium dioxide because upon heating, germanium dioxide will be converted to germanium monoxide which sublimes at 950 K

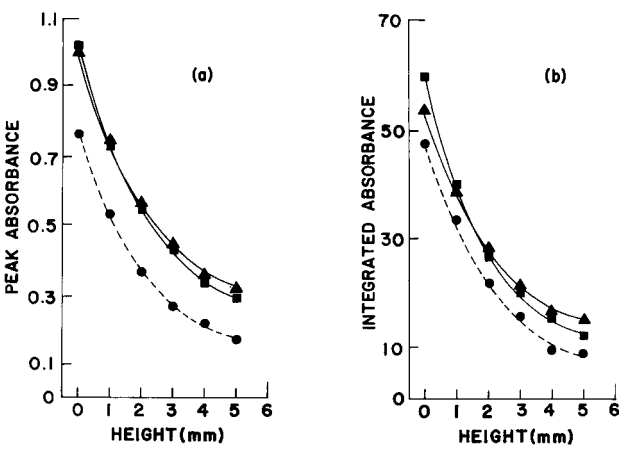


Fig. 4. Lead (a) peak and (b) integrated atomic absorbance—height profiles for Pb only (•), Pb with a 10-fold wt. excess of La (▲) and Pb with a 100-fold wt. excess of La (■).

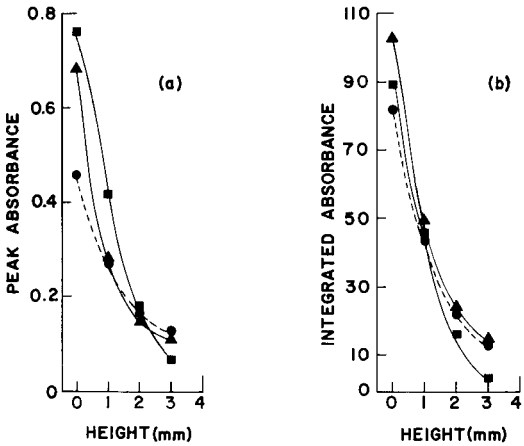


Fig. 5. Chromium (a) peak and (b) integrated atomic absorbance—height profiles for Cr only (•), Cr with a 10-fold wt. excess of La (▲) and Cr with a 100-fold wt. excess of La (■).

[22] and exhibits minimal dissociation to the metal prior to sublimation.

In order to simulate conditions that may be more realistic, the effects of a 10-fold and 100-fold excess of lanthanum on the absorbances of lead and chromium were examined. Figure 4a shows the peak absorbance—height profiles for lead with and without lanthanum. The integrated absorbance—height profile is presented in Fig. 4b. Again, signal enhancements of 30—60% were observed depending upon the spatial region being viewed. The enhancement appears to be independent of the lanthanum concentration and suggests that the 10-fold amount of lanthanum is sufficient to remove any traces of oxygen from the system.

Figure 5 shows the absorbance—height profiles for chromium with and without lanthanum. Signal enhancements of 25—65% were recorded depending on the spatial zone viewed and whether or not peak or integrated absorbance was measured. The signal depression seen at 3 mm is believed to be due to condensation processes in which the higher concentration of lanthanum may be undergoing homogeneous condensation and serving as nucleation sites for chromium. Unlike the trends observed for the lead signal with increasing lanthanum concentration, the 100-fold amount of lanthanum resulted in a larger chromium absorbance signal than a 10-fold amount when peak height was used. However, the opposite effect was observed when the chromium absorbance signal was integrated. This observation is similar to that made by Smeyers-Verbeke et al. [23] using a carbon furnace atomizer where sharper and narrower peaks were recorded when a positive interference was encountered. Additional studies are required before a definitive statement about the cause of this anomaly can be made.

Figure 6 shows the absorbance—height profile for chromium with a 10- and 100-fold amount of vanadium. Unlike lanthanum, vanadium caused a depression in the analyte signal in regions less than 2 mm above the filament

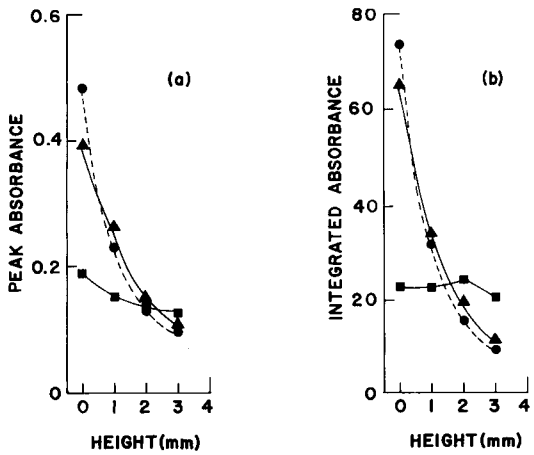


Fig. 6 Chromium (a) peak and (b) integrated atomic absorbance—height profiles for Cr only (•), Cr with a 10-fold wt. excess of V (▲) and Cr with a 100-fold wt. excess of V (■).

surface which cannot be fully explained at this time. The fraction of the sample that is atomized was better preserved at higher spatial regions when vanadium was present and resulted in signal enhancements of 25—100%. Sutter and Leroy [24] also found a vanadium depression of the nickel absorbance signal, which cannot be explained by the above mechanism.

CONCLUSIONS

In the light of the proposed enhancement mechanism, it is useful to examine those signal enhancements already reported in the literature. Recently, Sutter and Leroy [24] found that the presence of iron enhanced the nickel absorbance signal; this is in agreement with the proposed mechanism since the MO bond energy is 11.6 kcal mol^{-1} greater for iron than for nickel. Also, the enhancement increased with increasing iron concentration. There may be two reasons. First, there may have been significant amounts of oxygen present near the atomizer surface, and an increase in the nickel absorbance would occur as more oxygen is removed by increasing the iron concentration. Secondly, the iron—oxygen reaction is 100—1000 times slower than the oxidation of other metals for which kinetic data are available [25—28]. Thus, the relatively slow reaction rates may have resulted in rate-limited reaction conditions and, consequently, a continued increase in the degree of enhancement resulted as the iron concentration was increased.

Other examples of signal enhancement, which appear to result from oxygen scrubbing in the gas phase are included in the work of Maruta and Takeuchi [29] who investigated the effects of various ions on chromium absorbance. They found signal enhancements to be caused by the addition of vanadium and molybdenum. These elements form oxides whose bond strengths exceed that of chromium by 47 and 15 kcal mol^{-1}, respectively.

It must be mentioned that other examples of signal enhancement are known that do not fit this mechanism. Explanations of all these signal enhancements are complicated by inconsistent means of examining and reporting these interferences. Factors like the counter anion, the spatial zone being viewed, and the atomization conditions often are not reported. While the mechanism proposed here is simple, it forms a logical chemical basis for many signal enhancements in f.a.a.s.

The authors are grateful to the National Science Foundation for the financial support of this project under grant no. CHE 78-15438.

REFERENCES

1 W. C. Campbell and J. M. Ottaway, Talanta, 21 (1974) 837.
2 J. Aggett and A. J. Sprott, Anal. Chim. Acta, 72 (1974) 49.
3 R. E. Sturgeon, C. L. Chakrabarti and C. H. Langford, Anal. Chem., 48 (1976) 1972.
4 J. Aggett and T. S. West, Anal. Chem., 55 (1971) 349.
5 M. P. Newton and D. G. Davis, Anal. Chem., 47 (1975) 2003.
6 R. D. Reeves, B. M. Patel, C. J. Molnar and J. D. Winefordner, Anal. Chem., 45 (1973) 246.
7 B. M. Patel, R. D. Reeves, R. F. Browner, C. J. Molnar and J. D. Winefordner, Appl. Spectrosc., 27 (1973) 171.
8 G. Guiochon, B. Hircq and C. Tailland, Anal. Chim. Acta, 99 (1978) 125.
9 R. D. Reeves, B. M. Patel, C. J. Molnar and J. D. Winefordner, Anal. Chem., 45 (1973) 246.
10 J. A. Holcombe and R. H. Eklund, Anal. Chem., submitted.
11 J. F. Alder and T. S. West, Anal. Chim. Acta, 51 (1970) 365.
12 J. A. Holcombe, Rev. Sci. Instrum., submitted.
13 F. J. Szydlowski, E. Peck and B. Bax, Appl. Spectrosc., 32 (1978) 402.
14 J. A. Holcombe, Appl. Spectrosc., 32 (1978) 405.
15 D. R. Strull and H. Prophet, JANAF Thermochemical Tables, 2nd edn., National Bureau of Standards, Washington, D.C., 1971.
16 R. C. Weast (Ed.), Handbook of Chemistry and Physics, 51st edn., Chemical Rubber Co., Cleveland, Ohio, 1970—1971.
17 R. Hultgren, P. D. Desai, D. T. Hawkins, M. Gleiser, K. K. Kelley and D. D. Wagman, Selected Values of the Thermodynamic Properties of the Elements, American Society for Metals, Metals Park, Ohio, 1973.
18 M. P. Bratzel, Jr. and C. L. Chakrabarti, Anal. Chim. Acta, 63 (1973) 1.
19 D. J. Frurip and S. H. Bauer, J. Phys. Chem., 81 (1977) 1007.
20 D. Clark, R. M. Dagnall and T. S. West, Anal. Chim. Acta, 63 (1973) 11.
21 B. V. L'Vov, Atomic Absorption Spectrochemical Analysis, American Elsevier, New York, 1970.
22 L. Barton and C. A. Heil, J. Less-Common Met., 22 (1970) 11.
23 J. Smeyers-Verbeke, Y. Michotte, P. Van den Winkel and D. L. Massart, Anal. Chem., 48 (1976) 125.
24 E. M.-M. Sutter and M. J.-F. Leroy, Anal. Chim. Acta, 96 (1978) 243.
25 A. Fontijn, W. Felder and J. Houghton, XIV Symposium (International) on Combustion, Pittsburgh, 1973, p. 775.
26 W. Felder and A. Fontijn, J. Chem. Phys., in press.
27 W. Felder, R. Gould and A. Fontijn, J. Chem. Phys., 66 (1977) 685.
28 A. Fontijn, S. Kurzius and S. Houghton, XV Symposium (International) on Combustion, Pittsburgh, 1975, p. 167.
29 T. Maruta and T. Takeuchi, Anal. Chim. Acta, 66 (1973) 5.

Analytica Chimica Acta, 108 (1979) 63—68
© Elsevier Scientific Publishing Company, Amsterdam — Printed in The Netherlands

CHEMICAL ANALYSIS OF MANGANESE NODULES
Part IV. Determination of Nickel after Anion-exchange Separation

J. KORKISCH* and I. STEFFAN

Institute for Analytical Chemistry, University of Vienna, Währingerstrasse 38, A-1090 Vienna (Austria)

M. B. FISK

University of California, Scripps Institution of Oceanography, Geological Research Division, La Jolla, California 92037 (U.S.A.)

(Received 25th January 1979)

SUMMARY

A method is described for the a.a.s. determination of nickel in manganese nodules after its separation from interfering metals. After dissolution of the sample in a mixture of perchloric and hydrofluoric acids, manganese, iron, cobalt, copper and other elements are adsorbed on the strongly basic anion exchange resin Dowex 1 (chloride form) from 95% ethanol—5% 12 M hydrochloric acid. The nickel passes into the effluent in which it is determined by a.a.s. with an air—acetylene flame. The method was used successfully for the determination of nickel in numerous samples of nodules from the Pacific Ocean.

For the determination of nickel, which is one of the most significant constituents of marine manganese nodules, a variety of methods can be used which include spectrography [1—3] and x-ray spectrometry [4]. Analytical techniques based on atomic-absorption spectrometry after the removal of interfering main constituents have not been described in the literature, although interferences in the a.a.s. determination of nickel have been observed in several matrices including ores [5, 6], steels [7, 8], silver alloys [9] and copper-based materials [10, 11] as well as in solutions containing copper, cobalt, iron, manganese, zinc and chromium [12].

The present paper reports a method for the atomic-absorption determination of nickel after its separation by anion exchange.

EXPERIMENTAL

Solutions and reagents

Ion-exchange resin. The strongly basic anion exchanger Dowex 1-X8 (Bio-Rad AGl-X8; 100—200 mesh; chloride form) was used. Slurry the resin (4 g) with a few ml of the ethanol—HCl mixture; after ca. 30 min, pour into an ion-exchange column filled with the same solvent system. Subsequently pretreat the resin as mentioned in the Procedure.

Standard solutions. From aliquots of stock solutions containing 1 mg of Ni(II), Fe(III), Mn(II) and other elements per ml of 6 M hydrochloric acid, prepare standard solutions of the elements in 6 M hydrochloric acid.

Ethanol—HCl mixture. To ethanol (96%) add concentrated hydrochloric acid so that the mixture obtained consists of 95% (v/v) ethanol and 5% (v/v) concentrated hydrochloric acid.

Apparatus

The Teflon "bombs" used for the dissolution of the samples have been described previously [13].

The separations of nickel from interfering elements were done in ion-exchange columns of the type and dimensions described earlier [14].

For the determination of nickel, a Perkin-Elmer atomic-absorption spectrometer Model 303 (equipped with a Hitachi Perkin-Elmer recorder connected to a read-out accessory) was used with the following instrumental settings: u.v. grating; wavelength 232.5 nm; scale expansion up to 2×; slit width 3 (0.3 mm 0.2 nm bandpass); nickel hollow-cathode lamp at 25—40 mA; standard burner head; acetylene pressure 8 psig (7.0 on flow meter scale); air pressure 30 psig (9.0 on flow meter scale); noise suppression up to 2.

When the measurements were done with 6 M hydrochloric acid solutions, a sensitivity (1% absorption) of 0.24 ppm of nickel was obtained.

Determination of distribution coefficients

The distribution coefficients (K_d values) of nickel, manganese, iron and of other elements were determined by using the batch method [15].

Procedure

For drying and dissolution of the samples, use the procedure described previously [13, 16]. Dilute the final filtrate with 6 M hydrochloric acid to 100 ml (sample solution).

Evaporate 10 ml of the sample solution (= 0.1 g of the original sample of manganese nodule) to dryness on a steam bath and dissolve the residue in 50 ml of the ethanol—HCl mixture. Pass the sorption solution through an ion-exchange column containing 4 g of the anion exchanger (pretreated by washing it with 50 ml of the ethanol—HCl mixture) at a flow-rate which corresponds to the back-pressure of the resin bed (about 0.33 ml min^{-1}). Collect the effluent quantitatively; subsequently wash the resin bed with 100 ml of the ethanol—HCl mixture and combine this effluent with that obtained when the sorption solution was passed.

Evaporate the combined effluents (150 ml) containing the nickel to dryness on a steam bath and dissolve the residue in 10 ml of 6 M hydrochloric acid. Aspirate this solution into the air—acetylene flame. Construct calibration curves by aspirating suitable standard solutions of nickel before and after each batch of samples.

Regeneration of resin. To elute the adsorbed elements, wash the resin bed

first with 100 ml of 6 M hydrochloric acid and then with 100 ml of the 1 M acid. Subsequently, pass through the column 50 ml each of the following solutions in the order stated: 2 M nitric acid, 6 M hydrochloric acid and ethanol—HCl mixture. Use this regenerated resin for the separation of nickel as described above.

RESULTS AND DISCUSSION

Ion-exchange separation

On the anion-exchange column, nickel is only very slightly adsorbed (K_d = 8) so that it readily passes into the effluent together with all other elements which do not form anionic chloride complexes under these conditions. Completely adsorbed from this ethanol—HCl mixture are most of the major and minor constituents of manganese nodule samples such as Mn(II), Fe(III), Co(II), Cu(II), Mo(VI), Zn(II), Cd(II) and Pb(II). These elements can therefore be separated quantitatively from the nickel.

Measurements of the batch distribution coefficients of nickel and the main constituents of manganese nodule samples (i.e., manganese and iron) in various alcohol—hydrochloric acid systems gave the results presented in Tables 1 and 2. From the data shown in Table 1, it can be seen that nickel is

TABLE 1

Results of determinations of distribution coefficents in alcohol—HCl mixtures (1 g Dowex 1-X8; 1 mg load)

Mixture	Distribution coefficients		
	Ni(II)	Mn(II)	Fe(III)
95% Ethanol—5% 12 M HCl	8.0	167	500
95% Isopropanol—5% 12 M HCl	73	8383	548
90% Isopropanol—10% 6 M HCl	49	1511	250

TABLE 2

Results of determinations of distribution coefficients in 95% ethanol—5% HCl mixtures containing varying concentrations of hydrochloric acid (1 g Dowex 1-X8; 1 mg load)

Hydrochloric acid (M)[a]	Distribution coefficients		
	Ni(II)	Mn(II)	Fe(III)
2	7.8	20	497
4	7.9	48	502
6	8.3	68	507
8	7.9	90	498
10	8.1	129	495
12	8.0	167	500

[a]With respect to the 5% aqueous phase of the mixtures.

only slightly retained by the anion exchanger from the ethanol—HCl mixture while it is relatively strongly adsorbed from the propanol media. Consequently, the latter systems are unsuitable for the separation of this element from manganese and iron which are also strongly retained by the resin. However, an isopropanol—HCl medium has been found to be very useful for the chromatographic separation of manganese, copper, cobalt, lead, uranium, zinc, and cadmium on a column of the same anion-exchange resin [17].

In comparison to aqueous hydrochloric acid systems, the main advantage of using this ethanol—HCl mixture is based on the fact that Mn(II), Co(II) (K_d = 2740), Cu(II) (K_d = 1720) and Pb(II) (K_d = 3210) are very strongly retained by the resin, which is not the case when pure aqueous media containing hydrochloric acid are employed [15]. Thus, when the ethanol system is used, it is possible to separate nickel from all elements interfering with its a.a.s. determination. No interferences were caused by the elements passing into the effluent together with nickel, e.g. aluminium, vanadium, alkali and alkaline earth elements.

A minor disadvantage of using the ethanol—HCl mixture is that complete elution of the nickel is achieved only after washing the resin bed with 100 ml of the mixture (see Procedure). If a pure aqueous hydrochloric acid medium were used for the nickel separation, the volume of washing solution could be reduced to a few milliliters because nickel does not show any measurable adsorption on the anion exchanger from aqueous hydrochloric acid media of any acid concentration, but suitable separations would not then be achieved.

On regeneration of the resin (see Procedure), the 6 M hydrochloric acid eluent provides quantitative elution of manganese, copper, cobalt and lead, which can be determined quantitatively in this eluate if required, by a.a.s. or any other suitable method. With the 1 M hydrochloric acid which is used next, iron and molybdenum are eluted quantitatively, and on treatment of the resin bed with 2 M nitric acid both zinc and cadmium are completely removed from the column. Subsequent treatment of the anion-exchanger with 6 M hydrochloric acid guarantees quantitative re-conversion of the resin to the chloride form.

Application to manganese nodules

Table 3 gives the results obtained when this procedure was applied to the analysis of five "standard and repeatedly analyzed samples" of manganese nodules. Comparison of the results for nickel in column A with those of columns B and C shows that direct a.a.s. gives results for this element which are invariably higher than those measured after application of the anion-exchange separation procedure. This was found to result from interferences in the a.a.s. measurements caused by the presence of copper, cobalt, iron and manganese; copper caused the highest, and manganese the lowest, increase in the absorption values.

Comparison of the nickel results listed in columns B and C of Table 3 shows that the amounts of nickel added (500 μg/0.1 g of nodule sample) were recovered quantitatively in all cases, i.e. nickel is not lost during the separation and

TABLE 3

Results for the determination of nickel in "standard and repeatedly analyzed samples" of manganese nodules
(A = Results obtained by direct a.a.s. of nickel in the 6 M hydrochloric acid sample solutions. B = Results obtained after anion-exchange separation of nickel. C = As under B, but after deduction of 500 μg Ni added to the sorption solutions before their passage through the resin columns. D = Results obtained in other laboratories.)

Sample	Nickel (%)				
	A	B	C	D	
Schafer 1 (112DK 20)	0.81	0.79	0.79	0.77[a]	Standard samples
				0.77[b]	
Schafer 2	1.47	1.42	1.44	1.46[a]	
				1.50[b]	
MR 33	1.21	1.15	1.18	1.07[b]	Repeatedly analyzed samples
				1.08[c]	
MR 58	1.17	1.14	1.16	1.18[b]	
				1.13[c]	
MR 8	1.24	1.23	1.22	1.03[b]	
				1.04[c]	

[a]Metallgesellschaft AG, Frankfurt, West Germany.
[b]Kennecott Exploration, Inc., San Diego, California.
[c]Scripps Institution of Oceanography, La Jolla, California (Dr. G. Arrhenius).

evaporation procedures. There is also reasonably good agreement between the present nickel results and those obtained in other laboratories (see column D), except for sample MR 8 in which the amount of nickel found here was over 15% more than that found by other investigators.

The results shown in Table 4 indicate that the nickel content varies by about a factor of 10 among the marine nodules. On average, however, the content is higher—by about two orders of magnitude—than the nickel concentration of the Lake Michigan nodule sample. In other samples of ferromanganese nodules from the Great Lakes, nickel contents of 55 ppm and 320 ppm were measured by Callender [18].

Comparison of the results of nickel determinations shown in column A with the data listed in column B once more demonstrates that direct a.a.s. usually gives results which are higher than those measured after anion-exchange removal of the interfering elements. The results obtained by x-ray spectrometry [19] (see Table 4, column C) are in several cases higher than those measured by a.a.s.

This research was sponsored by the Fonds zur Förderung der wissenschaftlichen Forschung, Vienna, Austria. Samples were supplied by the Lamont—Doherty Geological Observatory, T. Walsh at the Scripps Institution of Oceanography, Dr. Edward Callender (U.S. Geological Survey, Reston, Virginia) and Dr. John Mero (Ocean Resources Inc.); the Lake Michigan sample was supplied by Dr. David Edgington (Argonne National Laboratory). Generous support from these sources is gratefully acknowledged.

TABLE 4

Results of nickel determinations in manganese nodules from the Pacific Ocean and Lake Michigan
(A = Results obtained by direct a.a.s. of nickel in 6 M hydrochloric acid sample solutions. B = Results obtained after anion-exchange separation of nickel. C = Results obtained by x-ray spectrometry [19].)

Sample	Nickel (%)		
	A	B	C
AMPH 124C	0.361	0.378	0.42
CATO 10PB, outer crust	0.128	0.128	0.14
CHAIN 100B	0.324	0.313	0.34
COCOTOW, 2DA; 1/10 Nod.	0.685	0.666	0.65
RC 12-87, 25 cm	0.564	0.550	0.65
RC 13-66, 973 cm; 1/4 Nod.	0.348	0.339	0.36
STYX 46 FFGX-sect. Nod.	0.301	0.283	0.30
STYX 81 FF-42, 1/2 Nod.	0.420	0.413	0.41
7 TOW-123D, crust	0.405	0.386	0.40
V-18-277, Top	0.244	0.230	0.22
V-18-279, Top	0.324	0.324	0.33
V-18-280	0.378	0.372	0.41
DOMES 24B G-H	1.460	1.446	1.32
TRIPOD 9D	1.019	1.002	1.10
DPSNO 2-D2 Rock Top 1	0.679	0.667	0.66
DPSNO 2-D3-14	0.557	0.534	0.60
DPSNO 2-D3-18	0.209	0.209	0.22
DPSNO 2-D4-13	0.122	0.120	0.15
Lake Michigan nodule[a]	0.0063	0.0056	

[a]This sample contained 1.7% Mn and 25.6% Fe.

REFERENCES

1 J. L. Mero, Econ. Geol., 57 (1962) 747.
2 J. P. Willis and L. H. Ahrens, Geochim. Cosmochim. Acta, 26 (1962) 751.
3 J. P. Riley and P. Sinhaseni, J. Mar. Res., 17 (1958) 466.
4 G. H. W. Friedrich, H. Kunzendorf and W. L. Plüger, J. Geochem. Explor., 3 (1974) 303.
5 K. Kinson, J. E. Dickeson and C. B. Belcher, Anal. Chim. Acta, 41 (1968) 107.
6 V. Endo, T. Hata and V. Nakahara, Bunseki Kagaku, 18 (1969) 833.
7 K. Kinson and C. B. Belcher, Anal. Chim. Acta, 30 (1964) 64.
8 S. Sprague and W. Slavin, in E. N. Davis (Ed.), Development in Applied Spectroscopy, Vol. 4, Plenum Press, New York, 1965, p. 433.
9 J. M. Viebrock, Anal. Lett., 3 (1970) 373.
10 K. Itsuki, H. Komuro and T. Nagasawa, Bunseki Kagaku, 19 (1970) 1282.
11 B. Gandrud and J. C. Marshall, Appl. Spectrosc., 24 (1970) 367.
12 L. L. Sundberg, Anal. Chem., 45 (1973) 1460.
13 J. Korkisch, I. Steffan, G. Arrhenius, M. Fisk and J. Frazer, Anal. Chim. Acta, 90 (1977) 151 (Part 2).
14 W. Koch and J. Korkisch, Mikrochim. Acta, (1972) 687.
15 J. Korkisch, Modern Methods for the Separation of Rarer Metal Ions, Pergamon, Oxford, 1969, pp. 7, 8.
16 J. Korkisch, I. Steffan and G. Arrhenius, Anal. Chim. Acta, 94 (1977) 237 (Part 3).
17 J. Korkisch, H. Hübner, I. Steffan, G. Arrhenius, M. Fisk and J. Frazer, Anal. Chim. Acta, 83 (1976) 83 (Part 1).
18 E. Callender, Mich. Dep. Nat. Resour. Geol. Surv. Div., Miscellany, 1 (1970) 56.
19 J. Z. Frazer, M. B. Fisk, J. Elliott, M. White and L. Wilson, Scripps Institution of Oceanography (S10) Reference Series, 78-25, Annual Report, June 30, 1977—August 31, 1978.

Analytica Chimica Acta, 108 (1979) 69—74
© Elsevier Scientific Publishing Company, Amsterdam — Printed in The Netherlands

ATOMIC ABSORPTION SPECTROMETRY OF VANADIUM WITH A TUNGSTEN ELECTROTHERMAL ATOMIZER

KIYOHISA OHTA and MASAMI SUZUKI*

Department of Chemistry, Faculty of Engineering, Mie University, Kamihama-cho, Tsu, Mie-ken 514 (Japan)

(Received 31st January 1979)

SUMMARY

A detailed study of the atomic absorption characteristics of vanadium with a tungsten micro-tube atomizer is presented. The absolute sensitivities (1% absorption) were 2×10^{-10} and 4×10^{-11} g of vanadium for ammonium vanadate and the vanadium *N*-benzoyl-*N*-phenylhydroxylamine complex, respectively. Diverse elements and acids have pronounced depressive effects, but vanadium may be determined in rocks after selective extraction of the above complex into chloroform.

Graphite-tube atomizers are widely applied in electrothermal atomic absorption spectrometry. However, the determination of some elements, including vanadium, in a graphite tube furnace is impaired by carbide formation. A tantalum lining in a graphite tube has been used in an attempt to prevent carbide formation. Donega and Burgess [1] used a tantalum boat for atomization of vanadium and found a sensitivity of 6×10^{-10} g. This paper describes the electrothermal atomization of vanadium with a tungsten micro-tube atomizer, and its application for the determination of vanadium in rocks.

EXPERIMENTAL

Apparatus

Atomic absorption measurements were made with a Nippon Jarrell-Ash 0.5-m Ebert-type monochromator coupled to an R106 photomultiplier tube (Hamamatsu TV Co.) and a fast-response amplifier which was assembled in this laboratory. The output signal from the amplifier was monitored on an Iwatsu MS-5021 Memoriscope. A Hitachi 056-1001 chart recorder was also used.

The atomizer was a tungsten micro-tube (25 mm long, 1.5 mm bore) mounted in the absorption chamber (300 ml) which was purged (under recommended analytical conditions) with 480 ml Ar min^{-1} and 20 ml H_2 min^{-1}. The micro-tubes were fabricated from 0.05-mm thick tungsten sheet. The tube temperature was measured as described previously [2].

The radiation source was a vanadium hollow-cathode lamp (Hamamatsu TV Co). The wavelength used was 318.4 nm. Background absorption was

checked with a deuterium lamp (original Hanau D200F). All sample solutions were injected with glass micropipettes.

Reagents

A vanadium stock solution (1000 μg ml^{-1}) was prepared by dissolving ammonia metavanadate in 0.45 M sulphuric acid. Working solutions were freshly prepared by diluting the stock solution with water before use. All reagents were of analytical-reagent grade.

Procedure for the determination of vanadium in rocks

Decompose 0.5—1g of rock with 4—6 ml of 14 M nitric acid and 4—6 ml of 40% hydrofluoric acid in a Uni-Seal decomposition vessel by heating at 120°C in an electric oven for 2 h. After decomposition, transfer the solution to a Teflon beaker and evaporate to dryness on a water bath. Dissolve the residue in 0.1 M hydrochloric acid and dilute to 25 ml with the same acid. Transfer 1 ml of the solution to a separatory funnel and add 1 drop of 0.3% (w/v) potassium permanganate solution to oxidize vanadium. Add 1 ml of 11 M hydrochloric acid and 4 ml of a *N*-benzoyl-*N*-phenylhydroxylamine solution in chloroform (0.075% w/v). Extract the vanadium complex. Inject 1 μl of the organic phase into the atomizer. Dry at 100°C for 60 s and atomize at 2200°C for 1 s. Check for background absorption by use of the deuterium lamp, by measurement on a separate aliquot.

Prepare a calibration curve by extracting vanadium from standard solutions using the above procedure.

RESULTS AND DISCUSSION

Atomization characteristics

Vanadium was atomized from various compounds and complexes. Figure 1 shows the Memoriscope traces of the vanadium absorption obtained. Vanadium(IV) was prepared by evaporating a vanadium(V) solution in hydrochloric acid. Vanadium *N*-benzoyl-*N*-phenylhydroxylamine (BPHA), diethyldithiocarbamate (DDTC), 8-quinolinol and thiocyanate complexes were prepared as described in the literature [3—6]. The sample solution (1 μl) was placed in the micro-tube and dehydrated at 100°C. Then, vanadium was atomized by heating so as to give a final temperature of 2200°C. Although the charring step (300°C for 10 s) was included for the simple vanadium ions, this step led to lower sensitivity for vanadium in the complexes. Carbide formation may occur in the course of the breakdown of an organic matrix. Therefore, the charring step was omitted for the organic and thiocyanate complexes.

Small absorption peaks from organic species were observed at about 700—800°C during the atomization from the BPHA and 8-quinolinol complexes. The fast-response detection system facilitated the recording of the thermal separation of the production of vanadium and organic species. The thiocyanate

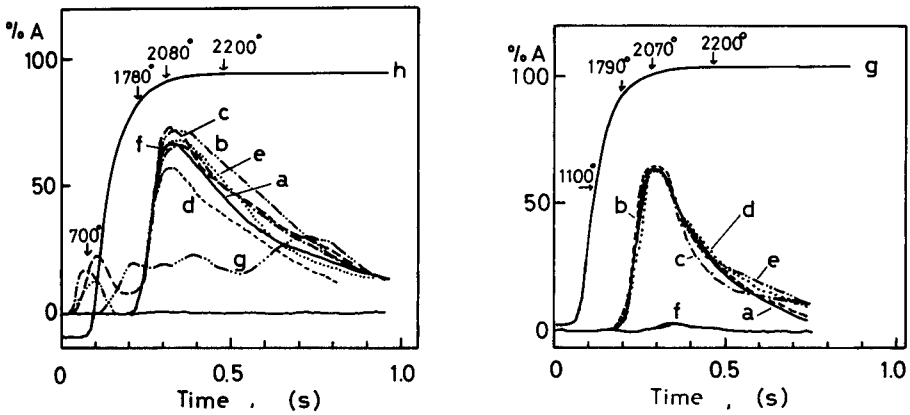


Fig. 1. Memoriscope traces of vanadium (10 ng) absorbance in the tungsten micro-tube atomizer. (a) Vanadate ion; (b) vanadyl ion; (c) BPHA complex; (d) as (c) with charring step; (e) DDTC complex; (f) 8-quinolinol complex; (g) thiocyanate complex; (h) curve of temperature increase (in °C). Gas flow-rates, 480 ml Ar min^{-1}, 20 ml H_2 min^{-1}. Charring step omitted for (c), (e), (f) and (g).

Fig. 2. Memoriscope traces of vanadium absorbance at different gas flow-rates. (a) 480 ml Ar min^{-1} and 20 ml H_2 min^{-1} (b) 400 ml Ar min^{-1} and 100 ml H_2 min^{-1}; (c) 300 ml Ar min^{-1} and 200 ml H_2 min^{-1}; (d) 200 ml Ar min^{-1} and 300 ml H_2 min^{-1}; (e) 100 ml Ar min^{-1} and 400 ml H_2 min^{-1}; (f) 500 ml H_2 min^{-1}; (g) curve of temperature increase. Vanadate (10 ng V) was used in all cases.

complex showed complex vanadium atomization characteristics. The appearance temperature (the temperature at which vanadium atom formation is first observed) and the peak temperature (the temperature at which maximum absorption is observed) were about 1780°C and 2070°C, respectively, for atomization of vanadium from all the compounds and complexes except the thiocyanate complex. Both temperatures are lower than those reported for a carbon atomizer (1877°C and 2417°C for the appearance and peak temperatures, respectively, when a carbon rod is used [7]).

The nominal appearance temperatures may be controlled by the rate of temperature increase of the atomizer; the tungsten atomizer allows a very fast temperature increase. Sturgeon et al. [8] demonstrated a carbon reduction mechanism for atom formation of vanadium. For a tungsten atomizer, it seems reasonable to postulate that the major pathway leading to gaseous vanadium atoms is thermal dissociation of the oxide.

Hydrogen was mixed with argon purge gas to protect the micro-tube atomizer from oxidation. Figure 2 shows the effect of hydrogen flow-rate on vanadium absorption. The amount of hydrogen added seems to have no effect on the atomization of vanadium except when all the argon has been excluded, when almost no atomization occurred. Thus reduction of vanadium(V) oxide by hydrogen, is unlikely to be a major mechanism of vanadium atom formation. Sturgeon et al. [7] reported that the presence of hydrogen did not affect the atomization of vanadium in a carbon rod atomizer.

Analytical considerations

Peak height measurements were used to obtain the calibration graph. The characteristic concentration (amount of vanadium giving 1% absorption) was 2×10^{-10} and 4×10^{-11} g for atomization from pure ammonium vanadate and the BPHA complex, respectively. A sensitivity of 2×10^{-10} g has been reported for atomization of vanadium in a graphite furnace [9]. The coefficient of variation for six determinations of 10 ng of vanadium was 2%.

The effects of arsenic(III), bismuth, calcium, chromium(III), chromium(VI), cobalt, copper, iron(III), lead, magnesium, sodium, tin(IV) and zinc on the absorption of vanadium were examined. They were added as their chlorides or nitrates, except for sodium arsenite and potassium dichromate. All the samples were checked for background effects. The Memoriscope traces for vanadium (10 ng) in the presence of 1000-ng amounts of these elements are shown in Fig. 3. All elements depressed the vanadium absorption. Only bismuth lowered the atomization temperature of vanadium; all the other elements increased the peak temperature.

Acids had some effect on vanadium absorption, as shown in Fig. 4, although the peak temperature was not altered. Perchloric acid depressed the vanadium absorption markedly.

Because of these interference effects, vanadium must be isolated from interferents for its accurate determination. Vanadium(V) can be extracted effectively into chloroform as its BPHA complex. This enables vanadium to be determined in complex samples.

The results obtained when the method is applied to rocks (Table 1) demonstrate the accuracy of the method. The measurement is only possible because

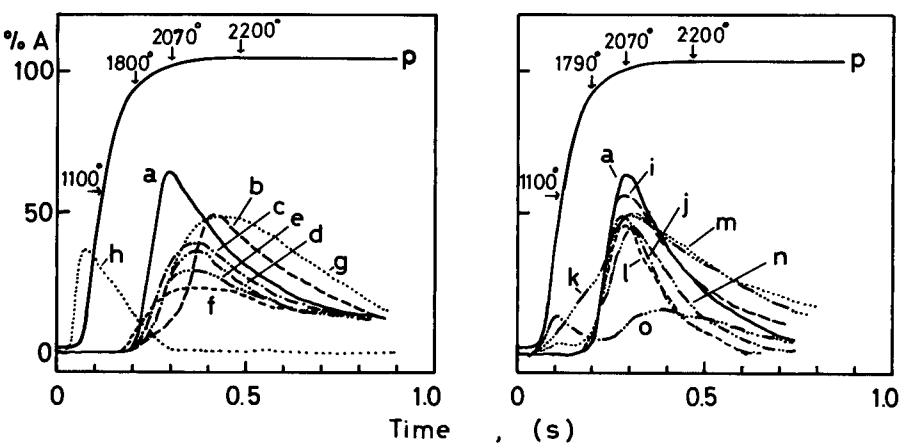


Fig. 3. Memoriscope traces of effects of 1000 ng of various elements on the absorbance of 10 ng of vanadium as vanadate. (a) V alone; the other curves relate to vanadium with (b) Ca; (c) Zn; (d) Cu; (e) As(III); (f) Cr(VI); (g) Sn(IV); (h) Bi; (i) Co; (j) Cr(III); (k) Na; (l) Fe(III); (m) Mg; (n) Ni; (o) Pb; (p) curve of temperature increase. Gas flow-rates as in Fig. 1.

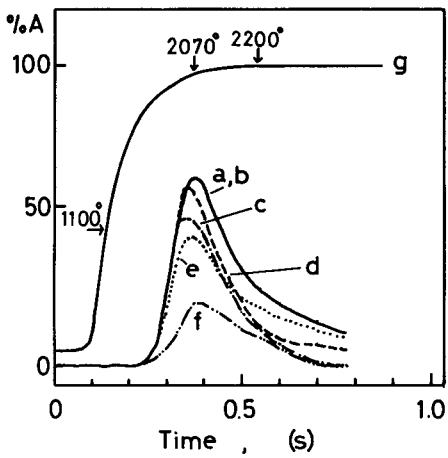


Fig. 4. Memoriscope traces of effects of acids on absorption from 10 ng of vanadium (as vanadate). (a) No acid added; (b) 0.05 M HCl; (c) 0.5 M H_3PO_4; (d) 0.05 M H_2SO_4; (e) 0.05 M HNO_3; (f) 0.05 M $HClO_4$; (g) curve of temperature increase. Gas flow-rates as in Fig. 1.

TABLE 1

Determination of vanadium in rock samples

Rock	Vanadium (ppm)	
	Found	Reported [10]
JG-1	21 (c.v. 9.5%)[a]	24[b]
JB-1	225 (c.v. 12%)[a]	211[b]

[a]Four determinations. [b]Arithmetic mean of the values within 2σ.

of the use of a fast-response detection system. With a conventional detection system the thermal separation of vanadium absorption from absorptions by organic species is not sufficient. Only small samples are needed for rocks in which vanadium is distributed homogeneously.

The donation of rock samples by Dr. A. Ando, Geological Survey of Japan, is gratefully acknowledged.

REFERENCES

1 H. M. Donega and T. E. Burgess, Anal. Chem., 42 (1970) 1521.
2 K. Ohta and M. Suzuki, Anal. Chim. Acta, 83 (1976) 381.
3 H. Nagatatsu and H. Ishii, Bunseki Kagaku, 17 (1968) 836.
4 H. Bode, Fresenius Z. Anal. Chem., 144 (1955) 165.

5 N. A. Talvitie, Anal. Chem., 25 (1953) 604.
6 H. Goto and S. Ikeda, Nippon Kagaku Zasshi, 79 (1958) 152.
7 R. E. Sturgeon, C. L. Chakrabarti, I. S. Maines and P. C. Bertels, Anal. Chem., 47 (1975) 1240.
8 R. E. Sturgeon, C. L. Chakrabarti and C. H. Langford, Anal. Chem., 48 (1976) 1792.
9 C. W. Fuller, Electrothermal Atomization for Atomic Absorption Spectrometry, The Chemical Society, London, 1977, p. 82.
10 A. Ando, H. Kurasawa, T. Ohmori and E. Takeda, Geochem. J., 8 (1974) 175.

Analytica Chimica Acta, 108 (1979) 75—85
© Elsevier Scientific Publishing Company, Amsterdam — Printed in The Netherlands

DIRECT DETERMINATION OF TRACE METALS IN SOLID SAMPLES BY ATOMIC ABSORPTION SPECTROMETRY WITH ELECTROTHERMAL ATOMIZERS

Part 3. Application of an Autosampler to the Determination of Silver, Bismuth, Cadmium and Zinc in Steels

ERIK LUNDBERG* and WOLFGANG FRECH

Department of Analytical Chemistry, University of Umeå, S-901 87 Umeå (Sweden)

(Received 9th February 1979)

SUMMARY

A modification of the Varian-Techtron autosampler ASD-53 to accept solid samples and to operate under non-isothermal as well as isothermal conditions is described. The performance of the autosampler is illustrated for the determination of silver, bismuth, cadmium and zinc in high- and low-alloy steels with the CRA 90 graphite cup and isothermal atomization. Good agreement with certified or reported values was obtained, with relative standard deviations of 3.8—30%. Peak height and peak area evaluations were compared; the use of peak area values gives considerably better precision for silver, bismuth and cadmium. The non-specific absorption caused by the matrix was measured in the region 200—350 nm. For the resonance lines used, the background level was found to be 0.00—0.03 units (absorbance × seconds) depending on element and the age of the cup.

In Part 1 of this series [1], it was shown that lead and antimony, taken as examples, are fairly evenly distributed in a number of metallurgical materials. It was concluded that samples weighing as little as 2 mg are sufficiently large to allow determination of these elements with a precision of 5—10%. In part 2 [2], the "solid sampling technique" was successfully applied to the determination of lead in metallurgical samples with the Varian-Techtron CRA 90 graphite cup. Both precision and accuracy were improved by recording the peak area instead of the peak height and by atomizing the samples under isothermal conditions, a prerequisite for obtaining accurate peak area values [3]. Headridge et al. [4—7] determined the concentrations of several trace metals in a variety of metallurgical materials by dropping the solid samples into a home-made induction furnace held at constant temperature. However, their results are based on peak height measurements. As discussed earlier [2], the main advantage of isothermal atomization and peak area evaluation is that accurate determinations are possible even if the metal is fractionally atomized from the sample.

This paper describes a simple modification of an autosampler which permits it to accept solid samples and to operate under isothermal conditions in

a commercially available system (Varian-Techtron). The use of an autosampler significantly extends the applicability of the solid sampling technique. Fully automatic operation is possible and, in addition, isothermal atomization can conveniently be utilized at temperatures above 2000°C. The performance of the autosampler is illustrated for the determination of silver, bismuth, cadmium and zinc in steels of different compositions. These metals were chosen since they are more or less completely extracted from the sample during reasonable atomization temperatures and times. The possibility of applying this technique to less volatile elements is currently under investigation.

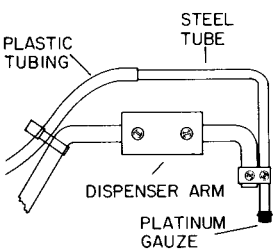
EXPERIMENTAL

Instrumentation

The instrumentation used has been described earlier [2]. In addition, an automatic sample dispenser, ASD-53 (Varian-Techtron) was installed to provide automatic insertion of the solid samples. A printer (Datel Systems Inc., Model DPP-7) was connected to the peak reader module [8].

Autosampler modification. The autosampler was modified to insert solid samples into a graphite cup. The capillary tubing used to dispense solutions was replaced by a stainless steel tube (o.d. 3.0 mm, i.d. 2.2 mm) mounted on the dispenser arm as shown in Fig. 1. A platinum gauze (40 mesh) was attached to the "sampling" end of the tube to retain the sample, while the other end was connected to a vacuum pump with plastic tubing via a magnetic valve. The simplicity of the modification allows the steel tube used for solids and the capillary tubing used for solutions to be interchanged within 1 min.

As isothermal atomization was used, the dispenser arm had to be positioned above the graphite cup when the atomization step started. This could not be accomplished with the ASD-53 control module operated in the normal way. A block diagram of a "solid sampling interface" providing both a NORMAL and an ISOTHERMAL atomization mode, is shown in Fig. 2. The NORMAL mode is used for solid samples that have to be inserted at ambient temperature, e.g. biological materials requiring an ashing step, while the ISOTHERMAL



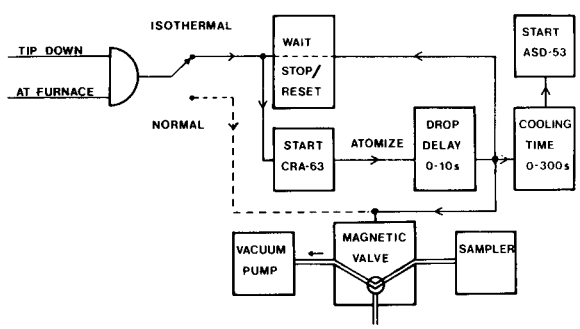


Fig. 1. Dispenser arm modified to accept solid samples.

Fig. 2. Block diagram of the "solid sampling interface".

mode is used for samples that do not require an ashing step, e.g. metallurgical materials. The operating principle for the latter mode is described below.

The vacuum pump was turned on and the sampling program initiated by pressing the autosampler start button (the magnetic valve was then in the position shown in Fig. 2). The dispenser arm travelled to the sample vial where the sample was lifted by means of suction. When the arm reached the position above the graphite cup, the ASD-53 TIP DOWN and AT FURNACE control signals "locked" the WAIT and STOP/RESET functions via the interface. At the same time the CRA 63 program was initiated. When the atomization step was reached, the DROP DELAY function of the interface, i.e. a preselected delay time (0—10 s), was triggered. At the end of this time, the magnetic valve changed position and the sample dropped into the cup (now at final temperature). At the same time the WAIT and STOP/RESET functions were "released", thereby causing the dispenser arm to leave the heated environment.

When the preselected COOLING TIME (0—300 s) was over, the sampling program proceeded automatically until all samples were analyzed. A detailed description of the interface, including circuit diagram and components used, can be obtained from the authors upon request.

Procedure for steel analysis

Single pieces of the materials (1—5 mg) were weighed on an electrobalance (Mettler, Model ME 30) and transferred with tweezers to small plastic vessels for storage before analysis. The sample carousel of the ASD-53 was loaded with polyethylene sample vials with conical bottoms (Perkin-Elmer, part no. 087-056) to facilitate the sampling. After transfer of the samples to the vials, the autosampler program was initiated by using the ISOTHERMAL mode. Peak heights as well as peak areas were automatically registered on the printer. The instrumental parameters are given in Table 1.

Samples and standards were run alternately and concentrations were calculated relative to one of the standards, based on the peak area values. To establish the "background" level with the element-specific lamp, at least every fifth run was a blank firing.

Non-specific absorption

The non-specific absorptions caused by a mild steel and a nickel-base alloy were measured with a hydrogen hollow cathode lamp (Varian-Techtron) in the region 200—350 nm. The instrumental parameters used are given in Table 1.

Dissolution procedure and instrumental parameters used for standardization of silver in steel

Samples (1g) of the materials SRM 361, SRM 364 and JK 2C were dissolved with gentle heating in 30 ml of 20% (v/v) nitric acid (Merck Suprapur) and diluted to 50 ml. Aliquots (2—10 μl) were pipetted into a Perkin-

TABLE 1

Instrumental parameters

	Ag	Bi	Cd	Zn	Background
Atomization,[a] time (s)	8	7	6	7	7
Atomization, temp (°C)	2400	2400	1700	2400	1400—2400
Wavelength (nm)	338.3	223.1	228.8	307.6	200—350
Spectral bandwidth (nm)	0.5	0.2	0.5	0.5	0.5
Lamp current (mA)	5	11	3	7	9[b]
Noise on signal (absorbance)	±0.004	±0.003	±0.006	±0.002	—
Drop delay[c] (s)	2.0	2.0	1.5	2.0	2.0
Integration delay[d] (s)	2.0	2.0	1.5	2.0	2.0
Integration time (s)	5.5	2.0—3.5	3.5	4.5	4.5
Argon flow (l min^{-1})	5	5	5	5	5

[a]The ashing step was on for 20 s at 600°C for correct performance of the peak reader module [8]. The mean heating rate during atomization was 900°C s^{-1}. [b]Hydrogen lamp (scale divisions). [c]Time from the start of the atomization step to when the sample was dropped. [d]Time from the start of the atomization step to when the integration started.

Elmer HGA 76 graphite furnace and the silver contents were determined at the 328.1-nm line by means of the standard addition technique. The instrumentation used was as described in Part 1 [1]. The following parameters were utilized: ashing temperature 500°C for 40 s; atomization temperature 2150°C for 5 s, gas stop; outburning at 2400°C for 3 s; lamp current 5 mA; spectral bandpass 2.0 nm; background corrector on.

Reagents and materials

The following metallurgical materials were used: British Chemical Standards BCS 330 (mild steel) and BCS 334-336 (austenitic stainless steels); National Bureau of Standards SRM 361, SRM 362 and SRM 364 (low-alloy steels); standards JK 1C, JK 2C (mild steels) and JK 8C, JK 8F (austenitic stainless steels), supplied by Institutet för Metallforskning, Sweden; SANICRO 72 (nickel-base alloy), supplied by Sandviken steel factory, Sweden.

The larger graphite cup (i.d. 4.5 mm) was used throughout.

RESULTS AND DISCUSSION

Atomization mode and signal evaluation

In part 2 of this series [2], it was shown that isothermal atomization gave better precision and accuracy than non-isothermal atomization for the determination of lead in steels. Theoretically, these advantages of isothermal atomization are valid for all elements. Therefore, only this atomization mode was used for the determination of silver, bismuth, cadmium and zinc.

A comparison of peak height and peak area evaluation for the direct determination of lead in metallurgical materials at constant temperature [2] showed

TABLE 2

Evaluation by peak height (in milliabsorbance units) and peak area (in milliabsorbance units × seconds) for the determination of bismuth, cadmium, zinc and silver in stainless steel BCS 336

	Bi		Cd		Zn		Ag	
	Peak height[a]	Peak area[a]	Peak height[a]	Peak area[a]	Peak height[a]	Peak area[a]	Peak height[a]	Peak area[a]
	304[b]	174[b]	314[b]	97.5[b]	93.3[b]	26.2[b]	354[b]	138[b]
	257	163	240	92.7	87.6	26.2	318	163
	308	159	306	111	86.7	20.1	220	150
	278[c]	165[c]	165	106	98.0	19.6	246	168
			275[c]	108[c]	80.1	22.0	191	172
					81.0	18.1	167[c]	161[c]
					91.3[c]	22.0[c]		
Mean value	287	165	260	103	88.3	22.0	249	159
S.d.	24	6	60	8	6	3	72	13
R.s.d. (%)	8.3	3.8	23	7.4	7.3	14	29	7.9

[a]Normalized to 1 mg; [b]Determinations number 1—5 in a given cup; [c]Determinations number 25—35 in a given cup.

that better precision was obtained by using the peak area values. A similar comparison was applied to the determination of silver, bismuth, cadmium and zinc in stainless steel BCS 336; the results are presented in Table 2. As can be seen, peak area evaluation is superior for silver, bismuth and cadmium. This is also true for the other steels analyzed for these elements. For the determination of zinc, however, peak area evaluation gave poorer precision. For other steels analyzed for zinc (Table 5), no significant difference in precision between peak height and peak area was found. The results presented in the following paragraphs are based on integrated values.

Non-specific absorption

In earlier experiments [2], lead was determined in metallurgical materials at an atomization temperature of 1800°C, by using the 283.3 and 205.4-nm lines. It was shown that for these parameters, the background absorption was insignificant. However, the determination of silver, bismuth and zinc required a higher atomization temperature, 2400°C, in order to extract these elements in reasonable times. At this temperature the steel matrix has a considerably higher vapour pressure than at 1800°C, which means that the probability of obtaining non-specific absorption is greatly increased. Therefore, in order to investigate the usefulness of available absorption lines with respect to non-specific absorption, the absorption caused by the main constituents of steel (Fe, Ni, Cr) in the region 200-350 nm were measured. Figure 3 shows the integrated signals obtained with a hydrogen lamp for the ultrapure steel JK

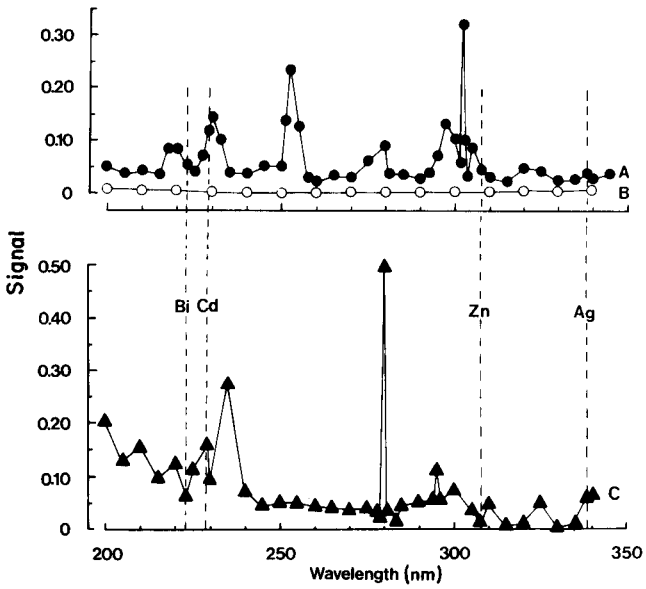


Fig. 3. Integrated signals (absorbance × *s*) obtained with a hydrogen lamp for the ultra-pure steel JK 1C (•), the nickel-base alloy SANICRO 72 (▲) and blank firings (○) at 2400°C

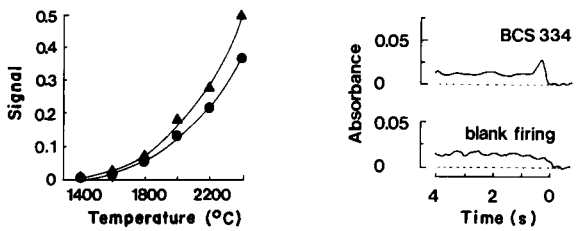


Fig. 4. Background signal (absorbance × *s*) as a function of temperature for JK 1C (•) at 302.5 nm, and SANICRO 72 (▲) at 280.0 nm.

Fig. 5. Recorder traces for bismuth in 2.5 mg of stainless steel BCS 334 and a blank firing.

1C, the nickel-base alloy SANICRO 72, and blank firings at 2400°C. As can be seen, the magnitude of the background varies strongly with wavelength for both materials, indicating the presence of molecular absorption. Of the resonance lines utilized for silver, bismuth, cadmium and zinc, only the 228.8-nm cadmium line coincided with a background absorption peak. However, cadmium was determined at 1700°C. At this temperature the background absorption at 228.8 nm was only 0.004 integrated units (absorbance × seconds). At the resonance lines used for the other elements, the background levels were low at 2400°C.

The effect of the atomization temperature on the background signal was investigated. Figure 4 shows the results obtained for JK 1C and SANICRO

72 at their most intense "bands" when the temperature was varied between 1400 and 2400°C. These results indicate that high background levels are to be expected for the determination of elements that require atomization temperatures higher than 2400°C.

As will be shown below, the blank firing signals obtained with the element-specific lamps were 2—3 times lower than the background signals seen in Fig. 3. Measurements of the specific absorption with the background corrector in operation resulted, as expected, in overcompensated values. A possible explanation for this observation is as follows. Background correction with a continuous source of radiation is correct only if the background absorption is itself continuous over the spectral bandpass used. The discrepancy between the background signals obtained with the element-specific lamps and the hydrogen lamp suggests that the background absorption is not continuous. This may arise from the presence of rotational lines of molecular spectra within the spectral bandpass. In the presence of such lines, background correction with a continuous source of radiation will give incorrect results [9, 10].

The blank firing signals obtained with the element-specific lamps were low (0.00—0.03 integrated units depending on the element and the age of the cup) and accurate determinations were possible without using the background corrector.

Determination of bismuth

Even the presence of small amounts (1—2 $\mu g\ g^{-1}$) of bismuth has adverse effects on the mechanical properties of stainless steels [11]. In order to obtain good accuracy at these low levels, it is therefore desirable to reach a detection limit of 0.1 $\mu g\ g^{-1}$ or better. Figure 5 shows the recorder trace for 2.5 mg of BCS 334, corresponding to ca. 0.2 ng of bismuth, and the recorder trace of a blank firing. As can be seen, the blank firing signal increases slightly during the atomization step, hence contributing to the integrated value for bismuth. It is therefore advantageous to minimize the integration time with respect to the duration of the peak. Considering the uncertainty of the blank values, a detection limit of 0.02—0.05 $\mu g\ g^{-1}$ can be obtained. The detection limit was defined as the concentration corresponding to twice the standard deviation of four blank firing values obtained between the determination of samples. It should be mentioned that the magnitudes of the blank values increased gradually during the lifetime of a cup, from zero for an unused cup to 0.02—0.03 integrated units after 35 determinations. In order to compensate for this blank contribution, the mean of two adjacent blank values was subtracted from the signals obtained for the samples.

Metallurgical materials with certified values for bismuth at concentrations lower than 5 $\mu g\ g^{-1}$ are not available. To overcome this lack of standards, Andrews and Headridge [5] utilized reported concentrations of bismuth for a mild steel, BCS 330, and took it to be 3.0 $\mu g\ g^{-1}$. Using BCS 330 as reference material, these authors analyzed 40 different steels with bismuth concentrations in the range 0.004—3.4 $\mu g\ g^{-1}$.

TABLE 3

Results for the determination of bismuth in steels (relative to BCS 330)

Designation	BCS 336	JK 8F	JK 8C	BCS 334	BCS 335	BCS 330
Reference value ($\mu g\ g^{-1}$)	3.3[a,b]	0.5[c]	0.2[d]	0.05[a]	0.06[a]	3.0
Mean value ($\mu g\ g^{-1}$)	3.4	0.6	0.2	0.1	0.1	—
R.s.d. (%)	3.8	6.6	15	26	30	3.9
No. of determinations	4	8	6	6	6	4

[a]See ref. [5]; [b]See ref. [12]; [c]See ref. [13]; [d]See ref. [14].

Table 3 shows the results obtained for the determination of bismuth in a number of stainless steels relative to BCS 330, adopting the value 3.0 $\mu g\ g^{-1}$. As can be seen, the mean values are in good agreement with results reported elsewhere [5, 12—14]. High precision was obtained for BCS 330, BCS 336 and JK 8F, whereas the uncertainty increased for steels with lower concentrations of bismuth, mainly because of the relatively high blank contributions at these low levels.

Determination of cadmium

Cadmium was determined at an atomization temperature of 1700°C. This temperature was chosen because below 1700°C cadmium became gradually more difficult to extract; this could be seen after approximately ten determinations, when the signal did not return to the baseline. At too high temperatures, however, the non-specific absorption increased markedly, as discussed above. In addition, the integrated specific absorbance values decreased because of higher diffusion rates, so that the detection limit deteriorated.

In Fig. 6, a recorder trace near the detection limit is shown for 2.8 mg of

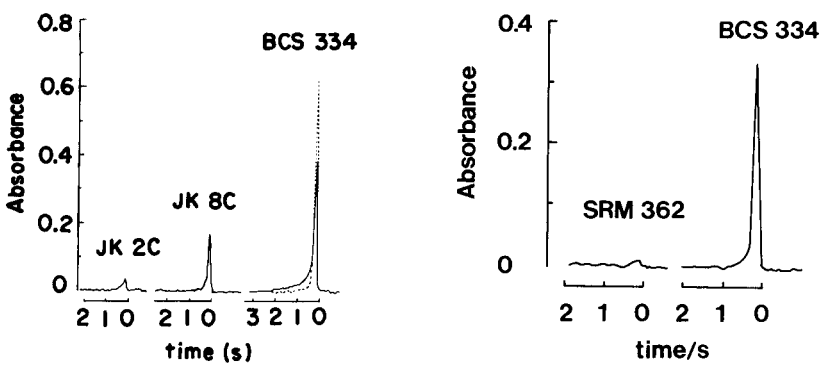


Fig. 6. Recorder traces for cadmium in 2.3 mg (dotted; new cup) and 1.4 mg (old cup) of stainless steel BCS 334, 1.2 mg of stainless steel JK 8C and 2.8 mg of mild steel JK 2C.

Fig. 7. Recorder traces for zinc in 2.2 mg of stainless steel BCS 334 and 1.2 mg of mild steel SRM 362.

TABLE 4

Results for the determination of cadmium in steels (relative to JK 8C)

Designation	JK 2C	BCS 334	BCS 335	BCS 336	JK 8C
Recommended value ($\mu g\ g^{-1}$)	0.03	—	—	—	0.2
Mean value ($\mu g\ g^{-1}$)	0.04	0.7	0.6	0.7	—
R.s.d. (%)	23	6.3	13	7.4	21
No. of determinations	6	5	5	5	7

JK 2C containing 0.1 ng of cadmium. The integrated absorbance was 0.018, which may be compared with 0.004 ± 0.002 integrated units obtained for a blank firing. A practical detection limit for cadmium can be estimated to be 0.01 $\mu g\ g^{-1}$.

The change in signal shape during the course of the determinations is illustrated for BCS 334 in Fig. 6. Although the signal always returns to the baseline, the decay time increases with the age of the cup. This stresses the importance of integrating the signal instead of measuring the peak height. A signal for cadmium in JK 8C is also shown in Fig. 6.

Table 4 shows the results obtained for the determination of cadmium in one mild and three austenitic steels. The mean values presented are given relative to JK 8C, determined to contain 0.2 $\mu g\ g^{-1}$ of cadmium [14]. Considering the low cadmium concentrations in all materials, the precision can be regarded as acceptable. However, no certified standard in this concentration range was available, which means that the accuracy of the determinations cannot be established.

Determination of zinc

Figure 7 shows a recorder trace for 2.2 mg of stainless steel BCS 334 (117 $\mu g\ g^{-1}$ of zinc) at the 307.6-nm line. As can be seen the signal returns rapidly to the baseline (this occurs even after 35 determinations). The detection limit can be estimated to be 10 $\mu g\ g^{-1}$ of zinc and is illustrated by the recorder trace for 1.2 mg of the mild steel SRM 362 (10 $\mu g\ g^{-1}$ of zinc) shown in Fig. 7.

For the determination of lower concentrations of zinc, the most sensitive line, 213.9 nm, has to be used. Atomization of the ultrapure steel JK 1C (2 $\mu g\ g^{-1}$ of zinc) at this line resulted in integrated values of approximately 0.8 units per mg. This sensitivity is too high for concentrations in the range 2—10 $\mu g\ g^{-1}$. However, as discussed earlier [2], the sensitivity can be decreased 10-fold by measuring the atom population above the cup. In this way, it should thus be possible to determine zinc in steels containing less than 10 $\mu g\ g^{-1}$.

Table 5 shows the results obtained for the determination of zinc at the 307.6-nm line in four steels (relative to BCS 334). No systematic deviation of the results from the certified values can be seen. This indicates that the zinc signal is not affected by the difference in composition of the materials.

TABLE 5

Results for the determination of zinc in steels (relative to BCS 334)

Designation	JK 2C	JK 8C	BCS 334	BCS 335	BCS 336
Certified value ($\mu g\ g^{-1}$)	29	18	117	112	64
Mean value ($\mu g\ g^{-1}$)	25	22	—	120	60
R.s.d. (%)	8.5	21	10	9.2	14
No. of determinations	7	7	6	6	7

TABLE 6

Results for the determination of silver in steels (relative to JK 2C)

Designation	JK 2C	JK 8C	BCS 334	BCS 335	BCS 336	SRM 364
Reference value ($\mu g\ g^{-1}$)	0.50[a], 0.36[b]	—	—	0.47[c]	0.70[c]	0.13[a,b]
Mean value ($\mu g\ g^{-1}$)	—	0.85	0.32	0.42	0.63	0.18[d]
R.s.d. (%)	6.6	8.0	5.3	7.5	7.9	7.0
No. of determinations	6	5	6	6	6	4

[a]Determined after dissolution, see text; [b]See ref. [6]; [c]See ref. [13]; [d]0.05 integrated units per mg.

Determination of silver

The change in signal shape obtained when silver was volatilized from a series of samples was similar to that for cadmium. The signals always returned to the baseline, although the decay time increased with the age of the cup.

The practical working range for the less sensitive 338.3-nm line was found to be 0.05—2 $\mu g\ Ag\ g^{-1}$. In this range, no metallurgical standards certified for silver were available. Therefore, the silver content of two reference materials, JK 2C and SRM 364 was determined, after dissolution as described above. JK 2C was found to contain $0.50 \pm 0.02\ \mu g\ Ag\ g^{-1}$ and SRM 364 $0.13 \pm 0.01\ \mu g\ Ag\ g^{-1}$. The dissolution procedure used was checked by analyzing a certified reference material, SRM 361. The concentration found — $3.8\ \mu g\ Ag\ g^{-1}$ — agrees well with the certified value ($4\ \mu g\ g^{-1}$) and with results reported by others [15, 16].

Table 6 shows the results obtained for the direct determination of silver in one mild and four austenitic steels relative to JK 2C, based on the value $0.50\ \mu g\ g^{-1}$. The relative standard deviation values are of the same order of magnitude as those reported recently by Aziz-Alrahman and Headridge [6].

Conclusions

Determinations of the volatile elements silver, bismuth, cadmium and zinc in steels under isothermal conditions give fairly accurate results, provided that standards are available and the peak area is evaluated. In order to extract these elements in reasonable times, atomization temperatures of up to 2400°C have to be used. At such and even higher temperatures, manual

sample introduction becomes very difficult and for that reason some kind of autosampler is necessary.

For the elements investigated, the use of isothermal atomization results in unchanged sensitivity during the lifetime of a graphite cup. This means that standardization with only a few calibration points is possible.

The authors thank Mr. Lars Lundmark and Mr. Svante Jonsson for help with the autosampler modification and Dr. Michael Sharp for linguistic revision of the manuscript.

REFERENCES

1 E. Lundberg and W. Frech, Anal. Chim. Acta, 104 (1979) 67. (Part 1.)
2 E. Lundberg and W. Frech, Anal. Chim. Acta, 104 (1979) 75. (Part 2.)
3 B. V. L'Vov, Atomic Absorption Spectrochemical Analysis, Adam Hilger, London, 1970.
4 J. B. Headridge and D. R. Smith, Talanta, 19 (1972) 833.
5 D. G. Andrews and J. B. Headridge, Analyst, 102 (1977) 436.
6 M. Aziz-Alrahman and J. B. Headridge, Talanta, 25 (1978) 413.
7 D. G. Andrews, M. Aziz-Alrahman and J. B. Headridge, Analyst, 103 (1978) 909.
8 E. Lundberg, Appl. Spectrosc., 32 (1978) 276.
9 H. Massman, Z. El Gohary and S. Gücer, Spectrochim. Acta, Part B, 31 (1976) 399.
10 C. Hendrikx-Jongerius and L. de Galan, Anal. Chim. Acta, 87 (1976) 259.
11 S.-E. Lunner, Avesta Jernverk, private communication.
12 W. Frech, Fresenius Z. Anal. Chem., 275 (1975) 353.
13 S. E. Bäckman, Lecture held at 6th Nordiska Konferensen i Spårelementanalys, Södertälje, Sweden, 1977.
14 Analysis Certificate for JK 8C, Institutet för Metallforskning, Sweden.
15 K. E. Burke, Talanta, 21 (1974) 417.
16 P. J. Paulsen, R. Alvarez and C. W. Mueller, Appl. Spectrosc., 30 (1976) 42.

Analytica Chimica Acta, 108 (1979) 87—92
© Elsevier Scientific Publishing Company, Amsterdam — Printed in The Netherlands

DETERMINATION OF MAJOR AND MINOR ELEMENTS IN SILICATES BY INDUCTIVELY COUPLED PLASMA EMISSION SPECTROMETRY

HIROSHI UCHIDA*

Industrial Research Institute of Kanagawa Prefecture, 3173, Showa-machi, Kanazawa-ku Yokohama 236 (Japan)

TETSUO UCHIDA and CHUZO IIDA

Laboratory of Analytical Chemistry, Department of Engineering Sciences, Nagoya Institute of Technology, Gokiso-cho, Showa-ku, Nagoya 466 (Japan)

(Received 12th February 1979)

SUMMARY

A simple rapid method for the determination of major and minor elements in silicates is reported. Powdered sample (50 mg) is treated with hydrochloric and hydrofluoric acids in a small sealed Teflon vessel. After addition of boric acid, silicon, aluminium, iron, titanium, manganese, calcium, magnesium, sodium, and potassium are determined by inductively coupled plasma emission spectrometry. The method is satisfactory for a variety of standard silicate materials.

The inductively coupled plasma (i.c.p.) is the best excitation source in emission spectrochemical analysis for major, minor and trace elements in various materials because of the high sensitivity, wide dynamic range and comparatively few interferences obtained, with respect to its use for the analysis of geological materials; determinations of copper, lead, nickel and cobalt in soil after dissolving with nitric and perchloric acids, have been reported [1]. Uranium in rocks has been determined after decomposition with a mixture of nitric and sulphuric acids [2], and metaborate fusion has been applied to the determination of major and minor elements in silicate rocks [3].

In i.c.p. procedures chemical and ionization interferences have seldom been observed, but solution viscosity affects the introduction rate of the sample solution to the plasma [4, 5]. Therefore, a low concentration of total salts in the solution was preferred for reproducible nebulization. A simple decomposition of silicates with a mixture of hydrofluoric acid and aqua regia in a sealed Teflon vessel has been reported for the determination of major [6, 7] and minor [8, 9] elements by atomic absorption spectrometry. Trace elements have also been determined after decomposition with the same acid mixture and chelating resin separation [10]. A similar method of decomposition of silicates would be well suited for the determination of major elements by an i.c.p. method, and the total salt concentration obtained would be less than with alkali and metaborate fusions.

In this paper, decomposition of silicate rocks with hydrochloric and hydrofluoric acids in a small home-made sealed Teflon vessel and determination of major elements by i.c.p. emission spectrometry are described. The method is simple and rapid, and has been applied successfully to the determination of major and minor elements in standard silicate samples.

EXPERIMENTAL

Instrumentation and operating parameters

The spectrometric instrumentation and operating parameters for the successive measurement of individual elements are summarized in Table 1. The wavelengths at which emissions were measured are given in Table 2. Although these conditions are not optimal for some elements, the conditions were kept constant throughout this work, in order to establish if the method could be used for simultaneous multi-element analysis with the polychromator used. The uptake rate of sample solution and the introduction rate to the plasma were 1.4 and 0.11 ml min^{-1}, respectively.

Reagents and standard solutions

Standard stock solutions of silica (10 mg SiO_2 g^{-1}) were prepared by dissolving quartz powder (prepared by crushing the tube; Toshiba Ceramics) in hydrofluoric acid. The silica content was determined gravimetrically from the ignition loss of a portion of the quartz powder on treatment with a mixture of hydrofluoric and sulphuric acids. Standard metal stock solutions (2 mg g^{-1}) were prepared by dissolution as follows: titanium metal (Japan Lamp Industrial) in hydrofluoric acid; aluminium metal and iron, manganese, and magnesium oxides (Johnson Matthey Specpure) and calcium carbonate (Merck G.R.) in hydrochloric acid; and sodium and potassium chlorides (Matsunaga Chemical Co., recrystallized) in water.

Working standard solutions for constructing calibration curves of every element were simply prepared by suitable dilution followed by appropriate mixing of the stock solutions described above. The concentrations in each working solution are shown in Table 3. All diluting procedures were carried out gravimetrically on a top-pan balance. The hydrochloric and nitric acids used were of super-special grade (Wako Pure Chemical Co.), boric acid was Merck G. R., and hydrofluoric acid was reagent grade (Toshiba).

Dissolution procedure

Into the Teflon vessel [10], 50 mg of powdered sample was weighed, and 1 ml of hydrochloric and 0.5 ml of hydrofluoric acids were added. After sealing the vessel and leaving it to stand for more than 4 h at room temperature, the contents were transferred to a polypropylene bottle with 6 ml of 4% (w/v) boric acid solution. The solution was finally diluted with water to 100 g and weighed.

TABLE 1

Instrumentation and operating parameters

I.c.p. source	Nippon Jarrel—Ash, Model ICAP-1	Monochromator	Japan Electron Optics Lab. Model JSG-125B
Frequency	27.12 MHz	Mounting	Asymmetric Czerny—Turner (1.25 m)
Output power	1.6 kW	Grating	1200 lines mm^{-1}
Coolant gas	Argon, 14.0 l min^{-1} (3.0 kg cm^{-2})	Linear dispersion	0.62 nm mm^{-1}
Plasma gas	Argon, 1.0 l min^{-1} (3.0 kg cm^{-2})	Entrance slit	10 μm width, 2 mm height
Carrier gas	Argon, 0.7 l min^{-1} (3.0 kg cm^{-2})	Exit slit	30 μm width, 10 mm height
Nebulizer	Cross-flow type	Photomultiplier	Hamamatsu TV, R 955
Viewing point	17.5 mm above work coil	Amplification	D.c. amp., V/f converter
		Integration time	8 s

TABLE 2

Analytical lines used

Species	Wavelength (nm)	Species	Wavelength (nm)	Species	Wavelength (nm)
Si(I)	288.1	Al(I)	396.1	Ti(II)	334.9
Fe(II)	259.9	Mg(II)	279.5	Ca(II)	393.4
Mn(II)	257.6	K(I)	766.5	Na(I)	588.9

TABLE 3

Composition of mixed standard solutions[a]

	Concentration (μg g^{-1})								
Std. Soln	SiO_2	Al	Fe	Ti	Mn	Ca	Mg	Na	K
1	0	0	0	0	0	0	0	0	0
2	50	5	5	1	0.1	5	5	5	5
3	100	10	10	2	0.2	10	10	10	10
4	200	20	20	4	0.4	20	20	20	20
5	300	30	30	6	0.6	30	30	30	30
6	400	40	40	8	0.8	40	40	40	40
7	500	50	50	10	1.0	50	50	50	50

[a]Each solution contained 1 ml HCl + 0.5 ml HF + 0.24 g H_3BO_3/ 100 g of solution.

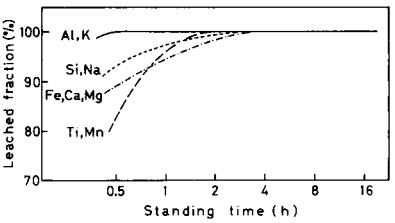


Fig. 1. Effect of time on sample dissolution by 1 ml of HCl and 0.5 ml of HF.

TABLE 4

Effect of acid composition on analytical results for JB-1 basalt[a]

Component	Certified value (%)	Values found (%)				
		HNO_3(ml) 1.00	0.75	0.50	0.25	0.00
		HCl (ml) 0.00	0.25	0.50	0.75	1.00
SiO_2	52.09	51.9	52.7	53.2	52.6	53.0
Al_2O_3	14.53	14.6	14.9	14.4	14.8	14.8
Fe_2O_3	9.04	8.53	8.69	8.96	8.87	8.96
TiO_2	1.34	1.23	1.28	1.30	1.31	1.37
MnO	0.16	0.18	0.17	0.16	0.16	0.16
CaO	9.21	9.13	9.11	9.18	9.19	9.13
MgO	7.70	7.48	7.58	7.72	7.66	7.57
Na_2O	2.79	2.64	2.71	2.81	2.73	2.68
K_2O[b]	1.42	1.3	1.6	1.6	1.3	1.4

[a]Sample 50 mg; HF 0.5 ml, decomposition time 16 h. [b]Precisions were limited by using HTV R 456 photomultiplier instead of R 955.

RESULTS AND DISCUSSION

The powdered silicates were completely dissolved with small volumes of hydrochloric, nitric, and hydrofluoric acids in the Teflon vessel at room temperature. That interferences were not caused by this mixture of acids was confirmed in preliminary experiments with synthetic sample solution. Table 4 shows the effect of acid composition on the analytical results obtained for basalt (JB-1). It can be seen that there is little difference in the results for major components regardless of the acid composition. The use of hydrochloric and hydrofluoric acids was preferred, to keep the procedure simple.

In previous work [6, 7], 50 mg of silicate was decomposed with 3 ml of hydrofluoric acid; after the dissolution, 2.8 g of boric acid was added to mask fluoride. However, 0.5 ml of hydrofluoric acid was sufficient for dissolution of the same amount of sample in the present procedure, and the amount of boric acid was reduced to 0.24 g, i.e., a 20% excess over the fluoride added. Consequently, the total salt concentration of the sample solution was lowered

TABLE 5

Accuracy and precision in the analysis of basalt JB-1

Component	Certified value %	Value found %	Recovery %	R.s.d.[a] %
SiO_2	52.09	52.3	100.4	0.88
Al_2O_3	14.53	14.8	101.9	0.67
Fe_2O_3	9.04	8.91	98.6	0.97
TiO_2	1.34	1.32	98.5	1.10
MnO	0.16	0.16	100	1.40
CaO	9.21	9.20	99.9	0.85
MgO	7.70	7.80	101.3	0.91
Na_2O	2.79	2.76	98.9	1.90
K_2O	1.42	1.40	98.6	1.85

[a]For 6 analyses.

TABLE 6

Analytical results (%) for standard silicate samples (duplicate analyses)

Component		JG-1 Granodiorite	AGV-1 Andesite	MRG-1 Gabbro	R 701 Feldspar	NBS No.91 Opal glass
SiO_2	found	72.6	60.1	38.5	68.1	67.0
	certified	72.24	59.00	39.24	67.98	67.53
Al_2O_3	found	14.6	17.1	8.22	17.6	5.80
	certified	14.21	17.25	8.56	17.31	6.01
Fe_2O_3	found	2.13	6.76	18.1	0.09	0.08
	certified	2.21	6.76	17.80	0.09	0.08
TiO_2	found	0.28	1.06	3.75	0.01	0.03
	certified	0.26	1.04	3.75	0.01	0.019
MnO	found	0.066	0.099	0.18	—	—
	certified	0.06	0.097	0.17	—	—
CaO	found	2.20	5.00	14.9	—	10.4
	certified	2.18	4.90	14.72	—	10.48
MgO	found	0.74	1.51	13.5	—	—
	certified	0.73	1.53	13.51	—	—
Na_2O	found	3.59	4.18	0.72	3.34	8.69
	certified	3.39	4.26	0.71	3.35	8.48
K_2O	found	4.05	2.96	0.19	10.8	3.37
	certified	3.96	2.89	0.18	10.41	3.25

enough for i.c.p. measurements. As fluoride was masked, silicon could be measured without difficulty even with a glass nebulization chamber and a quartz torch tube.

The effect of time on sample dissolution with 1 ml of hydrochloric and 0.5 ml of hydrofluoric acids is shown in Fig. 1. Aluminium and potassium were leached rapidly, but titanium and manganese were initially slow to dissolve.

After 4 h all elements were completely dissolved. For routine analysis a dissolution time of 16 h, i.e., overnight, is recommended for convenience and security.

Table 5 shows the accuracy and reproducibility of 6 analyses of the standard basalt, JB-1. The accuracy for each element was $\leqslant 2\%$ relative, and the relative standard deviations were also $\leqslant 2\%$ relative, including those for sodium and potassium. The low sensitivity for sodium and potassium arises from their low ionization potentials; the temperature of the plasma is too high to determine alkali metals sensitively based on atomic emissions. No ionization interferences were observed even in the determination of calcium.

The results for a variety of standard silicate samples, summarized in Table 6, agree well with the certified values. The calibration graphs obtained were linear up to high concentrations, so that the extrapolation of calibration lines is justified, judging from the results for iron and titanium in MRG-1.

Conclusion

The proposed method is not only simple but also well suited for the application of i.c.p. emission spectrometry to the determination of major elements in silicates. As the dissolved sample and simply mixed standard solutions are prepared in the same matrix solution, the introduction rate to the plasma is constant for all solutions. In addition, the gravimetric preparation of such solutions is simpler and faster than a volumetric procedure. The proposed method can be applied to silicates of various compositions, and to simultaneous interference-free multi-element analysis.

The authors express their gratitude to Dr. K. Goto for making the integrator with a V/f converter and to Dr. I. Kojima for useful discussions.

REFERENCES

1 R. H. Scott and M. L. Kokot, Anal. Chim. Acta, 75 (1975) 257.
2 R. H. Scott, A. Strasheim and M. L. Kokot, Anal. Chim. Acta, 82 (1976) 67.
3 J. Burman, C. Ponter and K. Bostrom, Anal. Chem., 50 (1978) 679.
4 S. Greenfield, H. M. McGeachin and P. B. Smith, Anal. Chim. Acta, 84 (1976) 67.
5 H. Uchida and H. Matsui, Bunko Kenkyu, 27 (1978) 110.
6 B. Bernas, Anal. Chem., 40 (1968) 1682.
7 T. Uchida, Y. Ono and C. Iida, Bull. Nagoya Inst. Tech., 28 (1976) 113.
8 R. T. T. Rantala and D. H. Loring, At. Absorpt. Newsl., 12 (1973) 97.
9 D. E. Buckley and R. E. Cranstone, Chem. Geol., 7 (1971) 275.
10 T. Uchida, M. Nagase, I. Kojima and C. Iida, Anal. Chim. Acta, 94 (1977) 275.

Analytica Chimica Acta, 108 (1979) 93—101
© Elsevier Scientific Publishing Company, Amsterdam — Printed in The Netherlands

SOIL ANALYSIS BY THIN-FILM ENERGY-DISPERSIVE X-RAY FLUORESCENCE

R. VAN GRIEKEN* and L. VAN'T DACK

Department of Chemistry, University of Antwerp (U.I.A.), B-2610 Wilrijk (Belgium)

C. COSTA DANTAS and H. DA SILVEIRA DANTAS

Department of Nuclear Energy, Federal University of Pernambuco, Recife, Pe. 50000 (Brasil)

(Received 15th January 1979)

SUMMARY

Energy-dispersive x-ray fluorescence is advantageous for trace analysis of soils present as thin films. A target thickness of about 2 mg cm^{-2} provides a compromise between optimal sensitivity and minimal absorption effect or optimal accuracy. Sample preparation involves only suspending the finely ground soil in water and drying this suspension on a thin mylar foil glued on a ring that fits into the x.r.f. spectrometer. The "effective sample weight" present in the exciting beam area is computed from the scatter peaks, a method that cancels out target heterogeneity problems. High accuracy is demonstrated for many elements in reference soil and rock materials; a precision around 5% and a detection limit around 10 ppm can be achieved. As an illustration, results for 16 trace elements and preliminary interpretation are given for a series of pedologically important soil samples from Brasil.

In its wavelength-dispersive form, x-ray fluorescence (x.r.f.) is applied routinely by many laboratories to thick specimens of silicate material. A dilution method is often used in which a homogeneous melt is produced by fusion with a matrix of low atomic number (see, e.g. ref. 1) in order to reduce absorption, enhancement and particle-size effects, at the expense of a less favourable sensitivity. Otherwise, finely ground powder is compressed into a pellet and for each type of sample a similar standard calibration pellet is required, intricate approximate numerical correction methods for matrix effects are applied, internal standards are added or the primary radiation scattered by the sample is used as an internal standard to correct for variations in matrix effects. The latter method was first suggested by Andermann and Kemp [2], who showed that, for a given concentration of a trace element, the ratio of the intensity of an analysis line to the intensity of the adjacent background remains relatively constant in wavelength-dispersive x.r.f. for samples of different mass absorption coefficient. Kalmann and Heller [3] showed that this method is particularly suitable for the determination of heavy metal traces in rocks and soils. The energy-dispersive x.r.f. method for thick geological targets presented by Giauque et al. [4] was partially based on a similar line of reasoning.

Price and Angell [5] demonstrated that wavelength-dispersive x.r.f. could well be applied to rock powders mounted as thin films. The thin-film technique requires only minute amounts of sample and, within limits, it offers advantages of increased sensitivity and lack of matrix effects; the main problem usually lies in the preparation of suitable targets. In the present work, the thin-film technique is combined with energy-dispersive x.r.f. for simple trace analysis of soil samples with highly variable compositions.

Thin-film technique

The thin-film method of x.r.f. consists of using samples which are relatively thin compared to the depth of penetration of the characteristic x-ray. In contrast to the more usual analytical conditions for x.r.f., enchancement effects can then be neglected. For samples of homogeneous thickness ρD (in g cm^{-2}), the x-ray absorption correction factor, t, is given by

$$t = \chi(\rho D)/[1 - \exp(-\chi \rho D)] \quad (1)$$

where $\chi = \mu_1 \operatorname{cosec} \theta_1 + \mu_2 \operatorname{cosec} \theta_2$; μ_1 and μ_2 are the mass attenuation coefficients (in cm^2 g^{-1}) for the characteristic and exciting radiation, respectively; and θ_1 and θ_2 are the angle of emergence of the characteristic beam and angle of incidence of the exciting beam, respectively.

Of course, when the sample to be analysed is thinner, the absorption effect is less important, the uncertainty on the μ factor is reflected in the final result to a lesser extent, and the simplicity and accuracy of the analysis are improved.

The detection limit also varies as a function of the sample thickness; it is commonly defined in x.r.f. as three times the square root of the background. In the wavelength-dispersive technique, the background is caused mainly by scatter of the fraction of the continuous tube spectrum with its energy close to the analytical line. In secondary fluorescer energy-dispersive x.r.f., incomplete charge collection in the detector of the scattered "monochromatic" exciting x-ray beam constitutes the main background contribution. Because the exciting radiation is more penetrating, the background will increase more quickly than the analytical line with increasing sample thickness, and the detection limit will increase above a certain thickness. It is easily shown that when the carrier blank contribution is small, a direct measure of the sensitivity is given by

$$S = \{1 - \exp[-\chi(\rho D)]\}/\{1 - \exp[-2\mu_2 2^{1/2}(\rho D)]\}^{1/2} \quad (2)$$

This sensitivity factor is inversely proportional to the detection limit. The sensitivity factors for some elements are plotted in Fig. 1 as a function of the target thickness, with Mo K_α as the exciting radiation. The μ values were obtained by transmittance measurements on typical soil samples. It appears that the detection limit is minimal for sample thicknesses near 12.5 mg cm^{-2} for an average element such as iron. Yet, in this work, the target thickness was usually limited to ca. 2 mg cm^{-2}. The absorption factors, t, were then only 1.91, 1.40, 1.15, 1.09 and 1.03 for K, Ti, Fe, Zn and Rb, respectively, in typical soil samples, versus 8.0, 4.0, 1.97, 1.55 and 1.18 respectively for

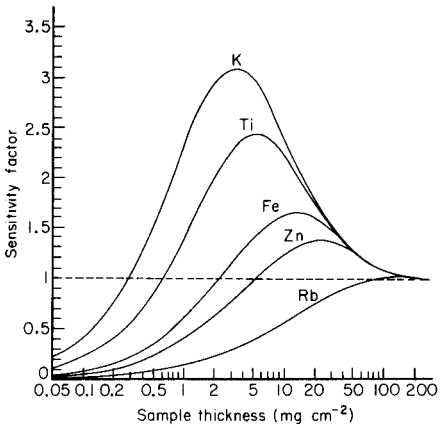


Fig. 1. Variation of the sensitivity factor (eqn. 2), which is inversely proportional to the detection limit, as a function of the target thickness for a typical soil.

12.5 mg cm^{-2} targets, and 225, 110, 42.8, 26.3 and 9.2 respectively for typical thick targets (350 mg cm^{-2}). While a 20% uncertainty in the μ values is almost completely reflected in the final result on a thick target, it results in uncertainties of only 8.9%, 5.3%, 2.3%, 1.5% and 0.5% for K, Ti, Fe, Zn and Rb, respectively, in the case of a 2 mg cm^{-2} target. Compared to thick samples, the detection limit will be lower for 2 mg cm^{-2} targets for elements lighter than iron (e.g., by a factor of 3 for K or 2 for Ti), but higher for heavier elements (e.g., by a factor of 1.6 for Zn or 4.3 for Rb). Because less material is required for analysis, and because enhancement effects are usually negligible and absorption corrections are less critical, the use of thin targets or targets of intermediate thickness is advantageous.

The main problem in thin-film x.r.f. usually lies in the preparation of suitable targets, i.e. films of metal or compounds. In energy-dispersive x.r.f., the excitation-detection efficiency usually varies quite strongly from point to point in the sample plane [6] and homogeneous vacuum-deposited films are often used for calibration purposes. Thus either samples of homogeneous thickness should be used for analysis, or the method applied should allow calculation of the effective sample weight weighted for the excitation-detection efficiency at every point in exactly the same way as the characteristic x-ray signal is weighted. Both methods were used in this work. While the former procedure will be described only briefly, the latter is discussed in more detail.

EXPERIMENTAL

Equipment

The x-ray fluorescence unit consisted of a Siemens Kristalloflex 2 high-voltage generator, a Kevex 0810 subsystem with a tungsten-anode Röntgen tube, a set of interchangeable secondary fluorescers and filters, a 16-position

automatic sample changer, a 30-mm^2 Si(Li) detector connected to a 4096-channel analyzer, and a magnetic tape recorder for off-line computer evaluation.

Sample preparation

Samples (ca. 1 g) were mixed with 7 ml of twice-distilled water either in a McCrone Micronizing Mill for 1 min or manually with a corundum pestle and mortar; microscope photographs showed particle sizes below 10 μm in the former case. The vessel was emptied and rinsed with another 7 ml of water. From the resulting suspension, which was shaken vigorously to make it as homogeneous as possible, a 0.5-ml fraction was immediately pipetted onto a mylar foil (<4 μm thickness; Somar Laboratories, New York) glued on a Teflon ring fitting in the sample changer of the x.r.f. unit. The target area within the Teflon ring was 12.6 cm^2. Careful evaporation at 80°C resulted in a target containing ca. 2 mg cm^{-2} of soil materials. The targets were homogeneous within a factor of two.

X.r.f. measurement and spectrum analysis

The sample powder prepared as described above was measured for 1000—3000 s by using the Mo secondary fluorescer and filter.

The characteristic x-rays were evaluated from the spectrum by a computer program based on non-linear least-squares fitting [7]. The spectra of the soil specimens (see, e.g. Fig. 2) are usually very complex and require an equally complicated analysis program. The x-ray intensities were converted to mg cm^{-2} amounts of the corresponding elements by using a series of homogeneous vacuum-deposited, thin-film standards (Micromatter Co., Seattle, U.S.A.); these results were, of course, weighted for the excitation detection efficiency at every point within the heterogeneous excitation beam.

The "effective sample weight per unit area", weighted in exactly the same way for the excitation-detection efficiency at every point, was obtained by

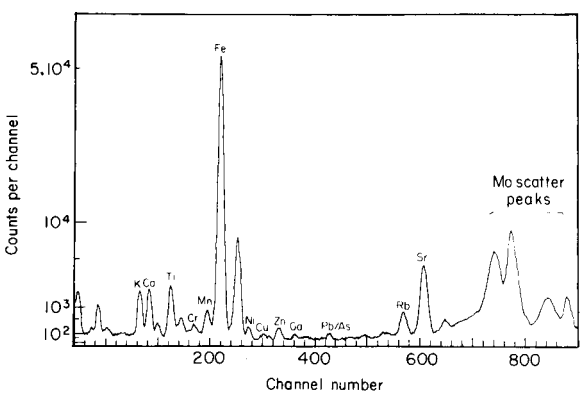


Fig. 2. Typical spectrum of a soil specimen.

the procedure recently developed by Van Espen et al. [8]. This method is based on the facts that the incoherent scatter intensity for samples of a certain composition is directly proportional to the weighted "effective sample weight" in the beam, and that both the specific incoherent scatter intensity and the coherent-to-incoherent scatter ratio vary smoothly with the average atomic number of the sample. After calibration with specimens of known composition, calculation of the coherent-to-incoherent scatter peak ratio leads to the average atomic number of the sample, and the relation between the specific incoherent scatter intensity and the atomic number can be used to compute the effective sample weight in the beam. The contributions to the effective sample weight and scatter intensities of the elements $Z > 20$ are separately calculated from their characteristic x-ray intensities. The accuracy of this effective weight determination procedure is around 5% for geological samples [8]. The advantages of this new method are as follows. No actual sample weighing is required. The effective sample weight in the beam (in g cm^{-2}) is weighted for the excitation-detection efficiency at every point in the same way as the amounts of element (in g cm^{-2}) are weighted; therefore relative results (in ppm) are independent, within certain limits, of the distribution of sample material within the beam and targets of inhomogeneous thickness can readily be analyzed.

RESULTS AND DISCUSSION

Table 1 lists some representative analyses on soil samples collected in the state of Pernambuco in the north east of Brasil. Samples A_1, A_2 and A_3 were reddish-brown podzolic soils of medium texture taken at the surface and at

TABLE 1

Typical results for soil profiles[a]

Element	Concentration (ppm)									
	A_1	A_2	A_3	B_1	B_2	B_3	B_4	C_1	C_2	C_3
K	278	303	347	9010	6040	7090	8090	5510	8470	4320
Ca	189	147	260	226	201	542	374	928	234	544
Ti	4400	5720	6820	5380	7200	7450	7600	11700	9070	7340
V	61	58	81	171	207	300	252	228	233	294
Cr	10	20	20	33	47	56	61	54	45	72
Mn	12	30	37	550	280	261	301	412	197	184
Fe	2710	4410	5510	37200	79000	70200	74300	26500	38300	59400
Ni	<7	<7	<7	11	26	22	29	11	14	24
Cu	<6	<6	<6	17	30	26	37	28	29	54
Zn	6.3	12	13	52	85	72	84	30	28	41
Ga	5.5	9.0	15	15	34	24	30	14	15	22
Rb	<4	<4	<4	36	43	41	58	26	40	40
Sr	6.3	9.7	12	49	39	39	30	16	11	14
Ba	63	89	135	809	632	422	567	42	396	185
Pb	3.7	12	11	26	56	41	47	16	15	25
Th	<10	10	<10	10	12	12	10	<10	19	12

[a]A, B and C refer to three different sampling sites (see text); samples 1—4 were taken at increasing depth.

different depths at one site near Goiana, in the humid coastal region. The major elements K and Ca (also the exchangeable K^+, Ca^{2+} and Mg^{2+}, as appeared from other measurements) and several trace elements are very low in concentration; manganese is almost deficient in the surface layer (A_1). Samples B_1—B_4 were taken in a hilly and drier region near Aliança, and are eutrophic red soils. There are relatively high levels of V, Mn, Cu, Zn, Ba and Pb; Ca^{2+} and Mg^{2+} appeared to be the dominating exchangeable bases. Soil samples C_1—C_3 were collected near the coast at Barreiros, a mountainous region; in these reddish-brown podzols with clayish texture the levels for several trace metals are relatively high, as would be expected for such soils.

A detailed pedological interpretation of these and 130 other samples collected over the State of Pernambuco and analysed by the proposed procedure will be presented elsewhere. Many of the trends in the data correspond to earlier observations on trace element concentrations in soils and their controlling factors [9], which points to the reliability of the method.

The overall accuracy and precision of the procedure was determined by analyses of standard soil and rock specimens available from the International Atomic Energy Agency and from the National Institute of Metallurgy (Johannesburg), Centre de Recherches Pétrochimiques et Géochimiques and Geological Survey of Japan. From each standard six targets were prepared; the effective sample thickness ranged from 0.9 to 2.3 mg cm^{-2}. In Table 2 the results are compared with the average results of the intercomparison run on the soil standard [10] and with the best values for the rock reference specimens quoted by Flanagan [11]. (For the soil reference specimen IAEA Soil-5, Table 2 includes the results of 11 additional analyses from the analysis of variance series.) As a measure of the overall precision, the standard deviations per single analysis are also given; these values should be multiplied by 0.82 to obtain the confidence intervals at the 95% probability level. The agreement appears to be quite satisfactory; there are no systematic deviations. Some aberrations (e.g. copper at low concentrations) can be attributed to spectrum analysis uncertainties and counting statistics.

A further test of accuracy was provided by the analysis of 33 of the soil samples by x.r.f. and by a colorimetric technique for copper and zinc after dissolution in HNO_3—H_2SO_4 mixtures. The Cu and Zn contents varied from the detection limits up to only 100 ppm. Linear regression analysis indicated satisfactory agreement, despite the low contents: $(\text{ppm Zn})_{\text{x.r.f.}} = (-4 \pm 7 \text{ ppm}) + (1.11 \pm 0.15)(\text{ppm Zn})_{\text{col.}}$, and $(\text{ppm Cu})_{\text{x.r.f.}} = (8 \pm 5 \text{ ppm}) + (0.87 \pm 0.09)(\text{ppm Cu})_{\text{col.}}$. (The significance of the calculated parameters may be rather low because the uncertainties in the chemical method are not very small compared to those of the x.r.f.)

The overall precision can be evaluated from the data in Table 2. The coefficient of variation averaged over all standards (except NIM-P) for the elements with high x-ray intensity (K, Ca, Ti, Mn, Fe, Zn and Sr) amounts to 4.6%.

An analysis of variance was carried out, involving 11 analyses on standard reference material IAEA Soil-5 and 5 analyses on NIM-S and on CRPG-GA.

TABLE 2

Analysis of standard reference samples. The results, given in ppm with the standard deviation in parentheses, are the average of 6 analyses (17 on IAEA Soil-5)

Element	Specimen											
	IAEA Soil-5 (soil)		GSJ-JB-1 (basalt)		GRP6-GA (granite)		NIM-L (lujavrite)		NIM-N (norite)		NIM-P (pyroxenite)	
	Given[a]	Found	Given	Found	Given	Found	Given	Found	Given	Found	Given	Found
K	18600 ± 1500	16270 (460)	11800	12900 (600)	33500	33600 (800)	46000	44500 (1400)	2200	2360 (370)	830	1060 (510)
Ca	22000	23400 (970)	65800	69600 (3700)	17500	18000 (500)	23600	22800 (300)	82550	86000 (3100)	19200	20200 (1000)
Ti	4700	4890 (400)	8030	8350 (520)	2300	2080 (70)	3060	2840 (90)	1140	1270 (60)	1200	1240 (180)
V	151	196 (32)	300	259 (32)	36	44 (24)	76	122 (12)	225	244 (8)	225	344 (43)
Cr[b]	29 ± 2.8	43 (11)	417	515 (47)	10	127 (19)	20	476 (12)	40	42 (13)	22000	24100 (1800)
Mn	852 ± 37	830 (26)	1240	1140 (80)	700	650 (25)	5500	5270 (170)	1320	1310 (60)	1630	1720 (80)
Fe	44500 ± 1900	43000 (1000)	63000	60600 (3560)	19800	20700 (800)	68300	67000 (3300)	62900	59300 (2500)	86000	86200 (5900)
Ni	13	20 (2)	139	144 (14)	7	83 (6)	11	25 (7)	78	124 (6)	470	610 (50)
Cu	77 ± 4.7	93 (7)	52	60 (7)	14	28 (6)	15	28 (4)	13	20 (4)	17	27 (4)
Zn	368 ± 8.2	390 (26)	83	90 (4)	75	68 (4)	320	394 (17)	80	61 (4)	100	119 (10)
Ga	18 ± 1.6	18 (1.9)	17	18 (3)	16	16 (2)	55	59 (5)	19	19 (4)	13	10 (2)
As	94 ± 7.5	87 (6)	—	6 (3)	—	5 (2)	—	11 (5)	—	<4	—	<8
Rb	138 ± 7.4	126 (5)	41	51 (14)	175	169 (2)	183	183 (10)	9	7 (2)	4	11 (8)
Sr	330	370 (12)	438	488 (22)	305	309 (12)	4480	4480 (180)	254	290 (11)	40	36 (10)
Y	21	28 (2)	—	20 (2)	18	19 (3)	30	15 (4)	7	6 (2)	—	<5
Ba	561 ± 53	422 (94)	400	535 (80)	850	765 (110)	448	290 (100)	90	96 (17)	56	220 (110)
Ce	60	<40	67	65 (26)	—	<35	240	220 (60)	14	<30	85	<45
Pb	129 ± 26	201 (13)	14	<8	—	34 (15)	45	51 (17)	<10	<7	<10	<10
Th	11 ± 0.73	11 (2.9)	9	<8	15	13 (5)	69	61 (9)	0.5	<7	1	<9
U	3.0 ± 0.51	<6	1.8	<7	—	<6	13	<10	0.5	<7	0.5	<9

[a] The reported uncertainties are confidence limits for a 0.95 probability level for the given Soil-5 values and standard deviations per measurement in all the x.r.f. results presented.

[b] Cr results can be subject to some contamination from the grinding unit.

The scheme for each standard involved treble measurements on the same target, three target preparations from the same batch of sample suspension, and treble sampling and suspension preparation from the same standard reference specimen supply. The analysis of variance included only those results that were at least ten times above the detection limit (to exclude the contribution of counting statistics) and were derived from characteristic x-ray peaks free from major spectral interferences (to exclude major uncertainties from spectrum fitting) and with absorption corrections below 30% (to exclude major uncertainties from matrix effects). The following conclusions were drawn.

(a) The average coefficient of variation for repeated measurements on one target is 1.8% (confidence interval at the 0.95 probability level, 1.2—2.4%).

(b) The average combined coefficient of variation for repeated target preparation from one batch of sample suspension and for the x-ray fluorescence measurement amounts to 2.3% (confidence interval, 1.5—3.1%). At the 0.95 probability level, this is not significantly above the uncertainty of the measurement step only. Thus pipetting part of a sample suspension onto a mylar carrier to prepare a thin target does not add significantly to the overall uncertainty.

(c) The average overall coefficient of variation for the sampling, the sample and target preparation and the measurement amounts to 5.2% (confidence interval, 2.4—7.1%). This is very significantly above the 2.3% uncertainty in the target preparation and measurement. The 4.7% difference might be due to heterogeneities at the 25-mg level and unrepresentative sampling of the standard reference materials, or to contamination in the sample preparation step.

The detection limits were calculated as three times the standard deviation on the background count rate, assuming no interelement interferences. Representative values are: 150 ppm for K, 90 ppm for Ca, 30—10 ppm for Ti, V, Cr, Mn, 7—3 ppm for Fe, Ni, Cu, Zn, Ga, As, Rb, Sr, Y; and, with *L*-radiation, 50—35 ppm for Ba, La, Ce and ca. 10 ppm for Hf, Pb, Th, U. In complex spectra with important overlap, realistic detection limits may become less favourable for some elements.

Alternative procedure

Several authors have recommended "puff techniques" or vacuum evaporation or laser evaporation—deposition to prepare homogeneous targets from solids. Quite homogeneous thin targets can also be prepared by simply filtering off a suspension through a membrane [12, 13]. In the initial stages of this work, 600 mg of ground soil was placed in 30 ml of water at pH 6.5 and shaken for 2 h at constant temperature. An aliquot (1 ml) of this slurry was pipetted into 50 ml of water; this diluted suspension was placed on a Nuclepore membrane (47-mm diameter, 0.4-μm pore) in a Gelman 4200 filter holder and drawn through, resulting in a membrane loaded with 2.1 mg cm^{-2} of soil material. To check whether, during the water suspension step, considerable

amounts of the trace metals had been leached out of the soil samples, the filtrates from several soil samples were analysed by x.r.f. after evaporating 2 ml on a Whatman filter provided with a hydrophobic ring [6] and after a pre-concentration step involving chelation by oxine and adsorption on activated carbon [14] with varying amounts of reagents. Less than 2—3% of the K, Ca, Br, Rb, Sr and Zn contents, and less than 0.1% of the other transition metals were detected in the leachate. The loaded filter analysis thus could be considered as a nearly total trace metal analysis. The precision of the overall procedure was measured by preparing three suspensions from each of six standard rock and three soil specimens, and analysing the resulting targets separately. The coefficient of variation for one determination was 11.2%, which is considerably less satisfactory than the value for the other procedure. When results relative to iron were considered, the corresponding coefficient of variation was still 8.9%, which is not significantly different at the 0.95 probability level. Hence, the difference in precision cannot be completely attributed to target heterogeneities. Probably the additional error can be explained by the soil powder suspension being heterogeneous and the pipetting of 1 ml of the suspension being somewhat unrepresentative of the soil weight included.

The homogeneity of the soil load on the filter was checked by analysing several filters numerous times both at the centre and at different peripheral locations. The diameter of the exciting beam was approximately 1.5 cm. The 5% coefficient of variation found for the most intense elements was close to what would be expected from counting statistics and geometry uncertainties, and indicated homogeneous loading of the filter near its centre. However, a significant enrichment close to the edge of the filter because of the conical shape of the Gelman filter holder cannot be ruled out; indeed, analyses (in the filter centre) of standard rock target on average yielded values that were 10% low. Because both the precision and accuracy of this alternative procedure were less favourable, it was not used in later stages of this work.

REFERENCES

1 K. Norrish and J. T. Hutton, Geochim. Cosmochim. Acta, 33 (1969) 431.
2 G. Andermann and J. W. Kemp, Anal. Chem., 30 (1958) 1306.
3 Z. H. Kalmann and L. Heller, Anal. Chem., 34 (1962) 946.
4 R. D. Giauque, R. G. Garrett and L. Y. Goda, Anal. Chem., 49 (1977) 62.
5 N. B. Price and G. R. Angell, Anal. Chem., 40 (1968) 660.
6 J. Smits and R. Van Grieken, Anal. Chim. Acta, 88 (1977) 97.
7 P. Van Espen, H. Nullens and F. Adams, Nucl. Instrum. Methods, 142 (1977) 243.
8 P. Van Espen, L. Van't Dack, F. Adams and R. Van Grieken, Anal. Chem., in press.
9 H. Aubert and M. Pinta, Trace Elements in Soils, Developments in Soil Science 7, Elsevier, Amsterdam, 1977.
10 R. Dybczynski, A. Tugsavel and O. Suschny, Report on the intercomparison run Soil-5 for the determination of trace elements in soil, Report IAEA/RL/46, January 1978.
11 F. J. Flanagan, Geochim. Cosmochim. Acta, 37 (1973) 1189.
12 J. R. Cann and C. K. Winter, Mar. Geol., 11 (1971) 33.
13 M. Vanderstappen and R. Van Grieken, Fresenius Z. Anal. Chem., 282 (1976) 25.
14 J. Verbeeck, B. Vanderborght and R. Van Grieken, Bull. Soc. Chim. Belges, 86 (1977) 23.

Analytica Chimica Acta, 108 (1979) 103—111
© Elsevier Scientific Publishing Company, Amsterdam — Printed in The Netherlands

EMISSION SPECTROGRAPHIC DETERMINATION OF TRACE ELEMENTS IN ATMOSPHERIC PARTICULATE MATTER

SAKINGO IMAI*

Public Health Research Institute of Kobe City, 1-5, Kano-Cho, Ikuta-Ku, Kobe-Shi, Hyogo 650 (Japan)

YUZURU KUSAKA, HARUO TSUJI and YOSHIKAZU HISHIYA

Department of Chemistry, Faculty of Science, Konan University, Okamoto-Cho, Higashinada-Ku, Kobe-Shi, Hyogo 650 (Japan)

(Received 30th October 1978)

SUMMARY

Air containing particulate material was passed continuously for one month through a low-volume air sampler equipped with a cyclone to exclude particulates greater than 10 μm in diameter. The samples and filters were ashed in a low-temperature plasma and, after addition of In_2O_3 support, palladium internal standard and graphite buffer, the ashes were analyzed by a.c. arc emission spectrometry. Standard samples were prepared from a commercial standard containing 49 elements. The procedure allows the determination of 14 trace metals (Ag, Al, Cr, Cu, Fe, Ga, Mn, Mo, Ni, Pb, Sn, Ti, V, Zn) with relative standard deviations of 1.4—15.1%. The procedure has been applied successfully to monthly determinations of the average atmospheric concentrations of these elements in Kobe City for the past three years.

Determinations of trace elements in atmospheric particulate matter is important in surveys of environmental pollution. Usually, the particulates are collected on a suitable filter, pretreated suitably and finally analyzed by atomic absorption spectrometry, emission spectrometry or neutron activation analysis. The emission method is particularly valuable because of its simplicity and multi-element capability.

The NASN method is used widely for emission spectrometric analyses of such samples [1]. This method involves sample collection on a glass fiber filter with a high-volume air sampler for 24 h at a flow rate of 1.5 m^3 min^{-1}, ashing at 500°C, extraction with warm hydrochloric acid, and addition of Sr or In as internal standard; cup-type carbon electrodes containing lithium chloride and graphite are used. Various modifications of this method with high-volume air samplers and glass fiber filters have been reported [2—5].

Since these methods use a high-volume samplers, they are unsuitable for determining the average concentrations of elements over relatively long periods. Moreover, impurities in the filters, e.g. Ti, Zn and Ba in glass fiber filters, often complicate the analyses [6—8]. Because of this difficulty, Yamane et al. [9] and Sugimae [10] proposed the use of chemically purer membrane filters.

For all these methods, however, standard samples are prepared by mixing aliquots from standard stock solutions of individual elements; this produces excellent uniformity but complicates the procedure and is time-consuming.

In earlier work [11, 12], a simplified emission spectrometric method was developed for determining average concentrations of several elements after collection for 15 days with a low-volume air sampler at a flow rate of 20 l min^{-1}. The collected particulates were subjected to low-temperature ashing and analyzed with a palladium internal standard.

This paper describes an extension of the earlier method to longer sampling periods, as well as a simplified procedure for preparing standard samples, a detailed study of the degree of dilution with In_2O_3 and optimum excitation conditions. The method developed permits quantitative analysis for 14 elements over a wide range of concentrations with high precision. It has been applied to investigations of atmospheric particulates in Kobe City over the last three years.

EXPERIMENTAL

Apparatus and conditions

The apparatus used for emission spectrometry, excitation conditions, carbon electrode, photographic plate and photometric conditions are summarized in Table 1.

Collection of atmospheric particulate matter

An all-weather low-volume air sampler (Type-S-2, Shintaku Machinery Works Ltd., Japan) which has a stainless steel cover and filter holder with plastic clamps, was equipped with a membrane filter (Gelman GA-3, 1.2-μm pore size, 110-mm diameter; Gelman Instrumental Company, U.S.A.), a

TABLE 1

Experimental apparatus and conditions

Spectrograph	Shimazu Littrow-type crystal spectroscope (QL-170)
Source unit	Shimazu universal source unit
Discharge	7.5-A, a.c. arc
Sample electrode	National Carbon L-4309, cup-type with a 3-mm diameter, 3-mm deep crater
Counter electrode	Hitachi-Kasei CTE-2006, 6-mm diameter, pointed
Analytical gap	2 mm held constant
Pre-arc time	None
Exposure time	20 s
Slit width	10 μm
Spectral region	250.0—350.0 nm
Plate and treatment	4 × 10-in Kodak SA-1 plate, processed with FD-131 developer for 2 min at 20°C, stopped in FS-1 stop bath, fixed with FF-H4 fixer for 20 min and air-dried
Comparator	Shimazu automatic microphotometer (Type-802)

Polyflon filter (PF-1, 20-μm pore size, 110-mm diameter; Toyo Roshi Kaisha Ltd., Japan) to support the membrane filter and to prevent contamination, a constant differential pressure valve, and a cyclone to exclude particles exceeding 10 μm in size. The sampler was positioned 10 m above the ground, and air was pumped through it at 20 l min^{-1} continuously for one month.

The Gelman GA-3 membrane filter used is made of cellulose acetate. Membranes made of cellulose nitrate and cellulose acetate tend to burn explosively during ashing, causing losses by scattering, but the Gelman filters burn smoothly. Like other filters the Gelman membranes contain various impurities [13]. In the present work, filters were analyzed by low-temperature ashing, dissolution of the ash in dilute nitric acid, and atomic absorption spectrometry. The following elements were found per 1 cm^2 of the filter: Cr, 29 ng; Cu, 19 ng; Fe, 75 ng; Mn, 3 ng; Ni, 5 ng; Pb, 2 ng; Zn, 10 ng. Flame photometry gave a result of 2100 ng Na cm^{-2}. Therefore, before use, the filters were immersed in 2 M nitric acid for 6 h, washed with double-distilled water, immersed in 2 M acetic acid for 6 h, placed on a glass filter, washed thoroughly with double-distilled water and dried in a desiccator over silica gel for 24 h. This operation removed 75—90% of the impurities in the filter, and the residual concentrations were negligible compared with the concentrations of the elements in the samples collected.

Standard sample series and standard atmospheric dust sample (AS-1)

The series of standard samples for emission spectrometry was prepared from Spex Mix No. 1000 (Spex Inc., U.S.A.), which contains 1.27% each of the following 48 elements: Ag, Al, As, B, Ba, Bi, Br, Ca, Cd, Ce, Cl, Co, Cr, Cs, Cu, F, Fe, Ga, Ge, Hg, I, In, K, Li, Mg, Mn, Mo, Na, Nb, Ni, P, Pb, Rb, Sb, Se, Si, Sn, Sr, Ta, Te, Th, Ti, Tl, U, V, W, Zn and Zr. Weighed amounts of this Spex Mix were diluted successively with In_2O_3 to give the following concentrations of each element (in ppm): 0.2, 0.5, 1, 2, 5, 10, 20, 50, 100, 200, 500, 1000, 2000, 5000, and 10000.

The analytical precision of the present method was checked with the AS-1 sample prepared by Hashimoto [14, 15] from dusts adhering to the air filter of the air conditioner installed in a high-rise building; the fraction that passed a 200-mesh sieve was dried at 105°C, mixed for 10 h in a Mixer Mill (Spex Inc.) and further mixed by the increment method. Before use, a weighed amount of the sample was transferred to a quartz boat and ignited for 24 h in a low-temperature asher (Trapelo PDS-504; 100-W r.f.; oxygen flow rate, 40 ml min^{-1}; 1 Torr vacuum); the ash was weighed, and a weighed portion was mixed thoroughly with a 5- or 50-fold amount of In_2O_3 (>99.999% pure) in an agate mortar.

Analytical procedure

The membrane filter with the collected sample was dried to constant weight in an Auto-desiccator (Sanko Plastic, Japan), weighed to determine the total weight of sample, transferred to a quartz boat and ashed in the low-temperature

asher for 2 h as described for AS-1. (An earlier study based on neutron activation analysis [16] showed that there were no volatilization losses of the elements determined during ashing.) The ash was weighed and mixed thoroughly and two weighed portions were diluted with In_2O_3, one 5-fold and the other 30-fold. The 5-fold diluted sample was used to determine Ag, Ga, Mo, Ni, Sn and V in relatively low concentrations, while the 30-fold diluted sample was used for Al, Cr, Cu, Fe, Mn, Pb, Ti and Zn.

Each ash (samples and standards) diluted with In_2O_3 was mixed well with an equal amount of graphite powder (Hitachi Kasei Inc.) containing 50 ppm of palladium (PdO, spectroscopically pure). About 12 mg of the mixture was loaded by tapping into the electrode crater for analysis. The analytical lines and the palladium internal standard lines were selected from the bright line spectrum recorded under the conditions specified in Table 1. The content of each element was established from the calibration curves prepared for each line pair by the density comparison method and the Seidel transformation method.

The difference in density, ΔD, and the difference in Seidel density, ΔW, were calculated from the equation $\Delta D = \log A_i/A_s$, where A_i and A_s are absorbances of the internal standard line and the analytical line, respectively; and from the equation $\Delta W = \log \{[(T_0/T_a) - 1]/[(T_0/T_i) - 1]\}$, where T_0, T_a and T_i are the transmittances of the unexposed portion of the photographic plate, the analytical line and the internal standard line, respectively.

RESULTS

Effect of buffer agents

For comparison of the performance of various buffer agents, several samples were prepared by mixing Spex Mix No. 1000 and the buffer agent to be tested so that the concentration of each element became 500 ppm. The changes in intensity of the analytical lines of the 14 test elements with exposure time were then followed by the photographic plate moving method. Fractional distillation occurred and the intensities were generally low when NaF with graphite powder was used as the buffer agent; each element showed maximum intensity 10 s after the start of excitation. In the case of LiCl, $NaHCO_3$, Li_2CO_3, or In_2O_3, the duration of excitation was longer and some fractional distillation was noted, but the intensities were generally high. In_2O_3 gave the highest intensities.

On the basis of the above findings, a powdered mixture of In_2O_3 and graphit (which suppresses fractional distillation) was selected. A study of the relationship between the proportion of In_2O_3 in the mixture and the line intensity indicated that, as long as the addition of In_2O_3 was kept above 37.5%, there were virtually no variations in line intensities for each element or in temporal changes. Therefore, a 1:1 mixture of In_2O_3 and graphite was used here. The plots of intensity against exposure time (I—T curves) are shown in Fig. 1. Given these I—T curves, and the lowering of the S/N ratio with increasing

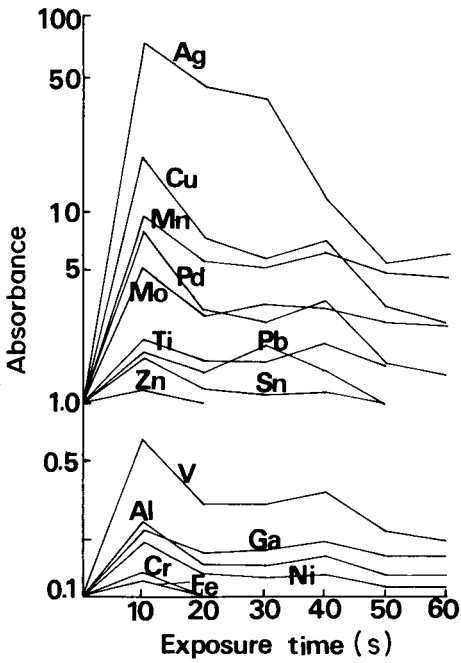


Fig. 1. *I—T* curves with graphite and In_2O_3 mixture (1:1) as buffer agent.

exposure time, exposure to the photographic plate was effected for 20 s after the start of excitation.

SAMPLE DILUTION WITH In_2O_3

The optimum degree of dilution of the ash with In_2O_3 was investigated for the AS-1 standard dust. In_2O_3 was added to ashed AS-1 at ratios of 5, 10, 15, 20, 25, 30, 40, 50 or 60 parts to 1 part of AS-1, and the line intensities of the 14 test elements were measured by applying the Seidel transformation method to lines of low intensity and the density comparison method to the intense lines.

The results showed that 5-fold dilution was suitable for determinations of Ag, Ga, Mo, Ni, Sn and V, which are either present in low concentrations or are of low sensitivity. For the other elements which are present in relatively high concentrations or are highly sensitive, 15- to 30-fold dilution gave line intensities within the ranges of the calibration curves; the *S/N* ratios were good and stable results were obtained. However, with dilutions greater than 30-fold, In_2O_3 began to cause interference, the *S/N* ratio dropped, and larger errors were produced in the results. For these reasons, the two-step dilutions, 5- and 30-fold, were adopted for quantitative work.

Working ranges and precision

Analysis of the emission spectra of AS-1 and the samples showed that the 14 elements could be determined. Correlation coefficients were computed for the calibration curves prepared from the results of five experiments. Working ranges were taken where these coefficients were 0.98 or better. Regression lines were obtained in these working ranges by the least-squares method; factors a and b were obtained from the usual equations: $\Sigma Y = na + b(\Sigma X)$ and $\Sigma XY = a(\Sigma X) + b(\Sigma X^2)$, where n is the number of portions of the standard sample over the working range, Y is ΔD or ΔW, and X is the concentration in the standard sample.

The analytical lines, regression factors and working ranges are presented in Table 2. As is apparent from Table 2, it is generally desirable to apply the Seidel transformation method to determinations of low-concentration elements (Ag, Ga, Mo, Ni, Sn and V) and the density comparison method to high-concentration elements (Al, Cr, Cu, Fe, Mn, Pb, Ti,and Zn).

To check the analytical precision, AS-1 was analyzed five times; the results are shown in Table 3. The relative standard deviations range from 2.7% to 8.4% for the 14 elements, which should be acceptable for a practical method.

Application

The recommended method was applied to determinations of the 14 elements in atmospheric particulate matter sampled in seven areas in Kobe City over the past 3 years. The sampling areas were as follows: (A) in Ogo-Cho, Kita-Ku, a farm area among hills; (B) in Suzurandai-Cho, Kita-Ku, and (C) in Hirano-Cho Tarumi-Ku, both suburban residential areas; (D) in Fukae-Cho, Higashinada-Ku, between a trunk motorway and an express highway; (E) in Sumiyoshi-Cho,

TABLE 2

Analytical lines, working ranges and regression lines

Elements	Line (nm)	Density comparison		Seidel transformation	
		Range (ppm)	Regression factors[a]	Range (ppm)	Regression factors[a]
Ag	328.02	1—10	a = —0.067, b = 0.863	0.5—100	a = 0.026, b = 0.99
Al	256.80	200—10000	a = —1.685, b = 0.613	200—2000	a = —4.771, b = 1.64
Cr	284.33	50—2000	a = —1.793, b = 0.938	5—2000	a = —2.696, b = 1.36
Cu	327.42	10—500	a = —0.743, b = 0.883	2—200	a = —0.747, b = 1.04
Fe	258.59	200—5000	a = —2.319, b = 0.947	200—5000	a = —3.314, b = 1.35
Ga	287.42	100—1000	a = —2.014, b = 1.084	50—2000	a = —2.164, b = 1.23
Mn	279.48	5—500	a = —0.713, b = 0.826	5—500	a = —0.756, b = 0.98
Mo	317.03	20—1000	a = —0.976, b = 0.863	2—500	a = —1.272, b = 1.13
Ni	300.25	50—1000	a = —1.642, b = 0.904	10—2000	a = —2.260, b = 1.22
Pb	283.31	50—1000	a = —1.728, b = 1.029	5—2000	a = —2.230, b = 1.31
Sn	284.00	50—2000	a = —1.638, b = 0.982	10—2000	a = —1.927, b = 1.20
Ti	337.28	20—2000	a = —0.871, b = 0.715	20—2000	a = —0.940, b = 0.85
V	318.40	10—500	a = —0.448, b = 0.584	5—500	a = —0.413, b = 0.69
Zn	328.23	200—10000	a = —1.430, b = 0.553	50—2000	a = —2.996, b = 1.13
Pd	324.27				

[a] Regression equation; $Y = a + bX$.

TABLE 3

Determination of fourteen elements in standard atmospheric dust sample (AS-1). Mean results ($\bar{x}$), standard deviations (s) and relative standard deviations (s_r) are given (n = 5)

Elements	$\bar{x}$ (ppm)	s	s_r (%)	Previous results [15][a] (ppm)
Ag	4.0	0.16	4.0	3, 3.7
Al	36400	1290	3.5	38000, 55000, 56000
Cr	412	21	5.1	370, 360, 330
Cu	441	21	4.8	600, 320, 340
Fe	36900	2490	6.7	47000, 48000, 39000
Ga	187	7.8	4.2	13
Mn	956	37	3.9	1200, 13000, 900
Mo	31.9	2.2	6.9	—
Ni	184	12	6.4	250, 210, 175
Pb	2100	87	4.1	1800, 2640
Sn	129	5.6	4.3	—
Ti	2020	55	2.7	5800, 3700, 2900
V	236	13	5.4	200, 290, 240
Zn	1710	140	8.4	2800, 3800, 3040

[a]Results from an interlaboratory test.

Higashinada-Ku, near a large ironworks; (F) in Omichi-Cho, Nagata-Ku, an area full of small and medium-size factories; and (G) in Hamabe-Cho, Fukiai-Ku, an office area in the center of the city. The results as a whole and their environmental implications will be reported separately; for illustration, some results are presented in Table 4.

The values measured in area A are lower than those in other areas for almost all the 14 elements; thus, area A is least affected by emission from both fixed and mobile sources and these values may be regarded as very close to the background values of the environmental atmosphere of Kobe City. Compared with area A, area B shows a marked increase in iron and some increases in Mn and Ni, both of which are known to show a relatively high correlation with iron. However, other elements are found in roughly equal amounts in both areas, which suggests that the higher iron values found in area B may be attributable to an electric railroad track running through this area. In area C, all the elements are at slightly higher concentrations than in area A, but none is singularly different, i.e. area C shows a typical suburban distribution of the elements. Compared with areas A—C the values found in areas D—G distinctly show a city-type distribution; the concentrations of all the elements increase markedly and the influences of both fixed and mobile emission sources are clearly recognizable.

TABLE 4

Emission spectrometric determination of fourteen elements in atmospheric particulate matter collected at seven locations[a]

Elements (ng m^{-3})	A		B		C		D		E		F		G	
	I	II	I	II	I	II	I	II	I	II	I	II	I	II
Ag	0.02	0.01	0.04	0.02	0.03	0.02	0.28	0.15	0.19	0.10	0.26	0.21	0.08	0.11
Al	1320	1340	1180	960	1540	1580	1790	1470	1150	1170	1160	1230	1720	1320
Cr	5.6	4.4	5.0	5.6	7.1	5.0	15	10	16	9.1	18	19	21	16
Cu	7.6	7.6	7.6	5.2	8.5	9.0	18	24	24	12	15	17	20	16
Fe	520	570	1080	820	620	560	1000	820	1190	840	980	1040	1150	1440
Ga	2.7	2.1	3.9	5.7	3.4	2.6	7.6	5.0	7.7	4.2	9.5	6.5	11	8.0
Mn	15	10	18	22	19	18	30	46	43	35	46	48	52	42
Mo	0.3	0.3	0.3	0.4	0.3	0.3	3.6	2.4	2.0	1.6	1.3	2.0	1.5	2.0
Ni	2.3	2.2	7.4	4.9	6.8	4.6	15	18	17	10	23	20	21	15
Pb	24	24	23	21	39	27	120	128	83	115	120	114	122	93
Sn	3.4	3.3	3.2	2.4	4.0	5.1	9.0	7.2	8.5	7.8	16	9.4	9.0	11
Ti	15	14	12	18	16	12	36	24	39	20	22	18	14	25
V	2.7	3.3	3.2	2.4	4.0	6.7	58	34	29	39	29	26	29	54
Zn	30	33	33	39	43	60	120	120	160	99	180	200	130	210
M ($\mu g\ m^{-3}$)	18.9	24.8	14.5	19.4	32.9	24.2	46.5	39.5	38.7	32.1	48.7	38.2	44.4	38.9

[a]Sampling dates: I = May 1976; II = June 1976. M is the concentration of atmospheric particulate matter.

DISCUSSION

The components of atmospheric particulate matter vary widely in concentration with the area, period and conditions of sampling. In emission spectrometric analysis of such samples, it is desirable to change the degree of dilution of the ashed sample with In_2O_3 according to the characteristics of each sample and to select either the density comparison method or the Seidel transformation method to accommodate the changes in intensity of the spectral lines. It is possible to analyze a wide range of samples by means of the two-step dilution method suggested.

Standard samples can be prepared simply and in large quantities at one time; they can be stored over long periods of time. In consequence, the reproducibility of calibration curves is good and the time required for analysis can be reduced.

The recommended procedure has been applied during three years to 222 samples of atmospheric particulate matter and has been found practical, simple and rapid.

REFERENCES

1 U.S. Public Health Service, Air Pollution Measurement of National Air Sampling Network, (1963) p. 213.
2 T. Hasegawa and A. Sugimae, Jpn. Anal. (Bunseki Kagaku), 20 (1971) 840.
3 A. Sugimae, Anal. Chim. Acta, 78 (1975) 107.
4 A. Sugimae, Anal. Chem., 47 (1975) 1840.
5 D. R. Scott, W. A. Loseke, L. E. Holboke and R. J. Thompson, Appl. Spectrosc., 30 (1976) 392.
6 W. H. Zoller and G. B. Gordon, Anal. Chem., 42 (1970) 257.
7 K. Mizuno, L. Yamada and F. Ota, Jpn. Anal. (Bunseki Kagaku), 20 (1970) 1235.
8 J. R. Kean and E. R. Fisher, Atmos. Environ., 2 (1968) 603.
9 Y. Yamane, M. Miyazaki and H. Nakazawa, Jpn. Anal. (Bunseki Kagaku), 22 (1973) 1135.
10 A. Sugimae, Anal. Chem., 46 (1974) 1123.
11 S. Imai, K. Ito, A. Hamaguchi, Y. Kusaka and M. Warashina, Jpn. Anal. (Bunseki Kagaku), 22 (1973) 551.
12 S. Imai, S. Furuya, Y. Kusaka and H. Tsuji, Jpn. Anal. (Bunseki Kagaku), 25 (1976) 549.
13 R. Dams, K. A. Rahn and J. W. Winchester, Environ. Sci. Technol., 6 (1972) 441.
14 Y. Hashimoto, Bunseki, 4 (1975) 250.
15 Y. Hashimoto, T. Otoshi and K. Oikawa, Environ. Sci. Technol., 10 (1976) 815.
16 S. Imai, Jpn. Anal. (Bunseki Kagaku), 27 (1978) 611.

Analytica Chimica Acta, 108 (1979) 113—118
© Elsevier Scientific Publishing Company, Amsterdam — Printed in The Netherlands

A DIRECT METHOD FOR THE DETERMINATION OF CARBONATE AND NON-CARBONATE CARBON IN GEOLOGICAL MATERIALS BY INFRARED SPECTROMETRY

S. TERASHIMA

Geological Survey of Japan, Hisamoto 135, Kawasaki 213 (Japan)

(Received 25th October 1978)

SUMMARY

A simple and direct infrared method for determining carbonate and non-carbonate carbon in geological samples is described. To determine carbonate carbon, hydrochloric acid is added directly to the heated samples; non-carbonate carbon is determined by combustion after digesting the samples with hydrochloric acid. The limit of detection is 2 ppm for carbonate carbon and 10 ppm for non-carbonate carbon; the relative standard deviations are 4% or less for 100—1000 μg of carbonate and non-carbonate carbon. The method has been applied to standard rocks, NBS minerals and geological exploration reference samples.

In studies of geochemical or geological processes, it is necessary to know the separate contents of carbonate and non-carbonate carbon for large numbers of geological samples. Recently, automatic determination of carbon and sulfur was achieved by combining combustion in a high-frequency induction furnace with i.r. spectrometry. The method is sensitive, precise and rapid and has been applied to total carbon and sulfur analyses of iron and steel [1], and geological materials [2]. The instrument, sample digestion and preparation of calibration standards have been modified so that the method can be applied to the separate determination of carbonate and non-carbonate carbon in geological samples. New data are presented for standard reference samples.

EXPERIMENTAL

Apparatus and reagents

The Kokusai Electric I.R.-Matic "C—S" VK-111 AS automatic carbon—sulfur analyzer used was described earlier [2]. Non-carbonate carbon was determined with oxygen as the combustion and carrier gas, and nitrogen as the purge gas, in a ceramic crucible. For the determination of carbonate carbon, the apparatus was similar to the classical arrangement for the determination of carbonate in rocks: the assembly consisted of a U-tube containing 10 g of ascarite; a 200-ml Pyrex digestion flask with a side arm connected to a separatory funnel fitted through the stopper of the flask (the flask is placed on a hotplate); a gas wash-bottle, containing 30 ml of 9 M sulfuric acid, in an ice

box; a U-tube containing 12 g of magnesium perchlorate; and a control valve for the carrier gas. The outflow from this valve was taken directly to the detector.

The reagents were as described earlier [2].

Recommended procedure for carbonate carbon

Pass nitrogen (0.4 l min^{-1}, 0.6 kg cm^{-2}) through the apparatus. Weigh the powdered sample (0.1 g for 0.05—5% carbon and 1.0 g for 0—0.05% carbon) into the dried digestion flask; by pipette, add 10 ml of 6 M hydrochloric acid to the separatory funnel, and connect up the apparatus. Adjust the flow rate of nitrogen to 2.5 l min^{-1} (0.5 kg cm^{-2}). Heat the digestion flask for ca. 3 min on the electric hot plate at about 150°C. Open the stopcock of the separatory funnel to allow the acid to flow into the digestion flask. Shake the mixture for 20—30 s, and allow to stand until carbon dioxide is not detected.

Recommended procedure for non-carbonate carbon

Place magnesium perchlorate (12 g and 8 g, respectively) in the drying tubes of the automatic carbon analyzer. Pass oxygen (2.5 l min^{-1}, 1.5 kg cm^{-2}) and nitrogen (0.4 l min^{-1}, 0.6 kg cm^{-2}) through the apparatus.

Weigh out the powdered sample (0.1 g for 0.05—0.05—5% carbon and 0.5 g fc 0—0.05% carbon) into a ceramic crucible. Add 2 ml of 11 M hydrochloric acid and place on an electric hot plate at about 130°C in a fume hood. If the samples are igneous rocks and minerals, cover the crucible with a filter funnel while heating for 15—20 min. After evaporating to dryness, place for 20—30 min in a drying oven at about 150°C to remove residual hydrochloric acid. Cover the residue with ca. 0.6 g of iron powder and add ca. 1.3 g of tungsten chips. Place the crucible on the pedestal of the furnace. Introduce the crucible into the cold combustion tube by raising the locking mechanism handle. Combust for 35—60 s at ca. 1800°C.

RESULTS AND DISCUSSION

Analysis for carbonate carbon

For the digestion of the samples, the concentration (4—8 M) and amount (6—12 ml) of hydrochloric acid were not critical. After heating for 3 min on the hot plate at 150°C, the temperature of the bottom of the digestion flask was about 100°C; temperature variation between 95 and 110°C did not affect the determination of carbonate carbon in JG-1 and JB-1 rock standards. On average, the blank value was 1 μg carbon.

In the determination of total carbon [2], the calibration standards were prepared by adding calcium carbonate to silicon dioxide; this procedure yielded values ca. 6% higher than those obtained from actual samples (e.g. JG-1, JB-1 and JA-1) to which calcium carbonate was added. In this study, therefore, calibration standards were prepared from known amounts of calcium carbonate and rock standard JA-1; the samples were ground and mixed in an agate mortar. The amount of carbonate carbon in JA-1 was determined by

the standard addition method; the linearity of the calibration graph was as reported earlier [2].

The analysis time depends on the carbon content. In general, 50 s was required for 0.05% carbon and 80 s for 5% carbon. The limit of detection is 2 μg of carbon at the 2 σ confidence level. The results are better than those given by gravimetric [3], titrimetric [4, 5], gasometric [6] and potentiometric [7] methods.

Analysis for non-carbonate carbon

For the direct determination of non-carbonate carbon in geological samples, the digestion method of Foscolos and Barefoot [8] was simpler and more convenient than others [3, 7] and was adopted after slight modification. The internal temperature of the crucible, which was important for digestion of the samples, reaches ca. 95°C when covered by a funnel, but only ca. 65°C without a cover. In general, 95°C provided good results for igneous samples, and 65°C for sediments (Table 1). Organic carbon moves to the upper rim of the crucible during the digestion of sediments at 95°C and this gives imperfect combustion.

There was no clear difference in the results obtained for samples digested in air or under nitrogen; complete combustion can be obtained by adding iron powder (ca. 0.6 g) and tungsten chips (ca. 1.3 g) for less than 0.5-g samples. An average blank value of 10 μg carbon was found. The calibration graph was prepared as described earlier [2].

Precision study

The precision and recovery for carbonate carbon in rocks were examined. Known amounts of calcium carbonate were added to JG-1 and JB-1. The results are given in Table 2. Similarly, the determination of non-carbonate carbon was studied by adding graphite. The relative standard deviations for 100 and 400 μg of carbon were 4 and 2%, respectively, and the recovery was 97—101%.

TABLE 1

Comparison of results for non-carbonate carbon (ppm) in selected samples at different digestion temperatures

Samples	Expected[a]	Digestion temperature	
		95°C	65°C
JG-1 Granodiorite	47	50, 41	85, 62
JB-1 Basalt	119	110, 124	240, 275
MRG-1 Gabbro	129	148, 156	330, 288
NBS-97a Clay	597	560, 585	590, 570
NBS-120a Phosphate	2050	1960, 1800	2000, 2060
GXR-2 Soil	26400	25200, 24600	25900, 26300

[a]Values obtained by subtracting carbonate carbon from the total carbon.

TABLE 2

Precision and recovery in the determination of carbonate carbon

Sample[b]	Taken (g)	Carbon (μg)		s_r (%)	Recovery (%)
		Added	Found[a]		
JG-1	0.5	0	86	4	—
	0.5	100	189	4	103
	0.2	500	530	1	99
	0.2	1000	1033	1	100
JB-1	0.5	0	176	3	—
	0.2	500	558	2	98
	0.2	1000	1075	1	100

[a]Average (n = 5). [b]Carbonate-carbon contents are 172 μg g^{-1} for JG-1 and 353 μg g^{-1} for JB-1.

Analysis of geological samples

The results of this study and independent data [4, 9—11] for carbonate carbon in U.S. Geological Survey Standards are listed in Table 3. Marinenko and May's data [11] were obtained by the phosphoric acid digestion—gas chromatographic method; Sen Gupta's data [4] were obtained by hydrochloric acid digestion followed by non-aqueous titration. The agreement between the results for G-2 is generally good. The results for AGV-1 and BCR-1 are very varied; the present results agree with those of Marinenko and May [11].

The results for carbonate and non-carbonate carbon in a variety of igneous standard reference samples are given in Table 4. Data for non-carbonate carbon in these samples have not been reported [9, 10]. Hoefs' [7] data for non-carbonate carbon in granites and granodiorites lay in the ranges 110—420 ppm and 75—260 ppm, respectively; these values are significantly higher than those obtained for G-2 and NIM-G granites, and GSP-1 and JG-1 granodiorites in this study.

TABLE 3

Comparison of results for carbonate carbon (given as % CO_2) in six U.S.G.S. standard rocks

Sample	This study[a]	Abbey [9]	Flanagan [10]	Marinenko and May [11]	Sen Gupta [4]
G-2	0.078	0.08	0.08	0.062	0.08
GSP-1	0.109	0.12	0.15	0.098	0.10
AGV-1	0.0033	0.01	0.06	0.0038	0.02
PCC-1	0.132	0.16	0.12	0.16	0.18
DTS-1	0.089	0.06	0.08	0.065	0.07
BCR-1	0.0037	0.03?	0.03	0.0041	0.02

[a]Average (n = 3).

TABLE 4

Analytical results for carbonate carbon and non-carbonate carbon in standard rocks and comparison with total carbon

Sample		Carbonate carbon (ppm)[a]	Non-carbonate carbon (ppm)[a]	Total carbon (ppm)	
				Present work	From ref. [2]
USGS	G-2 Granite	214	24	238	246
	GSP-1 Granodiorite	297	33	330	336
	AGV-1 Andesite	9	15	24	48
	PCC-1 Peridotite	360	112	472	543
	DTS-1 Dunite	243	90	333	314
	BCR-1 Basalt	10	20	30	67
CSRM	MRG-1 Gabbro	2883	154	3037	3012
	SY-1 Syenite	890	320	1210	1290
	SY-2 Syenite	1328	128	1456	1430
	SY-3 Syenite	1093	75	1168	1202
NIM	NIM-D Dunite	936	178	1114	1150
	NIM-G Granite	102	39	141	144
	NIM-L Lujavrite	358	84	442	432
	NIM-N Norite	111	87	198	222
	NIM-P Pyroxenite	124	111	235	283
	NIM-S Syenite	67	31	98	132
GSJ	JG-1 Granodiorite	172	43	215	219
	JB-1 Basalt	353	114	467	472
	JA-1 Andesite	6	21	27	40
	JB-2 Basalt	11	10	21	31

[a]Average (n = 3—5).

The results for limestone, feldspar, clay and phosphate (National Bureau of Standards samples) and soils, sediments and copper ore (Geochemical Exploration Reference samples) are listed in Table 5. High carbon contents were determined after the reference samples had been diluted with silicon dioxide. The NBS values for non-carbonate carbon in NBS-1a limestone are 0.53—0.69%; the lower value agrees with this study. For the NBS-98a plastic clay, 0.90% of total carbon was detected after grinding and drying (1 h at 150°C) to remove the water in the sample. The earlier value [2] of 0.81% is considered to have resulted from the presence of water.

The agreement between the values for carbonate plus non-carbonate carbon and the earlier values for total carbon is generally good (Tables 4 and 5) although samples such as AGV-1, BCR-1, NIM-S, JA-1, JB-2 and NBS-99a give values of carbonate plus non-carbonate carbon that are slightly lower than the total carbon values. The difference may arise from the presence of volatile carbon species.

TABLE 5

Analytical results for carbonate carbon and non-carbonate carbon in N.B.S. minerals and Geochemical Exploration Reference samples (GXR) and comparison with total carbon

Samples	Carbonate carbon (%)[a]	Non-carbonate carbon (%)[a]	Total carbon (%)	
			Present work	From ref. [2]
NBS-1a Limestone, argillaceous	9.10	0.53	9.63	9.73
NBS-88a Limestone, dolomitic	12.68	0.012	12.692	12.83
NBS-70a Feldspar, potash	0.0033	0.0014	0.0047	0.005
NBS-99a Feldspar, soda	0.0008	0.020	0.0208	0.03
NBS-97a Clay, flint	0.0003	0.058	0.0583	0.06
NBS-98a Clay, plastic	0.0010	0.91	0.911	0.90[b]
NBS-120a Phosphate	0.835	0.20	1.035	1.04
GXR-1 Jasperoid	0.124	0.016	0.14	0.17
GXR-2 Soil	0.0029	2.61	2.6129	2.64
GXR-3 Hot spring deposit	1.31	0.030	1.34	1.33
GXR-4 Porphyry copper ore	0.038	0.0083	0.0463	0.06
GXR-5 Soil	0.0063	1.56	1.5663	1.65
GXR-6 Soil	0.0036	0.16	0.1636	0.18

[a]Average (n = 3—5). [b]Determined after grinding and drying.

The author is grateful to Dr. A. Ando and Dr. S. Ishihara for helpful suggestions and critical reading of the manuscript.

REFERENCES

1 A. Ohnuma, S. Ihara and E. Oguchi, Gakushin Open-file Report (Jpn.), 19-9847 (1975).
2 S. Terashima, Anal. Chim. Acta, 101 (1978) 25.
3 R. W. Kotsch, F. M. D'itri and S. B. Upchurch, J. Sediment. Petrol., 46 (1976) 1026.
4 J. G. Sen Gupta, Anal. Chim. Acta, 51 (1970) 437.
5 J. L. Bouvier, J. G. Sen Gupta and S. Abbey, Geol. Surv. Can. Paper, 72-31 (1972).
6 L. Shapiro, U.S. Geol. Surv. Prof. Paper, 750-B (1971) B161.
7 J. Hoefs, Geochim. Cosmochim. Acta, 29 (1965) 399.
8 A. E. Foscolos and R. R. Barefoot, Geol. Surv. Can. Paper, 70-11 (1970).
9 S. Abbey, Geol. Surv. Can. Paper, 77-34 (1977).
10 F. J. Flanagan, Geochim. Cosmochim. Acta, 37 (1973) 1189.
11 J. Marinenko and I. May, U.S. Geol. Surv. Prof. Paper. 700-D (1970) D103.

Analytica Chimica Acta, 108 (1979) 119—125
© Elsevier Scientific Publishing Company, Amsterdam — Printed in The Netherlands

RAPID NON-DESTRUCTIVE DETERMINATION OF THIN FILMS OF PLATINUM BY PARTICLE BACK-SCATTERING

J. ROSENFARB* and H. A. LAITINEN

Department of Chemistry, University of Florida, Gainesville, Florida 32611 (U.S.A.)

J. T. SANDERS, and H. A. VAN RINSVELT

Department of Physics and Astronomy, University of Florida, Gainesville, Florida 32611 (U.S.A.)

(Received 23rd November 1978)

SUMMARY

Rutherford back-scattering of α-particles is used to determine trace amounts of thin films of platinum. The method is sensitive to 0.3 ng of platinum and the response is linear from at least 0.01 to 80 μg Pt cm^{-2} of substrate surface area. Calibration with weighed standards reveals good accuracy and precision throughout the linear range. Up to at least 80 μg cm^{-2}, no matrix effects can be observed for platinum determinations on Mylar, carbon, glass, and glass or quartz coated with up to 0.5 μm thicknesses of tin oxide. Particle-induced x-ray emission spectra are included to show their utility in surface composition analysis. The analytical procedure for the determination of platinum is rapid and non-destructive, and requires minimal sample preparation.

Analytical methods used to determine trace levels of platinum have included; colorimetry [1], atomic absorption (a.a.s.) [2, 3], polarography [4], neutron activation analysis (n.a.a.) [5], and electrochemical analysis of the total charge arising from the re-oxidation of chemisorbed hydrogen on platinum sites [6]. The first three of these techniques preclude sample retrieval for further manipulations. Neutron activation is relatively slow and is subject to a variety of interferences. The last method suffers from not necessarily being totally quantitative because of covered sites. A non-destructive and rapid determination of thin films of platinum on various substrates down to levels of less than 1 μg Pt cm^{-2} of surface area has proven to be a rather difficult problem. Furthermore, it is often desirable to be able to check for platinum homogeneity over the sample surface. Table 1 lists the practical detection limits for platinum obtainable by conventional methods for platinum determination and the limitations for each.

High-energy ion beams have become increasingly useful in surface science [8], medical research [9], environmental problems [10, 11] and to some degree for specific analytical determinations [10, 12—15]. Recently, it was pointed out that Rutherford back-scattering (RBS) was a useful technique for analyzing thin films [12]. Although RBS has been known for some time, the chemist has traditionally not utilized this technique even though thin

TABLE 1

Conventional methods for determination of platinum

Method	Practical det'n[a] limit ($\mu g\ cm^{-2}$)	Disadvantage	Reference
N.a.a.	2×10^{-6}[b]	Slow and background interferences	16
A.a.s.	2×10^{-3}	Requires removal of Pt	2,3
Colorimetry	2×10^{-1}	Requires removal of Pt sensitivity	1
Polarography (Pulse, d.p.p.)	6×10^{-4}	Requires removal of Pt	4
Adsorbed hydrogen re-oxidation	1×10^{-3}[c]	Only surface-exposed Pt	6
X-ray fluorescence	5×10^{-1}[d]	Lack of spatial distribution	16
P.i.x.e.	2×10^{-2}	Large background; requires standards	15

[a] Relevant to a 5-cm^2 surface area; platinum is dissolved and concentrated into 1 ml, in the cases where applicable.
[b] Assuming 10^{-5} $\mu g\ g^{-1}$ and about 6-cm^2 surface area.
[c] Assuming a sensitivity corresponding to a hundredth of a monolayer.
[d] Assuming 1 $\mu g\ g^{-1}$ and an area of 0.25 cm^2.

metal films are of frequent concern. The analytical method reported here satisfies the above requirements for detection and determination of trace levels of platinum as thin films on a number of different substrates. Included are particle-induced x-ray emission (p.i.x.e.) data which when coupled with RBS, enable the system to be described more completely.

EXPERIMENTAL

Instrumentation

Particles were accelerated to 2.5 MeV with a 4-MV Van de Graaff accelerator The beam was collimated and focused onto the target in a 3-mm^2 beam spot. Normally 150—200 nA of beam current was used to perform the analysis except for the more fragile Mylar targets, for which the current was kept as low as 2 nA. The scattered ^4He particles in the RBS experiments were detected in a 50-μm thick silicon surface-barrier detector located at 155° from the beam direction. The x-rays, produced for the particle-induced x-ray emission analysis (p.i.x.e.) were detected with a lithium-drifted silicon detector (80-mm^2 surface area, 5-mm thick) positioned at 135° from the beam direction. Protons were used in the p.i.x.e. experiments since they provided a lower overall background and therefore better counting statistics. The p.i.x.e. results were analyzed by using a General Automation 1830 on-line computer, equipped with magnetic tape, disk, plotter, graphics display, and line printer. For all RBS experiments, α-particles were used; for they provided enough energy resolution

to separate the platinum peak from the tin peak. Here, however, because of the simplicity of the energy spectra, no computer assistance was required for the data acquisition and manipulation, and a 512-multichannel analyzer was used.

Platinum targets

Platinum standards obtained from Micromatter (Seattle, Washington) were prepared by vacuum deposition through a precision mask onto a 2.5-μm Mylar substrate or a 30 $\mu g\ cm^{-2}$ carbon substrate. The amount of the deposit per unit area was then determined by using the weight difference and the mask area. All weighings were done with a Sartorius Model 1802 two-pan micro balance with a precision of ± 0.001 mg and an optical range accuracy of ± 0.0005 mg. A rolled Pt foil (700 $\mu g\ cm^{-2}$) standard was also used. Sample targets were either electrolytically-deposited or vapor-deposited on Mylar, Pyrex glass, quartz, carbon and tin oxide (1% antimony) on glass and quartz. All chemicals were of the purest available grade and were used without further preparation. Tin oxide preparations have been previously described [17].

Calculations

For the RBS experiments, two major equations are of concern [18]. The elastic scattering differential cross-section may be defined and calculated as follows:

$$d\sigma/d\Omega = [Z_1 Z_2 e^2/2E \sin^2\theta]^2 \{\cos\theta + [1 - (M_1/M_2 \sin\theta)^2]^{1/2}\}^2/ \quad (1)$$
$$[1 - (M_1/M_2 \sin\theta)^2]^{1/2}$$

where Ω is the solid angle subtended by the particle detector, Z_1 and Z_2 are the atomic numbers of the accelerated particle and the element determined, respectively. E is the energy of the incident particles just before scattering, θ is the angle between the detector and the beam direction, M_1 and M_2 are the masses of the projectile and element, respectively, and e is the electron charge. The amount of platinum is then given by:

$$N_{Pt} = N_c/(d\sigma/d\Omega)\, N_P \Omega \quad (2)$$

where N_{Pt} is the number of platinum atoms per unit area and by appropriate conversion yields the total number of μg of platinum per unit area; N_c is the number of elastically scattered particles and N_P is the number of incident particles. The angles, θ and Ω, determined by mechanical measurement, were estimated to be accurate to within 1% and 10%, respectively.

RESULTS AND DISCUSSION

Energy loss

Historically, investigators using RBS have tried to distinguish between "thick" and "thin" targets [13, 18]. A thick target may be described as one

in which there is an appreciable energy loss of the scattered particles because of non-elastic interactions in the sample as particles try to escape after collision. The thicker the sample is, the greater the loss of energy of the particles trying to escape from the lower depths. Figure 1 shows a broad flat-topped tin peak for a sample of platinum on a tin oxide film (about 0.5-μm thick as estimated from interference fringes [17]) on glass, indicating that for this target, the tin represents a "thick" layer or target. In this case the treatment of the data is more complicated although still solvable [19]. However, the resolved platinum peak in Fig. 1a is quite sharp and shows the characteristics of a "thin" target — or the lack of significant energy losses for elastically scattered particles. Theoretical calculations [18] show that about 300 μg Pt cm^{-2} is required for a full-width half-maximum broadening of 21 keV for incident 2.5-MeV α-particles. The resolution of the equipment used in this study was approximately 20 keV for RBS. However, floated and supported platinum loadings greater than 80 μg cm^{-2} showed line broadening of 50 keV or more. This observation indicates that at loadings greater than 80 μg cm^{-2} inelastic collisions are significantly increased. Thus, loadings under this limit must be regarded as thin targets and can be treated by using eqns. (1) and (2) To demonstrate the absence of energy loss arising from errors in the platinum films under 80 μg cm^{-2} used in this study, various loadings of platinum were analyzed at different target angles to the beam path in order to yield differen depths for beam penetration through the film for an identical amount of tota incident charge. Figure 2 indicates that although the tin peak, for tin oxide-supported platinum as an example, is significantly broadened at increasing angles, the platinum peak retains its sharp contour. The decrease in platinum peak intensity in Fig. 2(c) is due to spreading of the beam spot. Experiments showed that platinum loadings up to 80 μg cm^{-2} may still be regarded as "thin" platinum films and that errors arising from beam angle error are negligible.

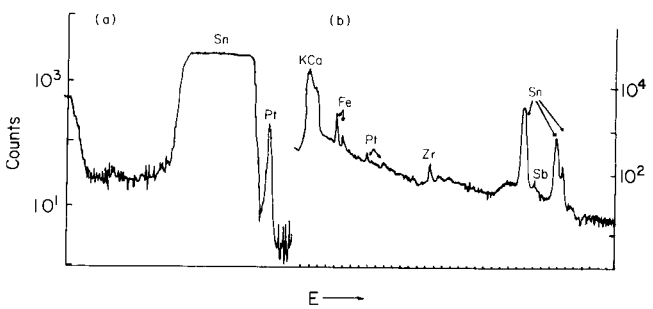
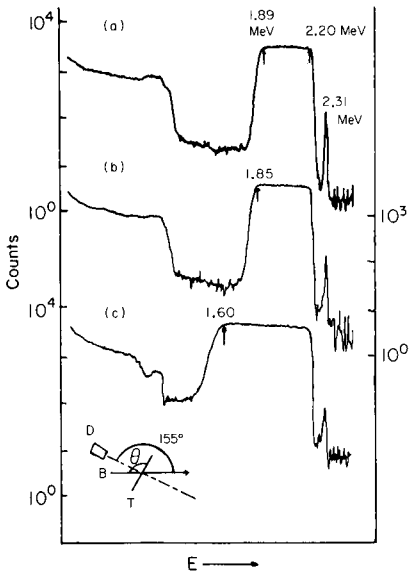


Fig. 1 (a) RBS spectra of 0.1 μg Pt cm^{-2} on tin oxide (1% Sb)—glass substrate. (b) P.i.x.e. spectra is in (a). The Pt L_α, L_{β_1}, L_{β_2}, and L_γ lines are normally located at 7.44, 11.07, 11.25 and 12.94 keV, respectively.



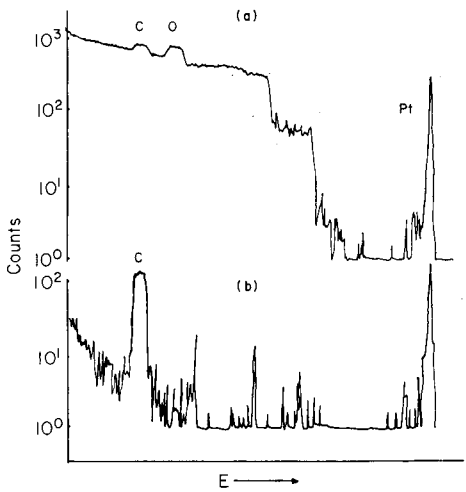


Fig. 2. RBS spectra of 1.0 μg Pt cm^{-2} on tin oxide—glass at varying θ values: (a) 90°; (b) 135°; (c) 160°. D is the detector, T the target, and B the beam direction.

Fig. 3. Comparison of RBS spectra for 1.3 μg Pt cm^{-2} on carbon on tin oxide (1% Sb)—glass (a) and for Pt—carbon after removal from the substrate (b).

Matrix effects

Several types of substrates for platinum films were studied in regard to their possible effect on platinum peak shapes and quantification. Figure 3, curve a, shows the RBS results for a platinum film prepared by vapor deposition on carbon, supported by a Pyrex sheet. After measurement by RBS, the carbon—platinum film was floated off on water, collected as a self-supported film and analyzed again. As seen in Fig. 3, curve b, the glass background is now missing, the carbon peak is still present, and the platinum peak retains the same line shape characteristics and gives quantitative results. Mylar, carbon and tin oxide coatings on glass and quartz did not have noticeable effects on the determination of platinum up to about 80 μg cm^{-2}.

Calibration and interferences

Table 2 compares the deviation of the RBS analysis from the values of standards. The total cumulative error was estimated to be about 15%; however, values in every case agree to within 10% in the range 1—80 μg Pt cm^{-2}, with a precision to within 1% at all loading levels. At least three points were used to determine precision. The 700 μg Pt cm^{-2} foil is not presented in Table 2, since this standard must be considered a "thick" target. No interferences were encountered for the types of samples and concentration ranges used in this study. Within the 9-mm^2 limitation of lateral resolution, samples investigated

TABLE 2

Calibration for platinum with RBS

Actual ($\mu g\ cm^{-2}$)	0.97 ± 25%	4.8 ± 10%	11.1 ± 5%	80 ± (<5%)
Found ($\mu g\ cm^{-2}$)	0.90	4.3	11.0	77

in this study were normally found to be macroscopically homogeneous by moving the beam around the sample surface and determining the platinum content at various locations about the sample.

Sample preparation and sampling time

Except for normal laboratory precautions such as beginning with clean surfaces [17] and reagents, little sample preparation preceded epoxying the samples to the target holder. The entire target preparation was accomplished by manual manipulation under normal laboratory conditions. After analysis, the sample in most cases was observably browned at the points of beam impact. The darkening was attributable mainly to organic material in the scattering chamber which was between 1.3×10^{-3} and 1.3×10^{-4} Pa (10^{-5} —10^{-6} torr). Target cooling was found to be unnecessary; the targets were not degraded by the beam, as evidenced by the identical results obtained from the same sample at the same location on different days. Table 3 indicates the relatively small sampling times required for various loadings of platinum under the typical conditions stated previously. Times listed in Table 3 correspond to those necessary to obtain distinct platinum peaks and good counting statistics for 150—200 nA of beam current. These times do not include approximately 5 min for target preparation and loading into the target chamber.

Complementary x-ray data (Fig. 1) show RBS to be more sensitive for platinum than is p.i.x.e., since the large background (compared to RBS) in the energy range of Pt x-ray lines decreases the signal-to-noise ratio when the same time scale is used. RBS has the advantage of giving direct counts with very low background counts whereas, because of background correction problems, p.i.x.e. requires significant background corrections and a standard, e.g. the use of RBS, for calibration. The low background for platinum with RBS also eliminates the need for the more extensive computerized data manipulations needed for p.i.x.e. spectra. However, p.i.x.e. data appear to be a significant complement to RBS spectra because elemental compositions at the surface may be studied. Such dual experiments may be done at the same time, thus providing determination of platinum and/or its macroscopic spatial distribution

TABLE 3

Sampling times for typical samples of platinum on glass matrices

Loading ($\mu g\ cm^{-2}$)	0.05	0.50	5.00
Time (min)	30	15	3

on a surface. A determination of surface compositions through elemental ratios of the substrate is also possible and is normally reliable to 1%.

Conclusions

Rutherford scattering has been shown to be a non-destructive, rapid analytical method for determining platinum films with good accuracy and precision in the range 0.01—80 $\mu g\ cm^{-2}$ of surface area. The sensitivity is comparable to, and in some cases better than, that of conventional techniques (Table 1). The quantitative limit of 0.01 $\mu g\ Pt\ cm^{-2}$ corresponds to a sensitivity of 0.3 ng Pt in the 3-mm^2 beam. With longer counting times and modified detectors, this limit may be significantly reduced. By doubling the longest counting time (Table 3), one still retains a relatively rapid analysis considering the lack of sample preparation and direct output of the data. The method lends itself to applications requiring the analysis of a large number of samples at trace platinum loadings. Energy losses for platinum films on tin oxide, glass, quartz, and Mylar surfaces appear to be negligible for coverages under 80 $\mu g\ cm^{-2}$, and are thus found to behave as "thin" films. RBS and p.i.x.e. appear to be powerful analytical tools for trace amounts of surface platinum and it is expected that their extension to other elements will also prove fruitful.

This research was supported by the U.S. Department of Energy (ERDA) grant EY-76-S-05-4947.

REFERENCES

1 E. B. Sandell, Colorimetric Determination of Traces of Metals, 2nd edn., Interscience, New York, 1950.
2 R. J. Coombes, A. Chow and R. Wageman, Talanta, 24 (1977) 421.
3 G. L. Everett, Analyst, 101 (1976) 348.
4 P. W. Alexander, R. Hoh and L. E. Smythe, Talanta, 24 (1977) 543; 24 (1977) 549.
5 W. Mielke, J. Electrochem. Soc., 122 (1975) 965.
6 T. Biegler, D. A. J. Rand and R. Woods, J. Electrochem. Soc., 24 (1977) 549.
7 S. A. E. Johansson and T. B. Johansson, Nucl. Instrum. Methods, 137 (1976) 473.
8 S. A. E. Johansson, Nucl. Instrum. Methods, 142 (1977) 1.
9 R. R. Zombola, P. A. Kitos and R. C. Bearse, Anal. Chem., 49 (1977) 2203; H. A. Van Rinsvelt, R. D. Lear and W. R. Adams, Nucl. Instrum. Methods, 142 (1977) 171.
10 J. A. Cooper, Nucl. Instrum. Methods, 106 (1973) 525.
11 R. L. Walter, R. D. Willis, W. F. Gutknecht and J. M. Joyce, Anal. Chem., 46 (1974) 843.
12 J. Buch and N. L. Balalikin, Mikrochim. Acta, 1 (1978) 19.
13 W. Reuter and A. Lurio, Anal. Chem., 49 (1977) 1737.
14 T. B. Johansson, R. A. Kselsson and S. A. E. Johansson, Nucl. Instrum. Methods, 84 (1970) 141.
15 J. V. Gilfrich, P. G. Burkhalter and L. S. Birks, Anal. Chem., 45 (1973) 2002.
16 Ulf Lindh, Ph.D. thesis, University of Uppsala, Sweden, 1978.
17 H. A. Laitinen and H. Kim, J. Am. Ceram. Soc., 58 (1975) 23.
18 Ion Beam Handbook for Material Analysis, J. W. Mayer and E. Rimini (Eds.), Academic Press, New York, 1977, pp. 5—11, 42—43 and 55—60.
19 J. F. Ziegler and W. K. Chu, Atomic Data and Nuclear Data Tables, 13 (1974) 463.

Analytica Chimica Acta, 108 (1979) 127—135
© Elsevier Scientific Publishing Company, Amsterdam — Printed in The Netherlands

THE DETERMINATION OF CARBON IN THE REFRACTORY METALS ZIRCONIUM, NIOBIUM, TANTALUM AND TUNGSTEN BY INSTRUMENTAL DEUTERON ACTIVATION ANALYSIS

C. VANDECASTEELE**, K. STRIJCKMANS and J. HOSTE*

Institute for Nuclear Sciences, Rijksuniversiteit Gent, Proeftuinstraat 86, B-9000 Gent (Belgium)

(Received 30th January 1979)

SUMMARY

Instrumental activation analysis is used for the determination of carbon in the refractory metals zirconium, niobium, tantalum and tungsten, based on the $^{12}C(d, n)^{13}N$ reaction induced by 5—7-MeV deuterons. $^{13}N(t_{\frac{1}{2}} = 10.0$ min) is detected via its annihilation radiation. The contribution of ^{13}N to the annihilation activity is separated from that of other β^+-emitters by decay-curve analysis. The method is free of nuclear interferences. The possible spectrometric interferences are discussed. Concentrations of 65.1, 24.8, 1.04 and <0.015 μg $C\,g^{-1}$, with relative standard deviations of 4.0, 5.9 and 14.0%, were obtained for zirconium, niobium, tantalum and tungsten, respectively.

The physical and especially the mechanical properties of the refractory metals are influenced [1] even by trace amounts of carbon. The determination of carbon in these materials is therefore of great technological and economic significance [2, 3]. The reference bureau of the European Communities (BCR, B-1049 Brussels, Belgium) organized a round-robin test to study the possibilities for the preparation and analysis of a certified reference material for carbon in zirconium. The refractory metals group of the "Gesellschaft Deutscher Metallhütten und Bergleute" carried out intercomparisons concerning the determination of carbon in molybdenum and tungsten. It appeared that the classical determination of carbon by combustion in an oxygen stream is subject, at least for these refractory metals, to important systematic errors. Below 10 μg $C\,g^{-1}$, analysis is not feasible by this technique [2].

Other analytical methods for determining low carbon concentrations in refractory metals are therefore needed. These methods should preferably be purely instrumental to avoid the difficult chemical separation of carbon (or, e.g., nitrogen) from such materials. Photon activation analysis can be applied to determine carbon in refractory metals but often requires elaborate chemical separation of the ^{11}C formed [4, 5], which is of course a source of possible systematic errors. Activation analysis with charged particles allows an instrumental determination of carbon in many refractory metals.

**"Bevoegdverklaard Navorser" of the N.F.W.O.

TABLE 1

Nuclear reactions for the determination of carbon

Nuclear reaction	Threshold (MeV)	Nuclear interferences	Threshold (MeV)	$A/10^{-6}$ [a] (cpm)
$^{12}C(d,n)^{13}N$	0.3	$^{14}N(d,t)^{13}N$	4.9	1500[b]
$^{12}C(^3He,\alpha)^{11}C$	$Q > 0$	$^{9}Be(^3He,n)^{11}C$	$Q > 0$	950[b]
		$^{10}B(^3He,d)^{11}C$	$Q > 0$	
		$^{16}O(^3He,2\alpha)^{11}C$	6.3	
$^{12}C(^3He,n)^{14}O$	1.4	$^{14}N(^3He,t)^{14}O$	6.2	8.4[c]
		$^{16}O(^3He,\alpha n)^{14}O$	9.9	

[a] Activity at the end of irradiation for a zirconium sample containing 1 μg C g^{-1}, irradiated for 1 $t_{\frac{1}{2}}$ with a 1-μA beam of 5-MeV deuterons or 10-MeV ^{3}He. [b] For a γ,γ-coincidence set-up with two 7.6 × 7.6-cm NaI(Tl) detectors. [c] For a Ge(Li) detector.

Several nuclear reactions can be used to determine carbon. Table 1 summarizes some useful reactions, with their thresholds, the nuclear interferences and the activity for an irradiated zirconium sample containing 1 μg C g^{-1} under defined conditions. The $^{12}C(^3He,n)^{14}O$ reaction leads to $^{14}O(t_{\frac{1}{2}} = 70.6$ s) which emits 2313-keV γ-rays that allow a very selective analysis if a Ge(Li) detector is used. The sensitivity is, however, rather low. The other two reactions are more sensitive but lead to pure β^+-emitters. The $^{12}C(^3He,\alpha)^{11}C$ reaction suffers interference from reactions on boron and beryllium. The $^{12}C(d,n)^{13}N$ reaction was preferred, since it is free of nuclear interferences if the energy is below 4.9 MeV.

If a purely instrumental determination is required, the particle energy should be sufficiently low that the matrix is activated only to a negligible extent. For zirconium and niobium, the Coulomb barrier is about 7 MeV, and for tantalum and tungsten about 11 MeV. The incident energy chosen was between 4.9 and 3.8 MeV, which is not only well below the Coulomb barrier but also below the threshold of the interfering reactions.

EXPERIMENTAL

Samples, standards and irradiation

The samples were cylindrical disks (15 or 20 mm diameter, 1 mm thick). The standards used were pellets of graphite, polyethylene or nylon 6.

The samples and standards were irradiated in vacuum (10^{-2} Pa) with a 5- or 7-MeV deuteron beam extracted from the CGR-MeV 520 isochronous cyclotron of Gent University. The beam was collimated with a collimator of 12-mm diameter. A nickel foil (11.15 mg cm^{-2} for the irradiation of Zr, 11.7 mg cm^{-2} for Ta and W and 11.8 mg cm^{-2} for Nb) was placed in front of the sample to monitor the beam intensity. For the Ta and W samples, a molybdenum foil (24.5 mg cm^{-2}) was placed between the nickel foil and the sample to stop recoil nuclei from the monitor foil. Table 2 summarizes the irradiation conditions. For the standards the irradiation time was 1 min and the intensity 0.1 μA.

TABLE 2

Irradiation conditions

	Zr	Ta, W	Nb
Deuteron energy (MeV)	5.00	7.00	7.00
Energy after monitor (Ni) and recoil catcher foil (Mo) (MeV)	4.12	4.92	6.26
Energy corresponding to depth of etching (MeV)	3.4—3.8	3.5—3.8	4.7—4.9
Beam intensity (μA)	1	2	1
Irradiation time (min)	3	5	2

Chemical etching after irradiation

After irradiation, the samples were etched in acid mixtures to remove a 5—30 mg cm^{-2} surface layer. The etching conditions are summarized in Table 3. The thickness removed was determined by weighing and checked by means of a micrometer.

Measurements

The samples were measured with a γ,γ-coincidence measuring set-up consisting of two 7.6 × 7.6-cm cylindrical NaI(Tl) detectors at 180°. The niobium samples and the corresponding standards were measured with a Ge(Li) detector coupled to a multichannel analyser. Measurements started 2—25 min after irradiation. For niobium, the waiting time was kept short (2 min) to allow the simultaneous determination of oxygen and nitrogen. Each sample was measured repeatedly for 1 or 2 min during a 100—250-min period. This made it possible to obtain the decay curve of the measured activity.

For the standards, the measuring cycle was similar but was started 80—120 min after irradiation.

The flux monitors for the samples and the standards were measured, respectively, for 1—5 min, 250—500 min after irradiation and for 5—20 min, 80—220 min after irradiation. The 283-keV peak of ^{61}Cu ($t_{\frac{1}{2}}$= 3.41 h) formed by the ^{60}Ni(d,n)^{61}Cu reaction was integrated and used as a measure of the beam intensity.

TABLE 3

Etching conditions

Sample	Mixture	Temperature	Duration (s)	Thickness removed (mg cm^{-2})
Zr	HF/H_2O (1 + 40)	room	2 × 60	5—10
Nb	HF/HNO_3 (1 + 1)	room	5	18—28
Ta	HF/HNO_3 (3 + 2)	room	2 × 50	25—30
W	HF/HNO_3 (1 + 1)	room	2 × 50	24

Standardization

The carbon concentration is obtained from the equation

$$C_X = C_S \frac{A_X}{A_S} \frac{I_S}{I_X} \frac{S_S}{S_X} \left[\int_{E_i}^{0} \sigma_E \frac{dE}{(dE/dl)_S} \Big/ \int_{E_i}^{0} \sigma_E \frac{dE}{(dE/dl)_X} \right] \quad (1)$$

where C is the concentration ($\mu g\ g^{-1}$); A the ^{13}N activity at the end of the irradiation; I the beam intensity obtained from the ^{61}Cu activity of the flux monitor; S the saturation factor for ^{13}N production; σ_E the cross-section at energy E; and dE/dl the stopping power (MeV g^{-1} cm^2). The subscripts X and S refer to the sample and the standard, respectively.

The last factor in the equation is calculated as a function of the incident energy E_i by numerical integration, based on the excitation function for the $^{12}C(d,n)^{13}N$ reaction [6] and the stopping powers tabulated in the literature [7].

In eqn. (1), it is assumed that the sample and the standard are irradiated with particles of energy E_i. In practice, this cannot easily be realised as post-irradiation etching does not always remove the same thickness from the sample. Therefore the activity A_S is deduced from a calibration curve where $A_S/I_S S_S$ is given as a function of E_i; typical curves are shown in Fig. 1. For the experimental establishment of such curves, graphite pellets were irradiated behind different numbers of nickel foils (11.8 mg cm^{-2}), the first of which served as a beam intensity monitor. The first point corresponds to 2 nickel foils, the second to 3 foils and the third to 4 foils. For zirconium, a more detailed curve was obtained by using aluminium foils (4.80 mg cm^{-2}) to degrade the energy. This curve is also shown in Fig. 1. For niobium, a similar curve was obtained between 4.0 and 5.4 MeV.

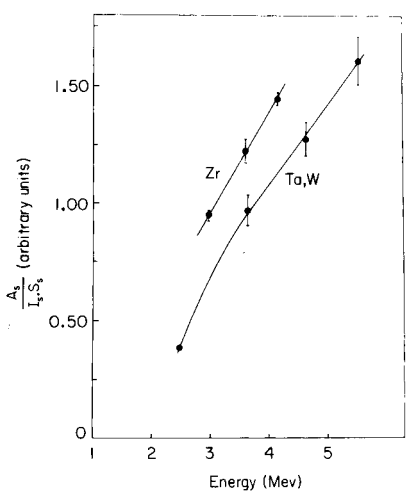


Fig. 1. Calibration curve used for the determination of carbon in Ta and W and in Zr (see text). The curve for Zr has arbitrarily been shifted towards higher ordinate values.

TABLE 4

Analysis of decay curves

Sample	Waiting time[a] (min)	Components[b]	$t_{\frac{1}{2}}$ for ^{13}N (min)
Zr	15	^{13}N, ^{61}Cu	10.14 ± 0.27
Nb	2	^{17}F, ^{15}O, ^{13}N	10.6 ± 1.5
Ta	16—25	^{15}O, ^{13}N, (^{61}Cu?)	10.57 ± 0.19
W	7—11	^{15}O, ^{13}N	—

[a]Time between end of irradiation and start of the first measurement used for the analysis of the decay curve. [b]Components used for the resolution of the decay curves by means of the CLSQ-program.

RESULTS AND DISCUSSION

Analysis of decay curves

When the appropriate waiting times were observed, the decay curves contained the components mentioned in Table 4. ^{17}F ($t_{\frac{1}{2}}$ = 66 s) is formed by the $^{16}O(d,n)^{17}F$ reaction, ^{15}O ($t_{\frac{1}{2}}$ = 2.05 min) by the $^{14}N(d,n)^{15}O$ reaction, ^{13}N ($t_{\frac{1}{2}}$ = 9.97 min) by the $^{12}C(d,n)^{13}N$ reaction, and ^{61}Cu ($t_{\frac{1}{2}}$ = 3.41 h) by the ^{60}Ni $(d,n)^{61}Cu$ reaction.

In each case a good fit to the experimental data was obtained when the components indicated were used to resolve the decay curves by means of the CLSQ program [8]. Furthermore, it was verified that, when the first 2 or 3 measurements, for example, were not used in the calculations, the same result was obtained within experimental error. Iterative calculation of a best value for the half-life of ^{13}N yielded the values shown in Table 4. In general, the agreement with the literature value of 9.97 min is satisfactory. Figure 2 shows the decay curves for zirconium and tantalum.

Interferences

Nuclear interferences have already been mentioned in Table 1. Below 4.9 MeV, there are no nuclear interferences Various radionuclides that emit β^+-radiation and have a half-life close to 10 min can be formed, however. Most of these emit γ-rays to a significant extent, so that they can be detected by Ge(Li) γ-spectrometry. As shown in Fig. 3, a Ge(Li) spectrum of zirconium contains the 658-keV peak of ^{97}Nb ($t_{\frac{1}{2}}$ = 72 min) formed by the $^{96}Zr(d,n)^{97}Nb$ reaction and the 1779-keV peak of ^{28}Al ($t_{\frac{1}{2}}$ = 2.31 min) from the $^{27}Al(d,p)^{28}Al$ reaction. None of these radionuclides emits β^+-radiation.

Figure 4 shows a Ge(Li) spectrum for tantalum, where a 511-keV peak and peaks of ^{182}Ta ($t_{\frac{1}{2}}$ = 115 d) and of ^{182m}Ta ($t_{\frac{1}{2}}$ = 16.0 min) are evident. These radionuclides do not emit β^+-radiation. An analogous spectrum for tungsten showed the ^{187}W peaks ($t_{\frac{1}{2}}$ = 24 h) from the $^{186}W(d,p)^{187}W$ reaction and the ^{28}Al peaks.

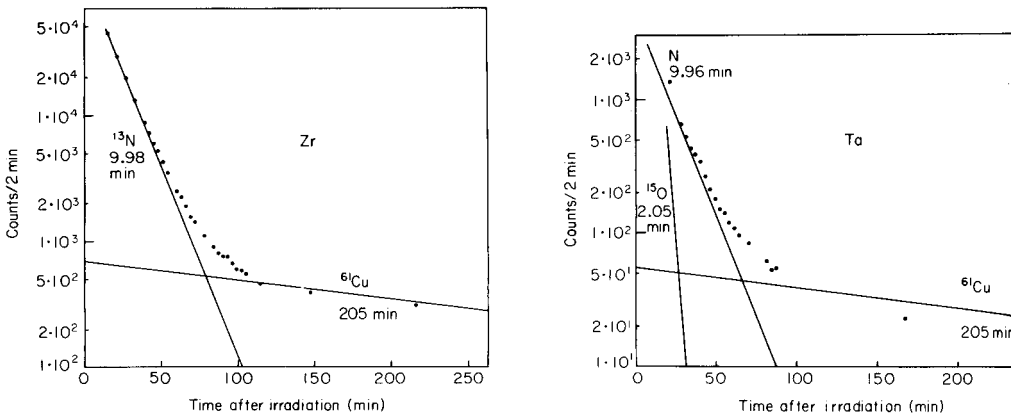


Fig. 2. Decay curves for zirconium and tantalum after irradiation for 5 min at a beam intensity of 2 μA.

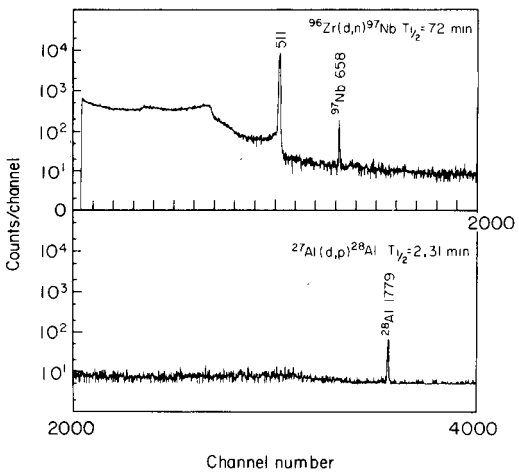


Fig. 3. Ge(Li) spectrum for zirconium after irradiation for 3 min at a beam intensity of 1 μA; measurement time, 3 min.

Some pure or practically pure β^+-emitters with half-lives between 5 and 20 min can also be formed by deuteron reactions with stable elements, e.g. ^{136}La, ^{162}Ho, ^{62}Cu, ^{134}La and ^{120}Sb. Except for ^{62}Cu, all of these are formed from heavy elements. At the low energies used, the cross-sections for deuteron reactions with heavy elements are very small, so that the interferences can be neglected as long as the interfering radionuclide cannot be formed from the matrix. ^{62}Cu ($t_{\frac{1}{2}}$ = 9.73 min) can be formed by the ^{61}Ni(d,n)^{62}Cu and ^{64}Zn(d, α)^{62}Cu reactions. However, from nickel, ^{61}Cu ($t_{\frac{1}{2}}$ = 3.41 h, E_γ = 283 and 656 keV) is formed by the ^{60}Ni(d,n)^{61}Cu reaction; from zinc, ^{65}Ga ($t_{\frac{1}{2}}$ = 15.2 min, E_γ = 115 keV) is formed by the ^{64}Zn(d,n)^{65}Ga reaction. By means of pure nickel samples irradiated under the same conditions as the samples, the ratio of the

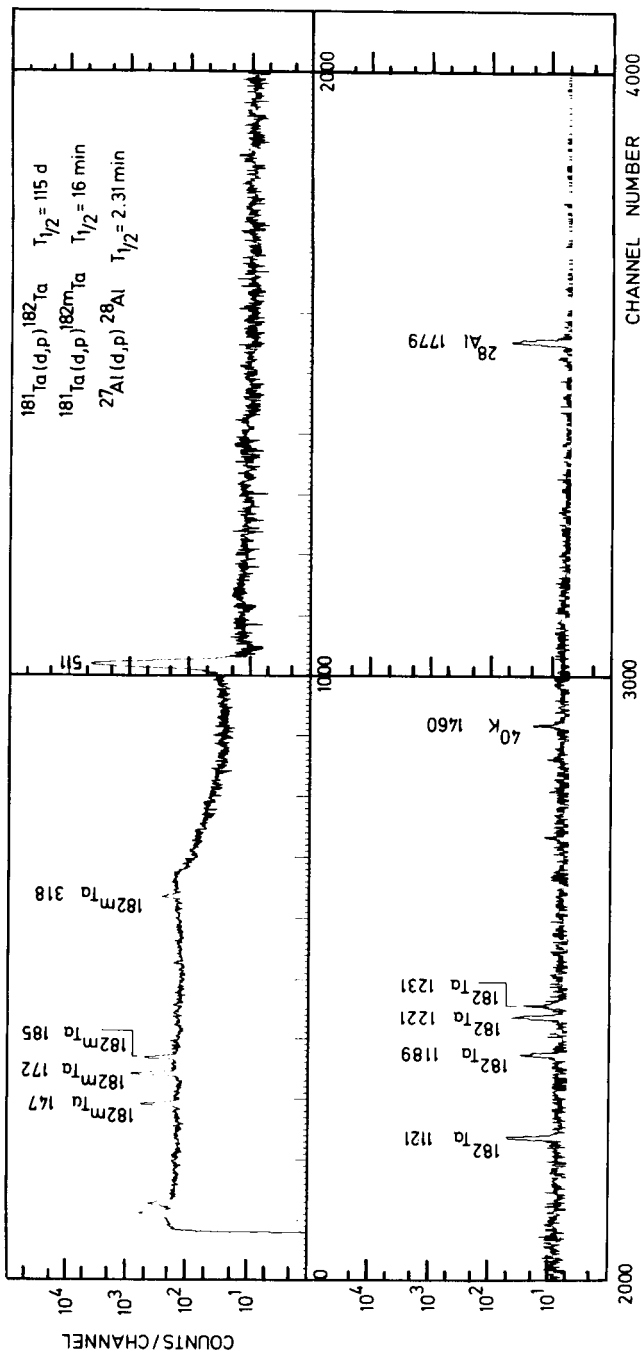


Fig. 4. Ge(Li) spectrum for tantalum after irradiation for 5 min at a beam intensity of 2 μA; measurement time, 5 min.

283-keV and 656-keV peaks in the Ge(Li) spectrum to the ^{62}Cu contribution to the 511-keV peak, i.e. the 9.73-min component in the decay curve of this peak, was deduced for a given waiting time after irradiation. With pure zinc samples, the ratio of the 115-keV peak from ^{65}Ga to the 511-keV peak was determined for a given waiting time and for the same irradiation conditions as the samples. From the Ge(Li) spectra of the analysed materials, it was deduced that the interference of ^{62}Cu from zinc with the determination of carbon is at most 0.4, 7 and 5% for Zr, Nb and Ta, respectively. For ^{62}Cu from nickel the corresponding figures are 0.6, 0.5 and 4%.

Analysis of samples

Table 5 summarizes results obtained by repeated analysis of the refractory samples involved. The precision can be considered as satisfactory. The results for carbon in zirconium were compared during a preliminary round-robin test organized by BCR with those obtained by the classical combustion method. The results from the latter method ranged from 61 to 92 μg C g^{-1} with a mean value of 75 μg g^{-1} and a standard deviation of 9 μg g^{-1}.

For tungsten the carbon concentration was very low. The resulting activity was so low that it was impossible to determine with certainty the half-lives of the components of the decay curve; therefore, only upper limits for carbon are given. These limits were calculated from a 2-min measurement 15 min after irradiation, by means of the equation $L = A + 3A^{1/2}$, where L is the upper limit for the ^{13}N activity (counts per 2 min), and A is the recorded number of counts per 2 min. The corresponding upper limit for the carbon concentration is given in Table 5. This limit is surprisingly low, for chemical methods such as combustion in an oxygen stream usually yield results for tungsten at the 1—10 μg C g^{-1} level, probably because of blank problems.

In general, the sensitivity of this method greatly exceeds that of other analytical methods (except perhaps for photon activation analysis), whilst the precision is at least similar to that of the combustion method.

TABLE 5

Results for carbon in refractory metals

Matrix	Mean (μg g^{-1})	n	s (μg g^{-1})	s_r (%)
Zr	65.1	14	2.6	4.0
Nb	24.8	5	1.5	5.9
Ta	1.04	6	0.15	14.0
W	<0.015	5	—	—

Thanks are due to R. Kieffer and J. Dewaele for technical assistance and to J. Pauwels (BCR and BCMN, Geel) and H. Ortner (Metallwerk Plansee) for providing the samples. The financial support of the N.F.W.O. and I.I. K.W. is gratefully acknowledged.

REFERENCES

1 E. Fromm and E. Gebhardt, Gase und Kohlenstoff in Metallen, Springer Verlag, Berlin, 1976.
2 H. Ortner, The analysis of O, N and C-traces in the refractory metals Mo and W. An international effort, Euroanalysis III, Dublin, Aug. 1978.
3 Technological and economic significance of the determination of carbon in molybdenum and tungsten, BCR, Commission of the European Communities, Brussels, 1978.
4 M. Fedoroff, C. Loos-Neskovic and G. Revel, J. Radioanal. Chem., 38 (1977) 107.
5 C. Engelmann, J. Gosset and C. Grumet, J. Radioanal. Chem., 28 (1975) 185.
6 R. Jaszczak, R. Macklin and J. Gibbons, Phys. Rev., 181 (1969) 1428.
7 C. Williamson, J. Boujot and J. Picard, Tables of range and stopping power of chemical elements for charged particles of energy 0.05 to 500 MeV, Rapport CEA-R 3042, 1966.
8 J. Cumming in G. O'Kelley (Ed.), Applications of Computers to Nuclear and Radiochemistry, NAS-NS 3107, 1963.

Analytica Chimica Acta, 108 (1979) 137—147
© Elsevier Scientific Publishing Company, Amsterdam — Printed in The Netherlands

DETERMINATION OF THE TOTAL AMOUNT OF ORGANICALLY BOUND CHLORINE, BROMINE AND IODINE IN ENVIRONMENTAL SAMPLES BY INSTRUMENTAL NEUTRON ACTIVATION ANALYSIS

J. GETHER and G. LUNDE

Central Institute for Industrial Research, Oslo (Norway)

E. STEINNES*

Institutt for Atomenergi, Kjeller (Norway)

(Received 18th December 1978)

SUMMARY

The determination of chlorine, bromine and iodine present as non-polar, hydrophobic hydrocarbons in environmental samples is reported. The organohalogen compounds are separated from water into an organic phase by on-site liquid—liquid extraction, and from biological material by procedures based on lipid phase extraction and codistillation. After removal of inorganic halides by washing with water and concentration of the sample by evaporation of the solvent, the resulting extracts are analyzed for their chlorine, bromine and iodine contents by instrumental neutron activation analysis. Strict attention is paid to the possibility of contamination in every step of the procedure. Background values in routine analysis are approximately 100—200 ng of chlorine, <5 ng of bromine and <3 ng of iodine.

Chlorinated hydrocarbons are introduced to the environment through a large variety of technical processes, and have received ever-increasing attention as environmental pollutants in recent years. The best-known chlorinated micro-pollutants are various insecticides (e.g. dieldrin and DDT) and industrial chemicals such as polychlorinated biphenyls (PCB). These compounds may occur at concentration levels of about 1 ng l^{-1} in water [1—3] and about 1 μg g^{-1} in marine biological material [4, 5]. Organically bound bromine and iodine are known to occur in water [1] and in marine organisms [6], but very little is known about the origin and composition of such substances. Compared to chlorine, much smaller amounts of organic bromine and iodine are introduced to the environment by man.

Because of the widespread technical use of chlorine, chlorinated hydrocarbons and chlorinating processes, the level of chlorinated hydrocarbons in the environment may constitute a general index of exposure to man-made micro-pollutants. While individual components can be determined at very low concentration levels by gas chromatography, no generally applicable methods have been reported for the determination of the total amount of organically bound chlorine in a sample. In this paper, neutron activation analysis (n.a.a.)

is proposed as a suitable technique for the determination of total amounts of organically bound halogens in environmental samples after appropriate separation and concentration procedures. This kind of approach was first described by Schmitt and Zweig [7] who used n.a.a. for the determination of "total organic chloride" in butterfat by a procedure somewhat similar to the one described here. More recently [1], the possibility of monitoring the total amount of non-polar chlorinated hydrocarbons in the environment through measurement of their chlorine content by n.a.a. was suggested. This approach has been found very useful in our studies related to halogenated hydrocarbons in recent years. The present paper gives a description and discussion of the experimental procedures used for the determination of organically bound chlorine, bromine and iodine in environmental samples.

A complete analysis consists of sampling, sample preparation, removal of inorganic halides, and simultaneous determination of organically bound Cl, Br and I by instrumental n.a.a. In the sample preparation step the halogenated hydrocarbons are isolated from the bulk sample by extraction into an organic phase. In the case of water, this is accomplished on the site by liquid—liquid extraction with hexane in a continuous stirred extractor as described by Ahnoff and Josefsson [8]. In the analysis of biological material, the halogenated compounds are isolated along with the lipid phase by extracting the homogenized sample material with a mixture of isopropanol and hexane [9, 10] For a separation of the more volatile fraction of the halogenated hydrocarbons [10], codistillation with cyclohexane is used. After removal of possible traces of inorganic halides by washing with water and concentration by evaporation, the residual organic extracts are usually divided in two parts, one being used for the activation analysis, and the other for the determination of individual chlorinated hydrocarbons by gas chromatography.

To obtain meaningful results at the low levels at which organically bound halogens occur in environmental samples, strict attention to the control of contamination is essential. This applies to the whole analytical procedure including the sampling and the transport of samples to the laboratory.

EXPERIMENTAL

Purification of solvents

The solvents to be used, i.e. cyclohexane, n-hexane, isopropanol and acetone (for cleaning apparatus) are purified by distillation in the apparatus shown in Fig. 1. Column (1) is a rectification column (1500 mm length, 25 mm diameter) filled with stainless-steel turnings produced in a lathe, and insulated with a 30-mm thick layer of expanded polystyrene foam. The solvent to be purified is introduced through the inlet of a 1-l flask (2) equipped with a Teflon stopcock in the bottom, which allows the apparatus to be drained and cleaned without dismantling. Condenser (3) is fitted with an adapter (4) to the 1-l funnel (5) used as receiver. This funnel may be detached from the apparatus and used elsewhere in the laboratory, in which case a "swan-neck"

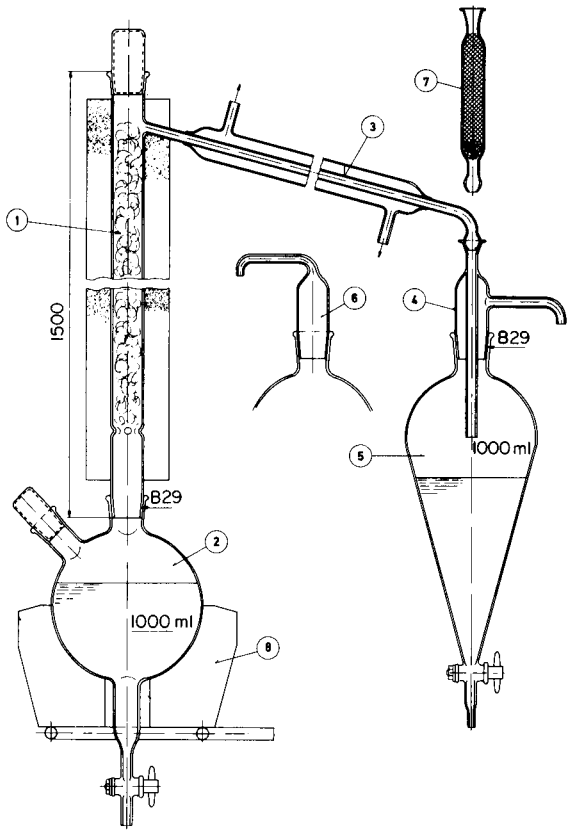


Fig. 1. Distillation apparatus. See text for key to numbering.

adapter (6) prevents dust from entering. An activated carbon trap (7) may be inserted behind the condenser. Heating is done with a normal mantle (8). When 80—90% of the solvent has been distilled off, the residue is drained through the bottom stopcock of flask (1). The apparatus is completely closed to the atmosphere, and may be operated with an inert gas such as highly purified nitrogen.

If heat-labile solvents or benzene are to be purified, the heating mantle is replaced by an aluminium block (see below), and the apparatus is purged with nitrogen. Circulating water or oil-baths tend to contaminate the work area, and should not be used.

When n-hexane or cyclohexane is to be distilled, 10 ml of a 10% (w/v) solution of sodium metal in anhydrous ethanol per liter of solvent is added prior to distillation. In the case of isopropanol, 0.1 g of sodium metal is added directly. Acetone is purified without any additions. Technical-grade solvents are used as starting materials. Blanks are run on all solvents before use. Although the apparatus may be rinsed from the top of the rectification column,

the lowest and most reproducible blank values are obtained when rinsing and dismantling of the apparatus are reduced to a minimum.

Distilled water is prepared in an all-glass apparatus over alkaline potassium permanganate. Small sliced pieces of Teflon sheet efficiently prevent bumping.

Cleaning of apparatus

Materials for which proven cleaning procedures do not exist should not be used in this kind of work. Two suitable procedures are as follows. Centrifuge tubes and flasks of a volume less than about 1 l are kept overnight at 550°C in an oven used for annealing glassware. The glassware is placed in large beakers with raised lids, where it is exposed to the atmosphere but protected from dust. It is subsequently stored in the same beakers with a large Petri dish as cover, and treated as if sterile. All flasks are stoppered as soon as they have cooled sufficiently. For apparatus that cannot easily be placed in the annealing oven, thorough rinsing with purified acetone is employed. This method was tested with low levels of PCB, and found to give satisfactory results with glass and with smooth surfaces of stainless steel.

No procedure has been found that will satisfactorily clean any type of plastic surface without destroying it. The use of plastic equipment, except for the Teflon stopcocks mentioned above, should therefore be avoided in this type of trace analysis.

Sample preparation

On-site liquid—liquid extraction. The apparatus used consists of three main parts: an extraction unit, a magnetic stirring device and a pump. The extraction unit has been described by Ahnoff and Josefsson [8]. The water is continuously pumped into an 800-ml extraction chamber and mixed vigorously with 200 ml of an organic solvent less dense than water. The resulting emulsion is separated in the lower part of the chamber and the water extracted is drained off at constant flow. The flow rate is about 4 l h^{-1} and the total volume of water extracted is typically about 200 l. The organic extract, usually in n-hexane, is transported to the laboratory in glass flasks with glass stoppers.

Lipid phase extraction. About 50 g of tissue is homogenized in a Waring-type blender, transferred to a glass-stoppered flask to which twice the weight of a 1:1 isopropanol/hexane mixture is added, and placed in an ultrasonic bath for 15 min. The flask is subsequently placed in a shaking apparatus or on a ball mill (100—200 rpm) for 24 h at 20°C. The mixture is allowed to settle and the hexane phase is separated.

Codistillation. About 500 g of tissue is homogenized in a Waring-type blender with 1 l of distilled water and transferred to a distillation apparatus equipped with a condenser and a receiving flask. Then 10 ml of cyclohexane is added, the sample is carefully brought to boiling, and about 25 ml of water is distilled over along with the cyclohexane. The apparatus is cooled to 20°C, another 3 ml of cyclohexane is added, and distillation is continued for 4—5 min to flush out traces of volatile compounds remaining in the condenser.

To obtain a better idea of the volatility of the halogenated hydrocarbons, this distillation sequence may be repeated, and the second distillate analyzed separately [10].

Concentration of extracts. In most cases, the extracts are evaporated to a volume of a few ml in a modified Kuderna-Danish apparatus (Fig. 2). The modifications provide better retention of volatile material through an efficient column with provision for regulating the reflux rate, an aluminium heating body of known and controllable temperature to prevent overheating of the glass walls and possible destruction of sample material, and facilities for operation under vacuum or in inert gas. The distillation column (1, 2) is constructed from two pieces of concentric glass tubing with a glass rod wound as a coil in the space between them; the diameter of the inner tube is about 20 mm, and the space between the inner and the outer tube is about 2 mm.

The column is insulated with expanded polystyrene foam. The inserted tube (3) is an inverted condenser, the length of which may be varied by lifting or lowering the central tube and the bottom closure attached to it. The sample

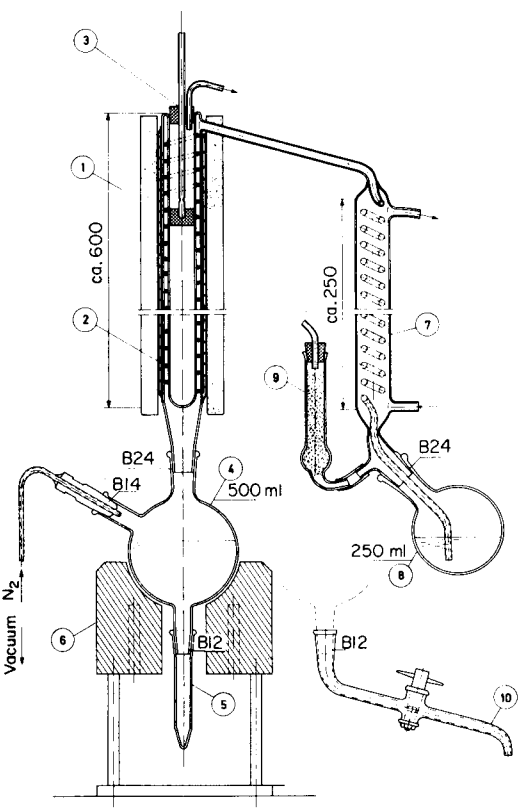


Fig. 2. Modified Kuderna-Danish apparatus. See text for key to numbering.

is distilled from a 500-ml round-bottom flask (4) to which a 10-ml centrifuge tube may be attached by means of a B12 ground-glass joint. Heating is effected by an aluminium block (6) machined to fit the flask, and fitted with three 150-W soldering iron elements connected to an adjustable mains supply. The block also has a thermometer and a spring under the centrifuge tube to keep it in position (neither is shown in Fig. 2). A second ground-glass joint allows introduction of nitrogen gas into the flask, or application of vacuum for cleaning (see below). An ordinary condenser (7) is fitted to a 250-ml receiving flask (8), and a tightly packed glass wool filter (9) prevents access of particulate material. This filter may be connected to a vacuum line for operation at reduced pressure.

In operation, the sample to be concentrated is introduced into the evaporation flask through a funnel attached to the B14 ground-glass joint. (For complete closure to the atmosphere a separating funnel equipped with a Teflon stopcock and a male glass joint may be used.) The aluminium block is set at a suitable temperature (60—70°C for hexane), and the reflux condenser is adjusted to give a suitable reflux ratio. A flow of nitrogen (30—50 ml min^{-1}) is started simultaneously. With most of the sample removed, the round-bottom flask is rinsed by applying vacuum momentarily to the nitrogen inlet, so that a portion of the distillate is sucked back into the distillation column. This is repeated twice as the surface of the liquid becomes visible beneath the aluminium block. Evaporation of the sample will stop at this stage, and the sample is left in an unheated state until removed from the apparatus. This is done simply by removal of the centrifuge tube. The concentration of one 200-ml sample to 4 ml requires about 90 min, and about 5 min of attention and supervision.

Smaller final volumes can be achieved by using centrifuge tubes with greater taper at the bottom. Accurate determination of the concentrated sample is best achieved by weighing.

The apparatus is rinsed by substituting the draining attachment (10) for the centrifuge tube and a flask containing purified acetone for the receiver, and applying vacuum from a water aspirator to the nitrogen inlet. Two such rinses were found to be sufficient. The acetone is drained and the draining attachment replaced by a clean centrifuge tube to prepare the apparatus for a new sample. Traces of acetone remaining in the apparatus do not affect further analyses as described in this paper.

Removal of inorganic halides. Traces of inorganic halides are eliminated by washing the extracted phase with distilled water. This is always done before, and in some cases also after, the concentration step. Washing of sample volume larger than a few millilitres with water is done in glass-stoppered separatory funnels equipped with Teflon taps and with the tapered outlets. For smaller volumes glass-stoppered (B12) centrifuge tubes are used. About equal volumes of water and organic phase are employed. Separatory funnels are placed for 10—20 min in a reciprocating shaker (Edmund Bühler, type SM2, Tübingen, Germany); the contents of centrifuge tubes are intimately mixed by means of a "Whirlimixer" (Fison's Scientific Apparatus, Loughborough, England).

Extractions are repeated three times. Emulsions should be avoided. They normally cause no problems with hexane extracts, but may be encountered with oils that contain much phospholipid; in such cases, the addition of some isopropanol will help.

Neutron activation analysis

After the final work-up of samples, the part of the sample intended for the determination of total organically bound halogens is sealed in a glass ampoule and stored in a refrigerator until n.a.a. can be done.

For irradiation, 1—2 ml of the sample is sealed in an ampoule made from polyethylene tubing. These ampoules are cleaned batchwise as follows: washing with distilled water, washing with cyclohexane, storage under cyclohexane overnight, and drying in an oven at 60°C. The cleaned ampoules are stored in air-tight containers until used. Testing for blanks with pure cyclohexane is carried out separately for 4 ampoules from each cleaned batch.

Immediately after sealing, the samples are packed in pairs in polyethylene "rabbits" and then stored at —20°C until the start of the irradiation. This procedure is used to prevent appreciable diffusion of solvent or organohalogen compounds through the walls of the vial during the pre-irradiation and irradiation period.

The irradiations were performed in the pneumatic-tube facility of the JEEP-II reactor (Kjeller, Norway) at a thermal neutron flux of about 1.5×10^{13} n cm^{-2} s^{-1}. The irradiation time employed was usually 10 min, and the transfer time from the reactor to the laboratory was 25 s. Immediately after return, the vials are cut and 1.00-ml aliquots are pipetted into counting vials.

After exactly 5 min, recording of the γ-energy spectra is started with two Ge(Li) solid-state detectors with associated electronics interfaced to a NORD-1 digital computer which takes care of the simultaneous data accumulation from the two detector systems and also of the subsequent peak-area calculations. A counting time of 5 min is usually employed. The analyses are based on γ-peaks from ^{38}Cl ($t_{\frac{1}{2}}$ = 37.2 min, E_γ = 1643 keV), ^{80}Br ($t_{\frac{1}{2}}$ = 17.6 min, E_γ = 617 keV, and ^{128}I ($t_{\frac{1}{2}}$ = 25.0 min, E_γ = 443 keV). Calibration is done with an aqueous solution (1 M NH_4OH) of the halides in question, irradiated and counted under the same condition as the samples. Simultaneous detection of ^{24}Na ($t_{\frac{1}{2}}$ = 15.0 h, E_γ = 2754 keV) induced in sodium may serve as a check for contamination by inorganic halides.

RESULTS AND DISCUSSION

Removal of inorganic halides

Results from radiotracer experiments with ^{38}Cl as chloride and ^{82}Br as bromide to check the efficiency of the washing procedure for the removal of inorganic halides from hexane extracts are summarized in Table 1. In some of the experiments the hexane had been treated with concentrated sulfuric acid, which is a procedure used in the analysis of chemically persistent

TABLE 1

Removal of inorganic chloride and bromide by washing of hexane extracts with water, indicated by the ratio of the activity in hexane extract to the activity in the aqueous phase (H:aq)

Organic phase	Aqueous phase	H:aq ($\times 10^{-5}$)
n-Hexane	0.05 M Cl^-	18
	0.05 $\times 10^{-3}$ M Cl^-	8
	0.05 M Br^-	$\leqslant 10$
n-Hexane + H_2SO_4	0.05 M Cl^-	8
n-Hexane + TMA[a,b]	0.05 M Cl^-	10
	0.05 M Br^-	$\leqslant 10$
n-Hexane + TMA + conc. H_2SO_4	0.05 M Cl^-	10
n-Hexane + DPA[a,b]	0.05 M Cl^-	$\leqslant 5$
	0.05 M Br^-	$\leqslant 10$
n-Hexane + DPA + H_2SO_4	0.05 $\times 10^{-3}$ M Cl^-	8
	0.05 M Cl^-	7
	0.05 M Br^-	$\leqslant 10$
Water extr. from poll. river	0.05 M Cl^-	11
	0.05 $\times 10^{-3}$ M Cl^-	14
n-Hexane + herring oil[b]	0.05 M Cl^-	75
	0.05 M Br^-	$\leqslant 10$
n-Hexane + herring oil + H_2SO_4	0.05 M Cl^-	11

[a]TMA = trimethylamine; DPA = diphenylamine. [b]100 μg ml^{-1} added in each case.

chlorinated hydrocarbons. In other cases, certain other situations encountered in practical work were simulated, as indicated in Table 1. In all cases, a single washing was found to reduce the level of chloride and bromide by a factor of more than 4 decades, even in the presence of fairly high concentrations of oil-soluble amines. These results are in accordance with those reported by Schmitt and Zweig [7], and with all previous experience from work with marine oils.

Blanks from ampoules and solvents

In the initial work, the polyethylene ampoules used for irradiation of samp were found to be a serious source of contamination with chlorine. When samples of pure hexane were stored in polyethylene ampoules not subjected to special pretreatment and subsequently analyzed, values up to several μg Cl ml^{-1} of hexane were observed, evidently because of extraction of chlorinated compounds from the polyethylene. After introduction of the washing proced described, the blank from this part of the analysis became a minor problem. For chlorine, values obtained by testing the ampoules with pure cyclohexane are typically about 50 ng Cl ml^{-1} and negligible for bromine and iodine.

The role of treatment of solvents is indicated from the results given in Table 2. The use of sodium ethylate in distillation of the solvents seems to be crucial. Results not reported here indicate that chlorinated solvents should not be used in rooms where this analytical work is carried out.

TABLE 2

Effects of purification procedures on organically bound chlorine in hexane and cyclohexane

Solvent[a]	Cl in final extract (μg ml^{-1})	
	A	B
Merck analytical-grade cyclohexane (glass bottle)	2.1	1.4
Merck puriss.-grade cyclohexane (can)	0.94	
Merck puriss.-grade n-hexane (can)	0.66	
Merck puriss.-grade n-hexane (can) + Na-ethylate	0.18	0.14
Merck puriss.-grade n-hexane (can) + Na-ethylate, equilibrated with puriss. isopropanol (glass bottle)	0.31	0.26
As above, isopropanol purified over sodium	0.16	0.13
Merck puriss.-grade n-hexane (can) + Na-ethylate treated also with concentrated sulphuric acid	0.11	0.13

[a]Samples were prepared in a room where chlorinated solvents were not used, and were concentrated from 200 to about 4 ml. For further details of analysis, see text.

Recoveries from extraction and blank levels

The recovery of the on-site liquid—liquid extraction is normally quite satisfactory in clean waters, but may be poor in waters with a high content of particulate material [8]. Losses may also occur in the concentration step, particularly with volatile material. Some results to indicate the degree of such losses are given in Table 3; losses are quite low for compounds with boiling points above 200°C.

TABLE 3

Recovery of various compounds during the concentration step
(Experimental conditions: 200 ml of hexane concentrated to 4 ml; distillate flushed back 3 times for washing; reflux ratio ca. 50%, final volume obtained in ca. 90 min; 25 ml N_2 min^{-1} passed through the apparatus.)

	B.p. (°C)	Amount added (μg)	Amount found (μg)	Recovery (%)
Dichloromethane	40	138	14	11
Chlorobenzene	132	110	83	75
1,2-Dichlorobenzene	180.5	127	103	81
Hexachlorobenzene	322	160	147	92
DDT	260	118	107	91
n-Alkanes C-10	174	75	53	71
C-16	287	75	69	92
C-23		75	72	96

TABLE 4

Blank levels obtained for different types of separation procedures

Type of separation	Element/ compound	Concentration in final extract (ng ml^{-1})	Concentration, calculated to normal sample size (ng kg^{-1})[a]
Water/extraction	Total Cl	100—150	4—6
	Total Br	2—5	0.08—0.2
	Total I	0.5—1	0.02—0.04
	PCB	1—2	0.05—0.1
Herring/extraction	Total Cl	100—200	1000—2000
	Total Br	1—5	
	Total I	0.5—3	
	PCB	1—2	
Herring/co-distillation	Total Cl	200—300	1000—2000

[a]200 l for water; 100-g wet weight for herring tissue.

Table 4 lists typical blank levels estimated from about 35 values obtained in between actual samples, at different times and by different personnel, and relating to both water and biological material. The values are given in terms of the contribution they would make to an actual sample. Values for PCB, determined by gas chromatography on aliquots of the same extracts, are included. The relative standard deviation of the chlorine blank values is generally about 20% for both water and biological material. For bromine and iodine, the blank levels are insignificant.

Table 5 shows some results from activation analysis of solutions with known concentrations of chlorinated hydrocarbons. The precision attained at the 1—5 $\mu g\ ml^{-1}$ level of chlorine is of the order of 1.5—3%. Experiments with 1,2-dichlorobenzene show that there is a loss of about 20%, referred to an inorganic chloride standard solution. Similar results were obtained in other experiments, where solutions of CCl_4 in hexane gave results in the range 76—84% of the nominal values when analyzed at different times. Corresponding analyses of hexane solutions of $CHBr_3$ analyzed simultaneously showed no

TABLE 5

Recovery and reproducibility of the n.a.a. method for organically bound chlorine

	No. of samples	Mean ($\mu g\ ml^{-1}$)	R.s.d. (%)	Recovery (%)
1,2-Dichlorobenzene in hexane[a]	10			
with ammonium chloride as reference		3.73	1.7	78
with 1,2-dichlorobenzene as reference		4.70	1.7	97
PCB in hexane[b]	2	0.95	—	103

[a]Corresponding to 4.83 μg Cl ml^{-1}. [b]Corresponding to 0.92 μg Cl ml^{-1}.

similar loss. Possibly a certain fraction of the radioactive chlorine atoms released from their molecular sites on activation by the Szilard—Chalmers process is lost by sorption to the inner walls of the polyethylene ampoule. It appears that the fraction lost is relatively constant for different chlorinated compounds, and a recovery of about 80% may therefore be generally assumed with the present experimental set-up, at least when hexane is used as solvent. Alternatively, a solution of a known amount of a suitable organochlorine compound in the same solvent as employed for the samples should be used as the standard. In the case of bromine or iodine compounds, there was no indication of losses during irradiation under the experimental conditions used.

The detection limits of the activation analysis as used here are about 0.02 μg Cl ml^{-1}, 0.005 μg Br ml^{-1}, and 0.003 μg I ml^{-1}. At high levels of chlorine, the detection limits for bromine and iodine are somewhat higher because of the Compton continuum from ^{38}Cl in the γ-spectra.

Conclusion

One person can put 30 samples through the n.a.a. procedure in one day, including the packaging work. As far as sampling and preparation of extracts, is concerned, the amount of work involved depends on the type of sample, and is about the same as required in analysis for PCB of DDT. Operation of the continuous extractors requires about 30 min of work at the sampling site.

The methodology described has now been used routinely for about 3 years for the analysis of large series of environmental samples. The results obtained have provided significant information on the extent of environmental pollution, especially when combined with investigation of specific compounds such as PCB. This work has also provided some insight into the field of naturally occurring organochlorine and organobromine compounds.

REFERENCES

1 G. Lunde, J. Gether and B. Josefsson, Bull. Environ. Cont. Toxicol., 13 (1975) 656.
2 E. V. Holden, in PCB Conference II, Stockholm 1972, Almänna Förlaget, Stockholm, 1973, pp. 23—24.
3 B. Ahling and S. Jensen, Anal. Chem., 23 (1970) 1483.
4 V. Zitko and P. M. K. Choi, Techn. Report No. 272, Fisheries Research Board of Canada (1971).
5 J. E. Bjerk, Nord. Vet.-Med., 24 (1972) 451.
6 G. Lunde, J. Am. Oil Chem. Soc., 48 (1971) 517.
7 R. A. Schmitt and G. Zweig, J. Agric. Food Chem., 10 (1962) 481.
8 M. Ahnoff and B. Josefsson, Anal. Chem., 46 (1974) 658.
9 G. Lunde and E. Steinnes, Environ. Sci. Technol., 9 (1975) 155.
10 G. Lunde, J. Gether and E. Steinnes, Ambio, 5 (1976) 180.

Analytica Chimica Acta, 108 (1979) 149—154
© Elsevier Scientific Publishing Company, Amsterdam — Printed in The Netherlands

CATHODE RAY POLAROGRAPHY AND DIFFERENTIAL PULSE POLAROGRAPHY OF THE CATALYTIC MOLYBDENUM(VI) WAVE

GARY D. CHRISTIAN,** JEAN L. VANDENBALCK and GASTON J. PATRIARCHE*

Institut de Pharmacie, Universite Libre de Bruxelles, Campus Plaine B.P. 205/1, 1050 Bruxelles (Belgium)

(Received 9th November 1978)

SUMMARY

The optimum conditions of electrolyte composition and pH were studied for the cathode ray polarography (c.r.p.) of the catalytic molybdenum(VI) wave; 1—2 M potassium nitrate at pH 1.6—2.2 is optimum, the detection limit is 3×10^{-9} M (0.3 ppb) molybdenum(VI). Equal molar concentrations of foreign electroactive substances do not interfere at the potential of the molybdenum wave and 500-fold amounts of these can be tolerated if their c.r.p. peaks are separated from the molybdenum wave by 0.1 or 0.2 V. Similar conditions were used for the differential pulse polarography of the catalytic wave. The detection limit is 2×10^{-8} M (2 ppb). being limited in part by lead impurities which contribute to the background.

Molybdenum(VI) exhibits a catalytic wave in the presence of perchloric acid [1] or nitric acid [2] at the conventional dropping mercury electrode (DME). Violanda and Cooke [3] investigated these waves in detail and found the optimum supporting electrolyte to be 2.4 M nitric acid; the limit of detection was 5×10^{-8} M molybdenum, about 100 times more sensitive than diffusion-controlled processes. Stach and Schoene [4] investigated the catalytic wave produced in sulfuric acid solution containing 2 M sodium perchlorate or 1 M sodium nitrate, achieving a detection limit of 9×10^{-8} M in the latter electrolyte at a temperature of 40°C. The catalytic wave in nitrate solutions has been used for the determination of as little as 5×10^{-6} % molybdenum in soils and plant ash, with no interference from 1500-fold amounts of tungsten(VI), 100-fold amounts of copper(II), or 40-fold amounts of iron(III) [5]. Molybdenum also exhibits a catalytic wave at the DME in the presence of carboxylic acids [6], and two catalytic waves in the presence of chlorate and hydroxyacids [7, 8]. A catalytic wave has been reported in the presence of bromate at a graphite disk electrode [9] and in the presence of hydrogen peroxide at a rotating graphite electrode [10].

Cathode ray polarography [11, 12] offers added sensitivity over conven-

**Permanent address: Department of Chemistry, University of Washington, Seattle, WA 98195 (U.S.A.).

tional polarography. This report describes a study of the cathode ray polarographic characteristics of the molybdenum catalytic wave. Optimum conditions of electrolyte are discussed. These conditions are applied for differential pulse polarography. Savéant and Vianello [13] have presented a theoretical discussion of catalytic waves in oscillographic polarography.

EXPERIMENTAL

Cathode ray polarograms were obtained on a Southern Analytical A1660 Davis differential cathode ray Polarotrace with a single cell. The potential scan extended —0.5 V from the starting potential. A mercury pool anode was used as reference. The DME had a capillary constant of 7.15 $mg^{2/3}\ s^{-1/2}$ and a drop time of 8.68 s (open circuit). The potential was scanned for 2 s beginning 6 s after the start of drop formation.

Pulse polarograms were obtained on a Tacussel polarograph (type PRG 34) operated under the following conditions: drop time 3.00 s, pulse amplitude 40 mV, pulse duration 19 ms, delay 2.98 s, scan rate 2 $mV\ s^{-1}$. A saturated calomel electrode (SCE) was used as the reference.

Controlled-current electrolysis was done with a Princeton Applied Research Potentiostat/Galvanostat Model 173 and electrolyte purification apparatus Model 9500.

Working standard solutions of molybdenum(VI) were prepared by serial dilution from a stock solution of ammonium molybdate. Water was triple distilled and then deionized on a mixed-bed ion-exchange column. Solutions were deaerated for 10 min with nitrogen and a nitrogen atmosphere was maintained above the solution while the polarograms were recorded. Solutions were thermostatted at 25.0 ± 0.1°C. The cell was cleaned between each series of runs by boiling in aqua regia.

The pH of potassium nitrate solutions was adjusted with acetate buffers of sulfuric acid [3].

RESULTS AND DISCUSSION

Cathode ray polarography

Initial work was done with a 2.4 M nitric acid supporting electrolyte as recommended by Violanda and Cooke [3]. A catalytic molybdenum peak was obtained at —0.1 V vs. the mercury pool anode. When the starting potential was +0.2 V, a rounded peak at 0.0 V preceded the molybdenum peak; this rounded peak was also obtained with the blank and was apparently due to appreciable dissolution of the mercury pool by nitric acid. Mercury is known to dissolve in nitrate solutions [14] and highly acidic electrolytes [15]. When the potential scan was initiated at 0.0 V, the mercury peak decayed before the scan had started and did not interfere with the wave from a 7×10^{-7} M molybdenum solution if the polarogram was run within 7—8 min. However, results under these conditions were not as reproducible or sensitive as could

TABLE 1

Catalytic molybdenum waves for 7×10^{-7} M molybdenum(VI) solution in 2 M potassium nitrate at different pH values.
(All potentials are given in V vs. Hg pool electrode)

pH	E_p (V)	$E_{1/2}$ (V)	Peak height (μA)	Starting potent. (V)
(1.9 M HNO_3)	−0.1	—	0.005	0
0.65	−0.73	−0.64	0.35	−0.4
1.6	−0.75	−0.65	0.50	−0.4
2.2	−0.87	−0.78	0.50	−0.5

be obtained with a less acidic solution. A saturated calomel reference electrode can be employed in more acidic solutions [3].

The molybdenum wave in 2 M potassium nitrate was then investigated at different pH values. The results are summarized in Table 1. A peak was obtained in nitric acid, but in potassium nitrate a sigmoidal wave drawn out about 0.2V was obtained. The half-wave potential of this wave is given in Table 1 as well as the "peak" potential (the top shoulder of the wave). Both the peak potential and the height of the wave changed markedly as the pH was increased. This contrasts with the results obtained in conventional polarography where the wave height was nearly independent of pH up to 2; above pH 2, the height decreased markedly [3]. The half-wave potential in conventional polarography shifted −0.115 V/pH unit from 3 M nitric acid to pH 3 in sodium nitrate (−0.1 to −0.5 V vs. SCE); it should be recalled that the potential of the mercury pool depends on the electrolyte employed.

The peak height was about 1.3 times greater in 2 M potassium nitrate than in 1 M potassium nitrate at pH 1.6. Violanda and Cooke [3] found that the height of the catalytic wave was nearly doubled in going from 2 M to 4 M nitric acid. The slight enhancement here may not warrant the added danger of increased impurities. However, the calibration curves in Fig. 1 illustrate that the linear range is almost doubled when the nitrate concentration is doubled.

A concentration of 3×10^{-9} M molybdenum(VI) (0.3 ppb) could be determined in 2 M potassium nitrate at pH 1.6. This is about 15 times more sensitive than the possibilities of the catalytic wave with d.c. polarography, and 1500 times more sensitive than anodic stripping voltammetry [16–18]. Linear calibration curves were prepared over 10-fold ranges from 5×10^{-9} to 5×10^{-6} M molybdenum, with standard deviations of 5% or less.

A study was made of the tolerance for other electroactive species in 2 M potassium nitrate at pH 1.6 for the determination of 7×10^{-7} M molybdenum. Copper(II) at 2.8×10^{-4} M exhibited a peak at −0.35 V with a height 10 times that of the catalytic molybdenum wave. If the potential scan was started at

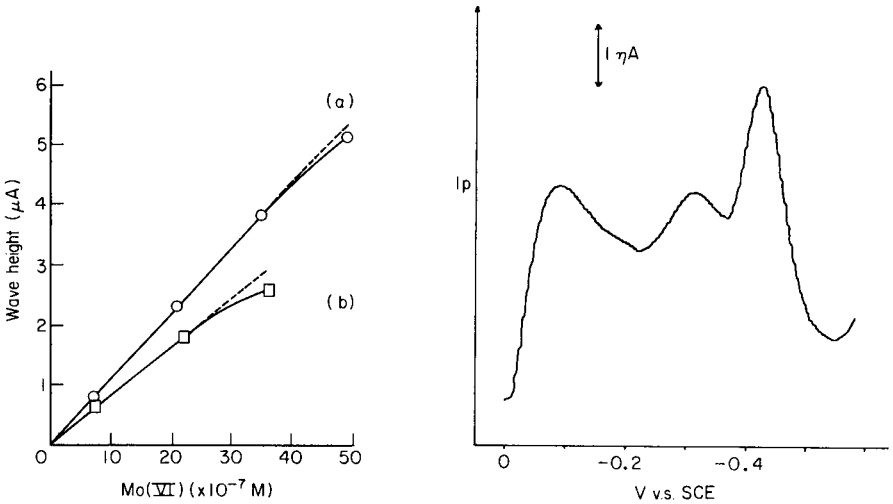


Fig. 1. Calibration curves for molybdenum(VI) by cathode-ray polarography at pH 1.6: (a) 2 M potassium nitrate; (b) 1 M potassium nitrate.

Fig. 2. Differential pulse polarogram of 20 ppb molybdenum in 2 M KNO_3, pH 1.6 (with H_2SO_4). Conditions: drop time 3.00 s; delay 2.98 s; pulse amplitude 40mV; pulse duration 19 ms; sweep speed 2mV s^{-1}. E_p of Mo, −0.32 V vs. SCE. E_p of Pb (100 ppb), −0.42 V vs. SCE.

−0.4 V, the copper current decayed early in the drop life (before the potential was scanned) and did not interfere. The sensitivity for the molybdenum wave was 41 times that of the copper. Cadmium (1.5×10^{-4} M) gave a peak after the molybdenum wave at −0.9 V; this 210-fold amount of cadmium did not alter the height of the molybdenum wave.

Since equimolar concentrations of copper and cadmium give peaks that are only about 1/40th the height of the molybdenum wave, errors of 2% or less would be expected to result from equimolar concentrations of other electroactive substances which have similar diffusion coefficients and *n*-values and are reduced or oxidized at or near the potential at which the molybdenum wave occurs. Based on the results with copper and cadmium, it appears that substances that give peaks ten times greater in magnitude than the molybdenum wave can be tolerated if their peaks are separated at least 0.1—0.2 V from the foot or top of the molybdenum wave. For substances similar to copper or cadmium, then, about 400-fold excesses could be tolerated. Thus, for example, 3×10^{-9} M molybdenum could be detected in a supporting electrolyte containing 1.5×10^{-7} M lead (see below, d.p.p.) with a peak potential about 0.1 V more negative than the molybdenum wave.

Advantage can be taken of the pH dependence of the molybdenum wave by shifting it to more positive or negative potentials to eliminate interferences, as in conventional polarography. An added advantage here is that the wave can be shifted to potentials more negative than a larger interfering peak, because

the initial current caused by the interfering peak will decay to a small value before the potential scan is initiated, as in the case of copper.

Differential pulse polarography

Differential pulse polarography (d.p.p.) of the catalytic wave was investigated for the optimum conditions found in cathode ray polarography. With 2 M potassium nitrate at pH 1.6, a catalytic peak was observed at —0.32 V vs. SCE (Fig. 2). A linear calibration curve was obtained for 20—125 ppb molybdenum with a standard deviation of 7%. A significant peak from a lead impurity (present in the potassium nitrate) followed the molybdenum peak at —0.42 V, the foot of which overlapped the molybdenum peak and limited its detectability and precision. The contribution of this lead to the background current in part prevented increasing the sensitivity setting of the instrument by causing it to "overload". In addition, the contribution of the residual current preceding the molybdenum wave, probably caused by mercury dissolution from the electrode [14], severely limited the sensitivity. The lead concentration in the 2 M electrolyte was about 100 ppb (5×10^{-7} M). Attempts were made to purify the electrolyte by controlled potential electrolysis at —0.8 V vs. SCE for 48 h; this reduced the lead concentration to about 30 ppb (1.5×10^{-7} M). Under these conditions, 2×10^{-8} M molybdenum (2 ppb) could be detected. This is five times lower than can be detected by d.p.p. based on the electrochemical reduction of dioxobis (8-quinolinol) molybdenum(VI) [19]. Perhaps a further improvement in detectability could be achieved with improved electrolyte purification (by longer electrolysis or solvent extraction or with a different source of potassium nitrate) but these results demonstrate the advantage of cathode ray polarography based on the catalytic wave when interfering substances are present. Even with improved purification, the background current preceding the molybdenum wave would be expected to limit the sensitivity.

Attempts to measure the molybdenum d.p.p. catalytic wave in 1 M nitric acid failed; no catalytic wave was observed with 200 ppb molybdenum probably because of the increased residual current at the beginning of the polarogram, which, in the case of cathode ray polarography could be allowed to decay away.

G.D.C. thanks the Commission for Educational Exchange between the United States of America, Belgium and Luxembourg for support, and G.J.P. acknowledges support from the Fonds National de la Recherche Scientifique (F.N.R.S. Belgium).

REFERENCES

1 G. P. Haight, Anal. Chem., 23 (1951) 1505.
2 M. G. Johnson and R. J. Robinson, Anal. Chem., 24 (1952) 366.
3 A. T. Violanda and W. D. Cooke, Anal Chem., 36 (1964) 2287.
4 B. Stach and K. Schoene, Mikrochim. Acta, 2 (1977) 565.

5 R. U. Bikbulatova and S. I. Sinyakova, Agrokhimiya, (1967) 123.
6 F. Pottkamp, F. Umland and H. Reimann, Fresenius Z. Anal. Chem., 26 (1972) 102.
7 E. G. Chikryzova and L. G. Kiriyak, Zh. Anal. Khim., 27 (1972) 1747.
8 E. G. Chikryzova and S. M. Bardina, Zh. Anal. Khim., 29 (1974) 2414.
9 V. F. Vekslina, S. A. Vashchenko and L. N. Kitaeva, Nov. Polyarogr., Tezisy Dokl. Vses, Soveshch, Polyarogr., 6th (1975) 183.
10 V. F. Toropova, N. G. Chovnyk, V. A. Vekslina and V. V. Vashchenko, Zh. Anal. Khim., 25 (1970) 2464.
11 J. E. B. Randles, Trans. Faraday Soc., 44 (1948) 344.
12 H. M. Davis and R. C. Rooney, J. Polarographic Soc., 8 (1962) 25.
13 J. M. Savéant and E. Vianello in I. Longmuir (Ed.), Advances in Polarography Vol. I, Pergamon Press, New York, 1960, p. 367.
14 S. Lal and G. D. Christian, Fresenius Z. Anal. Chem., 254 (1971) 363.
15 G. D. Christian, E. C. Knoblock and W. C. Purdy, Anal. Chem., 37 (1965) 425.
16 P. Lagrange and J. P. Schwing, Bull. Soc. Chim. Fr., (1970) 3170.
17 P. Lagrange and J. P. Schwing, Anal. Chem., 42 (1970) 1844.
18 V. V. Pnev, G. N. Popov and V. G. Nagarev, Zh. Anal. Khim., 28 (1973) 2050.
19 P. Bosserman, D. T. Sawyer and A. L. Page, Anal. Chem., 50 (1978) 1300.

Analytica Chimica Acta, 108 (1979) 155—160
© Elsevier Scientific Publishing Company, Amsterdam — Printed in The Netherlands

A MICROCOMPUTER-BASED DATA ACQUISITION AND PROCESSING SYSTEM FOR ELECTROCHEMICAL ANALYSIS

T. E. EDMONDS

The Macaulay Institute for Soil Research, Craigiebuckler, Aberdeen, AB9 2QJ (Gt. Britain)

(Received 2nd January 1979)

SUMMARY

The system described for electrochemical analysis includes ensemble averaging, boxcar integration and background subtraction. A digital storage oscilloscope interfaced to a microcomputer provides these data-processing techniques for the differential pulse polarographic determination of molybdenum. The system is easily interfaced to the polarograph. An approximately four-fold improvement in the detection limit for molybdenum — to 2.7×10^{-4} ppm — was achieved by using a combination of ensemble averaging and background subtraction.

The amenability of electrochemical techniques to computer control and data processing has been commented on by Kryger et al. [1] who described a minicomputer-controlled electroanalytical instrument. Other authors [2—7] have reported on minicomputer-controlled polarographs for specialized voltammetric or polarographic techniques, and Bond and Grabaric [8] have carried out differential pulse polarography and anodic stripping voltammetry using a commercial polarograph with a dedicated microcomputer.

The microprocessor has enabled data-processing techniques such as ensemble averaging, background subtraction and digital filtering to be carried out on analytical signals without recourse to a minicomputer. However, interfacing a microprocessor with an experiment can take a good deal of time and effort, which would not be justified for experiments used infrequently, or for continuous experiments where data processing is only required occasionally.

The instrument described in this paper has been designed to provide a versatile data-processing system that may be interfaced simply and rapidly with a range of electrochemical techniques.

EXPERIMENTAL

Data acquisition and processing system

The flexibility of the system derives from the use of a digital storage oscilloscope as the interface between the microcomputer and the experiment. The Gould Advance OS4000 oscilloscope, with the OS4001 output unit may

operate both as a normal 10-MHz oscilloscope and as a storage instrument. The relevant operating parameters of the oscilloscope are listed in Table 1. In the storage mode, the incoming signal is digitized at 1.8×10^6 to 4.5 Hz, by means of an 8-bit analog-to-digital (A/D) convertor. The digitized data are read into a store which can contain up to 1024 8-bit words. Subsequently the data are displayed on the cathode ray tube via an 8-bit digital-to-analog (D/A) convertor. The slowest rate of digitization can be reduced (see Fig. 1) by incorporating a single-pole single-throw switch into line L10 from S6, the time-base selector switch. When this switch is open, pin 13 of IC711 (Mostek 5009 decade divider) is forced high irrespective of the setting of S6. Thus over the last five settings of the time-base switch, a multiplication of 100 is achieved. Effectively this means that analog signals with duty cycles from a few microseconds to over 6 h may be accurately digitized.

The output option enables the store to be read out to external instrumentation in either digital or analog format. Three digital outputs are provided: two 8-bit ports for channels 1 and 2 and one 10-bit port, which contains the number of the storage location whose value is currently latched at one of the 8-bit ports. The same information is provided by the analog output. The store is read out at the rate determined by the time-base selector switch.

An Intel SBC 80/10 microcomputer was interfaced with the oscilloscope. The computer comprised an 8080A central processing unit (CPU), a system controller, 48 programmable parallel input/output lines, a programmable serial input/output port, 1 K of read/write random access memory (RAM) and provision for up to 4 K of programmable read-only memory (PROM).

TABLE 1

Gould Advance OS4000/OS4001 operating parameters

Display	8 × 10 cm rectangular CRT
Vertical deflection	Two identical input channels Bandwidth: d.c., 10 MHz Sensitivity: 5 mV cm^{-1} to 20 V cm^{-1} in 12 ranges, continuously adjustable Input impedance: 1 MΩ, 28 pF Input coupling: a.c.—GND—d.c.
Horizontal deflection	Time base: 1 μs cm^{-1} to 20 s cm^{-1} in 23 ranges X Expansion: continuously variable from 1 × to 10 ×
Trigger	Source: CH1±, CH2±, Ext±, Line± Coupling: a.c., l.f. Rej., h.f. Rej. Sensitivity: internal, 2 mm at d.c. — 2 MHz, 1 cm at 10 MHz; external, 1 V at d.c. — 2 MHz, 5 V at 10 MHz
Output	Digital: true binary from open collector TTL buffers, negative logic

Both bus control logic and the necessary drivers were also contained on the board. In the present application the system was expanded by the addition of a further 4 K of RAM. This memory was contained on a single board designed and built within the Institute. A monitor programme resided in 1 K of PROM.

The binary data from the digital output of channel 1 of the oscilloscope were led via an 8-way ribbon connector to eight of the SBC 80/10's parallel input/output lines. These eight lines were configured as an input port by the software of the computer. In the same manner a second input port, of only 4 bits, was also established. The least significant digit of the 10-bit digital output of the oscilloscope was connected to the least significant bit (LSB) of the 4-bit port. A software routine examined this LSB for a transition (either 0 to 1 or 1 to 0), and called a second routine whenever such a transition occurred. This latter routine fed the data that were present at the 8-bit input port to the CPU which performed the necessary mathematical operations on the data prior to storing them in the 4 K RAM. In this manner, each of the 1024 data words were sequentially acquired and stored by the microcomputer. Processed data were read out of the computer at an 8-bit latched output port and taken to the oscilloscope or an X-Y recorder via a laboratory-built D/A convertor. A GR Electronics pocket teletype was used to communicate with the computer.

The computer programme performed ensemble averaging, background subtraction and digital filtering. This filtering was achieved by including a scanning boxcar integrator (SBI) in the software. Essentially an SBI operates by cross-correlating a normalized rectangular pulse (amplitude = 1) with the signal to be filtered [9]. This function is carried out by the following algorithm. A window of width n points is moved along the stored signal, point by point, and at each location the sum is calculated for the n points. This calculated value is then used to replace the original value of one of the points within the window. The location of the window with respect to that of the replaced value determines whether a retrospective, current, or prospective sum is taken. Different degrees of filtering are achieved by varying the width of the window. In the present application an average of the points was taken to restore the data to an 8-bit format and the prospective sum of the points was taken. This produced a linear shift in the filtered signal which was proportional to the window width. This filter is conceptually similar to that recently described by O'Haver [10]. O'Haver's filter, although called a linear response time low pass filter, behaved as a scanning boxcar integrator.

The computer software was written to provide an interactive mode of operation, and it was possible to select the number of scans to be averaged and the degree of filtering to be applied to the signal. Provision was made for two distinct signals to be stored separately. Each signal or the difference between them may be displayed on the oscilloscope or on a chart recorder.

Electrochemical system

The differential pulse polarographic determination of molybdenum(VI) in 0.6 M nitric acid was used to evaluate the system. A PAR 174A polarographic analyser was used after two simple modifications had been made. First a connection was made between the + 15-V power rail and a spare terminal on the INITIAL switch, such that when this switch moved from the ON to OFF position, a 15-V trigger was sent to the oscilloscope. Secondly, the clock circuit was modified to include a push-button switch, which grounded the time constant capacitor. This ensured that whenever the SCAN switch was depressed the clock started from a reset position.

The electrolyte was prepared from Aristar nitric acid (BDH Chemicals Ltd.) and distilled—deionized water. Stock solutions of copper and molybdenum were prepared from analytical-grade $CuSO_4$ and $(NH_4)_6Mo_7O_{24}$, respectively: serial dilutions were used to prepare the working concentrations from the 1000-ppm stock solutions. All measurements were made in de-oxygenated solutions. The dropping mercury electrode (DME) was used at a reservoir height of 65 cm and a mercury flow rate of 2.76 mg s^{-1}. A saturated calomel electrode (SCE) was used as reference against a Pt wire counter electrode. A layer of chloroform separated the mercury pool that formed at the bottom of the polarographic cell from the electrolyte, thus minimizing the dissolution of trace impurities from the mercury. The conditions for all scans were: drop time 2 s, scan rate 5 mV s^{-1}, pulse height 100 mV.

RESULTS AND DISCUSSION

A typical signal for 2×10^{-2} ppm Mo is shown in Fig. 2. The rather broad catalytic peak has an $E_{1/2}$ value of −0.147 V vs. SCE and the signal terminates at the foot of the hydrogen peak. Comparison of curves (a) and (b) shows that filtering has removed the digitization noise, and has smoothed the steps caused by the 2-s drop time of the DME. A more striking example of the effect of filtering is given in Fig. 3; curves (a) and (b) were obtained from single scans of solutions containing 0.5 ppm Cu and 0.5 ppm Cu + 0.02 ppm Mo, respectively, and curves (c) were generated by subtracting (a) from (b). Because the reduction of copper occurs at a more positive potential than that for molybdenum, the trailing edge of the copper peak partially obscures the molybdenum peak. Clearly, the subtraction of the raw data curves (Fig. 3A) did nothing to improve the determination of the molybdenum peak height. Processing the curves with the digital filter, followed by subtraction, yielded useful information about the size of the molybdenum peak (Fig. 3B). Further evidence of the value of the background subtraction may be seen from Fig. 4. Statistical calculations on ten replicate determinations of 4×10^{-3} ppm Mo yielded a detection limit ($S:N$=2:1) for a single scan of 1×10^{-3} ppm Mo. Curve (b) of Fig. 4A shows the signal obtained from 16 averaged scans of 1×10^{-3} ppm Mo. The magnitude of the peak is difficult to assess, because of the non-linearity of the background. A measurable molybdenum peak was obtained by subtraction

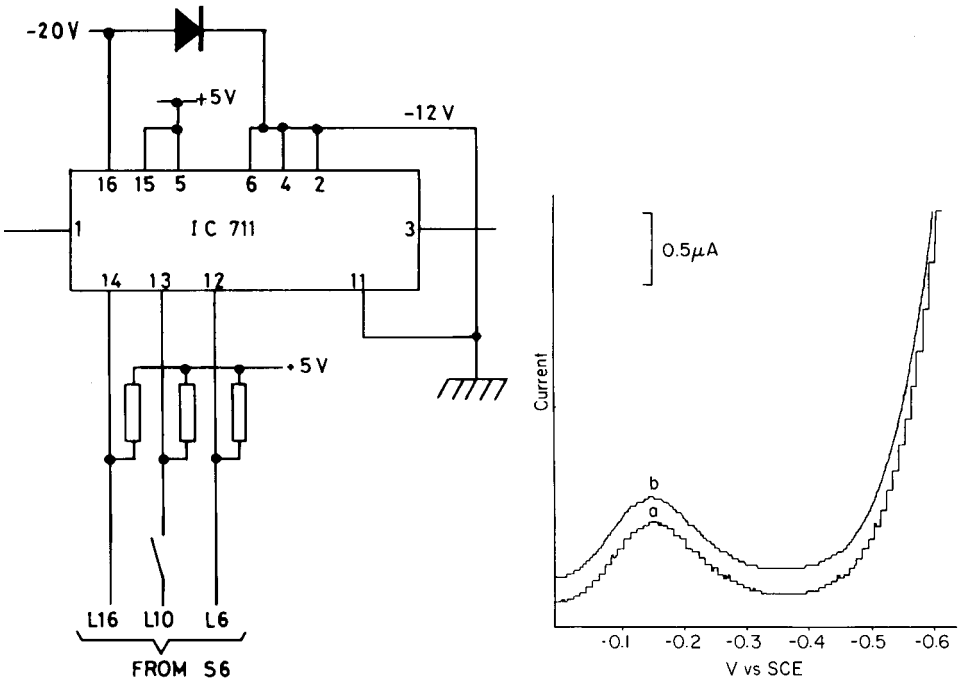


Fig. 1. Circuit diagram of modification to OS4000 time-base selection.

Fig. 2. Differential pulse polarogram of 2×10^{-2} ppm Mo: (a) raw data, (b) filtered data.

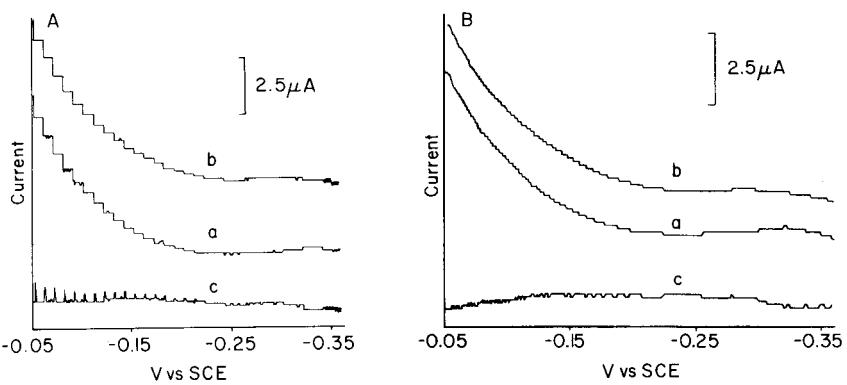


Fig. 3. Differential pulse polarograms of (a) 0.5 ppm Cu, and (b) 0.5 ppm Cu + 2×10^{-2} ppm Mo. (A) Raw data; (B) filtered data. Curves (c) represent the difference (b)—(a).

to give curve (c). The improvement in detection limit arising from ensemble averaging is demonstrated in Fig. 4B, where curve (c) shows a peak for 5×10^{-4} ppm Mo. Ten replicate determinations of 5×10^{-4} ppm Mo under these conditions yielded a relative standard deviation of 27%. Therefore, the

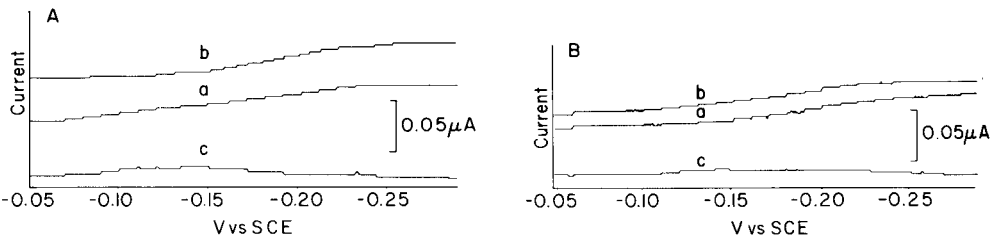


Fig. 4. Differential pulse polarograms of (A) 1×10^{-3} ppm Mo and (B) 5×10^{-4} ppm Mo. (a) 16 scans of background electrolyte; (b) 16 scans of the specified Mo solution. Curves (c) represent the difference (b)—(a).

detection limit may be calculated as 2.7×10^{-4} ppm Mo, a ca. 4-fold improvement on the single-scan detection limit. The theoretical improvement in detection limit for ensemble averaging is given by $n^{1/2}$ where n is the number of scans [9].

Clearly, the use of the microcomputer-based data acquisition and processing system, described here, has significantly improved the detection limit of the differential pulse polarographic determination of molybdenum; the background subtraction facility enables molybdenum to be determined in the presence of a larger amount of copper. Interfacing the system with the polarograph is a simple and rapid procedure.

Two further features of the system not specifically demonstrated here should be noted. First, other electrochemical techniques, such as stripping voltammetry, rapid-scan voltammetry and controlled-potential coulometry, can also be interfaced. The different data rates of these techniques can all be accommodated by the oscilloscope. Secondly, the data acquisition process takes place off-line so that the microcomputer is free to carry out other tasks during the experiment, such as controlling another experiment, or preparing a hard-copy report.

The author thanks B. L. Sharp and A. R. Morrisson for the design of the 4K RAM board.

REFERENCES

1 L. Kryger, D. Jagner and H. J. Skov, Anal. Chim. Acta, 78 (1975) 241.
2 S. C. Rifkin and D. H. Evans, Anal. Chem., 48 (1976) 2174.
3 Q. V. Thomas and S. P. Perone, Anal. Chem., 49 (1977) 1369.
4 J. A. Turner, J. H. Christie, M. Vukovic and R. A. Osteryoung, Anal. Chem., 49 (1977) 1904.
5 J. A. Turner, V. Eisner and R. A. Osteryoung, Anal. Chim. Acta, 90 (1977) 25.
6 J. A. Turner and R. A. Osteryoung, Anal. Chem., 50 (1978) 1496.
7 M. Bos, Anal. Chim. Acta, 81 (1976) 21.
8 A. M. Bond and B. S. Grabaric, Anal. Chim. Acta, 88 (1977) 227.
9 H. V. Malmstadt, C. G. Enke and S. R. Crouch, Electronic Measurements For Scientists, W. A. Benjamin, Menlo Park, 1974.
10 T. C. O'Haver, Anal. Chem., 50 (1978) 676.

Analytica Chimica Acta, 108 (1979) 161—167
© Elsevier Scientific Publishing Company, Amsterdam — Printed in The Netherlands

ION-SELECTIVE FIELD EFFECT TRANSISTORS WITH HETEROGENEOUS MEMBRANES

BRUCE SHIRAMIZU, JIŘÍ JANATA* and STANLEY D. MOSS

Department of Bioengineering, University of Utah, Salt Lake City, Utah 84112 (U.S.A.)

(Received 18th December 1978)

SUMMARY

Polyfluorinated polyphosphazene can be used as an elastomer for the preparation of heterogeneous membranes which can be applied to the ISFETs by solvent casting. The performance characteristics of such devices prepared with AgCl, AgCl—Ag_2S and AgI—Ag_2S membranes are very similar to those found for heterogeneous membranes based on silicone rubber, which have been used in the corresponding ion-selective electrodes. The sensor is suitable for direct determinations of chloride in sweat.

To a first approximation, the ion-sensitive field effect transistor (ISFET) can be described as an ion-selective membrane integrated with a pre-amplifier. The theory of these devices has been reviewed [1] and ISFETs sensitive to hydrogen [2—4], potassium [3], sodium [4], and calcium ions [3], have been described. While an ion-selective electrode is assembled from separately prepared parts, including the previously prepared membrane, the fabrication of ISFETs requires that ion-selective membranes be applied by a process which is compatible with the integrated circuit. Solvent casting proved to be suitable for manufacturing of K^+-, Ca^{2+}-, and H^+-selective ISFETs [3]. In this paper, the preparation of ISFETs with heterogeneous membranes is described.

The ion-selective properties and electrochemical properties of membranes composed of an inert elastomer and a semiconducting inorganic salt have been extensively studied by Pungor and Tóth [5]. The typical elastomer used in this membrane is silicone rubber which is made from the linear polymer and a suitable bi-functional silane for cross-linking. The finely divided inorganic salt is mixed with the elastomer before the cross-linking step. The finished membrane is then cut into pieces of a suitable size which are mounted on the electrode body. Electrodes selective to halides, cyanide, thiocyanate, and various heavy metals have been prepared in this way. It is impractical in the preparation of an ISFET to apply a preformed piece of a membrane to the gate. Instead, it is more convenient to cast the membrane in the form of a slurry which then forms a membrane.

EXPERIMENTAL

The fabrication technique for integrated-circuit sensors has been described by McBride et al. [3]. The same procedure was used to characterize ISFETs with heterogeneous membranes.

Membranes and Chemicals

The silver chloride—silicone rubber membrane described previously [5, 6] was adapted for use on CHEMFET gates. The membrane was prepared from silver chloride (Mathieson, Coleman and Bell, and prepared by precipitation) and silicone rubber (linear polymer, cross-linking agent, and catalyst). The three components of the silicone rubber were individually prepared in chloroform solvent. Just before the application of the membrane, the three components were thoroughly mixed and the appropriate amount of AgCl was added. The membrane was applied to the gate and the solvent allowed to evaporate.

For the initial polyfluorinated polyphosphazene membrane (PNF 200 lot RPP10132, kindly donated by Firestone Laboratories) [7], commercial silver chloride was also used. Two solvent systems were tested separately for the casting, an acetone—cyclohexanone mixture (1:1, v/v) and methyl isobutyl ketone (MIBK). The membranes were cast on the CHEMFET gates by applying the solution 4—5 times, the solvent being allowed to evaporate slowly each time.

Membranes in which a mixture of AgX (X = Cl, I) and Ag_2S were incorporated were tested next. Systems of this type have been discussed by Ross [8]. The inorganic salt was prepared by coprecipitation so that an accurate halide: sulphide ratio could be obtained. For the membranes with AgX—Ag_2S in the PNF matrix, the silver salts were prepared first by coprecipitation [9—12]. To an aqueous ethanolic solution of silver nitrate, salt solutions of iodide or chloride and sulfide were added in an appropriate ratio (see below). The resulting precipitate was washed with ethanol and deionized water, filtered and dried for 24 h at 60°C. The precipitate was finely ground and used to prepare the membrane mixture with PNF and solvent. As described above, 4—5 solution castings were applied to the CHEMFET gate, the solvent being allowed to evaporate slowly between castings.

Unless otherwise specified, all solutions were prepared from analytical-grade chemicals and de-ionized water. Solutions for chloride testing were prepared from sodium chloride dissolved in 0.01 M sodium sulfate solution to maintain constant ionic strength (μ = 0.03). Potassium chloride dissolved in 0.10 M potassium nitrate solution was also used. Chloride tests were carried out either by adding the sodium chloride solution to a background solution of 0.01 M Na_2SO_4 or by adding the potassium chloride solution to a background solution of 0.10 M KNO_3. Potassium iodide was used for the iodide tests with 0.10 M KNO_3 as the background solution; for cyanide tests, sodium cyanide and sodium hydroxide were used. Sodium hydroxide and silver nitrate solutions were prepared from J. T. Baker analytical concentrates.

The albumin solution was prepared from bovine albumin (Sigma) dissolved in 0.01 M sodium sulfate solution. The concentration was equivalent to the concentration of albumin in human serum (45 μg of albumin per 100 ml of human serum). Rejected human serum was used to test its effect on membrane response.

Sweat tests were carried out on collected human sweat.

Apparatus

An Ag/AgCl (saturated KCl) reference electrode with a 0.10 M KNO_3 salt bridge was used for solution tests. The salt bridge was needed to prevent contamination of the test solutions. A magnetic stirrer was used and all tests were done in a thermostated vessel at 37.0 ± 0.1°C.

Stock solutions were added from a precise micrometer burette (Gilmont Inst., model S 3100) and/or micropipettes.

Experimental results were obtained by operating the ISFETs with a negative feedback system, and recorded on a Soltec chart recorder. A Tektronix 7623A oscilloscope was used for the time-response experiments.

RESULTS

Chloride ISFET

The responses of the AgCl—silicone rubber membrane were irreproducible and the best response that was obtained was 27 mV/decade.

The response of the AgCl—PNF membrane to chloride is shown in Fig. 1 curve Cl_b^-). Figure 1 shows the experimental results for the chloride sensors

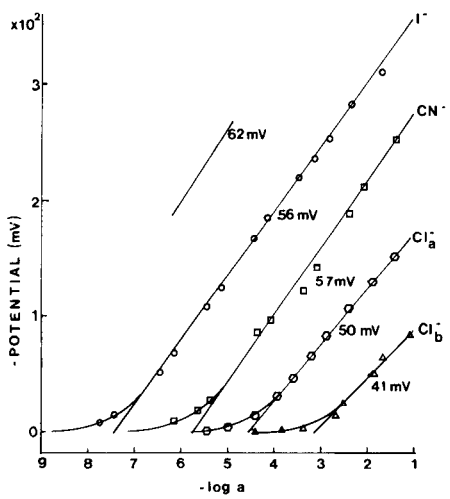


Fig. 1. Response curves showing the characteristics of the chloride, cyanide and iodide ISFETs. (Cl_a^-) AgCl—Ag_2S membrane; (Cl_b^-) AgCl membrane tested in KNO_3 solution. The theoretical Nernstian response is 62mV.

tested in potassium nitrate solution. There is a difference in sensitivity of the chloride sensors depending on the background solution, as can be seen by comparison with Table 1 which shows the results obtained in 0.01 M sodium sulfate solution. Other characteristics are summarized in Table 1. The average slope of the calibration graphs for the AgCl-PNF membranes was found to be 54 mV/decade; this was calculated from the results for ten separately prepared sensors tested in sodium sulfate solutions. The membrane was irreversibly poisoned by exposure to iodide ions and to serum proteins, and there was a loss in sensitivity with bovine albumin.

The AgCl—Ag_2S membrane was characterized by changing the molar ratio of chloride to sulphide during coprecipitation. No response was found for the ratio $2Cl^-:1S^{2-}$. The optimum response was obtained with precipitates from solutions containing 4 mol of chloride to 1 mol of sulfide; ISFETs prepared from mixtures of 75% of this salt to 25% PNF gave responses of 56 ± 2 mV/pCl. With 20% total salt in the membrane, there was no response to chloride. These membranes were also irreversibly poisoned by exposure to serum. The sensor showed no sensitivity to pH in the range 5—9.

Iodide (cyanide) ISFET

It was assumed that the optimum weight ratio for the components of this membrane would again be 75% salt—25% PNF. The optimum molar ratio during coprecipitation was found to be 6 mol I^-:1 mol S^{2-}. The responses of these membranes to iodide and cyanide were 56 mV/pI and 57 mV/pCN, respectively. Storage in human serum for 48 h had only a small effect on the slope, which decreased to 55 mV/pI, but considerably reduced the range of response, to 10^{-4}—10^{-1} M.

TABLE 1

Characteristics of the heterogeneous membrane ISFET at 37°C

Membrane	Principal Ion	Sensitivity mV/decade	Useful range [M]	Stability (mV h^{-1})	K_{ij}[a]	Interfering Ions Tested	Respon time [τ(63%)]
AgCl—PNF[b]	Cl^-	54	10^{-1} —3.16×10^{-5}	1.5	$K_{Cl/Br} = 1.87$ $K_{Cl/SO_4} = 1.00 \times 10^{-2}$ $K_{Cl/NO_3} = 1.33 \times 10^{-4}$	I^-, Br^-	
AgCl—Ag_2S —PNF[c]	Cl^-	56	10^{-1} —3.16×10^{-5}	1.5	$K_{Cl/Br} = 5.4$ $K_{Cl/I} = 0.42$ $K_{Cl/SO_4} = 4.48 \times 10^{-3}$ $K_{Cl/NO_3} = 5.07 \times 10^{-4}$	I^-, Br^-	120 ms
AgI—Ag_2S[d]	CN^-	57	10^{-1} —1.58×10^{-6}	2.5	$K_{CN/Cl} = 2.00 \times 10^{-4}$ $K_{CN/OH} = 2.22 \times 10^{-4}$	I^-	1.3 s
AgI—Ag_2S[e]	I^-	56	10^{-1} —3.55×10^{-8}	2.0	$K_{I/Cl} = 1.14 \times 10^{-5}$ $K_{I/NO_3} = 5.31 \times 10^{-7}$	CN^-	1.3 s

[a]Calculated for $a_{OH} = 9.0 \times 10^{-3}$; $a_{Br} = 7.54 \times 10^{-4}$; $a_I = 7.54 \times 10^{-5}$; $a_{SO_4} = 5.0 \times 10^{-3}$; $a_{NO_3} = 7.5 \times 10^{-2}$ calculated from the Debye—Hückel equation. [b]Characterized in Na_2SO_4 solution. [c]Characterized in Na_2SO_4 solution; insensitive to pH changes. [d]Characterized in NaOH solution; the range decreased after storage in serum. [e]Characterized in KNO_3 solution.

Response times

The response of the drain current of the transistor to stepwise changes in the gate voltage tests the electrical characteristics of the ISFET. The gate capacity of the transistors used was approximately 5 pF and the gate area was 8×10^{-5} cm^2. With the AgCl—Ag_2S—PNF membranes, both voltage steps and concentration steps (up or down) produced a drain current change which reached 63% of its maximum value in 120 ms. This corresponds to a specific resistance of 1.9×10^8 Ω cm for the membrane. The response time of the drain current in transferring from stationary to a stirred solution was approximately 150 ms. This is as expected, because the relatively high solubility of silver chloride is responsible for the formation of a concentration gradient near the surface of the electrode which is affected by stirring. In that sense, the difference between stirred and stationary solutions represents a concentration step change.

The response time of the AgI—Ag_2S—PNF membrane was substantially different. The electrical response time, $\tau_{63\%}$ was only 10 ms which corresponds to a specific resistance of 1.6×10^7 Ω cm for these membranes. However, the concentration step produced drain current response times ($\tau_{63\%}$) of 1.3—1.5 s. This large discrepancy suggests that the rate-determining step for this membrane is the ion-exchange process at the membrane—solution interface and not the displacement current through the more resistant membrane.

DISCUSSION

With these heterogeneous membranes composed of an inert elastomer and silver halides with and without silver sulphide, the weight ratio of the polymer to the salt is critically important for the proper functioning of the ISFET. Membranes based on coprecipitated salts also depend on the mole ratio of the two components of the precipitate. Table 2 shows the dependence of the response of the AgCl—PNF membrane on the amount of silver chloride in the membrane. Similar results were found for the other membranes. A satisfactory, though sub-theoretical, response was found for the highest practical loading of the membrane (75% AgCl:25% PNF). This is consistent with the model of point-point grain contact of the semiconducting salt suggested earlier [5]; salt contents exceeding 75% (w/v) resulted in mechanically unstable membranes. The detection limit of these silver chloride sensors was about 3×10^{-5} M (Table 1) when tested in sodium sulfate solutions, but the linear portion of the response curve began near 10^{-4} M. In agreement with previous observations

TABLE 2

ISFET Response as a function of the percentage of silver chloride in the PNF membrane

AgCl (% w/w)	20	50	60	75
Slope (mV/pCl)	0	4	7	54

[13, 14], these membranes were irreversibly poisoned by exposure to iodide ions and to serum proteins.

The silicone rubber membranes were prepared from a linear silicone rubber bi-silane. Each component was initially fluid, though very viscous, and required dilution with a suitable solvent to achieve proper mixing of the inorganic and organic phases. Incomplete mixing may have contributed to the irreproducible and sub-Nernstian response of these membranes. In order to achieve better control over the final composition of the membrane, an elastomer which would be completely soluble in an organic solvent was sought. PNF was found to be highly suitable for this purpose, as it dissolves in ketones and other solvents. In initial experiments, a mixture of acetone and cyclohexanone was used, but this was later replaced with MIBK.

The potentiometric selectivity coefficients were determined by the fixed interference method, i.e. potential measurements were made with a constant level of the interfering ion, a_B, varying the activity of the primary ion, a_A. Table 1 shows the ions that affect the response of the membrane. In the case of the chloride sensors, iodide and bromide irreversibly poisoned the sensor. The AgI—Ag_2S membranes responded to the presence of either cyanide or iodide in the usual way for these electrodes.

All measurements were made at 37°C. The reason for this temperature is that it is hoped to apply the devices for in vivo clinical analysis.

APPLICATION

One of the important applications of the chloride sensor is in the determination of chloride ion in sweat for the early diagnosis of cystic fibrosis [15, 16]. In order to assess the potential value of the proposed sensor for this application, its performance in sweat was studied both in the presence and in the absence of pilocarpine. The method adopted was a modified Gran plot technique which has been described previously by Buffle et al. [17]. In order to minimize the effect of the change of the sample matrix on the liquid junction of the reference electrode and on the sensor itself, the following procedure was adopted. A sample of sweat with an unknown concentration of chloride was used as the "solvent" for preparation of the "standard" solution of chloride ion. An exactly known amount of solid sodium chloride was dissolved in this sweat sample to make the total concentration of chloride $C_S = (C_A + C_X)$ M, where C_X is the unknown molarity of chloride and C_A is the molarity corresponding to the addition of the salt. This solution was then used as the "standard" solution in constructing the usual Gran plot. The equation for the potential response can be written as

$$\psi = [V_X + V_S] \exp [(E - E_0)/S] = C_S V_S + C_X V_X$$

where V_X and V_S are the initial and added volumes, respectively, S is the slope and E is the potential of the electrode. Substituting $C_S = C_A + C_X$ and extrapolating for $\psi = 0$ (V_S^0) then yields $C_X = -C_A V_S^0/(V_X - V_S^0)$.

This procedure was used to analyze a sweat sample from one of the authors (B. S.). The standard chloride solution was 1.053 M which included the concentration of the chloride initially present in the sweat (calculated after back-extrapolation). The result of this determination was 31.6×10^{-3} M as opposed to 30.3×10^{-3} M found by titration with silver nitrate. No interference from pilocarpine nitrate (3.68×10^{-5} M) was found.

This work was partly supported by NIGMS grant no. 22952. We thank Dr. D. Owen for his advice on the choice of encapsulants and Dr. E. Klein for suggesting PNF as the polymer matrix.

REFERENCES

1 J. Janata and R. J. Huber in J. D. R. Thomas (Ed.), Ion-Selective Electrode Reviews, Pergamon Press, 1979, in print.
2 S. D. Moss, J. B. Smith, P. A. Comte, C. C. Johnson and L. Astle, J. Bioeng., 1 (1977) 11.
3 P. T. McBride, J. Janata, P. A. Comte, S. D. Moss and C. C. Johnson, Anal. Chim. Acta, 101 (1978) 239.
4 M. Esashi and T. Matsuo, IEEE Trans. BME-25 (1978) 184.
5 See, e.g., E. Pungor and K. Tóth, Analyst, 95 (1970) 625.
6 G. A. Rechnitz and M. R. Kresz. Anal. Chem., 38 (1966) 1786.
7 H. R. Allcock, Angew. Chem. Int. Ed., Engl., 16 (1977) 147.
8 J. W. Ross in R. A. Durst, (Ed.), Ion Selective Electrodes, Nat. Bur. Stand., Spec. Publ. 314, Washington D.C., 1969, p. 57.
9 M. H. Sorrentino and G. A. Rechnitz, Anal. Chem., 46 (1974) 943.
10 I. C. Popescu, E. Hopirtian, L. Savili and R. Vlad, Rev. Roum. Chim., 20 (1975) 993.
11 G. A. Rechnitz, Chem. Eng. News, June 12 (1967) 146.
12 J. F. Lechner and I. Sekerka, J. Electroanal. Chem., 57 (1974) 317.
13 A. K. Covington in R. A. Durst (Ed.), Ion Selective Electrodes, Nat. Bur. Stand., Spec. Publ. 314, Washington, D.C., 1969, p. 89.
14 R. M. Khuri in R. A. Durst (Ed.), Ion Selective Electrodes, Nat. Bur. Stand., Spec. Publ. 314, Washington, D.C., 1969, p. 287.
15 P. T. Bray, G. C. F. Clark, G. J. Moody and J. D. R. Thomas, Clin. Chim. Acta, 80 (1977) 333.
16 L. Webster and H. Lochlin, Med. J. Aust., 1 (1977) 923.
17 J. Buffle, N. Parthasarathy and D. Monnier, Chimia, 25 (1971) 223.

Analytica Chimica Acta, 108 (1979) 169—178
© Elsevier Scientific Publishing Company, Amsterdam — Printed in The Netherlands

THE FORMATION AND PROPERTIES OF MIXED CADMIUM SULFIDE—SILVER SULFIDE, AND MIXED MERCURY SULFIDE—SILVER SULFIDE MEMBRANES FOR ELECTRODES SELECTIVE TO CADMIUM(II) AND MERCURY(II)

W. E. van der LINDEN* and R. OOSTERVINK

Laboratory for Analytical Chemistry, University of Amsterdam, Nieuwe Achtergracht 166, Amsterdam (The Netherlands)

(Received 30th January 1979)

SUMMARY

The preparation and behavior of cadmium(II)-selective and mercury(II)-selective electrodes made from mixed metal sulfide-silver sulfide precipitates are discussed. The performance of the cadmium-selective electrode is satisfactory in accordance with similar electrodes described in the literature. Responses to cadmium(II), alone as well as in the presence of complexing agents such as EDTA, NTA, trien and tetren, were determined as a function of pH. Selectivity coefficients are presented. The mercury(II)-selective electrodes generally did not behave reproducibly; at best, the limit of detection was about 10^{-5} M.

To complete recent studies on the formation and properties of mixed sulfide membranes for ion-selective electrodes, mixed cadmium sulfide—silver sulfide and mercury sulfide—silver sulfide precipitates have been examined. The electrochemical behavior of membranes pressed from these materials has been studied, special attention being given to the influence of complexing agents. The results for cadmium and mercury are discussed below.

CADMIUM SULFIDE—SILVER SULFIDE MEMBRANES

The preparation of cadmium(II)-selective electrodes based on membranes pressed from the mixed sulfide has been reported in several papers [1—8]. The procedure of bulk coprecipitation originally given in the Orion patent [1] was also recommended by Rechnitz and co-workers [2, 3] and by Růžička and Hansen [5]. In their procedure, a mixture of the metal solutions was added to an excess of sodium sulfide with vigorous stirring to ensure that an excess of sulfide was present in the entire solution throughout the precipitation procedure. Mascini and Liberti [7] added the sulfide solution to the mixture of metal solutions, but did not obtain good results in this way, probably because silver sulfide precipitated first followed by post-precipitation of cadmium sulfide leading to a precipitate with the properties of pure cadmium sulfide. Membranes pressed from cadmium sulfide alone do not show an

electrochemical response. Mascini and Liberti claimed good results by precipitation with hydrogen sulfide from acidic medium. The precipitate thus obtained was subsequently heated to 600°C for 3 h under a stream of hydrogen sulfide.

Gordievskii et al. [4] started from the two separate sulfides and heated the mixture in a vacuum furnace at 1200°C; membranes were cut from the slowly cooled melt. Hirata and Higashiyama [6] also started from the separate sulfides, but pressed the mixture at 200—500°C for 1—3 h at a pressure of 3000—7000 kg cm^{-2}. They found a faster response and better mechanical properties after the addition of some copper(I) sulfide. Finally, van de Leest [8] prepared electrodes by covering ionic conductors such as silver sulfide with thin metal sulfide layers (including cadmium sulfide) followed by heating under part pressure of sulfur. The favourable influence of elevated temperatures was confirmed by Rechnitz and co-workers [2, 3], who pressed their pellets at 750 MPa (7600 kg cm^{-2}) for 4—8 h at 150—250°C.

In the work described here, the procedure recommended by Frant and Ross [1] and later by other workers yielded good electrodes. With some minor changes this procedure was therefore adopted in further experiments.

Preparation of the precipitate and the membrane electrode

A solution containing 0.1 mol of cadmium nitrate and 0.1 mol of silver nitrate per liter was added to a 1 M solution of sodium sulfide, the amount of sulfide being 30% in excess with respect to the total amount of cadmium and silver. The solution was added very slowly by means of a peristaltic pump; the mixture was stirred vigorously throughout the whole procedure. When the addition was complete, the temperature was gradually raised to about 75°C and maintained at 75°C for 0.5—1 h. After settling and centrifugation, the precipitate was washed twice with 200 ml of 10^{-3} M HNO_3, once with 100 ml of 0.1 M HNO_3 and twice with 200 ml of redistilled water. As peptization occurred easily at higher temperatures, all washings were done at room temperature. The final product was washed with acetone, dried at 70°C, and powdered in a mortar. About 0.5 g of the material was used to press a pellet in a die (13-mm diameter) at 150°C under a pressure of 980 MPa (10000 kg cm^{-2}) for at least 2 h.

The electrode was made by sealing the pellet to a glass tube and filling the tube with an inner solution of 10^{-3} M cadmium nitrate in 0.1 M potassium nitrate. For comparison, a solid-state cadmium(II)-selective electrode (Orion model 94-48) was used. The experimental arrangement for testing the electrodes was similar to that described previously [9—12].

Solutions were prepared as described previously [9—12]. Calibration solutions were prepared in 0.05 M maleate buffer, pH 6.5. The ionic strength was adjusted to 0.1 with potassium nitrate. Metal nitrates were used except for iron(II) which was used as its sulfate.

General aspects of electrode behaviour

X-ray diffraction analysis of the precipitate and the pellet revealed the presence of acanthite (Ag_2S) and greenockite (CdS) only [13]. A difference

between the diffractograms of the precipitate and the pellet was the enhanced intensity of the cadmium sulfide reflections of the pellet compared with the intensity of the silver sulfide reflections. This can be attributed either to more favorable orientation of the cadmium sulfide crystals because of the heating under pressure or to decreased crystallinity of the silver sulfide because of the transition to argentite (cubic) followed by reconversion to polycrystalline acanthite.

The surface of the cadmium membrane had to be polished regularly to maintain acceptable response times; for a change of concentration from 10^{-7} M to 10^{-4} M, 95% of the total potential change was reached within 10 s. At least a ten-fold increase in the response time was observed for the reverse concentration change. In general, the electrode response was less reproducible than that of the copper(II)-selective electrode [9—11]. The slope of the calibration graph (E vs.—log $a_{Cd^{2+}}$) varied between 27.2 and 27.8 mV/decade within one day, but somewhat larger fluctuations were observed at intervals of several days.

The limit of detection of the electrode depended to some extent on the pretreatment. In maleate buffer (pH 6.5), the average value observed was about 6.5, expressed in terms of—log $a_{Cd^{2+}}$. The selectivity coefficients determined at this pH by the fixed interference method are summarized in Table 1 together with those obtained with the Orion cadmium(II)-selective electrode. The latter electrode shows a slightly better selectivity.

Like all metal sulfide electrodes, good sensitivity to sulfide ions was observed. From the intersection of the E vs.—log $a_{Cd^{2+}}$ and the E vs.—log $a_{S^{2-}}$ curve, the solubility product was calculated as $pK_{SO}^{CdS} \sim 26.4$ at $I = 0.1$. This value compares reasonably well with values found in the literature [14].

Response of the electrode as a function of pH

Figure 1 shows the response of the electrode as a function of pH in a solution containing 10^{-3} M cadmium(II) and 0.1 M KNO_3. The decrease above pH 9 must be due to the hydrolysis of cadmium(II); the slope of this part of the curve (56 mV/decade) suggests the precipitation of $Cd(OH)_2$. The E—pH curve calculated with the literature value for the solubility product of $Cd(OH)_2$, $pK_{SO} = 13.2$ [15], almost coincides with the experimental curve. At this concentration level, there is evidently no substantial amount of $CdOH^+$ formed.

Response of the electrode in the presence of complexing agents

The influence of the complexing agents EDTA, NTA, trien and tetren on the electrode response was studied. For this purpose, E—pH curves were recorded for solutions containing 2×10^{-3} M ligand and 10^{-3} M cadmium(II), and for solutions containing 10^{-3} M ligand only (Fig. 2a—d). Theoretical curves were calculated from the equation

$$-\log a_{Cd^{2+}} = \log \beta_{CdL} + \log \{\alpha_{ML(H)} / \alpha_{L(H)}\} + \log \{[L'] / [CdL']\} \qquad (1)$$

where β_{CdL} is the stability constant of the complex and $\alpha_{X(Y)}$ denotes the side-reaction coefficient of the species X with Y; the primed concentrations

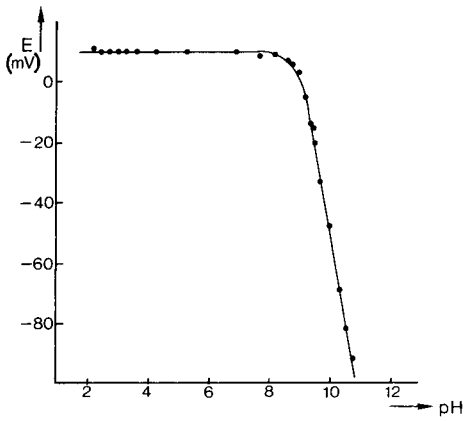


Fig. 1. Response of the cadmium i.s.e. vs. pH in a solution containing 10^{-3} M cadmium nitrate and 10^{-1} M potassium nitrate (•). Solid curve calculated with log $K_{SO} = -13.2$ for $Cd(OH)_2$

TABLE 1

Selectivity coefficients log $k^{pot}_{Cd,N}$ of the cadmium(II)-selective electrode in acidic medium for $C_N = 10^{-3}$ M, $I = 0.1$ and $C_{Cd^{2+}} = 10^{-3}$ M

Metal N	log $k^{pot}_{Cd,N}$ present electrode	log $k^{pot}_{Cd,N}$ Orion electrode
Pb^{2+}	−1.5	−1.8
Zn^{2+}	−3.1	−3.2
Mn^{2+}	−3.4	−3.4
Ni^{2+}	−3.4	−3.5
Fe^{3+}	−3.3	−4.0
Fe^{2+}	−2.7 (under N_2)	−3.4 (under N_2)
Cu^{2+}	—	—

TABLE 2

Logarithmic values of the stability constants used for the calculation of free cadmium concentrations [14, 15]

Complexing agent	β^{H}_{HL}	$\beta^{2H}_{H_2L}$	$\beta^{3H}_{H_3L}$	$\beta^{4H}_{H_4L}$	$\beta^{5H}_{H_5L}$	β^{L}_{CdL}	$\beta^{2L}_{CdL_2}$		
Hydroxide						4.3	7.7	β_3	= 103
Sulfide	12.6	19.5							
EDTA	10.3	16.6	19.3	21.4		16.5		β^{H}_{CdLH}	= 2.9
NTA	9.8	12.4	14.4			10.1	14.5		
Trien	10.0	19.3	26.0	29.4		10.75	13.9		
Tetren	9.7	18.8	26.9	31.6	34.6	14.0			

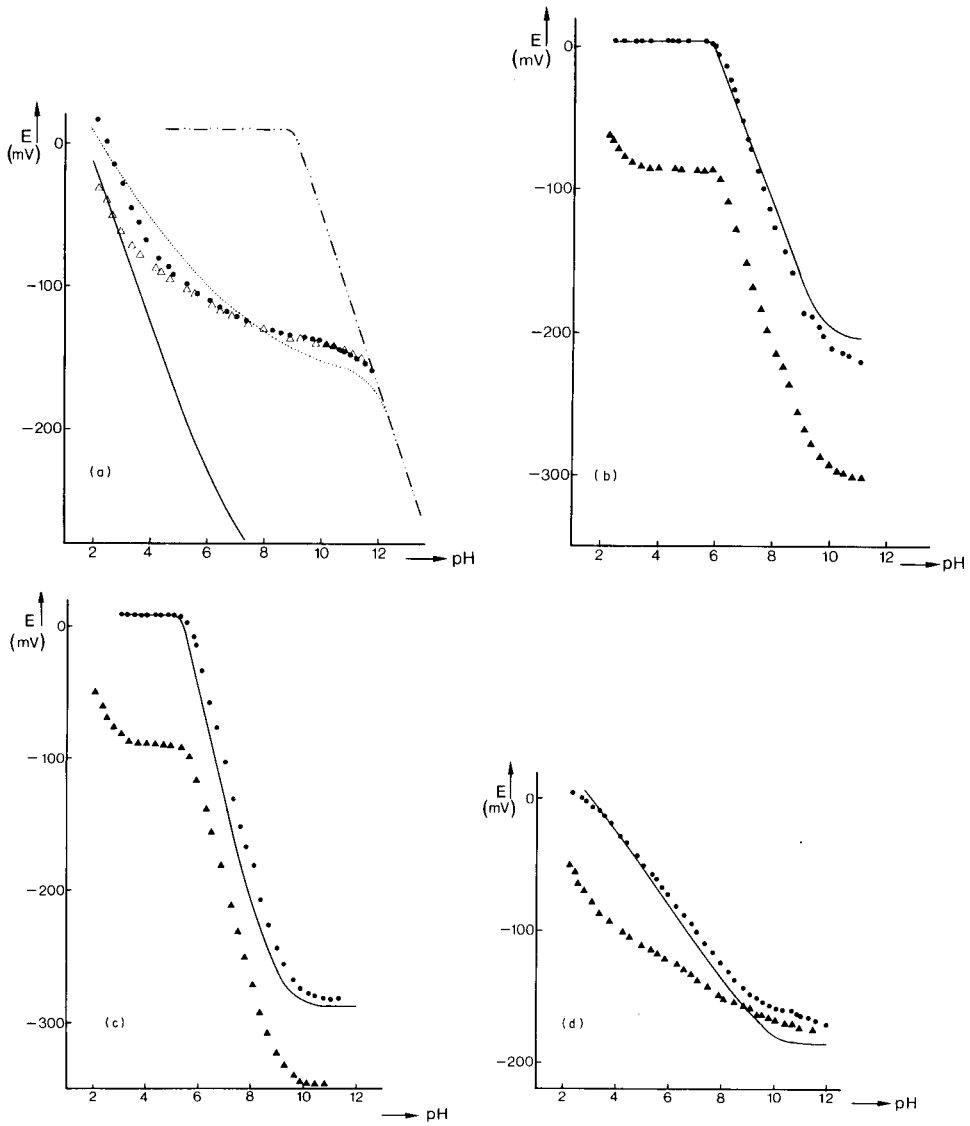


Fig. 2. Response of the cadmium-i.s.e. vs. pH in the presence of different ligands. (a) With 10^{-3} M EDTA (Δ), and 2×10^{-3} M EDTA + 10^{-3} M cadmium nitrate (•) and 10^{-3} M cadmium nitrate without EDTA (— · · —); the theoretical curves were calculated according to eqn. (1) (—) and to eqn. (2) (. . .). (b) With 10^{-3} M trien (▲), and 2×10^{-3} M trien + 10^{-3} M cadmium nitrate (•); the theoretical curve was calculated according to eqn. (1) (—). (c) As for (b) with tetren as the ligand. (d) As for (b) with NTA as the ligand.

include all species formed by side-reactions. The values of the constants used are summarized in Table 2.

Like the copper(II)- and lead(II)-selective electrodes based on the respective mixed sulfide membranes [11, 12], the cadmium(II)-selective electrode seems

to respond fairly correctly to the cadmium ion activity in the bulk solution as far as trien or tetren are concerned. In the case of EDTA, the experimental curve seems to be independent of the presence of the cadmium—EDTA complex. Apparently, the response of the electrode is determined by the excess of ligand alone instead of the ratio [L'] / [CdL']. The experimental curve roughly fits the equation

$$E = -180 + 27.6 \log \alpha^{\frac{1}{2}}_{EDTA(H)} \quad (2)$$

as can be seen from Fig. 2 (a). Such a dependence on the logarithm of the square root of $\alpha_{EDTA(H)}$ was also observed with the other metal sulfide electrodes. In contrast to the copper(II)-selective electrode, the cadmium electrode shows the same behavior towards NTA and polyamines such as trien and tetren. Similar observations have been made with the Orion cadmium electrode [17].

Applicability

The cadmium(II)-selective electrode was tested in the dismountable flow-through cell described in a previous paper [16]. The response time of the membrane is somewhat too long for application to flow injection analysis, but the electrode can be used for continuous monitoring quite well.

The electrode is also useful as a sensor in complexim etric titrations for concentrations down to 10^{-5} M. In the direct titration of cadmium(II), ideal behavior was observed before the equivalence point; especially in the case of EDTA, deviations from ideality were observed after the equivalence point because of the different response mechanism.

MERCURY SULFIDE—SILVER SULFIDE MEMBRANES

Little has been published about mixed mercury sulfide—silver sulfide membranes. Růžička and Lamm [18] mentioned the preparation of a mercury(II)-selective electrode by activating the surface of a graphite rod with pure mercury(II) sulfide or its admixture with silver sulfide. No details were given abou the preparation of the sulfides. Anfält and Jagner [19] prepared a mercury-selective electrode by coating a silver rod with silver sulfide by anodic oxidation in sulfide medium followed by precipitation of mercury(II) sulfide on the surface; this was accomplished by immersing the electrode in a solution of sodium sulfide and then adding a solution of mercury(II) nitrate until the free mercury ion concentration was about 0.01 M. A similar procedure was proposed by van de Leest [8]. None of these electrodes behaved in a manner suitable for the direct determination of mercury.

In his study of the suitability of different compounds for the preparation of solid-state selective membranes, Kahr [20] found that it was difficult to press good pellets from the black cubic HgS (metacinnabar) whereas the red hexagonal HgS (cinnabar) could not be pelletted at all. Pellets with good mechanical properties were obtained with precipitates made from mercury(I) nitrate sol-

utions containing nitric acid; on pressing such precipitates, some elemental mercury was formed because of disproportionation of mercury(I) sulfide. Mixed precipitates containing HgS and Bi_2S_3 were also easily pelletted and membranes prepared in this way showed a better response.

The present report deals with attempts to prepare mixed mercury sulfide—silver sulfide membranes. Although the actual pelletting of the different precipitates did not give trouble, the electrodes showed varying responses, and an irritating lack of stability.

Preparation of the membranes

Two 0.1 M mercury solutions were prepared: the first by dissolving mercury in nitric acid (solution A) and the second by dissolving mercury(II) oxide in nitric acid (solution B). To avoid hydrolysis, dilution was carried out very carefully so that the nitric acid concentration did not fall below 5×10^{-2} M. The presence of mercury(I) in solution A was proved by means of the ammonia test [21]. Mixed silver sulfide—mercury sulfide precipitates were prepared, from both mercury solutions, by the procedure described above for the mixed cadmium sulfide precipitates. For comparison, the "pure" mercury sulfides were also prepared. All chemicals used were of analytical-reagent grade.

Pellets were pressed from the mixed sulfides in a 13-mm die at 150°C by applying a pressure of 980 MPa for at least 2 h. The internal solution of the electrode consisted of 10^{-4} M mercury(II) nitrate in 0.05 M acetate buffer containing 0.1 M KNO_3.

General aspects of electrode behavior

All powdered precipitates and pellets were analyzed by x-ray diffraction analysis. The diffractograms of the "pure" mercury sulfides showed that the precipitate prepared from solution B consisted of metacinnabar only [22], whereas the sulfide made from solution A contained cinnabar [13] in addition to metacinnabar.

The mixed silver sulfide—mercury sulfide precipitates prepared from solutions A and B yielded diffractograms that did not differ significantly from each other; both showed the presence of acanthite as well as cinnabar and metacinnabar. In addition to these materials, another compound has to be present and in fact must be the major component of the precipitate, witness the strong reflections at, e.g., $2\theta = 17.95, 32.50, 37.40$ and 41.30 (Fig. 3). These reflections cannot be attributed to either silver sulfides or mercury sulfides. Probably these unidentified reflections should be attributed to a ternary sulfide that has not so far appeared in any of the standard files. The pellets pressed from the precipitates gave diffractograms similar to those of the powdered precipitates, the only difference being that the peaks were somewhat sharper for the pellets. Under the microscope, some inhomogeneities in the surfaces of the pellets were observed, but diffractograms taken from these parts of the surface showed no differences. The appearance of the inhomogeneities suggests the presence of some elemental sulfur.

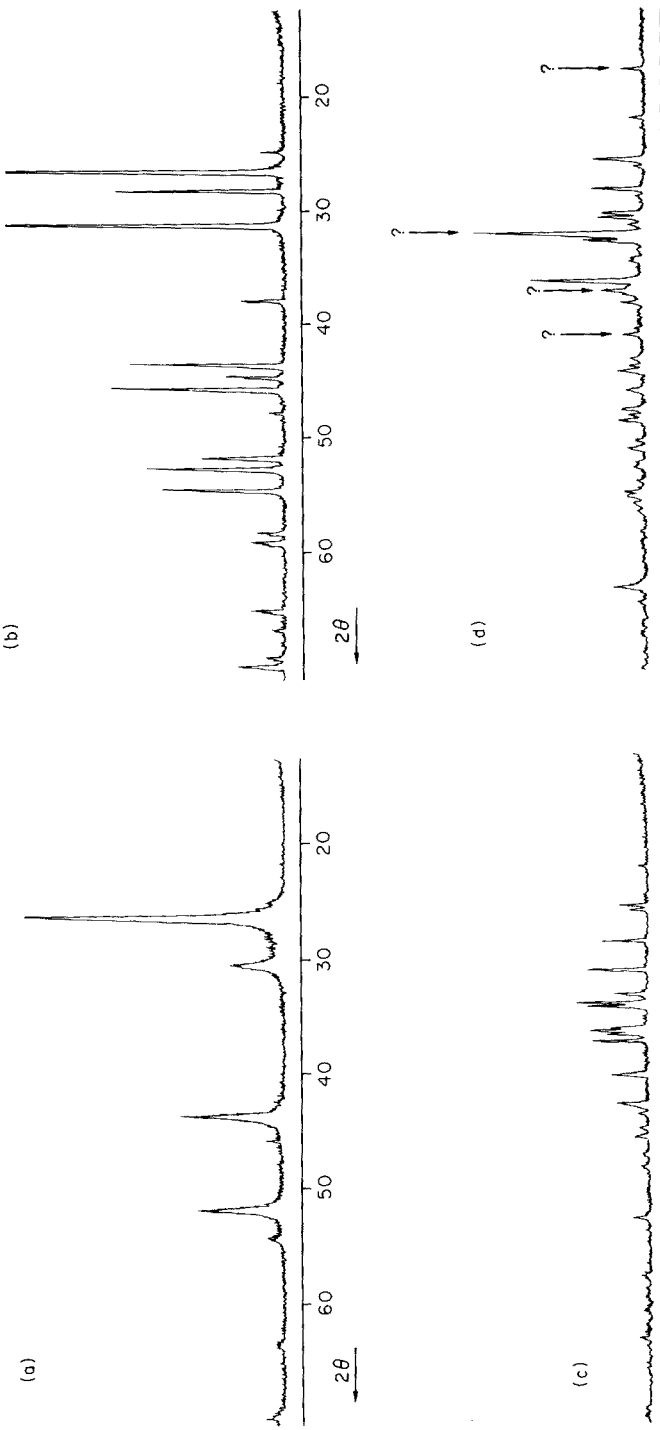


Fig. 3. X-ray diffractograms of some precipitates (Cu $K\alpha$-radiation). (a) "Pure" metacinnabar prepared from mercury solution B (see text); (b) pure cinnabar; (c) acanthite; (d) mixed mercury sulfide—silver sulfide.

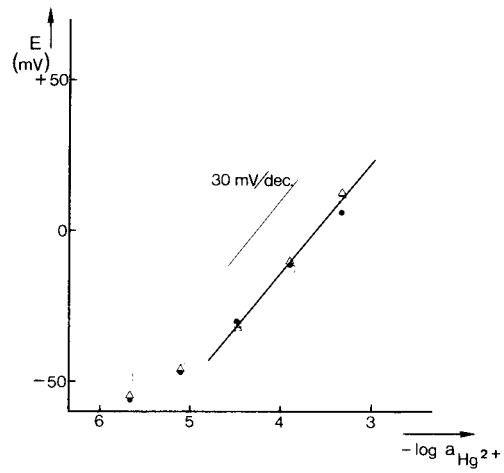


Fig. 4. Calibration curve for the Hg-i.s.e. in acetate buffer (pH 4.8) containing 10^{-1} M KNO_3 : (•) Hg^{2+} only; (□) in the presence of 10^{-4} M copper nitrate; (Δ) in the presence of 10^{-3} M copper nitrate.

Electrodes made with pellets pressed from precipitates prepared from mercury solution A gave the best response to mercury(II) ions. In general, it was very difficult to obtain electrodes that behaved reproducibly and so it was not profitable to test these electrodes as extensively as was done for the other mixed metal sulfide electrodes. Testing was therefore confined to the preparation of calibration graphs and the assessment of the interference by copper(II) ions. Figure 4 shows a typical calibration curve in the absence and the presence of copper(II). The interference by copper is obviously of little importance. The limit of detection expressed in terms of—log $a_{Hg^{2+}}$ is only about 5, which is worse than the other mixed metal sulfide electrodes investigated.

The authors express their gratitude to Mr. W. Ozinga for his assistance with part of the electrochemical experiments, and to Dr. B. Koch and W. Molleman for all the work done on the x-ray diffraction analysis of the samples.

REFERENCES

1 M. S. Frant and J. W. Ross, German Offen. 1 942 379 (CL. G 01 n) 12 Mar 1970.
2 H. Thompson and G. A. Rechnitz, Chem. Instrum., 4 (1972) 239.
3 J. D. Czaban and G. A. Rechnitz, Anal. Chem., 45 (1973) 471.
4 A. V. Gordievskii, V. S. Shterman, A. Ya. Syrenckov, N. I. Savvin, A. F. Zhukov and and Yu. I. Urusov, Zh. Anal. Khim., 27 (1972) 2170.
5 J. Růžička and E. H. Hansen, Anal. Chim. Acta, 63 (1973) 115.
6 H. Hirata and K. Higashiyama, Fresenius Z. Anal. Chem., 257 (1971) 104.
7 M. Mascini and A. Liberti, Anal. Chim. Acta, 64 (1973) 63.
8 R. E. van de Leest, Analyst, 102 (1977) 509.
9 G. J. M. Heijne, W. E. van der Linden and G. den Boef, Anal. Chim. Acta, 89 (1977) 287.

10 G. J. M. Heijne and W. E. van der Linden, Anal. Chim. Acta, 93 (1977) 99.
11 G. J. M. Heijne and W. E. van der Linden, Anal. Chim. Acta, 96 (1978) 13.
12 G. J. M. Heijne, W. E. van der Linden and G. den Boef, Anal. Chim. Acta, 100 (1978) 193.
13 Powder Diffraction File, Joint Committee on Powder Diffraction Standards, Swarthmore Penn., U.S.A. Acanthite, ref. 14-72; greenockite, ref. 6-0314; cinnabar, 6-0256.
14 L. G. Sillén and A. E. Martell, Stability Constants, Spec. Publ. no. 17 (1964) and suppl. no. 1, Spec. Publ. no. 25 (1971), The Chemical Soc., London.
15 A. Ringbom, Complexation in Analytical Chemistry, Interscience, New York, 1963.
16 W. E. van der Linden and G. J. M. Heijne, in E. Pungor and I. Buzás (Eds.), Ion-Selective Electrodes, Akademiai Kiado, Budapest, 1978.
17 W. E. van der Linden and R. Oostervink, Anal. Chim. Acta, 101 (1978) 419.
18 J. Růžička and C. G. Lamm, Anal. Chim. Acta, 53 (1971) 206.
19 T. Anfält and D. Jagner, Anal. Chim. Acta, 55 (1971) 477.
20 G. Kahr, Diss. ETH-Zürich, no. 4927, 1972.
21 C. J. van Nieuwenburg and J. W. L. van Ligten, Kwalitatieve Chemische Analyse, 4th edn., D. B. Centen's Uitgev. Mij., Amsterdam, 1956.
22 NBS- circular 539 (IV) 22.

Analytica Chimica Acta, 108 (1979) 179—191
© Elsevier Scientific Publishing Company, Amsterdam — Printed in The Netherlands

REDETERMINATION OF THE STANDARD pH VALUES FOR POTASSIUM HYDROGENPHTHALATE REFERENCE BUFFER SOLUTION FROM 0 TO 85°C

H. PIERRE BÜTIKOFER and ARTHUR K. COVINGTON*

Department of Physical Chemistry, University of Newcastle, Newcastle upon Tyne, NE1 7RU (Gt. Britain)

(Received 15th January 1979)

SUMMARY

Values of pH(S) for 0.05 mol kg^{-1} solutions of potassium hydrogenphthalate in the temperature range 0—85°C have been obtained from cells without transport. The results are compared with re-analysed results from previous investigations by a new method of multilinear regression of pH as a function of both temperature and added chloride concentration. The results fit the equation $pH(S) = 4.005 + 1.0068 \times 10^{-3} (T - 298.15) + 3.275 \times 10^{-5} (T - 298.15)^2$ where T is the temperature expressed in Kelvin; pH(S) = 4.005 at 25°C.

Most national and international scales of pH include amongst their standard reference buffers the solution of molality 0.05 mol kg^{-1} of potassium hydrogen-*o*-phthalate first suggested as a pH standard by Dodge [1] in 1920. The pH values adopted are derived from the work at the National Bureau of Standards (NBS) of Hamer and Acree [2] and of Hamer et al. [3] in 1944—6 which covered the temperature range 0—60°C, and the later work of Bower and Bates [4] which extended the range to 60—95°C. Guggenheim, in recalculating this work for the revision of the British Standard BS 1647 pH Scale in 1961, recognised that the two sets of data were inconsistent [5]. He was unable to his satisfaction to fit the data to a single polynomial and the British Standard Specification defined [5] pH by the two equations

$$pH = 4.000 - \tfrac{1}{2}[(t - 15)/100]^2 \text{ for } 0 < t < 55 \quad (1)$$

and

$$pH = 4.000 - \tfrac{1}{2}[(t - 15)/100]^2 - (t - 55/500) \text{ for } 55 < t < 95 \quad (2)$$

with the value at 25°C being 4.005. Bates, however, when he revised [6] the standard pH values, pH(S), for a number of reference buffers adopting the Bates—Guggenheim convention [7] for the chloride-ion activity coefficient, fitted the two sets of data to a single polynomial. The value at 25°C was 4.008. Recently Hetzer et al. [8] published the results of a redetermination of pH(S) carried out in 1966 at NBS in connection with the certification of a new batch of standard reference material (SRM 185d). They quoted an experimental value of 4.007 and a smoothed value 4.005_8 for 25°C.

The British Standard pH Scale [5], unlike all other national scales except the Japanese [9], adopts a single primary standard which is the 0.05 mol kg^{-1} solution of potassium hydrogenphthalate. It is therefore of greater importance for the British Scale than for multistandard scales that the assigned pH(S) values for the primary standard be known accurately. In connection with the current revision of BS 1647, pH(S) has been redetermined from 0 to 85°C, and the existing data have been re-analysed for the phthalate reference buffer solution from the cell

$$\text{Pt} \mid \text{Pd} \mid \text{H}_2 \mid \text{KHPh (0.05 mol kg}^{-1}\text{), KCl } (m) \mid \text{AgCl} \mid \text{Ag} \qquad \text{(I)}$$

where Ph = phthalate and m = 0.005—0.05 mol kg^{-1}.

EXPERIMENTAL

Potassium hydrogenphthalate was either AnalaR grade (B.D.H., Poole, Dorset) or primary pH standard grade material certified at the National Physical Laboratory (NPL). A few determinations with this material alongside NBS SRM 185e did not reveal any detectable difference between results. Potassium chloride was AnalaR grade (B.D.H.). Both this and the phthalate samples were dried overnight at 110°C. Solutions were prepared on a mass basis with nitrogen-purged distilled water. The cell vessels used were those described earlier [10] and were filled under nitrogen pressure. Silver—silver chloride electrodes were prepared as described earlier [11]. Before assembly of each cell, these electrodes were soaked overnight in the appropriate cell electrolyte. Palladized platinum electrodes, the use of which is necessary to avoid reduction of phthalate by hydrogen gas, were prepared by plating 1-cm^2 platinum foil substrates at 10 mA cm^{-2} for 10 min in a solution of 2 g of $PdCl_2$ in 100 ml of 1 mol l^{-1} hydrochloric acid. These electrodes had a greyish appearance compared to platinized platinum electrodes.

Six cells were measured at a time in a water bath maintained at the appropriate temperature by two Techne (Cambridge) Tempunits Type TU8, with cooling when necessary supplied by a Grant (Cambridge) refrigerator unit. The temperature was indicated by a quartz crystal thermometer (Hewlett-Packard Dymec Model 2801 A). Measurements were made to ±0.05 mV with a digital voltmeter (Type 701; Fenlow Electronics, Weybridge, Surrey) calibrated against an NPL-certificated Weston cell. Measurements were made first at 25°C and the temperature was then changed by 5°C intervals up or down. Some cells were studied over the whole temperature range and others over restricted ranges. Initial equilibrium at 25°C was reached in 60—90 min and within 20—30 min after change in temperature. Measurements were corrected to 1 atm partial pressure of hydrogen gas by using the table published by Bates [12].

RESULTS

The function $p(a_H\gamma_{Cl})$ is calculated from the e.m.f. of Cell I by the equation

$$p(a_H\gamma_{Cl}) = -\log (m_H\gamma_H\gamma_{Cl}) = [(E - E^\ominus)/k] + \log m \qquad (3)$$

where $k = RT(\ln 10)/F$, m is the KCl molality, and E° is the standard potential of the reference electrode. The chloride ion activity coefficient was calculated from the Bates—Guggenheim convention [7]: $\log \gamma_{Cl} = -AI^{\frac{1}{2}}/(1 + 1.5\, I^{\frac{1}{2}})$, where I is the ionic strength, taken as $0.0534 + m$ at all temperatures. The values of A used were those listed by Bates [12] appropriate to the molality scale. Thus $pa_H = pa_H\gamma_{Cl} + \log \gamma_{Cl}$. and $pH(S) = pa^0_H$ is obtained by linear regression analysis of pa_H values against m to $m = 0$. It was ascertained that this procedure yielded the same result for pa^0_H as regression of $pa_H\gamma_{Cl}$ values and the use of the Bates—Guggenheim convention [7] for the $m = 0$ value only.

The majority of the e.m.f. values obtained are listed in Tables 1 and 2, which also include the values of pa_H. The pa_H values were calculated by using standard potential values E° obtained from a recalculation of the data of Bower and Bates [4] described elsewhere [13], to which was added 0.1 mV at each temperature to bring the values into line with the E° value at 25°C repeatedly obtained in this laboratory. This procedure is recommended by Bates and Robinson [14]. The values of pa^0_H at each temperature obtained by linear regression analysis are shown in Table 3, column 20. It was noted in one particular run, with freshly remade silver—silver chloride electrodes (Table 4) restricted to 25°, 45° and 60°C, that the slopes of the regression analyses were much lower than in the other runs (see Fig. 1). High values of the slopes were obtained only after the silver—silver chloride electrodes had been subjected to temperatures above 60°C or to prolonged exposure to phthalate.

All the results, except the few that gave low slopes, were analysed by a multilinear regression analysis method described elsewhere [13]. Briefly this method makes use of the fact that the slopes B_t of the linear plots of pa_H against m are a uniform function of temperature. Assuming that B_t is a linear function of temperature:

$$B_t = B_{25} + b(t - 25) \tag{4}$$

(where b is a constant), then

$$pa_{H(t)} = pa^0_{H(t)} + B_t m \tag{5}$$

and

$$pa_{H(t)} = pa^0_{H(t)} + B_{25}m + bm(t - 25) \tag{6}$$

For the variation of pH with temperature, a fitting equation of the form

$$pH = (A/T) + B + CT + DT^2 \tag{7}$$

has usually been adopted [6]. Inserting $T = 298$ K (an abbreviation for 298.15 K) and subtracting the resulting equation from eqn. (7) gives

$$(T - 298)\, pH = B(T - 298) + C(T - 298)^2 + D(T - 298)^3 \tag{8}$$

or

$$pH = pH_{25} + C(t - 25) + D(t - 25)^2 \tag{9}$$

TABLE 1

Results for e.m.f. (in mV) of cell I and pa_H in the ranges 0—25°C and 25—50°C

m KCl ($\times 10^{-2}$ mol kg^{-1})	0°C	5°C	10°C	15°C	20°C	25°C
1.0057	566.53[a]	569.46	572.71	575.87	579.16	
	3.989	3.985	3.984	3.984	3.988	—
1.0064	566.43	569.63	572.73	—	—	582.03
	3.993	3.989	3.985	—	—	3.988
1.4970	556.67	—	562.85	—	—	571.76
	3.983	—	3.979	—	—	3.984
1.5035	557.33[a]	559.96	563.01	566.07	569.16	—
	3.991	3.985	3.984	3.985	3.989	—
1.9308	551.43[a]	553.96	556.91	559.87	562.76	—
	3.989	3.983	3.981	3.983	3.985	—
2.0066	549.73	552.73	555.63	—	—	563.93
	3.984	3.997	3.975	—	—	3.997
2.5078	544.93[a]	547.16	550.21	553.17	555.96	—
	3.981	3.971	3.973	3.977	3.979	—
2.5952	543.63	546.33	549.13	—	—	557.13
	3.977	3.971	3.969	—	—	3.971
3.0016	540.43[a]	542.96	545.61	548.47	551.16	—
	3.974	3.971	3.967	3.970	3.972	—
3.0027	539.87	—	545.35	—	—	553.11
	3.969	—	3.963	—	—	3.965
3.5061	536.33	538.93	541.53	—	—	549.11
	3.969	3.963	3.960	—	—	3.962
	25°C	30°C	35°C	40°C	45°C	50°C
0.9976	528.43	585.68	588.68	591.83	594.87	597.91
	3.991	3.999	4.005	4.015	4.025	4.036
1.5534	571.23	574.18	577.08	580.03	582.87	585.81
	3.986	3.992	3.999	4.009	4.019	4.032
2.0141	566.88	569.68	572.43	575.27	578.01	—
	3.987	3.994	4.002	4.014	4.026	—
2.4749	561.38	564.08	566.73	569.37	572.01	—
	3.982	3.990	3.998	4.008	4.020	—
3.0167	555.38	557.98	560.53	563.17	565.81	—
	3.966	3.974	3.981	3.992	4.006	—

[a]At 0.5°C.

Combining eqns. (9) and (6) gives

$$pa_{H(t)} \equiv pH_t = pH_{25} + B_{25}m + (C + bm)(t - 25) + D(t - 25)^2 \qquad (10)$$

If the linear variation of slope in eqn. (4) is inadequate, quadratic variation can be assumed. Equation (10) was used in a multilinear regression analysis [13] based on a program for the IBM 370 written in APL. The parameters obtained for this equation are given in Table 5. Values of pH_t are given in the final column of Table 3. Plots of residuals against predicted values or temperature

TABLE 2

Results for e.m.f. (in mV) of cell I and pa_H at 25°C, 45°C and 55—85°C

m KCl ($\times 10^{-2}$ mol kg^{-1})	25°C	45°C	55°C	60°C	65°C	70°C	75°C	80°C	85°C
0.7292	—	603.62	—	613.29	616.58	619.38	—	—	—
	—	4.029	—	4.070	4.088	4.099	—	—	—
1.0016	582.47	595.02	601.14	604.19	607.28	610.28	613.42	616.51	619.35
	3.994	4.029	4.054	4.069	4.085	4.102	4.122	4.142	4.159
1.0160	582.12	—	600.90	—	606.43	609.33	612.58	—	619.94
	3.996	—	4.057	—	4.079	4.094	4.116	—	4.174
1.4987	571.72	—	588.89	591.79	596.67	597.83	600.58	603.68	606.94
	3.984	—	4.038	4.054	4.069	4.091	4.108	4.131	4.157
1.5024	571.71	583.63	589.41	592.18	—	597.80	—	—	—
	3.9853	4.022	4.047	4.060	—	4.092	—	—	—
1.5060	571.77	582.52	589.44	—	595.08	—	—	603.66	—
	3.987	4.021	4.049	—	4.078	—	—	4.133	—
1.9883	—	575.22	580.94	583.59	586.38	589.08	591.92	594.71	597.55
	—	4.008	4.036	4.050	4.066	4.083	4.103	4.123	4.145
2.0026[a]	564.11	575.18	581.09	583.23	—	588.98	—	—	—
	3.972	4.010	4.042	4.047	—	4.045	—	—	—
2.4939	—	569.08	574.31	576.63	—	582.10	—	—	—
	—	4.007	4.031	4.040	—	4.076	—	—	—
2.4988	558.36	568.98	573.89	576.43	—	581.78	—	—	—
	3.976	4.006	4.025	4.038	—	4.073	—	—	—
2.9220[a]	553.86	564.23	569.39	571.73	—	576.78	—	—	—
	3.966	3.997	4.022	4.033	—	4.065	—	—	—
3.0052	553.32	—	568.79	—	579.83	576.13	578.68	581.58	584.44
	3.969	—	4.024	—	4.054	4.067	4.085	4.110	4.134
3.0065	—	563.48	568.61	571.08	—	576.10	—	—	—
	—	3.997	4.022	4.035	—	4.067	—	—	—
3.4952	549.22	—	563.99	—	—	—	—	—	—
	3.963	—	4.014	—	—	—	—	—	—

[a]NBS SRM 185e.

are shown in Fig. 2. These plots show that the residuals are randomly distributed and that the fit of eqn. (10) to the data is very good (residual mean sum of squares = 1.16×10^{-8}). The pa_H^0 values by multilinear regression may be compared with those obtained by linear regression at each temperature and smoothed with eqn. (10) given in column 20 of Table 3. Differences do not exceed 0.001 except at the extremes of the temperature range.

RECALCULATION OF PREVIOUS DATA

The results of Hamer et al. [2, 3] were converted from international to absolute volts by multiplying by 1.00033 and analysed by linear regression analysis at each temperature and by the multilinear regression method. The results are shown in columns 6—8 of Table 3. The E° values taken were either the values assumed for analysis of the present data or those of Harned and Ehlers (see [13]) converted to absolute mV. The parameters of eqn. (10) are shown in Table 5. Plots of residuals shown in Fig. 3 show a sigmoidal tendency which is indicative of some systematic error in the results, or the failure of eqn. (9) to fit the temperature variation of the results.

TABLE 3

Summary of pH(S) values for phthalate buffer[a]

Temp. (°C)	B.S. 1647 [4]	NBS [12]	Hamer et al. [2, 3]					Bower and Bates [4]	Bates [6]		Etz [15]				Hetzer et al. [8]				This work		
			(1)	(2)	(3)[b]	(5)[b]	(3)[c]	(1)	(1)	(2)	(1)	(2)	(4)[d]	(5)[d]	(1)	(2)	(3)[e]	(5)[e]	(1)[c]	(2)[c]	(5)[c]
0	4.011	4.003	4.007	4.012	4.007	4.000	4.002	—	4.006	4.003	—	4.003	4.004	4.001	4.010	4.010	4.010	4.008	3.998	3.998	4.000
0.5	—	—	—	—	—	3.999	—	—	—	4.003	4.001[f]	4.002[f]	4.003[f]	4.000[f]	—	4.009	—	—	4.001	3.998	4.000
5	4.005	3.999	4.005	4.005	4.000	3.997	3.997	—	3.999	3.999	3.998	3.998	3.999	3.998	4.003	4.004	4.005	4.004	3.998	3.997	3.998
10	4.001	3.998	3.999	4.001	3.997	3.995	3.994	—	3.996	3.998	3.997	3.996	3.997	3.997	4.000	4.000	4.001	4.002	3.994	3.996	3.997
15	4.000	3.999	4.000	4.000	3.996	3.996	3.994	—	3.997	3.999	3.995	3.996	3.997	3.998	3.999	3.999	4.001	4.002	3.994	3.998	3.998
20	4.001	4.002	4.003	4.001	3.999	3.999	3.997	—	4.000	4.002	3.998	3.999	4.000	4.000	4.001	4.001	4.002	4.003	3.999	4.000	4.001
25	4.005	4.008	4.008	4.005	4.005	4.004	4.005	—	4.008	4.008	4.005	4.004	4.005	4.005	4.007	4.006	4.007	4.007	4.004	4.005	4.005
30	4.011	4.015	4.016	4.011	4.012	4.011	4.012	—	4.016	4.015	4.011	4.011	4.012	4.011	4.012	4.012	4.012	4.013	4.011	4.011	4.011
35	4.020	4.024	4.025	4.019	4.023	4.020	4.021	—	4.024	4.024	4.018	4.020	4.020	4.019	4.018	4.021	4.018	4.021	4.022	4.019	4.018
37	—	—	4.032[g]	4.027[g]	—	4.024	—	—	—	4.028	—	4.024	4.024	4.022	—	4.025	—	4.024	—	4.023	4.022
40	4.031	4.035	4.036	4.030	4.034	4.031	4.032	—	4.035	4.035	4.031	4.030	4.030	4.028	4.032	4.031	4.033	4.031	4.032	4.028	4.027
45	4.045	4.047	4.050	4.043	4.047	4.045	4.045	—	4.047	4.047	4.043	4.042	4.042	4.039	4.043	4.043	4.044	4.043	4.040	4.039	4.038
50	4.061	4.060	4.068	4.059	4.064	4.060	4.061	—	4.063	4.060	4.057	4.055	4.055	4.053	4.056	4.056	4.057	4.056	4.053	4.051	4.050
55	4.080	4.075	4.084	4.077	4.081	4.077	4.078	—	4.080	4.075	—	4.070	4.070	4.067	4.071	4.071	4.073	4.072	4.067	4.065	4.064
60	4.091	4.091	4.101	4.097	4.097	4.096	4.094	4.082	4.095	4.091	4.082	4.085	4.086	4.084	4.087	4.087	4.089	4.090	4.078	4.081	4.080
65	4.105	—	—	—	—	4.118	—	—	—	4.108	—	4.102	4.102	4.102	—	4.104	—	4.110	4.098	4.098	4.097
70	4.121	4.126	—	—	—	4.141	—	4.124	4.124	4.126	4.120	4.119	4.120	4.122	—	4.122	—	4.132	4.112	4.116	4.116
75	4.140	—	—	—	—	4.166	—	—	—	4.145	—	4.137	4.139	4.144	—	4.141	—	4.156	4.135	4.136	4.137
80	4.161	4.164	—	—	—	4.194	—	4.162	4.162	4.164	—	4.156	4.158	4.168	—	4.160	—	4.183	4.160	4.158	4.159
85	4.185	—	—	—	—	4.223	—	—	—	4.185	—	4.175	4.178	4.193	—	4.181	—	4.211	4.183	4.181	4.183
90	4.211	4.205	—	—	—	4.225	—	4.202	4.202	4.205	—	4.195	4.199	4.220	—	4.201	—	4.241	—	4.206	4.208
95	4.240	4.227	—	—	—	4.289	—	4.231	4.231	4.227	—	4.215	4.221	4.249	—	4.222	—	4.273	—	4.233	4.236

[a](1) Original data; (2) original data smoothed; (3) experimental data recalculated; (4) recalculated, smoothed, usual method; (5) recalculated, smoothed, new method.

[b]E° calculated from data of Harned and Ehlers, see [13].

[c]E° calculated by Bütikofer et al. [13] + 0.1 mV at all temperatures.

[d]E° calculated by Etz [15]

[e]E° calculated from data of Bates and Bower [16] + 0.04 mV at all temperatures.

[f]At 1°C.

[g]At 38°C.

TABLE 4

Results for e.m.f. (in mV) of cell I and pa°_{H} at 25°C, 45°C and 60°C

m KCl ($\times 10^{-2}$ mol kg^{-1})	25°C	45°C	60°C
1.0057	582.26	594.92	604.20
	3.992	4.029	4.071
1.5035	572.06	583.62	592.20
	3.992	4.022	4.066
1.9308	565.66	577.02	585.40
	3.990	4.024	4.065
2.5078	558.66	569.62	577.70
	3.982	4.017	4.059
3.0016	553.76	564.22	—
	3.975	4.008	—

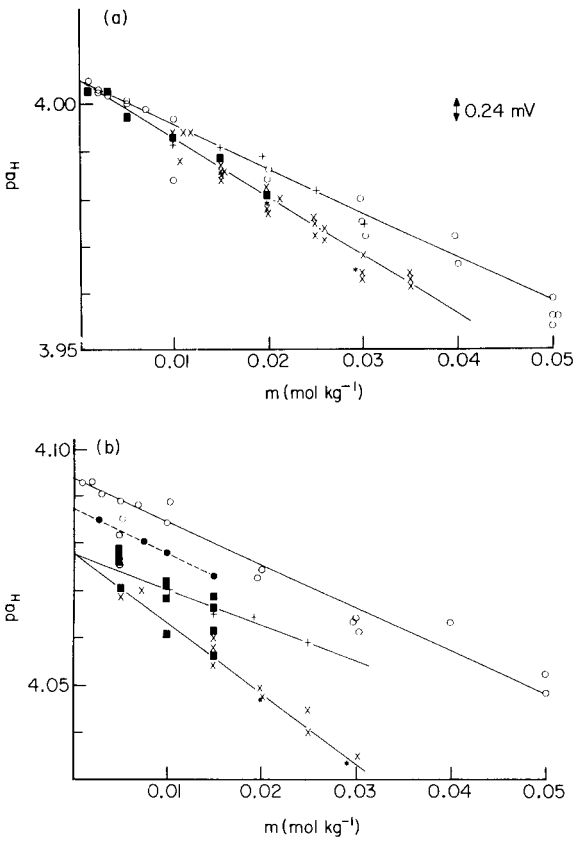


Fig. 1. Recalculated results for 0.05 mol kg^{-1} potassium hydrogenphthalate solution at (a) 25°C and (b) 60°C. (○) Hamer et al. [2, 3]; (▪) Covington and Ferra (unpublished) in (a) and Bower and Bates [4] in (b); (●) Etz [15]; (+) this work, new silver—silver chloride electrodes; (×) this work, old silver—silver chloride electrodes; (∗) old silver—silver chloride electrodes with NBS SRM 185e material.

TABLE 5

Parameters of the eqns. (10) for the 0.05 mol kg^{-1} potassium hydrogenphthalate buffer solutions

Workers	No. of obs.	A	$10B$	10^3C	10^4D	10^5E	$10^6 \times$ RMS
Hamer et al. [2, 3]	117	4.0041936 $\pm 0.2869 \times 10^{-3}$	−9.403845 $\pm 10.92 \times 10^{-3}$	1.19924 $\pm 0.013 \times 10^{-3}$	−3.155341 $\pm 0.5642 \times 10^{-3}$	4.091084 $\pm 0.000528 \times 10^{-3}$	3.139
Etz [15]	143	4.004684 $\pm 0.4948 \times 10^{-3}$	−9.016825 $\pm 47.72 \times 10^{-3}$	1.03846 $\pm 0.0233 \times 10^{-3}$	−2.231069 $\pm 2.235 \times 10^{-3}$	3.504155 $\pm 0.000499 \times 10^{-3}$	6.048
Hetzer et al. [8]	39	4.0071109 $\pm 0.6508 \times 10^{-3}$	−12.17154 $\pm 56.27 \times 10^{-3}$	0.959014 $\pm 0.03219 \times 10^{-3}$	−46.307692 $\pm 2.906 \times 10^{-3}$	4.055571 $\pm 0.000715 \times 10^{-3}$	1.921
This work	205	4.0047976 $\mp 0.8035 \times 10^{-3}$	−11.738406 $\pm 35.88 \times 10^{-3}$	1.000685 $\pm 0.03063 \times 10^{-3}$	−96.178308 $\pm 1.208 \times 10^{-3}$	3.274523 $\pm 0.00422 \times 10^{-3}$	0.0116

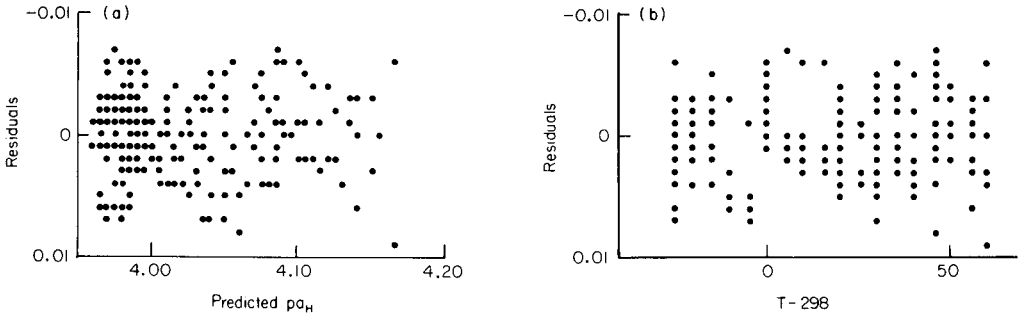


Fig. 2. Residual plots from fitting the results of the present work to eqn. (10). (A) Against predicted pa_H; (B) against $(T - 298)$. Plots are computer-produced and do not show all points because of superposition.

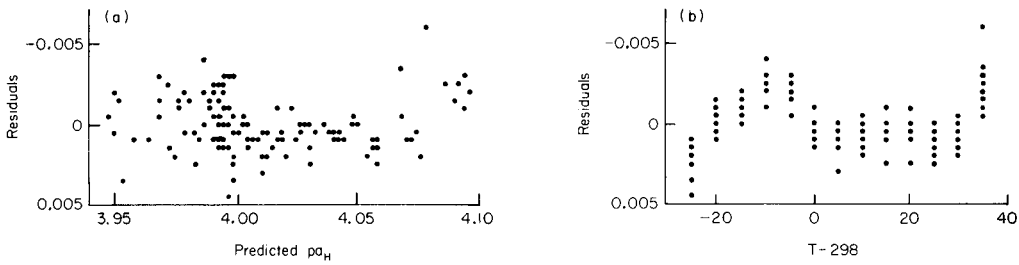


Fig. 3. As for Fig. 2 but for the results of Hamer et al. [2, 3].

Bower and Bates [4] did not report their raw e.m.f. data, but gave the slopes and intercepts from their regression analysis of points for three chloride concentrations. Their raw data at 60°C (obtained from Professor Bates) are compared with those of Hamer et al. [2, 3] in Fig. 1 which shows well the nature of the discrepancy referred to earlier between the two sets of data. The results reported by Hetzer et al. [8], also for three chloride concentrations only, were analysed by the new method with the results shown in column 19 of Table 3. Parameters of the fitting eqn. (10) are shown in Table 5 and the residual plots in Fig. 4. The $E^{\ominus}$ values used in the calculations were derived by adding 0.04 mV to the values of Bower and Bates [4], to bring them into line with the values adopted by Hetzer et al. [8].

After the experimental work described in this paper was finished, an investigation of potassium hydrogenphthalate by Etz [15] at NBS carried out in connection with the certification of SRM 185e came to our attention. Etz obtained the $E^{\ominus}$ values of his silver—silver chloride electrodes by making measurements in 0.01 mol kg^{-1} hydrochloric acid at each temperature and by assuming values for $\gamma_{\pm}$ of HCl at each temperature as calculated by Bower and Bates. Etz's raw results were analysed by both the methods of analysis described above with the results shown in columns 14 and 15 of Table 3. Parameters of eqn. (10) are shown in Table 5. Plots of residuals (Fig. 5) show a

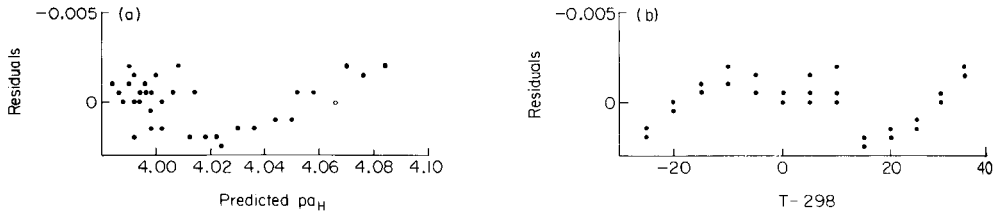


Fig. 4. As for Fig. 3 but for the results of Hetzer et al. [8].

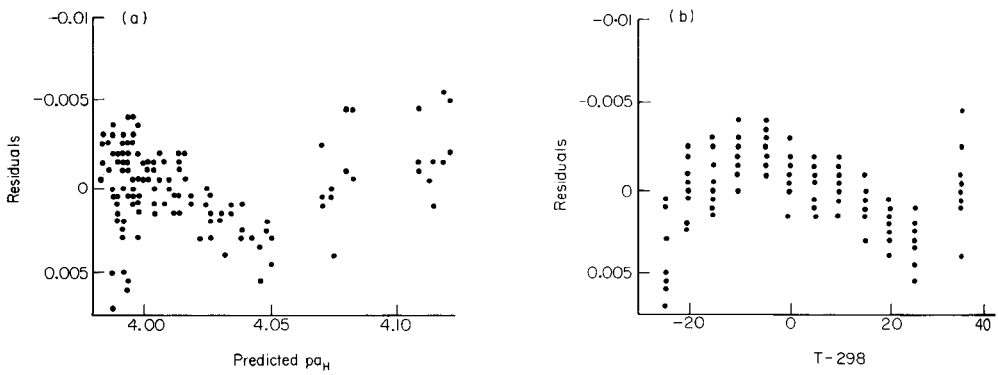


Fig. 5. As for Fig. 3 but for the results of Etz [15].

sigmoidal tendency. The results from all recalculations are shown in the form of a deviation plot in Fig. 6; the base line chosen is that given by the present data smoothed by means of eqn. (10).

Table 3 summarizes all previous results available for potassium hydrogenphthalate solutions, both those given or recalculated previously and those recalculated in the present work.

DISCUSSION

Figure 1(a) summarizes the present situation at 25°C. The NBS determinations of Hamer et al., of Hetzer et al. and of Etz (although only the first of these is shown on Fig. 1) are in agreement with the present investigations with newly prepared silver—silver chloride electrodes. The results for SRM 84a are noticeably less scattered than those of 84b [2, 3]. Although the present results with silver—silver chloride electrodes which have been exposed to phthalate solutions at high temperature or for long periods lie on a line of higher slope, the intercept pa_H^0 value is not affected. The two determinations illustrated, which were made with SRM 185e, are not different from those with the British-produced material.

The situation at 60°C is markedly different. The results of Bower and Bates [4] lie scattered in the region of the low and high slope values from the present

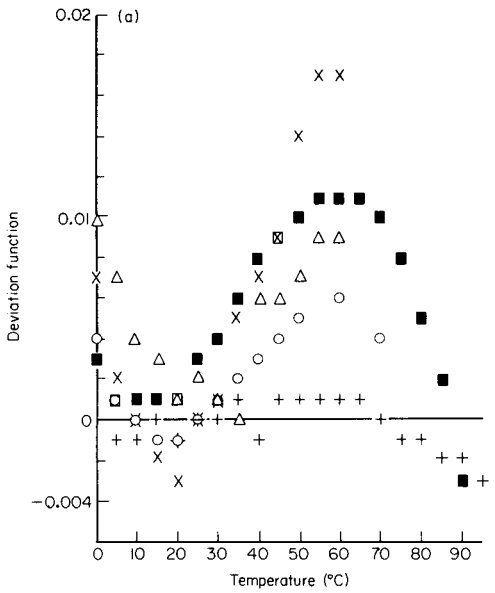


Fig. 6. pH deviation plot for recalculated results by multilinear regression at each temperature and smoothing by eqn. (9). (×) Hamer et al. [2, 3]; (○) Etz [15]; (△) Hetzer et al. [8]; (▪) Hamer et al. [2, 3], Bates and Bower [4, 16]; (+) this work.

work. Those of Hamer et al. [2, 3] lie on a distinctly higher line displaced by 0.016. Etz's results and those of Hetzer et al. (not shown) lie between these and the "low" slope results. Although our "low" and "high" slope results have been extrapolated to a common intercept, the "low" slope results could lead to a pa_H^0 value higher by 0.004. Smoothing the intercept values tends to reduce the differences between the data.

The sigmoidal tendency in the residual plots of Figs. 3—5 is not present in Fig. 2 but it may be noted that in this last case the residuals are greater by almost a factor of 2. The method of determining the results by the procedure of thermal cycling could be one factor which produces the sigmoidal residual plots but another may be the failure of eqn. (10) to fit the pH(S) variation with temperature adequately.

Table 3 shows the discrepancy in pa_H^0 = pH(S) values between the data of Hamer et al. and all other determinations. Bates [6], using a single smoothing equation on the combined data of Hamer et al. [2, 3] and Bower and Bates [4], reduced the increasing deviation of the results of Hamer et al. at 50—60°C to about 0.006 in pH. The results of Etz [15] are in closer agreement with those of the present work, the deviation at 60°C being 0.006. Slightly greater deviations are apparent in the results of Hetzer et al. [8], particularly at temperatures below 15°C. These workers found it necessary to use a separate set of cells in the range 40—60°C and this is very apparent from the form of the residual plots shown in Fig. 4. The rather large number of results rejected by

these workers, on the basis of their criteria that (a) differences between pairs of electrodes in the same cell should not exceed 0.1 mV, and (b) recovery of the cells at 25°C after exposure to 60°C should be better than 0.3 mV, is rather worrying. It is certainly true that the overall reproducibility of cells containing phthalate is not as good as for other Harned-type cells. Hetzer et al. attribute this to reduction of phthalate at palladized hydrogen electrodes [8]. These electrodes tend to be more sluggish in response than platinized platinum hydrogen electrodes, but their use alongside platinized electrodes in cells, where there is no risk of chemical reduction, gives identical results. The behaviour of silver—silver chloride electrodes in phthalate solutions seems not to be entirely reliable as shown by the different values of the slopes found for old and freshly prepared electrodes. All NBS determinations were made with freshly prepared electrodes and the slopes of plots of eqn. (4) are in agreement with the present low slope values. This problem with silver—silver chloride electrodes is being investigated further, but it does not affect values of the intercept, pa^0_H.

Figure 7 shows a deviation plot of results obtained by analysis by the single-stage method and reveals somewhat more clearly the discrepancies between the four principal determinations. Examination shows that below 35°C all determinations, except for those of Hetzer et al. [8], lie within ±0.002. In the region 40—95°C the uncertainty may be as great as ±0.006 but this is entirely adequate because it is doubtful whether operational pH measurements to better than ±0.01 are possible in this temperature range. Some of the uncer-

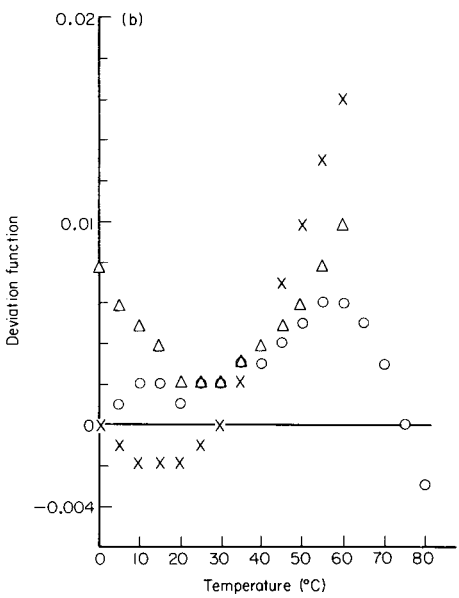


Fig. 7. pH deviation plot for recalculated results by multilinear regression based on eqn. (10). (×) Hamer et al. [2, 3]; (○) Etz [15]; (△) Hetzer et al. [8].

tainty is due to variations in E° of the silver—silver chloride electrode. A difference of 0.1 mV leads to a variation of 0.0017 in pH. At 0°C the E° value is particularly uncertain by perhaps ±0.2 mV.

Very recently, Manning [17] has published values for 0.05 mol kg^{-1} potassium hydrogenphthalate solution obtained from measurements on cell I over the temperature range 93—200°C. The raw results were not given but it may be noted that extrapolation of the results of the present work to 100°C gives pH(S) = 4.264 compared with 4.254 ± 0.03 given by Manning [17]. The agreement is entirely satisfactory.

We thank ICI Mond Division for financial support of this work and in particular Dr. P. O. Kane for his interest and encouragement. We are grateful to Drs. R. G. Bates, R. A. Durst and E. Etz for providing original data.

REFERENCES

1 F. D. Dodge, J. Am. Chem. Soc., 42 (1920) 1655.
2 W. J. Hamer and S. F. Acree, J. Res. Nat. Bur. Stand., 32 (1944) 215.
3 W. J. Hamer, G. D. Pinching and S. F. Acree, J. Res. Nat. Bur. Stand., 36 (1946) 47.
4 V. E. Bower and R. G. Bates, J. Res. Nat. Bur. Stand., 59 (1954) 261.
5 British Standards Institution, Specification for pH Scale BS 1647 (1961).
6 R. G. Bates, J. Res. Nat. Bur. Stand., 66A (1962) 179.
7 R. G. Bates and E. A. Guggenheim, Pure Appl. Chem., 1 (1961) 163.
8 H. B. Hetzer, R. A. Durst, R. A. Robinson and R. G. Bates, J. Res. Nat. Bur. Stand., 81A (1977) 21.
9 Japanese Industrial Standard, Method for Determination of pH, Z8802 (1964).
10 C. P. Bezboruah, M. F. G. F. C. Camoes, A. K. Covington and J. V. Dobson, J. Chem. Soc. Faraday Trans. 1, 69 (1973) 949.
11 A. K. Covington and J. E. Prue, J. Chem. Soc., (1955) 3696.
12 R. G. Bates, Determination of pH. Theory and Practice., 2nd edn., Wiley, New York, 1973, p. 283.
13 H. P. Bütikofer, A. K. Covington and D. A. Evans, submitted.
14 R. G. Bates and R. A. Robinson, private communication (1976).
15 E. Etz, unpublished work (1973), private communication from Drs. R. A. Durst and E. Etz (1977).
16 R. G. Bates and V. E. Bower, J. Res. Nat. Bur. Stand., 53 (1954) 283.
17 G. D. Manning, J. Chem. Soc. Faraday Trans. 1, 74 (1978) 2434.

Analytica Chimica Acta, 108 (1979) 193—204
© Elsevier Scientific Publishing Company, Amsterdam — Printed in The Netherlands

DIFFERENTIAL PULSE VOLTAMMETRIC OXIDATION OF POLYINOSINIC ACID AND ITS COMPONENTS

LIONEL G. KARBER and GLENN DRYHURST*

Department of Chemistry, University of Oklahoma, Norman, Oklahoma 73019 (U.S.A.)

(Received 29th January 1979)

SUMMARY

The differential pulse voltammetric oxidation of polyinosinic acid (poly(I)), inosine-5′-monophosphate, inosine and hypoxanthine at a pyrolytic graphite electrode has been studied. Poly(I) gives a single, pH-dependent voltammetric oxidation peak which is well separated from the single peak observed for very low concentrations of hypoxanthine. An electroanalytical method for the detection and determination of trace amounts of hypoxanthine in poly(I) samples is described.

The electrochemical oxidation behavior of a number of natural and biosynthetic polynucleotides has been discussed in recent papers [1—4]. The compounds investigated have included various DNA's and RNA's, poly(A), poly(G) and poly(X). The only major purine polynucleotide which has not previously been investigated is polyinosinic acid, poly(I), which is the subject of this report. Poly(I) is one of the least studied biosynthetic polynucleotides [5] and its structure has not yet been unequivocally determined. Rich [6] has proposed that poly(I) has a three-stranded right-handed helical structure. Thiele and Guschlbauer [5], however, have proposed that the structure of the polynucleotide is a four-stranded, left-handed helix. The most recent work, by Arnott et al. [7] supports the suggestion of a four-stranded, right-handed helix.

Poly(I) is the polymeric form of inosine-5′-monophosphate and in solution its structure is thought to be highly dependent upon pH, temperature and ionic strength [5, 6]. As the pH increases from 6.7 to 10.2 the sedimentation coefficient for poly(I) decreases, indicating that some breakdown of the organized helical structure takes place [6]. In contrast, as the ionic strength of a solution containing poly(I) increases, the concentration of the organized form increases. Thus, below an ionic strength of 0.006 M in NaCl at 3—20°C, it is considered to exist as a single stranded, poorly stacked helix [5], while above an ionic strength of 0.7—0.8 M it is thought to be largely in its organized form [5, 6]. Owing to the fact that poly(I) can assume several protonation states it exhibits melting curves which show at least two steps [5].

Earlier investigations of poly(X) [4] revealed that commercial samples of

this compound are often contaminated with traces of xanthine and xanthosine-5′-monophosphate. Thus, this investigation was carried out not only to survey the basic electrooxidation behavior of poly(I) and its constituents, i.e., hypoxanthine, inosine and inosine-5′-monophosphate, but also to investigate the possibility of developing electroanalytical methods for detection and determination of traces of the latter monomeric species in the presence of polymeric poly(I).

EXPERIMENTAL

Chemicals

Poly(I) (5′-potassium salt), inosine and inosine-5′-monophosphate (disodium salt) were obtained from Sigma. Hypoxanthine was obtained from Calbiochem.

Buffer solutions were prepared from reagent-grade chemicals. Phosphate buffers having an ionic strength of 0.5 M were generally used. However, for studies at high pH values (>12) the supporting electrolytes consisted of sodium hydroxide with sufficient sodium sulfate added to obtain an ionic strength of 0.5 M.

Apparatus

The pyrolytic graphite electrode (PGE) of 2-mm diameter was fabricated as described earlier [8]. Differential pulse voltammetry was done with a Princeton Applied Research Corporation (PAR) Model 174A Polarographic Analyzer. All differential pulse voltammograms were obtained at a sweep rate of 5 mV s^{-1} with a modulating amplitude of 25 mV and with the drop timer control set at 0.5 s. An initial potential of 0.2 V was applied to the PGE for 30 s prior to the voltage sweep. Voltammograms were recorded on a Hewlett-Packard Model 7015A X-Y recorder. The water-jacketed voltammetric cell had a capacity of ca. 5 ml and was maintained at 25 ± 0.1°C. A pool of clean mercury at the bottom of the cell served as the counter electrode. Electrical contact to the saturated calomel reference electrode (SCE) was made through a double salt bridge arrangement with the tip of a Luggin capillary positioned very close to the surface of the PGE. The arrangement prevented any significant contamination of the test solution with chloride ions from the SCE. All potentials are referred to the SCE at 25°C.

Controlled potential electrolysis was done with a PAR Model 373 Potentiostat/Galvanostat. The three-compartment cell used had salt bridges made of agar and phosphate buffer pH 7.0, ionic strength 0.5 M. The counter and reference electrode compartments contained the latter buffer solution. The reference electrode was a Fisher Fiber-Tip SCE; the counter electrode was platinum foil.

Test solutions for differential pulse voltammetry or for controlled potential electrolysis were not deaerated.

It was noted that all the hypoxanthine derivatives studied were strongly adsorbed to the inner surface of the voltammetric cell such that contamina-

tion of subsequent blank or test solutions was noted. The cells, therefore, were rinsed thoroughly at least ten times with double-distilled water between solutions.

Procedure for detection of hypoxanthine in poly(I)

Typically, about 3 mg of poly(I) is dissolved with stirring in 2 ml of phosphate buffer pH 7.0 with an ionic strength of 0.5 M at room temperature. This solution is transferred to the voltammetric cell. An initial potential of 0.2 V is applied to the PGE for 30 s after which time the positive-going voltage sweep is started. Poly(I) exhibits a single, well-formed differential pulse voltammetric oxidation peak, close to the background discharge, with a peak potential of 1.28 V at 25°C. Poly(I) concentrations of ca. 1.5 mg ml^{-1} give peak currents of about 6 μA at the 2-mm diameter PGE. If hypoxanthine is present in the poly(I) sample, it may be detected by the appearance of a voltammetric oxidation peak having a peak potential of 0.94—0.96 V.

Procedure for determination of hypoxanthine in poly(I)

A calibration curve of peak current vs. hypoxanthine concentration is prepared by obtaining voltammograms for a series of solutions, prepared in phosphate buffer pH 7.0, ionic strength 0.5 M, with a fixed concentration of hypoxanthine-free poly(I) typically ca. 5 mM (1.53 mg ml^{-1}) containing hypoxanthine concentrations ranging from 1 μM to ca. 25 μM; here the weights of poly(I) refer to the monopotassium salt. These solutions should be freshly prepared because of the tendency for hypoxanthine to decompose.

The ionic strength of the supporting electrolyte solution is not of critical importance provided that all standards and unknowns are made up with identical buffers. Traces of hypoxanthine in poly(I) can be removed by electrooxidation under controlled-potential conditions at 0.96 V in pH 7.0 phosphate buffer, ionic strength 0.5 M at a PGE of large area.

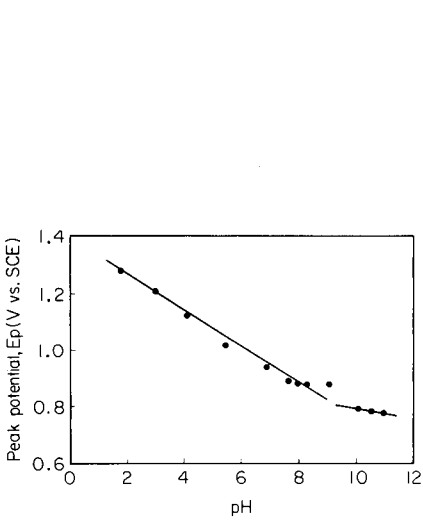
At least three voltammograms of each solution should be run and the average hypoxanthine peak current used for the calibration curve.

The concentration of hypoxanthine in samples of poly(I) is determined by dissolving ca. 3.0 mg of the poly(I) in 2 ml of pH 7.0 phosphate buffer. At least three voltammograms are run on this solution. The concentration of hypoxanthine is then determined by reference to the calibration curve obtained under identical experimental conditions.

RESULTS AND DISCUSSION

Differential pulse voltammetry of hypoxanthine

At hypoxanthine concentrations below ca. 2 mM, only a single, well-defined differential pulse voltammetric (d.p.v.) oxidation peak is observed. The peak potential (E_p) for this peak at the 37 μM hypoxanthine concentration level is pH-dependent up to about pH 8.4 (Fig. 1) according to the relationship E_p (pH 1.8—8.4) = [1.34 − 0.056 pH] V. At around pH 9 the peak becomes



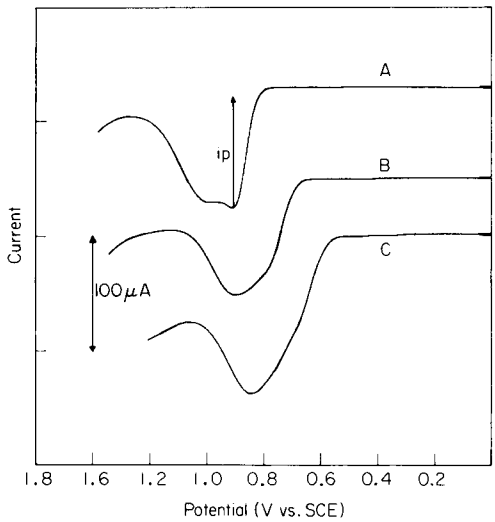


Fig. 1. Peak potential (E_p) vs. pH relationship for the d.p.v. oxidation peak of hypoxanthine observed in phosphate buffers of ionic strength 0.5 M. Data obtained at a hypoxanthine concentration of 37 μM.

Fig. 2. Differential pulse voltammograms of 3.68 mM hypoxanthine in phosphate buffers at (A) pH 4.94, (B) pH 7.00 and (C) pH 9.03. Axis marker at start of each voltammogram indicates zero current.

almost independent of pH at E_p = 0.78 ± 0.02 V (Fig. 1). The peak potential for the oxidation peak of hypoxanthine shifts to more positive values with increasing concentration. For example, at the 37 μM concentration level at pH 7.0, the peak potential is 0.92 V; at the 2 mM concentration level E_p = 0.99 V. Similar shifts of peak potential with concentration were observed at other pH values. The break in the E_p vs. pH plot for hypoxanthine at about pH 9 coincides with the pK_a value of this compound (pK_a = 8.94 [9]) corresponding to dissociation of the neutral compound to its monoanion.

At hypoxanthine concentrations exceeding 2 mM the oxidation peak of hypoxanthine becomes distorted and has the appearance of two or more overlapping peaks. This effect is particularly noticeable at pH values greater than 4. Some typical voltammograms of 3.68 mM hypoxanthine solutions are presented in Fig. 2. In view of the pK_a values of hypoxanthine (pK_{a1} = 1.98, pK_{a2} = 8.94 and pK_{a3} = 12.33 [9]), the peak distortion noted at relatively high concentrations cannot be due to dissociation effects. A careful inspection of voltammograms of hypoxanthine at various concentrations suggests that the distortion of the peaks is caused by the presence of a very poorly resolved adsorption prepeak. This indicates that the product of electrooxidation of hypoxanthine is adsorbed at the electrode surface [10, 11]. Peak current vs. concentration plots for hypoxanthine (Fig. 3) are linear at low concentrations (10—200 μM), but have the general appearance of a Langmuir isotherm at

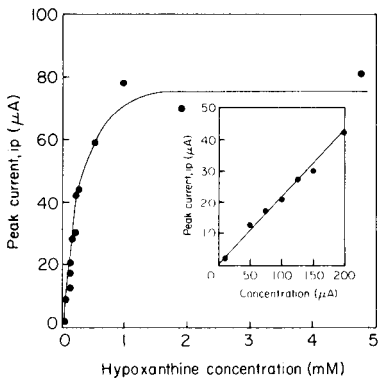


Fig. 3. Peak current (i_p) vs. concentration curves for the d.p.v. oxidation of hypoxanthine at the PGE in phosphate buffer pH 7.0, ionic strength 0.5 M. The inset is an expanded view of the low concentration region of the curve.

higher concentrations. Indeed, at concentrations greater than 2 mM, the peak current becomes virtually independent of the hypoxanthine concentration (Fig. 3). Such i_p vs. concentration behavior also supports the view that adsorption processes are involved in the oxidation of hypoxanthine. It should be noted that the currents measured at concentrations above 2 mM in Fig. 3 are those corresponding to the maximum value on the distorted voltammogram. The procedure for measuring i_p for such voltammograms is shown in Fig. 2A.

Differential pulse voltammetry of inosine

Inosine gives rise to a maximum of two d.p.v. oxidation peaks. Below pH 6 and at low concentrations, only one peak (peak I) appears, but at higher concentrations peak II appears. Both peaks are pH-dependent (Fig. 4). The peak potential for peak I at the 2 mM concentration level is described by the equation E_p (pH 6.3—11.5) = [1.73 — 0.078 pH] V; for peak II, E_p (pH 2.9—11.5) = [1.62 — 0.043 pH] V. A peak current vs. concentration study on inosine was carried out at pH 11.0 to investigate the effects of concentration on peaks I and II. The latter pH was selected because the separation of the two peaks is greatest (Fig. 4). This study showed that inosine peak I becomes virtually independent of concentration at about the 0.2 mM concentration level, whereas inosine peak II increases linearly with concentration (Fig. 5). Similar but less well-defined behavior was observed at other pH values where there are two inosine peaks. The i_p vs. concentration behavior of inosine peak I strongly supports the view that it is an adsorption prepeak. Such peaks are usually characteristic of an electrode reaction where the product of the electrode process is more strongly adsorbed than the reactant [10, 11].

Differential pulse voltammetry of inosine-5'-monophosphate

Commercial samples of inosine-5'-monophosphate (IMP) exhibit up to

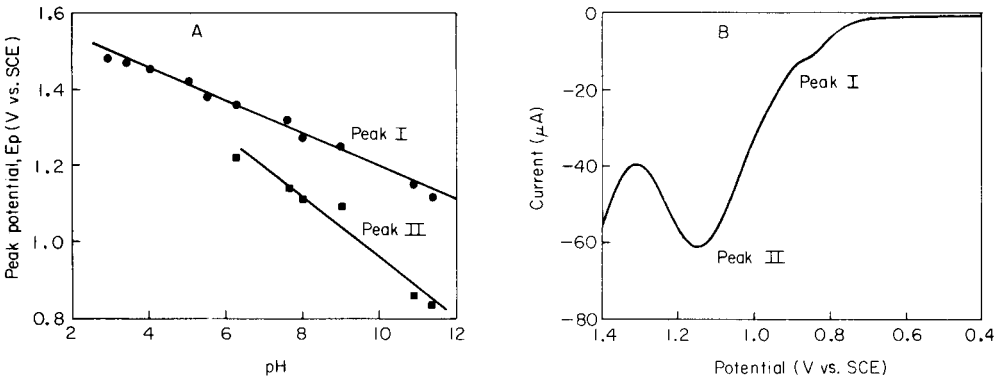


Fig. 4. (A) Peak potential vs. pH for the d.p.v. oxidation peaks of 2.03 mM inosine in phosphate buffers of ionic strength 0.5 M. (B) Differential pulse voltammogram of 2.03 mM inosine at pH 10.9.

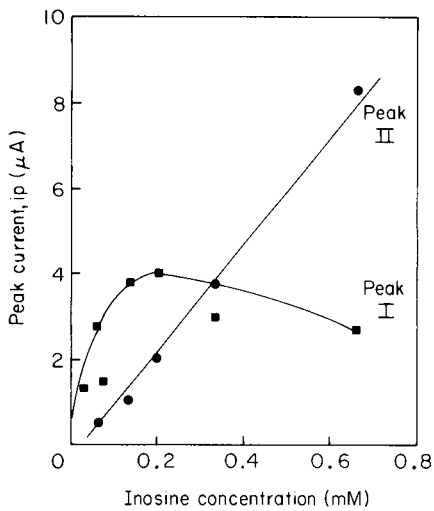


Fig. 5. Peak current vs. concentration curves for the d.p.v. oxidation peaks of inosine in phosphate buffer pH 11.0 of ionic strength 0.5 M.

three d.p.v. oxidation peaks. All three oxidation peaks are observed only above pH 6 and at IMP concentrations at or above about 1 mM. At the latter concentration level, all three peaks are pH-dependent (Fig. 6A). The pH-dependence for the most negative peak A is given by the relationship E_p (pH 2.9—11.6) = [1.20 — 0.048 pH] V. For peak I, E_p (pH 6.3—7.1) = [1.71 — 0.075 pH] V; E_p (pH 7.8—11.6) = [1.47 — 0.039 pH] V. For peak II, E_p (pH 2.9—8.2) = [1.65 — 0.052 pH] V; E_p (pH 8.2—11.6) = [1.44 — 0.026 pH] V. The peak equations given above for the pH dependence of peak I (Fig. 6A) should be regarded as very approximate because peak I occurs as a shoulder on the rising portion of peak II.

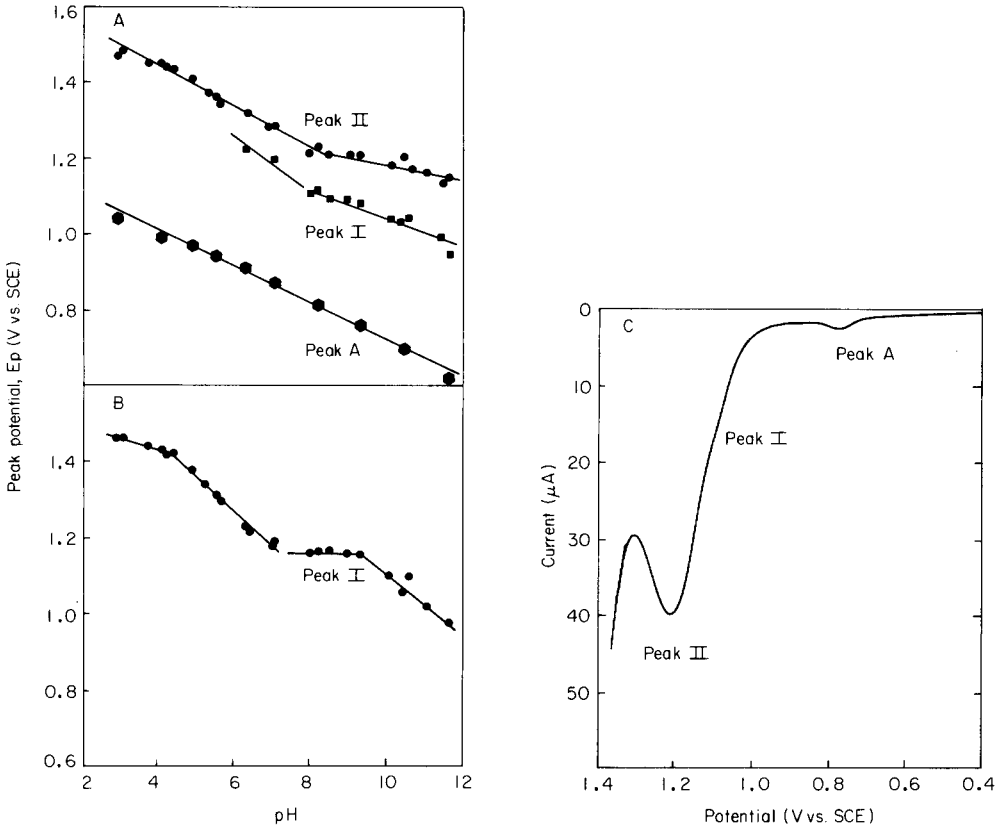


Fig. 6. Peak potential vs. pH relationship for the three d.p.v. oxidation peaks of inosine-5'-monophosphate in phosphate buffers of ionic strength 0.5 M. IMP concentration: (A) 0.95 mM, (B) 0.095 mM, (C) differential pulse voltammogram of 0.95 mM IMP at pH 8.45.

At low concentrations of IMP only a single oxidation peak is observed (see Fig. 6B). The E_p vs. pH relationships for this peak are given by the expressions: E_p (pH 2.5—4.2) = [1.54 — 0.029 pH] V; E_p (pH 4.2—7.1) = [1.80 — 0.090 pH] V; E_p (pH 7.1—9.4) = [1.17 ± 0.01 pH] V; E_p (pH 9.4—11.6) = [1.98 — 0.087 pH] V. The obvious break in the E_p vs. pH plots noted in Fig. 6A at about pH 8 agrees approximately with the pK_a of IMP (8.88 [9]) corresponding to dissociation of the $N(1)$ hydrogen. Careful examination of voltammograms of IMP at high and low concentrations proved that the single peak observed at low concentrations corresponds to peak I observed at higher IMP concentrations. Because peaks I and II are so close together at concentrations where they are both observed, it is essentially impossible to measure their individual peak heights as a function of concentration. Thus, peak I is so distorted by peak II that it generally appears as an ill-defined inflexion on the rising portion of peak II (Fig. 6C). With increasing IMP concentration peak II clearly becomes dominant. Accordingly, it is concluded that peak I is an adsorption prepeak.

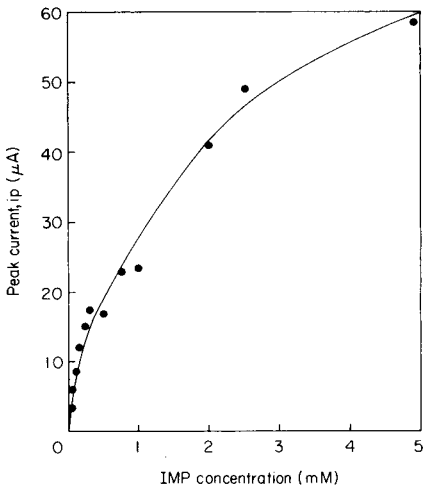


Fig. 7. Peak current vs. concentration curves for d.p.v. oxidation peaks I plus II of IMP observed in phosphate buffer pH 7.0.

When both peaks are present, only the maximum current on the voltammogram can be measured. When this current is plotted as a function of IMP concentration, curves similar to that shown in Fig. 7 are obtained. The linear range extends only to 50 μM. The overall non-linear relationship supports the view that IMP and/or its electrooxidation product are adsorbed at the PGE.

Peak A observed on differential pulse voltammetry of IMP samples was considerably smaller than peaks I and II (Fig. 6C). For example, at an IMP concentration of 1 mM, i_p for peaks I plus II is ca. 25 μA, whereas the i_p for peak A is only ca. 1.5 μA. Because of the rather large separation of the peak potential for peak A from the others, it was suspected that peak A was caused by electrooxidation of some impurity in IMP. Initially, it was thought that peak A might be due to the presence of hypoxanthine in IMP. However, when a 0.5 mM IMP solution at pH 7.0 was made 5 μM in hypoxanthine, both peak A and the single peak of hypoxanthine were observed. That peak A was due to an impurity in IMP was supported by the fact that controlled potential electrolysis of a 2.0 mM solution of IMP at pH 7.0 at a potential of 0.88 V (cf. Fig. 6C) resulted in elimination of all traces of peak A. However, peaks I and II were unaffected and u.v. absorption spectra of the IMP solution before and after electrolysis were essentially identical, i.e., IMP was not electrooxidized. Several purine bases were examined by differential pulse voltammetry at pH 7.0 and it was found that adenine (6-aminopurine) at concentrations of 27 μM or less gave a single peak at a peak potential identical to that of peak A. This, of course, does not prove conclusively that peak A is due to adenine. However, the results strongly support the view that peak A arises from a trace impurity in IMP samples.

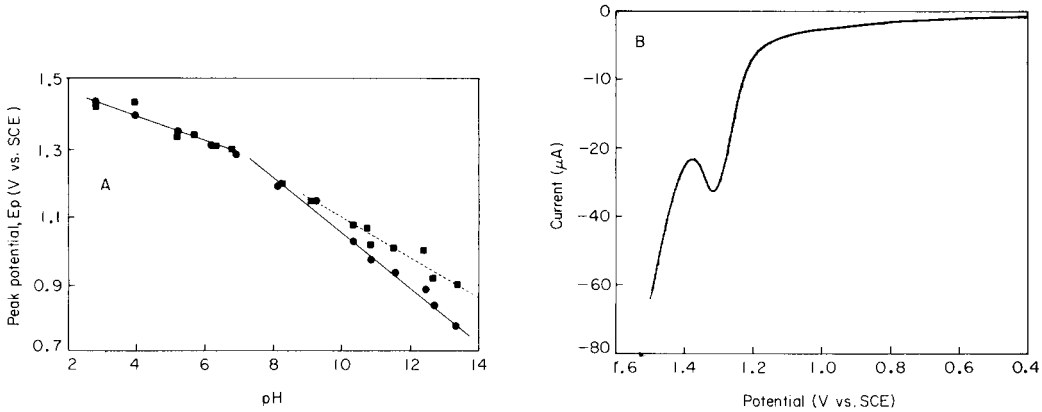


Fig. 8. (A) Peak potential vs. pH relationships for the single d.p.v. oxidation peak of poly(I) obtained in phosphate buffers of ionic strength 0.5 M at a concentration level of (•) 1.65 mM and (▪) 0.165 mM. (B) Differential pulse voltammogram of 1.65 mM poly(I) at pH 6.25.

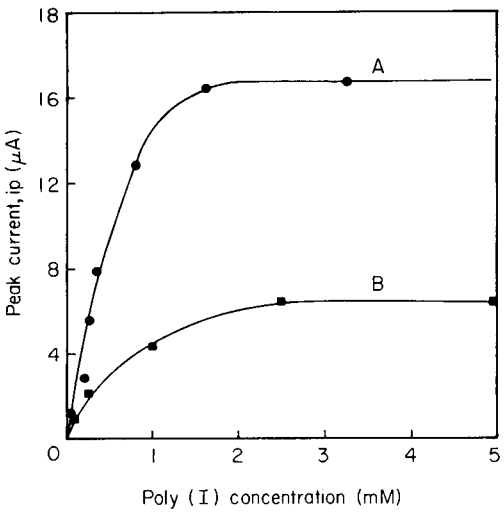
Differential pulse voltammetry of poly(I)

Poly(I) gives rise to a single, well-defined differential pulse voltammetric oxidation peak between pH 2 and 14 (Fig. 8). At concentrations* of 0.165 mM and 1.65 mM, the peak potential is independent of concentration between pH 2.9 and 7.2 and is described by the equation E_p (pH 2.9—7.2) = [1.56 — 0.039 pH] V. At higher pH values the peak potential is somewhat dependent on concentration (Fig. 8). At the 0.165 mM level, E_p (pH 7.2—14) = [1.87 — 0.082 pH] V, while at the 1.65 mM level, E_p (pH 7.2—14) = [1.66 — 0.057 pH] V.

The effect of the ionic strength of the supporting electrolyte on the peak current for poly(I) is quite pronounced. Thus, in phosphate buffer pH 6.3, for example, the peak current for a constant (1.65 mM) concentration of poly(I) increases quite steeply with ionic strength up to a value of about 0.4 M, and the peak current then becomes essentially independent of ionic strength. Accordingly, to obtain the greatest analytical sensitivity, buffers with an ionic strength of 0.5 M were used for all further studies of poly(I) and its monomeric components. This ionic strength also has the advantage that small variations in ionic strength do not influence the peak current for poly(I).

The peak current vs. concentration curves for poly(I) are non-linear and the peak current is highly dependent on pH. In general, the peak current is largest at low pH and systematically decreases with increasing pH. Similar behavior was noted with hypoxanthine, inosine and inosine-5′-monophosphate. This suggests that the adsorption of all species is greatly increased at

*Concentrations of poly(I) were determined from its molar absorptivity in pH 7.0 phosphate buffer (7.6×10^3 l mol^{-1} cm^{-1}). A 1.0 mg ml^{-1} solution of poly(I) is, therefore, 3.3 mM.



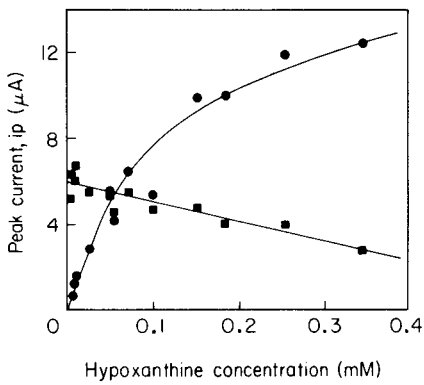


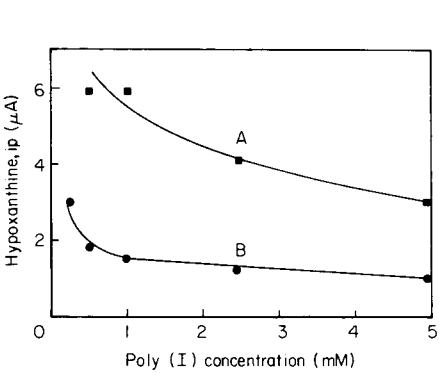
Fig. 9. Peak current vs. concentration for the d.p.v. oxidation of poly(I) in (A) phosphate buffer pH 5.3 and (B) phosphate buffer pH 7.0. Ionic strength of buffers, 0.5 M.

Fig. 10. Peak current vs. hypoxanthine concentration in phosphate buffer pH 7.0 of ionic strength 0.5 M containing 2.0 mM poly(I). (•) Peak current for hypoxanthine peak I; (▪) peak current for poly(I) peak.

low pH with a resulting increase of the experimental peak current. Some typical results obtained for poly(I) at pH 5.3 and pH 7.0 (Fig. 9) indicate that at concentrations of poly(I) above 2 mM the peak current is independent of concentration. Such behavior is also indicative of strong adsorption of poly(I) or its electrooxidation product at the electrode surface.

Inspection of the peak potential vs. pH relationships for hypoxanthine (Fig. 1), inosine (Fig. 4), IMP (Fig. 6) and poly(I) (Fig. 8) reveals that the major peaks of inosine, IMP and poly(I) occur at almost the same potential over the entire pH range. This implies, therefore, that it is impossible to determine traces of inosine and/or IMP in poly(I) samples by differential pulse voltammetry. However, it has been our experience that nucleosides, nucleotides and polynucleotides are generally contained primarily with traces of the corresponding base. For example, xanthosine and poly(X) have been shown in previous reports to be contaminated with xanthine [4, 12]. Accordingl it was decided to investigate the determination of hypoxanthine as a trace contaminant of poly(I).

Because most of our mechanistic studies of the electrochemical oxidation of purine systems are now carried out at physiological pH, the hypoxanthine/ poly(I) mixtures were investigated at pH 7.0. The peak current for poly(I) reaches its maximal value at about the 2 mM concentration level (Fig. 9), i.e., adsorbed poly(I) or its electrooxidation product entirely covers the PGE surface. It was thought that at this poly(I) concentration hypoxanthine would



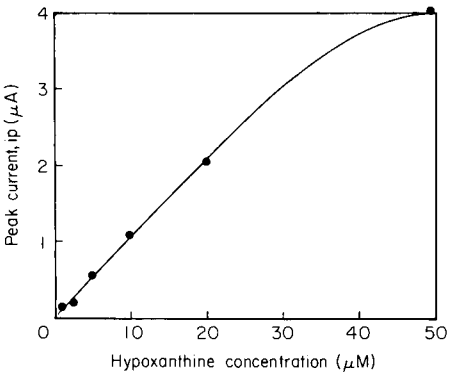


Fig. 11. Variation of hypoxanthine peak current with poly(I) concentration in phosphate buffer pH 7.0 of ionic strength 0.5 M. Hypoxanthine concentration: (■) 40 μM; (●) 10 μM.

Fig. 12. Peak current vs. hypoxanthine concentration relationship in phosphate buffer pH 7.0, ionic strength 0.5 M containing 5 mM poly(I).

not be adsorbed and would give rise to a linear peak current vs. concentration relationship. However, under these conditions, the relationship was linear only up to the 25—50 μM concentration level (Fig. 10). In addition, it was observed that the peak current for poly(I) systematically decreased with increasing hypoxanthine concentrations (Fig. 10). This behavior suggests that competitive adsorption occurs at the electrode surface. The phenomenon was further examined by investigating the effect of relatively high poly(I) concentrations (0.25—5 mM) on the peak currents for 10 μM and 40 μM hypoxanthine. The results (Fig. 11) suggest that at poly(I) concentrations approaching 5 mM the hypoxanthine peak current approaches a constant minimal value. It thus appears that at poly(I) concentrations around 5 mM and at micromolar hypoxanthine concentrations the adsorption of hypoxanthine is minimized. The relationship between the peak current for hypoxanthine and its concentration in the presence of 2 mM and 5 mM poly(I) is shown in Fig. 12; the linear range extends only to ca. 25 μM. Thus under the conditions specified, the differential pulse voltammetric oxidation is limited analytically to the determination of hypoxanthine which contaminates poly(I) to a maximum extent of 0.5%.

In order to test the usefulness of the differential pulse voltammetric tech nique at the PGE for determination of traces of hypoxanthine in poly(I), series of solutions were prepared containing 5 mM poly(I) and hypoxanthine concentrations ranging from about 9 μM to 24 μM. When these were analyzed as specified, calibration curves similar to that shown in Fig. 12 were obtained. The results are presented in Table 1 where it may be seen that very low concentrations ($\leqslant$ 0.5%) of hypoxanthine can be readily determined in poly(I) samples with an accuracy of about ±0.4%. Such analyses have not previously been possible even by spectrometric methods. This is so because the u.v. absorption spectrum of poly(I) is very similar to

TABLE 1

Determination of hypoxanthine in poly(I) samples[a] by differential pulse voltammetric oxidation at the PGE

Sample No.	Concentration of hypoxanthine	
	Actual (μM)	Found (μM)[b]
A	24.1	23.1
B	16.9	17.5
C	9.6	9.2

[a]Determination run in pH 7.0 phosphate buffer containing 5 mM poly(I). [b]Average of 3 determinations.

that of hypoxanthine; for example, at pH 7.0 the λ_{max} for poly(I) is 247 nm while that for hypoxanthine is 249.5 nm.

This work was supported by the National Institutes of Health through Grant No. GM-21034-04. One of us (L.G.K.) expresses his appreciation to the Karcher Endowment of the University of Oklahoma for award of the Karcher Fellowship.

REFERENCES

1 V. Brabec and G. Dryhurst, J. Electroanal. Chem., 89 (1978) 1978.
2 V. Brabec and G. Dryhurst, J. Electroanal. Chem., 91 (1978) 219.
3 V. Brabec and G. Dryhurst, Stud. Biophys., 67 (1978) 23.
4 G. Dryhurst and L. G. Karber, Anal. Chim. Acta, 100 (1978) 289.
5 D. Thiele and W. Guschlbauer, Biophysik, 9 (1973) 261.
6 A. Rich, Biochim. Biophys. Acta, 29 (1958) 502.
7 S. Arnott, R. Chandrasekaran and C. M. Martilla, Biochem. J., 141 (1974) 537.
8 G. Dryhurst, Anal. Chim. Acta, 57 (1971) 137.
9 A. Albert and D. J. Brown, J. Chem. Soc., 157 (1954) 2060.
10 L. Meites, Polarographic Techniques, 2nd edn., Interscience, New York, 1965, pp. 187—189.
11 R. H. Wopschall and I. Shain, Anal. Chem., 39 (1967) 1514.
12 J. L. Owens and G. Dryhurst, Anal. Chim. Acta, 89 (1977) 93.

Analytica Chimica Acta, 108 (1979) 205—211
© Elsevier Scientific Publishing Company, Amsterdam — Printed in The Netherlands

DIFFERENTIAL PULSE POLAROGRAPHIC DETERMINATION OF CEPHALOSPORINS AND THEIR DEGRADATION PRODUCTS

A. G. FOGG* and N. M. FAYAD

Department of Chemistry, Loughborough University of Technology, Loughborough, Leicestershire (Gt. Britain)

C. BURGESS and A. McGLYNN

Glaxo Operations (U.K.) Ltd., Barnard Castle, Co. Durham (Gt. Britain)

(Received 15th November 1978)

SUMMARY

The differential pulse polarography (d.p.p.) of several cephalosporins — cephalothin, cephalosporin C, cephaloridine, cephalonium, cefuroxime, cephoxazole, cephalexin, cephradine, desacetylcephalosporin C, 7-aminocephalosporanic acid and 7-aminodesacetoxycephalosporanic acid — and some degradation products has been studied. Cephalexin, cephradine and 7-aminodesacetoxycephalosporanic acid, which contain an unsubstituted 3-methyl group but no reducible group, do not give d.p.p. peaks at the dropping mercury electrode, whereas certain of their degradation products do. The other cephalosporins, in which the 3-methyl group is substituted, give a d.p.p. peak at about—1 V (pH 2—4). Although these peaks are near the cathodic limit under the conditions used, these cephalosporins can be determined down to about 0.1 μg ml^{-1}. Cephaloridine exhibits two d.p.p. peaks in this region, and can be determined. Cefuroxime, in addition to the peak at —1V, has a larger peak at —0.45 V (pH 2). Cephalonium shows a large well-defined peak at —0.72 V (pH 3) and two overlapping peaks. D.p.p. data for several degradation products including the diketopiperazines formed from cephalexin and cephradine are reported.

The β-lactam rings of cephalosporins and penicillins readily hydrolyse in aqueous solutions. The opening of the β-lactam ring of penicillins gives the pencilloates but the analogous cephalosporoates are generally unstable and undergo further reaction. Cephalosporins are more resistant to hydrolysis than are penicillins, but cephalosporins with the α-aminophenylacetamido group at the 7 position undergo intramolecular aminolysis which makes them more labile at pH 7 than other cephalosporins. Diketopiperazine products formed in these latter reactions have been isolated by Indelicato et al. [1], Cohen et al. [2] and Bundgaard [3].

To follow these degradation reactions, reliable analytical methods for determining the cephalosporins and their degradation products are required. The classical methods of determining cephalosporins have been reviewed [4, 5]; these include hydrolysis followed by iodimetric titration, aminolysis with hydroxylamine followed by spectrophotometry of the hydroxamic acid complex formed with iron(III), and the ninhydrin and nicotinamide methods for selected cephalo-

sporins. In studying the kinetics of degradation of cephalosporins, Yamana et al. [6] used iodimetric titrations and u.v. spectrophotometry: Bundgaard [3, 7] used u.v. spectrophotometry. Magnem et al. [8] found it more reliable to use u.v. spectrometry in conjunction with t.l.c. Yamana and Tsuji [9] later used h.p.l.c., iodimetric and hydroxamic acid assays. Further studies [10, 11] have been made of the h.p.l.c. determination of cephalosporins. A spectrofluorimetric method has been used to determine cephalexin degradation in plasma or serum [12, 13].

Hall et al. have used a.c. and d.c. polarography and coulometry in a study of the degradation of 3-(5-methyl-1,3,4-thiadiazol-2-ylthiomethyl)-7-[2-3-sydnone)acetamido]-3-cephem-4-carboxylic acid [14]; cyclic voltammetry was also applied in their study of cephalothin [15]. The first report of the d.c. polarographic determination of cephalosporins seems to be that of Jones et al. [16]. Benner [17] determined cephalothin, cephaloridine and cephalexin by cathode-ray polarography, the latter compound after hydrolysis. Preparative electrochemical reductions of cephalosporanic acids have been described by Ochiai et al. [18].

The present paper describes the differential pulse polarography (d.p.p.) of several cephalosporins, and gives the optimum solution conditions for their determination. Details are given of the polarographic behaviour of several hydrolysis products. The sensitivity and selectivity of differential pulse polarography are superior to those of d.c. and cathode-ray polarography.

EXPERIMENTAL

Equipment and reagents

Measurements were made with a PAR 174 polarographic analyser (Princeton Applied Research Corp.). For d.p.p. operation, a forced drop time of 1 s, a scan rate of 2 mV s^{-1} and a pulse height of 50 mV were used except where otherwise stated. Three-electrode operation was employed with a dropping mercury electrode (d.m.e.), a platinum counter electrode and a saturated calomel reference electrode. The water-jacketed polarographic cell similar to that described by Smyth et al. [19] was kept at 25°C except where otherwise indicated. Solutions for polarography were deoxygenated with nitrogen gas which had previously been passed through a vanadium(II) scrubber.

Polarography was carried out in Britton—Robinson universal buffer. The stock buffer solution (pH 2) was 0.04 M in boric acid, orthophosphoric acid and glacial acetic acid: pH adjustments were made with 0.2 M sodium hydroxide solution as required.

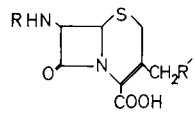
Samples

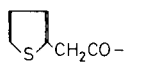
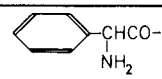
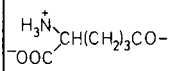
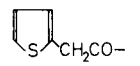
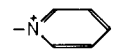
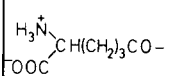
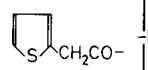
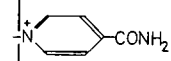
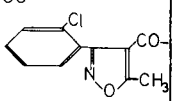
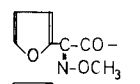
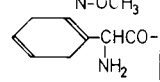
The samples listed in Table 1 were provided by Glaxo Operations (U.K.) Ltd, except for cephradine which was kindly provided by E. R. Squibb and Sons Ltd.

Except for 7-aminocephalosporanic acid (7-ACA) and 7-aminodesacetoxycephalosporanic acid (7-ADCA), these compounds were freely soluble in water.

TABLE 1

Structures of the compounds examined



Name	SUBSTITUENT		Name	SUBSTITUENT	
	R	R′		R	R′
Cephalothin		$-OCOCH_3$	Cephalexin		$-H$
Cephalosporin C		$-OCOCH_3$	Cephaloridine		
Desacetyl-cephalosporin C		$-OH$	Cephalonium		
Cephoxazole		$-OCOCH_3$	Cefuroxime		$-OOCNH_2$
7-Aminoceph-alosporanic acid	H-	$-OCOCH_3$	Cephradine		$-H$
7-Aminodesacetoxy-cephalosporanic acid	H-	$-H$			

7-ACA and 7-ADCA were dissolved in 2 ml of 0.2 M sodium hydroxide solution and the resulting solutions were immediately made up to volume in pH 2 Britton–Robinson buffer: prolonged contact with sodium hydroxide solution caused extensive degradation, as indicated by the appearance of polarographic peaks of degradation products, and decrease in the height of the 7-ACA peak.

Methods

The effects of pH on the d.p.p. curves were studied by using test solutions that were individually prepared from buffer solutions at the required pH. D.c. polarograms were also run at various mercury pressures to check that reductions were diffusion-controlled. Data for calibration graphs were obtained by successive syringe injections of concentrated sample solutions into a deoxygenated buffer solution at the optimum pH. All peaks used in obtaining calibration curves were shown to be diffusion-controlled.

Preliminary degradation studies were made directly in the polarographic cell; with cephalexin, the peak at −0.56 V was reduced considerably in height when the degradation was carried out in the presence of mercury. Solutions used for degradation studies reported here were stored in separate flasks, fresh portions of the solution being added to the polarographic cell for each measurement point, except where indicated otherwise.

TABLE 2

D.p.p. data for cephalosporins

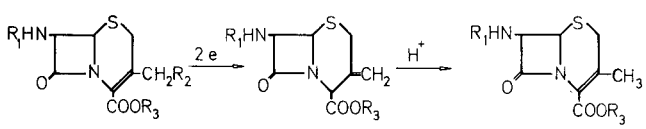
Sample	Optimum pH	E_p (V)	Comments
Cephalothin	2.0	−1.00	$i_p = 0$ at pH>4
Cephalosporin C	2.0	−1.00	$i_p = 0$ at pH>3
Cephaloridine	4.0	−1.06[a], −1.28	
Cephalonium	3.0	−0.72[a], −1.00, −1.12	
Cefuroxime	2.5	−0.39[a], −1.02	
Cephoxazole	2.0	−0.95	
Desacetylcephalosporin C	2.0	−0.99	$i_p = 0$ at pH>6
7-ACA	2.0	−0.99	$i_p = 0$ at pH>3

[a]Wave used for analysis.

DIFFERENTIAL PULSE POLAROGRAPHY OF CEPHALOSPORINS

Data for those cephalosporins studied which give polarographic peaks are summarized in Table 2; cephalexin, cephradine and 7-aminodesacetoxycephalosporanic acid do not give polarographic peaks. Table 2 shows the peak potentials at the optimum pH for measurement. Calibration curves (typically 0—2 μg ml^{-1}) were rectilinear in all cases and the coefficient of variation was typically <2% at the 0.1 μg ml^{-1} level. The peak currents are highly dependent on pH and standards and samples should be measured in the same buffer. In general, peak currents decreased with increasing pH.

All the cephalosporins which have a substituted 3-methyl group give a differential pulse peak at about −IV at pH 2—4. Cephaloridine exhibits two peaks in this region but only the first peak [E_p = (−0.79—0.068 pH) V] is useful for analytical purposes. At pH 8 a polarographic maximum of the first kind was observed on the d.c. polarogram. Ochiai et al. [18], using preparative electrochemical reduction, have shown that cephalosporins substituted at the 3-methyl position are reduced according to the scheme:



Cefuroxime gives two peaks: the first peak is about twice the height of the second peak and is more suitable for analytical purposes. Cephalonium exhibits three polarographic peaks in Britton—Robinson buffer. The second and third peaks overlap and the first peak [E_p = (−0.51—0.069 pH) V], which is twice the height of the other two, is the most suitable for analytical purposes.

DIFFERENTIAL PULSE POLAROGRAPHY OF DEGRADATION PRODUCTS

The potentiality of d.p.p. for studying the degradation of cephalosporins and for stability testing is most clearly seen in the case of cephalexin and cephradine. These two cephalosporins which have similar structures do not exhibit polarographic peaks themselves but several of their degradation products do (see Fig. 1). The initial degradation product, the diketopiperazine(I) gives a distinct wave at —0.9 V (pH 7.4). A polarographic peak, caused by hydrogen sulphide [20], appears at —0.56 V as the diketopiperazine itself is degraded. Two further peaks, which were not identified, appear at —0.78 and —1.26 V. The changes in the heights of these peaks are shown in Fig. 1 (b).

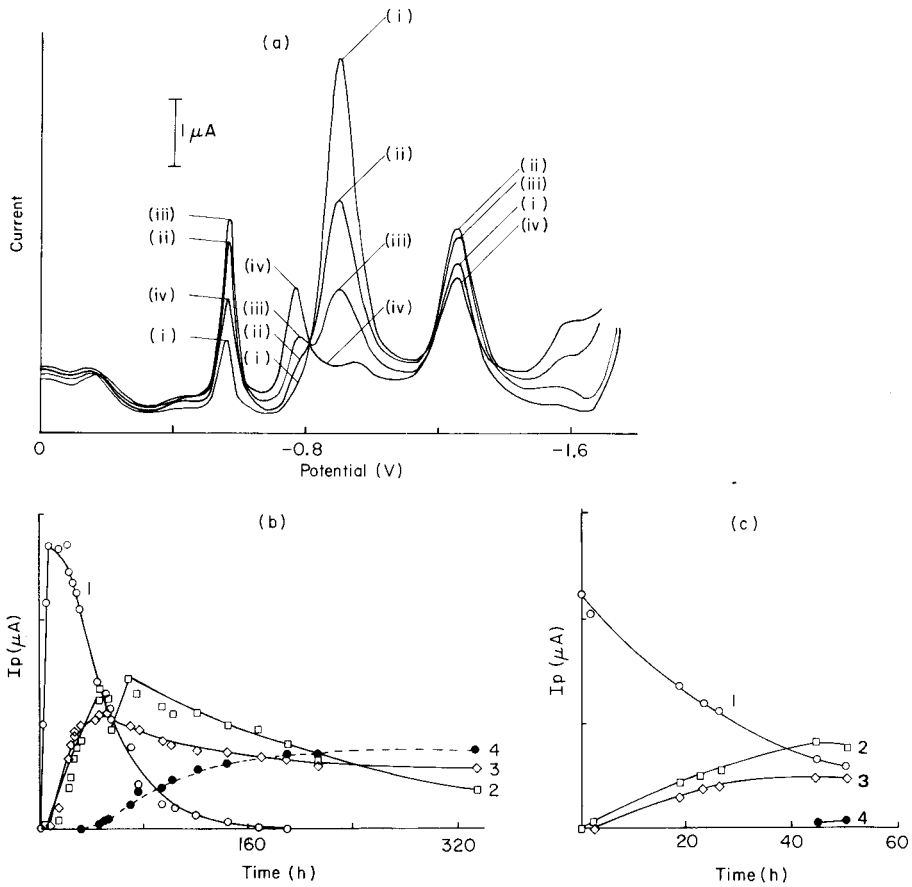
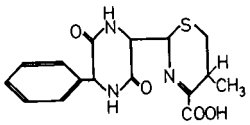


Fig. 1. (a) D.p.p. curves showing part of the degradation of a 100 μg ml^{-1} solution of cephalexin in B—R buffer at pH 7.4 at 37°C. Measurement times: (i) 24, (ii) 46.5, (iii) 70, (iv) 190 h. (b) Plot of peak heights of cephalexin degradation products versus measurement time: curve (1) diketopiperazine derivative; (2) hydrogen sulphide; (3) and (4) unidentified products. (c) Plot of peak heights of the diketopiperazine derivative and its degradation products versus measurement time. Key as (b). Curve 3, peak at —1.26 V. Curve 4, peak at —0.78 V.



(I)

The diketopiperazine formed from cephalexin was isolated; its u.v. and i.r. spectra were in accord with the findings of previous workers for structure I [1, 3]. The melting point (145—148°C) was less than that quoted by Bundgaard [3], (160—162°C). A d.p.p. study of this compound is summarized in (Fig. 1(c), the degradation products being the same as those finally observed in the degradation of cephalexin.

During the initial degradation of cephalexin, a strong smell of hydrogen sulphide was apparent. The question arises as to whether this hydrogen sulphide comes from degradation of cephalexin or diketopiperazine or both. A comparison of the maximum height reached by the diketopiperazine peak after 7 h in the degradation of cephalexin with peaks of standard diketopiperazine solutions indicate a maximum yield of diketopiperazine of about 55%. This does

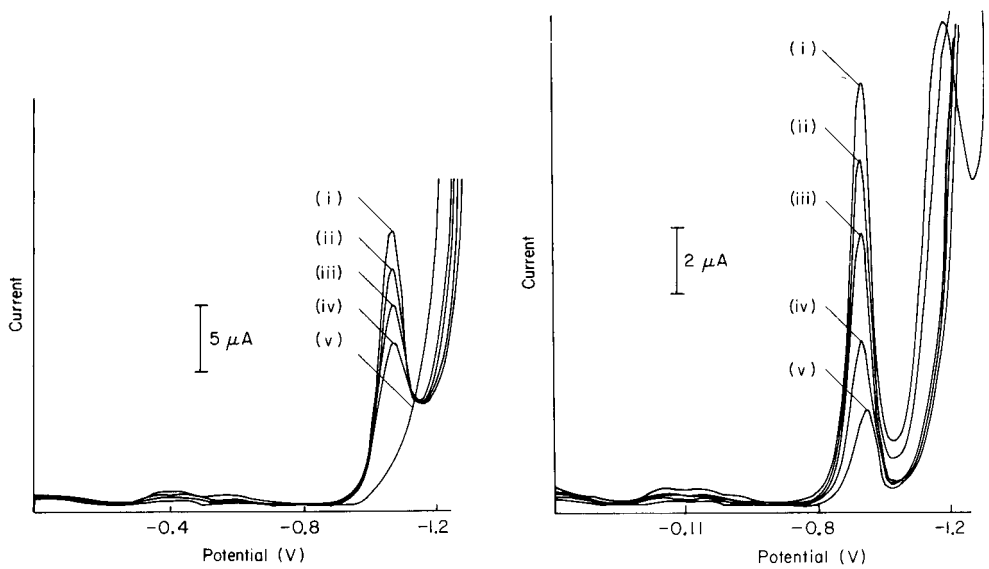


Fig. 2. D.p.p. curves showing degradation of a 140 μg ml^{-1} solution of cephalothin in B—R buffer at pH 2 at 50°C. Measurement times: (i) 0.5, (ii) 2.0, (iii) 2.5, (iv) 4.5, (v) 18.5 Degradation was carried out in the polarographic cell and the polarograms were obtained at 50°C.

Fig. 3. D.p.p. curves showing degradation of 100 μg ml^{-1} of solution of cephaloridine in B—R buffer at pH 2 at 37°C. Measurement times: (i) 0, (ii) 17.5, (iii) 27, (iv) 48, (v) 96 h. Polarograms obtained at 25°C.

not resolve the question, however, and further studies are being made to determine the amount of hydrogen sulphide formed and the mechanism of its formation.

Cephradine was found to behave in a similar manner to cephalexin, as was expected.

Preliminary studies of the degradation of cephalothin and cephaloridine are shown in Figs. 2 and 3. In these cases the degradation can be followed by using the d.p.p. peaks of the cephalosporins. Some small peaks produced by degradation products are observed but the major degradation products do not give peaks.

REFERENCES

1 J. M. Indelicato, T. T. Norvilas and W. J. Wheeler, J. Chem. Soc. Chem. Commun., (1972) 1162.
2 A. I. Cohen, P. T. Funke and M. S. Puar, J. Pharm. Sci., 62 (1973) 1559.
3 H. Bundgaard, Arch. Pharm. Chem. Sci., 5 (1977) 149.
4 L. P. Marrelli in E. H. Flynn (Ed.), Cephalosporins and Penicillins: Chemistry and Biology, Academic Press, New York, 1972.
5 D. W. Hughes, A. Vilim and W. L. Wilson, Can. J. Pharm. Sci., 11 (1976) 97.
6 T. Yamana, A. Tsuji, K. Kanayama and O. Nakano, J. Antibiot., 27 (1974) 1000.
7 H. Bundgaard, Arch. Pharm. Chem. Sci., 4 (1976) 25.
8 T. M. Magnem, P. H. Villmo and J. Karlsen, Medd. Nor. Farm. Selik., 39 (1977) 221.
9 T. Yamana and A. Tsuji, J. Pharm. Sci., 65 (1976) 1563.
10 M. A. Carroll, E. R. White, Zs. Jancsik and J. E. Zarembo, J. Antibiot., 30 (1977) 397.
11 E. R. White, M. A. Carroll and J. E. Zarembo, J. Antibiot., 30 (1977) 811.
12 R. H. Barbhaiya and P. Turner, Proceedings of the B.P. S., (1977) 734P.
13 R. H. Barbhaiya, R. C. Brown, D. W. Payling and P. Turner, J. Pharm. Pharmacol., 30 (1978) 224.
14 D. A. Hall, J. Pharm. Sci., 62 (1973) 980.
15 D. A. Hall, D. M. Berry and C. J. Schneider, J. Electroanal. Chem., 80 (1977) 155.
16 I. F. Jones, J. E. Page and C. T. Rhodes, J. Pharm. Pharmacol., 20 (1968) 45S.
17 E. J. Benner, Antimicrob. Agents Chemother., (1970) 201.
18 M. Ochiai, O. Aki, A. Morimoto, T. Okada, K. Shinozaki and Y. Ashahi, Tetrahedron Lett., 23 (1972) 2341; J. Chem. Soc. Perkin Trans. 1, (1974) 258.
19 W. F. Smyth, M. R. Smyth, J. A. Groves and S. B. Tan, Analyst, 103 (1978) 497.
20 M. Youssefi and R. L. Birke, Anal. Chem., 49 (1977) 1380.

Analytica Chimica Acta, 108 (1979) 213—219
© Elsevier Scientific Publishing Company, Amsterdam — Printed in The Netherlands

PULSE POLAROGRAPHIC DETERMINATION OF NITROSAMINES
Part 2. Methods for the Determination of *N*-Nitrosodiphenylamine and *N*-Nitrosodibutylamine

ROBERT SAMUELSSON

Department of Analytical Chemistry, University of Umeå, S-901 87 Umeå (Sweden)

(Received 2nd January 1979)

SUMMARY

Differential pulse polarographic methods are reported for the determination of *N*-nitrosodiphenylamine and *N*-nitrosodibutylamine in aqueous media. Optimum conditions for analysis were obtained with acetate buffer (pH 3.74) and 0.01 M H_2SO_4, where reduction peak separations were of the order of 300 mV and 200 mV, respectively. Detection limits were approximately 3×10^{-8} M for each compound. Methods for the extraction of these nitrosamines from iso-octane to aqueous solutions were quantitatively examined.

During the last ten years evidence has been collected which indicates that *N*-nitrosamines may contribute significantly to the widespread occurrence of human cancer. Numerous determinations of such compounds in a variety of environmental samples have been reported [1—5], although only a few of these papers deal directly with their presence and formation in industrial conditions [4, 5]. The rubber industry, in particular, is a cause of recent serious concern, because in certain processes *N*-nitrosodiphenylamine is employed as a retarding agent. Although this nitrosamine is itself not carcinogenic, its reaction with dibutylamine, which is a commonly used vulcanizing catalyst, may lead to the generation of considerably more hazardous species at a later stage in the manufacturing process. It is extremely likely that under the conditions in which such substances are permitted to come into contact, i.e. in n-octane solution at elevated temperatures, a transnitrosation reaction [6] occurs which produces the highly carcinogenic *N*-nitrosodibutylamine.

The occurrence of this reaction under laboratory conditions has been recently confirmed and the kinetic parameters evaluated. The result of this study will be published elsewhere.

The present report summarizes the development of the pulse polarographic method for the determination of *N*-nitrosodiphenylamine and *N*-nitrosodibutylamine which was employed in the above investigation of transnitrosation. The applicability of polarographic techniques for the identification and determination of *N*-nitrosamines at trace levels has already been discussed in the literature [5, 7—9].

EXPERIMENTAL

Materials

All chemicals used were of analytical grade. Tetrabutylammonium perchlorate (TBAP) was purified as described elsewhere [10]. The buffer solutions used in the pH investigation were prepared as described by Perrin and Dempsey [11] and contained 20% (v/v) ethanol and 0.1 M LiCl. *N*-nitrosodiphenylamine (Eastman Kodak Co., m.p. 66–67°C) and *N*-nitrosodibutylamine (Eastman Kodak Co., b.p. 104–105°C/8 mm Hg) were used to prepare stock solutions (about 10^{-3} M) in ethanol or iso-octane. Calibrated micropipettes were used for the additions of samples and standards.

Instrumentation

The instrument and electrodes were the same as described earlier [5]; the instrumental parameters were as follows: scan rate 2 mV s^{-1}, modulation amplitude—50 mV, drop time 1 s and h_{uncorr} 57 cm. High-purity nitrogen was used to purge oxygen from the solutions. Measurements of pH were carried out directly in the ethanol—water buffers with a glass electrode which had been calibrated against aqueous standard buffer solutions [5]. The temperature during the measurements was 21 ± 1°C.

RESULTS AND DISCUSSION

Poor selectivity constitutes one of the major disadvantages of the polarographic method. In general, the successful simultaneous analysis of two different species requires a separation of at least 0.1 V between the corresponding reduction peak potentials. Different nitrosamines are normally reduced in aqueous solution at pH 1 within a potential range of only 0.6 V and the reduction peaks show pH dependencies which may differ for the various compounds present, as noted earlier [5, 7, 12]. In addition, the magnitudes of the peak currents observed, i_p, will also depend upon pH, so that a careful choice of pH is necessary to achieve satisfactory selectivity and sensitivity for a given sample. In order to establish optimum conditions for the analyses of *N*-nitrosodiphenylamine and *N*-nitrosodibutylamine, the effect of pH on the peak currents, i_p, and peak potentials, E_p, for reduction of these compounds was examined in eight different buffer solutions over the range pH 0—11. Figure 1A shows the pH dependence of E_p for *N*-nitrosodiphenylamine. Below pH 2 the slope is 99 ± 1.5 mV/pH, which is about 30 mV lower than reported earlier [12]. Between pH 2 and pH 8 the average slope is 61 ± 2.2 mV/pH except for the potassium hydrogenphthalate buffer below pH 4.5, where the slope is 75 mV/pH, and the Tris buffer which gives a slope of 29 mV/pH. Above pH 8, E_p is independent of pH. These results agree substantially with those reported by Lund [12]. In Fig. 1, it may also be noted that E_p is shifted by about 50 mV anodically in the phthalate buffer with respect to the other buffer solutions at pH values below 4.5.

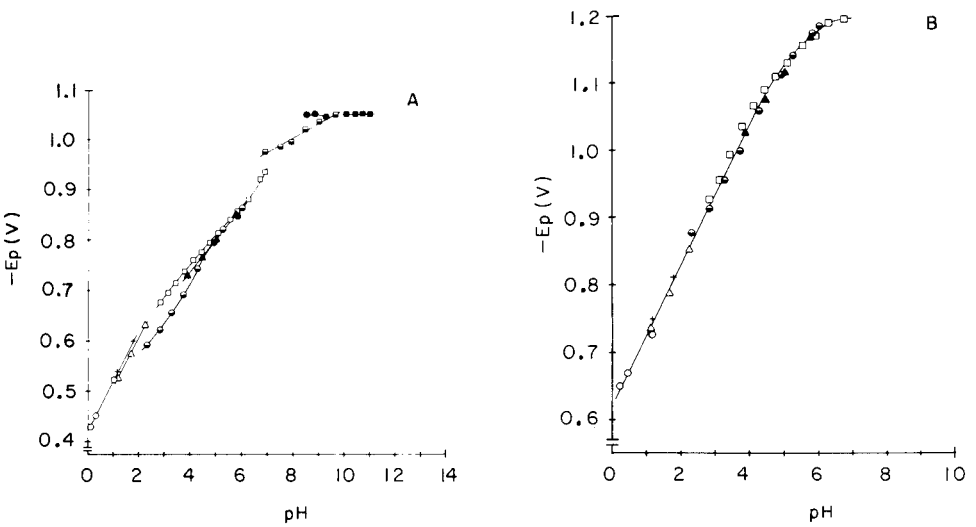


Fig. 1. Effect of pH on peak potentials for (A) 5.3×10^{-6} M *N*-nitrosodiphenylamine and (B) 6.1×10^{-6} M *N*-nitrosodibutylamine. (○) H_2SO_4; (+) H_2SO_4 + 0.1 M LiCl; (△) HCl—KCl buffer; (□) B—R buffer; (◒) KH-phthalate; (▲) HAc; (●) borate; (◙) Tris; (■) Na_2CO_3.

Figure 1B shows the effect of pH on E_p for *N*-nitrosodibutylamine. The plot is linear up to pH 4.5, where the slope starts to decrease gradually. In the linear region the average slope in the buffers used is 98 ± 9.4 mV/pH. This result is about 30 mV lower than that reported by Borghesani et al. [13] for the same *N*-nitrosamine. Above pH 7 a well-defined peak is not observed. It has been shown [13] that the reduction of *N*-nitrosodibutylamine is rather irreversible at pH values above 7 and the charge transfer becomes too irreversible to give a measurable peak in the differential pulse mode.

Figure 2 shows the effects of pH on the reduction peak currents, i_p, for *N*-nitrosodiphenylamine and *N*-nitrosodibutylamine. Similar results for both the *N*-nitrosamines were obtained below pH 7, but with a doubled i_p value and a greater variation in i_p for *N*-nitrosodiphenylamine.

Examination of the effect of ionic strength on i_p showed a linear decrease of about 10% for *N*-nitrosodiphenylamine with increasing ionic strength between 5×10^{-3} and 1.0 M. The i_p for *N*-nitrosodibutylamine was independent of ionic strength in this range.

These results indicate that the reduction mechanism for these *N*-nitrosamines is rather complex. The mechanism depends not only on pH but also on the composition of the buffer solution and even the concentration of ethanol present [14]. In addition, the behaviour of different *N*-nitrosamines in various supporting electrolytes varies considerably, which means that an extensive examination in a number of supporting electrolytes at different pH values must be carried out for every single *N*-nitrosamine to obtain optimum conditions for analysis. In the case of *N*-nitrosodiphenylamine and *N*-nitrosodibutyl-

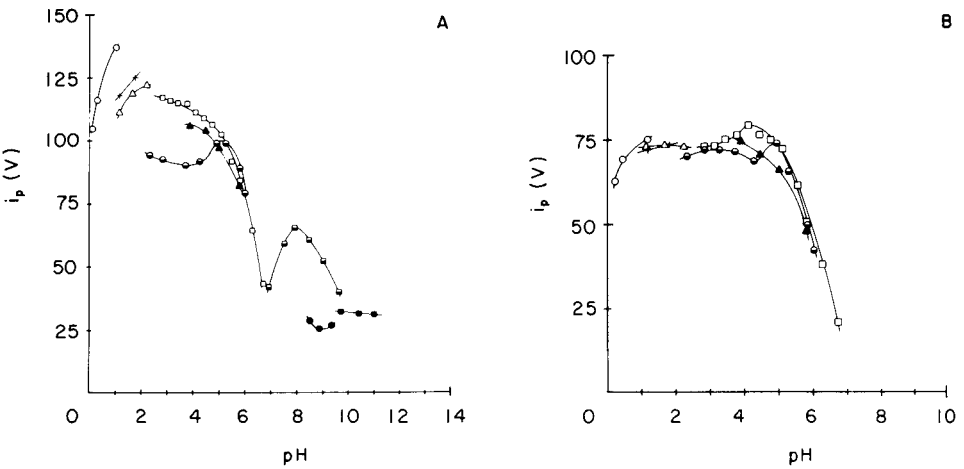


Fig. 2. Effect of pH on the peak currents for (A) *N*-nitrosodiphenylamine and (B) *N*-nitrosodibutylamine. Conditions and symbols as in Fig. 1.

amine, the separation in peak potentials was found to be sufficiently large for adequate selectivity. Analytical conditions were therefore chosen to obtain optimum sensitivity.

Effect of ethanol concentration on linearity and detection limit

From the pH investigation, acetic acid buffer (pH 3.74) and 0.01 M sulfuric acid were considered to be suitable supporting electrolytes for the reduction of *N*-nitrosodiphenylamine and *N*-nitrosodibutylamine, respectively. The background currents were low and constant and the sensitivity was sufficiently high for the analysis of concentrations below 10^{-7} M. These electrolytes were therefore used in the following experiments. Studies of the linearity of the calibration plots and the detection limits for the two *N*-nitrosamines were performed in solutions with varying concentrations of ethanol; 0.02 M KCl was added to reduce the *IR* drop and to prevent migration currents. The results are summarized in Fig. 3.

The calibration plots for *N*-nitrosodiphenylamine in the acetate buffer solutions and in sulfuric acid with 40% (v/v) ethanol were linear over the concentration range examined. In the sulfuric acid solutions with 5 and 20% (v/v) ethanol, however, the plots were not linear below concentrations of 8×10^{-7} M, although they were linear at higher concentrations. Addition of $2—5 \times 10^{-5}$ M TBAP to the solution eliminated this discrepancy. Weak adsorption of nitrosamines on the surface of the mercury electrode is a likely cause of non-linear response at low concentrations. Addition of the much more strongly adsorbed tetrabutylammonium ion [5, 15, 16] was found to remove this effect, and the adsorbed layer did not hinder the *N*-nitrosamine reduction.

N-nitrosodibutylamine behaves in a similar manner with non-linearity in

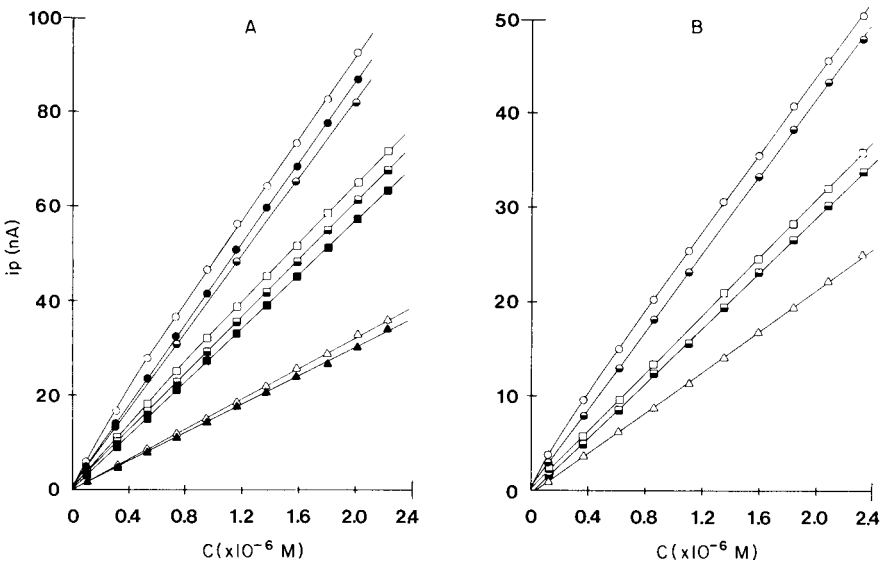


Fig. 3. Effect of ethanol concentration on linearity and sensitivity for (A) *N*-nitrosodiphenylamine and (B) *N*-nitrosodibutylamine. (○) 5% EtOH, 0.01 M H_2SO_4 (pH 1.9); (◒) 5% EtOH, 0.01 M H_2SO_4 (pH 1.9), 5×10^{-5} M TBAP; (●) 5% EtOH, HAc buffer (pH 3.6); (□) 20% EtOH, 0.01 M H_2SO_4 (pH 2.0); (◨) 20% EtOH, 0.01 M H_2SO_4 (pH 2.0); 2×10^{-5} M TBAP; (■) 20% EtOH, HAc buffer (pH 3.8); (△) 40% EtOH, 0.01 M H_2SO_4 (pH 2.2); (▲) 40% EtOH, HAc buffer (pH 4.3). All solutions contained 0.02 M KCl.

sulfuric acid—5% (v/v) ethanol. The concentration where the linearity starts is somewhat lower than for *N*-nitrosodiphenylamine. In the other solutions, the calibration plots were linear.

The sensitivities for *N*-nitrosodiphenylamine and *N*-nitrosodibutylamine decreased by factors of 3 and 2, respectively, when the ethanol concentration was increased from 5% (v/v) to 40% (v/v). Detection limits were calculated as usual [5] from the linear calibration plots and remained quite constant at values of $3.2 \pm 1.0 \times 10^{-8}$ M and $2.7 \pm 0.66 \times 10^{-8}$ M for *N*-nitrosodiphenylamine and *N*-nitrosodibutylamine, respectively. Higher sensitivities are preferable, however, because the evaluation of peak currents is then simplified.

Efficiencies of extraction methods for N-*nitrosodiphenylamine and* N-*nitrosodibutylamine prior to polarography*

Many *N*-nitrosamines exhibit lipophilic properties, so that an organic solvent extraction may be necessary to separate the nitrosamines from the environmental system of interest. In some cases, e.g. the rubber industrial process, the systems are themselves solutions in organic solvents. For analysis by pulse polarography, the species have subsequently to be transferred from the organic solvent to an aqueous phase for determination.

In the present investigation, two extraction methods were used depending on the volume of the iso-octane sample added. The supporting electrolyte employed for the determination of *N*-nitrosodiphenylamine was acetate buffer (pH 3.74), 0.02 M KCl, 2×10^{-5} M TBAP together with 5% (v/v) and 20% (v/v) ethanol in Method 1 and Method 2, respectively. For *N*-nitrosodibutylamine 0.01 M H_2SO_4 was used with 10% (v/v) ethanol, 0.02 M KCl and 2×10^{-5} M TBAP. The methods are described in detail below.

Method 1. For samples less than 0.2 ml. The sample was added to 20.0 ml of supporting electrolyte in the polarographic cell and stirred thoroughly for 10 min by bubbling nitrogen. A standard addition plot was constructed by precise additions of ethanolic 10^{-3} M *N*-nitrosamine standards. The successive peak currents for *N*-nitrosodiphenylamine were measured from the background current recorded in the pure electrolyte. For *N*-nitrosodibutylamine the currents were measured from an approximated baseline as discussed earlier [5]. The unknown sample concentration was calculated graphically and four determinations were carried out for each sample volume.

Method 2. For samples greater than 0.2 ml. Predetermined volumes (1 or 2 ml) of the organic sample were added to each of three separate polarographic cells. To two of the cells different amounts of *N*-nitrosamine standards in iso-octane were added and the samples were homogenized for 5 min ultrasonically. Supporting electroyte (20.0 ml) was added and the solutions were stirred thoroughly for 20 min. A polarogram was recorded for each solution and a standard addition plot was constructed. The evaluation was performed with an approximated baseline and three determinations were carried out for each sample volume.

The efficiencies of the two methods are summarized in Table 1. In almost all cases the relative error and precision for the methods used were better than 5%.

The need for two extraction procedures arises because of the wide differences in sample volumes employed. For small sample volumes, the extraction

TABLE 1

Efficiencies of extraction methods for *N*-nitrosodiphenylamine(I) and *N*-nitrosodibutylamine(II) from iso-octane to an aqueous phase for polarography

Iso-octane sample added (ml)	Concentration (μM) of I in			Concentration (μM) of II in		
	Iso-octane phase	Aqueous phase		Iso-octane phase	Aqueous phase	
		Calc.	Found		Calc.	Found
0.047	98.0	0.23	0.23 ± 0.0093	124	0.29	0.28 ± 0.0079
0.095	9.80	0.046	0.045 ± 0.00026	124	0.59	0.60 ± 0.015
0.19	9.80	0.093	0.088 ± 0.0035	12.4	0.12	0.11 ± 0.0056
1.0	9.80	0.49	0.48 ± 0.031	12.4	0.62	0.59 ± 0.025
2.0	9.80	0.98	0.94 ± 0.082	12.4	1.2	1.1 ± 0.01

of the *N*-nitrosamine into the aqueous phase will be virtually complete, i.e. the amount which remains in the organic phase is negligible. Under such conditions, normal standard addition methods can be used with an ethanolic *N*-nitrosamine standard solution. When larger organic samples are taken, however, a much greater fraction of the total nitrosamine content will remain in the organic phase and is therefore effectively removed from the analysis. The standard addition techniques used in Method 1 will then lead to erroneous results. The modified procedure outlined in Method 2, in which standard additions to the organic samples were made before extraction, proved to be satisfactory. It should be remarked that examinations of the influence of stripping times and tests for the establishment of equilibrium were not carried out. Provided that the experiments were performed in exactly the same manner, however, acceptable precision was obtained.

I thank Dr. Michael Sharp for many valuable discussions. This work was supported financially by the Swedish Work Environment Fund.

REFERENCES

1 D. H. Fine, D. P. Rounbehler, N. M. Belcher and S. S. Epstein, Science, 192 (1976) 1328.
2 R. A. Scanlan, CRC Crit. Rev. Food Technol., 5 (1975) 357.
3 S. S. Hecht and R. M. Ornaf, J. Nat. Cancer Inst., 54 (1975) 1237.
4 P.-A. Zingmark and C. Rappe, Ambio, 6 (1977) 237.
5 R. Samuelsson, Anal. Chim. Acta, 102 (1978) 133.
6 S. S. Singer, W. Lijinsky and G. M. Singer, Environmental Aspects of *N*-Nitroso Compounds, IARC Scientific Publications No. 19, Lyon, 1978, p. 175.
7 K. Hasebe and J. Osteryoung, Anal. Chem., 47 (1975) 2412.
8 W. F. Smyth, P. Watkiss, J. S. Burmicz and H. O. Hanley, Anal. Chim. Acta, 78 (1975) 81.
9 S. K. Changand and G. W. Harrington, Anal. Chem., 47 (1975) 1857.
10 C. K. Mann, in A. J. Bard (Ed.), Electroanalytical Chemistry, Vol. 3, M. Dekker, New York, 1969, p. 132.
11 D. D. Perrin and B. Dempsey, Buffers for pH and Metal Ion Control, Chapman and Hall, London, 1974, p. 123.
12 H. Lund, Acta Chem. Scand., 11 (1957) 990.
13 G. Borghesani, F. Pulidori, R. Pedriali and C. Bighi, J. Electroanal. Chem., 32 (1971) 303.
14 F. Pulidori, G. Borghesani, C. Bighi and R. Pedriali, J. Electroanal. Chem., 27 (1970) 385.
15 S. R. Missan, E. I. Becker and L. Meites, J. Am. Chem. Soc., 83 (1961) 58.
16 E. Bou Karam, R. Bennes and D. Bellostas, J. Electroanal. Chem., 84 (1977) 21.

Analytica Chimica Acta, 108 (1979) 221—226
© Elsevier Scientific Publishing Company, Amsterdam — Printed in The Netherlands

APPLICATION OF A GLOW DISCHARGE DETECTOR TO THE DETERMINATION OF TRIMETHYLSILYL-DERIVATIZED COMPLEX ORGANIC MIXTURES

A. D. HORTON, R. A. JENKINS* and C. FELDMAN

Analytical Chemistry Division, Oak Ridge National Laboratory P.O. Box X, Oak Ridge, TN 37830 (U.S.A.)

(Received 23rd November 1978)

SUMMARY

A helium glow discharge is employed as a gas chromatographic detector which is selective for silicon. Operated with spectral background compensation at 251.6 nm or 288.2 nm, the detector shows a lower limit of detection of 5 ng of silicon per injection. The detector is applied to the rapid screening of trimethylsilylated fractions of shale-derived liquids being prepared for biossay.

Trimethylsilyl derivatization of compounds containing active hydrogen to simplify their gas chromatographic determination is a universally accepted procedure. The technique is used routinely in this laboratory for the analysis of cigarette smoke condensate [1] and other complex mixtures. Esterification of a pyridine solution of the analyte with a silylating reagent, such as bis-trimethylsilyltrifluoroacetamide (BSTFA) [2] under mild heating conditions is the usual procedure. While silylation is a powerful tool for the resolution of complex mixtures, most gas chromatographic detector systems routinely in use cannot readily discriminate between naturally occurring compounds and those which are synthesized during the derivatization procedure.

Several workers have reported element-selective detectors for gas chromatographic systems, many of which are capable of element-selectivity for silicon [3—8]. However, most of these detectors exhibit significant levels of sensitivity toward pure hydrocarbons, which makes the interpretation of chromatograms of complex mixtures somewhat ambiguous. Feldman and Batistoni [9] have recently reported innovations in an element-selective glow discharge detector system which employs dynamic background correction [9]. Because of the background correction method, extremely high selectivity for silicon (compared with hydrocarbons) is achieved. The purpose of this paper is to describe the potential applications of the glow discharge detector for silicon-selective detection in complex organic matrices. While the application presented is restricted to synthetic fossil fuel mixtures, the technique should be applicable to such problems as the identification of polar constituents in the particulate matter of cigarette smoke or organic concentrates of physiological fluids.

EXPERIMENTAL

Equipment

The element-selective glow discharge detector (GDD) used is that described by Feldman and Batistoni [9]. Essentially, the detection system consists of a helium glow discharge, the image of which is focused on the entrance aperture of the collimating mirror of an Ebert monochromator. The exit beam is split, so that a portion of the beam provides sensitivity to the element in question, while the remainder of the beam provides for spectral background correction. A gas chromatograph (Perkin-Elmer Model 3920, Norwalk, CT) was adapted for use with a GDD and a flame ionization detector (FID) in parallel. Effluent from the column was split 4:1 by means of a capillary restrictor and a T-joint of zero dead volume, with the larger fraction being directed to the GDD. The output of the two detectors was displayed simultaneously on a dual pen recorder (Linear, Model 385); the FID responded to all organic compounds, while the GDD responded only to compounds containing silicon.

Sensitivity maximization

Prior to the analysis of a sample, the following procedure was used to maximize GDD sensitivity to silicon. First, exact focusing of the GDD image on a paper target mounted at the entrance of the paraboloid mirror of the monochromator was verified. Next, response to repeated injections of a silicon-containing compound, such as tributylsilane, at wavelengths of either 251.6 or 288.2 nm, was maximized by careful adjustment of the wavelength guide of the monochromator. Spectral background compensation was then obtained by injecting solutions of the silicon-containing compound and pure hydrocarbons which eluted near the tributylsilane and adjusting the wavelength, at which spectral background was monitored, with the micrometer screw drive. Once maximum silicon selectivity was achieved, samples were injected with the expectation of similar selectivity for other silicon-containing compounds.

Trimethylsilyl derivatization procedure

All samples were dissolved in appropriate amounts of redistilled pyridine. A 0.4-ml aliquot of the pyridine solution was mixed with 0.2 ml of BSTFA (Regis Chemical Co., Morton Grove, IL) in a 1-dram bottle sealed with a Teflon-lined septum. The bottle was heated for 30 min at 60°C. Occasionally, some samples required a longer reaction time before the silylation procedure was complete. (This could be recognized by an increase in the response of the GDD to silicon-containing compounds with repeated injections of identical volumes over a period of time.) Usually, heating for 1 h at 100°C was sufficient reaction time for these more difficult samples.

RESULTS AND DISCUSSION

Simultaneous chromatographic detection

For qualitative screening, spectral background compensation, while perhaps desirable, is not always necessary, since the selectivity of the GDD for silicon at wavelengths of 251.6 and 288.2 nm is relatively good. This is illustrated in Fig. 1, which compares the response of the conventional flame ionization detector with that of the GDD for a solution of normal hydrocarbons and trimethylsilyl-derivatized long-chain carboxylic acids. While there is a small response caused by broad-band spectral radiation from hydrocarbon molecular fragments, relative selectivity for the silicon-containing materials is substantial (greater than 37).

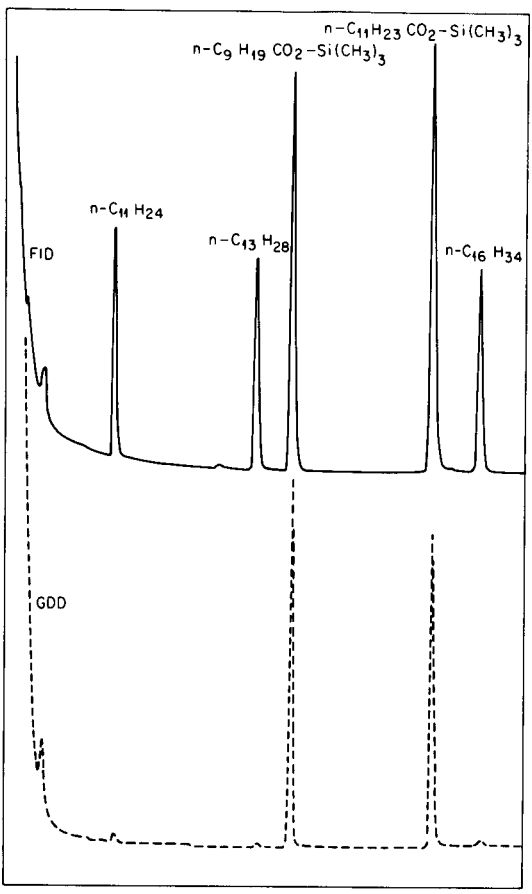


Fig. 1. Comparison of response of the FID and GDD to a mixture of n-alkanes and TMS-derivatized carboxylic acids. GDD wavelength, 288.2 nm; without spectral background compensation.

For quantitative work or for profiling of very complex mixtures, spectral background correction or compensation is necessary. It acts to prevent broadband radiation from various molecular fragments being recorded as a response to the element in question. Actual chromatograms taken under background-compensated and uncompensated conditions are compared in Fig. 2. Without compensation, a small false positive response can be observed; with compensation, this response disappears. To simulate a worst possible case, where the spectral background would be steeply sloped in the region of the line emission of silicon, the spectral bandpasses of the main channel and background channel were caused to overlap. This had the effect of reducing the apparent silicon response because part of the silicon "line" emission was compensated along with the background. Generally, putting the main and background channels in such close spectral proximity is not required, and the apparent silicon-selective response is decreased to a much smaller extent by the background compensation process.

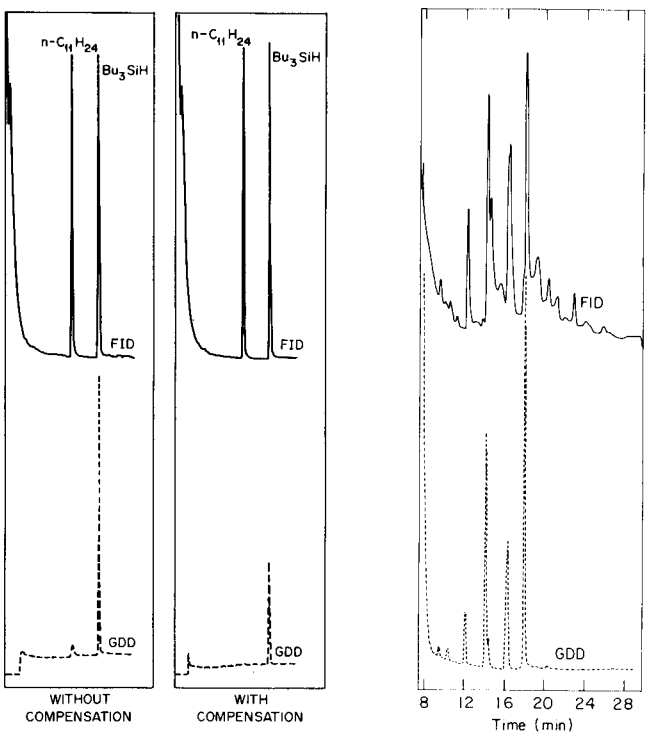


Fig. 2. Comparison of chromatographic traces with and without spectral background compensation. GDD wavelength, 288.2 nm. Background compensation conditions involve overlapping spectral bandpass.

Fig. 3. Comparison of chromatographic traces for the TMS-derivatized strong acid fraction of shale oil product water. GDD wavelength, 251.6 nm. Background compensation conditions involve an adjacent spectral bandpass. Chromatographic conditions: 20 ft. × 1/8 in. 4% OV-101 on Chromosorb G-HP; flow, 28 ml min^{-1}; program, 120°C hold for 4 min, program at 4°C min^{-1} to 190°C, hold for 8 min.

Sensitivity

A plot of GDD response (peak height measurements) as a function of the amount of silicon injected as tributylsilane was linear over the range 40—300 ng of silicon per injection. The absolute sensitivity of the GDD to silicon depends on many factors, including gas chromatographic conditions, carrier gas (helium) purity and flow rate through the discharge, detector temperature, monochromator slit width, etc. These have been discussed in detail [9]. For most practical applications, the lower limit of detection was found to be ca. 5 ng Si.

Co-elution of silicon-containing contaminants

During repeated use, the gas chromatographic column is exposed to a large amount of the unreacted silylating reagent (BSTFA). It was found that after a large number of repeated injections of silylated mixtures in pyridine, even materials which would not normally incorporate the $-Si(CH_3)_3$ group were responsible for positive responses when the GDD was used in the silicon-detection mode at either of the two important silicon emission wavelengths. These responses could not be eliminated with spectral background compensation, which suggested that the response was not a false positive. Gas chromatographic—mass spectrometric analysis with the same column verified that the normally non-derivatizable compounds giving rise to the silicon response did not actually contain silicon in their molecular structure. The problem was less important when other derivatizing solvents such as tetrahydrofuran or trifluoroacetic acid were used, but these solvents were much less satisfactory for the derivatization procedure. It was found that treatment of the column and transfer lines with Freon, followed by further cleaning of the plumbing with methylene chloride eliminated the problem. Presumably, the column treatment removed small amount of adsorbed impurities which enabled trace amounts of the BSTFA silylating reagent to cling to the column-packing material.

Application of silicon-selective screening of organic fractions

A significant portion of the work in this laboratory is directed toward the chemical characterization of complex organic mixtures in order to understand the nature of their biological impact. To this end, fractionations of cigarette smoke condensate and of liquids derived from fossil fuels are carried out under various schemes prior to both chemical analysis and bioassay by the Ames *Salmonella* mutagenicity assay [10]. The bioassay is used both as a measure of biological impact and as a screen for identifying those fractions which may warrant more detailed chemical characterization. Fractions are often described according to their acid—base character. Ideally, the fraction should contain only those species of similar character.

Silicon-selective detection was applied to the rapid screening of both strong and weak acid fractions of coal-derived liquids. Small amounts of these materials were TMS-derived by the procedures described above.

Silicon should be incorporated as $-Si(CH_3)_3$ into all compounds within the fractions that possess active hydrogens. If the fractionation scheme is completely effective, all compounds present in an acidic fraction should fall into this category. Under rigorous and exhaustive silylation conditions, any compounds present in the fraction which do not elicit a silicon response with the GDD probably do not possess active hydrogens, and so are neutral or basic species.

Responses of a conventional FID and GDD under simultaneous detection conditions are compared in Fig. 3 for a trimethylsilylated portion of the strong acid fraction [10] of a shale oil product water [11]. While most of the compounds eluting at the beginning of the chromatogram have incorporated silicon, and thus contained active hydrogens, several of the higher boiling constituents in the fraction did not contain silicon. This finding indicated that further sub-fractionation of the strong acid fraction would be necessary before biological activity of the sample could be ascribed to only acidic components. In contrast, a GDD—FID dual profile of the weak acid fraction of the same shale oil product water indicated that all the visualized constituents had incorporated silicon in the TMS derivatization; this implied that these components possessed active hydrogens, i.e. some acidic functionality. Because of the rapidity of the chromatographic procedure and the selectivity of the silicon response of the GDD, this procedure can be routinely applied to screening of complex mixtures prior to mutagenicity bioassay.

This research was sponsored by the Division of Biomedical and Environmental Research, U.S. Department of Energy under Contract W-7405-eng-26 with the Union Carbide Corporation.

REFERENCES

1 M. R. Guerin and P. Nettesheim, ORNL Tobacco Smoke Research Program Summary Report, ORNL-5008, March, 1975 (available from National Technical Information Service).
2 K. Blau and G. S. King, Handbook of Derivatives for Chromatography, Heyden, London 1977.
3 A. J. McCormack, S. C. Tong and W. D. Cooke, Anal. Chem., 37 (1965) 1470.
4 R. S. Braman and A. Dynako, Anal. Chem., 40 (1968) 95.
5 R. W. Morrow, J. A. Dean, W. D. Shults and M. R. Guerin, J. Chromatogr. Sci., 7 (1969) 572.
6 W. R. McLean, D. L. Stanton and G. E. Penketh, Analyst, 98 (1973) 432.
7 Y. Talmi and A. W. Andren, Anal. Chem., 46 (1974) 2122.
8 D. T. Bostick and Y. Talmi, J. Chromatogr. Sci., 15 (1977) 164.
9 C. Feldman and D. A. Batistoni, Anal. Chem., 49 (1977) 2215.
10 I. B. Rubin, M. R. Guerin, A. A. Hardigree and J. L. Epler, Environ. Res., 12 (1976) 358
11 C. H. Ho, B. R. Clark and M. R. Guerin, J. Environ. Sci. Health, A11 (7) (1976) 481.

Analytica Chimica Acta, 108 (1979) 227—231
© Elsevier Scientific Publishing Company, Amsterdam — Printed in The Netherlands

OPTIMIZED SEPARATION OF SCOPOLETIN AND UMBELLIFERONE AND *cis-trans* ISOMERS OF FERULIC AND *p*-COUMARIC ACIDS BY REVERSE-PHASE HIGH-PERFORMANCE LIQUID CHROMATOGRAPHY

WILLIAM PHILLIP PRICE, JR.** and STANLEY NORRIS DEMING*

Department of Chemistry, University of Houston, Houston, TX 77004 (U.S.A.)

(Received 20th November 1978)

SUMMARY

A systematic optimization strategy for reverse-phase h.p.l.c. is used to produce complete separation of all components of a mixture containing two coumarins, umbelliferone and scopoletin, and the *cis-trans* isomers of two cinnamic acids, *p*-coumaric and ferulic. A series of experiments gives retention time data for each of these substances in four citric acid-buffered mobile phases. A mathematical model fitted to this data gives model parameters that provide the basis for a window diagram of relative retentions vs. mobile phase pH. The window diagram gives an estimate of the mobile phase pH required for optimum separation.

The separation of coumarins and the separation of cinnamic acids are treated extensively in the literature [1, 2]. Although paper chromatography is the technique most commonly used, reverse-phase h.p.l.c. has several potential advantages, among them ease of quantification and short analysis time. More important from the point of view of method development however, is the large number of variables associated with the mobile phase that may be readily changed to improve the separation of complex mixtures.

Generally, it is more efficient to adopt systematic optimization strategies rather than to rely on experiential approaches for the development of new separation methods. This paper describes the application of a systematic reverse-phase h.p.l.c. optimization strategy [3] to the separation of a mixture of umbelliferone, scopoletin, and the *cis-* and *trans-* isomers of *p*-coumaric and ferulic acids

EXPERIMENTAL

Instrumentation

The chromatographic system was composed of a Model 6000A pump (Waters Associates, Milford, MA 01757), a Model U6K injector (Waters), a C_{18} Bondapak/Porasil precolumn (10-cm × 2-mm i.d.; Waters), and a

---

**Welch Foundation Pre-Doctoral Fellow.

C_{18} μBondapak high efficiency main column (30-cm × 4-mm i.d.; Waters). Injection volumes were 5 μl and flow rate was 2.0 ml min^{-1} throughout the study. Precolumn and main column temperature [4] was held at 25.0 ± 0.1°C with a constant temperature circulating water bath (Model FK, Haake, Inc., Saddle Brook, NJ 07662). A SP8200 u.v. detector (Spectra Physics, Santa Clara, CA 95051) was operated at 254 nm; the absorbance signal output was sent to a strip-chart recorder (Model 281, Soltec, Encino, CA 91316) and, simultaneously, to an analog-to-digital converter (Model ADC-12QZ, Analog Devices, Norwood, MA 02062) interfaced [5] to a digital computer (Model 9830A, Hewlett-Packard Calculator Products Division, Loveland, CO 80537). The absorbance signal was digitized at 0.5-s intervals. The time equivalent of the void volume (t_0 = 1.30 min) was estimated by measuring the time from injection to the first small deviation in signal baseline. Retention times (t_R) for all samples were measured from strip-chart records. Chromatograms shown in this paper were reproduced on a plotter (Model 9862A, Hewlett-Packard) from the digitized data.

Solutes

Umbelliferone, scopoletin, *p*-coumaric acid (4-hydroxycinnamic acid), and ferulic acid (4-hydroxy-3-methoxycinnamic acid) were purchased from the Fisher Scientific Company or Sigma Chemical Company. Isomeric solutes were obtained as the pure *trans* form. Solutions of the four individual solutes were prepared at a level of approximately 2.5 mg ml^{-1} in 10% (v/v) methanol—water.

Ferulic and *p*-coumaric acid solids were protected from light and stored at 5°C. A portion of each of the two cinnamic acid solutions was exposed to direct u.v. light for 15 min; both exposed and unexposed portions were stored in the dark and refrigerated until used. Samples were exposed to room lights only briefly and for equal intervals during solute injection.

Mobile phases

Table 1 shows the composition of the citric acid-buffered mobile phases used. Spectroscopic-grade methanol (Gold Label, Aldrich Chemical Company) was added, 10% (v/v), to produce faster elution. Ionic strength was 0.06 M. Each buffered mobile phase was filtered through a 0.45-μm Millipore cellulose acetate filter and degassed. The pH values of the mobile phase reported are those calculated for aqueous buffers and are based on citric acid pK_a values of 3.128, 4.761, and 6.396 [6]. Reported pH values probably do not accurately describe the true pH of the buffered mobile phases; the calculated pH values do, however, serve as an appropriate operational scale for this study [7].

RESULTS AND DISCUSSION

A previously described model [3, 8]

$$k'_R = [k'_{HA} + k'_A\, 10^{(pH - pK_a)}]/[1 + 10^{(pH - pK_a)}] \quad (1)$$

TABLE 1

Composition of buffered mobile phases

Apparent pH[a]	Citric acid[a] 2.0 M (ml)	NaOH[a] 2.0 M (ml)	NaCl[a] (g)
3.0	10.00	4.10	6.502
4.0	10.00	10.23	5.661
5.0	10.00	16.56	4.276
6.0	10.00	22.38	2.624

[a]In a final 2.00 l of solution containing 200 ml of methanol.

was fitted to the experimental data for each of the solutes by means of a non-linear least-squares simplex program [9]; calculated model parameters were used to construct the solute retention time vs. mobile-phase pH curves shown in Fig. 1. From these, the "window diagram" of relative retention vs. mobile phase pH [10, 11] was constructed (Fig. 2).

The window diagram provides an estimate of the mobile phase pH required to give the best separation of the worst separated pairs in the mixture of all solutes. Best predicted conditions fall between about pH 5.1 and 5.4, the top of the tallest shaded window in Fig. 2. The shape of the window provides additional information: a window with a broad top, like that between pH 4.75 and 5.80, indicates a region where a small change in mobile phase pH will not adversely affect the separation. By contrast, a sharply peaked window, like that between pH 4.2 and 4.75, indicates that tight control of mobile-phase pH is necessary to prevent serious deterioration of resolution between worst separated pairs.

A citric acid buffer pH 5.3 was prepared by mixing 10.00 ml of 2.0 M citric acid, 18.43 ml of 2.0 M NaOH, 3.80 g of NaCl, 200.0 ml of methanol, and sufficient distilled water to make 2.00 l of solution. The upper chromatogram in Fig. 3 was obtained with this mobile phase for the mixed solute sample. The initial solute mixture, spiked with *cis*- and *trans-p*-coumaric acid and with umbelliferone, produced the lower chromatogram shown in Fig. 3.

Equation 1, originally proposed as a model for the retention behavior of monoprotic Brønsted acids and bases in reverse-phase h.p.l.c. systems [3, 8], adequately describes the behavior of the acidic compounds studied but the retention times for each of the two neutral, strongly retained solutes (umbelliferone and scopoletin) remain essentially constant over the pH range studied. Thus, analysis time for these solutes cannot be significantly reduced by changing pH; nevertheless, because of the pH dependence of the acids, optimal separation is given at pH 5.1.

Support for this study was provided by Grant E-644 from the Robert A. Welch Foundation. Samples of the solutes were kindly provided by Ms. Bonnie Carpenter and Dr. Donald L. Hendrix, Department of Biology.

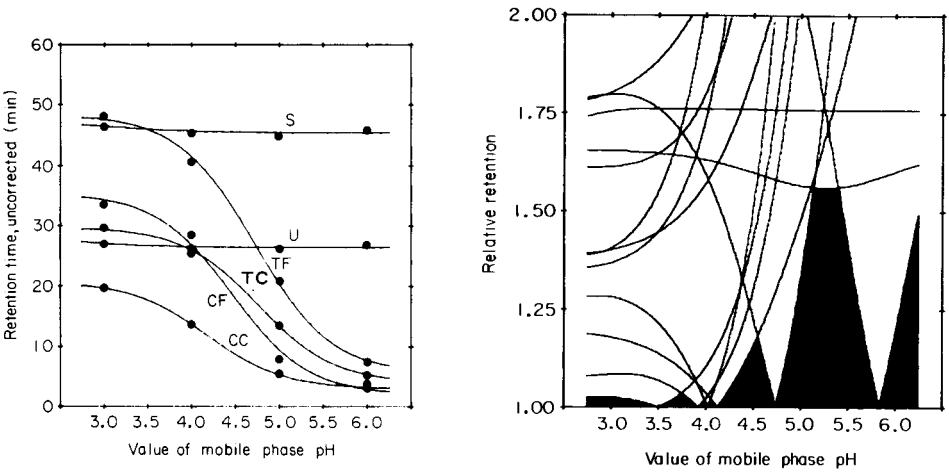


Fig. 1. Observed experimental points and calculated retention times vs. mobile-phase pH for each of the six solutes. (S) Scopoletin; (U) umbelliferone; (TF) *trans*-ferulic acid; (TC) *trans-p*-coumaric acid; (CF) *cis*-ferulic acid; (CC) *cis-p*-coumaric acid.

Fig. 2. Window diagram of relative retentions vs. mobile-phase pH.

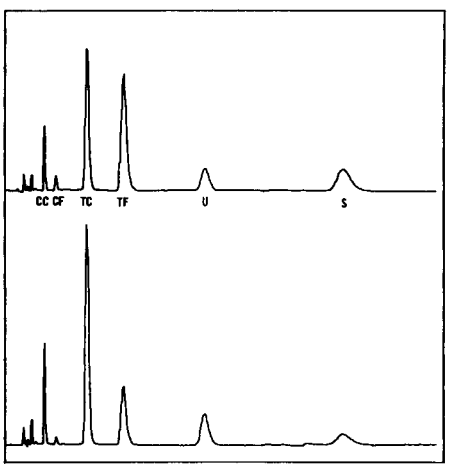


Fig. 3. Chromatograms of six-component mixture at pH 5.3. Upper chromatogram: original mixture. Lower chromatogram: 50% original mixture plus 25% u.v.-exposed *p*-coumaric acic and 25% umbelliferone.

REFERENCES

1 J. B. Harborne, Phytochemical Methods, Chapman and Hall, London, 1973, pp. 41–46.
2 E. Soczewinski, G. Matysik and Z. Grodzinska-Zachwieja, J. Chromatogr., 137 (1977) 182.
3 S. N. Deming and M. L. H. Turoff, Anal. Chem., 50 (1978) 546.

4 J. J. Kirkland, in J. J. Kirkland (Ed.), Modern Practice of Liquid Chromatography, Wiley, New York, 1971, p. 181.
5 A. S. Olansky, Ph. D. Dissertation, University of Houston, Houston, TX, 1978, p. 81.
6 G. Kortum, W. Vogel and K. Andrussow, Dissociation Constants of Organic Acids in Aqueous Solution, Butterworths, London, p. 314.
7 W. P. Price, Jr., R. Edens, D. L. Hendrix and S. N. Deming, Anal. Biochem., 93 (1979) 233.
8 C. Horvath, W. Melander and I. Molnar, Anal. Chem., 49 (1977) 142.
9 R. O'Neill, Appl. Statist., 20 (1971) 338.
10 J. R. Laub and J. H. Purnell, J. Chromatogr., 112 (1975) 71.
11 J. R. Laub and J. H. Purnell, Anal. Chem., 48 (1976) 799.

Analytica Chimica Acta, 108 (1979) 233—239
© Elsevier Scientific Publishing Company, Amsterdam — Printed in The Netherlands

DETERMINATION OF MORPHINE IN POPPY STRAW BY HIGH-PERFORMANCE LIQUID CHROMATOGRAPHY

C. Y. WU*, M. S. MICHAILIDIS and J. J. WITTICK

Merck Chemical Manufacturing Division, Merck & Co., Inc., Rahway, N. J. 07065 (U.S.A)

(Received 19th February 1979)

SUMMARY

A simple high-performance liquid chromatographic method for determining morphine in poppy straw is reported. The sample (ca. 2g) is ground and extracted with 0.02 M HCl; after suitable treatment, the morphine is extracted into chloroform—propan-2-ol (3:1), the acidified extract is evaporated, the residue is dissolved in dilute acid, and after further extraction, 100-μl aliquots are injected into the chromatograph. The method is specific and gives a precision of ± 2% relative.

As a result of shortages of gum opium, the unlanced poppy capsule (*Papaver somniferum)*, commonly called poppy straw, has become of industrial importance for the production of morphine and other alkaloids which have been traditionally extracted from gum opium. Poppy straw contains relatively low levels of morphine — ca. 0.5% as compared to 10—16% in gum opium. In the past, therefore, it was not economically feasible to process this material. However, several establishments are at present involved in extracting morphine, codeine, and thebaine from poppy straw to supplement world-wide supplies and there is growing interest in determining the alkaloid content, especially morphine, in this raw material. Classical wet methods are available [1—4] but they are tedious and subject to errors, and many improved modern analytical instrumental procedures have been described [5—22]. The h.p.l.c. method described here for the determination of morphine in poppy straw is based on earlier work dealing with the analysis of gum opium for its major alkaloid contents [23].

EXPERIMENTAL

Apparatus

A Waters Model ALC/GPC-244 liquid chromatograph equipped with a 280-nm detector, a Schoeffel variable-wavelength detector, and a Hewlett-Packard Model 3380A reporting integrator were used.

A Spectra-Physics injection valve equipped with a 100-μl injection loop was used for precise injections. A Millipore Swinny adaptor and MF-Millipore

filters (HAWP 01300; pore size, 0.45 μm) were used for sample solutions, and a Millipore all-glass filter apparatus (XX1504700) and MF-Millipore filters (HAWP04700) were used for distilled water and salt solutions. A Tekmar analytical mill (Model A-10) was used to grind the poppy straw samples.

Reagents

Morphine sulfate pentahydrate, U.S.P. grade of known alkaloid content, was available. Reagent-grade propan-2-ol, chloroform, dichloromethane, sodium hydroxide, sodium chloride, calcium hydroxide, sodium perchlorate, sodium dihydrogenphosphate monohydrate and glacial acetic acid (all from J. T. Baker) and acetonitrile (u.v. grade; Burdick and Jackson) were used.

Chromatographic conditions

Two μ-Bondapak C_{18} columns (30-cm × 4.0-mm i.d.; Waters Associates) were connected in series. The mobile phase was 0.1 M NaH_2PO_4 in aqueous 6% acetonitrile. The flow rate was 1.2 ml min^{-1} (ca. 1,900 psig). The injection volume was 100 μl.

The mobile phase was prepared as follows: 27.6 g of sodium dihydrogenphosphate monohydrate were dissolved in ca. 600 ml of distilled water in a 1-l beaker and filtered. The filtrate was transferred to a 2-l volumetric flask, and 120 ml of acetonitrile was added. The solution was diluted to volume with prefiltered distilled water and mixed. After mixing, the mobile phase was degassed under vacuum for 15 min prior to use.

Standard preparation

The stock solution containing the equivalent of 24 mg of morphine was prepared by weighing an appropriate amount of morphine sulfate pentahydrate standard into a 25-ml volumetric flask and diluting to volume with water. The working standard solution was prepared by pipeting 10 ml of the stock standard solution into a 100-ml volumetric flask containing 5 drops of glacial acetic acid and 10 drops of 2 M HCl and diluting to volume with water; 15 ml of this solution was then pipeted into a 50-ml polypropylene centrifuge tube containing 0.5 g of $Ca(OH)_2$ and thereafter handled as described below under Sample Preparation. (The standard and sample were treated in the same manner to compensate for any volume changes which occur during their preparation for chromatography).

Sample preparation

About 2 g of poppy straw powder (ground to a particle size of ca. 45 μm) was accurately weighed into a 50-ml polypropylene centrifuge tube; 25 ml of 0.02 M HCl was added to the tube and mixed, and the slurry was allowed to stand overnight. On the following day, the tube was shaken mechanically for 1 h and centrifuged at 16,000 rpm for 8 min, and the supernatant liquid was transferred to a 100-ml volumetric flask (flask I). The residue was washed sequentially with three 20-ml portions and one 18-ml portion of 0.02 M HCl by

mixing mechanically or ultrasonically. Each wash was centrifuged and the supernatant solutions were transferred to flask I; the solution was finally diluted to volume with water (ca. 8 ml of 0.02 M HCl are not recoverable from the slurry). A 50-ml aliquot of the extract from flask I was pipeted into a 150-ml beaker and the solution was adjusted to pH 9.0 ± 0.1 (isoelectric point of morphine) with 1 M NaOH. The solution was transferred quantitatively to a 250-ml separatory funnel containing 18 g of NaCl. To the aqueous extract in the separatory funnel, 50.0 ml of a chloroform—propan-2-ol solvent (3:1 v/v) were added, and the mixture was shaken vigorously for ca. 30 s. After phase separation, the organic phase was collected in a 150-ml beaker. When complete phase separation could not be achieved because of emulsions, the cloudy organic phase was centrifuged to effect separation. Five drops of glacial acetic acid were added and mixed with the contents of the beaker. The acidified organic extract was then evaporated to dryness at ambient temperature with a stream of air. The residue was dissolved (with the aid of ultrasonics, if necessary) in 6 drops of 2 M HCl and 5 ml of water. The solution was then transferred to a 25-ml volumetric flask (flask II). The beaker was rinsed with two 6-ml portions of water (containing 2 drops of 2 M HCl for each 6 ml), the rinsings were added to flask II, and this solution was diluted to volume with water. A 15-ml aliquot of the solution from flask II was pipeted into a 50-ml polypropylene centrifuge tube containing 0.5 g of calcium hydroxide.

The standard and sample preparation were then treated as follows: to each tube 10.0 ml of dichloromethane was added; the tubes were shaken vigorously for ca. 30 s and centrifuged at 2,500 rpm for 5 min. A volume of 8 ml of the top aqueous phase of each was pipeted into separate 10-ml volumetric flasks containing 5 drops of 2 M HCl. The solutions were diluted to volume with water and filtered before chromatographic analysis.

Quantification.

Quantification was achieved by injecting the sample and the standard solution and comparing the sample area response with that of the standard, taking into account all the dilution factors. Sample loop injection was used exclusively to achieve high precision. All the quantitative analyses were carried out within the linear response range (0 to at least 20 μg per 100-μl injection) established through calibration.

RESULTS AND DISCUSSION

Earlier work [23] suggested that an aqueous solvent might be effective for the quantitative extraction of morphine from poppy straw. Investigations showed that both water and 0.02 M HCl can be used, the latter being the more efficient. The data presented in Table 1 were obtained by analyzing successive extractions of a single sample with the specified solvent; quantitative extraction of morphine from poppy straw was achieved with 5 extractions when 0.02 M HCl was used as the solvent, and this was further substantiated

TABLE 1

Extractions of poppy straw with successive 30-ml portions of water or 0.02 M HCl

Extract no.	Morphine found in extract (mg)	Volume of extract recovered (ml)	Extract no.	Morphine found in extract (mg)	Volume of extract recovered (ml)
Poppy straw (3.0446 g) extracted with water			*Poppy straw (3.0203g) extracted with 0.02 M*		
1	6.72	19.6	1	6.94	19.7
2	3.36	30.8	2	3.54	31.5
3	1.11	30.9	3	1.21	30.0
4	0.49	30.0	4	0.46	30.9
5	0.23	30.8	5	0.21	29.8
6	0.1	30.3	6	Negligible	32.7
Total	12.01	172.4	Total	12.36	174.6

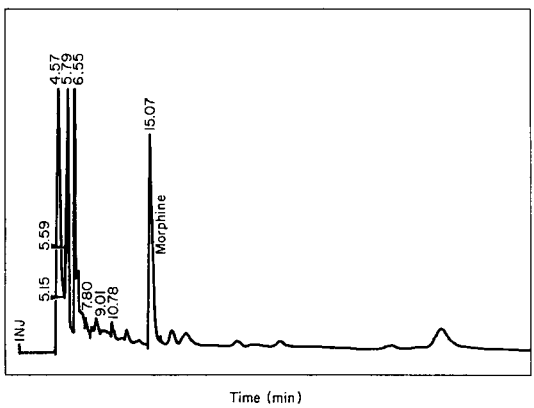


Fig. 1. Chromatogram of an unpurified 0.02 M HCl extract. (See text for chromatographic conditions.)

by analyzing the solid residue which remained after exhaustive extraction. The solid residue was dried at 40°C in vacuum and reground to create new surfaces to facilitate further extraction. The reground solid residue was then soaked in 25 ml of 0.02 M HCl and mechanically shaken overnight. The residue slurry was centrifuged at high speed and the supernatant solution was examined by h.p.l.c. Less than 0.1% of the total amount of morphine recovered was detected in this final extract. The combined extracts from five successive extractions with 0.02 M HCl may be determined directly by h.p.l.c. (see Fig. 1). It was considered impractical, however, to determine morphine in this manner because too many components are eluted after morphine; excessive time would be needed to clean the column after each analysis and, because of column con-

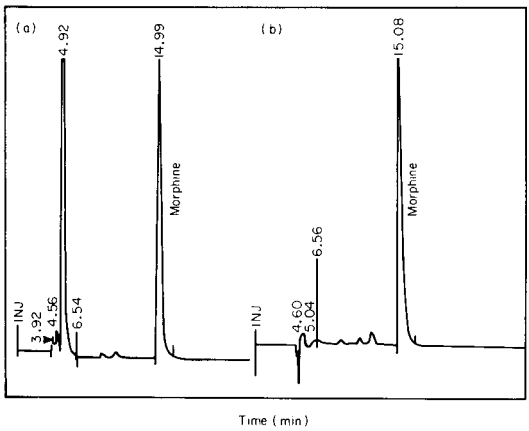


Fig. 2 (a) Chromatogram of chloroform—propan-2-ol extract residue resolubilized in acidified water (see text for chromatographic conditions.) (b) Chromatogram of the same solution after washing with dichloromethane.

contamination, frequent regeneration would be required. Further purification of the acidic aqueous extract was obviously necessary; extraction with a chloroform—propan-2-ol mixture purified the sample significantly (Fig. 2A) although two minor components were still eluted long after morphine (as shown in Fig. 1). Fortunately, these later components and the earlier large peak were decreased greatly by making the solution basic and washing with dichloromethane (Fig. 2B).

Despite the need for the two purification steps, the recovery of morphine was excellent, as established by adding known quantities of morphine to the original acidic aqueous extract before the chloroform—propan-2-ol extraction then following the sample preparation procedure. The recovery data (Table 2) show that one extraction with the specified volume ratio of organic to aqueous phase (1:1) gave quantitative extraction of the morphine.

Replicate analyses of a poppy straw sample indicated that the reproducibility of the method on the same day was excellent; direct injection of the unpurified acidic extract gave 0.423% morphine compared with 0.421% (average of 5 determinations with range 0.417—0.424; r.s.d = 0.6%) following the complete procedure. The day-to-day reproducibility was also good; direct injection of the unpurified acidic extract of this different sample gave 0.45% morphine, and the average value obtained with the complete procedure on 5 successive days was 0.45% (range 0.43—0.46, r.s.d. = 1.9%).

To demonstrate that the morphine peak consists of only one component, two approaches were used. In the first approach the object was to determine whether any impurities separated from morphine by t.l.c. are eluted at or near the morphine peak when those impurities are injected into the h.p.l.c. column. A t.l.c. system described by Stahl [24] was used. The solvent was carbon tetrachloride: methanol: n-butanol: 6 M ammonia = 40:30:30:2; the plate was

TABLE 2

Recovery of morphine from 30 ml of 0.02 M HCl poppy straw extract containing originally 2.74 mg of morphine.

Solution	Morphine (mg)			
	Added	Total present	Total found	Recovery (%)
Sample	0	2.74	2.74	—
1	1.86	4.60	4.63	101.8
2	2.79	5.53	5.57	101.4
3	3.72	6.46	6.50	101.1
				Av. 101.5

silica gel GF (Analtech). The sample applied (20 μl) was the chloroform—propan-2-ol extract from 2 g of poppy straw, concentrated to ca. 2 ml. The plate, developed in two dimensions to improve separation, was dried and the silica along the 45° diagonal of the plate both below (including the origin) and above the morphine spot ($R_F \approx 0.4$) was collected in two separate 15-ml centrifuge tubes. A mixed solvent (methanol and dilute hydrochloric acid) was used to extract the separated material from the silica. The extracts were dried with nitrogen, reconstituted with the mobile phase, and injected into the column. None of the impurities separated from morphine by t.l.c. were eluted at or near the morphine peak by h.p.l.c. In the second approach, the h.p.l.c. peak area response ratio of standard to sample should remain constant (within experimental error) at various wavelengths if the sample peak is as pure as the standard peak. The five wavelengths investigated included the absorption maximum at 285 nm and the minimum at 260 nm. The ratios obtained were 1.19 (254 nm), 1.18 (260 nm), 1.20 (271 nm), 1.18 (285 nm) and 1.19 (291 nm). These tests are considered adequate to demonstrate the specificity of the method.

REFERENCES

1 H. Bohme and R. Strohecker, Arzneim. Forsch., 3 (1953) 468.
2 F. Gstirner and K. Vollmer, Apoth. Ztg., 61 (1949) 57.
3 C. Mannich, Arch. Pharm. (Weinheim, Ger.), 280 (1942) 386.
4 K. Paech and M. V. Tracey (Eds.), Modern Methods of Plant Analysis, Vol. IV., Springer-Verlag (1955) 448 pp.
5 F.-F. Wu and R. H. Dobberstein, J. Chromatogr., 140 (1977) 65.
6 G. Fisher and R. Gillard, J. Pharm. Sci., 66 (1977) 421.
7 P. C. Cheng and N. J. Doorenbos, J. Miss. Acad. Sci., 21 (1976) 13.
8 A. I. Dumitrashko and F. V. Babilev, Izv. Akad. Nauk Mold. SSR. Ser. Biol. Khim. Nauk, (1) (1976) 83.
9 M. D. Grove, G. F. Spencer, M. V. Wakeman and H. L. Tookey, J. Agric. Food Chem., 24 (1976) 896.

10 J. W. Fairbairn and K. Helliwell, J. Pharm. Pharmacol., 27 (1975) 217.
11 M. Paris, J. P. Gramond and R.-R. Paris, Ann. Pharm. Fr., 32 (1974) 97.
12 D. W. Smith, T. H. Beasley, R. L. Charles and H. W. Ziegler, J. Pharm. Sci., 62 (1973) 1691.
13 J. Schou and B. Eriksen, Bull. Narcotics, 25 (1973) 57.
14 J. W. Fairbairn and F. Hakim, J. Pharm. Pharmacol., 25 (1973) 353.
15 V. A. Danelýant and Yu. V. Shostenko, Farm. Zh. (Kiev), 27 (1972) 48; 28 (1973) 79.
16 V. A. Danelýant, S. Kh. Mushinskaya and Yu. V. Shostenko, Khim.-Farm. Zh., 7 (1973) 47.
17 R. V. D. Rondina, A. L. Bandoni and J. D. Coussio, J. Pharm. Sci., 62 (1973) 502. (1973) 502.
18 A. V. Gaevskii and P. M. Loshkarev, Khim.-Farm. Zh., 6 (1972) 54.
19 B. Zsadon and T. Paal, Herba Hung., 8 (1969) 157; Acta Chim. Hung., 57 (1968) 323.
20 R.-R. Paris and G. Faugeras, Ann. Pharm. Fr., 24 (1966) 613.
21 R.-R. Paris, G. Faugeras, L. Balard and M. Campal, Ann. Pharm. Fr., 24 (1966) 411.
22 N. A. Izmailov, S. Kh. Mushinskaya and V. A. Danelýants, Med. Prom. SSSR, 18 (1964) 47.
23 C. Y. Wu and J. J. Wittick, Anal. Chem., 49 (1977) 359.
24 E. Stahl (Ed.), Thin-Layer Chromatography, Springer-Verlag, New York, (1969) p.440.

Analytica Chimica Acta, 108 (1979) 241—247
© Elsevier Scientific Publishing Company, Amsterdam — Printed in The Netherlands

DIFFERENTIAL KINETIC ANALYSIS AND FLOW INJECTION ANALYSIS
Part 2. The (2.2.1) Cryptates of Magnesium and Calcium

DORRIT ESPERSEN and ARNE JENSEN*

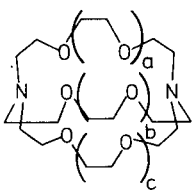
Department of Chemistry AD, The Royal Danish School of Pharmacy, 2 Universitetsparken, DK-2100 Copenhagen Ø (Denmark)

(Received 18th December 1978)

SUMMARY

Simultaneous differential kinetic analysis for magnesium and calcium ions in solution has been adapted to the flow injection system. The two-point kinetic assay is based on dissociation of the cryptand (2.2.1) complexes of magnesium and calcium ions with sodium ion as scavenger. The ions could be determined reproducibly with phthalein complexone as indicator, at a sampling rate of 80 samples per h with 200-μl sample injections and low reagent consumption. Rules derived from f.i.a. theory were confirmed experimentally.

Flow injection analysis (f.i.a.) can be utilized in connection with differential kinetic analysis [1]. The limiting factor of the method is that the difference between the rates of reaction of the metal complexes involved must be pronounced. A suitable difference exists between the metal complexes of ligands of the type I—III (cryptands) synthesized by Lehn [2]. The macrobicyclic ligands give 1/1 complexes with alkali and alkaline earth cations, called (2)-cryptates, the cation being contained inside the molecular cavity.



I, $a = 1; b = c = 0$ (2.1.1)
II, $a = b = 1; c = 0$ (2.2.1)
III, $a = b = c = 1$ (2.2.2)

The stability of the cryptate complexes depends largely on the relationship in size between the three-dimensional cavity of the cryptand and the diameter of the complexed ion. Ligand (2.2.1) displays very high Ca^{2+}/Mg^{2+} selectivity compared to other known ligands [3].

Kinetic studies of complex formation and dissociation between cryptands and alkaline earth ions in water have previously been published. The results suggest that the dissociation rates vary more from one system to another than the association rates [4—6]. The rates of dissociation of the cryptates of calcium and magnesium ions with (2.2.1) are very different because of the

pronounced selectivity of the ligand; thus the concentrations of the ions can be determined by differential kinetic analysis [7]. The reaction mechanism [6] is

$$MCry^{2+} + H^+ \underset{k_M^{HCry}}{\overset{k_H^{MCry}}{\rightleftharpoons}} HCry^+ + M^{2+} \quad (1)$$

$$HCry^+ + Na^+ \xrightarrow{k_{Na}^{HCry}} NaCry^+ + H^+ \quad (2)$$

Reaction (1) is the rate-determining step with a characteristic rate of dissociation for each metal complex, and reaction (2) is fast. The scavenger, sodium ion, is chosen so that $k_{Na}^{HCry}[Na^+] \gg k_M^{HCry}[M^{2+}]$ and application of the steady-state approximation to $[HCry^+]$ gives $-d[MCry^{2+}]/dt = k_d[MCry^{2+}]$. The rate of dissociation, k_d, can be calculated from $k_d = k^{MCry} + k_H^{MCry}[H^+]$. The rate of dissociation of the cryptand (2.2.1) complex of magnesium is fast, although the mechanism is not known in detail. The extent to which reactions (1) and (2) proceed can be followed spectrophotometrically by means of the reaction of the metal ion with phthalein complexone. The equilibrium between M^{2+} and phthalein complexone is rapidly established [8].

Phthalein complexone [9, 10] is an acid—base as well as an alkaline-earth metal indicator. This compound (metalphthalein, *o*-cresolphthalein complexone, phthalein purple) is a phenolphthalein derivative having iminodiacetate functional groups. The compound is colourless below pH 6.5 and gradually changes colour with increasing alkalinity. Above pH 11 the pink colour change to deep red ($pK_1 = 2.2$, $pK_2 = 2.9$, $pK_3 = 7.0$, $pK_4 = 7.8$, $pK_5 = 11.4$, $pK_6 = 12.0$) [9]. With magnesium and calcium the dye gives complexes with absorption maxima practically in the same range as that of the dye itself.

The f.i.a. method [11] utilizes direct injection of the sample into a continuously moving, unsegmented carrier stream. The well defined sample zone disperses during its passage through the system, the degree of dispersion being strictly controlled by the choice of the flow parameters [12]. This paper describes the combination of f.i.a. with differential kinetic analysis for determinations of magnesium and calcium ions with cryptand (2.2.1) as the ligand. The colour intensity of the M (phthalein complexone)$^{2+}$ complex is measured at two consecutive points in the flow stream at suitable time intervals.

EXPERIMENTAL

Reagents

All chemicals were of analytical-reagent grade and redistilled degassed water was used throughout.

The cryptand (2.2.1) was used as received (E. Merck). Standard aqueous solutions of the ligand were checked by potentiometric titration with 0.1 M hydrochloric acid. The solutions were protected from light in a brown bottle; potentiometric titrations showed the solutions to be stable for 6 weeks. The metal salts used were all nitrates and solutions were standardized by titration with EDTA.

The reagent solution in the flow system contained 1.50 M $NaNO_3$, 1.05×10^{-1} M triethanolamine and 1.50×10^{-3} M phthalein complexone, to which was added 2% (v/v) glycerine, before adjustment to pH 8.50 with nitric acid. The solution was found to be stable for at least 2 months. Cohen and Gordon [13] stated that a solution of phthalein complexone in triethanolamine showed no signs of decomposition after 4 months.

The carrier solution in the flow system was 3.00×10^{-3} M triethanolamine, containing 2% (v/v) glycerine and adjusted to pH 8.50 with nitric acid.

The standards consisted of metal nitrates in the concentration range 2.00×10^{-4}–1.00×10^{-3} M containing 1.38×10^{-3} M of cryptand (2.2.1). The standard aqueous solution of the ligand was adjusted to pH 10.00 with nitric acid prior to addition of the magnesium salt. The standards were subsequently adjusted to pH 9.50 with nitric acid. This adjustment of pH was unnecessary for the calcium standards. The mixed solutions were also adjusted to pH 9.50 with nitric acid. The pH chosen represents a compromise between avoiding precipitation of $Mg(OH)_2$ and dissociation of the calcium cryptate complex before measurement in the flow system. Similarly, the pH value of the reagent stream (8.50) represents a compromise, because any increase in alkalinity increases the absorption for a given concentration of M^{2+}.

Apparatus

Two Beckman DU spectrophotometers, modified by means of d.c. amplifier to a digital display [14], were each equipped with a Hellma flow-through cuvette (type OS-178.10, light path 10 mm, volume 80 μl) and connected to a Servo-Graph RE C61 recorder, furnished with a REA 112 high-sensitivity unit (Radiometer, Denmark). A Heto thermostat 05 E 623 (Heto, Denmark) was used to supply the circulating water as required.

An Ismatec Model mp-4 pump (Ismatec, Switzerland) was operated at a constant speed corresponding to 1.2 ml min^{-1}, with a servospeed regulator; the tubing was Technicon black (0.7-mm i.d).

Samples were injected by an injection port [15] consisting of a precisely made rotary valve and a loop with a total volume of 200 μl with a bypass of higher flow resistance (210 cm long, 1.0-mm i.d.). The sample was filled into the valve and loop with a syringe while the carrier solution flowed through the bypass.

The manifold (Fig. 1) was made from polyethylene tubing (0.5-mm and 1.0-mm i.d.) and Lego building blocks [11]. The different connections were made by drilling conical holes in perspex blocks of appropriate size. The second coil and flow-through cell were thermostated at 60°C. A confluence system was used to obtain effective and rapid mixing.

Measuring procedures

For the determination of magnesium and calcium ions as outlined above, the rate of dissociation of the calcium cryptate was increased by using a temperature of 60°C (Fig. 1). The manifold allows the first measurement to

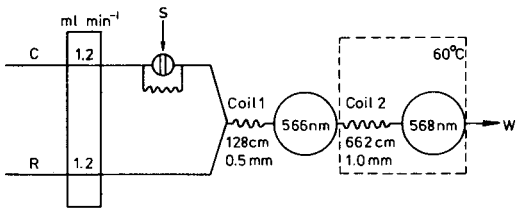


Fig. 1. Flow injection manifold. (S) point of injection (200-μl sample volume); (W) waste The second reaction coil and the flow-through cell are thermostated at 60°C. R represents the reagent stream and C the carrier stream, both at 21°C. All tube lengths are given in cm and the internal diameters in mm (D'_r = 1.3, T' = 19 s and D''_r = 5.2, T'' = 153 s).

be made after complete dissociation of the magnesium cryptate without dissociation of the calcium cryptate. The segment to be analyzed is completely mixed. Thus it is possible, after coil 1, to obtain an absorbance reading which can be directly related to the concentration of magnesium ions.

The absorbance reading obtained after the thermostated coil 2, i.e. after a fixed time interval, corresponds to the dissociation of a constant fraction of calcium cryptate, thus the reaction is carried out under pseudo first-order conditions. The absorbances after coil 2 can be directly related to the concentrations of calcium and magnesium ions and must be corrected for the absorbance corresponding to the magnesium ions in order to obtain the calcium concentration.

Samples and standards were injected in triplicate in all experiments. Calibration graphs were calculated from the absorbances read on the two spectrophotometers by the least-squares method on a Wang 370-2 programmable calculator.

RESULTS AND DISCUSSION

Figure 2 (a—c) shows a photographic reproduction of a routine run with the manifold from Fig. 1. The calibration graphs are linear in the range 2.00×10^{-4}—1.00×10^{-3} M. The total dispersion D'_t was 2.6 and the residence time T' was 19 s after the first measurement position [12]. The total dispersion D''_t and residence time T'' for the whole flow system were 10.4 and 153 s, respectively; with a coloured reagent stream, however, it is more practical to express the dispersion in relation to the reaching stream which has been dispersed in the ratio 1:1, i.e. $D_r = D_t/2$. D_f is the dispersion of the flow arrangement, and D''_f can be calculated from the first and second measurements cf. Figs. 2a and 2b. The value found was 4.1, so that the total dispersion found experimentally agrees well with the theoretical value, $D''_r = D'_r \times D''_f$ [12].

The maximum sampling frequency depends on the sample zone width. A routine run at the theoretical sampling frequency of 80 samples per hour with approximately 1% carryover from one sample to the next [12] is shown in Fig. 3. The rate of analysis in this work was about 40 determinations per hour, but it is unnecessary to reach the base-line between each determination. Excel-

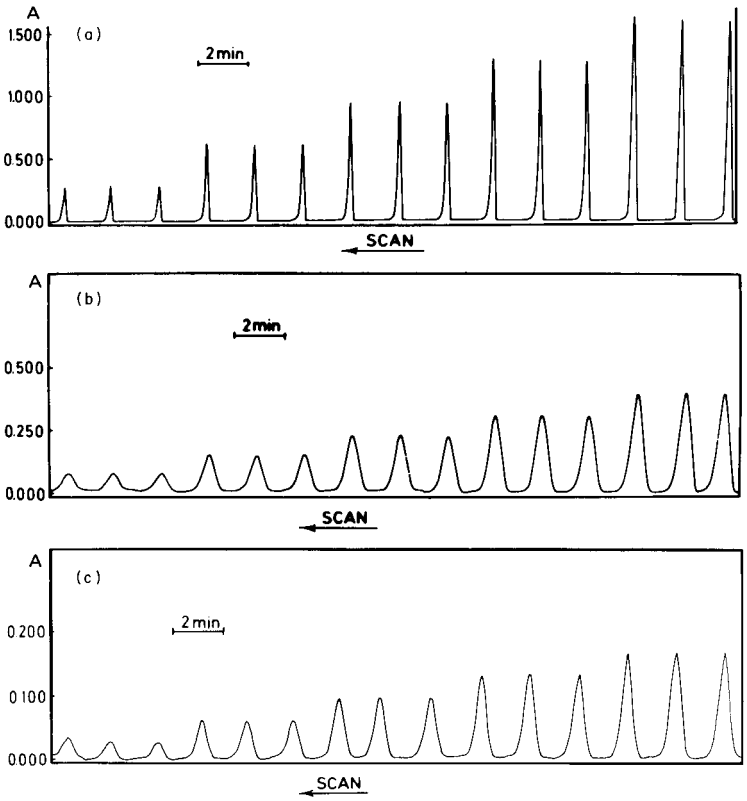


Fig 2. Analysis of standard solutions of magnesium and standard solutions of calcium ions at a rate of approximately 40 determinations per hour with the manifold of Fig. 1. From right to left are shown a set of aqueous magnesium (Fig. 2a and 2b) and calcium standards (Fig. 2c) covering the range 2.00×10^{-4} M—1.00×10^{-3} M $M(NO_3)_2$ with 1.38×10^{-3} M cryptand (2.2.1). All solutions were analyzed in triplicate. (a) Absorbance readings after coil 1; (b) and (c) absorbance readings after coil 2.

lent reproducibility of measurement and high base-line stability were obtained.

Table 1 shows the results obtained for the concentrations of magnesium and calcium nitrates. The relative errors from the correct concentration are also given. The concentrations of magnesium and calcium ions were determined with a satisfactory degree of accuracy except for the sample containing much less magnesium than calcium. The difference between the stability constants of the magnesium and calcium cryptates causes a slight double exchange to occur between these two complex ions. This double exchange is pronounced for the two concentrations mentioned and occurs to an even larger extent when this 1:4 concentration ratio is still smaller.

The cryptand consumption can be further reduced by using the recently developed principle of merging zones [16, 17]. Both the reagent (cryptand)

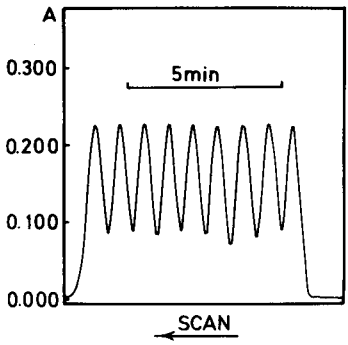


Fig. 3. Absorbance readings after coil 2 (Fig. 1) of a magnesium standard [6.00×10^{-4} M $Mg(NO_3)_2$ with 1.38×10^{-3} M cryptand (2.2.1)] at a rate of 80 samples per hour with approximately 1% carryover from one sample to the next.

TABLE 1

Spectrophotometric determinations of magnesium and calcium ions by differential kinetic analysis with the flow injection system.
(Each result is the average of 3 measurements)

Sample		$[Mg(NO_3)_2]$ found	Relative error	$[Ca(NO_3)_2]$ found	Relative error
$[Mg(NO_3)_2]$ ($\times 10^{-4}$ M)	$[Ca(NO_3)_2]$ ($\times 10^{-4}$ M)	($\times 10^{-4}$ M)	(%)	($\times 10^{-4}$ M)	(%)
2.00	2.00	2.05	2.5	2.08	4.0
4.00	4.00	4.02	0.5	4.16	4.0
2.00	4.00	2.10	5.0	4.10	2.5
4.00	2.00	3.96	−1.0	2.11	5.5
4.00	6.00	4.06	1.5	6.07	1.2
6.00	4.00	6.06	1.0	3.98	−0.5
2.00	8.00	2.16	8.0	8.16	2.0
8.00	2.00	8.02	0.3	2.00	0

and the sample (metal nitrate) zones can be injected into the carrier under controlled conditions. The metal cryptate and the scavenger then merge downstream.

Dispersion of the sample zone will decrease if a flow cell of small volume is used, i.e. the hold-up volume will be less important. The maximum sampling frequency will be increased simultaneously because the linear flow velocity in the flow cell will be higher [12]. Dispersion of the sample zone stops if the carrier stream remains stationary, and is then independent of the residence time [12]. The stopped-flow injection principle with only one flow cell can also be applied to the differential kinetic analysis of the magnesium and calcium ions. The absorbance reading can be related directly to the concentration of the magnesium ions. After the sample zone has been stopped in the

flow cell, the chemical reaction, i.e. dissociation of the calcium (2.2.1) cryptate, can be continuously monitored and used in determining the ions [18].

Cryptand (2.2.1) cannot be used for simultaneous differential kinetic determinations of magnesium, calcium and strontium ions by f.i.a., because the difference between the rates of dissociation of these calcium and strontium cryptates is not sufficiently pronounced. Simultaneous determinations of strontium ions and calcium or magnesium ions are possible with cryptand (2.2.2) [18]. The rate of dissociation of the barium (2.2.1) cryptate is fast, so that magnesium and barium will be determined together when barium is present. The rate of dissociation of the barium (2.2.2) cryptate is, however, too slow for the f.i.a. method to be used for determinations of barium [5, 6].

The authors express their appreciation for fruitful discussions with Professor J. Růžička and Dr. E. H. Hansen, Chemistry Department A, The Technical University of Denmark, and their thanks to Dr. P. Specht of Merck, Denmark, for donating a sample of cryptand (2.2.1).

REFERENCES

1 J. H. Dahl, D. Espersen and A. Jensen, Anal. Chim. Acta, 105 (1979) 327.
2 J. M. Lehn, Struct. Bonding (Berlin), 16 (1973) 1.
3 J. M. Lehn and J. P. Sauvage, J. Am. Chem. Soc., 97 (1975) 6700.
4 V. M. Loyola, R. G. Wilkins and R. Pizer, J. Am. Chem. Soc., 97 (1975) 7382.
5 V. M. Loyola, R. Pizer and R. G. Wilkins, J. Am. Chem. Soc., 99 (1977) 7185.
6 B. G. Cox and H. Schneider, J. Am. Chem. Soc., 99 (1977) 2809.
7 J. B. Pausch and D. W. Margerum, Anal. Chem., 41 (1969) 226.
8 G. Czerlinski, H. Diebler and M. Eigen, Z. Phys. Chem. (Frankfurt am Main), 19 (1959) 246.
9 G. Anderegg, H. Flaschka, R. Sallman and G. Schwarzenbach, Helv. Chim. Acta, 37 (1954) 113.
10 G. Schwarzenbach, Analyst, 80 (1955) 713.
11 J. Růžička and E. H. Hansen, Anal. Chim. Acta, 78 (1975) 145.
12 J. Růžička and E. H. Hansen, Anal. Chim. Acta, 99 (1978) 37.
13 A. I. Cohen and L. Gordon, Anal. Chem., 28 (1956) 1445.
14 B. Nielsen and K. Eberth, Arch. Pharm. Chem. Sci. Ed., 2 (1974) 130.
15 J. Růžička, E. H. Hansen, M. Mosbæk and F. J. Krug, Anal. Chem., 49 (1977) 1858.
16 J. Mindegård, Anal. Chim. Acta, 104 (1979) 185.
17 H. Bergamin F°, E. A. G. Zagatto, F. J. Krug and B. F. Reis, Anal. Chim. Acta, 101 (1978) 17.
18 H. Kagenow and A. Jensen, to be published.

Analytica Chimica Acta, 108 (1979) 249—254
© Elsevier Scientific Publishing Company, Amsterdam — Printed in The Netherlands

FLUORIMETRIC DETERMINATION OF DISSOCIATION CONSTANTS OF ARYL-SUBSTITUTED ALKYLAMMONIUM IONS

STEPHEN G. SCHULMAN* and WILLY J. M. UNDERBERG**

College of Pharmacy, University of Florida, Gainesville, Florida 32610 (U.S.A.)

(Received 2nd February 1979)

SUMMARY

Although the absorption spectra of aryl-substituted alkylammonium ions are insensitive to prototropic dissociation, the fluorescence quantum yields of these ions are often very different from those of their uncharged conjugate bases. This is shown to be the result of different rates of non-radiative deactivation in excited acid and conjugate base and is analytically useful for the determination of pK_a values. The pK_a values of six drugs (procaine, butacaine, benoxinate, cinchonine, propranolol and dibucaine) which are aryl-substituted alkylammonium ions were evaluated fluorimetrically and are presented here.

A great many drugs are, at physiological pH, alkylammonium ions with aryl moieties substituted on the alkyl groups. The dissociation constants (pK_a values) of the alkylammonium groups of these cations may be determined potentiometrically if solubility permits, but are not generally amenable to photometric determination because the electrostatic and electromeric perturbation of the π-electronic system of the aryl substituent, resulting from prototropic dissociation, is insufficient to have an appreciable effect on the absorption spectrum of the chromophore. Fluorescence spectroscopy has only recently been shown to be widely applicable to the determination of the dissociation constants of aromatic acids and bases [1—3]. The principal reason that fluorimetry has not heretofore gained wide acceptance as a means of determining dissociation constants is the interference derived from the imposition of the kinetics of excited-state proton transfer upon the pH dependences of the fluorescences of acid and conjugate base [4]. However, this problem has been shown to be manageable by instrumental and chemical means [1—3]. Because the dissociating group of an aryl-substituted alkylammonium ion is well removed from the aromatic system, changes in the electronic configuration of the aryl moiety accompanying electronic excitation should not alter the prototropic properties of the alkylammonium group; thus the pH dependence of the fluorescence of the arylalkylammonium ion should depend only on the relative fractions of the ammonium ion and its conjugate base directly excited.

**Present address: Farmaceutisch Laboratorium, Rijksuniversiteit Utrecht, Catharijnesingel 60, Utrecht, The Netherlands.

Although fluorescence is similar in origin to electronic absorption, there is good reason to expect that the fluorescence spectrum of an arylalkylammonium ion may well differ in intensity from that of the corresponding amine. The spectral position and intensity of an absorption band are determined, respectively, by the separation of the energy levels and the spatial overlap of the occupied and unoccupied orbitals of the aromatic ring involved in the electronic transition giving rise to the spectral band of interest. Since in an aryl-substituted alkylammonium ion the ammonium group is several atoms removed from the aromatic ring, the electrical perturbation of the electronic orbitals and states of the aryl group accompanying dissociation is minimal. The spectral position of a fluorescence band also depends on the separation of electronic states involved in the transition and accordingly would not be expected to be very different in the amine from that in the ammonium ion. The intensity of fluorescence is, however, governed by the rates of processes competing with fluorescence for the deactivation of the lowest excited singlet state. These competitive processes include internal conversion and intersystem crossing to the triplet state. Internal conversion in condensed media is particularly sensitive to solvation of the excited molecule and freedom of vibrational motion of substituents on the aromatic fluorophore. It was felt that if the solvation or the density of vibrational states of an aryl-substituted alkylammonium ion would be sufficiently different from those of the corresponding amine, the quantum yield and hence the fluorescence intensity of the ammonium ion might be sufficiently different from that of the amine to make the determination of the dissociation constant of the former feasible.

EXPERIMENTAL

Reagents

Dibucaine (Pfaltz and Bauer, Inc., Stamford, CT), procaine hydrochloride, butacaine sulfate (Winthrop Laboratories, New York), benoxinate hydrochloride (Dorsey Laboratories, Lincoln, NE), propranolol hydrochloride (Ayerst Laboratories, New York), cinchonine sulfate (Amend Drug, New York) and procainamide hydrochloride (E. R. Squibb and Sons, New York) were purified by recrystallization from 95% ethanol. A sample of dibucaine was converted to the hydrochloride with hydrochloric acid in ethanol, and samples of the other drugs were converted to their respective free base forms by neutralization with dilute sodium hydroxide in ethanol. The ethanol was evaporated and the free bases separated from sodium sulfate or sodium chloride by dissolution and reclamation from chloroform.

Spectroquality acetonitrile and ethanol (Matheson, Coleman and Bell) and distilled deionized water were employed as solvents.

Apparatus and procedures

Absorption spectra were taken on a Beckman DB-GT spectrophotometer. Fluorescence spectra were taken on a Perkin-Elmer MPF-2A fluorescence

spectrophotometer whose monochromators were calibrated against the xenon line emission spectrum. Total luminescence spectra were taken at 77 K in a cryogenic sample compartment in the fluorimeter. Fluorescence decay times were measured on a TRW decay-time fluorimeter interfaced with a Tektronix model 556 dual beam oscilloscope.

For the fluorimetric titrations, 2.00 ml of drug solution, in a silica cell, was titrated with microliter quantities of dilute sodium hydroxide or perchloric acid solution. The total volume change in each titration was less than 25 μl and only in the case of butacaine did the ionic strength reach 0.01. Volume corrections were therefore deemed unnecessary. The temperature was maintained at 25 ± 1°C throughout by means of a thermostated cell compartment with a circulating water bath.

Calculations

Dissociation constants were calculated, each from eight points in the appropriate fluorimetric pH titration. Relative quantum yields of fluorescence of the cations and free amines were calculated from the ratios of the fluorescence intensities at the maxima to the absorbances at the exciting wavelengths. The absorbances at the exciting wavelengths were made <0.02 to insure the linearity of the fluorescence signal to within 5%.

Dissociation constants were calculated from the fluorescence intensity, F, at the analytical emission wavelength at any given pH

$$F = F^0_{BH^+}([BH^+]/C_B) + (F^0_B[B]/C_B) \quad (1)$$

where $F^0_{BH^+}$ and F^0_B are the fluorescence intensities of the isolated arylalkylammonium ion, BH^+ (at the low pH extreme of the titration) and the isolated arylalkylamine, B (at the high pH extreme of the titration), respectively; $[BH^+]$ and $[B]$ are the equilibrium concentrations of BH^+ and B, respectively, at the pH at which F is measured, and C_B is the formal concentration of the analyte. The dissociation constant, K_a, is related to C_B, $[BH^+]$ and $[B]$ by the equations $[BH^+] = C_B[H^+]/([H^+] + K_a)$ and $[B] = C_BK_a/([H^+] + K_a)$, where $[H^+]$ is the hydronium ion concentration at the pH where F is measured. Combination of these three equations and subsequent rearrangement yields $K_a = [H^+](F^0_{BH^+} - F)/(F - F^0_B)$ or $pK_a = pH - \log[(F^0_{BH^+} - F)/(F - F^0_B)]$.

RESULTS

The long-wavelength absorption and fluorescence maxima of the drugs studied are presented in Table 1. In all cases the spectral maxima of the cations are either identical or nearly identical to the corresponding spectra of the neutral molecules. The quantum yields of fluorescence of the cations and neutral molecules, however, are generally quite different as reflected in their non-unity ratios (Table 2). Only in the case of procainamide was the intensity of the emission of BH^+ so close to that of B, in water, that pK_a could not be calculated from the pH dependence of the fluorescence. The pK_a values of the other

TABLE 1

Long-wavelength absorption (λ_a) and fluorescence (λ_f) maxima of the singly protonated cations (BH^+) and neutral amines (B) derived from procaine, butacaine, benoxinate, procainamide, cinchonine, propranolol and dibucaine in water, ethanol and acetonitrile

Drug	Solvent	BH^+		B	
		λ_a (nm)	λ_f (nm)	λ_a (nm)	λ_f (nm)
Procaine	Water	292	352	288	352
	Ethanol	296	334	296	333
	Acetonitrile	294	334	288	332
Butacaine	Water	280	354	277	354
	Ethanol	301	344	297	343
	Acetonitrile	290	333	287	331
Benoxinate	Water	310	375	307	369
	Ethanol	314	362	308	361
	Acetonitrile	310	354	304	347
Procainamide	Water	280	356	276	356
	Ethanol	294	350	285	345
	Acetonitrile	287	342	276	334
Cinchonine	Water	317	379	317	379
	Ethanol	317	339	317	339
	Acetonitrile	317	347	317	351
Propranolol	Water	322	327	322	326
	Ethanol	322	323	322	323
	Acetonitrile	322	327	322	327
Dibucaine	Water	330	408	330	398
	Ethanol	332	393	330	382
	Acetonitrile	329	397	328	386

drugs, along with the wavelengths of excitation and the analytical emission wavelengths, are presented in Table 3. In each case, the precision and accuracy obtained here is equal to, or superior to, those for values already in the literature (Table 3), all of which were obtained potentiometrically [5—8].

Although it was possible to determine the pK_a of singly protonated cinchonine in this study, surprisingly and unfortunately, it was not possible to do the same for its diastereomer cinchonidine because the fluorescence of the latter was too weak to be analytically useful.

In order to investigate the origin of the differences between the quantum yields of fluorescence of the arylalkylammonium ions and the corresponding arylalkylamines, the fluorescence spectrum of each species in absolute ethanol (which freezes to a clear glass) frozen to 77 K in liquid nitrogen and the fluorescence decay time of each species in absolute ethanol at room temperature were measured.

In rigid ethanol, the fluorescence intensities of each arylammonium ion and conjugate base were found to be essentially identical. This indicates that the differences between the quantum yields of fluorescence of each conjugate

TABLE 2

Ratios of the fluorescence efficiencies ($\phi^0_{BH^+}/\phi^0_B$) of the cations and neutral amines derived from procaine, butacaine, benoxinate, procainamide, cinchonine, propranolol and dibucaine in water, ethanol and acetonitrile. Also presented are the fluorescence decay times $\tau^0_{BH^+}$ and τ^0_B and their ratios, measured in ethanol at 298 K.

Drug	Solvent	$\phi^0_{BH^+}/\phi^0_B$	$\tau^0_{BH^+}$ (ns)	τ^0_B (ns)	$\tau^0_{BH^+}/\tau^0_B$
Procaine	Water	0.65 ± 0.05			
	Ethanol	0.71 ± 0.05	1.9 ± 0.1	2.9 ± 0.2	0.66 ± 0.06
	Acetonitrile	1.7 ± 0.1			
Butacaine	Water	0.70 ± 0.05			
	Ethanol	0.75 ± 0.05	2.5 ± 0.1	2.7 ± 0.1	0.93 ± 0.05
	Acetonitrile	1.20 ± 0.09			
Benoxinate	Water	0.60 ± 0.04			
	Ethanol	0.50 ± 0.04	<1.7	<1.7	—
	Acetonitrile	0.77 ± 0.05			
Procainamide	Water	1.0 ± 0.1			
	Ethanol	0.74 ± 0.05	—	—	—
	Acetonitrile	0.80 ± 0.06			
Cinchonine	Water	3.3 ± 0.2			
	Ethanol	1.0 ± 0.1	<1.7	<1.7	—
	Acetonitrile	0.24 ± 0.02			
Propranolol	Water	3.0 ± 0.2			
	Ethanol	0.80 ± 0.06	16.0 ± 0.5	20.5 ± 0.4	0.78 ± 0.06
	Acetonitrile	4.0 ± 0.3			
Dibucaine	Water	6.8 ± 0.5			
	Ethanol	7.0 ± 0.5	6.8 ± 0.2	<1.7	>4
	Acetonitrile	6.9 ± 0.5			

acid—base pair in fluid solution do not originate in the ground-state equilibrium structure and solvent cage of each, but rather occur as the result of relaxational processes occurring after absorption and before, or contemporaneously with, radiative decay.

Table 2 shows that the ratio of the fluorescence decay times, where calculable for acid and conjugate base, are equal or nearly equal to the ratio of the quantum yields of fluorescence of the same acid and conjugate base in each case. Because the absolute quantum yield and the fluorescence decay time of BH^+ are related by $\phi^0_{BH^+} = k_{BH^+}\tau^0_{BH^+}$ and those of B are related by $\phi^0_B = k_B\,\tau^0_B$ (where k_{BH^+} and k_B are the rate constants for fluorescence of BH^+ and B, respectively), the equivalence of $\phi^0_{BH^+}/\phi^0_B$ and $\tau^0_{BH^+}/\tau^0_B$ indicates that $k_{BH^+} = k_B$. This is of consequence here, because the rate constant for fluorescence is related to the probability of emissive transition in much the same way that molar absorptivity is related to the probability of absorptive transition [9]. The magnitude of the molar absorptivity depends on the overlap of orbitals involved in the electronic transition which is in turn related to the equilibrium geometry of the molecule in its ground electronic state [10]. The magnitude of the rate constant for fluorescence depends on the overlap of orbitals which

TABLE 3

Dissociation constants (pK_a) of singly protonated procaine, butacaine, benoxinate, cinchonine propranolol and dibucaine (a) determined fluorimetrically (this work) and (b) taken from the literature where possible. Also presented are the excitation (λ_e) and emission (λ_f) wavelengths employed in the fluorimetric pK_a determinations.

	pK_a (a)	pK_a (b)	Concn. of drug titrated (M)	λ_e (nm)	λ_f (nm)
Procaine	8.89 ± 0.04	8.85 [5]	8.1×10^{-6}	289	352
Butacaine	10.37 ± 0.04	—	8.8×10^{-6}	260	354
Benoxinate	8.80 ± 0.05	—	9.0×10^{-6}	304	369
Cinchonine	8.08 ± 0.03	8.15 [5] 8.5 [6]	2.7×10^{-5}	300	379
Propranolol	9.09 ± 0.06	9.45 [7]	7.5×10^{-6}	290	327
Dibucaine	8.11 ± 0.04	8.3 [8]	1.1×10^{-5}	312	408

is governed by the equilibrium geometry of the molecule in its lowest excited singlet state [10]. The equivalence of k_{BH^+} and k_B indicates that the difference in fluorescence efficiency between BH^+ and B in ethanol (and probably in the other solvents as well) is not appreciably due to differences between their equilibrium excited-state geometries but rather to differences between the rates of the various non-radiative processes (e.g., internal conversion, intersystem crossing) which deactivate BH^+ and B in their respective lowest excited singlet states. This suggests that the dependence of $\phi^0_{BH^+}/\phi^0_B$ on the solvent (Table 2) is derived from some combination of the differences between the efficiencies of internal conversion of excited B and BH^+ (involving vibrational energy transfer to the solvent), and between the efficiencies of intersystem crossing in B and BH^+ resulting from the influence of the solvent on the relative separation of the $^1n, \pi^*$ and $^1\pi, \pi^*$ states (as well as between these states and the lowest triplet states). It is possible that the occurrence of intramolecular hydrogen bonds in BH^+ but not in B (or vice versa) may account for the difference in non-radiative deactivation rates between excited BH^+ and B. This should prove an interesting area for further research.

REFERENCES

1 L. S. Rosenberg, G. Lam, C. Groh and S. G. Schulman, Anal. Chim. Acta, 106 (1979) 81.
2 L. S. Rosenberg, J. Simons and S. G. Schulman, Talanta, in press.
3 W. J. M. Underberg and S. G. Schulman, Anal. Chim. Acta, 105 (1979) 311.
4 S. G. Schulman, in E. L. Wehry (Ed.), Modern Fluorescence Spectroscopy, Vol. 2, Plenum, New York, 1976, p. 239.
5 E. L. Parrott, Pharmaceutical Technology, Fundamental Pharmaceutics, Burgess, Minneapolis, 1970, p. 220.
6 I. M. Kolthoff, Biochem Z., 162 (1925) 289.
7 G. S. Avery (Ed.), Drug Treatment, Publishing Sciences Group, Littleton, Mass., 1976, p. 890.
8 J. D. Martucci and S. G. Schulman, Anal. Chim. Acta, 77 (1975) 317.
9 N. J. Turro, Molecular Photochemistry, Benjamin, New York, 1967, p. 48.
10 T. C. Werner, in E. L. Wehry (Ed.), Modern Fluorescence Spectroscopy, Vol. 2, Plenum, New York, 1976, p. 277.

Analytica Chimica Acta, 108 (1979) 255—260
© Elsevier Scientific Publishing Company, Amsterdam — Printed in The Netherlands

A SPECIFIC SPECTROPHOTOMETRIC DETERMINATION OF OZONE IN AIR IN THE PRESENCE OF SULFUR DIOXIDE AND NITROGEN OXIDES

RANDLE S. COLLARD** and WILLIAM A. PRYOR*

Department of Chemistry, Louisiana State University, Baton Rouge, Louisiana 70803 (U.S.A.)

(Received 14th December 1978)

SUMMARY

A sensitive, specific spectrophotometric method for the determination of ozone in air by the ozonolysis of 1,1-di-phenylethylene (DPE) is described. The yield of formaldehyde from the ozonolysis of several terminal olefins was determined, and DPE was found to give the highest yield, 90%. The method was checked against the EPA iodimetric method, and gives a consistent yield of formaldehyde over the ozone range 0.05—5.00 $\mu g\ g^{-1}$ of air. As sulfur dioxide is used as a reagent, its presence in air does not interfere. Interference by nitrogen oxides and other free radical oxidants is prevented by the addition of mesitol (2,4,6-trimethylphenol). Formaldehyde in air interferes, but can be determined by using the method with DPE omitted from the sampling train, and so accounted for. In the procedure, formaldehyde is determined by the reverse of the West—Gaeke method for sulfur dioxide.

Ozone is a reactive and toxic species [1], and its accurate determination at the ppm-level has proved exceedingly difficult. Determinations have been based on ozonolysis [2—4] chemiluminescence [5—7], u.v. photometry [8], and various redox techniques [9, 10] including iodimetry [5, 11, 12]. The iodimetric methods have enjoyed wide use despite the controversy concerning their stoichiometry; indeed, until recently superseded by a u.v. photometric method [8], one of them [5] served as the EPA-approved reference standard method. Unfortunately, most methods for ozone, including iodimetry, are subject to interference from oxidants, reductants, and free radical initiators present in polluted air, such as peracids, peresters, and nitrogen oxides. However, one of the ozonolysis methods — that of West and co-workers [3] — is not subject to interference from sulfur dioxide or free radical oxidants. Additionally, the immediate separation of the formaldehyde produced in the ozonolysis step ensures that there are no side-reactions.

The present paper describes a study of the mechanism of the ozonolysis with the aim of developing a more sensitive procedure than the West method while retaining its inherent advantages. The reaction of 1,1-diphenylethylene (DPE) with ozone is used to produce formaldehyde in 90% yield (a 34% improvement

**Present address: Dow Chemical Louisiana Division, Plaquemine, LA 70784 (U.S.A.).

over the West method); the formaldehyde is determined by a slight modification of the method of Lyles et al. [13]. Interference by free radical oxidants is prevented by the addition of a free radical inhibitor, mesitol (2,4,6-trimethyl phenol).

EXPERIMENTAL

Apparatus

Midget impingers (No. 7531 Code 10) and fritted bubblers (No. 7530 Code 05) were obtained from Ace Glass, Inc. Flowmeters (No. 448-118; Fisher and Porter Corp.) were accurate to within 2% of full scale. A Beckman DU spectrophotometer equipped with a Gilford power supply, sample changer, and detector was used.

Reagents

Water was distilled, deionized, and boiled.

Sodium tetrachloromercurate(II) solution. Dissolve 27.2 g of mercury(II) chloride and 11.6 g of sodium chloride in water to make exactly 1 l of solution.

Sodium dichlorosulfitomercurate(II) solution. Dissolve 0.25 g of sodium sulfite in 25 ml of the sodium tetrachloromercurate(II) solution; prepare daily.

Pararosaniline solution. Add 0.448 g of pararosaniline acetate (Eastman Kodak 1376) to 67.5 ml of concentrated hydrochloric acid and dilute to exactly 250 ml with water.

1,1-Diphenylethylene. Purify DPE (Aldrich Chemical Co. D20,680-6) by passing an inert gas such as nitrogen through the impinger containing DPE for 10 min before placing the impinger in the trapping train; this process removes any formaldehyde present.

Ozone generation and trapping

Tank breathing air was passed over activated charcoal and silica gel and then into the ozone generating chamber (Fig. 1). The ozone concentration delivered was adjusted by varying the number of lamps and the voltage with a variable voltage transformer. The ozonized air was passed from the generating chamber to the sampling apparatus through an all-glass system (with ground-glass or Tygon butt joints) and then to the flowmeter. For iodimetric determinations, the ozonized air was trapped in a fritted bubbler containing 10 ml of the usual iodide-containing phosphate buffer [5]. For the olefin method, the ozone trapping apparatus consisted of a midget impinger containing 1 ml of olefin followed by a fritted bubbler containing 10 ml of water. Flow through the system was varied between 250 and 2000 ml min^{-1}.

Analytical procedure

Pass air containing ozone through a sampling apparatus consisting of an impinger containing 1 ml of the purified DPE and 0.1 ml of mesitol solution

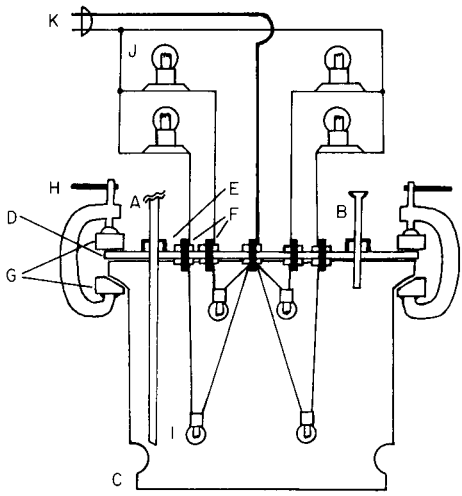


Fig. 1. Ozone generating apparatus. (A) Purified air inlet; (B) ozonized air outlet (to trapping apparatus); (C) 250-cm desiccator base; (D) 0.25-in Teflon plate; (E) 0.375-in. Kelvar fittings; (F) threaded brass rods (with nuts on each end); (G) aluminum rings (lower ring beveled to fit desiccator); (H) C clamps (8 equidistant around rings); (I) 4-W germicidal lamps (GE 4W-S11); (J) 40-W ballast lamps; (K) a.c. line to variable transformer.

(20% w/v in xylene), and pass the effluent through a fritted bubbler containing water to trap the formaldehyde. After a suitable sampling time, remove the fritted bubbler, and quantitatively transfer its contents to a 25-ml volumetric flask. Add 1 ml of the sodium dichlorosulfitomercurate(II) solution, mix, and add 2 ml of the pararosaniline reagent. Mix thoroughly, and dilute to the mark with water. Between 22 and 28 min after addition of the pararosaniline reagent, determine the absorbance at 580 nm vs. a water reference. Subtract the absorbance of a blank obtained by sampling the air stream without the DPE impinger in the sampling train, the determine the formaldehyde concentration by comparison to a calibration curve. The equation for calculation of the ozone concentration is: $O_3\ (\mu l\ l^{-1}) = \mu g\ CH_2O \times 22.4/30.02 \times 0.90 \times V$, where V is the volume of air (in l) corrected to NTP.

RESULTS AND DISCUSSION

Ozone standardization and formaldehyde determination

Ozone concentrations were determined by the neutral buffered iodimetric method described in the Federal Register [5] which was the EPA-approved reference method when this work was started.

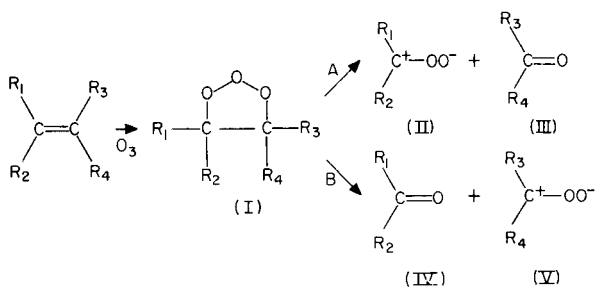
Formaldehyde was determined by a slight modification of the reverse West—Gaeke method developed by Lyles et al. [13]; formaldehyde reacts with sulfur dioxide to form an adduct that reacts with pararosaniline to produce a dye with an absorbance maximum between 540 and 580 nm, depending on pH

[14]. Investigating the West—Gaeke method for sulfur dioxide, Saltzman et al. [15] found that temperature affected the rate and extent of color development. The present study showed that maximum absorbance was attained for the modified Lyles method 22—28 min after addition of pararosaniline, when the temperature was 20—25°C; the absorbance increased steeply during the first 15 min and decreased gradually after 30 min. If determinations are carried out at other temperatures, the time required to achieve maximum absorbance must be established, and timing and temperature must be kept the same throughout the series.

The formaldehyde determination was calibrated with aliquots of commercial formaldehyde solution, which had been standardized by the sulfite method [16].

Factors affecting the direction of cleavage of a terminal ozonide

An ozonide, I, produced by the reaction of ozone with an olefin, ionizes to give a zwitterion and a carbonyl fragment as follows:



The yield of formaldehyde from the decomposition of a terminal olefin (Scheme A, $R_3 = R_4 = H$) is enhanced by R_1 and R_2 substituents that stabilize the zwitterion, II. Thus, the yield of formaldehyde from the ozonolysis of a tertiary terminal olefin (2,2,4-trimethylpentene) is 99% [17], while the yield from a secondary terminal olefin (eugenol) is only 67% [3]. In the ozonolysis of aromatic terminal olefins (styrene derivatives) [18, 19], the yield of formaldehyde is greatest when electron-donating substituents are present on the aromatic ring. For example, Fliszar and Granger [19] found a 60% yield of formaldehyde from styrene and an 80% yield from *p*-methoxystyrene. The ozonolysis of several commercially available styrenoid molecules was therefore investigated in an attempt to obtain a higher yield of formaldehyde than the 67% obtained from eugenol by the West procedure.

Since several of these compounds were solids, three solvents were examined for their suitability. 1-Hexanol produced highly colored blanks. Hexadecane, which was used in early experiments, proved sufficiently unreactive and nonvolatile; however, aromatic olefins were not very soluble in it, and it was later replaced by xylene. Xylene proved an excellent solvent, being unreactive, nonvolatile, and almost completely miscible with all of the aromatic olefins.

TABLE 1

Yields of formaldehyde from the ozonolysis of several terminal olefins
(Trapping for 10 min at a flow rate of 500 ml min^{-1} and an ozone concentration of 6.25 $\mu g\ g^{-1}$, as determined by the neutral buffered iodimetric method.)

Terminal olefin	(In solvent)	CH_2O yield (mol CH_2O/mol O_3)[a]
Vinyl anisole	1.0 (hexadecane)	0.23
Eugenol	1.0 (hexadecane)	0.22
	neat	0.67 [3]
Vinyl naphthalene	0.1 (hexadecane)	0.26
	0.5 (hexadecane)	0.29
	1.0 (hexadecane)	0.52
	10.0 (xylene)[b]	0.60
DPE	neat	0.90

[a]Each value is an average of at least three determinations, ozone being determined by the neutral iodimetric method and formaldehyde by the Lyles method.
[b]Highest convenient concentration.

Determination of the yield of formaldehyde from several terminal olefins

Yields of formaldehyde are given in Table 1 for several substrates. The greatest yield was obtained from neat DPE, hence the stoichiometry was further investigated.

The yield of formaldehyde from DPE was investigated for ozone concentrations in the range 0—9 $\mu g\ g^{-1}$ of air. It was found to be constant, with an average value of 0.90 ± 0.02, for the range 0.05—5.00 $\mu g\ g^{-1}$, above which negative deviations occurred.

Interferences

Although other ozonolysis methods are subject to interference from free radical initiators such as nitrogen oxides and organic peroxides [2, 20], the eugenol method developed by West and co-workers [3] is not. Since many free radical inhibitors, such as BHT (butylated hydroxytoluene) and BHA (butylated hydroxyanisole) are phenols, it was thought that the phenolic group of eugenol protected the olefin from reaction with free radical initiators.

When neat DPE was used, it was found that nitrogen dioxide levels as low as 0.2 $\mu g\ g^{-1}$ interfered with the ozone determination method, and that the stoichiometry of the reaction with nitrogen dioxide was 2.5:1.0 formaldehyde: NO_2, indicating that a chain mechanism was occurring. When mesitol was added as inhibitor, levels as low as 1% protected against 2 $\mu g\ NO_2\ g^{-1}$ and a level of 2% protected against 5 $\mu g\ NO_2\ g^{-1}$; levels as high as 20% did not interfere in the DPE method. The addition of 2% mesitol was, therefore, incorporated into the procedure to eliminate interferences from free radical initiators.

As in the method of West and co-workers [3], sulfur dioxide does not interfere, for it is used as a reagent.

Formaldehyde is the only species which was found to interfere with the DPE method for ozone. The formaldehyde contained in the air stream is trapped in the same way as the formaldehyde produced from ozonolysis. This interference can easily be accounted for, however, simply by determining a blank without the impinger in the sampling train and subtracting this blank from the amount of formaldehyde determined by the method. This procedure simultaneously accounts for solvent blank, and can also be used, with a separate solvent blank determination, to measure the amount of formaldehyde in the air stream, i.e., the method of Lyles et al. [13].

This work was carried out under grant HL-16029, from the National Institute of Health.

REFERENCES

1 H. E. Stokinger, Arch. Environ. Health, 10 (1965) 719.
2 H. A. Bravo and J. P. Lodge, Jr., Anal. Chem., 36 (1964) 671.
3 S. L. Sachdev, J. P. Lodge, Jr. and P. W. West, Anal. Chim. Acta, 58 (1972) 141.
4 T. R. Hauser and D. W. Bradley, Anal. Chem., 38 (1966) 1529.
5 Fed. Regis., 36, 228 (Nov. 25, 1971) 22392.
6 D. H. Stedman, E. E. Darby, F. Stuhl and H. Niki, J. Air Pollut. Control Assoc., 22 (1972) 260.
7 R. K. Stevens and A. E. O'Keeffe, Anal. Chem., 42 (1970) 143A.
8 Fed. Regis., 43 (June 22, 1978) 26971.
9 I. R. Cohen, T. C. Purcell and A. P. Altshuller, Environ. Sci. Technol., 1 (1967) 247.
10 J. J. Buffalini, Environ. Sci. Technol., 2 (1968) 703.
11 N. Gilbert and B. E. Saltzman, Anal. Chem., 31 (1959) 1914.
12 D. L. Flamm, Environ. Sci. Technol., 11 (1977) 978.
13 G. R. Lyles, F. B. Dowling and V. J. Blanchard, J. Air Pollut. Control Assoc., 15 (1965) 106.
14 R. V. Nauman, P. W. West and F. Tron, Anal. Chem., 32 (1960) 1307.
15 F. P. Scaringelli, B. E. Saltzman and S. A. Frey, Anal. Chem., 39 (1967) 1709.
16 J. F. Walker, Formaldehyde, 3rd edn., ACS Monograph Series, Reinhold, New York, 1964, pp. 485—8.
17 J. Knights and E. S. Waight, J. Chem. Soc., (1955) 2830.
18 S. Fliszar, Tetrahedron. Lett., 49 (1966) 6083.
19 S. Fliszar and M. Granger, J. Am. Chem. Soc., 91 (1969) 3330.
20 T. R. Hauser and D. W. Bradley, Anal. Chem., 39 (1967) 1184.
21 B. E. Saltzman, Environ. Health Ser. Air Pollution, Selected Methods for the Measurement of Air Pollutants, U.S. HEW, PHS No. 99-AP-11, May 1965.

Analytica Chimica Acta, 108 (1979) 261—266
© Elsevier Scientific Publishing Company, Amsterdam — Printed in The Netherlands

SENSITIVE FLOTATION—SPECTROPHOTOMETRIC DETERMINATION OF RHODIUM WITH MALACHITE GREEN

Z. MARCZENKO* and E. KOWALCZYK

Department of Analytical Chemistry, Technical University, Warsaw (Poland)

(Received 8th January 1979)

SUMMARY

Two sensitive, precise spectrophotometric methods for the determination of rhodium with malachite green are proposed. The anionic rhodium complex with tin(II) chloride yields an ion associate with malachite green; on shaking the solution (in 6.5 M HCl) with benzene, the sparingly soluble ion associate (rhodium: malachite green = 1:2) precipitates at the phase boundary. The precipitate is dissolved in a mixture of acetone and water (3 + 1). The molar absorptivity is 1.44×10^5 l mol^{-1} cm^{-1} at 627 nm. When test solutions (0.65 M HCl) are shaken with diisopropyl ether, an ion associate of a different composition is formed (rhodium:malachite green = 1:5) and the molar absorptivity is 3.4×10^5 l mol^{-1} cm^{-1}. Platinum, palladium and iridium interfere except in small amounts.

Although many spectrophotometric determinations of rhodium have been reported recently, there are few sensitive methods for this metal [1—3]. In a search for such methods, the formation of sparingly soluble compounds of the anionic rhodium complex with tin(II) chloride and some basic dyes has been examined. Such ion-pair complexes with malachite green have been used to develop a flotation—spectrophotometric method for the determination of rhodium. Many highly sensitive, flotation—spectrophotometric methods for determination of various elements have been developed recently [4]. On shaking the aqueous solution with a slightly polar solvent the sparingly soluble ion associate precipitates at the phase boundary. After separation of the liquid phases, the precipitate can be dissolved in a polar solvent for absorbance measurements.

EXPERIMENTAL

Reagents and apparatus

A standard solution of rhodium (1 mg Rh ml^{-1}) was prepared by dissolving 1.3660 g of $RhCl_3 \cdot 4H_2O$ in 500 ml of 1 M hydrochloric acid. Working solutions were prepared by diluting this solution with 1 M hydrochloric acid. Standard solutions of platinum, palladium, iridium and tin were prepared as described previously [3].

Malachite green was purified by recrystallization. The preparation was dissolved in ethanol and precipitated by adding a four-fold volume of diethyl

ether. A 0.001 M solution was obtained by dissolving a suitable amount of this crystalline dye in water.

A SPEKOL spectrocolorimeter and a SPECORD spectrophotometer were used with 1-cm cells.

Procedures

With benzene. To the test solution in 1 M HCl, containing less than 20 μg of rhodium, add 1 ml of tin(II) chloride solution (20% w/v in 1 M HCl) and sufficient hydrochloric acid to give ca. 10 ml of a solution 4 M in HCl. Heat the solution on a boiling water bath for 10 min. Allow to cool and transfer the solution to a separatory funnel. Rinse with 8 ml of 11 M HCl into the separatory funnel. Add 2 ml of malachite green solution and 5 ml of benzene. Shake the solution for 15 s. Allow the phases to separate; carefully remove the aqueous and organic phases. Dissolve the precipitate adhering to the walls of the separatory funnel in a mixture of acetone and water (3 + 1). Transfer the solution to a 25-ml volumetric flask, dilute to the mark with the mixture of acetone and water, and measure the absorbance at 627 nm against a reagent blank prepared in the same manner.

With diisopropyl ether. To the test solution in 1 M HCl, containing less than 8 μg of rhodium, add 0.6 ml of the tin(II) chloride solution and sufficient hydrochloric acid to give 10 ml of final solution 1.4 M in HCl. Heat the solution on a boiling water bath for 10 min. Allow the solution to cool and transfer it to a separatory funnel. Add 4 ml of malachite green solution and 5 ml of diisopropyl ether. Proceed as described above for the method with benzene.

RESULTS AND DISCUSSION

In hydrochloric acid media, rhodium yields anionic complexes with tin(II) which differ in colour and composition depending on the applied conditions (tin concentration, acidity and temperature). The red complex (λ_{max} 475 nm) has been the basis of a relatively insensitive spectrophotometric method for rhodium ($\epsilon = 3.7 \times 10^3$ l mol^{-1} cm^{-1}) [5—9].

The possibility of formation of extractable ion associates with basic dyes (e.g., malachite green, brilliant green, crystal violet, rhodamine B, safranine T, and Nile blue A) was examined. The studies were carried out in 6, 2 and 0.5 M HCl solutions with benzene, toluene, carbon tetrachloride, chloroform and diisopropyl ether. In all these cases, the extraction of the rhodium ion associate was accompanied by high blank values. In the majority of the systems examined, the sparingly soluble ion associate precipitated at the phase boundary. The precipitate was readily isolated from the aqueous and organic phases, because it adhered to the walls of the separatory funnel. Systems involving malachite green (and the related brilliant green) with benzene (in 6 M HCl) and diisopropyl ether (in ca. 0.6 M HCl) as flotation agents proved to be the most satisfactory.

The precipitate of the ion associate was readily soluble in ethanol, methanol or acetone; acetone—water mixtures were selected because the absorbances of these solutions did not change with time. The isolated precipitate gives the

basis for a flotation—spectrophotometric method for the determination of rhodium; blank values are relatively low. The absorption spectrum of the ion associate in aqueous acetone is identical with that of the pure dye in this solvent.

Benzene—6 M hydrochloric acid system

Preliminary experiments showed that flotation of the ion associate precipitate could be achieved with benzene from relatively concentrated (6 M) hydrochloric acid solution. The optimum conditions were established as follows. The absorbance of the solution of the precipitate in aqueous acetone was higher if the anionic complex of rhodium was formed by heating the solution containing rhodium, tin(II) chloride and hydrochloric acid for several minutes. Changes in hydrochloric acid concentration (in the range 1—7 M) did not affect the final result. A concentration of 4 M HCl was chosen. When the tin(II) chloride concentration was varied in the range 0.02—0.2 M, the absorbances did not change when more than 0.1 M tin(II) chloride was added. A study of the dependence of the absorbance of the final aqueous acetone solution on the acidity of the medium during flotation with benzene showed that the separation of rhodium as the ion associate was practically quantitative in the range 6.5—7.5 M HCl.

The absorbance attained a maximum and did not change with time when the molar ratio of malachite green to rhodium exceeded 10. At such dye concentrations, the absorbance of the blank was negligible (ca. 0.02). The blank value increased slightly with increasing concentration of the dye in solution.

The flotation of the ion associate precipitate occurred rapidly — shaking for 15 s was sufficient. Changes in the ratio of the phase volumes had no effect on the final result.

Beer's law was obeyed over the concentration range 0—1 μg Rh ml^{-1}. The molar absorptivity (ϵ) was 1.44×10^5 l mol^{-1} cm^{-1}. The precision of the results obtained for three rhodium concentrations is shown in Table 1.

The effects of iridium, platinum and palladium on the determination of rhodium are of importance. Ruthenium and osmium can easily be separated from other platinum metals by distilling their tetroxides [1, 2]. Results for the determination of rhodium in the presence of platinum, palladium and

TABLE 1

Precision of the results for the determination of rhodium with malachite green (n = 5)

Rhodium added (μg)	Rhodium found (μg)	Standard deviation (μg)	Relative standard deviation (%)	Confidence limits (probability level 0.95)
2.50	2.51	0.051	2.05	2.51 ± 0.06
10.00	9.96	0.136	1.36	9.96 ± 0.17
17.50	17.56	0.235	1.34	17.56 ± 0.29

TABLE 2

Effects of platinum, palladium and iridium on the determination of rhodium with malachite green

Metal	Metal-to-rhodium ratio (w/w)	Rhodium recovery (%)		
		Flotation with benzene		Flotation with diisopropyl ether
		With pre-heating	Without pre-heating	
Pt	0.5	—	126, 130	—
	1	124, 123	157, 155	138
Pd	1	101, 100	102, 102	198
	2	—	108, 106	—
	2.5	104, 106	—	—
	5	113, 114	137, 133	—
Ir	0.5	—	—	106
	1	107	100, 102	111
	2	117, 117	102	119
	5		106, 106	—
	8		114, 116	—
	10		116, 118	—

iridium are shown in Table 2. Palladium did not interfere at concentrations less than that of rhodium; platinum and iridium each influenced the determination if present in amounts equal to that of rhodium.

The molar ratio of rhodium to malachite green is 1:2 (Fig. 1). The same ratio was obtained from a comparison of the absorbances of the solution of the rhodium ion associate with those of corresponding amounts of the pure dye. A known amount of rhodium was converted to the ion associate which was then separated and dissolved in the mixture of water and acetone. A solution containing a two-fold molar excess of the dye with respect to rhodium

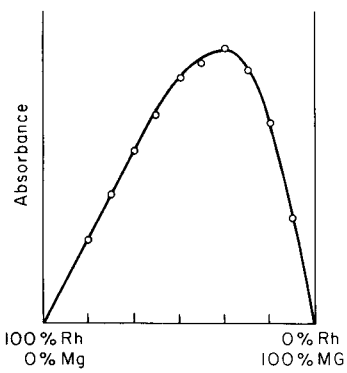


Fig. 1. Determination of the ratio of rhodium to malachite green in the ion associate by the isomolar series method.

was prepared separately. The absorbances of both the solutions were practically identical.

The tin content of the isolated ion associate was determined. The results showed poor reproducibility, but it was possible to estimate the molar ratio of rhodium to tin as 1:(5—6).

Diisopropyl ether—0.6 M hydrochloric acid system

From dilute hydrochloric acid (ca. 0.6 M HCl), there was no flotation of the rhodium ion associate with benzene. Quantitative isolation of the rhodium compound at the phase boundary could be obtained on shaking the aqueous solution with diisopropyl ether. The rhodium ion associate separated in this way differed in colour and composition from that described above.

In this variant of the method, the absorbance increased with increase in the concentration of tin(II) chloride. Within an intermediate concentration range (0.06—0.09 M) the absorbances were practically identical. Further increase in the $SnCl_2$ concentration caused increasing absorbance but the reproducibility of the results decreased progressively (Fig. 2). This is presumably caused by precipitation (above a certain $SnCl_2$ concentration) of an ion associate containing only an anionic tin complex and malachite green.

A study of the effect of the hydrochloric acid concentration on the flotation separation of the rhodium ion associate during shaking with diisopropyl ether showed that quantitative separation was obtained in the range 0.6—0.75 M HCl.

The dependence of the absorbance of the aqueous acetone solution on the molar excess of the dye is shown in Fig. 3. Above a 50-fold molar excess of malachite green with respect to rhodium the increase was very small. Curve 2 (Fig. 3) shows the absorbance of the blank. As with benzene, shaking the aqueous phase with diisopropyl ether for 15 s was sufficient.

The absorbance was directly proportional to the rhodium concentration in the range 0—0.2 μg Rh ml^{-1}. As the rhodium concentration increased a small

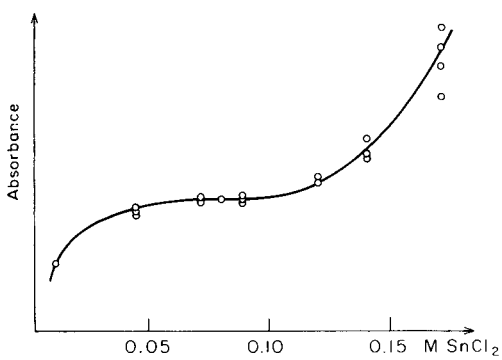


Fig. 2. Dependence of the absorbance of the aqueous acetone solution of the ion associate on the concentration of tin(II) chloride (flotation with diisopropyl ether).

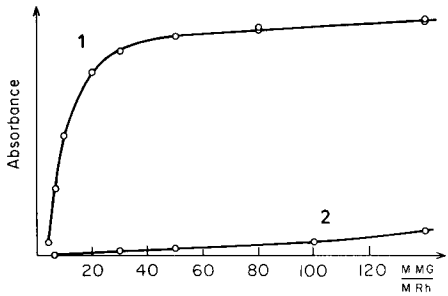


Fig. 3. Dependence of the absorbance of the aqueous acetone solution of the ion associate on the excess of dye (flotation with diisopropyl ether). Curve 1, absorbance of the solutions measured against the blank; curve 2, absorbance of the blank measured against water.

positive deviation from Beer's law was observed; the molar absorptivity was 3.4×10^5 l mol^{-1} cm^{-1} at 627 nm. The precision of the results was poorer than that for flotation with benzene. Table 2 shows that the influence of other platinum metals on the rhodium determination was higher than when benzene was used.

Attempts to determine the composition of the ion associate (without using the isomolar series method) indicated that the molar ratio of rhodium to malachite green was 1:5. Results for the rhodium-to-tin ratio in the separated ion associate were not reliable, but the ratio of tin to rhodium atoms was lower than in the compound obtained in the benzene variant of the method.

Studies of the application of the bromide [10—12] and iodide [13] systems to the flotation—spectrophotometric determination of rhodium with malachite green showed that only the bromide system was suitable; this method provided results similar to these obtained for the chloride system. The iodide system was completely unsuitable; the results were irreproducible.

REFERENCES

1 F. E. Beamish and J. C. Van Loon, Analytical Chemistry of the Noble Metals, Pergamon, Oxford, 1972.
2 S. I. Ginzburg, Analiticheskaya Khimiya Platinovykh Metallov, Izd. Nauka, Moskva, 1972.
3 Z. Marczenko, Spectrophotometric Determination of Elements, Ellis Horwood, Chichester, 1976.
4 Z. Marczenko, Mikrochim. Acta, (1977 II) 651.
5 A. D. Maynes and W. A. McBryde, Analyst, 72 (1954) 230.
6 G. H. Ayres, B. L. Tuffly and I. S. Forrester, Anal. Chem., 27 (1955) 1742.
7 I. F. Young, R. D. Gillard and G. Wilkinson, J. Chem. Soc., (1964) 5176.
8 S. K. Kalinin, K. P. Stolarov and G. A. Yakovleva, Zh. Anal. Khim., 25 (1970) 132.
9 S. K. Kalinin and G. A. Yakovleva, Zh. Anal. Khim., 25 (1970) 332.
10 S. S. Berman and R. Ironside, Can. J. Chem., 36 (1958) 1151.
11 F. Pantani and G. Piccardi, Anal. Chim. Acta, 22 (1960) 231.
12 G. G. Tertipis and F. E. Beamish, Anal. Chem., 34 (1962) 623.
13 E. W. Berg and H. L. Youmans, Anal. Chim. Acta, 25 (1961) 366.

Analytica Chimica Acta, 108 (1979) 267—275
© Elsevier Scientific Publishing Company, Amsterdam — Printed in The Netherlands

A STUDY OF THE DIRECT SPECTROPHOTOMETRIC DETERMINATION OF URANIUM(VI) IN TRIALKYLAMINE EXTRACTS WITH 2-(5-BROMO-2-PYRIDYLAZO)-5-DIETHYLAMINOPHENOL

SAMUEL J. LYLE* and MASSOUD TAMIZI

The Chemical Laboratories, The University of Kent at Canterbury, Kent CT2 7NH (Gt. Britain)

(Received 20th November 1978)

SUMMARY

A straightforward spectrophotometric method is described for the determination of uranium(VI) in trialkylamine sulphate extracts in kerosene diluent; 2-(5-bromo-2-pyridylazo)-5-diethylaminophenol (Br-PADAP) is used for colour formation without resort to back-extraction into an aqueous phase. The method provides good tolerance to sulphate ion and rapid colour development and appears to be free from interference when applied to extracts from uranium sulphate leach liquors.

Uranium leached from low-grade ore sources by sulphuric acid can be recovered by liquid—liquid distribution into an immiscible solvent system containing long-chain trialkylamines [1—3]. Usually the amines have normal hydrocarbon chains containing 8, 10 or 12 carbon atoms each and, as in the Purlex process operated in South Africa [4], a 5% (v/v) solution in kerosene is employed; additionally the kerosene is made 2% (v/v) in isodecanol or another long-chain alcohol to prevent third-phase formation and to help keep the amine salts in solution.

In order to control the extraction process, it is desirable to be able to analyse the kerosene phase for uranium content. Titrimetric [5], polarographic [6], x-ray fluorimetric [7] and spectrophotometric [8] methods which can be used for this purpose have been described.

Although not the most convenient, absorption spectrophotometry in the near u.v. and visible range of the spectrum is a technique readily available in most laboratories. Further, it is a convenient method of measurement in an automatic analytical procedure such as can be devised with the Technicon AutoAnalyzer. There is a case, therefore, for further exploration of potential spectrophotometric methods which will be applicable directly to the extract rather than those requiring the return of the uranium to an aqueous phase.

The azo dye, 2-(5-bromo-2-pyridylazo)-5-diethylaminophenol (Br-PADAP), has been shown to be a sensitive reagent for the determination of uranium in ores and waters [9]. Subsequently, Pakalns and McAllister observed [8] that

it gave a colour reaction with uranium(VI) in a single-phase system prepared by adding dimethylformamide to water, kerosene, ethanol and the trialkylamine. This was made the basis of a direct spectrophotometric determination of uranium in amine extracts. While the tolerance to many ions is good, unfortunately sulphate ion can interfere seriously. In the work described here, Br-PADAP has been re-examined with different reaction conditions for uranium determination in amine extracts, and an alternative method is presented. Likely interfering species and some aspects of the reaction system are considered.

EXPERIMENTAL

Reagents

Tri-n-octylamine (TOA; practical grade; Koch-Light Ltd.), kerosene (laboratory-reagent grade; Hopkin and Williams Ltd.), octan-2-ol (laboratory-reagent grade; Fisons Scientific Apparatus Ltd.), industrial methylated spirit (IMS 74.OP; Charles Tennant Co. (London) Ltd.) and $UO_2(NO_3)_2 \cdot 6H_2O$ (analytical-reagent grade; Fisons Scientific Apparatus Ltd.) were used as supplied. Br-PADAP (m.p 157—158°C; 97% purity; Aldrich Chemical Co.) was used as received. The chemical substances used in the interference tests were of analytical-reagent grade.

Apparatus

Absorbance measurements were made with a Hitachi Perkin-Elmer spectrophotometer model 139 and 1-cm matched glass cells. Spectra were measured with a Unicam SP800 recording instrument. An EIL pH meter, model 23A, equipped with glass and saturated calomel electrodes, was used to check the pH of aqueous phases.

Solutions

Br-PADAP. Dissolve the dye (0.0600 g) in methylated spirit (700 ml). Add TOA (20 ml) and, after mixing, distilled water (40 ml). Make up to 1 l with IMS.

Uranium-free solvent. Mix TOA (50 ml) and octan-2-ol (20 ml) and dilute to 1 l with kerosene. Convert to the amine sulphate by shaking with 1 M H_2SO_4 (100 ml); 1 ml of this solution contains about 7 mg of sulphate.

Uranium-containing solvent. Prepare a standard stock solution containing 4—5 g of U(VI) per litre from uranium-free solvent and solid $UO_2(NO_3)_2 \cdot 6H_2$(Addition of a further 10 ml of octan-2-ol per litre prevents the formation of a second organic phase ('third phase formation') at this stage. For calibration purposes, this latter solution is diluted with uranium-free solvent.

Recommended procedure

Transfer by pipette 1 or 2 ml of the amine extract containing up to 215 μg U(VI) and not more than 14 mg SO_4^{2-} into a 50-ml volumetric flask.

Adjust the volume to 50 ml with the Br-PADAP solution and mix well. Measure the absorbance at 575 nm with the Br-PADAP solution as reference. The colour develops within 5 min and remains stable for at least 12 h.

It should be noted that if 3 ml of amine extract containing about 21 mg of sulphate is taken, a 6% error arises in determining 88 μg U. The temperature coefficient at 575 nm is small; the absorbance decreases by less than 3% from 20°C to 30°C. If required, the uranium-loaded amine extract may be diluted with IMS.

Study of interfering ions

Method 1. An aqueous phase, 0.5 M in Na_2SO_4 adjusted to pH 1.5 with sulphuric acid and containing 2.22 g U(VI) l^{-1} and the potentially interfering ion, was equilibrated with one third of its volume of the uranium-free solvent. A portion of the extract was diluted with IMS by a factor of 50; 1 ml was then treated as described under Recommended Procedure and the absorbance measured. The absorbance was compared with that obtained in the absence of the ion under test.

Method 2. In this method the direct effect of extraneous ions on the colour reaction was tested by introducing them into the colour-forming medium through the water component of the Br-PADAP solution. Uranium-containing solvent was diluted with IMS made 2% (v/v) in TOA and 4% (v/v) in water so that 2 ml contained 88 μg uranium. In the test, 2 ml of this diluted uranium solution was mixed with the calculated volume of Br-PADAP solution containing the potentially interfering ion and the mixture was diluted to 50 ml with Br-PADAP solution

RESULTS AND DISCUSSION

Pakalns and McAllister [8] examined butyl cellosolve and dioxane as solvents compatible with water and kerosene. The former solvent appeared to prevent colour development between Br-PADAP and uranium(VI), and the latter was marginally inferior to dimethylformamide, the solvent they adopted to maintain homogeneity of the reaction mixture. In the course of the present work, Br-PADAP in xylene was found to prevent colour development when added to uranium-containing amine extracts. Further tests suggested that ethanol was a satisfactory diluent and consequently industrial methylated spirit, IMS, was used. It is compatible with a reasonable amount of amine extract, probably among the best solvents for the dye, and relatively cheap. The absorption spectra of ethanolic Br-PADAP and uranium(VI)—Br-PADAP solutions prepared as described in the Experimental section are recorded in Fig. 1. Since a large molar ratio of dye to uranium is maintained in the recommended procedure, measuring the absorbance of the uranium-containing coloured solution at 575 nm against Br-PADAP solution will involve negligible interference from changes in the dye concentration.

From Fig. 2, it is evident that the uranium—Br-PADAP reaction is sensitive

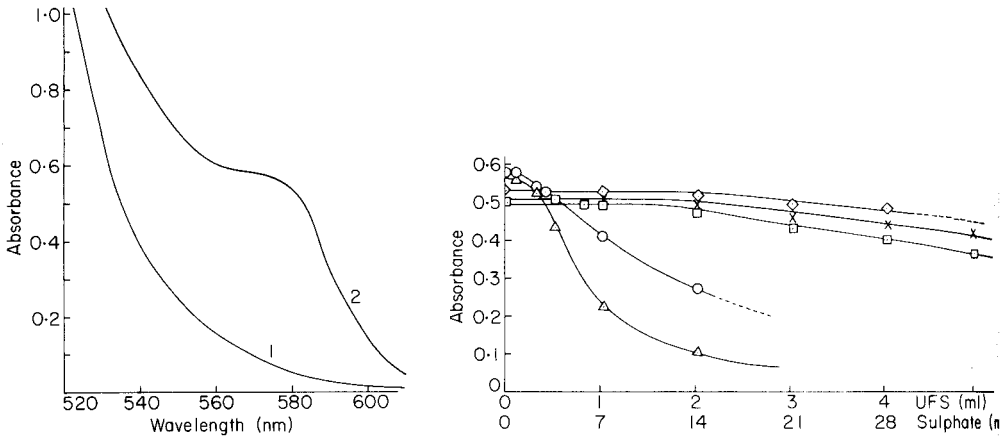


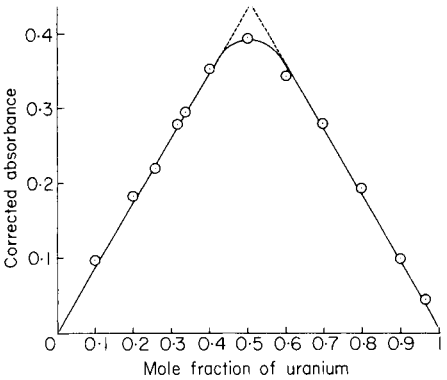
Fig. 1. Absorption spectra, with water as reference, for (1) 1.71 × 10^{-4} M Br-PADAP solution (see Experimental for composition); (2) uranyl—Br-PADAP complex at a uranium concentration of 7.47 × 10^{-6} M in the same solvent.

Fig. 2. Absorbance at 575 nm plotted as a function of uranium-free solvent (UFS) and of sulphate concentration in 50 ml of various colour-forming media (reference water). The solutions contained 7.38 × 10^{-6} M uranium and 1.48—1.65 × 10^{-4} M Br-PADAP (20—22-fold excess) (△) IMS; (⊙) 10% v/v water in IMS; (□) 2% TOA in IMS; (×) 2% TOA, 2% water in IMS; (◇) 2% TOA, 4% water in IMS. Broken lines indicate phase splitting.

to the sulphate salt of the amine. While water improves tolerance to this substance, the presence of 2% TOA(v/v) in the reaction mixture is more effective. Although water encourages 'phase splitting', it increases the absorbance of the uranium—Br-PADAP reaction mixture (Fig. 2), hence the compromise choice of an IMS medium 2% (v/v) in TOA and 4% (v/v) in water for colour development. When the recommended procedure is used, a rectilinear relation between absorbance and uranium content is observed for 0—215 μg of uranium per 50 ml of coloured solution. For a 1-ml aliquot sample, this corresponds to just over 0.2 g U l^{-1} in the amine extract. Maximum uranium loading of the amine sulphate phase in the extraction process is usually set at 5 g U l^{-1}. A considerable dilution may thus be necessary before colour development. This is best done with IMS, although uranium-free solvent could also be used. The molar absorptivity calculated on the basis of the uranium present is 6.58 × 10^4 l mol^{-1} cm^{-1}. This is a little lower than that reported by Pakalns and McAllister [8] (7.03 × 10^4 l mol^{-1} cm^{-1}). Full colour development occurs in less than 5 min from mixing; this compares favourably with the 20 min required in the Pakalns and McAllister method.

Job and mole ratio plots

The Job (Fig. 3) and mole ratio (Fig. 4) studies both point to the colour arising from a 1:1 uranium(VI): Br-PADAP reaction product. This is similar to the ratio found by Johnson and Florence [10] for (1 + 1) water—ethanol



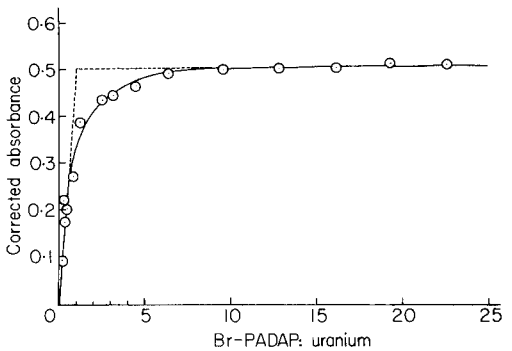


Fig. 3. Corrected absorbance at 575 nm plotted against mole fraction of uranium in the colour-developing medium with water as reference substance. The uranium and Br-PADAP concentrations were each 3.73×10^{-5} M.

Fig. 4. Plot of absorbance at 575 nm (water as reference) corrected for absorbance of free dye against mole ratio of Br-PADAP : uranium. The uranium concentration was 8.9×10^{-6} M.

solutions at pH 4.1. At pH 7.6 in a similar solvent mixture, Johnson and Florence concluded that a different, relatively unstable coloured complex of composition UO_2(Br-PADAP)OH was formed from which fluoride ion displaced hydroxyl to give UO_2(Br-PADAP)F. Fluoride may, therefore prevent polymerization of partially hydrolysed uranyl ion. The nature of the coloured complex at pH 4.1 is uncertain. However, with the IMS-based solvent, it was observed that the presence of relatively large molar ratios of amine sulphate to uranium inhibits colour development (Fig. 2) and that in the absence of sulphate colour development is sluggish and the ultimate colour intensity is impaired. For example, in the determination of 90 μg of uranium, mole ratios of sulphate to uranium in the range 4—400 gave colour development in less than 5 min without impairment of the intensity. Thus it is likely that sulphate plays an important role in the coloured uranium—Br-PADAP complex. This may be somewhat similar to that played by fluoride ion in the study by Johnson and Florence [10] but on present evidence it would be merely specula tive to suggest molecular species and structures.

Interference study

To be of practical value in the context of uranium recovery, the method requires evaluation with respect to the effect of extraneous substances present in aqueous sulphate leach liquors (see Table 1) and to changes in operating conditions in the uranium recovery plant. In studies of potential interferences, an immediate problem arises because the process involves phase transfer followed by colour development in the non-aqueous phase. On the one hand, a study in which the 'interfering' species is added to the aqueous phase requires

TABLE 1

The composition of various leach liquors

A. Synthetic Marysvale liquor [12] used to test the Amex process [3], U.S.A.
B. Used in the development of the Purlex process [4], S. Africa.
C. El Sherana leach liquor [13], Australia.
D. Milliken leach liquor [14], Canada.
E. Morro do Agostinho leach liquor [11], Brazil.
(Ion concentrations are given in $g\ l^{-1}$.)

	A	B	C	D	E
pH	0.85	1.5	1.3	—	—
U	1.25	0.25	1	0.6—1.0	0.5—1.5
Fe(II)	—	1.8	0.2	1.8—3.0	—
Fe(III)	5.8	0.5	0.2	0.3—0.4	—
Fe (total)	—	2.3	0.4	2.1—3.4	4-8
Al	3.3	—	—	0.60—1.14	—
SO_4^{2-}	50	16—20	10	13.7—19.2	—
PO_4^{3-}	2.0	—	0.27	0.3—0.4	—
F^-	1.7	—	—	—	—
Cl^-	—	—	0.2	0.22—0.27	—
SiO_2	—	1.5	0.2	—	—
SCN^-	—	0.02	—	—	—
Mo	—	—	—	0.001	0.2—0.6
V	—	—	—	—	0.02—0.06
Cu	—	—	0.05	—	—
Th	—	—	—	0.08—0.18	—
Ti	—	—	—	0.03—0.04	—
Zr	—	—	—	—	$\leqslant 1$

a knowledge of its partition ratio and its effect on uranium extraction; neither will be known with much reliability unless measured under the specified conditions. On the other hand, direct introduction of the species to the non-aqueous phase ignores inter-species effects in the aqueous phase and the partial selectivity derived from the phase transfer of the uranium. In the present work, the ions most likely to be encountered were examined by both procedures where considered appropriate.

While the composition of an aqueous leach liquor will vary with the mineral source, only a few ions are likely to merit special attention. Thus alkali and alkaline earth metals, magnesium, aluminium, zinc, vanadium(IV), chromium(III), manganese(II), iron(II), cobalt(II), nickel, copper(II) and thorium are not extracted to any significant extent from approximately 0.5 M Na_2SO_4 at pH 1.5. Iron(III) is partially extracted but uranium(VI) can displace it from tertiary alkylamine sulphate extracts [12]. Molybdenum(VI) is extracted at least as efficiently as uranium(VI). Floh et al. [11] reported that vanadium(V) initially enhances uranium(VI) extraction but when the concentration increases

sufficiently it assumes an inhibiting role. Vanadium(V) is extracted appreciably from aqueous sulphate media only at pH values higher than 1.5 [12]. Nitrate, chloride, fluoride and phosphate inhibit uranium extraction, the first three severely, the last only slightly or not at all if aluminium or iron(III) is present [12]. Thiocyanate, although less likely to be present except in ore sources derived from gold workings [4], can reduce uranium extraction.

The effects of commonly encountered potential interferences introduced into the aqueous phase before extraction are summarized in Fig. 5. Iron(II) and aluminium to about 3 g l^{-1} each, and phosphate and vanadium to about 1 g l^{-1} each in the aqueous phase could be tolerated for monitoring and extraction purposes. Beyond such concentrations, vandium(V) but not the others has a strongly depressing effect on colour intensity. Nitrate, fluoride, molybdenum(VI) and thiocyanate appear to interfere appreciably. Furthermore, phase splitting occurs with vanadium(V), molybdenum(VI) and thiocyanate at sufficiently high aqueous concentrations.

Results obtained after direct introduction of potentially interfering ions into the non-aqueous phase are collected in Fig. 6. Molybdenum(VI) at concentrations up to at least 40 mg l^{-1} in the medium used for colour development does not interfere. For a 1-ml aliquot of extract, this represents a molybdenum content of 2 g l^{-1}. Thus even if molybdenum extraction from the aqueous phase were virtually complete and allowing for a phase volume ratio (aqueous/organic) of 4, a concentration of 0.5 g l^{-1} in the aqueous phase should not interfere with colour development. Since uranium loading in plant operation will be in the region of several gram per litre of amine extract, a further dilution of the extract by a factor in the range 10—25 will be required before colour development. Thus the method should cope easily with liquors containing molybdenum at g l^{-1} concentrations (Table 1). Application of a similar argument to the fluoride data from Fig. 6 would lead to a similar conclusion. From Fig. 6, it is seen that either nitrate or thiocyanate could be tolerated up to 2 mg l^{-1} in the presence of moderate amounts (ca. 100 μg) of uranium in the colour-forming medium. Calculations on the above lines indicate that nitrate or thiocyanate would not interfere with the procedure for uranium. However, both would interfere with the partition of uranium from the liquor into the amine phase and along with chloride would have to be kept low in the liquor. Indeed, the evidence available suggests that the gross interferences shown in Fig. 5 arise largely from inhibition of uranium partition into the amine phase. Iron(III) forms a red colour with Br-PADAP under the conditions of reaction used here and thus makes a positive contribution to the absorbance at 575 nm. It can be tolerated to about 2 mg l^{-1} in the colour-forming medium; the organic/aqueous partition ratio is very small [3] (of the order of 0.01) so that a considerable concentration (several g l^{-1}) could be tolerated in the original aqueous leach liquor. Introduction of iron(III) or fluoride directly into the Br-PADAP system results in turbidity above the concentrations specified in Fig. 6; with fluoride, the effect on absorbance at 575 nm appears to be slight. Vanadium(V) reacts more slowly than uranium(VI)

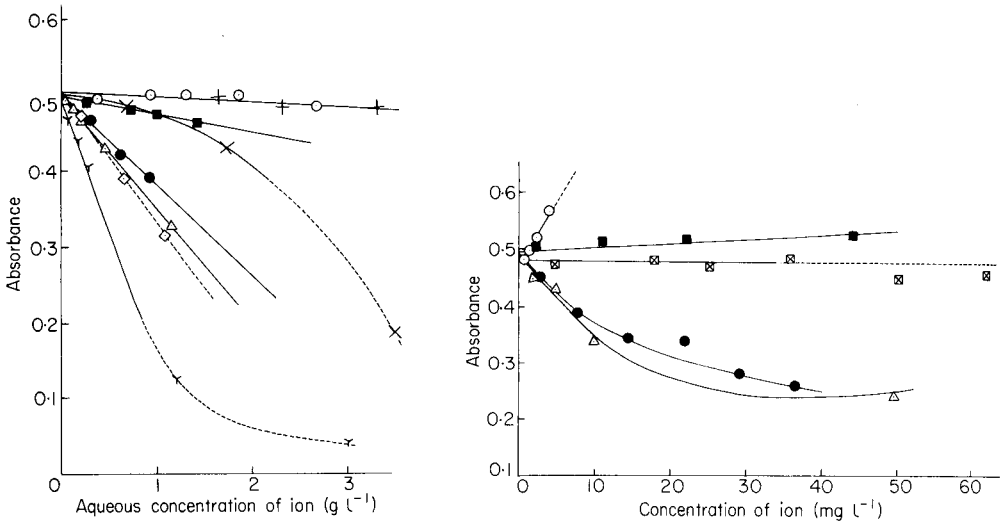


Fig. 5. Absorbance at 575 nm plotted against aqueous conentration of 'interfering' ion (see Method 1 under Experimental). (+) Al(III) added as $AlK(SO_4)_2 \cdot 12H_2O$; (○) Fe(II) as $FeSO_4 \cdot 7H_2O$; (■) PO_4^{3-} as $K_3PO_4 \cdot H_2O$; (×) V(V) as NH_4VO_3; (●) NO_3^- as $NaNO_3$; (△) F^- as KF; (◇) Mo(VI) as $(NH_4)_6Mo_7O_{24} \cdot 4H_2O$ and (Y), SCN^- as KSCN. A broken line indicates appearance of a third phase.

Fig. 6. Direct influence of potentially interfering ions (see Method 2). Absorbance plotted against concentration of ion in the colour-forming medium. Uranium concentration, 7.4×10^{-6} M. (○) Fe(III) added as $NH_4Fe(SO_4)_2 \cdot 12H_2O$; (■) Mo(VI) as $(NH_4)_6Mo_7O_{24} \cdot 4H_2O$; (⊠) F^- as NaF; (●) SCN^- as KSCN; (△) NO_3^- as $NaNO_3$. A broken line indicates a region of turbidity.

with Br-PADAP in the colour-forming medium, but inhibits the uranium reaction with Br-PADAP.

Table 1 provides a summary of the contents of leach liquors reported in the literature. If the recommended method is used, none of the elements listed at the concentrations given should interfere with the determination of uranium in the amine extract, with the possible exception of iron(III) in the Amex process [3] operated on Marysvale liquor [12]. In the event of large amounts of iron(III) and vanadium(V) being present, reduction to iron(II) and vanadium(IV) respectively, would be desirable; this could be accomplished with ascorbic acid.

When compared with the method of Pakalns and McAllister, the method recommended here represents a considerable simplification in terms of solvents, reagents and reaction conditions used. Tolerance to sulphate and phase splitting are improved and colour development is much more rapid (from 20 min to less than 5 min). The simplicity of the method and rapid colour development should make this procedure suitable for the development of an automatic method in, for example, an AutoAnalyzer.

REFERENCES

1 Processing of Low-grade Uranium Ores, Int. At. Energy Agency Panel Proc., I.A.E.A., Vienna 1966. Publ. 1967.
2 The Recovery of Uranium, Proc. Symp., São Paulo, 1970, I.A.E.A., Vienna, 1971.
3 C. F. Coleman, K. B. Brown, J. G. Moore and D. J. Crouse, Ind. Eng. Chem., 50 (1958) 1756.
4 T. H. Tunley and A. Faure, The Purlex Process — A Description of the Pilot Plant Leading to the Use of the Process in South Africa, Nat. Inst. for Metallurgy, Johannesburg, 1968.
5 W. Davies and W. Gray, Talanta 11 (1964) 1203.
6 S. J. Lyle, I. T. Salvadori and A. G. Stevenson, Anal. Chim. Acta, 62 (1972) 431.
7 A. Faure, private communication.
8 P. Pakalns and B. R. McAllister, Anal. Chim. Acta, 62 (1972) 207.
9 D. A. Johnson and T. M. Florence, Anal. Chim. Acta, 53 (1971) 73.
10 D. A. Johnson and T. M. Florence, Talanta 22 (1975) 253.
11 B. Floh, A. Abrão and E. Calmon Costa, in ref. 2, p. 267.
12 W. D. Arnold, K. B. Brown, D. J. Crouse, J. O. Denis and A. D. Kelmers, U.S. At. Energy Doc. ORNL-1959, 1955.
13 A. I. Bellingham, Proc. Australian Inst. Mining and Metallurgy, No. 198 (1961) 85.
14 N. Robb, V. Opratko and L. S. Price, Canadian Mining and Metallurgical Bull., 56 (1963) 476.

Analytica Chimica Acta, 108 (1979) 277—283
© Elsevier Scientific Publishing Company, Amsterdam — Printed in The Netherlands

RAPID SPECTROPHOTOMETRIC DETERMINATION OF PHENOTHIAZINES WITH MOLYBDOPHOSPHORIC ACID

H. SANKE GOWDA*, P. G. RAMAPPA and ANANT N. NAYAK

Department of Post-graduate Studies and Research in Chemistry, University of Mysore, Manasa Gangotri, Mysore 570006 (India)

(Received 8th December 1978)

SUMMARY

A simple and rapid spectrophotometric method for the determination of six phenothiazines can be based on the formation of a coloured compound between molybdophosphoric acid and phenothiazines. The i.r. and e.s.r. spectra of the coloured compounds showed that molybdophosphoric acid oxidizes phenothiazines to a radical cation with which it then forms a coloured compound. The proposed method is employed for the determination of phenothiazines in pharmaceutical preparations. Calibration graphs are linear over ranges of about 100—2000 μg of the phenothiazine.

Phenothiazines are of great importance because of their applications in chemotherapy, dye industry and lubrication. The importance of phenothiazine tranquilizers has prompted many investigators to work out methods for their rapid determination. Many proposed colorimetric methods [1—4] are unsatisfactory for one reason or another. In a comprehensive investigation on analytical methods for phenothiazines, molybdophosphoric acid was found to give a colour reaction with triflupromazine hydrochloride (TPH), trifluperazine hydrochloride (TFP), butaperazine dimaleate (BPDM), profenamine hydrochloride (PFH), mepazine hydrochloride (MH) and perphenazine hydrochloride (PPH). The present paper describes the investigation of these reactions for the rapid spectrophotometric determination of six phenothiazines (Table 1) with molybdophosphoric acid. The method offers the advantages of simplicity, stability and rapidity without the need for extraction or heating.

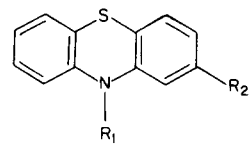
EXPERIMENTAL

Reagents and equipment

Solutions of phenothiazines. Stock solutions of TPH, TFP, PFH, MH and PPH were prepared by dissolving the requisite amount of the samples in doubly distilled water. BPDM solution was prepared in hot water. The stock solutions were standardized gravimetrically [5] and stored in amber bottles in a refrigerator. Working solutions were prepared as required by dilution.

TABLE 1

Phenothiazines studied



Derivative studied	Abbreviation	R_1	R_2
Triflupromazine[a]	TPH	$-CH_2-(CH_2)_2-N(CH_3)_2$	$-CF_3$
Trifluperazine[a]	TFP	$-CH_2-(CH_2)_2-N$(piperazine)$-N-CH_3$	$-CF_3$
Butaperazine[b]	BPDM	$-CH_2-(CH_2)_2-N$(piperazine)$-N-CH_3$	$-C(=O)-(CH_2)_2-CH_3$
Profenamine[a]	PFH	$-CH_2-CH(CH_3)-N(C_2H_5)_2$	$-H$
Mepazine[a]	MH	$-CH_2-$(piperidine)$-N-CH_3$	$-H$
Perphenazine[a]	PPH	$-CH_2-(CH_2)_2-N$(piperazine)$-N-(CH_2)_2OH$	$-Cl$

[a] As hydrochloride. [b] As maleate.

Molybdophosphoric acid solution. A 10% (w/v) solution was made by dissolution of molybdophosphoric acid in hot water with stirring, cooling, filtering and dilution. The solution was checked gravimetrically [6].

All reagents were of analytical quality.

Apparatus. A Beckman Model DB spectrophotometer with stoppered 1-cm silica cells was used for absorbance measurements. A pH meter Model L1-10, Perkin-Elmer model 257 i.r. spectrophotometer and a Varian E-4 X-band e.s.r. spectrometer were also used.

Standard procedure

Transfer an aliquot of the sample solution containing 100—1750 μg of TPH, 125—2875 μg of TFP, 75—1875 μg of BPDM, 100—2125 μg of PFH, 32—1400

of PPH or 100—2125 μg of MH to a 25-ml volumetric flask. Add 10 ml of 10% molybdophosphoric acid solution and dilute to the mark with doubly-distilled water. Mix well and set aside for about 5 min for complete colour development. Measure the absorbance at 510 nm for TPH and TFP; at 525 nm for BPDM, PFH and MH; and at 540 nm for PPH against a corresponding reagent reference solution. Deduce the amount of phenothiazine from the previously prepared calibration graph.

Determination of phenothiazines in pharmaceutical preparations

Grind 20 drug tablets in an agate mortar to a fine powder. Transfer an exactly weighed amount of the powder containing 5—25 mg of the drug to a 100-ml volumetric flask. Dissolve the drug in doubly-distilled water by thorough shaking, and dilute to the mark. Filter the solution. Determine the phenothiazine content in an aliquot of the filtrate by the standard procedure.

For the analysis of injection solutions, transfer the requisite volume of the injection solution to a 100-ml volumetric flask and dilute to the mark with doubly-distilled water. Determine the phenothiazine content in the diluted solution as described above.

RESULTS AND DISCUSSION

Molybdophosphoric acid reacts with TPH, TFP, BPDM, PFH, MH or PPH almost instantaneously in a solution of pH range 0.0—3.1 at room temperature. It oxidizes these phenothiazines to a radical cation which forms a coloured compound with the unreacted molybdophosphoric acid. Maximum intensity of the colour is obtained in 5 min in solutions of pH 0.7—1.7. The coloured solution becomes turbid below pH 0.7 and maximum colour intensity is not obtained above pH 1.7. Hence a medium of pH 1.3, which is readily obtained by mixing solutions of molybdophosphoric acid and the phenothiazine derivative, was selected in further studies.

The absorption spectra of molybdophosphoric acid and its coloured compounds with phenothiazines are shown in Fig. 1. BPDM, PFH and MH form brown compounds with absorption maxima at 525 nm. PPH with a chlorine atom at C-2 shows a bathochromic effect, the wavelength of maximum absorption being shifted to 540 nm. TPH and TFP with CF_3 at C-2 show a hypsochromic effect, λ_{max} being shifted to 510 nm. TPH, TFP, BPDM, PFH, MH and PPH and the reagent have negligible absorbance in this range, thus promoting excellent analytical conditions.

I.r. and e.s.r. spectra

The i.r. spectra of the coloured compounds of molybdophosphoric acid with phenothiazines were measured (KBr discs) in the region 650—4000 cm^{-1}. The R_3NH^+ group combined with halide ion, X^-, in the molecule of many phenothiazines gives rise to a broad band in the 2300—2500 cm^{-1} range [7]. For example, in the case of TPH, a broad band between 2420 and 2610 cm^{-1}

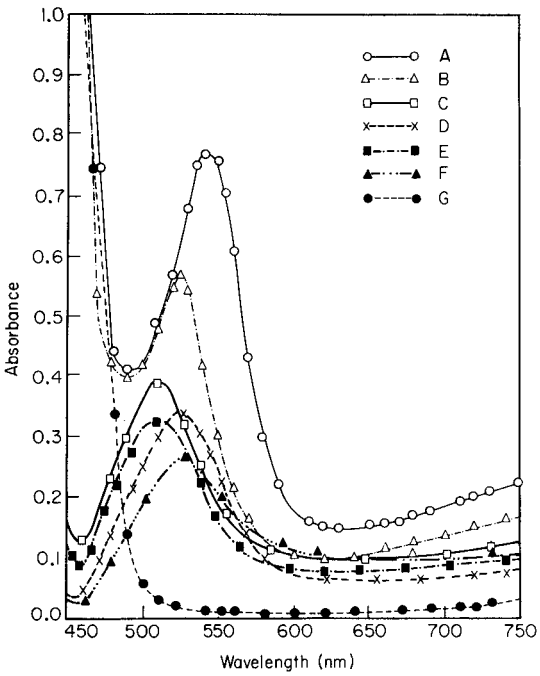


Fig. 1. Absorption spectra of coloured products of (A) PPH; (B) MH; (C) TPH; (D) BPDM; (E) TFP; (F) PFH; (G) molybdophosphoric acid; [molybdophosphoric acid] = 1.772 × 10^{-2} M. [Phenothiazines] = 40 ppm.

was observed in the i.r. spectrum of TPH, corresponding to the $-CH_2-N^+H(CH_3)_2$ group combined with chloride. In the i.r. spectrum of the molybdophosphoric acid—TPH product, however, this band disappeared completely, showing that the nitrogen of the side chain is a reaction site, as is the case with organic bases in general [8]. A band at 2880 cm^{-1} in the i.r. spectrum of TPH corresponds to the heterocyclic nitrogen to which the alkyl group is attached. This peak totally disappeared in the i.r. spectrum of the TPH—molybdophosphoric acid product, showing that this heterocyclic nitrogen is another reaction site. The i.r. spectra of the other phenothiazines and their coloured compounds with molybdophosphoric acid show similar behaviour.

The e.s.r. signals show that free radicals are formed by the oxidizing action of molybdophosphoric acid on the phenothiazine nucleus (Fig. 2). The *g* values calculated from the e.s.r spectra are 2.0071, 2.0047, 2.0047, 2.0059, 2.0053 and 2.0060 for the products of TPH, TFP, BPDM, PFH, MH and PPH, respectively. These values are in close agreement with the *g* value for free electrons (2.0023). It seems probable that the coloured product obtained on treatment of an aqueous solution of the phenothiazine derivative is the molybdophosphate of a cationic radical formed by oxidation. This conclusion is supported by the colour obtained which corresponds to that reported in the literature for free radicals formed by oxidation [9].

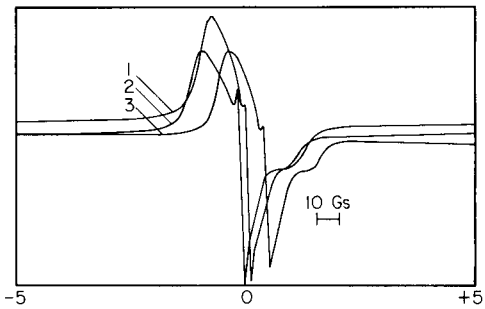


Fig. 2. E.s.r. spectra of phenothiazine—molybdophosphate products (1) BPDM; (2) TFP and (3) TPH. Field set: 3350, 3370 and 3360 G for BPDM, TFP and TPH, respectively. Microwave frequency: 9.395, 9.442 and 9.459 GHz for BPDM, TFP and TPH, respectively.

Effect of experimental variables

The maximum absorbance reading obtained 5 min after mixing of the reactants remained constant for periods of 0.7, 1, 3, 3, 6 and 18 h for PPH, MH, BPDM, PFH, TPH and TFP, respectively. The effect of changes in the concentration of molybdophosphoric acid was studied by measuring the absorbances at the wavelengths recommended in the procedure for solutions containing a fixed concentration of the phenothiazine and varying amounts of molybdophosphoric acid. The rate of formation and colour intensity of the product increased with increasing concentration of molybdophosphoric acid, but the stability of the coloured product decreased. The optimum amount of molybdophosphoric acid was 6—18 ml of 10% solution. A large excess of molybdophosphoric acid scarcely affected the sensitivity, hence 10 ml of 10% solution in a total volume of 25 ml was used in all subsequent work.

The maximum absorbance readings remained constant in the temperature range 5—40°C for TPH, TFP, PFH and MH, and 5—90°C for BPDM and PPH.

Calibration curve, range and sensitivity

The calibration curves were prepared by the standard procedure. Good linear relationships were obtained over the concentration ranges 4—70 ppm of TPH, 5—115 ppm of TFP, 3—75 ppm of BPDM, 4—85 ppm of PFH or MH, and 1.28—56 ppm of PPH. The calibration curve for BPDM did not pass through the origin. The optimum concentration ranges for effective spectrophotometric determinations of TPH, TFP, BPDM, PFH, MH and PPH, evaluated by Ringbom's method [10, 11], are 7—67, 9.5—110, 8—72, 8—80, 7—80 and 5—53 ppm, respectively. For $\log I_0/I = 0.001$, the sensitivities of the reactions calculated from Beer's law data are 101, 122, 111, 155, 71 and 55 ng cm^{-2}, and the corresponding molar absorptivities are 3.85×10^3, 3.93×10^3, 5.06×10^3, 2.19×10^3, 4.87×10^3 and 8.74×10^3 l mol^{-1} cm^{-1} for TPH, TFP, BPDM, PFH, MH and PPH, respectively.

TABLE 2

Effect of diverse ions on the determination of 40 ppm of TPH, 48 ppm of TFP, 32 ppm of BPDM, 40 ppm of PFH, 40 ppm of MH, and 24 ppm of PPH

Ion added	Tolerance limit[a] (ppm)					
	TPH	TFP	BPDM	PFH	MH	PPH
Fluoride	30	20	80	20	20	40
Chloride	200	200	1000	400	400	900
Bromide	400	400	2000	500	320	2000
Iodide	8	8	8	4	8	12
Nitrate	200	200	2000	400	300	1000
Sulphate	200	200	1200	500	200	1000
Sulphite	1.2	8	3	8	8	8
Carbonate	200	800	600	800	800	600
Phosphate	40	200	200	400	800	200
Acetate	40	20	40	200	50	50
Citrate	20	40	40	20	40	60
Formate	40	20	40	40	40	50
Oxalate	60	40	80	100	60	70
Tartrate	20	16	40	20	30	40
Ascorbic acid	0.8	6	2	4	6	2
Dextrose	1200	800	2000	1200	800	2000
Gum acacia	40	16	40	40	20	40
Sodium alginate	80	4	20	8	10	16
Barbitone	1600	1400	2000	200	1200	2000
Alcohol[b]	0.008	0.012	0.016	0.012	0.012	0.02

[a]Amount causing an error of less than 2%. [b]ml ml^{-1}.

TABLE 3

Determination of phenothiazines in pharmaceutical preparations

Tablet or injection	Drug present	Amount of drug		R.s.d. (%)
		Quoted (mg)	Found[a] (mg)	
Tablets				
Siquil[b]	TPH	10	9.95	1.38
Eskazine[c]	TFP	5	4.92	1.79
Eskazine[c]	TFP	1	0.98	1.70
Injections				
Siquil[b]	TPH	10	9.89	1.74
Eskazine[c]	TFP	1	0.97	2.56

[a]Average of ten determinations. [b]Marketed by Squibb, Inc. [c]Marketed by Smith, Kline and French, Ltd.

Effect of concomitants and application to pharmaceutical preparations

The effects of some ions and compounds which often accompany phenothiazines in pharmaceutical products were studied. The colour was developed

and the absorbance was measured as in the standard procedure. The results are summarized in Table 2. The interferences of some substances likely to be present in tablets and injections were also examined. Up to 70 mg of talc, 55 mg of magnesium stearate, 45 mg of starch, 30 mg of reserpine and 20 mg of gelatin did not interfere in the determination of 32 ppm of TPH, TFP, BPDM, PFH, MH or PPH.

The proposed method was successfully applied to the analysis of various pharmaceutical preparations. The results of the assay of tablets and injections presented in Table 3 compare favourably with the quoted values.

The authors thank Rhône-Poulenc, Paris; Smith, Kline and French Ltd., India; May and Baker Ltd., India; and Sarabhai Chemicals, India, for supply of pure phenothiazines. One of the authors (A.N.N.) is grateful to U.G.C., New Delhi, University of Mysore and Government of Karnataka for the award of a teacher fellowship under the U.G.C. Faculty Improvement Programme.

REFERENCES

1 H. Basinska, H. Puzanowska-Tarasiewicz and M. Tarasiewicz, Chem. Anal. (Warsaw), 15 (1970) 405.
2 R. P. Dzhorbenadze, V. S. Bostoganashvili and R. M. Pinyazhko, Soobshch. Akad. Nauk gruz. SSR., 77 (1975) 597; Anal. Abstr., 31 (1976) 264.
3 A. G. Davidson, J. Pharm. Pharmacol., 28 (1976) 795.
4 M. Stan, V. Dorneanu and Gh. Ghimicescu, Talanta, 24 (1977) 140.
5 J. Blazek and V. Mares, Cesk. Farm., 15 (1966) 349.
6 W. A. C. Campen and A. M. J. Sledsens, Analyst, 86 (1961) 467.
7 A. R. Katritzky and A. J. Boulton, Advances in Heterocyclic Chemistry, Volume 9, Academic Press, New York, 1968, p. 338.
8 P. Pascal, Nouveau Traite de Chimie Minerale Tome XIV, Masson, Paris, 1959, p. 914.
9 J. Meunier, B. Viossat, P. Leterrier and P. Douzou, Ann. Pharm. Franc, 25 (1967) 683.
10 A. Ringbom, Fresenius Z. Anal. Chem., 115 (1938) 332.
11 G. H. Ayres, Anal. Chem., 21 (1949) 652.

Analytica Chimica Acta, 108 (1979) 285—291
© Elsevier Scientific Publishing Company, Amsterdam — Printed in The Netherlands

A RE-INVESTIGATION OF PHENOL AS A SPECTROPHOTOMETRIC REAGENT FOR THE DETERMINATION OF NITRATE-NITROGEN

R. R. ELTON-BOTT

27 Regency Drive, Thornlie, Western Australia 6108 (Australia)

(Received 2nd January 1979)

SUMMARY

The advantages of phenol over isomers of dimethylphenol in the determination of nitrate-nitrogen are described. Linear calibration graphs are obtained for the ranges 0—100, 0—400 and 0—20 $\mu g\ ml^{-1}$ for nitrate-nitrogen; these ranges are suitable for analyses of plant materials, soil extracts and waters. For spiked samples, recoveries of 97.7 to 104.3% were obtained with relative standard deviations of 2.0 to 6.7%. Tolerance to chloride is good, and interferences by nitrite and hydrogen peroxide are easily controlled. A modified Markham microstill for use in automatic analyser systems is described.

Isomers of dimethylphenol are established reagents for the determination of nitrate ion [1] and the earlier history of their development has been fully reviewed in recent papers [2—4]. The substituent methyl groups increase the relative reactivity of the aromatic ring towards electrophilic attack, and direct the incoming nitro-group to a position which allows separation of the product by steam distillation. Solvent extraction has also been used to separate the nitroxylenols formed [1], but co-extraction of charred organic components can lead to errors in absorbance measurements. The classical phenol-disulphonic acid method [5—9] is convenient and rapid, but does not allow the product measured to be separated from interfering reaction products.

This paper reports a re-investigation of the use of phenol as the spectrophotometric reagent [5, 10]. Phenol is nitrated, and the nitrophenol formed is separated by steam distillation in a Markham still [11]. The method is essentially the same as previously described [2]. Phenol is considered superior to 3,4-dimethylphenol because it is cheap and readily available in high purity; the molar absorptivity for the nitro-derivative of phenol at 410 nm is higher; and the tolerance level for chloride is higher. Data are presented to demonstrate that phenol allows the excellent precision and rapidity inherent in the earlier method [2] to be retained.

EXPERIMENTAL

Apparatus

Spectra were recorded with a Unicam SP 800 spectrophotometer (1-cm

silica cells). Single-wavelength absorbance measurements were made with a Unicam SP 500. A Markham still was connected to a steam source (Büchi unit). Oxford dispensers were used for reagents; a vortex stirrer was used.

Reagents and standard solutions

A 5% (w/v) solution of phenol in ethanol and aqueous 2% (w/v) sodium hydroxide solutions were prepared. Diluted sulphuric acid (87.5% v/v; 7 + 1) was allowed to cool before use. A 2% (w/v) solution of silver sulphate in 87.5% sulphuric acid was prepared by adding 50 ml of water to 8 g of silver sulphate, followed by careful addition, with occasional stirring, of 350 ml of 18 M sulphuric acid. This reagent is stable for several months, and is needed only when chloride levels exceed certain limits.

Three sets of standard solutions containing 0, 25, 50, 100 μg ml^{-1} NO_3^--N and 0, 100, 200, 400 μg ml^{-1} NO_3^--N (for plants), and 0, 5, 10, 20 μg ml^{-1} NO_3^--N (for soils and water) were prepared by serial dilution of a stock standard 1000 μg ml^{-1} NO_3^--N containing 3.6107 g of potassium nitrate (dried at 105°C) in 500 ml of distilled water.

Procedure

Pipette aliquots (1 ml) of milled plant tissue extracts (500 mg in 10 ml of water) into 28 mm × 150 mm test tubes, and add 1 ml of phenol reagent. Mix with the vortex stirrer set at low speed. Place the test tube in a 250-ml conical flask containing cold tap water and introduce 9.0 ml of the diluted sulphuric acid slowly down the sides, while rotating the test tube. Remove the test tube from the flask, mix thoroughly (vortex stirrer) and transfer immediately into a clean Markham still with a few ml of distilled water. Ensure a fast flow of water through the condenser. Collect the distillate (20—22 ml) in a 25-ml graduated cylinder containing 2 ml of 2% sodium hydroxide solution, at 6—8 ml per min. Dilute to the mark with distilled water, mix, and measure the absorbance at 410 nm. Colour development is instantaneous; the colour is stable for several days. Treat similarly, as above, appropriate standards containing 0—100 μg NO_3^--N, or 0—400 μg NO_3^--N in a 1-ml aliquot.

Treat 5-ml aliquots of soil sample extracts (5.0 g with 10 ml of water), or 5 ml of water, with 1 ml of phenol reagent and 14.0 ml of the diluted sulphuric acid; the procedure is otherwise as for plant extracts. Treat similarly 5-ml aliquots of standard nitrate solutions containing 0, 5, 10, and 20μg N ml^{-1}. If different aliquots are used, adjust the volume of nitrating acid to keep the final concentration of acid in the reaction mixture constant.

With the above procedure, the use of 87.5% (v/v) sulphuric acid without added silver sulphate will tolerate up to 12% chloride in plant tissue and 2420 μg Cl^- g^{-1} or 1210 μg Cl^- ml^{-1} in soil or water, respectively. With 87.5% (w/v) sulphuric acid containing 2% (v/v) of silver sulphate, the tolerance levels for chloride ion are increased four-fold in each case. When chloride levels are expected to exceed these levels (e.g., in highly saline soils and sea water), prior removal of chloride ion by precipitation with a soluble silver

salt (e.g. silver lactate) in slightly acidified solution to coagulate silver chloride and filtration, is recommended.

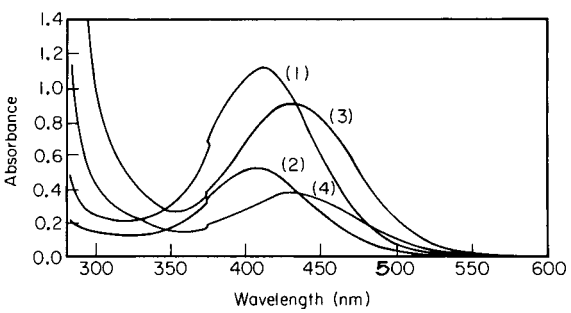
Procedure to give total nitrate plus nitrite

To a 5-ml aliquot of soil extract or water containing nitrite, add 0.3 ml of 1.0% (w/v) potassium dichromate solution, and mix (vortex stirrer). Introduce 14.0 ml of the diluted sulphuric acid, mix well, and allow to react for 30 min. Add 1 ml of phenol reagent, mix, and transfer the solution immediately to the Markham still with a few ml of water. Alternatively, nitrite in solution may be destroyed before nitration with sulphamic acid in the conventional manner.

DISCUSSION AND RESULTS

Phenol, first recommended by Sprengel [5] for the detection of nitrate, is easily nitrated, and yields derivatives with the nitro-groups almost entirely in the *ortho* and *para* positions. *o*-Nitrophenol is bright yellow and volatile in steam (b.p. 214°C); the other isomers of phenol are almost colourless and not volatile in steam (b.p. 290—300°C). These differences are attributed to hydrogen bonding in the *ortho*-compound [12].

Figure 1 shows that the absence of the methyl groups at C-3 and C-4 in the *o*-nitrophenoxide ion (the chromophore) gives a hypsochromic effect, with a shift in λ_{max} from 430 nm to 410 nm. A hyperchromic effect leading to ca. 20% increased absorption is also observed, possibly because of the absence of steric hindrance to nitration at both C-2 and C-6 in phenol.



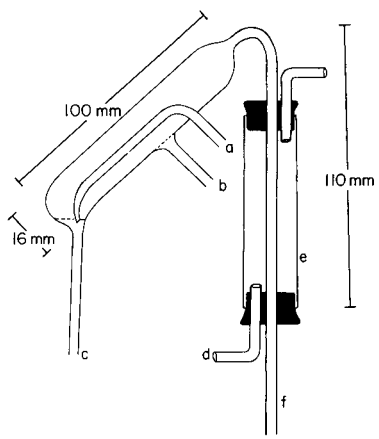


Fig. 1. Absorption spectra of the sodium salts of *o*-nitrophenol (1 and 2), and *o*-nitroxylenol (3 and 4) measured against distilled water. The spectra are for a standard solution containing 100 μg NO_3^--N in 25 ml of water (1 and 3), and for cabbage extracts containing 180 μg NO_3^--N in 100 ml of water (2 and 4).

Fig. 2. Microstill for the automated distillation of nitrophenol. (a) Steam entry; (b) sample entry; (c) to waste; (d) cooling water entry; (e) condenser; (f) distillate to colorimeter.

TABLE 1

Effect of acid strength on absorbances for plant and soil samples

Sample	87.5% (v/v) H_2SO_4 added (ml)	Absorbance	Final acid strength (% v/v)
Tomato leaf[a]	3	0.385	52.5
	5	0.410	62.5
	7	0.435	68.1
	9	0.470	71.6
	11	0.470	74.0
Soil[b]	2	0.005	21.9
	6	0.042	43.8
	8	0.136	50.0
	12	0.205	58.3
	14	0.215	61.2

[a]1-ml aliquot. [b]5-ml aliquot.

Effects of variation in reagent concentrations

The prior dilution of concentrated sulphuric acid to 87.5% (v/v) is necessary to modify the large heat of dilution that would otherwise occur during the nitration stage. The ratio of sulphuric acid to water affects the amount of nitrophenol produced and hence the sensitivity of the method. Table 1 shows that maximum colour formation is obtained when the final acid concentration in the reaction mixture is ca. 71.6% (v/v) for plants or ca. 61.2% (v/v) for soil and water.

Sodium hydroxide forms the salt of *o*-nitrophenol, thereby increasing its solubility in water, and extends the conjugation in the chromophore. Small amounts of 2% (w/v) sodium hydroxide (0.2—2 ml in 25 ml of water) develop the yellow colour fully.

To achieve maximum sensitivity, linearity, and reproducibility, sufficient phenol must be present during nitration. Different amounts of phenol were dissolved in ethanol, and studies made with different nitrate concentrations. The optimum concentration of phenol was 500 μg (not less than 125 μg) for each microgram of nitrogen (as nitrate).

Reaction rate, temperature of reactants and stability of chromophore

The nitration of phenol was as rapid as that for 3,4-dimethylphenol [2]. Maximum absorbances were obtained for standards and samples when the reactants were distilled immediately after mixing. External heating is not necessary for complete nitration; if the temperature becomes too high, loss of nitrophenol may occur and this is avoided by placing the test tube in cold water during the addition of sulphuric acid.

Absorbances of the distillates containing 0.2—4 μg N ml^{-1} (as nitrate) were monitored, and were found to remain constant for several days.

TABLE 2

Effect of diverse compounds on the determination of 100 μg of nitrate-nitrogen

Interferent added	Amount tolerated (μg)	Interferent added	Amount tolerated (μg)
NaCl	10000	H_2O_2	550
$MnSO_4 \cdot H_2O$	>50000	$K_2Cr_2O_7$	7500
Na_2SO_3	>15000	$HClO_4$	60000
$K_4Fe(CN)_6$	>10000	$K_3Fe(CN)_6$	>10000
		$NaNO_2$	—[a]

[a] 1-ml aliquot containing 100 μg NO_2^--N gives an absorbance of 0.08 at 410 nm in 25 ml of water.

Interferences

The nitration of phenol may be viewed as an oxidation—reduction system, with phenol as an electron-rich species, and the nitronium ion as an electrophilic species [13]. There may therefore be interferences from both oxidants and reductants. For example, chloride can interfere by reacting with nitric acid to give nitrosyl chloride [14]. The tolerance levels for possible interferences were determined (Table 2) by analyzing a 1-ml aliquot of a 100 μg ml^{-1} NO_3^--N standard spiked with 1 ml of a solution of the possible interferent. Except for hydrogen peroxide, which gives a deepening in colour of the distillate [4], phenol shows a remarkable tolerance to the other diverse ions studied. Hydrogen peroxide in acidic solution may be destroyed by adding 2% (w/v) $KMnO_4$ solution until a faint purple colour persists.

The tolerance level for chloride (Table 2) is equivalent to 12% chloride in plant tissue (calculated for a 1-ml aliquot) and 2420 μg Cl^- g^{-1} or 1210 μg Cl^- ml^{-1} for soil extracts or water (5-ml aliquots), respectively. A four-fold increase in these levels was achieved by using sulphuric acid (87.5% v/v) containing 2% (w/v) of silver sulphate.

Nitrite interferes by producing nitrosophenol [12]; a 1-ml aliquot containing 100 μg of nitrite-nitrogen gave an absorbance of 0.08 at 410 nm, in 25 ml of water. This is equivalent to 2000 μg N g^{-1} for nitrite in plants, and 40 μg N g^{-1} or 20 μg N ml^{-1} for nitrite in soil or water, respectively. These levels of nitrite-nitrogen are seldom encountered. Total nitrate-plus-nitrite nitrogen can be determined by oxidation of nitrite to nitrate with 1.0% potassium dichromate (see *Procedure*).

Precision, accuracy, and recovery for nitrate-nitrogen

Table 3 shows the precision of the method as evaluated by analysing two samples of plant tissue, one soil and one water sample. The recoveries for samples spiked with nitrate-nitrogen are shown in Table 4. Close agreement was obtained when the proposed method was compared with the u.v. absorption method [15, 16] for samples of water and 1 M KCl extracts of soil. The

TABLE 3

Precision of the method for different samples expressed as the mean of five analyses with standard deviation and relative standard deviation

	Sample			
	Cabbage	Tomato leaf	Soil	Water
$\bar{x}$ (μg N g^{-1})	4081	1065	8.4	2.8
s	133	21.2	0.5	0.2
s_r (%)	3.3	2.0	6.4	6.7

TABLE 4

Percentage recovery for nitrate-nitrogen in spiked samples

Sample	Aliquot (ml)	NO_3^--N present (μg)	NO_3^--N added (μg)	NO_3^--N found (μg)	Recovery (%)	Mean recovery (%)
Cabbage	1	229	25	252	92.0	97.7
			50	280	102.0	
			100	328	99.0	
Soil	5	20.4	10	30.2	98.0	100.2
			25	46.2	103.3	
			50	70.0	99.2	
Water	5	188.9	5	194.2	106.0	104.2
			25	214.6	102.8	
			50	241.0	104.2	

u.v. absorption method is rapid, accurate and precise, but suitable only for samples with a low correction factor for absorption by organic matter at 275 nm [15, 16].

An important aspect of the proposed method with phenol is the efficiency with which the Markham still separates the nitrophenol. Ordinary steam distillation of nitrophenol or nitroxylenol by boiling in a flask is an unsatisfactory way of removing all the required material from solution. The Markham unit, however, needs to be operated manually. A microstill for use in an AutoAnalyzer-type system is shown in Fig. 2. It can be operated continuously for several hours (solutions are gravity-fed), and is highly efficient for distillation of compounds such as nitrophenol or ammonia.

The author thanks J. Jago, S. Baseden and members of the Agricultural Chemistry Division, Government Chemical Laboratories, for helpful comments and facilities; F. E. Uren of the Industrial Hygiene Division for the use of facilities; J. Staniforth of the Water Division for skilful glassblowing; and Dr. R. Alexander, Western Australian Institute of Technology, for valuable discussions.

REFERENCES

1 Department of the Environment, Analysis of Raw, Potable and Waste Waters, H.M. Stationery Office, London, 1972.
2 R. R. Elton-Bott, Anal. Chim. Acta, 90 (1977) 215.
3 G. Norwitz and H. Gordon, Anal. Chim. Acta, 89 (1977) 177.
4 G. Norwitz and P. N. Keliher, Anal. Chim. Acta, 98 (1978) 323.
5 H. Sprengel, Poggendorffs Annalen, 121 (1863) 188.
6 A. Grandval and H. Lajoux, C. R. Acad. Sci., Paris, 101 (1885) 62.
7 E. M. Chamot and D. S. Pratt, J. Am. Chem. Soc., 31 (1909) 922.
8 J. E. Eastoe and A. G. Pollard, J. Sci. Food Agric., (9) 1950) 266.
9 American Public Health Association, American Water Works Association and Water Pollution Control Federation, Standard Methods for the Examination of Water and Wastewater, 12th edn., 1969.
10 See, e.g., W. F. Donkin, Chem. News, 28 (1873) 254. B. M. Margosches, E. Scheinost and V. Woyner, Ber., 58B (1925) 1850.
11 R. Markham, J. Biochem., 36 (1942) 790.
12 See, e.g., E. H. Rodd (Ed.), Chemistry of Carbon Compounds, Vol. III, Part A, Elsevier Publishing Company, 1958, p. 442.
13 R. Breslow (Ed.), Organic Reaction Mechanisms, 2nd edn., W. A. Benjamin, New York, 1969, p. 148.
14 L. Farcy, Bull. Soc. Chim. Fr., 5 (1909) 1088.
15 R. C. Hoather and R. F. Rackham, Analyst, 84 (1959) 548.
16 D. L. Miles and C. Espejo, Analyst, 102 (1977) 104.

Analytica Chimica Acta, 108 (1979) 293—296
© Elsevier Scientific Publishing Company, Amsterdam — Printed in The Netherlands

EXTRACTION-SPECTROPHOTOMETRIC DETERMINATION OF SULPHIDE AND SULPHITE IN WATERS BASED ON FORMATION OF THE BIS(2,9-DIMETHYL-1,10-PHENANTHROLINE)COPPER(I) ION

S. RAMA BHAT, J. M. ECKERT*, R. GEYER and N. A. GIBSON

Department of Inorganic Chemistry, University of Sydney, Sydney, N.S.W. 2006 (Australia)

(Received 5th January 1979)

SUMMARY

A spectrophotometric method is described for the determination of sulphide or sulphite. The bis(2,9-dimethyl-1,10-phenanthroline)copper(II) ion is reduced at pH 10 by sulphide in the presence of formaldehyde and by sulphide and sulphite in its absence. The resulting copper(I) complex is extracted into chloroform and measured. With any convenient sample volume between 1 and 100 ml, the limits of detection are 0.1 μg for sulphide and 0.25 μg for sulphite. The method is unaffected by iron(II) and nitrite, in concentrations of 100 and 1000 mg l^{-1}, respectively.

The determination of sulphide and sulphite in anoxic waters remains a challenging exercise because of the ease with which both ions are oxidized by air and because of interferences, notably by other reducing agents. In the titrimetric iodine and colorimetric methylene blue methods for sulphide, for example, interference by reducing agents, including sulphite, necessitates the preliminary separation of sulphide as zinc sulphide; and sulphide itself interferes with the determination of sulphite by iodide—iodate titration [1].

In this paper, an extractive method is reported for the separate determinations of sulphide and sulphite which should be suitable for ground and waste waters. The bis(2,9-dimethyl-1,10-phenanthroline)copper(II) ion is reduced to the corresponding copper(I) ion at pH 10 when sulphide or sulphite is added, but sulphite does not react in the presence of formaldehyde. After extraction of the copper(I) complex into chloroform, the determination is completed by spectrophotometry of the extract. The effects of likely contaminants on the method are assessed.

EXPERIMENTAL

Apparatus and reagents

Absorbance measurements were made with a Varian-Techtron Model 635 spectrophotometer.

Buffer solution, pH 10. Dissolve 3.21 g of ammonium chloride in water, add 70 ml of 2 M ammonia and dilute to 1 l with water.

Copper sulphate solution. Dissolve 1.87 g of copper sulphate pentahydrate in water, add 600 ml of the buffer solution and dilute to 1 l with water.

Copper–DMP reagent. Dissolve 0.11 g of 2,9-dimethyl-1,10-phenanthroline (DMP) hydrochloride (neocuproine HCl, Merck) in water, add 20 ml of the copper sulphate solution and dilute to 100 ml with water. This reagent should be used within 24 h.

Recommended procedure

Place suitable (and equal) volumes of the water for analysis in two 250-ml polythene bottles (A and B), add sufficient buffer solution to each to raise the pH to 9.8-10.0 and shake to mix. Any volume of water up to 100 ml may be sampled but it should contain not more than 15 μg of sulphide and 50 μg of sulphite. Immediately add 1 ml of formaldehyde solution (40% w/v) to bottle A, mixing well; then to each bottle add 5 ml of the copper–DMP reagent. The treated samples may, if necessary, be stored for up to 24 h at this stage.

Transfer the contents of the bottles, with rinsing, to two 250-ml separating funnels and adjust the volumes to about 100 ml with water. To each funnel add 10.0 ml of chloroform; shake the funnels for 1 min and allow to stand until the phases separate. Run the chloroform layers through glass wool plugs and measure the absorbances of the extracts (A and B) at 457 nm with chloroform in the reference cell.

Carry out a blank determination with 100 ml of distilled water. The blank absorbance should be not more than 0.02. The absorbance of extract A (corrected for the blank) is due to sulphide, and the difference between the absorbances (B − A), to sulphite. Calculate the concentrations of sulphide and sulphite in the water sample by comparison with standards run simultaneously.

RESULTS AND DISCUSSION

2,9-Dimethyl-1,10-phenanthroline has frequently been used in combination with reducing agents for the spectrophotometric determination of copper [2] and with copper(II) in the estimation of reducing agents (blood sugars [3] and iodide [4]). The orange-red colour produced in the reaction is due to formation of the bis (DMP) copper(I) ion ($\epsilon_{max} = 7.9 \times 10^3$ at 457 nm, with nitrate, perchlorate, or halide as the counter-ion in chloroform [5]). The high stability of this ion, relative to the copper(II) complex ion ($E_0 = 0.62$ V at 20° [6]) is attributed to steric interaction between the 2- and 9-methyl groups of adjacent ligand molecules which prevents the copper(II) complex from adoptir the energetically preferred square planar structure [7].

The copper–DMP reagent of the proposed method contains 1.5 mM copper(II) and 4.5 mM DMP, i.e., a Cu : DMP mole ratio of 1:3. The excess of DMP is included to inhibit dissociation of the bis- to the monochelate complex. The role of formaldehyde is to mask sulphite ions.

Calibration

Standard sulphide and sulphite solutions were prepared by dissolving the reagent grade sodium salts ($Na_2SO_3 \cdot 7H_2O$ and $Na_2S \cdot 9H_2O$) in oxygen-free water containing 5% v/v glycerol to enhance stability [8]. The solutions were prepared fresh and standardized iodimetrically [8] just before use.

In the range 0—25 μg, the amount of sulphide present (y μg) could be calculated from the absorbance (x), obtained with 1-cm cells and corrected for the blank, by means of the equation $y = 16.4x + 0.806x^2$. The corresponding equation relating the amount of sulphite (y μg) to the corrected absorbance (x) was $y = 62.2x$, in the range 0—80 μg. When sulphide and sulphite were both present, the calibration graphs were found to be additive, within experimental error, in the ranges 0—15 μg and 0—50 μg, respectively.

Precision and limits of detection

The precision of the proposed method was assessed by carrying out repeated determinations of sulphide and sulphite, present separately and together in solution. The results are shown in Table 1.

The limits of detection, taken to be the amounts which gave an absorbance equal to twice the standard deviation of a set of 12 absorbance readings at or near blank level, were found to be 0.1 μg for sulphide and 0.25 μg for sulphite (corresponding to concentrations of 0.001 mg l^{-1} and 0.0025 mg l^{-1} respectively, for a sample volume of 100 ml).

Interferences

The effects of various ions on the recovery of 5.00 μg of sulphide and 25.0 μg of sulphite are shown in Table 2. An attractive feature of the method is its relative freedom from interference by iron and nitrite ions, a consequence of the high pH of the aqueous phase.

TABLE 1

Precision of proposed method

Sulphide taken (μg)	Sulphite taken (μg)	Mean S^{2-} found[a] (μg)	s (μg)	s_r (%)	Mean SO_3^{2-} found[a] (μg)	s (μg)	s_r (%)
0.50	—	0.49	0.02	4	—	—	—
—	2.00	—	—	—	2.13	0.09	4
0.50	2.00	0.53	0.03	6	2.13	0.13	6
5.00	—	5.01	0.08	2	—	—	—
—	25.0	—	—	—	25.3	0.25	1
5.00	25.0	4.92	0.09	2	25.0	0.6	2

[a]Mean of 6 determinations.

TABLE 2

Allowable concentrations of foreign ions[a]

Concentration (mg l^{-1})	Ion
20 000	Cl^-, F^-, SO_4^{2-}
1 000	NO_2^-, I^-, Mg^{2+}
100	PO_4^{3-}, Fe^{2+}, Fe^{3+}
50	SCN^-, $C_2O_4^{2-}$, Ca^{2+}
20	$C_6H_5O_7^{3-}$ (citrate), NTA
10	Zn^{2+}

[a]100 (±3) % recovery of 5.00 μg of sulphide and 25.0 μg of sulphite, present together in solution, was obtained in the presence of the stated concentrations.

We acknowledge the support received by one of us (S.R.B.) from a University of Sydney Post-Graduate Studentship.

REFERENCES

1 Standard Methods for the Examination of Water and Wastewater, American Public Health Association, Washington, D.C., 14th edn., 1976, Sections 428, 9, pp. 499—509.
2 See, e.g., E. B. Sandell, Colorimetric Determination of Traces of Metals, 3rd edn., Interscience, New York, 1959.
3 M. E. Brown and M. S. Boston, Diabetes, 10 (1961) 60.
4 Y. Yamamoto, T. Kumamaru, Y. Hayashi and M. Yamamoto, Anal. Chim. Acta, 69 (1974) 321.
5 J. R. Hall, N. K. Marchant and R. A. Plowman, Aust. J. Chem., 15 (1962) 480.
6 C. J. Hawkins and D. D. Perrin, J. Chem. Soc., (1963) 2996.
7 B. R. James and R. J. P. Williams, J. Chem. Soc., (1961) 2007.
8 Official, Standardised and Recommended Methods of Analysis, Soc. Anal. Chem., London, 1973, pp. 460—465.

Analytica Chimica Acta, 108 (1979) 297—308
© Elsevier Scientific Publishing Company, Amsterdam — Printed in The Netherlands

ANALYSIS FOR CATECHOLAMINES AND RELATED COMPOUNDS BASED ON LUMINESCENCE AT ROOM TEMPERATURE AND AT 77 K

MASATOSHI YAMAGUCHI, YOSHITO YUTANI, KAZUYA KOHASHI and YOSUKE OHKURA*

Faculty of Pharmaceutical Sciences, Kyushu University 62, Maidashi, Higashi-ku, Fukuoka 812 (Japan)

(Received 22nd November 1978)

SUMMARY

The luminescence characteristics of 34 catecholamines and related compounds at room temperature and at 77 K are reported. Neutral, basic and acidic mixtures were used as solvents. Limits of detection, linear ranges and analytical precision were determined for each case. Analytically useful luminescence was obtained at 77 K. In neutral and acidic solutions, both fluorescence and phosphorescence could be used qualitatively and quantitatively; in basic solutions, the phosphorescence was valuable at concentrations as low as 10^{-6}—10^{-9} M, depending on the compound.

Although many fluorimetric methods for the detection and determination of catecholamines, and their precursors and metabolites in biological samples have been proposed [1—3], the fluorescence reactions utilized in the methods are not generally selective for the individual compounds, and therefore the methods have usually required complicated procedures for separation of the individual compounds from biological samples. Such separations can now be done easily by liquid chromatography [4] or high-performance liquid chromatography [5], and so the native luminescence (fluorescence and phosphorescence) characteristics of catecholamines and related compounds has become of greater analytical interest.

The phosphorescence at 77 K of some such compounds in ethanolic solutions [6] and in neutral, acidic and basic mixtures of water and methanol (90:10) [7] and their fluorescence at room temperature in 0.05 M sulfuric acid and 0.1 M phosphate buffer (pH 7) have been reported [8], but the fluorescence at low temperature has not been described. Furthermore, the analytical utility of the luminescence signals from individual compounds has not been compared.

This paper provides data on the fluorescence at room temperature (298 K) (room-temperature fluorescence) and at 77 K (low-temperature fluorescence), and the phosphorescence characteristics at 77 K of many varieties of catecholamines and related compounds in neutral, acidic and basic ethanolic solutions, and in neutral, acidic and basic aqueous solutions containing a

little methanol. The possibility of applying these luminescence characteristics in qualitative and quantitative microanalyses for these compounds is evaluated.

EXPERIMENTAL

Chemicals and solutions

All chemicals were of reagent grade, unless otherwise stated. Ethanol and methanol were distilled through a 4-ft. column filled with helical coils, and water was distilled after deionization.

Catecholamines and related compounds. L-Epinephrine, L-norepinephrine, Dopamine hydrochloride, L-Dopa, DL-3,4-dihydroxymandelic acid, 3,4-dihydroxyphenylacetic acid, DL-3,4-dihydroxyphenylethyleneglycol, 3-methoxytyramine hydrochloride, L-3-methoxytyrosine hydrochloride, DL-metanephrine hydrochloride, DL-normetanephrine hydrochloride, DL-3-methoxy-4-hydroxymandelic acid, homovanillic acid, vanillactic acid, vanilpyruvic acid, bis(3-methoxy-4-hydroxyphenylethyleneglycol) piperazine salt (piperazine does not affect the luminescence of the glycol in neutral, acidic and basic ethanolic and aqueous media even at a concentration of 1×10^{-4} M), L-tyrosine, DL-*p*-hydroxymandelic acid, *p*-hydroxyphenyllactic acid, L-phenylalanine, DL-phenyllactic acid, phenylpyruvic acid and homogentisic acid (all purchased from Sigma Chemical Co., U.S.A.), and *p*-hydroxyphenylacetic acid and *p*-hydroxyphenylpyruvic acid (Wako Pure Chemical Ind., Japan) were used without further purification. DL-3,4-Dihydroxybenzaldehyde, vanillin, tyramine hydrochloride, *p*-hydroxybenzaldehyde and phenylethylamine hydrochloride (all from Wako Pure Chemical Ind.) and vanillic acid, DL-octopamine hydrochloride, DL-phenylethanolamine and DL-mandelic acid (all from Sigma Chemical Co.) were purified by recrystallization. The ultraviolet absorption spectra of the compounds measured in ethanol, water or n-hexane were found to be in good agreement with the available literature data.

Neutral, acidic and basic ethanolic solutions of catecholamines and related compounds (1×10^{-9}—1×10^{-4} M). For neutral solutions, dissolve the compound in ca. 4.5 volumes of water, adjust the pH to 7 with sodium hydroxide or hydrochloric acid, dilute to 5 volumes with water and then dilute with ethanol to 100 volumes. For acidic and basic solutions, dissolve the compound in a mixture prepared by diluting 5 volumes of 1×10^{-4}—2 M hydrochloric acid or sodium hydroxide solutions with ethanol to 100 volumes. The concentrations of hydrochloric acid and sodium hydroxide are 5×10^{-6}—1×10^{-1} M, respectively.

Neutral, acidic and basic aqueous solutions of catecholamines and related compounds (1×10^{-9}—1×10^{-4} M). For neutral solutions, dissolve the compound in ca. 85 volumes of water, adjust the pH to 7 with sodium hydroxide or hydrochloric acid, dilute to 90 volumes with water and then dilute with methanol to 100 volumes. For acidic and basic solutions, dissolve the compound in a mixture prepared by diluting 90 volumes of 5.55×10^{-6}—1.11×10^{-1} M

hydrochloric acid or sodium hydroxide solution with methanol to 100 volumes; the concentrations of the acid or alkali are then 5×10^{-6}—1×10^{-1} M. The methanol in the solutions serves to form homogeneously frozen matrices at 77 K.

Apparatus and luminescence measurements

A Hitachi MPF-3 spectrofluorimeter equipped with a xenon arc-lamp and a Hitachi QPD33 recorder was used throughout. The slit widths in the exciter and analyser were set at 10 nm and 2 nm for the room- and low-temperature fluorescence measurements and at 10 nm and 10 nm for the phosphorescence measurements, respectively. The room-temperature fluorescence spectra and intensities of the ethanolic and aqueous solutions were measured at 298 K in conventional quartz cells of 1 × 1 cm optical path lengths. The phosphorescence spectra and intensities of the ethanolic solutions were measured in liquid nitrogen (77 K) in quartz tubes (4.0 mm i.d., 5.0 mm o.d., 200 mm long; sample volume required, ca. 150 μl) with the spectrometer equipped with a Hitachi phosphoroscope attachment. The low-temperature fluorescence spectra and intensities of the ethanolic solutions were obtained in the same way, but the chopper in the phosphoroscope was removed.

The low-temperature measurements on the aqueous solutions were made in the same way as those in the ethanolic solutions, but in open quartz sample tubes (1.0 mm i.d., 5.0 mm o.d., 200 mm long; sample volume required, ca. 20 μl) [9], which were rotated at ca. 1500 rpm by a rotating cell assembly [10] to minimize the fluctuations of signals resulting from inhomogeneities in the frozen aqueous solution and irregularities in the diameter of the sample tubes [10, 11]. Excitation spectra were corrected by the Melhuish method [12] and emission spectra by the method of Lippert et al. [13].

Phosphorescence lifetimes longer than 1 s were measured by recording the phosphorescence intensity as a function of time on the recorder (chart speed, 120 mm min^{-1}) after excitation had been stopped by closing the excitation shutter in the fluorimeter, lifetimes shorter than 1 s were determined with a Hitachi V-051 synchroscope in place of the recorder.

The calibration graphs were prepared in the usual manner. The ultraviolet absorption spectra were measured at room temperature with a Shimadzu UV 200S spectrometer in cells of 1-cm optical path length. The pH was measured at room temperature (298 K) with a Hitachi-Horiba pH meter M-7.

RESULTS AND DISCUSSION

Luminescences of neutral ethanolic and aqueous solutions

For each compound, the excitation and emission spectra of neutral ethanolic and aqueous solutions are identical in shape and wavelength maxima. The maxima of the spectra are shown in Table 1. The low-temperature fluorescence and phosphorescence excitation spectra for each compound are practically identical with those for room-temperature fluorescence, as might be expected.

TABLE 1

Excitation and emission maxima of the room-temperature and low-temperature fluorescence and phosphorescence of the compounds in neutral ethanolic (or aqueous) solution, with the phosphorescence lifetimes and detection limits[a]

Compound	Peak wavelengths (nm)				Phosphorescence lifetime (s)		Detection limits (M)		
	Excitation[b]	Fluorescence		Phosphorescence	Ethanolic (s)	Aqueous (s)	Fluorescence		Phosphorescence
		298 K	77 K				298 K	77 K	
3,4-Dihydroxyphenyl derivatives									
Epinephrine[c]	235, 280	309	304	419	0.4	0.9	1×10^{-6}	1×10^{-6}	1×10^{-6}
Norepinephrine[c]	237, 281	309	303	420	0.3	0.9	1×10^{-6}	1×10^{-6}	1×10^{-6}
Dopamine[c]	233, 281	310	306	417	0.3	0.8	8×10^{-7}	8×10^{-7}	1×10^{-6}
Dopa[c]	237, 283	310	307	417	0.4	0.8	5×10^{-6}	8×10^{-7}	5×10^{-7}
3,4-Dihydroxymandelic acid[c]	235, 281	309	305	409	0.5	0.8	5×10^{-6}	1×10^{-6}	3×10^{-7}
3,4-Dihydroxyphenylacetic acid[c]	235, 281	309	306	415	0.3	0.8	2×10^{-5}	7×10^{-7}	1×10^{-6}
3,4-Dihydroxyphenylethyleneglycol	235, 281	309	304	418	0.4	0.8	1×10^{-6}	1×10^{-6}	1×10^{-6}
3,4-Dihydroxybenzaldehyde	328	nd[d]	nd	458	0.1	0.2	nd	nd	6×10^{-8}
3-Methoxy-4-hydroxyphenyl derivatives									
3-Methoxytyramine	235, 281	307	299	415	0.3	0.8	1×10^{-6}	7×10^{-7}	1×10^{-6}
3-Methoxytyrosine[c]	233, 281	308	300	430	0.4	0.8	2×10^{-6}	2×10^{-6}	1×10^{-6}
Metanephrine[c]	235, 279	307	299	415	0.4	0.8	8×10^{-7}	8×10^{-7}	8×10^{-7}
Normetanephrine[c]	235, 279	307	298	423	0.4	0.8	8×10^{-7}	8×10^{-7}	8×10^{-7}
3-Methoxy-4-hydroxymandelic acid[c]	235, 280	306	298	417	0.5	0.8	5×10^{-6}	1×10^{-6}	2×10^{-7}
Homovanillic acid[c]	235, 280	307	300	409	0.3	0.8	2×10^{-5}	1×10^{-6}	5×10^{-7}
Vanillactic acid	235, 281	308	300	438	0.4	0.8	3×10^{-6}	2×10^{-7}	6×10^{-7}
Vanilpyruvic acid	235, 325	386	378	435	0.1	0.7	3×10^{-5}	5×10^{-8}	1×10^{-5}
3-Methoxy-4-hydroxyphenylethyleneglycol	235, 281	308	298	430	0.4	0.8	3×10^{-6}	3×10^{-7}	4×10^{-6}
Vanillic acid	268, 292	333	315	435	1.9	1.6	5×10^{-7}	5×10^{-7}	5×10^{-8}
Vanillin	328	nd	nd	457	0 1	0.2	nd	nd	2×10^{-8}
p-Hydroxyphenyl derivatives									
Tyramine[c]	233, 277	300	295	382	5.9	3.2	1×10^{-6}	1×10^{-7}	1×10^{-7}
Tyrosine	233, 277	300	295	383	2.7	3.2	2×10^{-6}	1×10^{-6}	1×10^{-7}
p-Hydroxymandelic acid	233, 275	298	293	380	1.7	2.1	5×10^{-6}	5×10^{-6}	1×10^{-7}

p-Hydroxyphenylacetic acid	231, 277	300	295	383	2.8	2.5	2×10^{-6}	1×10^{-6}	1×10^{-7}
p-Hydroxyphenyllactic acid	231, 277	300	295	382	2.7	3.0	1×10^{-6}	1×10^{-6}	1×10^{-7}
p-Hydroxyphenylpyruvic acid	235, 316	366	353	419	0.1	0.5	2×10^{-5}	7×10^{-8}	1×10^{-6}
Octopamine	233, 277	300	295	382	2.8	2.8	2×10^{-6}	1×10^{-6}	1×10^{-7}
p-Hydroxybenzaldehyde	295	nd	nd	440	0.1	0.2	nd	nd	2×10^{-8}
Phenyl derivatives									
Phenylethanolamine	220, 255	w[e]	w	370	5.1	5.9	nd	nd	4×10^{-6}
Phenylethylamine	220, 255	w	w	370	7.1	8.2	nd	nd	4×10^{-6}
Phenylalanine	220, 255	w	w	370	6.9	8.1	nd	nd	5×10^{-6}
Mandelic acid	225, 255	w	w	370	3.2	3.9	nd	2×10^{-5}	1×10^{-6}
Phenyllactic acid	225, 255	w	w	370	3.6	4.6	nd	8×10^{-6}	1×10^{-6}
Phenylpyruvic acid	235, 257	w	280	429	0.1	0.1	2×10^{-5}	2×10^{-5}	4×10^{-6}
Homogentisic acid	235, 297	328	282	413	3.0	3.2	1×10^{-7}	5×10^{-7}	8×10^{-8}

[a]Concentration, 1×10^{-6}—1×10^{-4} M according to the compound. [b]Excitation maxima for the room- and low-temperature fluorescence, and phosphorescence; the higher wavelengths were used for excitation in all cases. [c]Similar phosphorescence excitation and emission maxima and lifetimes in aqueous solutions have been previously described [7, 8]. [d]Not detectable at 1×10^{-4} M. [e]Weak fluorescence, intensities less than twice that of the background at 1×10^{-4} M. Detection limit is defined as the amount giving an intensity twice the background.

Benzaldehydes (e.g. 3,4-dihydroxybenzaldehyde, vanillin and *p*-hydroxybenzaldehyde) do not fluoresce even at the low temperature, but phosphoresce.

The phosphorescence lifetimes of neutral ethanolic and aqueous solutions are also shown in Table 1. In the ethanolic solutions, the compounds containing carbonyl groups (e.g. 3,4-dihydroxybenzaldehyde, vanillin, *p*-hydroxybenzaldehyde, vanilpyruvic acid, *p*-hydroxyphenylpyruvic acid and phenylpyruvic acid) have short lifetimes (below 0.1 s). In the other compounds, the lifetimes for the phenyl and *p*-hydroxyphenyl derivatives (1.7—7.1 s) are much longer than those for 3-methoxy-4-hydroxyphenyl derivatives (0.3—0.5 s), except for vanillic acid (1.9 s). The lifetimes for aqueous solution are about twice as long as those for the ethanolic solutions with some exceptions.

The luminescence characteristics of the neutral solutions, therefore, may be used in a complementary mode for the characterization of catecholamines and related compounds.

The detection limits of the compounds in neutral ethanolic solutions (Table 1) are practically the same as those obtained in neutral aqueous solutions. For many of the compounds, the low-temperature fluorescence and the phosphorescence are more intense than the room-temperature fluorescence (Table 1). In particular, the phosphorescence of 3,4-dihydroxybenzaldehyde, vanillin, *p*-hydroxybenzaldehyde, vanillic acid and homogentisic acid and the intense fluorescence at low temperature of vanilpyruvic acid and *p*-hydroxyphenylpyruvic acid serve to detect these compounds at concentration levels of 10^{-8} M. This sensitivity may also permit trace analysis for compounds which can be converted to these compounds. For example, metanephrine, normetanephrine, 3-methoxy-4-hydroxyphenylethyleneglycol and phenylethanolamine are easily converted to the corresponding benzaldehydes by periodate oxidation.

The calibration graphs of the compounds in neutral ethanolic and aqueous solutions are linear for concentrations from the detection limits to 10^{-4} M by phosphorimetry and low-temperature fluorimetry, and to 10^{-5} M by room-temperature fluorimetry.

The precision of the luminescence intensity measurements was established by performing 20 determinations on neutral ethanolic and aqueous solutions of each of the compounds at concentrations of 3 and 20 times the detection limits. The coefficients of variation of the phosphorescence and the low-temperature fluorescence measurements did not exceed 3.8 and 3.5% in the determinations of the ethanolic and aqueous solutions, respectively; those for room-temperature fluorescence measurements did not exceed 1%.

Luminescences of acidic ethanolic and aqueous solutions

Noticeable modifications of the shapes and maxima of the excitation and emission spectra for room-temperature and low-temperature fluorescence and phosphorescence were not observed in acidic ethanolic and aqueous solutions compared to those in neutral solutions. The phosphorescence lifetimes of the compounds in acidic ethanolic and aqueous solutions are closely

similar to those in neutral solutions (Table 1). The concentration of hydrochloric acid in the solutions does not affect the luminescence characteristics of the compounds. The similarity of the spectra and lifetimes of some catecholamine metabolites in acidic and neutral aqueous solutions has previously been observed [7].

The detection limits, the linear ranges of the calibration graphs and the precision of the luminescence intensity measurements of the compounds in acidic solutions were also very similar to those found for neutral solutions.

Luminescences of basic ethanolic and aqueous solutions

Phenyl derivatives in basic ethanolic and aqueous solutions show excitation and emission spectra and phosphorescence lifetimes practically identical with those observed in the corresponding neutral solutions. The concentration of sodium hydroxide in the solutions does not affect their luminescence characteristics. The detection limits, the linear ranges of the calibration graphs and the precision of the low-temperature fluorescence and phosphorescence measurements in basic solution are identical to those in neutral and acidic solutions. Thus luminescence analysis for the phenyl derivatives is possible in any aqueous or ethanolic medium.

The room-temperature and low-temperature fluorescence of 3,4-dihydroxyphenyl, 3-methoxy-4-hydroxyphenyl and *p*-hydroxyphenyl derivatives, and homogentisic acid in basic ethanolic or aqueous solutions decreases in intensity steadily as the concentration of sodium hydroxide is increased from ca. 5×10^{-6} to ca. 2×10^{-4} M without shift of the excitation and emission maxima from those in the neutral solutions. The fluorescences of 3,4-dihydroxyphenyl derivatives are stable for only a few minutes in basic ethanolic solutions and very unstable in basic aqueous solutions containing 5×10^{-3} M sodium hydroxide, but those of the 3-methoxy-4-hydroxyphenyl and *p*-hydroxyphenyl derivatives remain unchanged for at least 1 day in both these media. The fluorescence is, however, quenched completely at sodium hydroxide concentrations exceeding ca. 4×10^{-4} M, which indicates that the phenolates of those compounds are non-fluorescent. The decrease of the low-temperature fluorescence of normetanephrine and tyramine in basic ethanolic solution is shown in Fig. 1. This feature of the fluorescence at room- and low-temperatures may be applicable in the identification of these compounds, but not to their determination because of irregularities in the fluorescence intensities caused by slight changes of the alkali concentration.

Homogentisic acid in basic solutions shows no phosphorescence. The phosphorescence of the 3-methoxy-4-hydroxyphenyl and *p*-hydroxyphenyl derivatives in basic ethanolic and aqueous solutions increases greatly in intensity as the concentration of sodium hydroxide increases from ca. 5×10^{-6} to ca. 5×10^{-4} M with a red shift of the excitation maxima and a blue shift of the emission maxima from those in neutral solutions (Table 1) to new values (Table 2). Maximal constant phosphorescence is obtained when the solutions contain more than ca. 5×10^{-4} M of sodium hydroxide, indicating that the phenolate species are highly phosphorescent. This be-

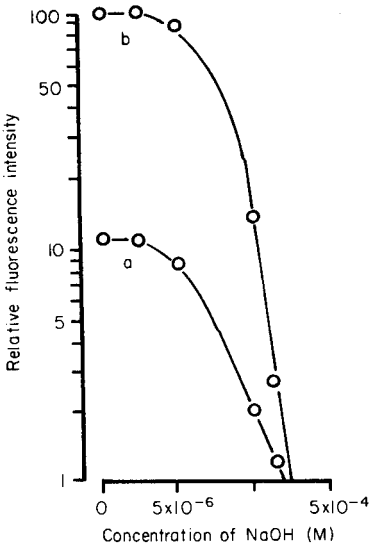


Fig. 1. Effect of sodium hydroxide concentration on the low-temperature (77 K) fluorescence intensities of 10^{-5} M solutions of (a) normetanephrine and (b) tyramine in basic ethanolic solutions, measured at the excitation and emission maxima (see Table 1).

havior of the phosphorescence of normetanephrine and tyramine in ethanolic solution is illustrated in Fig. 2. The resulting detection limits of most compounds (Table 2) are very small (10^{-8}—10^{-9} M). The phosphorescence of these basic solutions is stable for at least 60 min at room temperature. The phosphorescence lifetimes of the phenolate species of the compounds in basic ethanolic solution are slightly shorter than those in basic aqueous solution (Table 2), but longer than those of the species in neutral and acidic ethanolic solutions.

The phosphorescence intensities of 3-methoxy-4-hydroxyphenyl and *p*-hydroxyphenyl derivatives in basic (7×10^{-4} M NaOH) ethanolic and aqueous solutions are proportional to concentration from the detection limits up to ca. 1×10^{-4} M. The coefficients of variation for each compound at concentrations of 5 and 20 times the detection limits (freshly prepared solutions being used each time) were less than 4.0 and 3.5% ($n = 10$) for ethanolic and aqueous solutions, respectively. Similar results have been found [7] for the phosphorescence of tyrosine and some 3-methoxy-4-hydroxyphenyl derivatives in basic aqueous solutions.

The phosphorescence intensities of 3,4-dihydroxyphenyl derivatives other than 3,4-dihydroxybenzaldehyde in basic ethanolic solutions increase steadily as the concentration of sodium hydroxide increases from ca. 5×10^{-6} to ca. 5×10^{-4} M, again with shifts of the excitation and emission maxima (Table 3). Maximal (constant) phosphorescence intensity occurs when the ethanolic solution contains 5×10^{-4}—5×10^{-3} M of sodium hydroxide; an example is given in Fig. 2. The detection limits are given in Table 3. The compounds show phosphorescence lifetimes of 0.8 s.

TABLE 2

Excitation and emission maxima, lifetimes and detection limits for the phosphorescence of 3-methoxy-4-hydroxyphenyl and *p*-hydroxyphenyl derivatives, in basic ethanolic and aqueous solutions (5×10^{-4} M NaOH)

Compound	Peak wavelength (nm)		Lifetime		Detection limit[b] (M)
	λ_{ex}[a]	λ_{em}[b]	Ethanolic (s)	Aqueous (s)	
3-Methoxytyramine	245, 295	413	0.8	0.9	7×10^{-8}
3-Methoxytyrosine	243, 295	413	0.8	0.9[c]	8×10^{-8}
Metanephrine	243, 295	413	0.8	0.9[c]	8×10^{-8}
Normetanephrine	245, 295	413	0.8	0.9[c]	8×10^{-8}
3-Methoxy-4-hydroxy-mandelic acid	243, 295	413	0.8	0.9[c]	5×10^{-8}
Homovanillic acid	245, 295	413	0.8	1.0[c]	8×10^{-8}
Vanillic acid	245, 297	413	0.8	0.9	6×10^{-8}
Vanilpyruvic acid	245, 295	435	1.0	1.0	6×10^{-7}
3-Methoxy-4 hydroxyphe-nylethyleneglycol	245, 297	413	0.8	0.9	3×10^{-7}
Vanillic acid	305	440	1.4	1.5	3×10^{-8}
Vanillin	350	380	0.2	0.3	5×10^{-9}
Tyramine	241, 296	398	1.4	1.7	5×10^{-8}
Tyrosine	240, 297	400	1.4	1.6[c]	6×10^{-8}
p-Hydroxymandelic acid	240, 283	392	1.3	1.5	6×10^{-8}
p-Hydroxyphenylacetic acid	241, 295	395	1.3	1.6	6×10^{-8}
p-Hydroxyphenyllactic acid	240, 299	402	1.5	1.7	6×10^{-8}
p-Hydroxyphenylpyruvic acid	243, 328	398	1.2	0.5	5×10^{-7}
Octopamine	245, 295	392	1.3	2.0	6×18^{-8}
p-Hydroxybenazldehyde	333	413	0.2	0.2	5×10^{-9}

[a]The higher wavelengths were used for excitation in all cases. [b]Identical values were observed in both ethanolic and aqueous solutions. [c]Similar values have been reported in aqueous solutions containing 2×10^{-1} M or 5×10^{-1} M sodium hydroxide [7].

The native phosphorescence of 3, 4-dihydroxyphenyl derivatives in basic ethanolic solutions remains unchanged for only a few minutes (Table 3) when the solutions are allowed to stand in air at room temperature, and disappears after 30—40 min. However, a new phosphorescence appears with the excitation maxima at 302 and 365 nm and the emission maximum around 460 nm. As a typical example of the new phosphorescence, the spectra from norepinephrine are shown in Fig. 3. The new phosphorescence increases in intensity with time to reach a maximum after ca. 2 h at room temperature; it then diminishes gradually, but is stable at 77 K for at least 2 h. The maximal intensities of the phosphorescence from epinephrine, norepinephrine, Dopamine and Dopa are almost identical, and those from

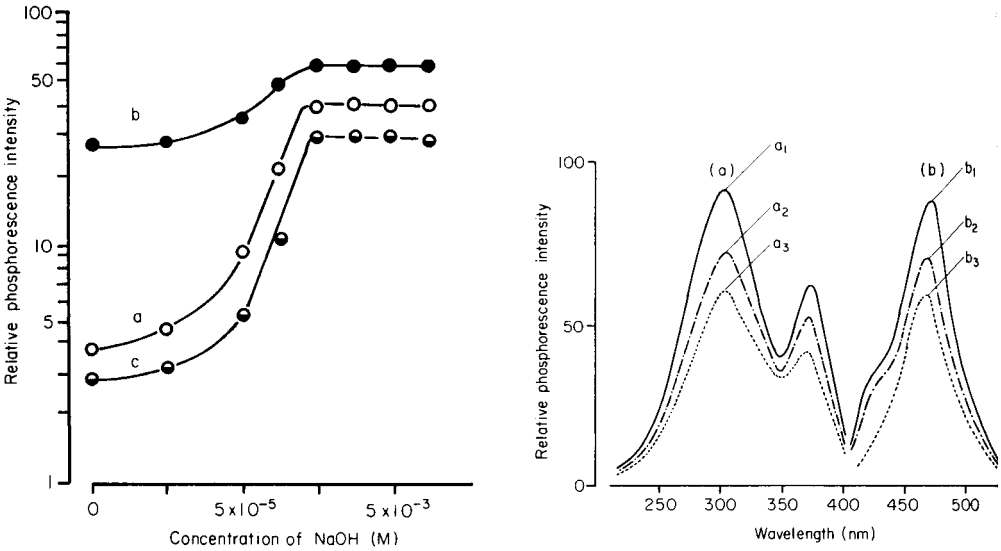


Fig. 2. Effect of sodium hydroxide concentration on the phosphorescence intensities of 10^{-5} M solutions of (a) normetanephrine, (b) tyramine and (c) epinephrine in basic ethanolic solutions, measured at the excitation and emission maxima (see Tables).

Fig. 3. (a) Excitation (302 and 365—366 nm) and (b) emission (460 nm) spectra of the phosphorescence from norepinephrine in basic ethanolic and aqueous solutions, and of the reaction mixture obtained by treating norepinephrine with hexacyanoferrate(III). (a_1 and b_1) 10^{-5} M norepinephrine in basic ethanolic solution (5×10^{-3} M NaOH) was left standing for 2 h at room temperature; (a_2 and b_2) 10^{-5} M norepinephrine in basic aqueous solution (5×10^{-4} M NaOH) treated as in (a_1 and b_1); (a_3 and b_3) a mixture of 0.2 ml of norepinephrine (5 μg ml^{-1}) in 0.4 M perchloric acid solution and 0.1 ml of 0.5 M phosphate buffer (pH 7.0) was mixed with 0.02 ml of 0.25% potassium hexacyanoferrate(III) solution, left standing for 1 min at room temperature, added to 0.2 ml of a mixture of 0.5 ml of aqueous 5 M NaOH solution, 0.1 ml of water and 10 mg of ascorbic acid, and diluted with 9.5 ml of ethanolic 5×10^{-3} M sodium hydroxide, and the phosphorescence was measured within 5 min.

3, 4-dihydroxymandelic acid, 3,4-dihydroxyphenylacetic acid and 3,4-dihydroxyphenylethyleneglycol are ca. 1/5th of that from norepinephrine. The lifetimes of the phosphorescence from those compounds are ca. 0.3 s. When more than 3×10^{-2} M sodium hydroxide is present, the disappearance of native phosphorescence and the appearance and disappearance of the new emisssion occur more rapidly.

In basic aqueous solutions of the 3,4-dihydroxyphenyl derivatives other than 3,4-dihydroxybenzaldehyde, the native phosphorescence disappears almost immediately, even when only 1×10^{-4} M sodium hydroxide is present. When solutions containing 5×10^{-5}—1×10^{-1} M of sodium hydroxide are exposed to air at room temperature for 5—20 min, another phosphorescence, which has the same characteristics as those observed in basic ethanolic solutions, begins to appear. The intensity of the latter solutions containing

TABLE 3

Duration times, excitation and emission maxima of the phosphorescence of 3,4-dihydroxyphenyl derivatives and their limits of detection in basic ethanolic solutions (5×10^{-4} M NaOH)

Compound	Duration time[a] at 298 K (min)	λ_{ex}[b] (nm)	λ_{em} (nm)	Detection limit (M)
Epinephrine	10	240, 295	413	1×10^{-7}
Norepinephrine	5	245, 295	413	1×10^{-7}
Dopamine	5	240, 297	411	2×10^{-7}
Dopa	10	245, 301	415	1×10^{-7}
3,4-Dihydroxymandelic acid	20	245, 299	413	1×10^{-7}
3,4-Dihydroxyphenylacetic acid	5	243, 298	411	2×10^{-7}
3,4-Dihydroxyphenylethyleneglycol	5	243, 299	416	2×10^{-7}

[a]Time for which the phosphorescence intensity remained unchanged. [b]The higher wavelengths were used for excitation in all cases.

5×10^{-4} M sodium hydroxide reaches a maximum after standing at room temperature for ca. 1 h and then decreases gradually with time, but is stable at 77 K for at least 5 h. The rate of change of the intensity depends on the alkali concentration. As an example, the phosphorescence spectra for norepinephrine are illustrated in Fig. 3. The appearance of this new phosphorescence in aqueous solution has been described previously [7].

The excitation and emission spectra and the lifetime of this phosphorescence from norepinephrine are closely similar to those of a reaction mixture obtained by treating norepinephrine with potassium hexacyanoferrate(III) at pH 7 in aqueous solution and then adding sodium hydroxide solution as in the procedure for the fluorimetric determination of catecholamines as trihydroxyindole derivatives [3], and diluting the resulting mixture with a basic ethanolic solution (Fig. 3). This indicates that the new phosphors from 3,4-dihydroxyphenyl derivatives might be trihydroxyindole derivatives formed by aerobic oxidation under the alkaline conditions.

However, phosphorescence with excitation maxima at 260—285 nm and an emission maximum around 400 nm which was reported for 3,4-dihydroxyphenyl derivatives in basic aqueous solutions after standing in air at room temperature for very long periods [7], was not observed in the present work even after 30 days at 298 K. 3,4-Dihydroxybenzaldehyde shows no phosphorescence in basic ethanolic and aqueous solutions.

The phosphorescence behavior of 3,4-dihydroxyphenyl derivatives in basic solutions may be applicable to their identification, but not to their determination.

A Grant-in-Aid for Scientific Research from the Ministry of Education, Science and Culture of Japan is gratefully acknowledged.

REFERENCES

1 S. Udenfriend, Fluorescence Assay in Biology and Medicine I, Academic Press, New York, 1962, pp. 129—160.
2 S. Udenfriend, Fluorescence Assay in Biology and Medicine II, Academic Press, New York, 1969, pp. 207—228.
3 A. H. Anton and D. F. Sayre, J. Pharmacol. Exp. Ther., 138 (1962) 360.
4 R. A. Wall, J. Chromatogr., 60 (1971) 195.
5 R. W. Stout, Anal. Biochem., 76 (1976) 330.
6 J. D. Winefordner, Methods of Biochemical Analysis, 15 (1968) 369.
7 W. J. Spann and J. D. Winefordner, Anal. Biochem., 15 (1973) 154.
8 D. E. Duggan, R. L. Bowman, B. B. Brodie and S. Udenfriend, Arch. Biochem. Biophys., 68 (1957) 1.
9 R. J. Lukasiewicz, P. A. Rozynes, L. B. Sanders and J. D. Winefordner, Anal. Chem., 44 (1972) 1339.
10 R. Zweidinger and J. D. Winefordner, Anal. Chem., 42 (1970) 639.
11 H. C. Hollifield and J. D. Winefordner, Anal. Chem., 40 (1968) 1759.
12 W. H. Melhuish, J. Opt. Soc. Am., 52 (1952) 1256.
13 F. Lippert, W. Naegels, I. Sheibold-Blankenstein, V. Steigner and W. Vass, Fresenius Z. Anal. Chem., 170 (1957) 1.

Analytica Chimica Acta, 108 (1979) 309—313
© Elsevier Scientific Publishing Company, Amsterdam — Printed in The Netherlands

TITRATION OF BINARY MIXTURES OF RARE EARTH METALS BASED ON MAGNETIC SUSCEPTIBILITY MEASUREMENTS

M. BOS*, J. A. LELY and W. LENGTON

Department of Chemical Technology, Twente University of Technology, Enschede (The Netherlands)

(Received 14th February 1979)

SUMMARY

Gouy balance weighings are used to monitor precipitation titrations of rare earth ions with standardized oxalate solutions. A procedure is described for the analysis of binary mixtures of these compounds. The accuracy of the determinations at the millimolar level depends on the magnetic moments of the components involved but is generally better than ±4%.

The determination of individual rare earths in mixtures still constitutes a major problem in chemical analysis. Even instrumental methods like x-ray fluorescence suffer from serious interelemental interferences within the group [1]. Numerous methods have been worked out for special cases, mainly based on redox processes, e.g. for cerium, europium and ytterbium. This paper also describes such a method, but one that is based on a property of the rare earth ions in which most of them differ widely, namely their magnetic moment. Except for lanthanum and lutetium, all the rare earth ions are paramagnetic in the trivalent state and so can be detected by Gouy balance measurements. Oxalate precipitates all rare earth ions selectively from solutions with carefully controlled pH [1]. This behaviour of the rare earth ions can be utilized in precipitation titrations which are monitored by either nuclear magnetic relaxation measurements [2] or Gouy balance weighing [3].

The method would not have any advantage over, say, the EDTA titration method, were it not that the titration curves provide information for the resolution of binary mixtures.

THEORY

If a solution of paramagnetic ions in a cylindrical glass tube is suspended between the poles of a magnet where an inhomogeneous field exists as in a Gouy balance, the force F acting on the sample and tube is given by

$$F = T_{\text{glass}} + \frac{1}{2}\mu_0 \chi A\ (H_2^2 - H_1^2) \qquad (1)$$

Here T_{glass} is the force acting on the glass tube caused by the diamagnetism

of glass, A is the cross-section of the tube, H_2 and H_1 are the magnetic field strengths at the upper and lower ends of the sample, μ_0 is the permeability of vacuum and χ is the volume susceptibility of the solution. The latter is related to the composition of the solution by $\chi = \chi_p + \chi_w$ and $\chi_p = \text{const.} N\mu^2$, where χ_p is the contribution of the paramagnetic ions to the susceptibility, χ_w the contribution of water, μ the magnetic moment of the paramagnetic ions, and N the number of these ions per unit volume. If it is assumed that the solutions of the various samples have been diluted to such an extent that their water content is equivalent to pure water, χ_w can be considered as a constant.

The force F is measured as an apparent difference in weight ΔW of the tube containing the sample with the magnetic field on and off: $F = \Delta W$. Combination of the above equations gives the following relation between ΔW and the concentration of a paramagnetic ion in a dilute solution: $\Delta W = \alpha C_p + \beta$. Here α and β are constants and C_p is the concentration of the paramagnetic ion. The constant α is characteristic for the paramagnetic ion under study whereas β is determined by the sample tube if all measurements are made at the same field strength. For mixtures of paramagnetic ions the apparent weight difference is given by $\Delta W = \Sigma_{i=1}^{n} \alpha_i C_i + \beta$. In this equation n is the number of paramagnetic species present in the solution.

For the precipitation titration of a binary mixture of the rare earths A and B with oxalate, it follows from the summation equation for ΔW that before the equivalence point

$$\Delta W = \alpha_a [C_a^* V_o - \frac{2}{3} V_{ox} M_{ox} C_a^* / (C_a^* + C_b^*)] / V_{tot}$$

$$+ \alpha_b [C_b^* V_o - \frac{2}{3} V_{ox} M_{ox} C_b^* / (C_a^* + C_b^*)] / V_{tot} + \beta \qquad (2)$$

In this equation, C^* denotes the concentration of the rare earth prior to addition of titrant, V_o is the starting volume, V_{tot} the volume of the sample plus titrant, V_{ox} the volume of titrant added, and M_{ox} the molarity of the oxalate solution. Rearrangement of this equation gives

$$(\Delta W - \beta) V_{tot} = \alpha_a C_a^* V_o + \alpha_b C_b^* V_o - \frac{2}{3} [M_{ox} / (C_a^* + C_b^*)] [\{\alpha_a C_a^* + \alpha_b C_b^*\} V_{ox}] \qquad (3)$$

Thus the part of the titration before the equivalence point can be plotted as a straight line. From the slope and intercept of this line, the separate concentrations C_a^* and C_b^* can be calculated if the values for α_a and β_b are known. These values can be established from separate titrations of the single components.

EXPERIMENTAL

Chemicals and equipment

Gadolinium oxide, samarium oxide, dysprosium oxide, neodymium nitrate

(all Fluka, puriss), neodymium oxide (Koch-Light, reagent grade) and dysprosium nitrate (Alfa, reagent grade) were used as received.

Standard solutions of these materials were prepared by dissolving the nitrates directly in doubly distilled water or by dissolving the oxides in diluted (1 + 1) concentrated nitric acid (Merck, reagent grade) and neutralizing the solution to pH 4 with ammonia. These solutions were standardized by EDTA titration with the use of xylenol orange indicator [4]. The oxalate titrant (about 1 M) was prepared by dissolving reagent-grade potassium oxalate (Merck) in doubly distilled water and standardizing with potassium permanganate (Merck, Titrisol). The Gouy balance was manufactured by Newport Instruments, England.

Procedures

Two procedures were adopted for carrying out the titrations. In the first, standard amounts of the buffered (0.05 M acetic acid—sodium acetate) solutions of the rare earth were pipetted into dry test tubes. Different amounts of titrant were added to these solutions, varying from 0 ml to volumes well beyond the estimated end-point. When the precipitate had settled, samples of the supernatant solutions were transferred by syringe to the measuring tube of the Gouy balance.

The second procedure differed from the first only in the use of 10-ml volumetric flasks instead of test tubes. These flasks were filled to the mark with water after addition of the titrant. Again the Gouy balance measurements were made on the supernatant liquid or filtrate of the precipitate. During the measurements a current of 1 A was used for the magnet, the maximum permitted for the instrument in use.

RESULTS AND CONCLUSIONS

An example of the titration of a single component (gadolinium) is given in Table 1 (volumetric flask method); the relevant titration plot is presented in Fig. 1. The end-point of the titration is found by calculating the intersection point of the two linear portions of the titration plot with the use of the least-squares technique.

For all the titrations, the weight differences after oxalate additions past the end-point corresponded to those of pure water, indicating that the contributions of the non-paramagnetic substances can be neglected.

Table 2 shows the relation between the slopes of the individual titration plots and the values of the magnetic susceptibility of the oxides of the trivalent state of the four rare earths examined [5]. From this table it can be concluded that if the Gouy measurements are calibrated with a paramagnetic reference substance like Mohr's salt, it is possible to use literature data for the magnetic susceptibilities of the rare earth ions in all but the most accurate titrations.

The data for the titration of a mixture of 1.978 mmol of samarium and 0.961 mmol of gadolinium in a total volume of 10.0 ml are presented in the lower part of Table 1. The results are summarized in Table 3, along with the

TABLE 1

Titrations of 0.961 mmol of gadolinium and of 0.961 mmol gadolinium plus 1.978 mmol of samarium by the volumetric flask method (V = 10.0 ml)

Oxalate added (mmol × 2/3)	ΔW (mg)	Oxalate added (mmol × 2/3)	ΔW (mg)	Oxalate added (mmol × 2/3)	ΔW (mg)
Gadolinium					
0.000	11.20	0.5325	−0.10	0.9984	−9.50
0.1331	8.60	0.5990	−1.50	1.065	−9.45
0.1997	7.15	0.6656	−3.20	1.132	−9.40
0.2662	5.60	0.7322	−4.52	1.198	−9.45
0.3328	4.15	0.7987	−5.85	1.265	−9.45
0.3994	2.70	0.8653	−7.30	1.331	−9.45
0.4659	1.40	0.9318	−8.90		
Gadolinium + samarium					
0.0000	12.90	1.493	2.45	2.986	−9.40
0.2986	11.20	1.792	0.10	3.285	−9.40
0.5972	9.15	2.090	−2.45	3.583	−9.40
0.8959	6.80	2.389	−4.70	3.882	−9.40
1.1950	4.65	2.688	−7.30		

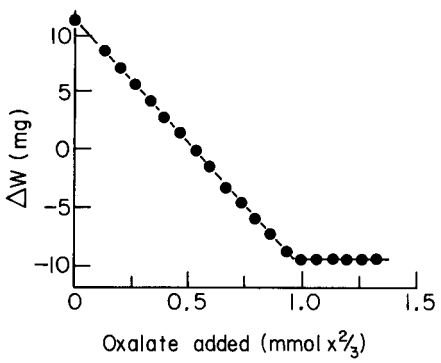


Fig. 1. Titration of 0.961 mmol of gadolinium by the flask method.

TABLE 2

Slope of individual titration plots of some rare earths compared to the magnetic susceptibilities of the oxides

Compound	Slope of plot (mg mmol^{-1})	Magn. susc. ($\times 10^{-6}$)	Quotient
Gd	−21.726	53200	−2448
Sm	−0.837	1988	−2375
Dy	−38.61	89600	−2320
Nd	−4.240	10200	−2405
			S.d. ± 2.3%

TABLE 3

Results of magnetic titrations of some rare earths

Compound	Added (mmol)	Found (mmol)	Rel. error (%)
Nd	2.387	2.431	+1.9
Nd	2.653	2.622	−1.1
Sm	2.986	2.926	−2.0
Sm	2.967	2.997	+1.0
Dy	2.970	3.038	+2.3
Dy	2.323	2.361	+1.7
Gd	0.961	0.962	+0.1
Dy/Nd	1.161/1.193	1.165/1.245	0.3/4.4
Sm/Gd	1.978/0.9607	2.009/0.9908	+1.6/+3.1
Sm/Nd	1.493/1.278	1.490/1.278	−0.2/4.4
Dy/Gd	0.551/1.280	0.554/1.280	+0.6/0.0

results obtained for other single components and mixtures. These results were calculated by using the least-squares slopes obtained from titrations of the individual elements. The accuracy of the method is somewhat dependent on the magnetic moments of the components of the binary mixtures and ranges from −1% to +5%.

The authors thank Ms. M. Muring for preparing the manuscript and Prof. E. A. M. F. Dahmen for his interest in this work.

REFERENCES

1 M. M. Woyski and R. E. Harris in I. M. Kolthoff, P. J. Elving and E. B. Sandell (Eds.), Treatise on Analytical Chemistry, Part II, Vol. 8, Interscience, New York, 1963.
2 A. Schlüter and A. Weiss, Anal. Chim. Acta, 99 (1978) 157.
3 H. G. Seltmann and W. Gunsser, Fresenius Z. Anal. Chem., 291 (1978) 39.
4 R. Pribil, Komplexometrie Band 1, VEB Deutscher Verlag für Grundstoffindustrie, Leipzig, 1963, p. 94.
5 R. C. Weast, S. M. Selby and C. D. Hodgman, Handbook of Chemistry and Physics, 45th edn., Chemical Rubber Co., 1964, p. E.59.

Analytica Chimica Acta, 108 (1979) 315—323
© Elsevier Scientific Publishing Company, Amsterdam — Printed in The Netherlands

CALIBRATION IN QUANTITATIVE ANALYSIS
Part 1. General Considerations

J. AGTERDENBOS

Analytisch Chemisch Laboratorium der Rijksuniversiteit, Croesestraat 77A, 3522 AD Utrecht (The Netherlands)

(Received 22nd December 1978)

SUMMARY

Mathematical procedures for calibration require assumptions to be made, e.g. the homogeneity of variances and the mathematical relationship between the analyte content x and the signal y. Little is known about the magnitude of errors arising from incorrect assumptions. The variation of the standard deviation of the analytical procedure with the content of the analyte, the selection of the type of mathematical relationship between x and y, and the types of errors made in testing hypotheses are discussed. In certain practical situations, the standard deviation (s.d.) is nearly independent of x if $x < 22p$ (p = detection limit) and the relative standard deviation (r.s.d.) is nearly independent of x if $x > 50p$. If the s.d. is constant, calibration relations of the type $y = a + bx$ are frequently to be preferred; with a constant r.s.d., relations of the type $\log y = a + b \log x$ have advantages.

In most types of quantitative instrumental analysis, calibration is vital. Generally a calibration curve is prepared or a corresponding mathematical relation between the content x (amount or concentration) of the analyte and the signal y is calculated and applied to the unknown sample. For the calculation of the relation between x and y, the mathematical procedures generally used are based on the "method of least squares". Only this type of procedure is discussed here. The calculation of the content x of the unknown sample frequently includes calculation of a confidence region for this content. The mathematical formulae applied in calibration have been given in many texts along with the mathematical criteria for their application [1—6]. The paper by Gottschalk [6] is part of a series on standardization in quantitative analytical procedures [7].

Analytical procedures do not generally obey the conditions imposed by mathematics, and some authors — recently Gottschalk [6] and Maessen et al. [5] — have therefore provided statistical methods to test the validity of the assumptions made. At least one point, however, seems to have escaped attention: a statistical test is not necessarily correct if it cannot be proved that it is incorrect. As has been shown by Agterdenbos [8], serious errors may result if this is not realized. Some other points are rarely discussed in analytical calibration. The mathematical relationship applied can be different from the

true relation between content x and signal y. Not much is known about the error caused by discrepancies, or about the way this error is influenced by factors such as the calibration range, or about the magnitude of the discrepancy. Calibrations made are justified only if certain mathematical conditions are fulfilled such as the homogeneity of variances (see below). Here, too, little is known about the error caused by unjustified assumptions and its dependence on the factors mentioned [8].

Another point rarely discussed is the importance of the location of the calibration points on the concentration axis if the number of these points is fixed. Shewell [9] calculated which location of five calibration points gave the best information (smallest confidence region) for the slope and intercept of a linear plot. However, he ignored the mutual dependence of these two parameters [10, 11]. In a recent paper, Franke and de Zeeuw [12] discussed a theory for achieving the optimum location of calibration points in the standard addition method. No general or more detailed discussion of the influence of the location of calibration points on accuracy seems to have been given.

A final point is "bracketing" the measurement of the concentration of an unknown sample by interpolation between two samples of known concentrations. The precision of such a procedure in dependence on some of the factors mentioned above was recently discussed by Schwartz [13].

GENERAL ASPECTS

Two steps may be distinguished in calibration: the preparation of the curve, i.e. calculation of the relation between x and y, and application of the relation to unknown samples. The preparation of the curve is sometimes preceded by or combined with an investigation of the type of mathematical relation between x and y. It always includes the calculation of the parameters a, b ....., and sometimes includes tests of the significance of the parameters [6] and of the homogeneity of variances [5, 6]. The application of the curve always includes the calculation of the analyte content of the unknown sample. Sometimes it also includes a comparison of the standard deviation found from the calibration measurements with the standard deviation found from the measurements of the unknown sample. Finally, a confidence region for the analyte content of the unknown sample is sometimes calculated [5, 6].

Types of mathematical relations in calibration

(The symbols and abbreviations used are listed in Table 1.)

Some mathematical relations that are frequently used are:

$$y = bx \tag{1}$$

$$y = a + bx \tag{2}$$

$$\log y = a + b \log x \tag{3}$$

(The Scheibe—Lomakin equation applied in emission spectrometry)

TABLE 1

Symbols and abbreviations

s.d.	= absolute standard deviation = σ or s in formulae[a,b]
r.s.d.	= relative standard deviation = σ_r or s_r in formulae (expressed as a fraction)
σ_t or s_t	= total s.d. in formulae
σ_{rt} or s_{rt}	= total r.s.d. in formulae
x	= content: y = signal
$\hat{a}$, $\hat{b}$, $\hat{c}$	are the best estimates and a, b, c are the population values of the calibration curve parameters
$\hat{a}_j$	= the same parameters, with special reference to equation j
Δ	= difference between the measured and calculated value of y
p	= limit of detection
k, q, z	= factors (see text)
α, β	= errors of the first and second kinds, respectively, in testing hypotheses

[a] "Standard deviation" in the text means that both s.d. and r.s.d. are considered. The terms "population" or "sample" are added if their omission may lead to confusion.
[b] σ is applied for population values, and s for sample values.

$$y = a + bx + cx^2 \tag{4}$$

(Found in atomic absorption spectrometry by Wagenaar et al. [14]; Agterdenbos and Vlogtman [15] found that it may be expected in absorption spectrometry if non-monochromatic light is the cause of non-linearity. The possible validity of eqn. (3) was not investigated by these authors.)

Other equations, rarely encountered, are:

$$\log y = a + \log x \tag{5}$$

$$\log y = a + b \log x + c (\log x)^2 \tag{6}$$

Calculations of the parameters in all the equations is based on the method of least squares, where for example, in eqn. (2) $\Sigma(\Delta_i)^2$ is a minimum for i measurements ($i > 2$) of y. The values calculated are the best estimates for the population parameters. Formulae for the calculation of the best estimates, their standard deviations and confidence intervals are given in standard texts. It should be remembered that these intervals are not independent of each other. For eqn. (2) this has been discussed in more detail [10, 11], and has been applied recently to practical analysis [5, 12]. More complicated relations between x and y may exist and the corresponding parameters can be calculated [13, 16].

With the procedure mentioned, good results are obtained only if some statistical conditions are fulfilled (see below) and if the true relation between x and y can be described adequately by a mathematical relationship.

Conditions to be fulfilled

Several conditions have to be fulfilled to justify the calculation procedure mentioned. One is that the precision of the measurement of the x values is

much better than the precision of the measurement of the y values. A second condition is that values found for y if parallel determinations are made at the same x value have a Gaussian distribution. In the present paper both conditions are assumed to be valid.

A third condition is the "homogeneity of variances" (variance = σ^2 or s^2), i.e. the s.d. of the measured y values must be the same for the whole range of x values covered by the calibration curve. The population s.d. should be considered, not the sample value or the r.s.d. Simple weighting procedures exist to take into account variations in the s.d. with x, if the values of $\hat{a}$ and $\hat{b}$ are calculated. However, if this is done, there is no good procedure for calculation of a confidence region for the analyte content in the unknown sample. Therefore such weighting procedures are not discussed here. The homogeneity of variances is discussed in more detail in the following section.

VARIATION OF THE S.D. OR R.S.D. IN y, WITH x

Some special cases

The condition that the s.d. of y should be independent of x was mentioned above. It will be shown below that by mathematical manipulation this condition may sometimes be changed to the condition that the r.s.d. of y should be independent of x. Therefore in the present section, the variation of the s.d. or r.s.d. of y within the range of x values applied for calibration is discussed in a more general way.

It seems difficult to give a single general discussion for all practical procedures, but some cases where the final measurement only is considered are well known. For counting errors, the s.d. increases with $N^{\frac{1}{2}}$, and the r.s.d. decreases with $N^{-\frac{1}{2}}$ (N = number of counts). In photometric analysis the Ringbom curve [17] is frequently cited, sometimes with some adaptations. In its original form, the Ringbom curve indicates that the r.s.d. in photometric measurements is reasonably constant if absorbance values between about 0.2 and 0.75 are considered. It seems unusual in the literature to consider the variation of the s.d. with absorbance; calculation shows that it is reasonably constant at lower absorbance values, but increases greatly at higher values (Table 2). (If the assumptions made are different from Ringbom's, other values are obtained, but the trend is similar.)

In many analytical procedures the sample preparation step may contribute more to the total error than the final measurement does. Here, too, a general theory for calculating the variation of the s.d. with the analyte content is not available. Agterdenbos [18] suggested that the total standard deviation may sometimes be found by (quadratic) addition of a s.d. and a r.s.d. component; quadratic addition is required because variances are additive. An obvious consequence of this consideration is that at smaller x values the s.d. is constant ("homogeneous") and at larger x values the r.s.d. is constant.

The situation considered here is similar to that discussed by Boumans [19, 20]. He suggests that inductively-coupled plasmas applied in emission

TABLE 2

Variation of s.d. and r.s.d. (both in arbitrary units) with absorbance A if the precision of the transmittance measurement is considered independent of transmittance

A	0.01	0.02	0.05	0.10	0.15	0.20	0.30
S.d.	0.444	0.455	0.487	0.547	0.613	0.688	0.867
R.s.d.	44.4	22.7	9.75	5.47	4.09	3.44	2.89
A	0.40	0.50	0.70	1.00	1.20	1.50	
S.d.	1.09	1.37	2.18	4.34	6.88	13.7	
R.s.d.	2.73	2.75	3.11	4.34	5.74	9.16	

spectroscopy behave as fluctuation-noise limited systems. Measurements with such a plasma, therefore, also give a total standard deviation composed of a s.d. and a r.s.d. component. For this consideration a relation between σ_{rt}, σ_r, p, k (see below) and x was derived [20].

Regions for constant s.d. and constant r.s.d.

The assumption that the total standard deviation is composed of a s.d. and a r.s.d. component seems useful for discussions of the homogeneity of variances in calibration. The following discussion shows which is the upper limit of the region where the s.d. is approximately constant and which is the lower limit of the region where the r.s.d. is approximately constant. By "approximately constant" is meant that σ_t or σ_{rt} does not vary by more than a factor $(z-1)$ where z is either 1.1 or 1.2 over the range of x values considered. Also $\sigma < \sigma_t < z\sigma$ and $\sigma_r < \sigma_{rt} < z\sigma_r$, with $z = 1.1$ or 1.2.

In the calculation the detection limit p may be introduced: $p = k\sigma$, where k depends on the risk accepted for drawing false conclusions (often, $k = 2$ or 3). The total standard deviation is then

$$\sigma_t = \left\{\left(\frac{1}{k}\cdot p\right)^2 + x^2\sigma_r^2\right\}^{\frac{1}{2}} \text{ or } \sigma_{rt} = \left\{\left(\frac{1}{k}\cdot\frac{p}{x}\right)^2 + \sigma_r^2\right\}^{\frac{1}{2}} \tag{7}$$

The equation for σ_{rt} is equivalent to that given by Boumans [20]. From eqns. (7) it follows that:

$\sigma < \sigma_t < z\sigma$ if $0 < x < p\,(z^2-1)^{\frac{1}{2}}/k\sigma_r$ and $\sigma_r < \sigma_{rt} < z\sigma_r$

if $\infty > x > p/k\,(z^2-1)^{\frac{1}{2}}$.

From these relations, limits for x can be calculated. Some examples for $k = 3$ are: $\sigma < \sigma_t < 1.1\sigma$ if $x < 0.153\,p/\sigma_r$; $\sigma < \sigma_t < 1.2\sigma$ if $x < 0.221\,p/\sigma_r$; $\sigma_r < \sigma_{rt} < 1.1\sigma_r$ if $x > 0.73\,p/\sigma_r$; and $\sigma_r < \sigma_{rt} < 1.2\sigma_r$ if $x > 0.50\,p/\sigma_r$.

One conclusion is that with $\sigma_r = 1\%$ and $z = 1.2$ (i.e. a variation of 20% in σ_t or σ_{rt}) σ can be considered as a constant if $x < 22p$ and σ_r as a constant if $x > 50p$. The region of x values where neither σ nor σ_r can be considered constant is only a factor $q = 50{:}22 = 2.3$. The value of q is independent of σ_r. If $z = 1.1$ (i.e. a variation of 10% in σ_t or σ_{rt}), $q = 73{:}15.3 = 4.8$. Actually q is proportional to (z^2-1).

SELECTION OF A CALIBRATION RELATION

In selecting a calibration relation, it is seldom realized that an important difference exists between the application of eqn. (1) or (2) on the one hand and eqn. (3) on the other hand, if the variation of the s.d. with x is considered. In Fig. 1 (a, b), linear relationships hold. In Fig. 1(a) the s.d. of y represented by vertical bars has the same value for all values of x; the conditions of homogeneity of variances is fulfilled. In Fig. 1(b) however, the s.d. increases regularly with y; the r.s.d. is constant, but the condition required is not fulfilled. Figure 1(c) is a logarithmic plot and the vertical bars show a constant value for the s.d. of log y. Therefore when eqn. (3) is applied, the homogeneity of variances is fulfilled in this instance. However, the situation that the s.d. of log y is independent of x implies that the r.s.d.of y is independent of x. This is the same situation as in Fig. 1(b) but now conditions for application of the usual type of calculation are fulfilled.

It is possible, therefore, to apply the usual method of calculation even if the r.s.d. is constant, but in this case the logarithmic eqn. (3) has to be used. A limitation of the latter equation, however, is that it cannot be used when $y \neq 0$ at $x = 0$. In such cases all y values measured can be diminished by the y value found for $x = 0$ ("blank"). This subtraction can be applied in many problems but it may suggest too high a precision in the results if the blank s.d. is too large. A difference between eqns. (2) and (3) is that eqn. (3) represents a non-linear relation between x and y in the general case that $b_3 \neq 1$. In this respect it seems somewhat equivalent to eqn. (4), and so it could be concluded that for non-linear relations between x and y, it is preferable to apply eqn. (3) if the r.s.d. of y is independent of x, and to apply eqn. (4) if the s.d. of y is independent of x.

Another important consideration in selecting eqn. (3) or (4) as a calibration equation is that the equation applied must represent correctly the true relationship between x and y. Some preliminary calculations [8] showed that if the curvature is only slight, the validity of one of these equations

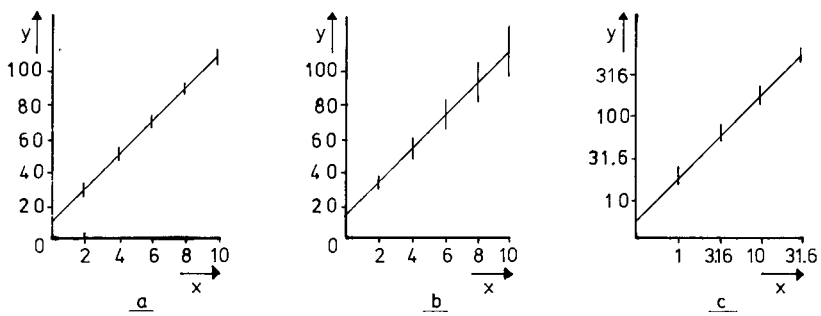


Fig. 1. Variation of the standard deviation in the signal y with the content x: (a) s.d. of y independent of x; (b) s.d. of y proportional to y, r.s.d. of y independent of x; (c) logarithmic plot with s.d. of log y independent of x, and r.s.d. of y independent of x.

implies that the other is also valid to a good approximation (of course after subtraction of any blank present). With large curvature, however, only one of the equations can be valid.

A relation that may be useful in the case of a constant r.s.d. of y if eqn. (3) does not apply, is eqn. (6), which was found satisfactory in some atomic absorption measurements [8]. For a linear relation between x and y and a constant r.s.d., eqn. (5) can be useful.

The conclusion that logarithmic calibration curves may be applied advantageously in situations where the r.s.d. is approximately independent of x, suggests that analytical instruments designed to perform the types of analyses where this situation can be expected, should be designed with appropriate calculation units.

Finally, it should be considered that for a straight-line plot (Fig. 1, a, b, c) a constant value of the s.d. of y or $\log y$ corresponds to a constant value of the s.d. of x or $\log x$. For a non-linear plot (eqn. 4 or 6), however, a constant value of s.d. or r.s.d. in y results in a gradually varying value of the s.d. or r.s.d. of x.

Errors in testing hypotheses

In calibration, statistical tests are sometimes applied to obtain information on the validity of assumptions or approximations. Such tests have been applied [5, 6] in testing the homogeneity of variances, in testing if a relation between x and y is curved, and in testing if the s.d. of the calibration procedure differs from the s.d. of the analysis of the real sample.

If hypotheses are tested, two types of errors can be made. First, the hypothesis is correct but it is assumed that it is false. This is an error of the first kind, and its probability is represented by α. Secondly, the hypothesis is incorrect but it is not rejected and is assumed to be correct (an error of the second kind with probability β). The maximum acceptable values for α and β should depend on the consequence of making a false decision. For α, a value of 0.10, 0.05 or 0.01 is often considered acceptable. Acceptable values for β are seldom given, however. This may be due partly to the fact that calculation of β is possible only for rather simple cases. An important reason why calculation of β is difficult is that it depends on the degree of incorrectness of the hypothesis, and this degree is difficult to describe in most cases.

An unwanted consequence of the difficulty of calculating β is that in many cases the existence of β is completely ignored. In such cases the hypothesis is considered correct if it cannot be proved that it is incorrect, even if β is large. This way of drawing statistical conclusions is comparable in some respects to drawing the analytical conclusion that a component is not present in a mixture because it cannot be detected, if one is not aware of the detection limit of the analytical method applied. Application of a different analytical method may give a positive result. Analogously, if it is considered necessary to test the hypothesis that homogeneity of variance exists, the result may depend on the type of statistical test applied [8]. It

is clear that other factors such as the number of observations also influence the probability that inhomogeneity will be detected. In the literature on analytical calibration no attention seems to have been given to this point.

A last point to be mentioned is that Gottschalk [6] applied a "heuristic" procedure. This can be demonstrated with an example: if eqn. (4) is applied and parameter c is found to be significantly different from zero, the conclusion may be that the application of the simpler eqn. (2) is not allowed. However, if c is so small that it may be neglected without significantly influencing the conclusions drawn about the analyte content of the sample, it may be preferable that eqn. (2) is applied. It seems that this is a good philosophy but good criteria for neglecting c must be given.

CONCLUSIONS

Calibration curves can be prepared in several ways. The simplest seems to be the graphical presentation, but very often mathematical procedures are applied, which can have different degrees of complexity. A discussion and comparison of graphical presentation and several mathematical procedures has been given by Kelly [21].

One limitation of the present paper is that only calibrations based on the method of least squares have been discussed. A second limitation is that the mathematical relations between x and y are rather simple. More complex relationships may be required in some practical situations. Some of these have been discussed recently by Schwartz [13]. However, the limitation of the present paper seem justified for at least two reasons: (a) the method of least squares is applied frequently in practice; (b) too frequently, analysts are not sufficiently aware of the assumptions and approximations made in their calculations and of the errors made in the final conclusions on the content of the unknown sample, if deviations arising from the assumptions made are too large.

The problem has been discussed only qualitatively here, and a more quantitative discussion is required. Some of the points to be included in such a more quantitative discussion, which will be discussed in further papers are the following: methods of detecting non-linearity of calibration curves and if possible a comparison of the "quality" of such methods; errors caused by the application of an improper calibration curve; dependence of the error on the degree of curvature and of the range of the calibration curve; methods of detecting inhomogeneity of variances and errors caused by unjustified assumptions of homogeneity; optimum location of calibration points on the x-axis if the number of observations is fixed.

REFERENCES

1 W. J. Dixon and F. J. Massey, Jr., Introduction to Statistical Analysis, 2nd edn., McGraw-Hill. New York, 1957.
2 W. J. Youden, Statistical Methods for Chemists, J. Wiley, New York, 1951.

3 K. Doerffel, Beurteilung von Analyseverfahren und Ergebnissen, Springer, Berlin, 1962.
4 V. V. Nalimov, The Application of Mathematical Statistics to Chemical Analysis, Pergamon, Oxford, 1963.
5 F. J. M. J. Maessen, J. W. Elgersma and P. W. J. M. Boumans, Spectrochim. Acta, Part B, 31 (1976) 179.
6 G. Gottschalk, Fresenius Z. Anal. Chem., 276 (1975) 81.
7 G. Gottschalk, Fresenius Z. Anal. Chem., 275 (1975) 1; 276 (1975) 257; 278 (1976) 1; 280 (1976) 205; 282 (1976) 1.
8 J. Agterdenbos, Unpublished work presented at XXth C.S.I., 7 I.C.A.S., Strbske Pleso, 1977 and Euroanalysis III, Dublin 1978.
9 C. T. Shewell, Anal. Chem., 32 (1960) 1535.
10 J. Mandel and F. J. Linnig, Anal. Chem., 29 (1957) 743.
11 J. Mandel, The Statistical Analysis of Experimental Data, Interscience, New York, 1964.
12 J. P. Franke and R. A. de Zeeuw, Anal. Chem., 50 (1978) 1374.
13 L. M. Schwartz, Anal. Chem., 49 (1977) 2062.
14 H. C. Wagenaar, I. Novotny and L. de Galan, Spectrochim. Acta, Part B, 29 (1974) 301.
15 J. Agterdenbos and J. Vlogtman, Talanta, 21 (1974) 231.
16 L. M. Schwartz, Anal. Chem., 48 (1976) 2287.
17 A. Ringbom, Fresenius Z. Anal. Chem., 115 (1938) 332.
18 J. Agterdenbos, Fresenius Z. Anal. Chem., 154 (1957) 401; 157 (1957) 161; 159 (1958) 202.
19 P. W. J. M. Boumans, Spectrochim. Acta, Part B, 31 (1976) 147.
20 P. W. J. M. Boumans, Fresenius Z. Anal. Chem., in press
21 P. C. Kelly, Anal. Chem., 44 (1972) 28A.

Analytica Chimica Acta, 108 (1979) 325—332
© Elsevier Scientific Publishing Company, Amsterdam — Printed in The Netherlands

CONTAMINATION OF WATER AND ORGANIC SOLVENTS STORED IN PLASTIC BOTTLES WITH PHTHALATE ESTER PLASTICIZERS

SADAO MORI

Department of Industrial Chemistry, Faculty of Engineering, Mie University, Tsu, Mie 514 (Japan)

(Received 3rd January 1979)

SUMMARY

Migration of phthalic acid esters into water, n-hexane, and methanol kept in polyethylene bottles or PVC tubes was investigated by high-performance liquid chromatography with a variable wavelength u.v. detector. The content of esters in water kept in contact with PVC for one day was 0.44 ppm and the migration rate of dibutyl phthalate was 4.8×10^{-5} mg h^{-1} cm^{-2} of PVC tube. n-Hexane stored in a polyethylene bottle for 7 days contained 6 ppm esters; the migration rate of dibutyl phthalate was 6.4×10^{-5} mg h^{-1} cm^{-2} of polyethylene. PVC tubing connected to ion-exchange resin columns contaminates deionized water with the esters.

Phthalic acid esters are added to plastic resins to improve flexibility; their content varies widely with the end use but can be ca. 30% by weight. Besides these plasticizers, other additives, e.g., antioxidants, colorants, flame retardants and stabilizers, may also be incorporated into plastics; these additives diffuse and dissolve in solvents in contact with the polymer surface. Phthalates have been detected in deionized water stored in a polyethylene bottle [1].

Phthalic acid esters, which account for over half the plasticizers used, are toxic to vital organisms and are widely dispersed in the environment [2]; they are, of course, present in common plastic laboratory ware. In analysis of many organic substances, contamination by plasticizers must be avoided, but detailed studies of this problem have not been reported. This study was undertaken to investigate the contamination with phthalic acid esters of water and organic solvents kept in plastic bottles.

Phthalic acid esters in environmental samples have been determined by gas chromatography with an electron capture detector [2] and by high-performance liquid chromatography (h.p.l.c.) with a u.v. detector [1]. The latter technique is employed here.

EXPERIMENTAL

Apparatus

A Jasco (Japan Spectroscopic Co., Ltd., Hachioji, Tokyo 192) Trirotar high-performance liquid chromatograph was used with a Jasco Model Uvidec-100 variable-wavelength u.v. detector, operated at 224 nm with a 10-mm microcell. The stainless-steel column (50 cm × 2.3 mm i.d.) was packed with Shodex HP-255 porous polystyrene gel (25 ± 3 μm).

Samples and reagents

Polyvinyl chloride (PVC) soft tubing (5 mm i.d., 7 mm o.d.) and 100-ml polyethylene bottles were used as sample plastics, with methanol, n-hexane (both reagent grade), and water as solvents. Water was distilled in glass apparatus and stored in a glass bottle. These three solvents were checked for contamination by phthalic acid esters before use.

Procedure

The sample plastics were rinsed with n-hexane and methanol to eliminate surface contaminants. Two 5-cm lengths of PVC tube were immersed in 100 ml of each of the three solvents in glass-stoppered Erlenmeyer flasks. Polyethylene bottles, each filled with 100 ml of a solvent, and the Erlenmeyer flasks were stored in a dark place at room temperature for a specified time. Then the n-hexane solution was transferred to a 100-ml volumetric flask and the volume was made up to the mark with n-hexane (henceforth referred to as the n-hexane sample). The methanol solution was concentrated on a rotary evaporator at room temperature; the concentrate was transferred to a 100-ml volumetric flask and made up to the mark with n-hexane (henceforth referred to as the methanol sample). The organic content of the water solution was extracted with 10 ml of n-hexane, after addition of 1.0 ml of purified 10% (w/v) sodium chloride solution, for 10 min on a mechanical shaker; the organic layer was transferred to a 10-ml volumetric flask and the volume was made up with n-hexane. These n-hexane extracts (henceforth referred to as the water sample) were examined by h.p.l.c.

To check the original phthalic acid ester content of the sample plastics (1-cm squares), Soxhlet extraction and extraction with boiling methanol or n-hexane for 6 h were operated in parallel. Contamination of water from deionization with ion-exchange resins was a major problem [1]. Samples (100 ml) taken from several points of the deionization apparatus, as shown in Fig. 1, were extracted with slight modifications of the procedures described above.

Methanol and n-hexane (reagent grade) were used without further purification as the mobile phases in h.p.l.c. at a flow rate of 1.0 ml min^{-1}. All measurements were made at room temperature. Sample injection volumes were 0.1 or 0.01 ml and attenuation was between 0.16 and 0.02 AUFS as required. A calibration curve for each phthalic acid ester was constructed by plotting peak height against the concentration of the standard solution.

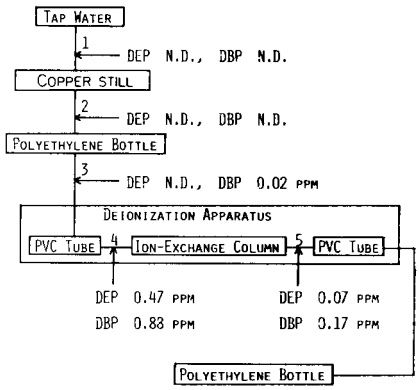


Fig. 1. Block diagram of the deionization process and the phthalate contents at the sampling points. N.D. means not detected.

RESULTS AND DISCUSSION

A variety of organic and inorganic materials may be present in plastics as additives; this discussion is focussed on phthalic acid esters because they are among the most abundantly used additives and can dissolve in both aqueous and non-aqueous solvents.

Most of the h.p.l.c. analyses were done with n-hexane as the mobile phase; if necessary to eliminate interferences between peaks, and for complete qualitative analyses, methanol was used. The chromatograms for the solvent samples showed two to three peaks; these were shown to correspond to the diethyl (DEP), dibutyl (DBP), or di-2-ethylhexyl (DEHP) phthalates, by fractionating these peaks and comparing their i.r. spectra with those of standard phthalates. This qualitative analysis was confirmed by direct comparison of the retention volumes with n-hexane and methanol as the mobile phases.

Examples of the chromatograms for the solvent samples are shown in Figs. 2 and 3. Phthalic acid esters were the only u.v.-sensitive constituents detected in the PVC tube extracts. Extracts from polyethylene bottles, however, gave u.v.-sensitive materials in addition to phthalic acid esters. These materials eluted around the DEHP peak (Fig. 3A), and hence reverse-phase chromatography with methanol as the mobile phase was used simultaneously (Fig. 3B).

Tables 1 and 2 show the amounts of contamination leached from the PVC tubes and polyethylene bottles. The extraction of phthalate esters by n-hexane was greater than that by methanol. Contamination of water was slight but could not be ignored. Table 1 indicates that the extent of the migration of DBP into water was 1 μg per cm^2 of PVC tube per day (3.8 μg in a week). Similarly, 0.022 μg of DBP per cm^2 of polyethylene bottle migrated into water in a week. For DBP, the extraction into n-hexane was 5.05 mg per cm^2 of PVC

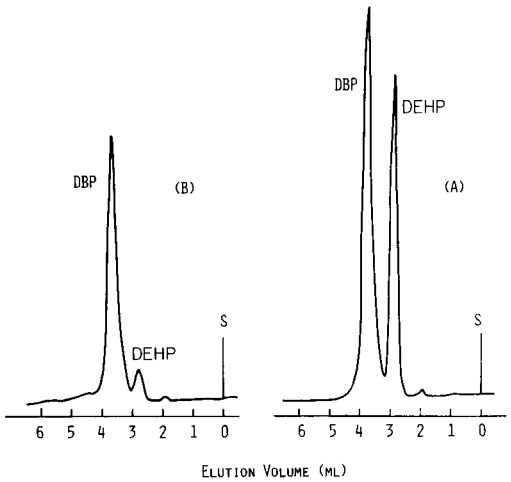


Fig. 2. Chromatograms of the u.v.-sensitive constituents in the methanol (A) and water (B) samples from PVC tubing. Immersion periods: (A) 1 day; (B) 30 days. Injection volume: (A) 0.01 ml, (B) 0.10 ml. Mobile phase, n-hexane; attenuation, 0.08 AUFS.

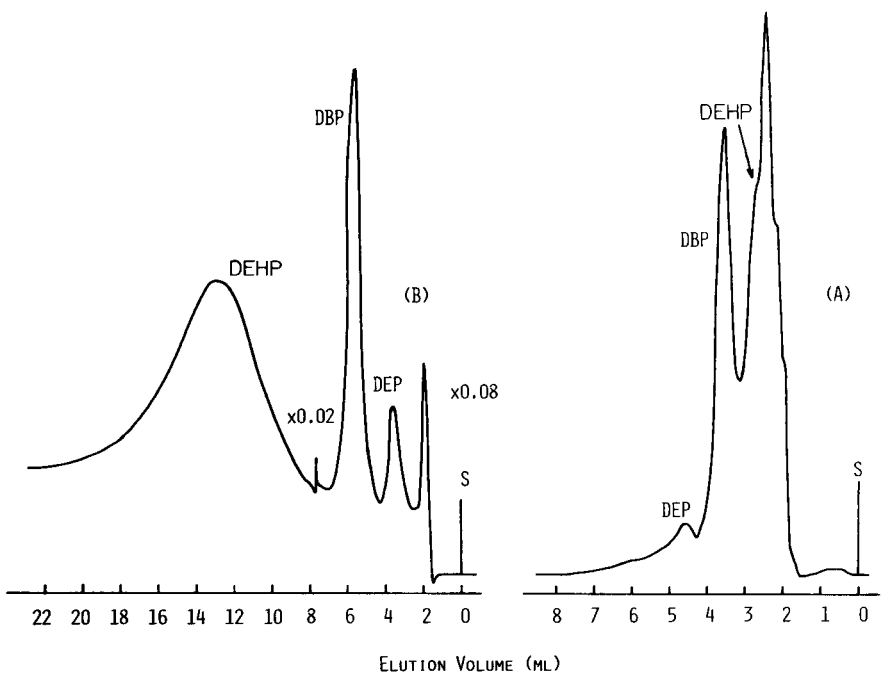


Fig. 3. Chromatograms of the u.v.-sensitive constituents in the n-hexane sample from polyethylene bottles after immersion for 30 days. Mobile phase: (A) n-hexane, (B) methanol; sample injection volume: (A) 0.01 ml, (B) 0.10 ml; attenuation: (A) 0.02 AUFS, (B) 0.08 and 0.02 AUFS.

TABLE 1

Migration of phthalic acid esters from PVC tubes to solvents

Solvent	Immersion period (day)	DBP content[a] (ppm)	DBP/PVC tube (% w/w)[b]	DBP/PVC tube ($mg\ cm^{-2}$)[c]	DEHP content[a] (ppm)	DEHP/PVC tube (% w/w)[b]	DEHP/PVC tube ($mg\ cm^{-2}$)[c]
Water	1	0.39	1.5×10^{-3}	0.001	0.045	2×10^{-4}	0.0001
	7	1.52	6.1×10^{-3}	0.0038	0.074	3×10^{-4}	0.0002
	30	2.88	1.09×10^{-2}	0.0071	0.155	6×10^{-4}	0.0004
n-Hexane	0.125	410	3.21	2.03	556	4.3	2.75
	1	1020	8.05	5.05	1390	11.0	6.88
	7	1320	10.40	6.53	2110	16.7	10.44
	Hot extn.[d]	1066	8.45	5.28	924	7.32	4.57
	Soxhlet extn.[d]	1090	8.85	5.40	980	7.95	4.85
Methanol	0.125	170	1.38	0.84	139	1.13	0.69
	1	422	3.35	2.09	336	2.67	1.66
	7	935	7.37	4.63	693	5.47	3.43
	Hot extn.[d]	908	7.26	4.50	816	6.53	4.04
	Soxhlet extn.[d]	763	6.26	3.78	616	5.05	3.05

[a]Phthalic acid ester content in solvent samples. [b]Weight of phthalic acid esters migrated from 1 g of PVC tube. [c]Weight of phthalic acid esters migrated from 1 cm^2 of PVC tube. [d]Immersion period, 6 h.

tube per day and 1.24 μg per cm^2 of polyethylene bottle per day. PVC tube immersed in n-hexane decreased in weight by ca. 27% in 7 days. The migration of esters is governed by the solubility of the esters in the solvent and by the diffusion rate in the plastics. Complete extraction of the esters in a polymer matrix was impossible even by exhaustive Soxhlet extraction and/or extraction by boiling solvent. DEHP in PVC tube was shown to be present to a greater extent than DBP by size-exclusion chromatography. However, regardless of the original content of esters in PVC tube, the migration of DEHP into water was significantly less than that of DBP.

The phthalic acid ester content in polyethylene is slight, but the problem of contamination by these esters is serious. They are most efficiently extracted by boiling solvent. DEP was detected in all the n-hexane samples and in the methanol sample after hot extraction.

The migration rate of the esters into solvents increased with decreased immersion time. The value obtained by plotting immersion time vs. the values in Tables 1 and 2 divided by immersion time, and by extrapolating to zero time, corresponds to the approximate initial migration rate of the esters at the start of the immersion of the plastics in the solvent. The results are shown in Table 3. From these results, it may be possible to estimate the extent of contamination of solvents in contact with plastics.

TABLE 2

Migration of phthalic acid esters from polyethylene bottles to solvents

Solvent	Immersion period (day)	DBP content[a] (ppm)	DBP/polyethylene		DEHP content[a] (ppm)	DEHP/polyethylene		DEP content[a] (ppm)	DEP/polyethylene	
			($\mu g\ g^{-1}$)[b]	($\mu g\ cm^{-2}$)[c]		($\mu g\ g^{-1}$)[b]	($\mu g\ cm^{-2}$)[c]		($\mu g\ g^{-1}$)[b]	($\mu g\ cm^{-2}$)[c]
Water	7	0.022	0.32	0.022	0.022	0.31	0.022			
	30	0.029	0.41	0.028	0.052	0.73	0.050			
n-Hexane	1	1.28	18.2	1.24	1.43	20.3	1.38	0.309	4.39	0.30
	7	3.59	51.0	3.47	2.15	30.5	2.07	0.402	5.71	0.39
	30	5.05	71.7	4.88	3.45	49.0	3.34	0.675	9.58	0.65
	Hot extn.[d]	8.75	43.8	1.27	15.3	76.6	2.22	1.60	8.01	0.23
	Soxhlet extn.[d]	7.52	61.5	2.31	4.68	38.3	1.43	0.725	5.93	0.22
Methanol	1	0.096	1.41	0.09	0.072	1.02	0.07			
	7	0.221	3.14	0.21	0.114	1.62	0.11			
	30	0.192	2.73	0.19	0.288	4.09	0.28			
	Hot extn.[d]	8.1	37.6	1.18	2.60	12.0	0.38	1.50	9.5	0.30
	Soxhlet extn.[d]	1.58	14.4	0.48	1.21	11.0	0.37			

[a,b,c,d] As in Table 1.

TABLE 3

The approximate initial migration rates of the phthalic acid esters from plastics

Solvent	DBP		DEHP		DEP	
	(ppm h^{-1})	(mg cm^{-2} h^{-1})	(ppm h^{-1})	(mg cm^{-2} h^{-1})	(ppm h^{-1})	(mg cm^{-2} h^{-1})
PVC tube						
Water	0.018	4.8×10^{-5}	0.0024	5.5×10^{-6}		
n-Hexane	190	1.10	225	1.40		
Methanol	120	0.59	90	0.45		
Polyethylene bottle						
Water	2.0×10^{-4}	2.0×10^{-7}	2.0×10^{-4}	2.0×10^{-7}		
n-Hexane	0.065	6.4×10^{-5}	0.08	8.0×10^{-5}	0.022	2.2×10^{-5}
Methanol	5.2×10^{-3}	5.0×10^{-6}	4.0×10^{-3}	4.0×10^{-6}		

Distilled water from a copper still was stored in a polyethylene bottle for 4 weeks before it was subjected to the deionization process. The stored water, which contained 0.02 ppm DBP (the third sampling point, Fig. 1), was poured into the deionization apparatus for 1 h and then the water was collected at the fourth and fifth sampling points. The phthalic acid ester contents of the samples are shown in Fig. 1. The ratio of water to n-hexane for solvent extraction was 20: 1 (v/v) and the extract was concentrated to about one-third of its initial volume. DEHP was not detected; the detection limit was 0.007 ppm of phthalate in the water. Phthalic acid esters were shown not to be eluted from the ion-exchange column in a separate experiment; this implies that the small quantities of esters in the water at the fifth sampling point originated from the esters at the fourth sampling point, so that the contamination of the deionized water by the phthalic acid esters was caused mainly by the PVC tube used in the apparatus.

The author thanks Professor A. Mizuike (Nagoya University) for many helpful suggestions and discussions; this work was supported in part by funds from Ministry of Education, Japan grant 235049.

REFERENCES

1 S. Mori, J. Chromatogr., 129 (1976) 53.
2 C. S. Giam, H. S. Chan and G. S. Neff, Anal. Chem., 47 (1975) 2225.

Analytica Chimica Acta, 108 (1979) 333—345
© Elsevier Scientific Publishing Company, Amsterdam — Printed in The Netherlands

ETUDE DES COMPLEXES SULFOSALICYLATE DE CUIVRE(II), NICKEL(II), COBALT(II) ET URANYLE(II) A L'AIDE D'UNE RESINE ECHANGEUSE DE CATIONS

F. CHOUAIB[‡] et C. POITRENAUD*

Institut National des Sciences et Techniques Nucléaires, B.P. n° 6, 91190 Gif-sur-Yvette (France)

(Reçu le 24 Novembre 1978)

RESUME

Les constantes conditionnelles des complexes 1:1 que donnent les ions sulfosalicylate (L^{3-}) avec les cations du cuivre(II), du nickel(II), du cobalt(II) et de l'uranium(VI) ont été déterminées en milieu perchlorate de sodium 0,1 M et à différents pH, à l'aide d'une méthode d'échange d'ions déduite de celle de Schubert. Les conditions dans lesquelles cette méthode doit être utilisée ainsi que les limites de ses possibilités ont été étudiées en détail. La variation avec le pH des constantes conditionnelles obtenues a permis de mettre en évidence l'existence des complexes 1:1 suivants: CuH_2L^+, $CuHL$, CuL^-; NiH_2L^+, $NiHL$, NiL^-; $CoHL$, CoL^-; $UO_2H_2L^+$, UO_2HL, UO_2L^- et UO_2LOH^{2-}. Les constantes de stabilité de ces complexes ont été mesurées. Les diagrammes de répartition des différents complexes de chaque élément en fonction du pH et de la concentration totale de sulfosalicylate en solution ont été tracés.

SUMMARY

Study of the sulphosalicylate complexes of copper(II), nickel(II), cobalt(II) and uranyl(II) by means of cation-exchange resins.

The conditional stability constants of the 1:1 complexes of the sulphosalicylate ions (L^{3-}) with copper(II), nickel(II), cobalt(II) and uranyl ions have been determined in a sodium perchlorate solution (0.1 M) and at various pH values by a cation-exchange method based on Schubert's procedure. The limits of application of the method are discussed. The variation with pH of the conditional stability constants can be explained by the existence of the complexes: CuH_2L, $CuHL$, CuL^-; NiH_2L^+, $NiHL$, NiL^-; $CoHL$, CoL^-; $UO_2H_2L^+$, UO_2HL, UO_2L^-, UO_2LOH^{2-}. The stability constants of these complexes are reported. Distribution diagrams of the various complexes of each element with pH and total concentration of sulphosalicylate parameters are given.

Les acides organiques solubles dans l'eau et capables de donner des complexes avec les éléments métalliques peuvent être utilisés pour masquer ces éléments en solution. Les conditions (pH, concentration de complexant) dans lesquelles un masquage sélectif peut être obtenu sont à déterminer par un calcul qui nécessite la connaissance précise de la nature et des constantes de stabilité des complexes.

[‡] Adresse actuelle: Facultad de Quimica, UNAM, Ciudad Universitaria, Mexico 20 DF.

Dans le cas des complexes que donne l'acide sulfosalicylique (H_3L) avec les éléments métalliques (M) les tables de constantes [1, 2] fournissent principalement les constantes des complexes 1:1 (ML); 1:2 (ML_2) et éventuellement 1:3 (ML_3). Or, dans certains cas il a été montré que ces complexes simples avaient des propriétés acides ou basiques et pouvaient coexister avec des complexes mixtes protonés MH_jL_i ou hydroxylés ML_iOH_j. Des constantes de stabilité de tels complexes mixtes ont déjà été publiées pour quelques éléments tels que Be(II) [3], Ce(III) [4], Cu(II) [5], les terres rares [4], Ti(IV) [6], U(VI) [7—9] et V(IV) [10]. Pour compléter les connaissances déjà acquises sur les complexes sulfosalicyliques nous avons effectué une étude détaillée des complexes de plusieurs éléments: le cuivre(II) qui nous a servi d'élément de référence et le nickel(II), le cobalt(II) et l'uranyle(II), éléments dont les complexes mixtes protonés ou hydroxylés ont été peu étudiés.

Les constantes de stabilité des complexes d'un élément métallique peuvent être déterminées à partir de la variation du coefficient de partage de cet élément entre la solution et une résine échangeuse de cations en fonction de la concentration du complexant en solution. Cette méthode a été mise au point par Schubert [11] qui a envisagé le cas simple où l'élément métallique M ne donne qu'un seul complexe en solution et n'existe dans la résine que sous forme de cation M^{n+}. Elle a ensuite été développée par de nombreux auteurs, en particulier par Fronaeus [12]. Les améliorations apportées à la méthode de Schubert consistent essentiellement à tenir compte des réactions secondaires qui se superposent aux réactions principales d'échange d'ions et de formation de complexes.

Les phénomènes pris en considération sont: la variation des constantes d'échange d'ions avec la composition ionique de la résine; la pénétration dans la résine des complexes cationiques de l'élément étudié; la pénétration dans la résine des ions H^+ aux faibles pH en solution; l'hydrolyse des cations métalliques en solution; la formation de complexes entre les anions du complexant et le cation en général alcalin de l'électrolyte; et la formation de complexes entre l'élément métallique et les ions du tampon qui impose le pH en solution.

Actuellement cette méthode est suffisamment bien au point pour être utilisée à la place ou comme vérification des autres méthodes classiques de détermination des constantes de stabilité des complexes. Nous l'avons appliquée au cas des complexes sulfosalicylate de Cu(II), Co(II), Ni(II) et U(VI) en nous efforçant de tenir compte de tous les phénomènes cités plus haut.

PRINCIPES THEORIQUES DE LA METHODE

Description du système utilisé

Supposons que l'on mette en contact une résine échangeuse de cations sous forme ionique Na^+ et une solution contenant par exemple du perchlorate de l'ion M^{2+} et de l'acide sulfosalicylique en présence de perchlorate de sodium à la concentration 0,1 M, le pH de la solution étant imposé par un tampon B.

Les espèces, autres que H^+, OH^-, Na^+ et ClO_4^-, pouvant exister en solution sont: (a) les ions sulfosalicylate L^{3-}, LH^{2-} et LH_2^- et éventuellement les paires d'ions qu'ils donnent avec les ions Na^+; (b) les ions métalliques M^{2+} et leurs complexes autres que sulfosalicyliques (avec OH^-, avec les ions apportés par le tampon ...); et (c) les complexes sulfosalicylate métalliques ML^-, ML_2^{4-} ... et leurs dérivés protonés ou hydroxylés $MH_iL(OH)_j$ ou $MH_iL_2(OH)_j$.

Dans ce qui suit les propriétés acide—base de l'acide sulfosalicylique seront caractérisées par les constantes conditionnelles:

$$K_2 = [H^+]([HL^{2-}] + [NaHL^-])/([H_2L^-] + [NaH_2L])$$

et $$K_3 = [H^+]([L^{3-}] + [NaL^{2-}])/([HL^{2-}] + [NaHL^-])$$

La stabilité des complexes sulfosalicylate sera mesurée par les constantes conditionnelles:

$$\beta_{1L} = [ML^-]/[M^{2+}]([L^{3-}] + [NaL^{2-}]) \quad \text{et} \quad \beta_{2L} = [ML_2^{4-}]/[M^{2+}]([L^{3-}] + [NaL^{2-}])$$

et par les constantes de dissociation $K^{iH,jOH}_{MH_iL(OH)_j}$ et $K^{LHjOH}_{MH_iL_2(OH)_j}$ des complexes $MH_iL(OH)_j$ et $MH_iL_2(OH)_j$ en H^+, OH^- et ML^- ou ML_2^{4-}.

Dans la solution qui imbibe la résine, outre les groupements fonctionnels ionisés, les seules espèces qui peuvent exister sont les ions Na^+, les ions M^{2+} et H^+ résultant d'échanges entre la solution et la résine initialement saturée en ions Na^+, des complexes cationiques du type MX^+ qui, dans les conditions choisies, restent en concentration faible devant celle des ions M^{2+} et enfin des anions provenant du partage de solutés ioniques, phénomène que l'on peut ignorer aux faibles concentrations ioniques utilisées (0,1 M).

Expression du coefficient limite de partage global d'un élément M

D'après ce qui précède, le coefficient de partage global de l'élément métallique, rapport des concentrations totales de l'élément dans la résine (R) et la solution (s) s'exprime donc par:

$$D = [M^{2+}]_R/\{[M^{2+}]_s + [MOH^+]_s + ... + [MB]_s + ... + [ML^-]_s + \sum_{ij}[MH_iL(OH)_j] + [ML_2^{4-}]_s + \sum_{ij}[MH_iL_2(OH)_j]\} \quad (1)$$

Le dénominateur de cette expression représentant la concentration totale $[M]_{Ts}$ de l'élément M en solution peut s'écrire:

$$[M]_{Ts} = [M^{2+}]_s\left(\alpha_{MOH} + \alpha_B - 1 + \frac{[L]_T\beta_{1L}}{\alpha_{HL}}\sum_{ij}\frac{(K_{H_2O})^j[H^+]^{i-j}}{K^{iH,jOH}_{MLH_i(OH)_j}} + \frac{[L]_T^2\beta_{2L}}{\alpha_{HL}^2}\sum_{ij}\frac{(K_{H_2O})^j[H^+]^{i-j}}{K^{iH,jOH}_{ML_2H_i(OH)_j}}\right) \quad (2)$$

Dans cette expression α_{MOH}, α_T et α_{LH} sont les coefficients de complexation de M^{2+} par OH^- et les ions du tampon et de L^{3-} par H^+ tels que les définit

Ringbom [2]. $[L]_T$ est la concentration totale en solution des ions sulfosalicylate non complexés par M et K_{H_2O} est le produit ionique de l'eau. Si l'on définit δ et γ par:

$$\delta = \frac{\beta_{1L}}{\alpha_{HL}} \sum_{ij} \frac{(K_{H_2O})^j [H^+]^{i-j}}{K^{iH,jOH}_{MLH_i(OH)_j}} \quad \text{et} \quad \gamma = \frac{\beta_{2L}}{(\alpha_{HL})^2} \sum_{ij} \frac{(K_{H_2O})^j [H^+]^{i-j}}{K^{iH,jOH}_{ML_2H_i(OH)_j}}$$

on peut écrire

$$D = [M^{2+}]_R/[M^{2+}]_s \{\alpha_{MOH} + \alpha_B - 1 + \delta \cdot [L]_T + \gamma \cdot [L]_T^2\}$$

Dans cette expression, le numérateur représente le coefficient-limite de partage D_0^0 de l'ion M^{2+} libre. En l'absence d'ions sulfosalicylate le coefficient-limite de partage s'écrit $D^0 = D_0^0/(\alpha_{MOH} + \alpha_B - 1)$. On parvient donc à la relation:

$$(1/D) = (1/D^0) + (1/D_0^0)(\delta \cdot [L]_T + \gamma \cdot [L]_T^2) \qquad (3)$$

Initialement la résine était sous forme Na^+. A l'équilibre des ions M^{2+} et H^+ peuvent s'y trouver par suite d'échanges entre les ions Na^+ de la résine et les ions M^{2+} et H^+ de la solution, équilibres de constantes K^H_{Na} et K^M_{2Na}. La concentration des ions M^{2+} dans la résine est toujours faible dans les conditions de partage limite. Par contre, celle des ions H^+ peut être non négligeable devant celle des ions Na^+, en particulier lorsqu'on opère en milieu acide. Dans ces conditions, si C_E est la capacité d'échange de la résine, on montre que:

$$D_0^0 = K^M_{2Na} \cdot C_E^2/\{[Na^+]_s + K^H_{Na} [H^+]_s\}^2 \qquad (4)$$

A concentration donnée de Na^+ en solution D_0^0 dépend donc de $[H^+]_s$ tant que $K^H_{Na} [H^+]_s$ n'est pas négligeable devant $[Na^+]_s$. Des courbes $D_0^0 = f(\text{pH})$ à $[Na^+]_s$ donnée peuvent être facilement déterminées expérimentalement. On s'y reportera ensuite pour connaître D_0^0 dans des conditions données.

Méthode de détermination des constantes de stabilité des complexes

Cette méthode met à profit l'expression (3) reliant D, D^0 et D_0^0. On voit que dans des conditions choisies (pH, L_T, $[Na^+]_s$ donnés), il suffit de déterminer expérimentalement D et D_0 et de lire D_0^0 sur une courbe $D_0^0 = f(\text{pH})$ pour pouvoir calculer:

$$Y = \{(1/D) - (1/D^0)\} D_0^0 \qquad (5)$$

D'après la relation (3) on prévoit que Y dépend de $[L]_T$ selon $Y = \delta [L]_T + \gamma [L]_T^2$. L'exploitation de la courbe expérimentale $Y = f([L]_T)$ doit donc permettre de déterminer δ et γ dans les conditions (L_T, pH) choisies. Dans cette expression, le premier terme $\delta \cdot [L]_T$ représente la contribution des complexes 1:1 et le deuxième terme $\gamma \cdot [L]_T^2$ celle des complexes 1:2. Donc, si la courbe $Y = f([L]_T)$ est une droite passant par l'origine, seuls les complexes 1:1 existent dans le domaine étudié.

La connaissance de δ, γ et α_{HL} à différents pH permet d'atteindre les constantes de stabilité des complexes. En effet, d'après la définition de δ on peut écrire:

$$\delta \cdot \alpha_{HL} = \beta_{1L} \sum_{ij} (K_{H_2O})^j [H^+]^{i-j} / K^{iH,jOH}_{MLH_i(OH)_j}$$

Si l'on se limite aux cas où $i = 0, 1, 2$ et $j = 0, 1, 2$ et si l'on n'envisage que les complexes = MLH_2^+, MLH, ML^-, $MLOH^{2-}$ et $ML(OH)_2^{3-}$ l'expression de $\delta \cdot \alpha_{LH}$ s'écrit:

$$\delta \cdot \alpha_{HL} = \beta_{1L} \left[\frac{[H^+]^2}{K^{2H}_{MLH_2}} + \frac{[H^+]}{K^{H}_{MLH}} + 1 + \frac{K_{H_2O}}{[H^+] K^{OH}_{MLOH}} + \frac{(K_{H_2O})^2}{[H^+]^2 K^{2OH}_{ML(OH)_2}} \right]$$

L'étude de la variation de $\delta \cdot \alpha_{HL}$ avec le pH doit donc permettre de déterminer les constantes de stabilité des complexes 1:1 envisagés. On montrerait de même que l'étude de la variation de $\gamma \cdot \alpha^2_{HL}$ avec le pH permettrait de déterminer les constantes de stabilité des complexes 1:2.

Limites de la méthode

Lorsque l'on veut étudier un complexe par échange de cations, on doit tout d'abord se placer dans des conditions telles que le coefficient de partage soit mesurable.

Il ne doit pas être trop grand sinon d'une part la concentration du métal en solution peut alors devenir inférieure à la limite de détection de la méthode de dosage; d'autre part, la concentration du métal dans la résine peut devenir trop grande (supérieur à $C_E/100$) pour que l'on puisse admettre remplies les conditions de partage limite, c'est-à-dire admettre le coefficient de partage indépendant de la concentration du métal en solution. Ceci impose une limite supérieure au coefficient de partage et en particulier au coefficient D_0^0 qui est la plus grande valeur possible de D. Ceci se traduit par une limite supérieure imposée à $[Na^+]_s$ (c'est-à-dire à la force ionique à laquelle on peut étudier le complexe).

Le coefficient de partage ne doit pas être trop petit sinon il est déterminé avec une mauvaise précision. Cette limite entraîne l'impossibilité d'étudier les complexes supérieurs peu stables. En effet, ces complexes n'apparaîssent en solution que lorsque tout le métal est déjà sous forme du premier complexe, c'est-à-dire dans des conditions telles que tout le métal est maintenu en solution et que le coefficient de partage est très faible.

En outre, le domaine de concentration d'acide sulfosalicylique dans lequel on peut faire l'étude est limité. $[L]_T$ ne doit pas être trop grand car la force ionique imposée par une concentration C_1 de $NaClO_4$ doit être sensiblement constante. Donc $[L]_T$ ne doit pas excéder une certaine valeur (dépendant d'ailleurs de C_1), de façon que l'on puisse admettre que l'addition de complexant n'a pas modifié de façon notable les coefficients d'activité en solution. Cette condition empêche d'étudier les complexes trop peu stables. Neanmoins, $[L]_T$ ne doit pas être trop petit car on doit pouvoir négliger la concentration des complexes en solution devant celle de $[L]_T$. On doit donc avoir grossièrement $[L]_T > 100\ C_s$.

La sensibilité de la méthode de dosage de l'élément M limite inférieurement le domaine de C_s donc de $[L]_T$ dans lequel on peut travailler. Ceci rend donc

difficile l'étude de complexes très stables qui ne peut être réalisée qu'à de faibles valeurs de $[L]_T$. On peut remédier à cet inconvénient en utilisant des traceurs radioactifs qui permettent des dosages très sensibles de l'élément en solution.

En conclusion, on voit que les différentes conditions imposées limitent beaucoup le nombre de complexes que l'on peut étudier. En particulier on peut dire que la méthode ne permet en général que l'étude des complexes inférieurs.

PARTIE EXPERIMENTALE

La résine utilisée était la Dowex 50W-X8 (50—100 mesh) ayant subi plusieurs échanges Na^+/H^+ avant d'être mise sous forme ionique Na^+ et de capacité trouvée égale à 4,55 meq g^{-1} de résine Na^+ sèche.

Chaque échantillon (2 g) de résine a été lavé par une solution contenant toutes les espèces sauf l'élément métallique ($NaClO_4$ 0,1 M + H_3L + tampon). Puis la résine a été séparée de la solution de lavage et mise en contact avec 50 ml de solution du sel métallique ($M(ClO_4)_2$ + H_3L + tampon + $NaClO_4$ 0,1 M) et agitée pendant 24 h. Au cours de cette agitation seuls se produisent les équilibres d'échange des ions M^{2+} et Na^+, le pH de la solution ne varie pas.

Les coefficients de partage ont été déduits des valeurs de concentrations de l'élément métallique en solution avant et après l'équilibre. Ces concentrations ont été déterminées par les méthodes de dosage suivantes.

Dosage du cuivre. Le partage du cuivre ayant été étudié à l'aide de l'isotope ^{64}Cu dont la concentration a été déterminée par dosage radiométrique, les solutions de perchlorate de ^{64}Cu ont été préparées par attaque du carbonate de cuivre (activé pendant 48 h dans un faisceau de neutrons lents de 1,8 $\times 10^{13}$ n cm^{-2} s^{-1}) par l'acide perchlorique. La mesure de radioactivité a été réalisée sur le pic de désintégration β^- (0,511 MeV) du ^{64}Cu isolé à l'aide d'un sélecteur de 400 canaux Intertechnique SA 40.

Dosage du nickel et du cobalt. Le nickel et le cobalt ont été dosés par spectrophotométrie à l'aide respectivement de la diméthylglyoxine et du sel nitroso-R.

Dosage de l'uranium. Le dosage de l'uranium(VI) a été effectué par spectrophotométrie du complexe de l'uranium avec le 1-(2-pyridylazo)-2-naphtol (PAN) extrait par le chloroforme.

Remarque. Dans toutes nos expériences, la concentration totale du sodium en solution a été maintenue égale à 0,1 M. Mais, en présence d'ions sulfosalicylate la formation de paires d'ions NaL^{2-}, $NaHL^-$ et NaH_2L entraîne que la concentration des ions libres Na^+ était inférieure à 0,1 M. Nous avons donc été amenés à corriger les valeurs expérimentales des coefficients de partage pour les ramener à des valeurs correspondant à $[Na^+]_s$ = 0,1 M. Cette correction est possible lorsque les constantes de formation des paires d'ions NaL^{2-}, $NaHL^-$ et NaH_2L sont connues [13].

RESULTATS EXPERIMENTAUX

Les conditions de travail choisies sont indiquées dans le Tableau 1. Dans ces conditions, nous avons en premier lieu déterminé les coefficients de partage D_0^0 (en l'absence de sulfosalicylate et de tampon) en fonction du pH. Les résultats obtenus sont regroupés sur la Fig. 1. Puis nous avons étudié la variation du coefficient de partage D de chaque élément en fonction de L_T et à différentes valeurs de pH. Pour tous les éléments étudiés les courbes $1/D = f(L)_T$ se sont révélées être des droites comme le montrent quelques exemples représentés sur la Fig. 2. Ceci indique que dans les conditions choisies seuls les complexes 1:1 se forment en solution. Les valeurs de δ relatives à ces complexes et déduites des pentes des droites $1/D = f(L)_T$ ont été déterminées aux différents pH choisis pour chacun des éléments étudiés (Tableau 2).

Du pH ont été déduits la concentration des ions H^+ en solution (en tenant compte du coefficient d'activité de ces ions) et le coefficient α_{HL}. Les courbes $\delta \cdot \alpha_{HL} = f([H^+])$ ont été tracées (Fig. 3). Dans le cas du cuivre(II) et du nickel(II), l'analyse mathématique des courbes obtenues a montré qu'elles vérifiaient une équation de la forme: $\delta \cdot \alpha_{HL} = a[H^+]^2 + b[H^+] + c$. Ceci indique que dans le domaine de pH étudié les seuls complexes existant en solution sont CuL^-, $CuHL$ et CuH_2L^+ dans le cas du cuivre, et NiL^-, $NiHL$ et NiH_2L^+ dans le cas du nickel.

Dans le cas du cobalt(II), la courbe $\delta \cdot \alpha_{HL} = f([H^+])$ est une droite ce qui conduit à admettre la seule existence des complexes CoL^- et $CoHL$ dans le

TABLEAU 1

Les conditions de travail

Cation	C_M[a] (M)	$[L]_T$[b] (M)	Tampons de pH ($\sim 10^{-2}$ M)
Cu^{2+}	10^{-5} (traceur)	5×10^{-3}—4×10^{-2}	$1{,}9 < pH < 4{,}5$ Sulfosalicylique Formique Acétique
Ni^{2+}	4×10^{-4}	5×10^{-3}—4×10^{-2}	$2{,}8 < pH < 6{,}4$ Sulfosalicylique Formique Acétique Succinique
Co^{2+}	4×10^{-4}	4×10^{-3}—2×10^{-2}	$2{,}8 < pH < 7{,}1$ Sulfosalicylique Formique Acétique Succinique
UO_2^{2+}	$3{,}32 \times 10^{-4}$	5×10^{-3}—4×10^{-2}	$2{,}8 < pH < 3{,}6$ Sulfosalicylique Formique

[a]Concentration totale de l'élément métallique en solution.
[b]Concentration totale des ions sulfosalicylate libres en solution.

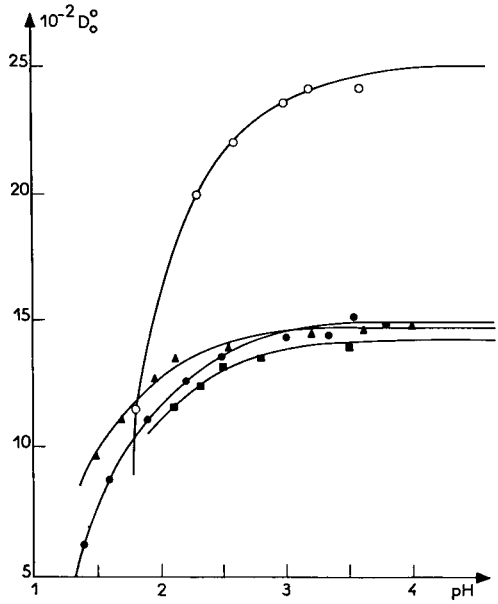


Fig. 1. Variation de D_0^0 en fonction du pH (Dowex 50W-X8, $NaClO_4$ 0,1 M); (○) UO_2^{2+}, (▲) Co^{2+}, (●) Cu^{2+}, (■) Ni^{2+}.

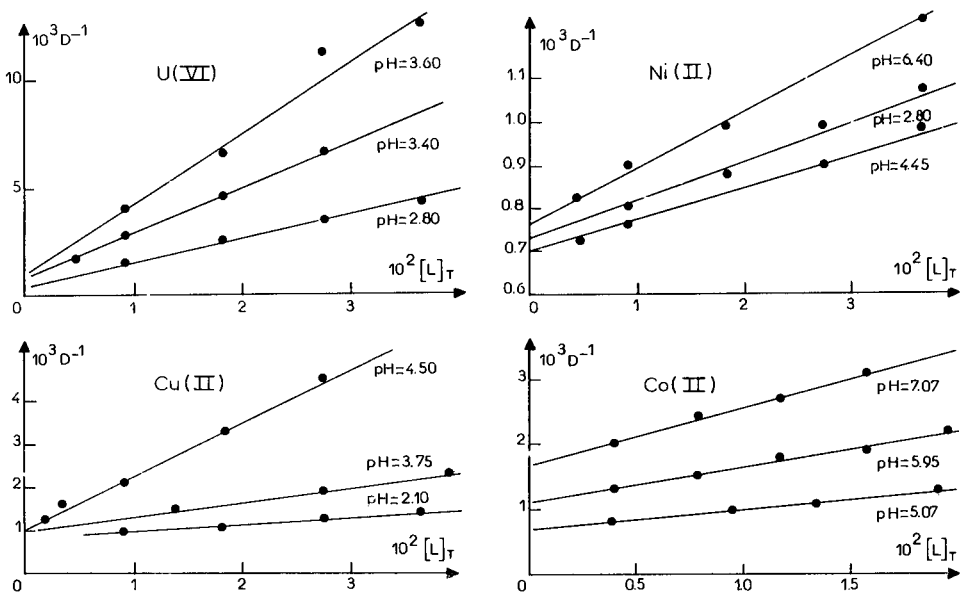


Fig. 2. Variation de $1/D$ en fonction de $[L]_T$ à différents pH.

TABLEAU 2

Les valeurs de δ et les coefficients α_{HL}

Elément	pH	D_0^0	δ	$-\log [H^+]$	$\log \alpha_{HL}$	Elément	pH	D_0^0	δ	$-\log [H^+]$	$\log \alpha_{HL}$
Cu(II)	1,90	1 100	18	1,8	11,94	Co(II)	2,78	1 450	35,1	2,68	10,81
	2,10	1 210	19	2,0	11,61		3,07	1 470	44,6	2,97	10,53
	2,70	1 410	24	2,6	10,75		3,75	1 475	55,6	3,65	9,85
	3,10	1 475	28,5	3,0	10,30		4,06	1 475	61,9	3,96	9,59
	3,75	1 495	54	3,65	9,84		4,47	1 475	61,7	4,37	9,16
	4,50	1 500	194	4,4	9,63		5,02	1 475	64,2	4,92	8,63
Ni(II)	2,80	1 360	12	2,70	10,32		5,30	1 475	62,1	5,20	8,33
	2,85	1 375	11	2,75	10,21		5,95	1 475	78,0	5,85	7,78
	3,55	1 420	11	3,45	9,37		6,46	1 475	88,2	6,36	7,32
	4,45	1 430	10	4,35	8,39		7,07	1 475	133,4	6,97	6,89
	4,95	1 430	12	4,85	7,97	U(VI)	2,80	2 300	250	2,70	9,24
	5.25	1 430	12,5	5,15	7,69		2,90	2 330	235	2,80	9,10
	5,55	1 430	14,5	5,45	7,45		3,15	2 380	280	3,05	8,79
	6,40	1 430	19	6,30	6,72		3,40	2 425	506	3,30	8,50
							3,58	2 450	820	3,48	8,30

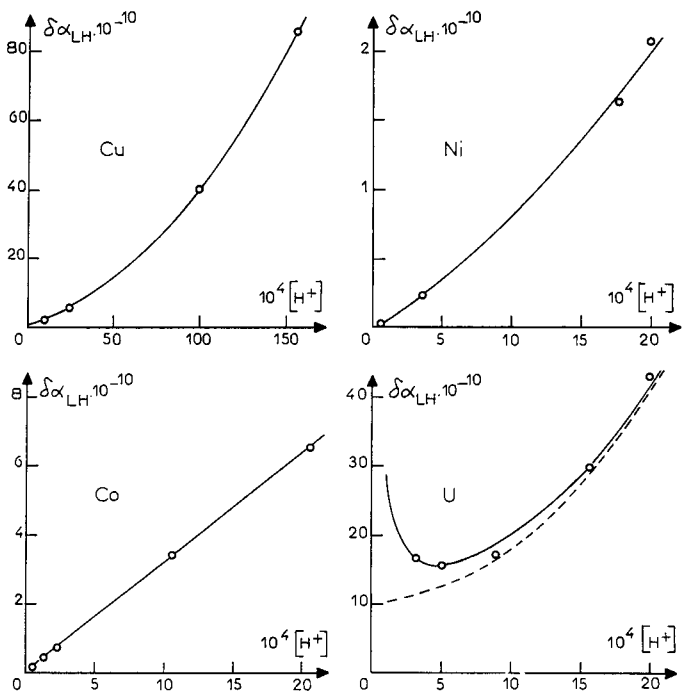


Fig. 3. Variation de $\delta \cdot \alpha_{HL}$ en fonction de $[H^+]$.

domaine de pH étudié. Dans le cas de l'uranium(VI), si l'on compare la courbe $\delta \cdot \alpha_{HL} = f([H^+])$ à la relation établie dans la partie théorique on est amené à supposer l'existence non seulement des complexes acides UO_2HL et $UO_2H_2L^+$ mais aussi de complexes hydroxylés pour expliquer l'allure de la courbe aux faibles valeurs de $[H^+]$. L'analyse mathématique de la courbe montre qu'elle

vérifie une équation de la forme: $\delta \cdot \alpha_{HL} = a[H^+]^2 + b[H^+] + c + d/[H^+]$. Ceci indique que les complexes 1:1 de l'uranyle sont: $UO_2H_2L^+$, UO_2HL, UO_2L^- et UO_2LOH^{2-}.

Sur la Fig. 3 et dans le cas de l'uranium, la courbe en traits pleins représente $\delta \cdot \alpha_{HL} = f([H^+])$. Elle est calculée point par point à partir de ces valeurs de constantes. On voit que les points expérimentaux sont voisins de cette courbe. La courbe en tireté représente la fonction $\beta_{1L}\{1 + ([H^+]/K^{H}_{UO_2HL}) + ([H^+]^2/K^{2H}_{UO_2H_2L})\}$. C'est la courbe que l'on obtiendrait s'il n'y avait pas de complexes basiques.

La détermination des paramètres des courbes obtenues a permis d'atteindre les valeurs des constantes de stabilité des complexes (Tableau 3).

DISCUSSION

On ne trouve mention du complexe CuHL dans la littérature que dans le travail de Turner et Anderson [5] qui font l'hypothèse de ce complexe dans la zone de pH où l'espèce sulfosalicylate stable est HL^{2-}. En fait, dans le domaine où ces auteurs ont travaillé (pH = 5, L_T très faible) l'espèce complexe qui prédomine est CuL^- mélangé à de petites quantités de CuHL. La valeur de constante conditionnelle égale à $10^{-2,7}$ qu'ils ont trouvée et attribuée à $k = [Cu][HL]/[CuHL]$ correspond en fait à $k' = [Cu^{2+}][HL^{2-}]/([CuL] + [CuLH])$.

A partir de nos résultats, on peut calculer k' à pH 5, on trouve $10^{-2,84}$, valeur voisine du résultat expérimental de Turner et Anderson.

Dans le cas du cuivre(II) la comparaison de notre valeur de β_{1L} avec celles données dans la littérature [14—26] est difficile puisque très souvent ces valeurs publiées ont été déterminées par potentiométrie (titrage de l'acide sulfosalicylique en présence de cation métallique) donc à pH variable et dans des domaines de concentration en complexant où en général plusieurs complexes coexistent alors que les calculs étaient faits en ne supposant l'existence que du seul complexe CuL. Les mesures faites par spectrophotométrie à pH

TABLEAU 3

Les valeurs des constantes de stabilité des complexes à I = 0,1 ($NaClO_4$)

($\beta_{iL} = [ML^-]/[M^{2+}]([L^{3-}] + [NaL^{2-}])$, $K^{H}_{MHL} = [ML^-][H^+]/[MHL]$, $K^{2H}_{MH_2L} = [ML^-][H^+]^2/[MH_2L^+]$ et $K^{OH}_{MLOH} = [ML^-][OH^-]/[MLOH^{2-}]$)

Cation	Log β_{1OH}	Log β_{2OH}	Log β_{1L}	Log β_{2L}	Log K^{H}_{MHL}	Log $K^{2H}_{MH_2L}$	Log K^{OH}_{MLOH}
Cu^{2+}	6		9,5	16,45[a]	3,7	5,9	
Ni^{2+}	4,6		6,4	10,24[a]	6,4	9,0	
Co^{2+}	5,1	10,2	6,8	9,82[a]	6,7	<7	
UO_2^{2+}	9,41[b]		11,0	19,20[a]	2,1	5,85	10,25

[a] D'après ref. 16; [b] D'après ref. 8.

fixé peuvent être considérées comme valables si le pH choisi est voisin de 5,2 puisque pratiquement à ce pH le seul complexe du cuivre est CuL. C'est le cas des mesures de Nair [17] qui dans des conditions voisines des nôtres (I = 0,2 $NaClO_4$, 25°C) et à pH = 5,1 trouve $\log \beta_1 = 9{,}65$, valeur proche de la valeur 9,6 que nous avons trouvée.

En ce qui concerne le nickel et le cobalt, toutes les valeurs de β_{1L} données dans la littérature [14, 16, 19] ont été déterminées à pH variable et dans des conditions où les complexes MHL et MH_2L pouvaient exister et ont été négligés. La même remarque est valable dans le cas de l'uranium(VI) [16, 24, 27—32] sauf pour deux études dans lesquelles il a été tenu compte des complexes protonés. L'une d'elles réalisée par Bartusek [7] a été faite par potentiométrie et a conduit à une valeur de $\log \beta_{1L}$ égale à 11,25 (I = 0,1, KNO_3, 20°C) proche de la valeur 11,1 que nous avons trouvée. En plus des espèces simples UO_2L^- et $UO_2L_2^{4-}$, Bartusek a été amené à admettre l'existence de l'espèce $UO_2HL_2^{3-}$ de constante $K^H_{UO_2HL_2} = 10^{5{,}19}$. Dans les conditions que nous avons utilisées cette espèce aurait dû exister en quantité notable dans nos solutions. Or, nous avons montré qu'il n'existait que des complexes 1:1 dans ces solutions. Par ailleurs, une autre étude [9] des complexes sulfosalicylate d'uranyle par spectrophotométrie n'a pas mis en évidence le complexe $UO_2HL_2^{3-}$ cité par Bartusek, mais a montré l'existence du complexe UO_2HL de constante: $[UO_2HL]/([UO_2^{2+}]\ [HL^{2-}]) = 10^{2{,}07}$. Cette valeur correspond à une valeur de $K^H_{UO_2HL}$ de $10^{2{,}5}$, peu différente de celle ($10^{2{,}1}$) que nous avons trouvée.

Aucune étude n'avait encore mis en évidence le complexe UO_2LOH^{2-} dont nous avons été amenés à admettre l'existence en milieu peu acide. Cahuzac [8] a fait l'hypothèse de l'existence du complexe $UO_2L_2OH^{5-}$ dans des solutions plus alcalines (pH > 10) que celles que nous avons étudiées.

A l'aide des constantes que nous avons déterminées, auxquelles nous avons ajouté les constantes β_{2L} déterminées à I = 0,1, $NaClO_4$, 25°C, par Banks et Singh [16] nous avons pu dresser le Tableau 3. Nous y avons fait figurer les constantes de formation des complexes d'hydrolyse du cation métallique [2]. Ces valeurs nous ont permis de tracer les diagrammes de répartition représentés sur les Figs. 4—6. Figure 4 donne les proportions des différentes espèces en fonction du pH, pour une concentration totale de sulfosalicylate libre égale à 0,02 M. La concentration totale de l'élément métallique est supposée inférieure à 2×10^{-4} M (excès de complexant) et la force ionique égale à 0,1 ($NaClO_4$).

Les diagrammes de Fig. 5 sont plus généraux et indiquent les domaines de prédominance des différentes espèces en fonction du pH et de la concentration du complexant libre. Les courbes délimitant ces domaines représentent les milieux dans lesquels les concentrations des deux espèces contigües sont égales. Les calculs ont été faits en supposant la force ionique égale à 0,1 ($NaClO_4$). C'est pourquoi les courbes ont été tracées en tiretés dans les domaines où cette condition ne peut être vérifiée. Les diagrammes ne sont valables que si l'élément métallique est en solution à l'état de traces puisque le complexant est toujours supposé en grand excès sur le métal et que les

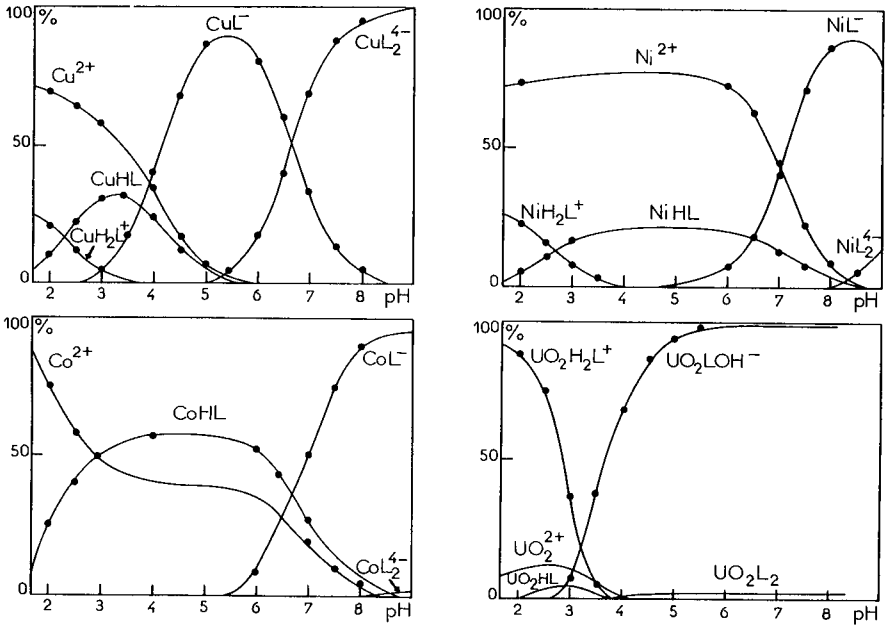


Fig. 4. Courbe de répartition des complexes sulfosalicylate de Cu(II), Ni(II), Co(II) et U(VI) en fonction du pH à 25°C et I = 0,1 M ($NaClO_4$).

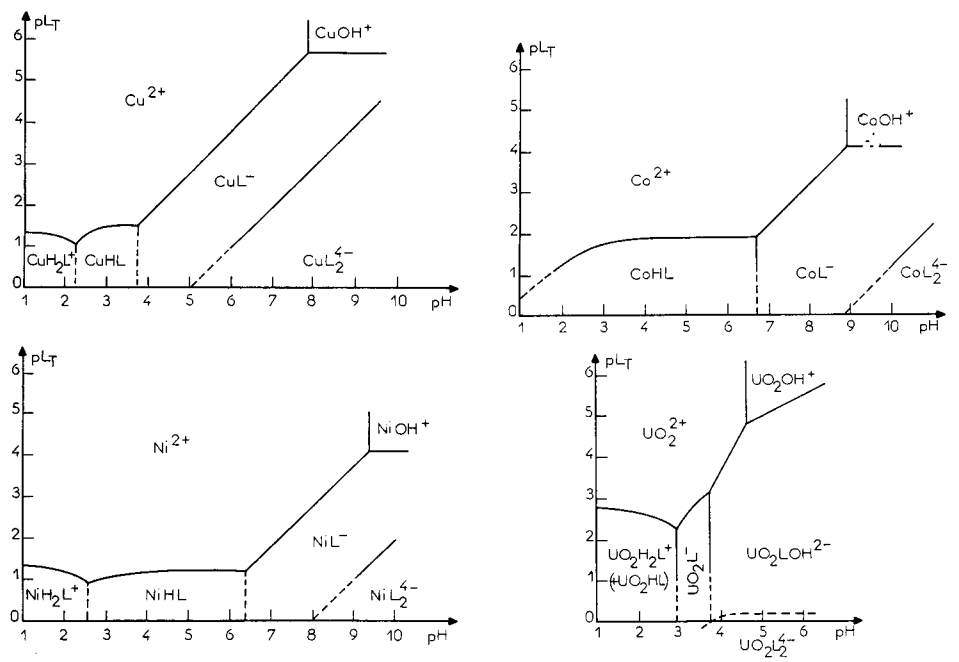


Fig. 5. Diagramme $pL_T = f(pH)$ des complexes sulfosalicylate de Cu(II), Ni(II), Co(II) et U(VI) (25°C, I = 0,1).

composés polynucléaires d'hydrolyse du cation métallique ont été négligés (en particulier pour l'uranium).

Les diagrammes de Fig. 5 font le bilan des connaissances actuelles sur les complexes sulfosalicylate du cuivre(II), nickel(II), cobalt(II) et uranyle. D'autres complexes que ceux qui y figurent peuvent toutefois exister; en particulier d'autres complexes protonés ou hydroxylés en milieux plus acides ou plus alcalins.

BIBLIOGRAPHIE

1 L. G. Sillen et A. E. Martell, Stability Constants of Metal—Ion Complexes, Special Publication of the Chemical Society, London, 1964; supplément (1974).
2 A. Ringbom, Les complexes en chimie analytique, Dunod, Paris, 1967.
3 J. Schubert et A. Lindenbaum, J. Biol. Chem., 208 (1954) 359.
4 C. R. Kanekar, N. V. Thakar et S. M. Jogdeo, Bull. Chem. Soc. Jpn., 41 (1968) 759.
5 S. E. Turner et R. C. Anderson, J. Am. Chem. Soc., 71 (1949) 912.
6 L. Sommer, Collect. Czech. Chem. Commun., 28 (1963) 2716.
7 M. Bartusek, J. Inorg. Nucl. Chem., 29 (1967) 1089; Collect. Czech. Chem. Commun., 32 (1967) 116.
8 S. Cahuzac, Rapport C.E.A. no. R3826, France (1969).
9 J. Haveland et L. Sommer, Collect. Czech. Chem. Commun., 32 (1968) 529.
10 G. E. Mont et A. E. Martell, J. Am. Chem. Soc., 88 (1966) 1387.
11 J. Schubert, J. Phys. Chem., 56 (1952) 114.
12 S. Fronaeus, dans H. B. Jonassen et A. Weissberger (Eds.), Technique of Inorganic Chemistry, London, 1963.
13 F. Chouaib et C. Poitrenaud, Analusis, à paraître.
14 D. D. Perrin, Nature, 182 (1958) 741.
15 C. V. Banks et R. S. Singh, J. Am. Chem. Soc., 81 (1959) 6159.
16 C. V. Banks et R. S. Singh, J. Inorg. Nucl. Chem., 15 (1960) 25.
17 V. S. K. Nair, Trans. Faraday Soc., 57 (1961) 1988.
18 R. Nasänen et P. Merilainen, Suomen Kemistilehti, 35 B (1962) 79.
19 V. S. K. Nair, Talanta, 9 (1962) 27.
20 R. P. Martin et R. A. Paris, Compt. Rend., 257 (1963) 3932; Bull. Soc. Chim. France, (1964) 80.
21 R. C. Das, R. K. Nanda et S. Aditya, J. Indian. Chem. Soc., 42 (1965) 307.
22 M. Bonnet et R. A. Paris, Bull. Soc. Chem. France, (1966) 747.
23 G. A. L'Heureux et A. E. Martell, J. Inorg. Nucl. Chem., 28 (1966) 481.
24 V. T. Athavale, N. Maha Devan, B. K. Mathur et R. M. Sathe, J. Inorg. Nucl. Chem., 29 (1967) 1947.
25 G. F. Condike et A. E. Martell, J. Inorg. Nucl. Chem., 31 (1969) 2455.
26 M. M. Petit-Ramel et M. R. Paris, Bull. Soc. Chem. France, (1969) 3070.
27 J. Hàla, Collect. Czech. Chem. Commun., 29 (1964) 905.
28 K. S. Rajan et A. E. Martell, J. Inorg. Nucl. Chem., 26 (1964) 789.
29 J. M. Rao et U. V. Seshaiah, Bull. Chem. Soc. Jpn., 39 (1966) 2668.
30 A. Bismondo, R. Portanova, P. Di Bernardo et L. Magnon, Energ. Nucl., 19 (1972) 402.
31 D. V. Jahagirdar et D. D. Khanolkar, J. Inorg. Nucl. Chem., 25 (1973) 921.
32 V. D. Khanolkar, D. V. Jahagirdar et D. D. Khanolkar, J. Inorg. Nucl. Chem., 35 (1973) 931.

Analytica Chimica Acta, 108 (1979) 347—350
© Elsevier Scientific Publishing Company, Amsterdam — Printed in The Netherlands

Short Communication

CONTROLLED TEMPERATURE-GRADIENT ATOMIC SPECTRAL LAMP

D. S. GOUGH and J. V. SULLIVAN*

CSIRO Division of Chemical Physics, P.O. Box 160, Clayton, Victoria 3168 (Australia)

(Received 14th December 1978)

Summary. The lamps are based on excitation of a thermally-produced vapour in a low-pressure gas discharge. For arsenic and selenium, the resonance line intensities are five times higher than those emitted by electrodeless discharge lamps for the same line-widths. Limits of detection are 16 ng ml^{-1} for arsenic and selenium in non-dispersive atomic fluorescence measurements; sensitivities are also improved in atomic absorption.

The most commonly used light sources for the production of narrow resonance lines of arsenic and selenium are the hollow-cathode lamp and the electrodeless discharge lamp (EDL). The former is far from satisfactory with respect to life-time and stability of output. The latter is an intense source and may be used for absorption and fluorescence measurements, but suffers from the disadvantages of a long warm-up time and a tendency for the ouput intensity to drift.

A new type of lamp, the controlled temperature-gradient lamp (CTGL; patent applied for) has been developed. In this lamp, a thermally-produced vapour is excited in a low-pressure gas-discharge. This type of lamp is suitable for elements with high vapour pressures at relatively low temperatures, such as arsenic, selenium, zinc, cadmium, potassium, sodium, sulphur and phosphorus.

Construction of the lamps

The lamp (Fig. 1) consists of a glass tube approximately 1 cm in diameter and 15 cm in length. It has a tungsten anode, A, and an electron-emitting filament, B, which forms the cathode of an exciting discharge. The central portion, C, which is slightly constricted to increase current density, is made of silica to permit transmission of u.v. wavelengths. A furnace, D, made by winding approximately 6 ohms of resistance wire on to a silica tube, surrounds the lower part of the lamp and provides the heat necessary to vaporize the element, E, which is housed in the anode compartment.

The temperature of the furnace is kept constant at a predetermined value by using a thermistor and feedback loop. A viewing port is provided in the wall of the furnace opposite the constriction C. The discharge provides some additional heat, mainly in the region of C, and ensures that no condensation occurs there. Temperature gradients exist between the filament and the bulb, F, and between the anode and the bulb. This ensures that the elemental vapour, dis-

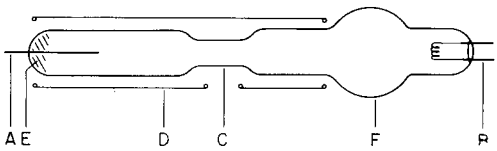


Fig. 1. Schematic diagram of the controlled temperature-gradient lamp. A, anode; B, oxide-coated filament; C, constriction; D, furnace; E, element; F, bulb. The lamp is run in a vertical position with the anode, A, at the bottom.

tilled continuously from the lower compartment, will condense on the surface of the relatively cool bulb. Thus the vapour pressure of corrosive material is very low in the region of the filament, thereby preventing poisoning of the electron emitter. The pressure of elemental vapour in the lamp is determined by the temperature of the furnace and not by the excitation discharge as it is with EDL's and Wotan-type lamps. In these lamps, increase in power input results in high elemental vapour pressure which leads to broadening of the resonance lines by self-absorption.

The lamp is filled to a pressure of approximately 2 Torr with argon. The power supply to the lamp incorporates a filament heater (6.3 V, 10 A) and two current-regulated power supplies, one capable of delivering 100 mA at 900 V and the other 750 mA at 120 V. The high-voltage supply causes the discharge to strike and thereafter provides a current of the order of 10 mA d.c., upon which is superimposed a modulated current of up to 750 mA. The frequency of modulation is 285 Hz and the output of the lamp is measured by using an amplifier tuned to this frequency.

Because the electron density in the exciting discharge is very high, emission is intense even when the elemental vapour pressure is low ($<10^{-6}$ Torr). Maximum intensity consistent with relatively narrow resonance lines is achieved at an elemental vapour pressure of approximately 10^{-5} Torr.

Performance of the arsenic and selenium lamps

Lamps for arsenic and selenium were compared with the corresponding EDL's with respect to line-width and intensity; the 4-m Czerny–Turner monochromator used incorporated a 76-mm, 600 grooves/mm grating in 8th order. The slit-width employed was 11 μm, which gave a theoretical resolution of 0.00105 nm. The EDL's were run at power inputs ranging from that recommended to the maximum possible consistent with stable operation. Approximate furnace temperatures for the CTGL's are shown in Table 1, which summarizes the results of the comparison made with the monochromator. Throughout the range of power input, the intensities of the resonance lines emitted by the CTGL's were higher than those emitted by the EDL's by a factor of about 5 for the same line-width.

Measurements were made with CTGL's and the corresponding EDL's as light sources with a non-dispersive atomic fluorescence spectrometer of the type described by Larkins [1]. The EDL's (Westinghouse) were operated with a power supply (also Westinghouse) which enabled them to be modulated at

TABLE 1

Line-widths and relative intensities of the As 193.7-nm and Se 196.0-nm resonance lines emitted by EDL's and CTGL's

	EDL			CTGL		
	Power (W)	Intensity	Line-width[a] (nm)	Furnace temp (°C)	Intensity	Line-width[a] (nm)
As	9	30	0.0014	140	100	0.0012
	11	90	0.0017	160	200	0.0014
Se	7	30	0.0016	100	70	0.0012
	8	60	0.002[b]	140	150	0.0015

[a]Measured at half-peak intensity and not corrected for the instrumental width of 0.0011 nm.
[b]Recorder traces showed evidence of self-reversal.

285 Hz. The arsenic and selenium lamps were run at 11 and 9 W, respectively, which are the maximum powers possible for stable operation These powers were greater than those recommended by the manufacturer for use in atomic absorption (7 W) because high output intensity was required. When the power supplied to the arsenic lamp was increased from 7 to 11 W, the intensity of the lamp was increased twenty-fold; when the power supplied to the selenium lamp was increased from 7 to 9 W, the lamp intensity was increased three-fold. For the corresponding CTGL's, the furnace temperatures were approximately 180°C and 140°C. Figure 2 shows the recorder traces obtained by this technique when an aqueous solution containing arsenic or selenium (300 ng ml^{-1}) was aspirated into a nitrogen-separated, slightly fuel-rich, air—acetylene flame. The fluorescence intensities indicate that the CTGL is three times as intense as the EDL under these conditions. The limits of detection (defined as the concentration giving a signal equal to twice the peak-to-peak fluctuation when only dilute acid or water is aspirated) were 16 ng ml^{-1} for both arsenic and selenium when the CTGL's were used, compared with 60 ng As ml^{-1} and 50 ng Se ml^{-1} for the appropriate EDL.

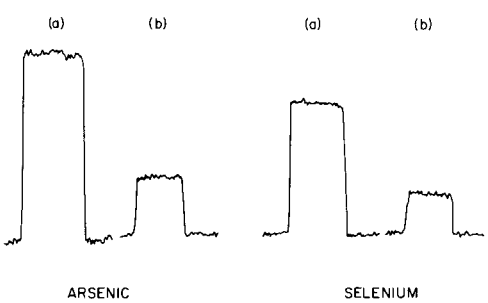


Fig. 2. Recorder traces of atomic fluorescence signals obtained with CTGL's and EDL's. (a) CTGL; (b) EDL at maximum permissible power, i.e. 11 W for arsenic and 9 W for selenium.

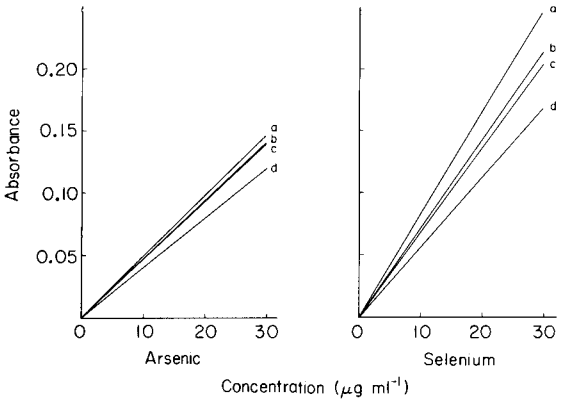


Fig. 3. Calibration curves in atomic absorption with CTGL's and EDL's. Monochromator bandpass, 0.15 nm; wavelengths, As 193.7 nm, Se 196.0 nm. (a) CTGL at emission intensity equal to that of EDL run at 7 W. (b) EDL run at 7 W (recommended power). (c) CTGL at emission intensity equal to that of EDL run at maximum power. (d) EDL run at maximum power (11 W for As, 9 W for Se).

Figure 3 shows the calibration curves of absorbance versus concentration when the CTGL's and EDL's were used as light sources in atomic absorption. Aqueous solutions of arsenic and selenium were sprayed into the 10-cm air—acetylene flame of a Techtron AA-4 atomic absorption spectrometer. It can be seen that the CTGL gives greater absorption sensitivity than that obtained with the EDL run under conditions giving the same lamp intensity. This confirms that the resonance lines emitted by the CTGL's are narrower than those emitted by the EDL run at the same emission intensity level.

Tests on the lifetime of the CTGL's are not yet complete. To date, arsenic and selenium lamps have operated satisfactorily for 1500 h.

Controlled temperature-gradient lamps containing sulphur and phosphorus have also been made. Their construction and use will be described in a later publication.

REFERENCE

1 P. L. Larkins, Spectrochim. Acta, Part B, 26 (1971) 477.

Analytica Chimica Acta, 108 (1979) 351—356
© Elsevier Scientific Publishing Company, Amsterdam — Printed in The Netherlands

Short Communication

A COMPARATIVE STUDY OF STANDARDS FOR DETERMINATIONS OF TRACE WEAR METALS IN JET ENGINE OILS

T. M. TUELL[a], A. H. ULLMAN[b], B. D. POLLARD[c], A. MASSOUMI[d], J. D. BRADSHAW, J. N. BOWER and J. D. WINEFORDNER*

Department of Chemistry, University of Florida, Gainesville, FL 32611 (U.S.A.)

(Received 5th January 1979)

Summary. The feasibility of using acid-treated metal powder standards for the determination of trace wear metals in spent jet engine oils is evaluated. The addition of 2:3:3 (v/v/v) HF—HCl—HNO_3 mixture to used lubricating oils did not cause any statistically reliable differences from results obtained with organometallic standards. Two sets of six correlation samples, one set being acid-treated, were analyzed for Cu, Cr, Mg, Fe, Mo and V by flame atomic absorption and flame atomic fluorescence spectrometry against each set of standards.

The Spectrographic Oil Analysis Program (more commonly known as SOAP) was initiated by the United States Air Force to monitor wear metals in the used lubricating oils of their aircraft. The idea is to detect excessively-worn components among the oil-wetted engine parts which might cause in-flight engine failure and loss of aircraft and personnel. The Air Force and Navy at present use approximately 120 laboratories across the world for the correlation of oil analyses. These SOAP laboratories are furnished with multi-element organometallic standards to prepare analytical calibration curves for evaluation of wear metal concentrations. Such standards are convenient in that the organometallic compounds used to prepare them dissolve completely in oils even at high concentrations [1]. Even though organometallic standards give linear analytical calibration plots with correlation coefficients very close to unity, they do not represent accurately the wear metals in the spent oils, i.e., they do not match the metal particles in the engine oils. Consequently, standards in which the analyte is present as a metal particle would appear to be more suitable for the oil analyses than the organometallic standards. The major purpose of this work was to determine the feasibility of using acid-treated metal powder standards for the determination of the wear metals.

The addition of a strongly oxidizing acid mixture to used lubricating oils has been shown to improve the signal for titanium in flame atomic absorption

[a]Present location: Syntex Lab., 3401 Hillview Ave., Stanford Indus. Park, Palo Alto, CA 94304, U.S.A.
[b]Present location: Industrial Chemicals Division, Proctor and Gamble Co., Sharon Woods Technical Center, Cincinnati, OH 45241, U.S.A.
[c]Present location: Department of Chemistry, Marquette University, Milwaukee, WI 53233, U.S.A
[d]Present location: Department of Chemistry, Pahlavi University, Shiraz, Iran.

spectrometry [2]. It is believed that the acids decrease the mean diameter of the metal particles resulting in atomization of a larger fraction of the wear metal, thus allowing measurement of metal particles too large to be completely atomized (without acid treatment) in a flame. Therefore, in this communication, the effect of treating used jet engine oils with a 2:3:3 (v/v/v) HF—HCl—HNO_3 mixture is examined for several wear metals by flame atomic absorption spectrometry (a.a.s.) and by flame atomic fluorescence spectrometry (a.f.s.). X-ray fluorescence spectrometry proved to have inadequate sensitivity, relatively high limits of detection, and thus poor precision in these studies.

Of the 120 SOAP laboratories, about half employ a.a.s. and the other half spark atomic emission spectrographs (s.a.e.s.) in the analysis of used jet engine oils for the determination of iron, silver, aluminum, chromium, copper, magnesium, silicon, titanium, and molybdenum. Discrepancies have been observed between the results obtained by a.a.s. and a.e.s. and also among a.a.s. results when different flame conditions have been used.

Choice of solvent, dilution ratio and acid mixture

Preliminary work indicated that of the four 1:3 (v/v) acid mixtures tested, i.e., HF—HCl, HF—HNO_3, HF—H_2SO_4 and HF—$HClO_4$, the latter two did not increase the analyte signal. Because the addition of HF—HCl or HF—HNO_3 to some oil samples increased the signal levels, and based on comparative studies with correlation samples, the acid mixture chosen for this study was a mixture of three acids HF—HCl—HNO_3 in the volume ratio of 2:3:3.

The effect of the solvent, dilution ratio, and aspiration rate on titanium absorbance in flame a.a.s. has been studied extensively by Eisentraut and Saba [2]. With the solvents studied, the highest sensitivity was obtained for one part of oil to two parts of methyl isobutyl ketone (MIBK). The solvents studied were: MIBK, *p*-xylene, acetylacetone, isopropanol, acetone, and ethanol; the sensitivity (absorbance/analyte concentration) decreased in that order. The optimum dilution ratio (largest signal with greatest linear range in the calibration plot) was found to be 1:2 (v/v); dilution ratios studied were 1:9, 1:5, 1:3, 1:2 and 1:1 (v/v, oil—MIBK). A dilution ratio of 1:1 gave the highest signal but also resulted in considerable deviation from linearity relative to the other dilutions.

Experimental

Preparation of standards and samples. A stock solution containing 90 ppm of each of the eight metals tested (Fe, Mg, Cu, Cr, Ti, V, Mo and Al) was prepared by treating 13.5 mg of each metal with 1 ml of the HF—HCl—HNO_3 mixture in 150 g of base oil. The stock solution was shaken for 15 min to insure homogeneous dispersion and maximum dissolution of the metal powders. A set of five oil standards ranging in concentration from 3 to 39 ppm was prepared by weighing a suitable quantity of the stock solution into a 2-oz Nalgene bottle and adding sufficient base oil to give a total weight of 15 g. Addition of 30 g of reagent-grade MIBK to each of the five standards gave working standards in the range 1—13 ppm.

The 325-mesh metal powders used were of high purity (>99%) (Ventron,

Alfa Division, Danvers, MA), and were dried at 120°C for ca. 5 h before use. The Conostan 85 base oil was a light-weight hydrocarbon oil (Continental Oil Co., Conostan Division, Ponca City, OK).

The preparation of the organometallic standards involved simple (1 + 1) dilution with MIBK of six specially prepared standards obtained from the Naval Air Rework Facility, Naval Air Station, Pensacola, Florida. Portions (15 g) of each standard (100, 50, 30, 3 and 0 ppm) were added to Nalgene bottles and diluted with 30 g of MIBK to give working standards with concentrations of 33.3, 17, 10, 3.3, 1 and 0 ppm. The 0-ppm standard was used as a blank for these standards.

Six correlation samples — for which the results were well documented — were mixed vigorously for 10 min in a Spex Mixer/Mill to insure good dispersion of the wear metals. Portions (15 g) of each sample were weighed into Nalgene bottles, and 30 g of reagent-grade MIBK was added to each sample. For one set, the samples were acid-treated by the addition of 0.15 ml of the HF—HCl—HNO_3 mixture to the diluted oils.

Instrumentation and experimental conditions. For the a.a.s. studies, a Perkin-Elmer Model 303 atomic absorption spectrometer was used. A laminar-flow slot burner (5.3 cm long) was used for both the acetylene—air (0.9 l min^{-1} and 17.0 l min^{-1}, respectively) and acetylene—nitrous oxide (3.0 l min^{-1} and ~8 l min^{-1}, respectively) flames. The former flame was used for Fe, Cr, Cu, and Mg measurements and the latter for Ti, V, Mo, and Al. The order of measurements in both a.a.s. and a.f.s. studies was sample—pure MIBK—blank—sample—pure MIBK—blank, etc. All instrumental components were operated in accordance with the manufacturer's recommendations. After several hours of operation (for both a.a.s. and a.f.s.), the burner head, nebulizer, and spray chamber were disassembled and soaked in a concentrated detergent solution overnight; the next day each section was rinsed in tap water and deionized water before reassembly.

For the a.f.s. studies, the automated multielement atomic fluorescence spectrometer described by Ullman et al. [3] was used. All experimental conditions were as described previously [3]; a sheathed-capillary burner with chamber nebulizer was used. Fe, Cu, Cr, and Mg were measured in a sheathed acetylene—air flame (2.1 l min^{-1} and 10.3 l min^{-1}, respectively, with a 17.9 l Ar min^{-1} sheath); Ti, V, Mo, and Al were measured in a sheathed acetylene—nitrous oxide flame (3.9 l min^{-1} and 7.3 l min^{-1}, respectively, with a 17.9 l Ar min^{-1} sheath).

X-ray fluorescence spectrometry was also tested (Siemens wavelength-dispersi x-ray spectrometer). However, the sensitivity and power of detection was inadequate for Mg, Cr, Al, V and Mo, and the precision was inadequate for Cr, Fe, and Ti.

In these studies, the concentration of wear metals in the jet engine oils is reported as parts per million on a weight basis, i.e. $\mu g\, g^{-1}$. In the SOAP studies, ppm refers to weight/volume basis, i.e. $\mu g\, ml^{-1}$; because the density of base oil is 0.85 g ml^{-1}, the values calculated in the present studies will be too high by a factor of 1/0.85 or 1.18.

Results and discussion

Of the eight elements of interest (Mg, Fe, Cr, Cu, Ti, V, Mo, and Al), analytically useful results were not obtained for Ti and Mo by either a.a.s. or a.f.s. Although analytically significant results were obtained for vanadium by both methods, no comparison with Tri-Services SOAP value was possible because vanadium was not included in the SOAP results.

Calibration plots were obtained for both the dispersed metal powder standards and the organometallic standards for all 8 metals by a.a.s. and a.f.s. In virtually all cases, the sensitivity (slope) of the calibration plot for the organometallic standards was greater than that for the dispersed metal powder standards; a typical case is shown in Fig. 1.

Analyses of the six correlation oil samples with and without acid treatment referred to acid-treated metal powder standards and organometallic standards gave the results shown in Table 1; the average values obtained by SOAP are also included. From these results and the calibration curves, several conclusions can be drawn. First, there was no definitive (statistically reliable) difference in the results whether acid was or was not added to the jet engine oil samples. Secondly, the a.a.s. and a.f.s. techniques with the organometallic standards gave approximately the same results for each element. Finally, the acid-"dissolved" metal powder standards did not give reliable calibration curves; Eisentraut and Saba [5] have, however, obtained reliable results with such standards.

The poor sensitivity and unreliable results obtained here with the acid-treated metal powder standards can be partially explained by incomplete dissolution (a sludge sometimes formed in the bottom of the bottles) and/or by hetero-

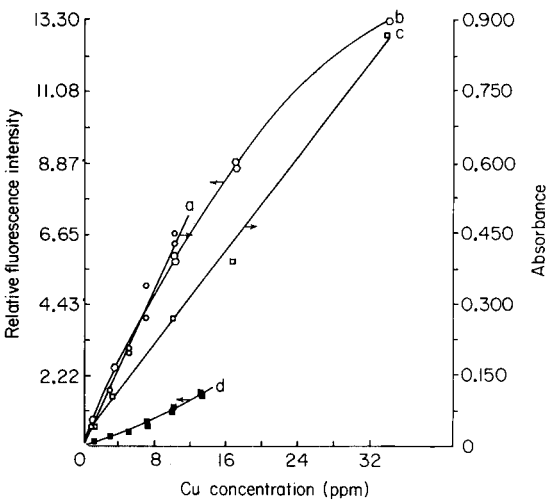


Fig. 1. Calibration curves for copper. (a) A.a.s. with organometallic standards; (b) a.a.s. with metal powder standards; (c) a.f.s. with organometallic standards; (d) a.f.s. with metal powder standards.

TABLE 1

Comparison of results for wear metals by a.a.s. and a.f.s. with the trimmed mean SOAP values
(All results are given as $\mu g\ g^{-1}$)

Sample[a]	Metal	Treatment[b]	A.a.s.		A.f.s.		SOAP[c]
			MP[d]	OM[e]	MP[d]	OM[e]	
129	Cu	Acid	13	4	47	9	21
		No acid	35	4	75	21	
	Cr	Acid	26	4	62	7	24
		No acid	63	18	163	23	
	Mg	Acid	123	4	165	5	13
		No acid	313	12	191	16	
	Fe	Acid	15	17	19	17	25
		No acid	26	17	24	22	
	Mo	Acid	12	15	21	17	19
		No acid	12	12	21	16	
	V	Acid	ND[f]	—[g]	3	—[g]	—[h]
		No acid	ND		7		
139	Cu	Acid	4	ND	9	ND	3
		No acid	4	ND	ND	ND	
	Cr	Acid	348	18	163	22	24
		No acid	390	16	—	23	
	Mg	Acid	84	3	43	3	4
		No acid	99	4	—	4	
	Fe	Acid	23	5	9	6	4
		No acid	10	7	—	6	
	Mo	Acid	ND	ND	5	ND	2
		No acid	ND	ND	5	ND	
	V	Acid	ND	—	4	—	—[h]
		No acid	ND	—	5	—	
144	Cu	Acid	40	21	107	33	40
		No acid	55	25	—	31	
	Cr	Acid	40	2	34	3	6
		No acid	40	3	—	3	
	Mg	Acid	147	10	150	11	14
		No acid	368	8	—	8	
	Fe	Acid	46	34	36	52	66
		No acid	36	35	—	43	
	Mo	Acid	ND	11	38	32	11
		No acid	ND	5	33	25	
	V	Acid	ND	—	61	—	—[h]
		No acid	ND	—	63	—	
146	Cu	Acid	38	11	87	24	26
		No acid	64	19	—	27	
	Cr	Acid	161	21	153	19	22
		No acid	199	22	—	22	
	Mg	Acid	275	8	195	23	14
		No acid	331	11	—	24	
	Fe	Acid	24	20	22	21	25
		No acid	29	19	—	24	

TABLE 1 continued.

Sample[a]	Metal	Treatment[b]	A.a.s.		A.f.s.		SOAP[c]
			MP[d]	OM[e]	MP[d]	OM[e]	
46	Mo	Acid	40	12	31	22	25
		No acid	29	10	31	21	
	V	Acid	ND	—	ND	—	—[h]
		No acid	ND	—	5	—	
151	Cu	Acid	12	ND	34	6	15
		No acid	23	2	44	ND	
	Cr	Acid	25	1	53	ND	8
		No acid	63	4	62	7	
	Mg	Acid	108	5	86	5	8
		No acid	454	5	108	ND	
	Fe	Acid	47	44	45	39	83
		No acid	48	33	42	7	
	Mo	Acid	ND	ND	20	11	0.3
		No acid	ND	ND	24	7	
	V	Acid	ND	—	3	—	—[h]
		No acid	ND	—	7	—	
153	Cu	Acid	5	—	139	23	53
		No acid	54	—	162	29	
	Cr	Acid	20	ND	143	5	22
		No acid	173	4	110	5	
	Mo	Acid	310	7	110	5	12
		No acid	291	5	150	6	
	Fe	Acid	31	49	36	19	53
		No acid	51	26	37	19	
	Mo	Acid	29	40	55	33	56
		No acid	37	25	50	36	
	V	Acid	ND	—	ND	—	—[h]
		No acid	ND	—	5	—	

[a]Correlation sample numbers refer to those from the Tri-Service SOAP studies. [b]Treatment refers to preparation (see Experimental section). [c]Trimmed mean values are from the interlaboratory SOAP studies. [d]Calibration with metal powder standards. [e]Calibration with organometallic standards. [f]ND, not detectable. [g]Standards not available. [h]No SOAP result.

geneous dispersion of the acid and oil phases. Either smaller volumes as used by Eisentraut and Saba [2, 5] and/or smaller particles (< 10-μm average diameter) might minimize these difficulties, especially as the acid treatment of the jet engine oils did not give significantly different results from the untreated oils.

This work was supported by grant AF-AFOSR-F44620-76-C-0005.

REFERENCES

1 National Bureau of Standards, Department of Commerce, Washington, D.C., April, 1964.
2 K. J. Eisentraut and C. S. Saba, Anal. Chem., 49 (1977) 454.
3 A. H. Ullman, B. D. Pollard, R. P. Bateh and J. D. Winefordner, Anal. Chem., in press.
4 J. H. Taylor, T. T. Bartels and N. L. Crump, Anal. Chem., 43 (1971) 1780.
5 K. J. Eisentraut and C. S. Saba, private discussion.

Analytica Chimica Acta, 108 (1979) 357—361
© Elsevier Scientific Publishing Company, Amsterdam — Printed in The Netherlands

Short Communication

DETERMINATION OF ARSENIC IN GEOLOGICAL MATERIALS BY ELECTROTHERMAL ATOMIC-ABSORPTION SPECTROMETRY AFTER HYDRIDE GENERATION

R. F. SANZOLONE, T. T. CHAO* and E. P. WELSCH

U.S. Geological Survey, Box 25046, Denver, Colorado 80225 (U.S.A.)

(Received 2nd January 1979)

Summary. Rock and soil samples are decomposed with $HClO_4$—HNO_3; after further treatment, arsine is generated and absorbed in a dilute silver nitrate solution. Aliquots of this solution are injected into a carbon rod atomizer. Down to 1 ppm As in samples can be determined and there are no significant interferences, even from chromium in soils. Good results were obtained for geochemical reference samples.

Arsenic commonly accompanies a number of ore elements so that it is a valuable pathfinder or indicator element in geochemical surveys [1]; arsenic distribution gives rise to broad primary as well as secondary halos around ore deposits. Rapid methods for the determination of arsenic in geological materials at or below the crustal abundance are therefore essential. It is well known that the direct determination of arsenic by atomic-absorption spectrometry after sample dissolution suffers from many interferences regardless of the method of atomization. Hydride generation has therefore been employed very extensively to isolate arsenic from possible interferences and for preconcentration prior to determination, but the generation of arsine and the final determination by flame or flameless methods may still be affected by various ions present in the sample solutions [2—9].

The proposed method makes use of a $HClO_4$—HNO_3 digestion, after which the residue is dissolved in hydrochloric acid. Arsine is generated from the resulting solution after addition of iodide, tin(II) and zinc, and is trapped in a dilute silver nitrate solution [10]. The arsenic in this solution is then determined by atomic-absorption spectrometry with a carbon-rod atomizer.

Experimental

Apparatus. A Varian AA6 atomic-absorption spectrometer equipped with a Model 63 carbon-rod atomizer, a simultaneous background corrector, and an arsenic electrodeless discharge lamp was used. Instrument settings were: wavelength, 193.7 nm; EDL, 7.5 W; slit width, 1.0 nm; nitrogen flow meter, 8.0; drying voltage, 7 (ca. 150°C for 30 s); ashing voltage, 6 (ca. 450°C for 15 s); and ramp cutoff voltage for atomization, 8 (ca. 2100°C at rate 2).

The generation—absorption apparatus was very simple: a 25 mm × 150 mm

pyrex test tube containing sample and reagents and fitted with a silicone rubber stopper connected to a 16 mm x 150 mm test tube (absorption tube) by glass tubing which was attached by tygon tubing to a 5 mm x 135 mm gas-dispersion tube with a porous tip (catalog no. 9435-C, Ace Glass Inc., Vineland, N.J.); this tube extended to the bottom of the absorption tube.

Reagents and standards. All chemicals were of analytical-reagent grade. Prepare a silver nitrate stock solution (1.0 M in 1 M HNO_3). Prepare the silver nitrate absorbing solution (0.01 M in 0.01 M HNO_3) by diluting 1 ml of the silver nitrate stock solution to 100 ml with water, immediately before use.

For the arsenic stock solution (1000 μg ml^{-1}), dissolve 0.132 g of As_2O_3 in 2 ml of 1 M NaOH, acidify with 1.0 ml of 10% (v/v) HCl and dilute to 100 ml with water. Prepare an arsenic working solution (10 μg ml^{-1}) by dilution with 1 M HCl. For the arsenic standard solutions, add 0, 10, 50, 100 200, and 500 μl of this arsenic working solution, using micro-pipettes, to 25 X 150 mm pyrex tubes containing 9 ml of 1 M HCl. These solutions contain, respectively, 0, 0.1, 0.5, 1, 2, and 5 μg As.

Procedure. Weigh 0.100 g of the rock, soil, or stream sediment samples (less than 100-mesh) into a 50-ml Teflon beaker. Add 5 ml of concentrated nitric acid and 4 ml of perchloric acid (70%), and heat on an oscillating hot plate set at 220°C for ca. 1.5 h to incipient dryness under a perchloric-acid hood. Transfer the moist residue to a 25 X 150 mm pyrex tube using two 4.5 ml portions of 1 M HCl. Add 0.5 ml of aqueous 40% (w/v) potassium iodide solution, mix and allow to stand for 10 min. Add 0.5 ml of 40% (w/v) tin(II) chloride solution in concentrated hydrochloric acid and mix well. Scoop 3 g of mossy zinc (analytical grade) into the sample solution and immediately connect to the absorption tube containing 5.0 ml of the silver nitrate absorbing solution, to prevent any possible loss of arsine being generated. The gas-dispersion tube should remain in contact with the bottom of the absorption tube to insure maximum absorption of the generated arsine. Allow the reaction to proceed for 10 min with occasional shaking. Remove the gas dispersion tube from the silver nitrate solution and cap the tube until analysis is performed. Duplicate or triplicate determinations in the peak-height mode are made with 10-μl aliquots of the silver nitrate solution. Standard solutions are treated identically as the sample solution for the construction of the calibration curve covering 0.2—10 ng As in the 10-μl aliquot.

A battery of 25 generation—absorption cells was constructed for this work. With this arrangement, combined with the automatic sample dispenser for the injection of the 10-μl aliquot of the sample solutions into the carbon rod, 50 samples can be analyzed for arsenic per 8-h working day.

Results and discussion

Sensitivity. The procedure outlined allows 0.1—5 μg As in the 5.0-ml absorbing solution to be determined; this range corresponds to 1—50 ppm As in the sample. Amounts of arsenic up to 200 μg in the absorbing solution can be

determined after dilution of this solution with 0.01 M $AgNO_3$ as required. For arsenic contents exceeding 2000 ppm in the sample, i.e. 200 μg in the absorbing solution, a smaller sample should be used, because more than 200 μg As cannot be recovered quantitatively by the proposed method.

Sample decomposition. The digestion with $HClO_4$—HNO_3 is a simplified version of the procedure of Terashima [5]. The results obtained correlate well with reported values, some of which were obtained after a HF—$HClO_4$—HNO_3—HCl digestion (Table 1); the good agreement between results with and without hydrofluoric acid in the digest may be explained by the fact that arsenic rarely occurs in the silicate lattice of geological materials.

Arsenic present in the sample is oxidized to arsenic(V) in the digestion; there is no apparent loss by volatilization as recoveries of arsenic spikes from samples were satisfactory. Evaporation of digests to dryness did not cause loss of arsenic but the dry deposits were difficult to remove from Teflon beakers. The proposed digestion is simple and efficient, yielding a moist residue which is easily transferable.

Interferences. There was no interference from as much as 25% Fe, 10% Mn, and 1000 ppm Bi, Cd, Co, Cu, Ni, Pb, Sb, and Te in the samples, even when the elements were present in various combinations. Samples containing more than 500 ppm selenium showed a 5% reduction in arsenic absorbance, but since the crustal abundance of selenium is less than 0.1 ppm [11], problems would not arise for most geological materials. Chromium suppressed the arsenic signal even with as little as 0.5 μg in the synthetic solution. The suppression increased with chromium concentration and tended to level off at 100 μg Cr. Maruta and Sudoh [4] reported a 30% reduction in arsenic signal with a 100-fold amount of chromium, using a similar arsine-generation technique. To investigate this problem, a soil-profile sample (PRP3-3.5) which contained more than 5000 ppm Cr was spiked with two levels of arsenic; the average recovery of the added arsenic was 98%. Possible explanations for the discrepancy may be that the $HClO_4$—HNO_3 digestion does not solubilize the chromium minerals in the sample and that chromium released during sample decomposition is adsorbed by the silica residue as suggested by Scott [12].

The most severe interference encountered was from nitric acid, which retards arsine formation; this confirmed earlier findings [4,5] that nitric acid must be completely removed by evaporation.

The proposed method does not suffer from as many interferences as most other atomic-absorption methods based on hydride generation. Many of the usual interfering elements probably affect the rate of arsine generation rather then the atomization process. The rate is very important in direct flame methods or flameless methods with heated cells, but is of no importance in the proposed method where the generated arsine is absorbed before determination.

Analysis of reference samples. Replicate analyses for arsenic of six geochemical reference samples with varying matrices for arsenic gave relative standard deviation ranging from1% to 6%. General agreement was obtained between means for these samples and arsenic values reported in the literature

TABLE 1

Replicate analyses (n=5) of arsenic in six geochemical reference samples [13] and comparison with reported values

Sample	Range (ppm)	Mean (ppm)	s_r (%)	Reported range[a] (ppm)	Other values (ppm)
GXR-1 (Jasperoid)	327—335	332	0.9	340—452	349[b], 335[c], 436[d]
GXR-2 (Soil)	17.0—19.7	18.2	6.0	19—42	16.25[b], 16.96[c], 23.3[d]
GXR-3 (Fe—Mn deposit)	4340—4820	4564	4.3	2790—3835	3980[d]
GXR-4 (Cu mill head)	83—93	89.0	4.1	75—121	103[d]
GXR-5 (Soil)	9.3—10.6	9.8	5.3	10—25	11.8[d]
GXR-6 (Soil)	315—343	329	3.8	215—312	304[b], 310[c], 297[d]

[a]Colorimetry after $HClO_4$—HNO_3 or HF—HCl—HNO_3—$HClO_4$ digestion [13]. [b]Aqua regia digestion [6]. [c]HF—$HClO_4$—HNO_3 digestion [6]. [d]Ref. [5].

TABLE 2

Recovery of known amounts of arsenic added to various samples (Results are averages of duplicates.)

Sample	Sample weight (g)	As present (μg)	As added (μg)	As found (μg)	Recovery (%)
GXR-1	0.1	34	40	75	101.4
	0.1	34	80	110	96.5
GXR-2	0.1	1.8	1	2.7	96.4
	0.1	1.8	2	3.5	92.1
GXR-3	0.025	109	50	159	100.0
	0.025	109	100	220	105.2
PRSP 3-3.5[a]	0.1	1.1	5	5.9	96.7
	0.1	1.1	10	11.0	99.1

[a]Containing more than 5000 ppm Cr.

(Table 1). Recoveries of two levels of arsenic added to samples ranged from 92% to 105% (Table 2).

REFERENCES

1 R. W. Boyle and I. R. Jonasson, J. Geochem. Explor., 2 (1973) 251.
2 F. D. Pierce and H. R. Brown, Anal. Chem., 49 (1977) 1417.
3 A. E. Smith, Analyst, 100 (1975) 300.
4 T. Maruta and G. Sudoh, Anal. Chim. Acta, 77 (1975) 37.

5 S. Terashima, Anal. Chim. Acta, 86 (1976) 43.
6 G. E. M. Aslin, J. Geochem. Explor., 6 (1976) 321.
7 R. G. Smith, J. C. Van Loon, J. R. Knechtel, J. L. Fraser, A. E. Pitts and A. E. Hodges, Anal. Chim. Acta, 93 (1977) 61.
8 J. Guimont, M. Pichette and N. Rheaume, At. Absorpt. Newsl., 16 (1977) 53.
9 G. F. Kirkbright and M. Taddia, Anal. Chim. Acta, 100 (1978) 145.
10 R. E. Madson, Jr., At. Absorpt. Newsl., 10 (1971) 57.
11 H. J. Rosler, 1972 Geochemical Tables, Elsevier, New York.
12 K. Scott, Analyst, 103 (1978) 754.
13 G. H. Allcott and H. Q. Lakin, Proc. 5th Int. Geochem. Explor. Symp., (1974) 659.

Analytica Chimica Acta, 108 (1979) 363—366
© Elsevier Scientific Publishing Company, Amsterdam — Printed in The Netherlands

Short Communication

THE DETERMINATION OF IODIDE IN THE PRESENCE OF OTHER HALIDES BY ENZYMATIC ENTHALPIMETRY

J. KEITH GRIME*

Department of Chemistry, University of Denver, Denver, Colorado 80208 (U.S.A.)

KENNETH R. LOCKHART

Department of Chemistry, University of Otago, P.O. Box 56, Dunedin (New Zealand)

(Received 6th November 1978)

Summary. Iodide in the range 0.7—9.2 mg can be determined rapidly in the presence of other halides by means of its peroxidase-catalysed oxidation with hydrogen peroxide; the relative standard deviations are 0.3—2%.

The enthalpimetric determination of iodide in admixture with other halides has been discussed in several monographs [1—4]. The relative magnitudes of the enthalpies of precipitation and the solubility products of the three insoluble silver halides indicate that it should be possible to titrate binary and ternary halide mixture successively with silver nitrate solution. In practice, however, thermometric titrations have produced conflicting results. The results obtained in a continuous titration with a mixed thorium nitrate—silver nitrate reagent [5] suggested that iodide could only be determined in the presence of chloride. Harries [6] titrated iodide in 1:1 iodide/bromide mixtures thermometrically with an accuracy of 1—2%, but the accuracy decreased significantly at higher proportions of bromide because of coprecipitation, as with other types of end-point detection. Takeuchi and Yamazaki [7] reported that iodide can be determined in binary or ternary halide mixtures with an error and precision of 1—3% by means of a differential thermometric technique. In a two-step procedure [8], iodide can be determined in the presence of bromide by thermometric titration of sample aliquots with silver nitrate and with potassium permanganate; the enthalpy of each titration reaction was determined and the results were obtained by solving linear equations. Iodide can be determined in admixture with bromide and chloride by direct injection enthalpimetry [9] based on selective oxidation of iodide by chloramine T at pH 8.0—9.0. Empirical direct injection procedures are, however, restricted to the analysis of sample solutions with identical thermal characteristics, unless a standard additions procedure is adopted. Moreover, strict adherence to experimental parameters must be maintained if frequent recalibration is to be avoided.

It has recently been shown [10] that iodide can be employed as the electron donor in the enthalpimetric determination of peroxidase activity.

The peroxidase-catalysed oxidation of iodide at pH 4.7

$$2H^+ + H_2O_2 + 2I^- \xrightarrow{\text{peroxidase}} I_2 + 2H_2O$$

has an enthalpy of reaction of -123.7 ± 0.6 kJ mol^{-1}. This reaction can be used to allow the accurate and precise determination of iodide in the presence of chloride, bromide and fluoride.

Experimental

Reagents. Type 1 horse-radish peroxidase (Lot No. 124C-9580; ca. 89 purpurogallin units per mg of solid; Sigma Chemical Co., St. Louis, Mo.) was used to prepare aqueous stock solutions containing ca. 2000 I.U. cm^{-3}. These solutions remained stable for at least four weeks when stored at 4°C. The aqueous stock solution (ca. 0.03 mol dm^{-3}) of hydrogen peroxide was stored in dark bottles at 4°C. Working solutions of iodide were prepared from potassium iodide. Buffer solutions of pH 3.9 were prepared by adjustment of a 0.1 mol dm^{-3} sodium acetate—acetic acid mixture. All solutions were prepared in distilled, deionized water from analytical-grade reagents.

Apparatus. All enthalpimetric measurements were performed at 25.0°C (short-term stability ± 0.0002°C) on a Tronac 450 calorimeter incorporating batch addition facilities. Details of the amplification, heating and recording systems have already been reported [10]. Reagents were injected from a gravimetrically calibrated Hamilton syringe with a Chaney adapter. Reagent and analyte solutions were thermostatted by immersion of the loaded syringe and the quasi-adiabatic reaction cell and contents in the thermostatted water-bath.

Procedure. Peroxidase solution (1.00 cm^3; ca. 2000 I.U.) and an accurately measured volume of iodide solution were introduced into the reaction cell. In halide interference experiments, 1.00—3.00 cm^3 of bromide, chloride or fluoride solutions or combinations thereof were added at this point. The analyte volume was then made up to 15 cm^3 with buffer solution. The syringe was loaded with 0.5 cm^3 of the hydrogen peroxide solution, containing a stoichiometric excess of reagent (ca. 10%). The entire cell assembly and syringe were then immersed in the thermostatted bath. After attainment of an isothermal baseline, the peroxide solution was injected while the temperature change was monitored. After an appropriate post-reaction baseline had been recorded, the cell and its contents were cooled. Then after re-equilibration the heat capacity of the system was determined by activation of the Joule heating circuitry. The amount of iodide in the solution was calculated in the usual manner from the molar enthalpy of reaction.

Results and discussion

A typical enthalpogram obtained in the assay of iodide ion alone or in the presence of chloride or bromide is shown in Fig. 1 (curve a). Neither chloride nor bromide affected the shape of the enthalpograms within the concentration ranges examined (Table 1). The enthalpogram obtained for the same mass of

TABLE 1

Analytical error (range) and precision data

Iodide taken (mg)	Other halide added (mg)			Range of iodide found (mg)	R.s.d.[a] (%)
	Br^-	Cl^-	F^-		
9.24	—	—	—	9.19 — 9.32	0.76(3)
5.07	—	—	—	5.01 — 5.14	0.99(5)
1.85	—	—	—	1.83 — 1.86	0.54(8)
0.68	—	—	—	0.67 — 0.69	1.48(4)
3.70	1.70	—	—	3.67 — 3.70	0.54(3)
3.70	5.10	—	—	3.65 — 3.74	1.35(3)
1.85	1.70	—	—	1.85 — 1.88	1.07(3)
1.85	5.10	—	—	1.83 — 1.88	1.61(3)
3.70	—	0.58	—	3.67 — 3.73	0.81(3)
3.70	—	1.75	—	3.69 — 3.74	0.81(3)
1.85	—	0.58	—	1.82 — 1.86	1.08(3)
1.85	—	1.75	—	1.84 — 1.86	0.54(3)
3.70	—	—	1.22	3.67 — 3.68	0.27(3)
3.70	—	—	3.67	3.66 — 3.68	0.27(3)
1.85	—	—	1.22	1.85 — 1.88	1.07(3)
1.85	—	—	3.67	1.82 — 1.89	2.15(3)
3.70	1.70	0.58	1.22	3.72	—
1.85	1.70	0.58	1.22	1.87	—
3.70	5.10	1.75	3.67	3.74, 3.69[b]	—
1.85	5.10	1.75	3.67	1.86, 1.89[b]	—

[a]Number of determinations in parentheses. [b]Results of duplicate determinations.

iodide in the presence of fluoride (Fig. 1, curve b) shows clearly that fluoride inhibits peroxidase activity; it does not affect the final degree of completion of the iodide oxidation but prolongs the time required. Consequently, within the limits defined by the adiabaticity of the instrumentation, a certain amount of fluoride can be tolerated with only a small loss in precision and accuracy. Analytical error (range) and precision data obtained for the determination of iodide alone and in binary, ternary or quaternary halide mixtures are presented in Table 1. Obviously, the technique provides an accurate and precise assay of iodide in the presence of other halides.

Small variations in hydrogen peroxide and peroxidase concentrations are acceptable, provided that the hydrogen peroxide is present in excess; the peroxidase concentration dictates only the rate of the enzymatic reaction. Reagent standardization is not necessary, nor is accurate replication of reagent volumes because heat capacity is measured in situ for each analysis. Thus, the method should be applicable to slurries and coloured or viscous solutions without recourse to time-consuming calibration or standard addition procedures.

Depending on the limiting reagent, the procedure could be used for the

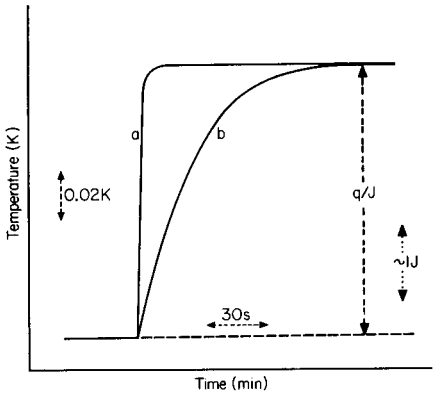


Fig. 1. Typical enthalpograms for 3×10^{-5} mol of iodide in the presence of (a) chloride and/or bromide, and (b) fluoride.

determination of either hydrogen peroxide or iodide. The possibilities of combining amplification reactions and enthalpimetric determinations on this basis are currently being studied.

REFERENCES

1 L. S. Bark and S. M. Bark, Thermometric Titrimetry, Pergamon Press, London, 1969.
2 H. J. V. Tyrrell and A. E. Beezer, Thermometric Titrimetry, Chapman and Hall, London, 1968.
3 G. A. Vaughan, Thermometric and Enthalpimetric Titrimetry, Van Nostrand—Reinhold, London, 1973.
4 J. Barthel, Thermometric Titrations, Wiley-Interscience, New York, 1975.
5 P. T. Priestley, W. S. Sebborn and R. F. W. Selman, Analyst 88 (1963) 797.
6 R. J. N. Harries, Proc. Soc. Anal. Chem., 3 (1966) 19.
7 T. Takeuchi and M. Yamazaki, Kogyo Kagaku Zasshi, 72 (1969) 1263.
8 P. Marik-Korda, Proc. Eur. Symp. Therm. Anal., 1st, (1976) p. 143.
9 L. S. Bark and A. E. Nya, Anal. Chim. Acta, 87 (1976) 473.
10 J. K. Grime and K. R. Lockhart, Anal. Chim. Acta, 106 (1979) 000.

Analytica Chimica Acta, 108 (1979) 367—370
© Elsevier Scientific Publishing Company, Amsterdam — Printed in The Netherlands

Short Communication

THE DETERMINATION OF CARBON IN ALUMINIUM BY DEUTERON ACTIVATION ANALYSIS

P. GOETHALS, C. VANDECASTEELE** and J. HOSTE*

Institute for Nuclear Sciences, Rijksuniversiteit, Proeftuinstraat 86, B-9000 Gent (Belgium)

(Received 8th January 1979)

Summary. Carbon can be determined in aluminium by deuteron activation analysis via the $^{12}C(d, n)^{13}N$ reaction. ^{13}N is separated from other activities by steam distillation. A carbon concentration of 0.25 $\mu g\ g^{-1}$ with a standard deviation of 0.05 $\mu g\ g^{-1}$ was obtained for aluminium of 99.5% purity.

The determination of carbon in aluminium has been the subject of numerous investigations by both non-nuclear and nuclear methods of analysis. The sensitivity of non-nuclear methods, such as combustion, is limited to concentrations of about 1 $\mu g\ g^{-1}$, mainly because of the presence of carbon at the sample surface and because of blank problems. Since the carbon concentration in aluminium is usually below this limit, more sensitive methods are needed.

Both photon [1] and charged-particle activation analyses allow the determination of carbon. A comparison of various charged-particle reactions [2] shows that deuteron activation is to be preferred for reasons of sensitivity and selectivity. When the deuteron energy is below 4.9 MeV, the determination is free from nuclear interferences. The $^{12}C(d, n)^{13}N$ reaction (threshold energy, 0.33 MeV) leads to ^{13}N, a pure β^+-emitter with a 10-min half-life. In the method reported here, ^{13}N is separated from other radionuclides by steam distillation. The method is applied to samples distributed by B.C.R. (Community Reference Bureau of the Commission of the European Communities, Brussels) in a program on the certification of reference materials for non-metals in non-ferrous metals. This material is commercially available as reference material for oxygen (R.M. No. 25).

Experimental

Samples and standards. Aluminium of 99.5% purity was analysed. The samples were cylindrical disks of 15-mm diameter and 1-mm thickness. Graphite and polyethylene disks were used as standards.

Irradiation. The samples and standards were placed in a water-cooled target holder and irradiated with a 7-MeV deuteron beam (8- or 12-mm diameter). The external beam of the isochronous cyclotron of Gent University

**Bevoegdverklaard navorser of the N.F.W.O.

was used. A nickel beam-intensity monitor (12.5-μm thick) and a 40-μm aluminium foil were inserted in front of the samples. Two series of standards were irradiated, placed behind a nickel foil and a 60 or 80-μm layer of aluminium foil. The irradiation conditions are summarized in Table 1.

Chemical etching and separation. To remove possible surface contamination, the samples were etched in a 7:2:1 (v/v) mixture of concentrated phosphoric, sulphuric and nitric acids for 5 min at 80°C. The etched thickness was determined by weighing and by measuring with a micrometer. The values obtained for the removed thickness were quite reproducible, namely 20—30 μm, corresponding to an energy of 4.90—4.70 MeV.

Samples were then placed in a conventional steam-distillation apparatus and dissolved with slight heating (50—60°C) in 25 ml of 10 M NaOH. After dissolution, the temperature was increased to 110—120°C and steam was introduced. The gases were passed through 20 ml of 0.03 M HCl, and 70 ml of the distillate was collected. This was sufficient for the quantitative recovery of the $^{13}NH_3$ as shown by tracer experiments. The chemical separation took 25—30 min.

Measurements. The annihilation photons of ^{13}N were measured by a γ,γ-coincidence system, with two 7.6 × 7.6 cm NaI(Tl)-detectors. Measurements of the samples were started 35—40 min after irradiation. Repeated 5-min measurements were made every 6 min for 30—40 min to obtain the decay curve. For the standard, a similar measuring cycle was started 40—50 min after irradiation.

Calculation of the results

The decay curve was analysed by the CLSQ program [3], assuming one component with a 10-min half-life. The program also determined, as a qualitative criterion for ^{13}N, a best estimate of the half-life. The values obtained ranged from 9.3 to 11.2 min with an average of 10.2 min. Figure 1 shows a decay curve.

The carbon concentration was calculated from

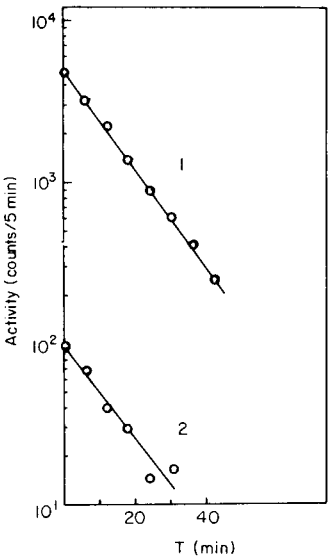
$$C_x = C_s(A_x/A_s)(I_s/I_x)(S_s/S_x)(R_s/R_x)\, g \qquad (1)$$

where C = carbon concentration ($\mu g\ g^{-1}$); A = ^{13}N-activity corrected for

TABLE 1

Irradiation conditions

	Sample	Standard
Beam energy corresponding to etching depth	4.9—4.7	
Beam intensity (μA)	4	0.05
Irradiation time (min)	10	0.5
Beam intensity normalization	$^{60}Ni(d, n)^{61}Cu$	



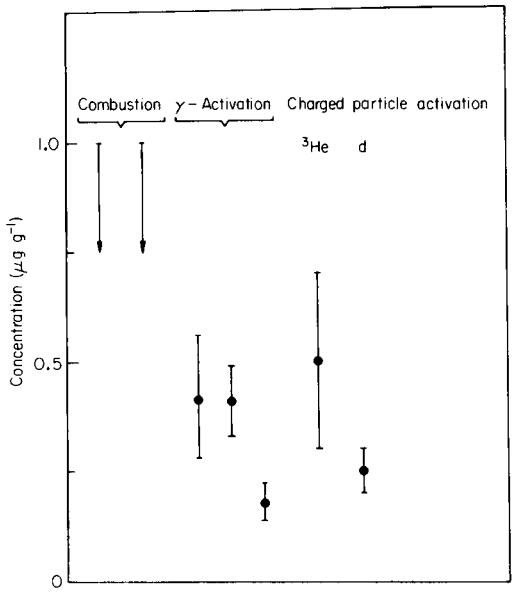


Fig. 1. Decay curves for graphite standard (1) and aluminium sample (2). Measurements were started 45 and 40 min after irradiation, respectively.

Fig. 2. Comparison of results obtained by different laboratories using different analytical methods. The length of the error bars corresponds to 2 standard deviations.

decay; I = beam intensity calculated from the 656-keV ^{61}Cu peak in the flux monitor; S = saturation factor for the production of ^{13}N; R = range (g cm^{-2}); and g = correction factor for the difference in detection efficiency between the sample (NH_3 solution) and the standard (disk). The subscripts x and s refer to the sample and the standards, respectively. In this equation, A_x and A_s must correspond to the same incident energy. Because of the chemical etching, the effective incident energy for the samples varies from 4.9 to 4.7 MeV. Therefore, A_s was obtained by interpolation from the activity of the standards irradiated behind 40 and 60 μm of aluminium, corresponding to incident energies of 4.97 and 4.48 MeV, respectively.

The energies of the particles after traversing the nickel flux monitor, the aluminium foil and the removed aluminium layer were deduced from the tables of Williamson et al. [4].

Results and discussion

The results are summarized in Table 2. Samples 2A—17A were taken from different places of the aluminium batch distributed by B.C.R.; the results given for 3A correspond to different samples taken from the same position of the batch. The F-test and the t-test indicated that both the standard deviation and the mean values for both sets of results did not differ significantly at the 95% confidence level. The entire aluminium batch can thus be assumed to

TABLE 2

Carbon concentration in aluminium 99.5

Sample	C ($\mu g\ g^{-1}$)		Sample	C ($\mu g\ g^{-1}$)	
	Individual results	Av. ± s		Individual results	Av. ± s
Al 99.5(3A)	0.19 ± 0.05[a]		Al 99.5(2A)	0.31 ± 0.03	
	0.23 ± 0.02		(5A)	0.25 ± 0.03	
	0.21 ± 0.03		(11A)	0.26 ± 0.04	
	0.20 ± 0.04		(14A)	0.32 ± 0.04	
	0.28 ± 0.03	0.22 ± 0.04 (n = 5)	(17A)	0.22 ± 0.02	0.27 ± 0.04 (n = 5)
	Overall mean:	0.25 ± 0.05 (n = 10)			

[a]Standard deviation calculated by the decay curve analysis program.

contain carbon homogeneously distributed, at least when samples of 15 mg are analysed. Comparison of the standard deviation expected from the decay curve analysis with the experimental standard deviation shows that counting statistics is the major source of imprecision.

Samples from the same batch were analysed by other laboratories using different analytical methods; Fig. 2 shows the results. It is apparent that results obtained by the present method agree (within experimental error) with those obtained by other methods.

Grateful acknowledgement is made to J. Pauwels (CBNM, Geel) for providing the samples and to the I.I.K.W. and N.F.W.O. for financial support.

REFERENCES

1 M. Fedoroff, C. Loos-Neskovic and G. Revel, J. Radioanal. Chem., 38 (1977) 107.
2 C. Engelmann, J. Radioanal. Chem., 7 (1971) 89, 281.
3 Y. Cumming, BNL Report 6470 (1963).
4 C. Williamson, J. Boujot and J. Pickard, Tables of Ranges and Stopping Power of Chemical Elements for Charged Particles of Energy 0.5—500 MeV, Rapport CEA-R 3042, Paris, 1966.

Analytica Chimica Acta, 108 (1979) 371—374
© Elsevier Scientific Publishing Company, Amsterdam — Printed in The Netherlands

Short Communication

DETERMINATION OF URANIUM BY NEUTRON ACTIVATION AND RADIOCHEMICAL SEPARATION OF THE TELLURIUM FISSION PRODUCT

I. KULEFF

Radiochemical Laboratory, Faculty of Chemistry, University of Sofia, 1126-Sofia (Bulgaria)

(Received 12th December 1978)

Summary. After irradiation and dissolution of the samples (minerals, rocks etc.), elemental tellurium is precipitated, redissolved, extracted for its diethyldithiocarbamate, and finally reduced again for measurement of the ^{132}Te 228-keV γ-peak. The chemical yield is 75% and the lower limit of determination is 2×10^{-7} g U.

Several authors have used ^{132}Te for the determination of uranium in minerals [1], pure aluminium [2], phosphate rocks, river and sea sediments [3], lunar samples, meteorites, rocks and minerals [4]. In all cases an appropriate chemical isolation of ^{132}Te is used, e.g. by ion exchange [2], precipitation [3] or both [4]. In this communication a radiochemical method for isolation of tellurium from a neutron-irradiated sample is proposed. The method is based on a combination of precipitation and extraction processes [5]. The content of ^{235}U or total uranium in minerals, rocks and environmental samples is determined by γ-spectrometry of ^{132}Te. High radiochemical purity of the final preparations is guaranteed although the procedure requires less working time than earlier methods [1—4].

Experimental

Irradiation and measurement. The powdered material (0.03—0.2 g) was placed in a polyethylene container and irradiated for 6—18 h at a neutron flux of 2×10^{12} n cm^{-2} s^{-1} (IRT-2000 reactor, Sofia). The standard U_3O_8 dissolved in nitric acid was irradiated simultaneously.

The γ-spectrum of the final product was measured with a Ge(Li) detector and a 4096-channel analyser. Peak areas were calculated by the TPA method [6].

Separation of tellurium. After a cooling time of 24 h, dissolve the irradiated sample in 11 M HCl, or in a mixture of H_2F_2 and H_2SO_4, or in 6 M HCl after fusion with Na_2O_2—NaOH, depending on the sample. For the Na_2O_2—NaOH fusion, use a nickel crucible previously prepared as follows: add 4 ml of 6 M NaOH to the crucible, evaporate to dryness under an i.r. lamp, add 3 ml of tellurium carrier (10 mg Te ml^{-1} in 3 M HCl, standardized gravimetrically by reduction with KH_2PO_2 [7]) to the dry residue and again evaporate to dryness. Store the crucible in a desiccator until required. Transfer the irradiated

sample to the crucible containing 0.5 g of NaOH and 1.5 g of Na_2O_2 and cover with 1.5 g of Na_2O_2 and 1 g of NaOH. Fuse at 600°C, homogenize the melt with a nickel rod, cover the crucible again and heat for another 15—20 min. Finally dissolve the melt in 6 M HCl.

When the irradiated samples can be dissolved in concentrated acids as mentioned above, add 3 ml of the tellurium carrier by pipette.

Transfer the solution obtained after dissolution of the irradiated sample to a centrifuge tube, adjust to 3 M in HCl, and add 1 ml of 0.04 M potassium iodate solution. Mix well, add 1 ml of 1.2 M potassium iodide and place the tube for a few minutes in a boiling water bath. A black precipitation is formed. Add 4 ml of a saturated solution of sodium sulfite and 2 ml of 2 M hydrazine hydrochloride to the hot solution and heat again in the water bath. Centrifuge, wash the precipitate with 15 ml of 1 M HCl and dissolve in 1 ml of aqua regia. Add 20 ml of water and transfer the solution to a separatory funnel. Add 2 ml of slightly acidified saturated sodium arsenite solution, shake vigorously, add 3—4 drops of cresol red solution (20% ethanolic). Add dilute (1 + 3) ammonia solution dropwise until the yellow solution turns crimson. Then add 5 ml of buffer pH 8.6 (4 g of H_3BO_3, 1 g of Na_2EDTA and 0.2 g of KCN in 100 ml of water, adjusted with 2.5 M NaOH to pH 8.6). Shake the solution, add 5 ml of aqueous 0.2 M sodium diethyldithiocarbamate solution and again shake vigorously. Add 20 ml of chloroform, shake for 1—2 min and transfer the organic phase to another funnel. Add 20 ml of 0.03 M $CuCl_2 \cdot 2H_2O$ solution in 3 M HCl and shake vigorously for 3—4 min. Transfer the aqueous phase to a centrifuge tube, add 10 ml of 11 M HCl and 5 ml of 1 M KH_2PO_2 and heat the mixture in a boiling water bath with constant stirring. Centrifuge the black elemental tellurium formed and wash with 10 ml of water, 20 ml of 0.03 M Na_2EDTA solution in acetate buffer pH 4.5 and 10 ml of water. Filter the precipitate on a fine filter paper previously treated with the wash solutions. Wash the precipitate with 20 ml of water, 10 ml of ethanol and 10 ml of ether, dry at 110°C for 10—15 min, and weigh for the determination of the chemical yield (which amounted to 75%). Measure the γ-spectrum of the sample, and evaluate the 228 keV γ-peak of ^{132}Te.

Results and discussions

Behaviour of interfering radionuclides. One of the most important sources of error for the γ-spectrometric determination arises from overlapping peaks. A critical review of the nuclear data of the radionuclides generated at the reactor flux used [8, 9] showed that the presence of ^{239}Np, ^{182}Ta, ^{177m}Lu, and ^{143}Ce would lead to systematic errors in the results. The present investigations indicate that the proposed radiochemical isolation ensures very good purification of radiotellurium. The decontamination factors and some nuclear data of the radionuclides which interfere with the γ-spectrometry of ^{132}Te are given in Table 1. It can be seen that very high decontamination factors are achieved for ^{143}Ce, ^{177m}Lu and ^{239}Np. The results for ^{182}Ta can be considered satisfactory, for this permits the analysis of rocks and other materials in which

TABLE 1

Nuclear data and decontamination factors (D) for interfering elements

Radio-nuclide	Nuclear reaction	Half-life	σ_{th}[a] (barn)	θ[b] (%)	Peak (keV)	I[c] (%)	D
^{143}Ce	(n, γ)	33.7 h	0.94	11.07	231	2.0	>8000
^{177m}Lu	(n, γ)	155 d	7	2.59	228	37.0	>10000
^{182}Ta	(n, γ)	115 d	19	99.99	229	3.8	150
^{239}Np	(n, γ) $\xrightarrow{\beta}$	2.35 d	2.71	99.27	228	9.5	>80000

[a]Thermal cross-section. [b]Isotopic abundance. [c]Absolute intensity (photons per 100 disintegrations).

the Ta : U ratio exceeds 500:1. The proposed method can be used for the analysis of samples with even higher tantalum concentrations, provided that γ-spectrometry is done 24 h after the ^{132}Te isolation by the 667- and 954-keV γ-peaks of the daughter ^{132}I. (The decontamination factor for the radio-iodine exceeds 10^6.)

Sensitivity, precision and accuracy. The applicability of the described method to various materials is demonstrated in Table 2. Under the experimental conditions used, the lower limit of determination, calculated as recommended by Currie [13], was 2×10^{-7} g U. The precision (relative standard deviation) of the method is 3 to 9%.

The results for the uranium content obtained by the proposed method are in very good agreement with certified values for the standard materials (S-2, S-4, S-12) as well as with the results obtained by other methods (Table 2).

TABLE 2

Uranium content in four minerals, two rocks and other samples

Sample	N[a]	s_r[b]	U content (g g^{-1})	
			This method	Other method[c]
Ishikawaite	6	5.2	0.190 ± 0.010	0.21 (IA); 0.200 (A); 0.200 (RF)
Autunite	4	4.0	(12.36 ± 0.50) × 10^{-3}	11.8 × 10^{-3} (A); 12.5 × 10^{-3} (IA).
S-2 (Torbernite)[d]	6	3.2	(2.78 ± 0.09) × 10^{-3}	2.65 × 10^{-3} (PC)[e]; 2.58 × 10^{-3} (IA); 2.70 × 10^{-3} (A); 2.57 × 10^{-3} (IA) [10]
S-4 (Uraninite)[a]	5	3.3	(3.00 ± 0.10) × 10^{-3}	3.13 × 10^{-3} (PC)[e]; 3.10 × 10^{-3} (A); 3.18 × 10^{-3} (IA); 3.21 × 10^{-3} (IA) [10]
S-12 (Pitchblende)[d]	6	3.6	(1.13 ± 0.04) × 10^{-4}	1.19 × 10^{-4} (PC)[e]; 1.53 × 10^{-4} (RM); 1.23 × 10^{-4} (IA)
Phosphate rock	6	4.9	(2.10 ± 0.08) × 10^{-5}	1.95 × 10^{-5} (IA); 1.90 × 10^{-5} (RF)
Monzodiorite	3	6.1	(2.32 ± 0.14) × 10^{-6}	2.7 × 10^{-6} (PC) [11]; 2.50 × 10^{-6} (A),
Sand	4	4.1	(2.18 ± 0.09) × 10^{-5}	1.90 × 10^{-5} (IA)
Soil	3	8.8	(1.25 ± 0.11) × 10^{-6}	0.90 × 10^{-6} (A)
Fertilizer	4	4.2	(4.30 ± 0.18) × 10^{-5}	4.6 × 10^{-5} (A); 4.2 × 10^{-5} (IA)

[a]Number of determinations. [b]Relative standard deviation (%). [c]A = neutron activation with radiochemical separation of ^{239}Np [12]; IA = instrumental neutron activation of ^{239}Np with Ge(Li)-detector; RF = x-ray fluorescence spectrometry; PC = spectrophotometry; RM = direct radiometric determination. [d]Standard materials with low uranium content, IAEA, Vienna. [e]Certified value.

REFERENCES

1 C. Fischer and J. Beydon, Bull. Soc. Chim. Fr., C, (1953) 102.
2 J. Gaittet, Ph. Albert, C.R.H. Acad. Sci., 247 (1958) 1861.
3 A. D. Suttle, Jr., B. C. O'Brien and D. W. Mueller, Anal. Chem., 41 (1969) 1265.
4 R. R. Keays, R. Ganapathy, J. C. Laul, U. Krähenbühl and J. W. Morgan, Anal. Chim. Acta, 72 (1974) 1.
5 I. Kuleff, K. Kostadinov and Y. Yanev, Sbornik Dokladov IIIth Symposiuma Stran Tshlenov SEW, November, Neubrandenburg, D.D.R., 1976, Vol. 2.
6 H. P. Yule, Anal. Chem., 40 (1968) 1480.
7 I. I. Nazarenko and A. N. Ermakov, Analytitshekaja Chimija Selena i Tellura, Nauka, Moskwa, 1971, p. 61.
8 F. Baumgärtner, Tabelle zur Neutronenaktivierung, Verlag Thiemig, München, 1967.
9 G. Erdtmann and W. Soyka, Die Gamma-Linien der Radionuklide, Ber. KFA-Jül-1003-AC (1974).
10 E. Mainka, H. Ruf, W. Goerdt, M. Friedrich and W. König, Ber. KFK-2458 (1977).
11 T. Hissina, M. Pavlova, Bull. Geol. Institute-Ser. Geochemistry, Mineralogy and Petrography, 17 (1968) 33.
12 I. Kuleff and D. Todorovsky, J. Radioanal. Chem., 21 (1975) 445.
13 L. A. Currie, Anal. Chem., 40 (1968) 586.

Analytica Chimica Acta, 108 (1979) 375—377
© Elsevier Scientific Publishing Company, Amsterdam — Printed in The Netherlands

Short Communication

KINETIC POTENTIOMETRIC DETERMINATION OF CITRIC ACID WITH A PERBROMATE-SELECTIVE ELECTRODE

L. A. LAZAROU and T. P. HADJIIOANNOU*

Laboratory of Analytical Chemistry, University of Athens, Athens (Greece)

(Received 5th December 1978)

Summary. Citric acid is determined in the 96—960-μg range with relative errors of about 1% by means of its iron(II)-induced reaction with perbromate. Each analysis takes about 8 min. Tartaric and lactic acids interfere.

Citric acid and perbromate do not react. However, when iron(II) is added, the iron is oxidized by perbromate, and this reaction induces the oxidation of citric acid by perbromate. The iron(II)-induced perbromate—citric acid reaction can be monitored with a perbromate-selective electrode [1]; under controlled conditions, there is a linear relation between the increase in electrode potential within a fixed period of time (6 min) and the amount of citric acid present.

Experimental

Apparatus. A perbromate-selective electrode [1] was used as the indicator electrode with a double-junction silver—silver chloride reference electrode (Orion Model 90-02-00). The electrode potential was measured and printed with an Orion Ionanalyzer (Model 801 digital pH/pIon meter) coupled to an Orion digital printer (Model 751) which was adjusted to print the potential every 6 min.

Reagents. All solutions were prepared with deionized distilled water and reagent-grade substances.

For the stock citric acid solution (0.1000 M) dissolve 21.01 g of citric acid in water and dilute to exactly 1 l. Store in a plastic bottle. Prepare working standards (1.00×10^{-4}, 5.00×10^{-4} and 1.00×10^{-3} M) by dilution as required. For the stock perbromate solution (0.01000 M), dissolve 0.1830 g of potassium perbromate in water and dilute to 100.0 ml. For the stock iron(II) solution (0.100 M), dissolve 39.2 g of $(NH_4)_2Fe(SO_4)_2 \cdot 6H_2O$ in 50 ml of 2 M sulfuric acid and dilute with water to 1 l; store in an amber bottle. Prepare a 2.00×10^{-3} M working solution by dilution with 0.005 M sulfuric acid.

During measurements all solutions were thermostated at 25° ± 0.1°C.

Procedure. Into the thermostated reaction cell [1], kept at 25.0°C, transfer 5.00 ml of acetate buffer pH 4.75 (total acetate, 0.20 M), 0.50 ml of potassium perbromate and 5.00 ml of the citric acid standard or sample solutions. Insert

the electrodes in the solution and start stirring at the maximum speed at which air bubbles are not formed. When the potential has stabilized (30—60 s), inject 50 μl of the 2.00×10^{-3} M iron(II) solution and immediately press the "start" switch of the printer to print the initial electrode potential, E_0. After 6 min, the new electrode potential, E_6, is automatically printed. Empty the cell by suction, rinse the electrodes and the cell with water and dry by suction. Repeat the procedure for each analysis.

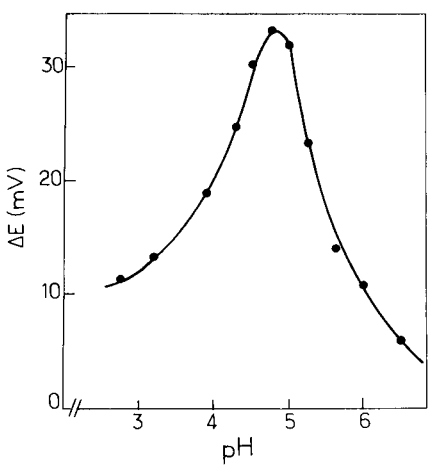
Working curves, μg of citric acid vs. ΔE ($\Delta E = E_6 - E_0$), were prepared by the least-squares method.

Results and discussion

The pH strongly affects the reaction rate; Fig. 1 shows the effect of pH on the value of ΔE, which is a measure of the reaction rate. A maximum is observed at about pH 4.75. Figure 2 shows the distribution of citrate species as a function of pH. From Figs. 1 and 2, it can be seen that the active citrate species are $C_6H_7O_7^-$ and $C_6H_6O_7^{2-}$. It is probable that iron(II) forms complexes with these species.

The concentration of perbromate chosen, 4.74×10^{-4} M, is a compromise to ensure a potential change of at least 50 mV before approaching the lower limit of the linear response of the perbromate-selective electrode. The rate of the iron(II)-induced perbromate—citric acid reaction increases with increasing ionic strength and temperature, which must therefore be kept constant.

Analysis of aqueous citric acid solutions of known concentrations gave the results shown in Table 1. The data indicate that citric acid in the range 96—960 μg



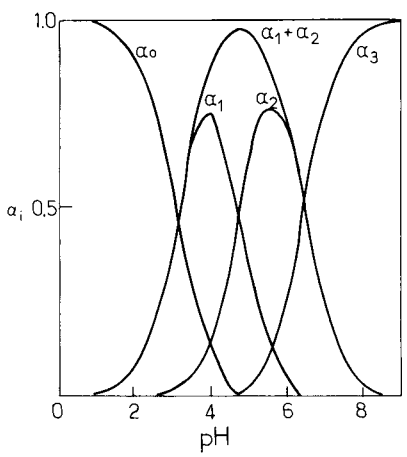


Fig. 1. Effect of pH on the iron(II)-induced perbromate—citric acid reaction for 1.00×10^{-3} M citric acid.

Fig. 2. Fraction of citrate present as different protonated species as a function of pH ($pK_1 = 3.13$, $pK_2 = 4.76$, $pK_3 = 6.40$) [3].

TABLE 1

Determination of citric acid in aqueous solutions

Citric acid in 5-ml sample (μg)		Error (%)
Taken	Found[a]	
96.0	95.7	−0.3
192	190	−1.0
288	288	—
384	391	+1.8
480	481	+0.2
672	687	+2.2
960	960	—
	Mean	0.8

[a]From working curve: μg citric acid = −7.3 + 22.4 ΔE (in mV). Single measurements.

(1.0×10^{-4}—1.0×10^{-3} M) can be determined with relative errors of about 1%. The relative standard deviation for the determination of 4.0×10^{-4} M citric acid sample was 1.0% (n = 5). Tartaric and lactic acids react with perbromate in the presence of iron(II) [2] and must be eliminated. Iron(III) and bromate do not interfere.

The authors thank O. Antonsen of the Eidgenössiches Institut für Reaktovforschung, Wurelingen, Switzerland, for provision of the potassium perbromate. This research was supported in part by a research grant from the Greek National Institute of Research.

REFERENCES

1 L. A. Lazarou and T. P. Hadjiioannou, Anal. Lett., in press.
2 L. A. Lazarou and T. P. Hadjiioannou, Anal. Chim. Acta, 100 (1978) 207.
3 H. Freiser and Q. Fernando, Ionic Equilibria in Analytical Chemistry, J. Wiley, New York, 1963.

Analytica Chimica Acta, 108 (1979) 379—383
© Elsevier Scientific Publishing Company, Amsterdam — Printed in The Netherlands

Short Communication

THE pH RESPONSE OF THE RETICULATED VITREOUS CARBON ELECTRODE

A. N. STROHL and D. J. CURRAN*

Department of Chemistry, GRC Tower I, University of Massachusetts, Amherst, Massachusetts 01003 (U.S.A.)

(Received 19th December 1978)

Summary. Reticulated vitreous carbon (RVC) electrodes show variable mV responses to changes in pH. The mV—pH slopes are Nernstian for the pH range 1—7 between 39 and 49°C. Treatment with permanganate solution greatly enhances the response. The RVC material was analyzed for carbon, hydrogen, and nitrogen and trace metallic impurities. Reasons for the response are discussed.

Reports in the literature concerning the hydrogen overpotential at various types of carbon electrodes are contradictory. Carbon voltammetric electrodes generally have cathodic potential limits in the vicinity of −1.0 V vs. SCE in 1 M $HClO_4$ [1]; a thin slice of reticulated vitreous carbon (RVC) has been used as an optically transparent electrode by Norvell and Mamantov [2], who reported a usable potential range at pH 7 from 1.2 to −1.0 V vs. SCE. Carbon electrodes can, however, also be used as potentiometric indicator electrodes for acid—base titrations and as pH monitors. Szepesváry and Pungor [3] have summarized much of the work in their report on a silicone rubber-based graphite electrode for use in acid—base titration [3]. The response of their electrode depended on the pretreatment, but in all cases the equivalence potential was considerably positive of the equivalence potential of the glass electrode for the identical titration.

During investigations of reticulated vitreous carbon (RVC) electrodes [4] for voltammetry in flowing streams, it was necessary to obtain current—voltage curves for several solutions of different acidities. These electrodes had very large surface areas and it was observed that the cathodic potential limit depended on the acidity and occurred at relatively positive potentials. This prompted an examination of the possible application of the RVC electrode as a pH electrode, as reported below.

Experimental

Chemicals. Buffer solutions were as follows: pH 2, 0.05 M potassium tetroxalate; pH 4 and pH 7, Fisher Scientific Gram Pacs; pH 9, Beckman Buffer 14049 or 0.01 M sodium tetraborate; and pH 12, calcium hydroxide solution

saturated at 25°C. Hydrogen (Airco prepurified, 99.995%), was used as received.

RVC electrode construction. RVC-4 (latest designation RVC 4X1-80-S; Chemotronics International, Inc., Ann Arbor, Mich.) was used for all experiments. A cylinder (8.0 cm long, 1.0 cm diameter) was cut from a RVC-4 block. For electrical contact, a platinum wire was pressed along the side of the cylinder and secured with Teflon tape. The platinum wire extended less than one third of the way down the cylinder and did not contact the test solution.

Equipment. Cell e.m.f.s were measured with a Corning Model 125 Digital pH Meter. A Fisher 13-639-50 reference electrode was used. Current—voltage curves were obtained with a Princeton Applied Research Model 170 Electrochemical System. For temperature control, a jacketed beaker was connected to a P. M. Tamson Model T-9 Circulating Bath. The thermometer used was calibrated against a second thermometer which had been calibrated by the National Bureau of Standards.

Emission spectra were obtained with a Jarrell-Ash Model 70,310 3.4-m Ebert Spectrograph.

E.m.f. measurements. A series of beakers containing the pH test solutions were placed in the temperature bath and allowed to equilibrate. In turn, each beaker was removed from the bath and placed into the jacketed beaker; a small amount of water in the inner portion of the jacket formed a thin film for heat transfer with the inserted beaker. The solution was mechanically stirred and hydrogen was bubbled into the solution continuously. The RVC electrode and the SCE were dipped into the solution, and the millivolt response was measured several times, the RVC electrode being removed from the solution and shaken dry before being replaced for the next measurement. When test solutions were changed, the RVC electrode was rinsed with distilled water, dried with acetone, and washed several times with the next solution to be measured. For most temperatures, only the pH 2—9 test solutions were measured; after all the test solutions had been measured, the temperature was changed and the procedure was repeated. However, for three temperatures, the calcium hydroxide pH 12 test solution was also measured; in this case, between sets, the RVC electrode was soaked in 2 M HCl for several hours. Strong base seemed to deactivate the response of the electrode to acidic solutions.

RVC spectroscopic analysis. Spectroscopic Harvey cups were packed with a piece of RVC-4 and inserted into the spectrograph. A d.c. arc (2—5 A) was applied for 15—60 s and the emission spectra were recorded on photographic plates. Spectra of carbon and iron were also recorded for background and calibration purposes.

RVC combustion analysis. A weighed amount of RVC-4 was placed in a ceramic crucible and ignited in air with a Meker burner. The weight loss was determined. Hot concentrated nitric acid was added to dissolve the residue. Spot tests [5] were run on the solution to attempt to confirm the results of the emission spectrochemical work. Carbon, nitrogen, and hydrogen in RVC

were determined by the University of Massachusetts RSCA Chemical Analysis Laboratory.

Results and discussion

Current—voltage curves were measured, as described previously [4], for solutions of several compositions and acidities (Fig. 1). In the absence of chloride ion, the anodic limit was shown to be due to the oxidation of water [4]. The electrode area was very large (515 cm^2 based on its dimensions) and the cathodic limits were positive of 0.0 V vs. SCE. On this basis, it was decided to perform some potentiometric studies with standard buffer solutions at different temperatures. The tabular summary of Robinson and Stokes [6] was used with linear interpolation to obtain the true pH of each solution at each temperature. The millivolt response was plotted vs. pH for eight different temperatures; six of these plots are shown in Fig. 2. In all but the most basic solution, the RVC electrode was the positive electrode of the cell. The slopes of the lines for all temperatures are presented in Table 1. Linearity is maintained over a wider pH range at lower temperature, but the slopes deviate the most from Nernstian response. In acidic solution, at 39—49°C, the response is Nernstian, but at still higher temperatures the slopes again are less than those predicted, assuming that the potential-determining process involves an equal number of protons and electrons. All these data were obtained in solutions saturated with hydrogen. Doležal and Štulík [7] performed acid—base titrations with glassy carbon electrodes and presented evidence to suggest that the electrode behaved as an oxygen electrode. The present work suggests that this is not the case with RVC electrodes, and perhaps with any carbon electrodes, since the solutions contained very little dissolved oxygen. Some of the measurements were repeated without the hydrogen bubbling, and the results

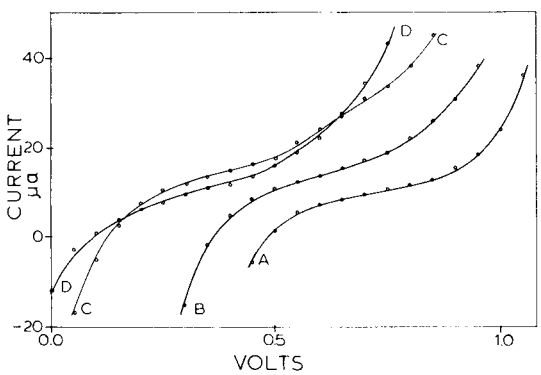


Fig. 1. Current—voltage curves at the RVC flow-through electrode. Potential vs. SCE; flow rate, 4 ml min^{-1}; data taken at fixed potential (every 50 mV). (A) 2.5 M H_2SO_4; (B) pH 0.3; (C) pH 3.9; (D) pH 6.2. Cathodic currents are shown as negative.

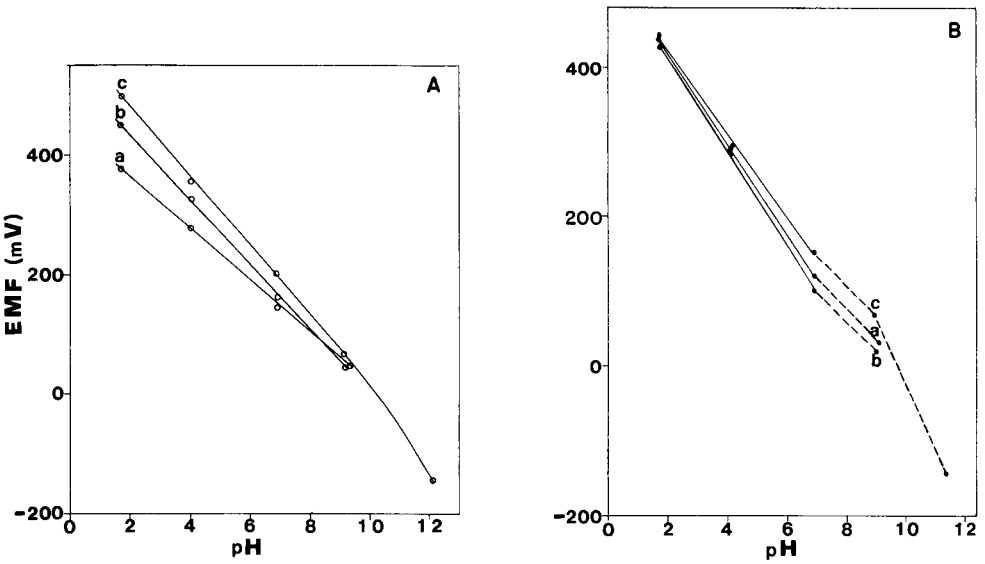


Fig. 2. Cell e.m.f. vs. pH. (A) a, 19°C; b, 29°C; c, 35°C. (B) a, 39°C; b, 49°C; c, 64°C.

TABLE 1

Slopes of the mV—pH curves at different temperatures

Temp. (°C)	pH range	Experimental slope (mV/pH)	Nernstian slope (mV/pH)
19	1—9	44.2	58.0
29	1—9	55.2	60.0
35	1—9	57.4	61.1
	9—12	69.7	
39	1—7	62.4	61.9
	7—9	40.5	
49	1—7	63.5	63.9
	7—9	38.7	
54	1—7	57.6	64.9
	7—9	31.6	
	9—12	56.8	
59	1—7	59.7	65.9
	7—9	46.4	
64	1—7	57.0	66.9
	7—9	39.5	
	9—12	88.0	

were identical to those obtained in its presence. Szepesváry and Pungor [3], following the lead of earlier work, found that their electrodes could be "activated" by immersion in solutions of strong oxidants; such electrodes pro-

duced much larger potential breaks than untreated electrodes in acid—base titrations. Similar results were found with RVC electrodes. Immersion of an RVC electrode for 10 min in a solution of permanganate produced an electrode which gave a response of 112 mV/pH at 48°C in the pH region 4—7.

The evidence above suggests that the potential-determining reaction for the acid—base response of carbon electrodes is neither the reduction of oxygen nor hydrogen ion. Clem [8] investigated the loss of hydrogen overvoltage on graphite electrodes used for anodic stripping, and concluded that to avoid the loss of overpotential, highly acidic solutions and acidic solutions containing oxidants should not be used. He suggested that the formation of surface carboxyl groups was the likely cause of the problem. It is not possible, on the basis of the present work, to state a mechanism for the acid—base response of RVC electrodes. However, the data are in accord with the presence of acidic functional groups on the electrode surface.

The weight loss on combustion in air showed that the material is principally organic (99.83%), but the elemental analyses (96.0% C, 0.5% H, 1.0% N) showed that it is not pure carbon. The change in slope of the curve shown in Fig. 2A can be qualitatively interpreted in terms of surface functional groups having pK_a values in the range 8—10. The shift in slope in this pH region with increasing temperature is in accord with the direction of change in pK_a with temperature. Emission spectroscopy showed that RVC contains Fe, Al, Cu and Ag impurities; the presence of Fe and Al was confirmed by spot tests. The role of these impurities is unknown. If they are present as their oxides, they could contribute to the acid—base behavior of the electrode. If they are present as metals, they would be dissolved on treatment with permanganate.

Despite the fact that the mechanism for the pH response of the RVC electrode is unclear, the material is useful for monitoring the acidity of solutions. It has been used in direct potentiometric measurements and can be used in acid—base titrations, or for continuous monitoring in flowing streams.

REFERENCES

1 D. T. Sawyer and J. Roberts, Jr., Experimental Electrochemistry for Chemists, J. Wiley, New York, 1974, p. 65.
2 V. E. Norvell and G. Mamantov, Anal. Chem., 49 (1977) 1470.
3 E. Szepesváry and E. Pungor, Anal. Chim. Acta, 54 (1971) 199.
4. A. N. Strohl and D. J. Curran, Anal. Chem., 51 (1979) 353.
5. F. Feigl and V. Anger, Spot Tests in Inorganic Analysis, 6th Eng. edn., Elsevier, New York, 1972.
6 R. A. Robinson and R. H. Stokes, Electrolyte Solutions, 2nd edn., Butterworths, London, 1959, p. 545.
7 J. Doležal and K. Štulíck, J. Electroanal. Chem., 17 (1968) 87.
8 R. Clem, Anal. Chem., 47 (1975) 1778.

Analytica Chimica Acta, 108 (1979) 385—388
© Elsevier Scientific Publishing Company, Amsterdam — Printed in The Netherlands

Short Communication

A PVC MATRIX MEMBRANE CALCIUM-SELECTIVE ELECTRODE BASED ON CALCIUM BIS-4-(1,1,3,3-TETRAMETHYLBUTYL)-2,6-DINITROPHENOXIDE

S. KAMATA**, G. J. MOODY and J. D. R. THOMAS*

Chemistry Department, UWIST, Cardiff CF1 3NU (Gt. Britain)

(Received 23rd November 1978)

Summary. The dinitrophenoxide specified shows calcium-selective properties similar to those reported earlier for the corresponding phosphate. The detection limit is 1.1×10^{-5} M. Selectivity coefficients are better for zinc, but poorer for barium and strontium than those obtained with electrodes based on phosphate esters.

Treatment of phosphorus oxide trichloride with an alcohol or 4-alkylphenol normally yields a mixture of di- and mono-phosphate esters [1, 2] and the products can be employed as calcium ion sensors [1, 3]. Recent work [4] has shown that the cumulative steric hindrance of the nitro groups in 4-(1,1,3,3-tetramethylbutyl)-2,6-dinitrophenol prevents measurable phosphorylation, although the singly nitrated material, 4-(1,1,3,3-tetramethylbutyl)-2-nitrophenol, is readily phosphorylated. This suggests that electrodes VA and VB of a previous paper [5] depended at least to some extent on the calcium salt of the unreacted phenol for their response instead of the postulated calcium salt of di[4-(1,1,3,3-tetramethylbutyl)-2,6-dinitrophenyl]-phosphate. Hence, the calcium ion-sensing property of calcium bis-4-(1,1,3,3-tetramethylbutyl)-2,6-dinitrophenoxide was investigated.

Experimental

Chemicals. Calcium bis-4-(1,1,3,3-tetramethylbutyl)-2,6-dinitrophenoxide was synthesized, the other chemicals being of analytical-reagent grade or reagent grade. For the phenoxide synthesis, 4-(1,1,3,3-tetramethylbutyl)-phenol was nitrated [6] with fuming nitric acid at —15°C. After separation and purification, the 4-(1,1,3,3-tetramethylbutyl)-2,6-dinitrophenol product (pK_a = 4.87) was added as a dilute solution in methanol (1 g in 100 cm^3) to a saturated, filtered solution of calcium hydroxide, and the resulting bright yellow phenoxide precipitate was separated by filtration [6].

Electrodes. Calcium-selective electrodes containing the calcium liquid ion-exchanger (0.40 g) [di-n-octylphenylphosphonate (0.36 g) plus sensor (0.04 g)] trapped in PVC (0.17 g) were prepared as previously described [7].

**Present address: Department of Applied Chemistry, Faculty of Engineering, Kagoshima University, Kagoshima, Japan.

Procedure. All e.m.f. measurements were made relative to an EIL Model RJ 23 saturated calomel reference electrode. A Beckman Research Model millivoltmeter-pH meter was used in conjunction with a Servoscribe potentiometric recorder. Selectivity coefficients, $k^{pot}_{Ca,B}$, were determined by the mixed solution method [8, 9] with a fixed level of interferent B. pH interference was assessed by the mixed solution method [8, 9] where the calcium ion level was fixed at 10^{-2} M and pH varied.

Interference potentials, E_M, defined as the difference between observed bi-ionic potentials and potentials calculated assuming no interference [10, 11] were also determined and their fit of the equation [10, 11] $E_M = -RTF^{-1} \ln [1 + K_M\, a_B/(a_{Ca})^{z_B/2}]$ was used to calculate the selectivity parameter, K_M. The test solutions contained m_1 and m_2 molal concentrations of $CaCl_2$ and BCl_2, respectively. Two series of test solutions were prepared at 3×10^{-3} and 3×10^{-2} M total ionic strength, with several solutions of varying $CaCl_2$:BCl_2 ratios being examined for each series.

Results and discussion

The main features of the electrode based on calcium bis-4-(1,1,3,3-tetramethylbutyl)-2,6-dinitrophenoxide sensor and di-n-octylphenylphosphonate solvent mediator (electrode I) are compared in Table 1 with those of established calcium ion-selective electrodes based on calcium bis-di[4-(1,1,3,3-tetramethylbutyl)phenyl] phosphate sensor and di-n-octylphenylphosphonate solvent mediator (electrode II) and a recent batch of Orion 92-20-02 liquid calcium ion-exchanger (electrode III). Table 2 summarizes K_M data for electrodes I,

TABLE 1

Comparison of properties of electrode I with electrodes II and III at 25°C (Electrode lifetimes exceed 2 weeks in each case.)

Property	Electrode I	Electrode II	Electrode III
Detection limit for Ca^{2+} (M)	1.1×10^{-5}	2.8×10^{-6}	5.0×10^{-6}
Slope (mV/decade)	30.5	30.5	33.5
Static response time[a]	10	20	40
Long term drift (mV d^{-1})	0.2	0.4	~2
pH range for 10^{-2} M $CaCl_2$ solutions	4.7—~10	4.7—~10	5.3—~9.0
Selectivity coefficient ($k^{pot}_{Ca,B}$)			
Na ($[B^+] = 5 \times 10^{-2}$ M)	1.0×10^{-2}	2.4×10^{-3}	1.1×10^{-2}
K	9.4×10^{-3}	2.6×10^{-3}	7.4×10^{-3}
Mg ($[B^{2+}] = 5 \times 10^{-4}$ M)	6.2×10^{-2}	1.6×10^{-2}	6.0×10^{-2}
Sr	3.0×10^{-1}	3.9×10^{-2}	8.6×10^{-2}
Ba	1.1	4.3×10^{-3}	2.6×10^{-2}
Mn	3.4×10^{-1}	1.8×10^{-2}	2.1×10^{-1}
Ni	4.8×10^{-2}	1.5×10^{-2}	2.1×10^{-2}
Zn	7.0×10^{-2}	3.0×10^{-1}	—[b]

[a] For 10^{-3} M to 10^{-2} M solutions.

[b] $k^{pot}_{Ca,Zn}$ could not be determined because the calibration graph in the presence of zinc(II) did not, at any stage, coincide with the normal calcium ion calibration.

TABLE 2

Slopes (K_M) and intercepts for $\exp(-E_M F/RT)$ versus a_B/a_{Ca} plots

Ionic strength (M)	B^{2+}	Electrode I		Electrode II		Electrode III	
		K_M	Intercept	K_M	Intercept	K_M	Intercept
3×10^{-3}	Mg	1×10^{-2}	1.0	-1×10^{-3}	1.0	-2×10^{-3}	1.0
	Sr	7×10^{-2}		7×10^{-3}		2×10^{-3}	1.0
	Ba	3×10^{-1}		-8×10^{-4}		-2×10^{-2}	0.91
3×10^{-2}	Mg	9×10^{-3}	1.0	-1×10^{-3}	1.0	-8×10^{-3}	0.88
	Sr	6×10^{-2}		7×10^{-3}		-4×10^{-3}	0.95
	Ba	3×10^{-1}		-8×10^{-4}		-1×10^{-2}	0.85

II and III, the intercepts being 1.0 for electrodes I and II, as required by eqn. (1) for plots of $\exp(-E_M F/RT)$ versus a_B/a_{Ca}, B being the bivalent interfering ions, magnesium, strontium and barium. The intercept deviated from 1.0 in many instances for electrode III, a phenomenon that has previously been observed [11].

Electrode I shows calcium-selective electrode qualities similar to those previously noted for electrode VA [5] and is in many respects similar to electrodes II and III (Table 1). There are, however, some significant differences, particularly that regarding the poor selectivity of electrode I with respect to calcium in the presence of barium ions (Table 1). The pH range is good (Table 1) and the dip in the e.m.f.—pH curve is present as for most calcium-selective electrodes containing dioctylphenylphosphonate. The minimum in the pH interference curve is at 2.8 pH.

The barium ion interference is also prominent in the K_M data, which also confirm low interference by strontium ions.

Occasional negative values for K_M have previously been noted for calcium-selective electrodes based on di[4-(1,1,3,3-tetramethylbutyl)phenyl] phosphate sensor when used with tri-n-pentylphosphate and with di-n-octylphenylphosphonate mediator [11]. They were attributed to possible complexation between the phosphate sensor, water and anions within the organic phase, as reported in the extraction of iron(III) from aqueous solutions [12], although a further factor may be the effect of a diffusion potential governed by an anion concentration gradient which may be countered by cation exchange [10].

Finally, plots of $\exp(-E_M F/RT)$ versus a_B/a_{Ca} for electrodes I and II obeyed eqn. (1) over the range 0—50 for the activity ratio a_B/a_{Ca} in all cases studied (Table 2) except for those of strontium and barium for electrode 1; a_B/a_{Ca} ratios exceeding 25 for strontium or 18 for barium led to curvature arising from limiting values of the exponential function. For electrode III, the plots were generally of a wide U-shape with linearity to the intercept being restricted to $a_B/a_{Ca} < 15$.

One of us (S. K.) thanks Kagoshima University and the Ministry of Education, Japan, for financial support, and the Chemistry Department, UWIST, for hosting a stay of nearly three months.

REFERENCES

1 G. H. Griffiths, G. J. Moody and J. D. R. Thomas, J. Inorg. Nucl. Chem., 34 (1972) 3043.
2 A. Craggs, P. G. Delduca, L. Keil, B. J. Key, G. J. Moody and J. D. R. Thomas, J. Inorg. Nucl. Chem., 40 (1978) 1483.
3 J. Růžička, E. H. Hansen and J. C. Tjell, Anal. Chim. Acta, 67 (1973) 155.
4 P. G. Delduca, G. J. Moody and J. D. R. Thomas, unpublished results.
5 L. Keil, G. J. Moody and J. D. R. Thomas, Anal. Chim. Acta, 96 (1978) 171.
6 P. G. Delduca, M. Sc. Thesis, University of Wales, 1978.
7 A. Craggs, G. J. Moody and J. D. R. Thomas, J. Chem. Educ., 51 (1974) 541.
8 G. J. Moody and J. D. R. Thomas, Lab. Pract., 20 (1971) 307; Talanta, 19 (1972) 623; Sel. Ann. Rev. Anal. Sci., 3 (1973) 59.
9 IUPAC, Recommendations for Nomenclature of Ion-selective Electrodes, Pure Appl. Chem., 48 (1976) 127.
10 J. Bagg, O. Nicholson and R. Vinen, J. Phys. Chem., 75 (1971) 2138.
11 G. J. Moody, N. S. Nassory and J. D. R. Thomas, Talanta, in the press.
12 C. F. Baes, J. Inorg. Nucl. Chem., 30 (1962) 1640.

Analytica Chimica Acta, 108 (1979) 389—393
© Elsevier Scientific Publishing Company, Amsterdam — Printed in The Netherlands

Short Communication

POLAROGRAPHIC ANALYSIS FOR CORTICOSTEROIDS
Part 2. Determination of Corticosteroids in Single-component Solutions, Suspensions, Ointments and Creams

H. S. de BOER, P. H. LANSAAT and W. J. van OORT*

Department of Analytical Pharmacy, Faculty of Pharmacy, State University of Utrecht, Catharijnesingel 60, 3511 GH Utrecht (The Netherlands)

(Received 11th December 1978)

Summary. Differential pulse polarographic methods are presented for corticosteroids in single-component pharmaceutical preparations. Adaptation of the supporting electrolyte to the lipophilicity of the preparation and standard addition methods give fast and reliable procedures. Standard deviations are about 1% for aqueous and alcoholic solutions and about 2% for creams, suspensions and ointments.

The electro-analytical properties of corticosteroids were described in Part 1 of this series [1]. This Part deals with the differential pulse polarographic (d.p.p.) determination of corticosteroids in single-component preparations of different lipophilicity. Direct current and d.p.p. methods have been reported for several corticosteroids in ointments and creams [2—5]. Chatten et al. [6] mentioned the determination of certain Δ^4-3 ketosteroids in some parenteral formulations by d.p.p., and h.p.l.c. has been applied [7] to the determination of triamcinolone acetonide in creams and suspensions. All these polarographic methods made use of calibration curves and supporting electrolytes which were mainly aqueous. Therefore, time-consuming clean-up procedures were needed or the excipients of the pharmaceutical preparation had to be added to the calibration solutions; the latter procedure cannot be applied to formulations of unknown content. Most h.p.l.c. methods also need an extended clean-up procedure. The h.p.l.c. method of Upton et al. [8] for steroid phosphates does not need a preliminary clean-up, but is applicable only to water-soluble phosphate esters.

In order to avoid these difficulties standard addition methods were applied here and the lipophilicity of the polarographic solvents was adapted to the lipophilicity of the formulations. D.p.p. offers the sensitivity required for this procedure.

Experimental

Apparatus. Three polarographs were used: a PAR model 174 polarograph and a Brucker E310 modular electrochemical system, both of which were equipped with a drop timer and a Houston model 2200-3-3 X-Y recorder, and

a Metrohm Polarecord E506 equipped with a polarographic stand E505. A water-jacketed 10-ml polarographic cell (Metrohm EA880-T-5) was employed with a dropping mercury electrode, a Metrohm EA432 Ag/AgCl reference electrode and a platinum wire auxiliary electrode. The cell was maintained at 20 ± 0.2°C. The "salt bridge" of the reference electrode was filled with the supporting electrolyte.

A piston microburette (Metrohm E457) was used for standard additions.

Chemicals. The steroid preparations used are listed, with their sources in Table 1. The solvents and materials for the supporting electrolytes were: methanol (Nanograde, Mallinckrodt); methanol (zur Analyse), dimethylformamide (DMF; Uvasol), tetramethylammonium hydroxide (TMAH; 10% zur Polarographie), acetic acid (99% reinst), phosphoric acid (99% reinst) (Merck); boric acid (Baker) and Dowex 1-X2 strongly basic anion exchanger (50—100 mesh, chloride; Fluka). All reagents were used without further purification.

Procedures. Because of the variety of dosage forms of corticosteroids, three solvents were used with different lipophilic properties: a (1 + 1) mixture of Britton—Robinson buffer pH 10 and methanol, 0.03 M TMAH in methanol, and 0.02 M TMAH in (87 + 13) DMF—water.

A d.p.p. curve of 10 ml of the supporting electrolyte (solvent) was recorded after deaeration with oxygen-free nitrogen [9] for 15 min. Then, a suitable amount of the sample was added, to obtain a concentration between 10^{-3} and 10^{-5} M steroid in the polarographic cell. After deaeration for 1 min the polarogram was recorded. A small volume of the standard solution containing about the same amount of steroid was then added and the polarogram was recorded again. Deaeration for 1 min was sufficient. Dilution by addition of the standard should not exceed 1%.

Standard solutions of the steroids were prepared in methanol or DMF depending on the supporting electrolyte used.

The normal scan parameters were: drop time 2 s, scan rate 2 mV s^{-1}, modulation amplitude 100 mV.

Results and discussion

Aqueous solutions. In general, the sample containing ionic steroid esters was added directly to the blank solution consisting of Britton—Robinson buffer pH 10 in 50% (v/v) methanol. The results are listed in Table 1. When 0.03 M TMAH in methanol was used as solvent, the average values were similar, but the standard deviation increased about five times. Some injections contain non-ionic compounds which increase the base line, such as non-ionic polar viscosity-increasing compounds (e.g., to improve the solubility of the corticosteroid—alcohol which appears after slow hydrolysis of the corticosteroid ester) or decomposition products of preservatives (e.g., benzaldehyde from oxidation of benzyl alcohol). The results then obtained are too high when the normal base line is used for calculation. A base line corrected for this interference can be obtained by addition of some anion exchanger (500 mg of Dowex 1) to the supporting electrolyte after addition of sample and standard solution: the ionic

TABLE 1

Results of assay of the dosage forms and standard deviations based on 5 determinations with separate sampling

Name	Source	Active constituent	Content (mg ml^{-1})	Found (mg ml^{-1})	R.s.d. (%)
Aqueous solutions					
Betnesol drops for eye, ear or nose	Glaxo	Betamethasone disodium phosphate[a]	1	1.00	0.5
Decadron-4 injection	MSD	Dexamethasone-21-phosphate[c] (as disodium phosphate)	4	4.04	0.8
Oradexon injection	Organon	Dexamethasone disodium phosphate[a]	5	5.02	1.1
Dexamethasone disodium phosphate	Organon	Dexamethasone disodium phosphate[a]	20	20.2	1.3
Celestone injection	Schering	Betamethasone (as disodium phosphate)	4	4.03	1.2
Alcoholic solution					
Celestoderm-V alcohol	Schering	Betamethasone (as 17-valerate)[d]	1[b]	1.09[b]	1.4
Solution in vegetable oil					
Neo-Hombreol	Organon	Testosterone propionate[c]	50	50.49	1.0
Solution in oleic acid					
Testosterone undecanoate in oleic acid	Organon	Testosterone undecanoate[a]	167	175	1.3
Suspensions					
Albicort-10	Labaz	Triamcinolone acetonide[a]	10	10.1	2.1
Hydro-Adreson	Organon	Hydrocortisone acetate[c]	25	24.9	2.7
Cream					
Betnelan-V	Glaxo	Betamethasone (as 17-valerate)[a]	1[b]	1.00[b]	2.2
Ointments					
Betnelan-V ointment	Glaxo	Betamethasone (as 17-valerate)[a]	1[b]	1.03[b]	2.5
Celestoderm-V ointment	Schering	Betamethasone (as 17-valerate)[d]	1[b]	0.94[b]	3.2

[a]Obtained in pure form from the manufacturer cited.
[b]Content in mg g^{-1}.
[c]Obtained in pure form from Nogepha.
[d]Obtained in pure form from Glaxo

corticosteroid ester is bound completely during the 10-min mixing time. Line (d) in Fig. 1A represents the "base line" obtained, which was used for calculation of the content. Addition of anion exchanger to a normal blank solution did not influence the normal base line (a), whereas addition to a standard solution gave a "base line" (d) which coincided with base line (a).

Alcoholic solutions. The samples were added directly to the blank solution consisting of 0.03 M TMAH in methanol.

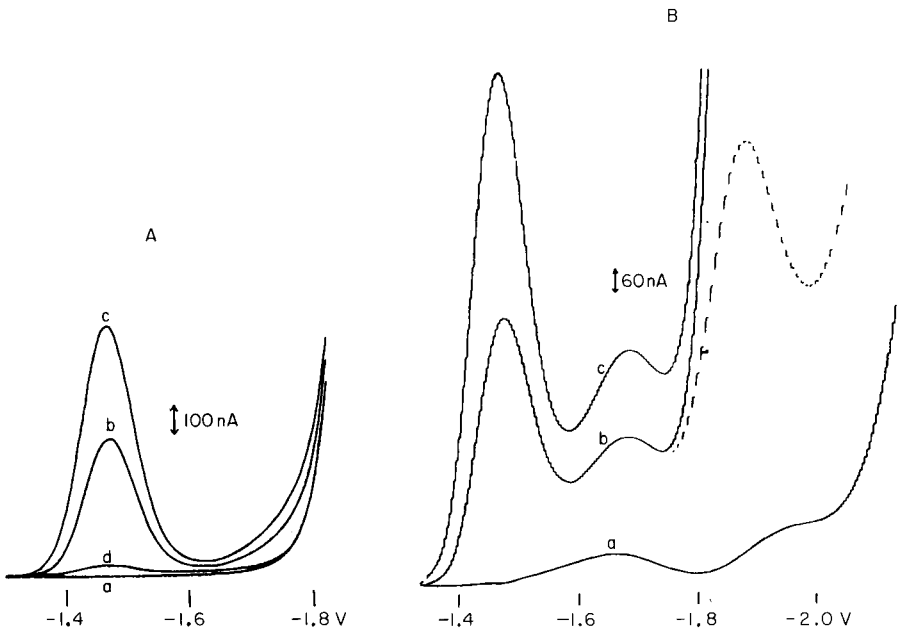


Fig. 1. Differential pulse polarograms for (A) Oradexon injection with methanolic Britton–Robinson buffer pH 10 and (B) Albicort 10 suspension with methanolic 0.03 M TMAH. (a) Blank solution; (b) blank solution + sample addition; (c) blank solution + sample + standard addition; (d) blank solution + sample + standard addition + Dowex. The final wave of triamcinolone (broken line in B) is overlapped by a sodium peak from NaCl and/or buffer in the sample.

Solution in vegetable oil. A suitable amount of the sample, diluted to 5.00 ml with toluene, was added to the blank solution consisting of 0.02 M TMAH in DMF (87% v/v). The oil was only partly miscible with the blank solution, but the steroid remained dissolved, obviously because of the large partition coefficient and the favourable phase–volume ratio (actually testosterone is a Δ^4-3 ketosteroid, not a corticosteroid).

Suspensions. The suspensions consisted of a dispersed system of lipophilic steroid esters in water. After the suspension had been shaken thoroughly, a suitable amount was added directly to the blank solution consisting of 0.03 M TMAH in methanol. The active compounds dissolved in this medium quickly and completely (Fig. 1B). The standard deviations were relatively high, probably because of the less reproducible sampling from the suspension.

Cream. The cream analyzed is an oil-in-water emulsion in which the steroid ester is dispersed. A suitable amount of the cream disintegrated on adding 5.0 ml of methanol and the active compound dissolved completely. An aliquot was pipetted into the blank solution consisting of 0.03 M TMAH in methanol. The emulsifying agent lost its properties in this non-aqueous medium, and there was no interference. A standard quantity of pure betamethasone-17-valerate was added to an amount of cream to determine the yield of the clean-up procedure. The recovery was 100%.

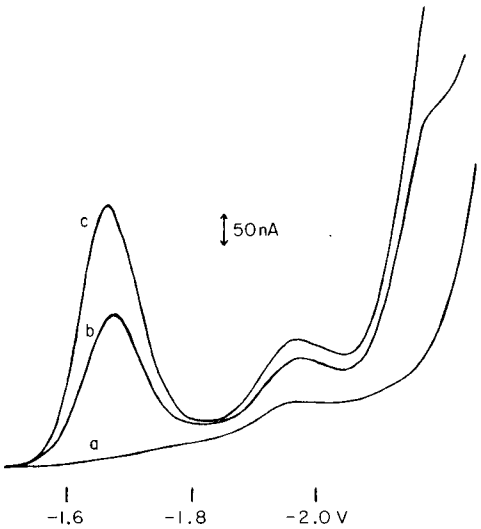


Fig. 2. Differential pulse polarogram of Betnelan-V ointment with 0.02 M TMAH in DMF (87% v/v). (a) Blank solution; (b) blank solution + sample addition; (c) blank solution + sample + standard addition.

Ointments. A suitable amount of ointment was dissolved completely in 5.00 ml of toluene. An aliquot was added to the blank solution, consisting of 0.02 M TMAH in DMF (87% v/v). The fatty constituents did not dissolve in the blank solution whereas the active compound remained dissolved (Fig. 2).

Testosterone undecanoate in oleic acid. In this preparation the steroid is dissolved in oleic acid, not in a vegetable oil. It appeared to be better to use 0.03 M TMAH in methanol as supporting electrolyte rather than the 0.02 M TMAH in DMF (87% v/v) preferred for the vegetable oil preparation. A suitable amount of the sample was added directly to the blank solution. Oleic acid is miscible with methanol.

The authors thank Organon International B.V., Oss, The Netherlands, for kindly supplying some of the examined preparations, Dr. H. Hindriks and Mr. J. van Gorp (Organon) for helpful discussions, and Mr. K. R. Kooistra for experimental assistance.

REFERENCES

1 H. S. de Boer, J. den Hartigh, H.H.J.L. Ploegmakers and W. J. van Oort, Anal. Chim. Acta, 102 (1978) 141.
2 P. Gantès and J. P. Juhasz, Ann. Pharm. Fr., 24 (1966) 687.
3 M. J. Haesman and A. J. Wood, J. Pharm. Pharmacol., 23 (1971) 1765.
4 D. Cantin, J. Alary and A. Coeur, J. Pharm. Belg., 32 (1977) 255.
5 E. Jacobsen and B. Korvald, Anal. Chim. Acta, 99 (1978) 255.
6 L. G. Chatten, R. N. Yadav and D. K. Madan, Pharm. Acta Helv., 51 (1976) 381.
7 G. Gordon and P. R. Wood, Analyst, 101 (1976) 876.
8 L. N. Upton, E. R. Townley and F. D. Sancilio, J. Pharm. Sci., 67 (1978) 913.
9 L. Meites, Polarographic Techniques, 2nd edn., Interscience, New York, 1964, p. 87.

Analytica Chimica Acta, 108 (1979) 395—399
© Elsevier Scientific Publishing Company, Amsterdam — Printed in The Netherlands

Short Communication

LEAD DIOXIDE-COATED CARBON PASTE ELECTRODES

C. EFRON and M. ARIEL*

Department of Chemistry, Technion - I.I.T., Haifa (Israel)

(Received 19th December 1978)

Summary. Lead dioxide electrodeposited under optimized conditions on carbon paste provides an electroanalytically useful electrode, with an anodic working range extending to 1.9 V. Voltammograms for sulphite are used to study electrode lifetime and reproducibility; calibration graphs are linear up to 10^{-3} M sulphite in 0.5 M sulphuric acid.

Electroanalytically useful electrodes with a potential range extending towards more positive values than those attainable with mercury are of interest. Gold and platinum electrodes are limited by oxide formation and carbon electrodes by surface group oxidation; regeneration (i.e. removal of parasitic surface films or contaminants) is not always easy. Lead dioxide electrodes, characterized by their good electrical conductivity and high oxygen overpotentials [1], have been widely employed in synthetic work, but to a far lesser extent for analytical purposes [2—7]. In some cases deposition periods of up to 100 h were involved [4]. This work was directed towards the development of a rapidly prepared, renewable PbO_2-coated carbon electrode, suitable for analytical use.

Two carbon substrates, spectrographic graphite and carbon paste, were investigated. The quality of the PbO_2 deposits was studied by scanning electron microscopy; electrode performance was evaluated by examining voltammograms recorded in standard sulphite solutions.

Experimental

A 3-electrode system was employed. Two types of working electrode were studied: (a) a rotated disc electrode made of graphite (Johnson Matthey, Ltd., Specpure graphite grade 1, JMC 2106) by glueing a graphite disc (6.4 mm diameter, 5 mm thick, to the end of a glass tube of appropriate width; and (b) a rotated carbon paste electrode [8] prepared by tamping the paste to a height of 10 mm into a glass tube (5.6 mm i.d.) The paste was prepared by mixing 15 g of graphite powder (grade 38, National Carbon Co., U.S.A.) and 9 ml of Nujol. Electrical contact to the electrodes was made by filling the glass tubes with graphite powder or mercury; they were placed in a synchronous rotator and rotated at 1450 rpm. An Ag/AgCl (saturated KCl) reference electrode and a platinum counter electrode completed the system. In the 50-ml cell used, the counter electrode compartment was separated by a sintered glass

partition; this prevented deposition of lead on the counter electrode and any attack of hydrogen on the PbO_2 deposit on the working electrode.

Analytical-grade reagents and triple-distilled water were employed.

Current—voltage curves, recorded on a Yokogawa 3077 x-y recorder, were obtained with the aid of a locally built linear potential scanner, 3-electrode potentiostat or dynamic compensator [9]. Before each experiment, the surface of the working electrode was renewed. Electrodes based on spectrographic graphite were polished with silicon carbide papers (grades 240, 400, 600) and in some cases also with diamond powder (15 μm); the carbon paste electrodes were renewed by extruding and removing about 3 mm of the paste from the glass tube and replacing by fresh paste.

Lead dioxide was best deposited on the carbon substrate from a 0.2 M lead nitrate solution at pH 3.0 by controlled-potential electrolysis for 20—30 min, with ohmic potential drop compensation. The optimum potential was 1.325 V for graphite discs and 1.350 V for carbon paste electrodes.

Results and discussion

The quality of the lead dioxide deposit on different substrates, obtained by electrodeposition at different potentials for various times, was judged by four criteria. First, good deposits are black and lustrous without macroscopic defects, whereas faulty deposits are dull and rough. Secondly, voltammograms in 0.5 M H_2SO_4 recorded cathodically do not show the reduction peak characteristic of graphite surface groups if the electrode is satisfactory, and residual currents are low throughout the scanned potential range (1.5—1.9 V). Thirdly, cycle widths up to 0.3 mA at +1.6 V for cyclic voltammograms recorded at 10 mV s^{-1} were considered to indicate a satisfactory deposit. Finally, voltammograms for sulphite served as a test of the completeness and quality of the PbO_2 deposit. On bare graphite, the voltammograms are drawn out, without a clear limiting current plateau, although there is proportionality between current and concentration in certain ranges [10]. On lead dioxide, the limiting current plateau extends over about 300 mV, and the current is proportional to sulphite concentration in the range 10^{-4}—10^{-2} M, exhibiting negative deviations from linearity at higher concentrations [4].

The base line and current—voltage curves recorded with sulphite solutions, at carbon paste electrodes before and after PbO_2 coating, are shown in Fig. 1. The resulting calibration graph showed a rectilinear relationship between current and concentration up to 10^{-3} M sulphite; at concentrations up to 2×10^{-3} M, the graph curved slightly but was still usable.

Lead dioxide deposits on graphite disc electrodes polished only with SiC papers lead to marked improvements in both the base line and the sulphite voltammograms. Imperfectly polished graphite surfaces show up as grooves on the PbO_2 deposit, which are visible under the microscope, and detract from the reproducibility of the electrode. Polishing with diamond powder markedly improves performance. Deposition of lead dioxide was tested at various deposition potentials (Table 1). Good deposits were obtained at +1.325 V after

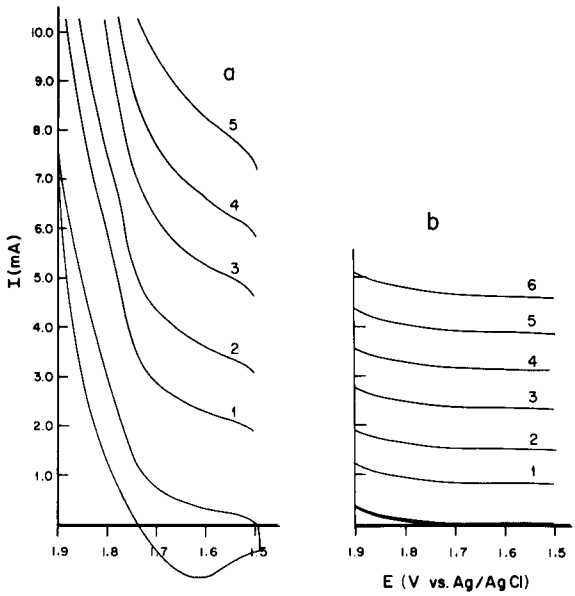


Fig. 1. Base line and current—voltage curves after successive additions of 0.1 ml of 1 M Na_2SO_3 to 50 ml of 0.5 M H_2SO_4. (a) Uncoated and (b) PbO_2-coated carbon paste electrode. Potential scan rate, 10 MV s^{-1}.

TABLE 1

Dependence of deposition current (I) on potential (E) for the graphite disc (GD) and carbon paste (CP) electrodes

E (V)	1.300	1.325	1.350	1.400	1.450
I (mA) for GD	0.7—0.8	0.7—1.2	0.9—1.3	1.6—2.3	3.0—3.7
I (mA) for CP	0.4—0.5	—	0.9—1.6	2.0—4.5	3.0—6.0

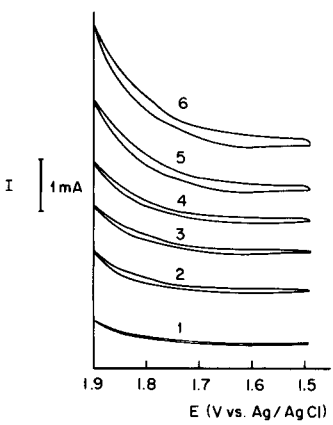
depositions lasting 20—30 min. Lower potentials or shorter deposition periods resulted in imperfect deposits, whereas higher potentials led to cracked deposits.

The preparation and renewal of the graphite disc electrodes involve appreciable effort and expertise. The carbon paste electrodes are far easier to prepare and were therefore chosen for further study. Table 1 shows the deposition currents obtained at different deposition potentials. Satisfactory deposits were obtained after deposition at +1.350 V for 30 min; in 15 experiments, only 2 imperfect deposits were obtained. Lower deposition potentials and shorter times gave imperfect deposits; at higher potentials, cracked deposits were obtained.

The stability of the deposits was tested as follows. After coating, the electrode was immersed in 0.5 M H_2SO_4, for periods of 6—95 min; it was then connected up and the potential was scanned (with rotation) between +1.5 V and +1.9 V. After 3 cycles, the blank voltammogram was recorded, and then voltammograms were recorded after successive additions of sulphite. There were no significant differences during the time interval specified. When the coated electrode was kept at +1.6 V, without rotation, for periods up to 145 min, the background currents observed in 0.5 M H_2SO_4 remained low. Finally, the coated electrode was rotated at the rate used during electrodeposition (1450 rmp) and continuously cycled between +1.5 V and +1.9 V, in 0.5 M H_2SO_4 (equivalent to continuous use as a working electrode). The blank voltammograms obtained over a period of time are shown in Fig. 2, and the results for different amounts of sulphite obtained 10 min and 90 min after coating are given in Fig. 3.

In all these treatments, the useful lifetime of the electrodes was found to be ca. 2 h; since the limiting currents increase slightly with time (Fig. 2), it is recommended that the electrodes be kept disconnected without rotation when not in use. Sulphuric acid was chosen because of its corrosive influence on lead dioxide; in media such as nitrate, perchlorate, etc., longer lifetimes would be expected.

The thickness of the lead dioxide deposit, calculated from the charge passed during electrodeposition, the electrode surface and PbO_2 density was about 10 μm, which is sufficient for the electrical properties of the deposit to be constant (i.e. unaffected by minor changes in its thickness) [11]. The deposits,



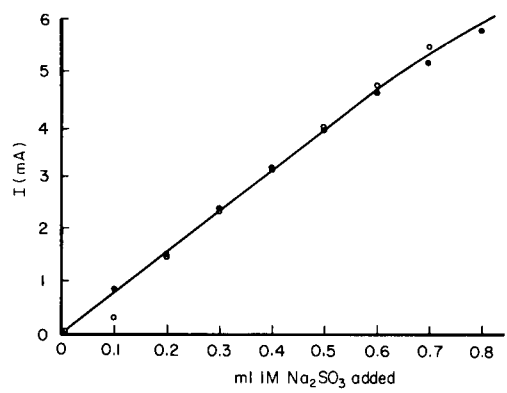


Fig. 2. Change of base line with time for the PbO_2-coated carbon paste electrode, immersed in 0.5 M H_2SO_4, rotated at 1450 rpm and cycled between 1.5 and 1.9 V. (1) 5; (2) 20; (3) 35; (4) 50; (5) 65 and (6) 80 min after coating.

Fig. 3. Dependence of limiting current on volume of sulphite added to 50 ml of 0.5 M H_2SO_4 for the PbO_2-coated carbon paste electrode treated as described (•) 10 and (○) 90 min after coating.

examined by scanning electron microscopy at 300× magnification, were free of pits or cracks; with some samples, crystals of lead sulphate were visible on the deposit.

The lead dioxide coating extends the useful anodic potential range by about 400 mV compared to the carbon substrate; species electroactive in this region should therefore become determinable.

REFERENCES

1 J. P. Carr and N. A. Hampson, Chem. Rev., 72 (1972) 679.
2 F. Strafélda and J. Krofta, Collect. Czech. Chem. Commun., 36 (1971) 1634.
3 C. N. Wang, P. J. Kinlen, D. A. Schoeller and C. O. Huber, Anal. Chem., 44 (1972) 1152.
4 G. Bélanger, Anal. Chem., 46 (1974) 1576.
5 G. Kainz and G. Sontag, Mikrochim. Acta, (1975) 171.
6 K. G. Schick, V. G. Magearu, N. L. Field and C. O. Huber, Anal. Chem., 48 (1976) 2186.
7 D. H. Karweik and C. O. Huber, Anal. Chem., 50 (1978) 1209.
8 R. N. Adams, Electrochemistry at Solid Electrodes, M. Dekker, New York, 1969, p. 280.
9 Ch. Yarnitzky and F. Friedman, Anal. Chem., 47 (1975) 876.
10 J. V. A. Novak, Collect. Czech. Chem. Commun., 25 (1960) 3068.
11 W. Mindt, J. Electrochem. Soc., 116 (1969) 1076.

Analytica Chimica Acta, 108 (1979) 401—403
© Elsevier Scientific Publishing Company, Amsterdam — Printed in The Netherlands

Short Communication

GAS CHROMATOGRAPHIC DETERMINATION OF XANTHINOL IN PLASMA

H. ROSEBOOM* and G. WIESE

Pharmaceutical Laboratories, University of Utrecht, Catharijnesingel 60, Utrecht (The Netherlands)

(Received 19th December 1978)

Summary. The determination of xanthinol in plasma is described. After extraction of the drug, together with the internal standard (papaverine hydrochloride), the extract is evaporated to dryness and the drug is derivatized with acetic anhydride for chromatography. The method is linear for 2—100 $\mu g\ ml^{-1}$; the coefficient of variation is 3% and the recovery 80%. The resulting stable solution allows large numbers of samples to be processed with an automatic injector.

Xanthinol nicotinate (Complamin), used in the treatment of peripheral vascular disorders, has been claimed to be of value in the treatment of angina of effort, of cerebral and other arteriosclerotic conditions, [1, 2] and of placental malfunctions [3]. Xanthinol is metabolized to a small extent (7—8%) and is largely excreted unchanged in urine [4]. The absorption of the drug from slow-release and plain tablets has been studied [5] by measuring plasma levels of nicotinic acid, but this is not the active species. A method for the determination of xanthinol in plasma does not seem to have been described; without such a method it is impossible to establish therapeutic blood levels or to evaluate the bio-availability from different formulations. This communication describes a gas chromatographic method for this purpose. The drug is extracted from the plasma together with the internal standard; after derivatization with acetic anhydride, it is injected into the gas chromatograph.

Experimental

Reagents. The reagents used were chloroform, isopropanol, methanol and acetic anhydride (Merck, Darmstadt), xanthinol nicotinate (Nogépha, Amsterdam) and papaverine hydrochloride (Brocacef, Maarssen). All solvents were of reagent grade.

Gas chromatography. A Packard-Becker Model 419 gas chromatograph, equipped with flame ionization detectors was used. The glass column (1.5 m × 2 mm i.d.) was packed with 10% SE 30 on Chromosorb WHP, 80—100 mesh (Chrompack, Middelburg). The operating conditions were: injection port temperature, 270°C; column temperature, 245°C; detector temperature, 270°C; carrier gas (nitrogen) flow, 20 ml min^{-1}; hydrogen flow 30 ml min^{-1}; air flow 300 ml min^{-1}. Peak areas were measured with the chromatography Data Analyser System IV B (Spectra Physics, Schijndel).

Assay procedure. To 1 ml of plasma in a centrifuge tube was added 100 μl of 0.1 M NaOH and 4 ml of chloroform—isopropanol (95 + 5), containing papaverine hydrochloride (2.5 μg ml^{-1}) as the internal standard. After shaking for 30 s and centrifugation for 10 min at 3000 rpm, the organic phase was transferred to another tube by means of a Pasteur pipette. The extract was evaporated to dryness under nitrogen in a metal heating block at 60°C after which 100 μl of acetic anhydride was added to the residue. After heating for 10 min at 80°C, the excess of reagent was evaporated under nitrogen and the residue was dissolved in 50 μl of methanol; 1 μl of this solution was injected into the gas chromatograph. Standard curves were obtained by spiking blank plasma with xanthinol nicotinate and subjecting these samples to the above procedure.

Recovery of xanthinol from plasma. First xanthinol nicotinate was dissolved in methanol to a concentration of 0.5 mg ml^{-1}, and 100 μl of this solution was added to 4 ml of chloroform—isopropanol containing the internal standard. This solution was then evaporated and derivatized as described for the assay procedure. Secondly, the solution of xanthinol nicotinate in methanol (100 μl) was added to 1 ml of plasma to which was then added 100 μl of 0.1 M NaOH. This solution was extracted with 4 ml of chloroform—isopropanol without internal standard. After separating the phases, 4 ml of chloroform—isopropanol containing the internal standard was added to the organic phase; this solution was then evaporated and derivatized as described.

Results and discussion

Injection of underivatized xanthinol on various columns resulted in strongly tailing peaks; losses as high as 500 ng per injection, probably through irreversible adsorption on the column support material, were noted. Derivatization of the two hydroxyl groups in xanthinol with acetic anhydride resulted in symmetrical peaks and no significant losses occurred. Acetic anhydride has the advantage that the reaction is complete within minutes and the excess of reagent can be easily removed by evaporation. Under the described chromatographic conditions, xanthinol and papaverine gave well-resolved symmetrical peaks (Fig. 1) with retention times of 4.5 and 5.5 min, respectively. Chromatograms of blank plasma samples showed no peaks at the retention times of xanthinol or the internal standard, although a peak with a retention time of 11 min occurred. When a column packed with 3% OV17 was used, the peaks of xanthinol and papaverine were further apart but the retention time of the plasma peak was very close to that of the xanthinol peak.

The calibration curves were linear over the range studied (2—100 μg ml^{-1}) with a small negative intercept of 0.3—0.5 μg ml^{-1}. The coefficient of variation, determined at 10 μg ml^{-1} and at 50 μg ml^{-1} by analyzing six plasma samples at each concentration, was calculated to be 3%. The recovery of xanthinol was 80% with a coefficient of variation of 5% (n = 6).

After injection into the gas chromatograph the solutions were occasionally

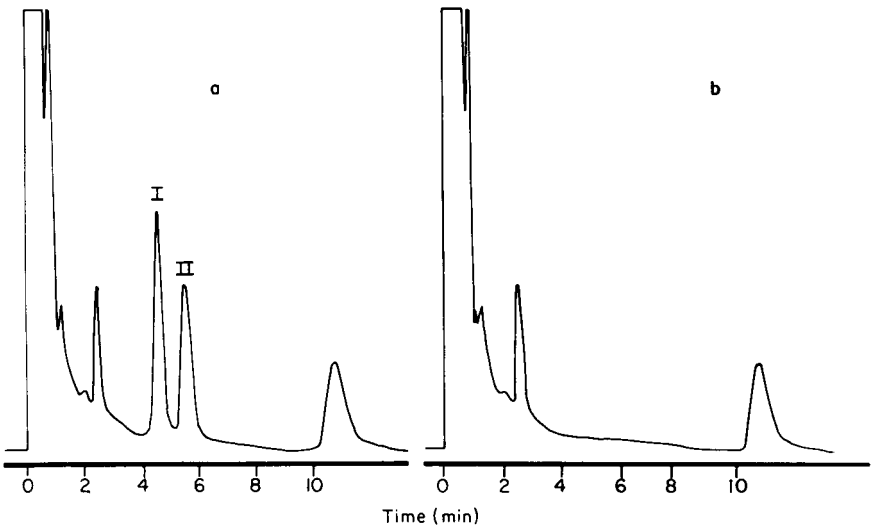


Fig. 1. Chromatograms of plasma samples; for conditions, see Experimental. (a) Blank plasma, spiked with xanthinol: (I) xanthinol; (II) papaverine. (b) Plasma blank.

stored in the dark at room temperature for 1 or 2 days; the peak area ratios did not change on storage. The stability of this solution should therefore allow the processing of a large number of samples with an automatic injector.

REFERENCES

1 A. Hedbom, Br. Med. J., (1965) 1554.
2 G. P. McNicol and A. S. Douglas, Br. Med. J., (1965) 1149.
3 N. A. M. Bergstein and H. I. J. M. van Kessel, Lancet, (1968) 111.
4 M. Tauscher, G. Eckhardt, B. Geisel and K. Credner, Arzneim, Forsch., 26 (1976) 1342.
5 P. L. Sharma, S. K. Garg and S. C. Sikka, Int. J. Clin. Pharmacol., 7 (1973) 299.

Analytica Chimica Acta, 108 (1979) 405—409
© Elsevier Scientific Publishing Company, Amsterdam — Printed in The Netherlands

Short Communication

EVALUATION OF ION CHROMATOGRAPHY FOR DETERMINATION OF SELECTED IONS IN GEOTHERMAL WELL WATER

R. P. LASH* and C. J. HILL

Allied Chemical Corporation, 550 Second Street, Idaho Falls, Idaho 83401 (U.S.A.)

(Received 29th January 1979)

Summary. Ion chromatography is evaluated as a technique for the separation and determination of selected anions (fluoride, chloride, bromide, and sulfate) and cations (lithium, sodium, potassium and ammonium) in geothermal well water samples. The results achieved are compared with those obtained by other methods of analysis in a round-robin test.

Geothermal energy is currently being studied as an alternative energy source. To tap this source, wells are drilled and the geothermal fluid is brought to the surface for energy recovery. The cooled effluent from this process may be returned to the ground through reinjection wells. The well-water samples must be thoroughly characterized in order to estimate corrosion and scaling problems as well as to establish any environmental impacts and potential for mineral recovery. Battelle Northwest Laboratory [1] conducted a round-robin program to evaluate analytical methods for the determination of various elements in geothermal well waters. Several of these elements lend themselves to determination by ion chromatography. The principles of separation and determination of inorganic ions by this technique have been demonstrated by Small et al. [2] and the technique has been applied to the determination of anions in boiler blow-down water [3].

This communication describes the ion-chromatographic determination of fluoride, chloride, bromide, sulfate, lithium, sodium, potassium and ammonium ions in geothermal well water. The feasibility of rapid, simultaneous, multi-ion analyses is also demonstrated.

Experimental

Instrumentation and columns. The ion chromatograph used was a Model 10 unit equipped with a 100-μl sample loop and an electrical conductivity detector (Dionex Corporation, 1228 Titan Way, Sunnyvale, California 94086). The prepacked columns (Dionex Corporation) were as follows. The anion separating column (3 mm i.d., 500 mm long) contained a low-capacity quaternary ammonium anion exchanger of the surface layer type; the stripping column (6 mm i.d., 250 mm long) contained a high-capacity sulfonic acid cation exchanger. The cation separating column (6 mm i.d., 250 mm long)

contained a low-capacity surface-sulfonated copolymer resin, and the stripping column (9 mm i.d., 250 mm long) was packed with a high-capacity quaternary ammonium anion exchanger. All the resins were of 55-μm particle size.

Reagents. All chemicals were analytical-reagent grade or better. The nitric acid used as the eluent for the cation determinations was Ultrex grade (J. T. Baker Chemical Company). Water from a Milli-Q water purification system (Millipore Corporation) was used throughout.

Mixed anion calibration standards were prepared by dissolving the appropriate sodium salts in water to yield the following concentrations of fluoride, bromide and sulfate: 4.0, 5.0, and 150 mg l^{-1} respectively, for test site A; and 12.5, 100, and 150 mg l^{-1}, respectively, for test site B. Separate chloride standards were prepared containing 2000 and 150000 mg l^{-1} for test sites A and B, respectively. Mixed cation calibration standards were prepared by dissolving the appropriate chloride salts in water to yield the following concentrations of lithium, sodium, ammonium and potassium ions : 4.0, 1000, 15, and 180 mg l^{-1}, respectively, for test site A; and 170, 50000, 350, and 11500 mg l^{-1}, respectively, for test site B.

A standard synthetic geothermal well-water sample was prepared to match the concentrations (Table 1) for water from test site A.

Procedure. Prior to injection into the chromatograph, the samples and standards were diluted as indicated in Table 2. The appropriate standards and samples were injected; changes in sensitivity settings (Table 2) were made between peaks where necessary, and results were calculated from the peak height ratios of samples to standards. The eluent for the anion determinations was 0.002 M $NaHCO_3$—0.0016 M Na_2CO_3 at a flow rate of 115 ml h^{-1}. The eluent for the cation determinations was 0.003 M HNO_3 at a flow rate of 184 ml h^{-1}.

Results and discussion

Figure 1 shows a typical ion chromatogram of anions in the synthetic test site A well water. The fluoride, bromide, and sulfate peaks are resolved well

TABLE 1

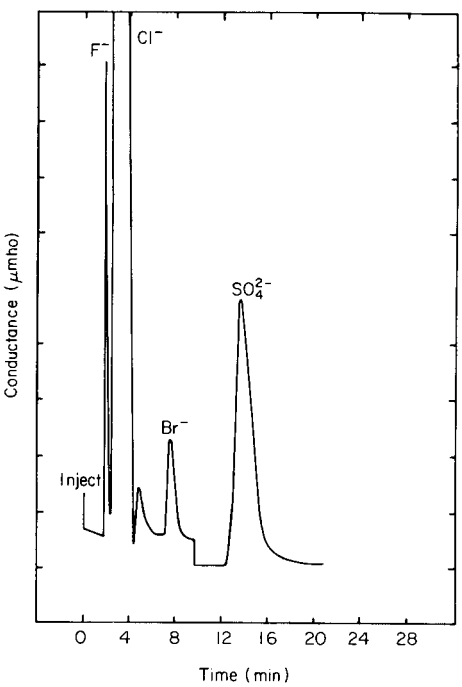
Typical contents of major and minor components of geothermal well water from test sites A and B

	Approximate content (mg l^{-1})							
	A	B		A	B		A	B
Li	4.0	150.0	Cs	0.4	15.0	Br^-	5.0	100.0
Na	1500.0	50000.0	Ca	15.0	23000.0	SO_4^{2-}	150.0	50.0
K	150.0	10000.0	B	8.0	300.0	Cl^-	2000.0	130000.0
NH_4^+	15.0	450.0	Pb	0.5	25.0	HCO_3^-	550.0	—
Rb	0.6	60.0	F^-	1.0	10.0	SiO_2	250.0	400.0

TABLE 2

Dilution and sensitivity settings for ion chromatography of geothermal well-water samples

Ion	Dilution		Sensitivity (μmho full scale)	
	Site A	Site B	Site A	Site B
Na^+	1: 50	1 :1000	30	100
K^+	1: 50	1: 1000	1	3
Li^+	1 :10	1: 1000	3	3
NH_4^+	1: 10	1: 1000	1	1
Cl^-	1: 20	1: 1000	300	300
F^-	1: 2	1: 25	10	3
Br^-	1: 2	1: 25	3	1
SO_4^{2-}	1 : 2	1 :25	30	1



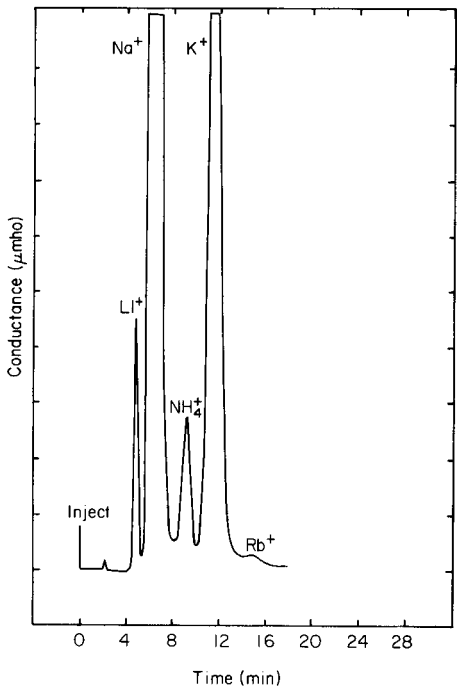


Fig. 1. Determination of anions in a synthetic geothermal well-water sample. Conditions as in Experimental.

Fig. 2. Determination of lithium and ammonium ions in a synthetic well-water sample. Conditions as in Experimental.

enough to allow their simultaneous determination in a single injection. Switching sensitivity settings before the bromide and sulfate peaks makes it possible to maximize peak heights and determine all three ions within 20 min. Figure 2 is an ion chromatogram of the cations in the synthetic test site A well water. It seems that the peaks are sufficiently resolved to permit simultaneous determinations of lithium, sodium, ammonium, and potassium ions. However, when sensitivity changes were made between the lithium and sodium peaks, their resolution was inadequate. Therefore, sodium and potassium ions were determined simultaneously on a separate injection of sample at the sensitivities shown in Table 2; excellent resolution and peak shapes were then obtained.

Figure 2 shows an additional small peak eluting at ca. 15 min, which was identified as rubidium, known to be present in the well-water samples (Table 1). Attempts to quantify it were unsuccessful because of the relatively large quantity of potassium present.

Results for the synthetic well water (Table 3) show that fluoride, bromide, sulfate, lithium, sodium, ammonium, and potassium ions can be determined with good precision and accuracy at the levels studied.

Table 4 shows a comparison of the results obtained by ion chromatography with the mean values calculated from the results obtained from all other methods and laboratories participating in the round-robin method evaluation [1, 4]. Agreement is generally good, but in some cases the values by ion chromatography differ considerably. A *t*-test applied to the results indicated that the values for fluoride from test site A and potassium from test site B were significantly different from the mean values. It appears that other results might be significantly different from the mean values (e.g., bromide from both test sites and fluoride and sulfate from test site B) but these differences cannot be considered significant because the individual values used to calculate the mean were widely scattered and the standard deviation of a single measurement for the pooled results was of the same order of magnitude as the mean value.

TABLE 3

Ion chromatographic determination of ions in a synthetic geothermal well-water sample

Ion	Taken ($mg\ l^{-1}$)	Found ($mg\ l^{-1}$)	Bias (%)	R.s.d. (%)
F^-	3.68	3.85	+4.6	0.6[a]
Br^-	10.12	9.90	−2.2	2.1[a]
SO_4^{2-}	300.0	296.0	−1.4	0.1[a]
Li	3.92	3.99	+1.0	1.4[b]
Na	1590.0	1560.0	−1.9	0.4[b]
NH_4^+	14.02	13.63	−2.8	1.8[b]
K	180.0	178.0	−1.1	1.2[b]

[a]For 3 determinations. [b]For 10 determinations.

TABLE 4

Comparison of results (in mg l^{-1}) for geothermal well water samples by ion chromatography (i.c.) and other methods

Ion	Test site A		Test site B	
	I.c.	Mean value[a]	I.c.	Mean value[a]
F^-	5.5	3.5 (14;6)	13.8	8.2 (12;6)
Cl^-	1980.0	1750.0 (19;7)	132000.0	130300.0 (15;6)
Br^-	1.6	4.1 (11;8)	95.0	254.0 (11;8)
SO_4^{2-}	159.0	151.0 (12;6)	33.0	59.0 (12;5)
Li	4.2	4.3 (17;5)	167.0	176.0 (17;5)
Na	1420.0	1430.0 (20;7)	48900.0	46120.0 (20;7)
NH_4^+	16.1	16.5 (16;7)	371.0	352.0 (14;7)
K	130.0	141.0 (19;7)	11300.0	9700.0 (17;5)

[a]The number of results used to calculate the mean value is given by the first value in parentheses and the second value indicates the number of methods used. The ion chromatographic value is included in the mean value.

As shown in Table 4, chloride was also determined by ion chromatography.

Its concentration was very high in comparison with that of other anions in the samples, so that it had to be determined on a separate injection. The precision and accuracy of the chloride ion determination by ion chromatography was not investigated, but the results (Table 4) were not significantly different from the mean values.

REFERENCES

1 J. C. Watson, E. M. Woodruff, J. G. Douglas, S. J. Thompson and R. J. Serne, U.S. Department of Energy, Battelle Pacific Northwest Laboratories, Report No. PNL-MA-572-UC-66d (1978).
2 H. Small, T. S. Stevens and W. C. Bauman, Anal. Chem., 47 (1975) 1801.
3 T. S. Stevens, V. T. Turkelson and W. R. Abe, Anal. Chem., 49 (1977) 1176.
4 J. M. Baldwin, Allied Chemical Corp., personal communication, 1977.

Analytica Chimica Acta, 108 (1979) 411—415
© Elsevier Scientific Publishing Company, Amsterdam — Printed in The Netherlands

Short Communication

DETERMINATION OF LYSINE IN ITS CEPHALEXIN SALT

J. L. FABREGAS* and J. E. BENEYTO

Analytical Department, Laboratorios Almirall, S.A., Cardoner 68-74, Barcelona (24) (Spain)

(Received 21st November 1978)

Summary. The determination of lysine in its cephalexin salt and in various pharmaceutical preparations can be done by separation of the two components by ion-exchange chromatography followed by colorimetric or fluorimetric determination of lysine.

The sodium salt of cephalexin is poorly absorbed after intramuscular injection [1, 2]; similar observations have been made with the related compound, cephradine [3]. Investigations with other soluble salts of cephalexin showed that some basic amino acid salts increased the absorption and bio-availability of cephalexin [4]. The extensive use of the lysine salt of cephalexin necessitated the development of methods for the determination of lysine in this salt. Alkalimetric determination of carboxylic groups and non-aqueous titration of α-amino groups cannot be used because these groups are also present, in the other component of the salt. For the same reason, the Folin reaction the sodium 1,2-naphthoquinone-4-sulphonate reaction, or hypobromite and α-naphthol [5] and the Saxena method [6] for microtitration of amino acid combinations were unsatisfactory and titration of the ϵ-amino group of lysine in aqueous media with sulphuric acid is insufficiently accurate.

The separation of lysine by ion-exchange, followed by colorimetric or fluorimetric assay, is suitable for the determination of lysine in its cephalexin salt and in pharmaceutical dosage forms.

Experimental

Apparatus and reagents. Absorption spectra were obtained with a Perkin-Elmer 323 double-beam spectrophotometer; fluorimetric assays were performed with an Aminco-Bowman spectrofluorimeter with a Riken Denshi Co. X-Y recorder. A 1.0-cm cell was used with both instruments. Elemental analyses and infrared spectra were obtained with Perkin-Elmer Models 240 and 257 instruments, respectively.

Amberlite CG50 (H^+; chromatographic grade; 200 mesh) was prepared as follows. The resin (40 g) was mixed with 0.5 M sodium hydroxide (200 ml), the liquid was decanted, and the resin washed with water until the eluate was neutral. Finally excess of water was removed by vacuum filtration. Lysine hydrochloride (Merck; standard biochemical grade) and lysine-cephalexin

salt (Laboratorios Almirall, S.A.) were used. The cephalexin content of the latter salt, determined by the British Pharmacopoeia method [7], was in agreement with the theoretical value (70.4%). The purity was confirmed by thin-layer chromatography. All the other reagents were of analytical-reagent grade.

Procedure A. An accurately weighed sample of the lysine—cephalexin salt, containing about 60 mg of lysine, was transferred to a 25-ml graduated flask and dissolved in water; 1 M sodium hydroxide (1.0 ml) was added and the solution made up to volume with water. (Freshly prepared solutions were used to avoid degradation of the cephalexin.) An aliquot (20.0 ml) of this solution was magnetically stirred for 5 min with 1 g of Amberlite resin (Na^+ form) and filtered (vacuum), and the resin washed with water (10 and 5 ml); the filtrates were discarded.

The resin was extracted with 0.1 M sodium chloride (4 × 20 ml) and the combined extracts were made up to 100 ml with 0.1 M sodium chloride. An aliquot (2 ml) of this solution was transferred to a 25-ml volumetric flask, followed by 0.1 ml of glacial acetic acid and 2.0 ml of aqueous 2% ninhydrin solution; after mixing, the well-stoppered flask was placed in a boiling water bath for exactly 5 min. When cool, the mixture was made up to volume with distilled water. The resulting suspension was centrifuged (3,000 r.p.m.) for 15 min and the absorption of the supernatant liquid was recorded at 490 nm against a similarly processed reference solution of sodium chloride.

The lysine content of the salt was calculated from a calibration curve prepared by submitting lysine hydrochloride solutions (1.70—2.80 mg ml^{-1}, initial concentration of free base) to the same procedure.

Procedure B. An accurately weighed sample of the lysine—cephalexin salt, containing about 25 mg of lysine, was transferred to a 25-ml calibrated flask and dissolved in water containing 1 M sodium hydroxide (1 ml); the lysine was separated by ion exchange as described above. An aliquot (50 μl) of the 0.1 M sodium chloride solution was added to 3.0 ml of borate buffer, pH 10 [8], followed by 50 μl of *o*-diacetylbenzene and 50 μl of ethanethiol; after 15 min the fluorescence was measured at 440 nm with excitation at 355 nm. The lysine content was calculated from a calibration curve prepared by submitting lysine hydrochloride solutions (0.60—1.30 mg ml^{-1} initial concentration of free base) to the same procedure.

Results and discussion

Studies of the influence of reaction conditions on the colorimetric and fluorimetric reaction indicated the importance of removing the cephalexin and its degradation products prior to carrying out the assay; only one of the amino groups of lysine reacts with ninhydrin to form a coloured product [9]. The lysine was separated from alkaline solutions of the salt by selective ion-exchange chromatography (lysine in acid solution was not retained by the resin; to avoid degradation of the cephalexin, freshly prepared alkaline solutions were used). Best results were obtained by a modification of the technique of Yamabe et al. [10]; a single resin (Amberlite, sodium form) was used and gradient

elution with sodium chloride (lysine is not eluted by sodium chloride concentrations of less than 0.1 M) was omitted. Lengthening the time of contact with resin to 1 h did not increase the amount of lysine extracted; an extraction time of 5 min is recommended.

Colorimetric reaction. The colorimetric reaction was studied at 100°C, 70°C and 50°C. Full colour development occurred after 5 min at 100°C and 35 min at 70°C; at 50°C, colour development was incomplete. Consequently, it is preferable to carry out the reaction at 100°C. Ninhydrin concentrations of 1 and 2% were compared; consistent results were obtained only at the higher concentration. In most analytical methods an excess of ninhydrin is recommended [11].

The reaction was studied with solutions of lysine—cephalexin salt in 2 M hydrochloric acid and in USP buffers [8] of pH 2.5, 3.5, 5.0 and 6.0. Cephalexin is most stable at pH 5.0 at moderate temperatures [12]. At pH 2.5 and 3.5, only very weak absorption bands were detected at 400 and 500 nm. Strong bands at 444 nm and 570 nm were observed when the reaction was carried out at pH 5 and pH 6. End absorption of the band at 570 nm was sufficient to prevent accurate determination of lysine at 444 nm. In hydrochloric acid, a single absorption band appeared at 490 nm. Maximum sensitivity was obtained by taking 2.0 ml of an aqueous solution of the sample, and adding 0.1 ml of glacial acetic acid before introduction of the ninhydrin reagent. Under these conditions, interference by cephalexin at 490 nm corresponded to less than 2% of the total lysine absorption; this interference was eliminated by prior ion-exchange treatment as described above. The main absorption peak for cephalexin under these conditions occurs at ca. 440 nm, and the degradation products of cephalexin, phenylglycine and 7-aminodesacetoxycephalosporanic acid, do not interfere.

A dark red precipitate was formed in the colorimetric reaction during the heating period. This residue was isolated by filtration, washed with water and dried at room temperature. Elemental analysis (71.0% C; 3.5% H; 1.6% N) and infrared spectrum (absorptions at 3400, 1710, 1625 and 1545 cm^{-1}) suggested that it is similar to Ruhemann's purple [13] (72.2% C; 4.7% N; 1.7% H).

Beer's law was obeyed by the supernatant liquid from centrifuged reaction solutions. The occurrence of the red precipitate could be avoided in an otherwise identical procedure by dissolving the ninhydrin reagent in dioxan or ethylene glycol monoethyl ether instead of in water. With these reagent solutions, the initial deep blue colour changed to a cherry-red colour after 5 min, without formation of a precipitate. The sensitivity of the reaction increased in these solvents, but cephalexin degradation products caused minor absorptions near 490 nm, which interfered; consequently the reaction with ninhydrin was carried out in aqueous solution.

Agreement with Beer's law was confirmed with a series of ten standard lysine hydrochloride solutions, covering the range $3.0—6.0 \times 10^{-3}$ M (initial concentration as free base). The solutions were treated as described in Procedure A; the absorbance at 490 nm was a linear function of concentration

fitting a straight line with slope 1920 (absorbance units per mole), $\log \epsilon = 3.284$, intercept 0.0005 absorbance units, correlation coefficient 0.999 ($P = 0.001$, Fisher and Yates Tables [14]). The coefficient of variation of the results was 1.93% for 10 sample solutions containing 40 $\mu g\ ml^{-1}$ lysine base.

Fluorimetric procedure. Roth and Jeanneret's method [15] was modified, to avoid residual interference by cephalexin, by introducing the previously described ion-exchange treatment and adjusting the working concentrations as described under Procedure B to improve accuracy. The intensity of the fluorescence was similar to that obtained with a solution (0.4 $\mu g\ ml^{-1}$) of quinine sulphate in 0.01 M sulphuric acid (excitation, 350 nm; emission, 450 nm). Recorded data, processed as above, yielded a correlation coefficient value of 0.999 ($P = 0.001$, [14]) with a slope of 0.101 (ratio of fluorescence to mass in milligrams). The coefficient of variation of the results was 1.55% for 10 sample solutions containing lysine base at the 3 $\mu g\ ml^{-1}$ level.

The results obtained for the determination of lysine in its cephalexin salt or in injectable dosage forms, containing preservatives such as ascorbic acid (0.2%) or EDTA (0.1%), are given in Table 1. Identical results were obtained for lysine determinations with and without the addition of the stated concentrations of these preservatives. The values obtained for lysine concentrations of 2.6×10^{-4} M and 2.2×10^{-5} M respectively indicate the suitability of these methods for quality control assays of lysine in its cephalexin salt.

TABLE 1

Determination of lysine in its cephalexin salt

	Nominal (%)	Found (%)	No. of detns.	Standard deviation (%)
Colorimetric method				
Raw Material	29.6	29.4—31.0	8	0.57
Injections A[a]	29.3	28.9—31.0	8	0.59
Injections B[a]	28.9	28.5—30.1	7	0.49
Fluorimetric method				
Raw Material	29.6	29.1—30.8	6	0.46
Injections A[a]	29.3	29.1—30.9	5	0.61
Injections B[a]	28.9	28.4—30.4	5	0.72

[a]Injections A and B are freeze-dried pharmaceutical formulations with different contents of lysine cephalexin salt.

The authors are indebted to Dr. J. Segura for the use of the spectrofluorimeter and thank Dr. R. G. W. Spickett for helpful discussions and Mr. C. Juliá for technical assistance.

REFERENCES

1 P. E. Gower, C. H. Dash and C. H. O'Callaghan, J. Pharm. Pharmacol., 25 (1973) 376.
2 P. Nicholas, B. R. Meyers and S. Z. Hirschman, J. Clin. Pharmacol., 13 (1973) 325.
3 T. W. Mischler, A. A. Sugerman, D. A. Villard, L. J. Braunick and E. S. Neiss, J. Clin. Pharmacol., 14 (1974) 604.
4 S. Barrios, J. H. Sorensen and R. G. W. Spickett, J. Pharm. Pharmacol., 27 (1975) 711.
5 J. W. Keyser, Biochem. J., 43 (1948) 488.
6 O. C. Saxena, Microchem. J., 18 (1973) 652.
7 British Pharmacopoeia, 1973, p. 87.
8 United States Pharmacopoeia XIX, 1975, p. 654.
9 E. Slobodian, G. Mechanic and M. Levy, Science, 135 (1962) 441.
10 T. Yamabe, K. Yamagata and M. Seno, J. Chem. Soc. Jpn. Pure Chem. Sect., 89 (1968) 772.
11 M. Friedman and L. D. Williams, Bioorganic Chem., 3 (1974) 267.
12 K. Florey, Analytical Profiles of Drug Substances, Vol. 4, Academic Press, New York, 1975, p. 33.
13 M. Friedman and G. W. Sigel, Biochemistry, 5 (1966) 478.
14 R. A. Fisher and F. Yates, Statistical Tables, Longman, Edinburgh, 1974, p. 63.
15 M. Roth and L. Jeanneret, Hoppe-Seyler's Z. Physiol. Chem., 353 (1972) 1607.

Analytica Chimica Acta, 108 (1979) 417—420
© Elsevier Scientific Publishing Company, Amsterdam — Printed in The Netherlands

Short Communication

SPECTROPHOTOMETRIC DETERMINATION OF TRACE AMOUNTS OF ANTIMONY(V) AFTER SELECTIVE PRECIPITATION WITH FERROIN AND DISSOLUTION IN NITROBENZENE

G. GOPALA RAO*, S. G. VISWANATH and G. SOMIDEVAMMA

Department of Chemistry, Andhra University, Waltair (India)

(Received 30th November 1978)

Summary. Antimony(V) in the range 24—240 μg can be determined very selectively in 8—10 M hydrochloric acid solutions by precipitation of its complex with ferroin; after dissolution in nitrobenzene, absorbances are measured at 510 nm. Antimony(III) and (V) can be determined successively in mixtures.

Recently, a new procedure [1] was reported for the determination of traces antimony(V) by solvent extraction—spectrophotometry of the $Fe(phen)_3^{2+}$—$(SbCl_6^-)_2$ ion-association complex. Because various cations interfere in this procedure, the present investigation was undertaken to ascertain if antimony(V) chloride could be selectively precipitated by ferroin. The work proved to be rewarding; relatively large amounts of several metals, arsenic(III) and arsenic(V) did not coprecipitate from 8—10 M hydrochloric acid solutions. The ion-association complex dissolved freely in nitrobenzene, and spectrophotometry of the resulting solution gave determinations of antimony(V).

Apart from the selectivity of the precipitation, this procedure has another advantage. The precipitates can be preserved for many hours without deterioration; the extracts obtained previously [1] were stable for only about 90 min. This stability is obviously a big advantage in routine analysis. A further advantage is that the separation of antimony(V) and antimony(III) and their individual determination can be made on a single aliquot of a mixture. The method has been applied to the determination of antimony in pharmaceuticals.

Experimental

Apparatus. A Gallenkamp microcentrifuge and a Hilger Uvispek spectrophotometer with matched 1-cm cells were used.

Antimony(V) solution (0.01 M). This was prepared in 10 M hydrochloric acid from potassium hexapyroantimonate. The solution was standardized by heating an aliquot with sodium sulphite [2] after addition of sufficient sulphuric acid to prevent volatilization of antimony(V) [3], cooling, passing carbon dioxide to expel sulphur dioxide, and titrating the resulting anti-

mony(III) with 0.025 M cerium(IV) sulphate with ferroin as indicator [4]. The stock antimony(V) solution was diluted to 0.001 M with 10 M hydrochloric acid as necessary.

Antimony(III) solution (0.01 M). This was prepared in 3 M hydrochloric acid from antimony(III) oxide and standardized with cerium(IV) sulphate [4]. This solution was diluted to 0.001 M with 10 M hydrochloric acid as necessary.

Other reagents. Antimony potassium tartrate solution (0.01 M) was standardized [5] with cerium(IV) sulphate, and diluted to 0.001 M as necessary. Ferroin solution (0.01 M) was prepared from iron(II) ammonium sulphate and 1,10-phenanthroline [2]. All the chemicals used were analytical-reagent grade.

Procedure. Accurately measure in aliquot (0.20—2.0 ml) of 0.001 M antimony(V) solution containing 24—240 μg of antimony into a micro-centrifuge tube, add 0.2 ml of 0.01 M ferroin solution and centrifuge for 5 min at 2000 rpm. Carefully remove the upper aqueous phase, add 1 ml of water, and centrifuge again. Repeat this procedure twice: as the antimony(V)—ferroin association complex is sparingly soluble in water, losses on washing will be negligible. Dissolve the precipitate in 2 ml of nitrobenzene and transfer to a small beaker containing 1 g of anhydrous sodium sulphate. Wash the centrifuge tube with two 1-ml portions of nitrobenzene and transfer to the same beaker. Transfer the nitrobenzene solution to a 10-ml volumetric flask. Wash the residual sodium sulphate with two 1-ml portions of nitrobenzene and add the washings to the flask. Make up carefully with nitrobenzene to 10 ml. Measure the absorbance at 510 nm (1-cm cells) against a nitrobenzene blank. Obtain the amount of antimony(V) from the calibration curve.

Calibration curve. Prepare the calibration curve by using ten different volumes (0.2—2.0 ml) of 0.001 M antimony(V) solution and applying the above procedure. Beer's Law is obeyed over the range 0—245 μg of antimony(V), the corresponding absorbance range being 0—1.000.

Results

The results of typical assays of antimony(V) are given in Table 1. In testing the effects of changes in hydrochloric acid concentration, it was found that the same calibration graphs were obtained for 8—10 M solutions. Precipitations made in hydrochloric acid concentrations lower than 8 M gave absorbance values that decreased with decreasing acid concentrations. Amounts of ferroin ranging from 1.5 to 4 times the theoretical required for the antimony(V) taken had no effect within the limits of experimental error.

The complex is soluble in nitrobenzene, 1,2-dichloroethane, chloroform, benzyl alcohol, n-butanol, and isobutyl methyl ketone. The colors are stable (ca. 50 min) in nitrobenzene and 1,2-dichloroethane but fade rapidly in the latter five solvents. The complex is also soluble in 2-chlorethanol, ethanol, isopropanol, ethylene glycol, and acetone, but insoluble in diethyl ether, diisopropyl ether, ethyl methyl ketone, carbon tetrachloride, chloroform, carbon disulphide, isoamyl alcohol, benzene, toluene, xylene, isobutanol, and isoamyl alcohol.

TABLE 1

Determination of antimony(V) in pure solutions

Sb(V) taken (μg)	43.83	87.66	121.75	182.63
Sb(V) found (μg)	45.05	90.09	124.19	181.41
Error (%)	+2.80	+2.77	+2.00	−0.67

Effects of diverse ions. A solution of the diverse metal ion in 10 M hydrochloric acid was added to the antimony(V) solution in 10 M hydrochloric acid before precipitation with ferroin. The results (Table 2) show that relatively large amounts of many cations do not interfere. When the interference of various anions was tested on the determination of 122 μg of antimony, citrate did not interfere up to 384 mg, tartrate up to 300 mg, succinate up to 118 mg, EDTA up to 15 mg and bromate up to 2.5 mg. The method can thus be used for the assay of tartar emetic after prior oxidation of antimony(III) with bromate.

Determination of antimony(III)

Antimony(III) is not precipitated by ferroin from 8—10 M hydrochloric acid, thus antimony(III) remaining in solution after the precipitation of antimony(V) can be determined by the recommended procedure after oxidation to antimony(V) with a slight excess of bromate. Some typical results for antimony(III) are presented in Table 3: the method can be used for the determination of antimony(III) in tartar emetic and other antimonial drugs.

Successive determination of antimony(V) and antimony(III) in mixtures

Antimony(V) is precipitated in 8—10 M hydrochloric acid with ferroin

TABLE 2

Determination of 122 μg of antimony(V) in the presence of diverse ions[a]

Diverse ion	Taken (mg)	Sb(V) found (μg)	Diverse ion	Taken (mg)	Sb(V) found (μg)
Cu(II)	12.7	121	Fe(III)	1.7	120
Mn(II)	22.0	120	Sb(III)	30.0	121
Ni(II)	23.5	119	As(III)	1.5	120
Co(II)	14.7	120	Sn(IV)	1.9	120
Zn(II)	10.0	121	Th(IV)	93.0	122
Hg(II)	21.7	123	V(IV)	2.5	121
Pb(II)	31.0	120	As(V)	18.6	123
			Cr(VI)	9.8	122

[a]Copper, manganese, nickel, tin, antimony were used as the chlorides; zinc, iron and vanadium(IV) as sulphates; lead and thorium as acetates; chromium(VI) as potassium dichromate; arsenic(V) as sodium arsenate; arsenic(III) as sodium arsenite.

and centrifuged. The centrifugate and the washings are treated with potassium bromate to oxidize the antimony(III) to antimony(V), which is precipitated with ferroin. The separate precipitates are then treated as in the recommended procedure. The results of assays of mixtures of antimony(V) and antimony(III) are presented in Table 4.

Although isopropyl ether [6, 7] and diisoamyl ether [8] are reported to separate Sb(V) from Sb(III), it is not known if other elements interfere. In the present procedure ferroin not only gives a clean separation of Sb(V) from Sb(III) but also provides the chromogenic reagent.

TABLE 3

Determination of antimony(III) after oxidation to antimony(V) with bromate, precipitation with ferroin and spectrophotometry in nitrobenzene solution

Sb(III) taken (μg)	48.7	97.4	121.8	146.1	194.8	243.5
Sb(III) found (μg)	48.1	97.4	119.3	148.5	199.7	238.6
Error (%)	−1.2	0.0	−2.1	+1.6	+2.5	−2.0

TABLE 4

Analysis of mixtures of antimony(V) and antimony(III)

Sb(V) + Sb(III) taken (μg)	Sb(V) found (μg)	Error (%)	Sb(III) found (μg)	Error (%)
97.4 + 146.1	97.4	0	141.2	−3.4
146.1 + 97.4	153.4	+5.00	99.8	+2.5
121.8 + 146.1	119.3	−2.1	146.1	0
146.1 + 121.8	143.7	−1.6	120.5	−1.1
170.5 + 121.8	165.6	−2.9	124.2	+2.0
121.8 + 170.5	120.5	−1.1	172.9	+1.4

REFERENCES

1 G. Gopala Rao and S. G. Viswanath, Anal. Chim. Acta, 94 (1977) 169.
2 I. M. Kolthoff and R. Belcher, Volumetric Analysis, Vol. III, Interscience, New York, 1957, pp. 74 and 127.
3 H. H. Willard and H. Diehl, Advanced Quantitative Analysis, D. Van Nostrand, New York, 1943, p. 346.
4 G. Gopala Rao and S. G. Viswanath, Anal. Chim. Acta, 92 (1977) 163.
5 G. Gopala Rao, S. G. Viswanath and M. Gandikota, Anal. Chim. Acta, 79 (1975) 273.
6 N. H. Bonner, J. Am. Chem. Soc., 71 (1949) 3909.
7 G. K. Schweitzer and L. E. Storms, Anal. Chim. Acta, 19 (1958) 154.
8 D. I. Ryabhikova and M. M. Privilova, Zh. Neorg. Khim., 3 (1958) 1694.

Analytica Chimica Acta, 108 (1979) 421—423
© Elsevier Scientific Publishing Company, Amsterdam — Printed in The Netherlands

Short Communication

FLUORIMETRIC DETERMINATION OF REDUCING CARBOHYDRATES WITH MALONAMIDE

SUSUMU HONDA*, YOSHIKAZU MATSUDA, MOTOME TERAO and KAZUAKI KAKEHI
Faculty of Pharmaceutical Sciences, Kinki University, Kowakae, Higashi-Osaka (Japan)
(Received 21st November 1978)

Summary. Samples are heated for 90 min with malonamide in carbonate buffer (pH 9.2) for measurement at 383 nm (excitation)/425 nm (emission). For D-glucose, relative standard deviations are 1—3% at the 10^{-6}—10^{-9} mol level. Relative fluorescence intensities are reported for 36 carbohydrates.

Of the fluorimetric methods for the determination of carbohydrates, those utilizing aliphatic amines, e.g. ethylenediamine [1] and taurine [2], proceed under weakly alkaline conditions, and are convenient for the determination of reducing carbohydrates and detection of liquid chromatographic eluates. This communication deals with the determination of reducing carbohydrates with a new reagent, malonamide.

Experimental

Reagents and apparatus. Deionized, distilled water was used; reagents and carbohydrate samples were of the purest grade commercially available. Carbonate buffers of various pH values were made by mixing x M sodium hydrogencarbonate and 0.5 x M sodium carbonate in the appropriate proportions.

Fluorescence spectra were recorded on a Shimadzu RF-500 spectrofluorimeter (1-cm quartz cell); intensities were referred to that of 10^{-4} M D-glucose at 383 nm (excitation)/425 nm (emission), measured under the recommended conditions.

Recommended procedure. Add 1 M carbonate buffer (pH 9.2, 5.00 ml) and 1.00 ml of 0.5 M malonamide to a solution (1.00 ml) containing the carbohydrate (10^{-9}—10^{-6} mol). Heat the mixture for 90 min on a boiling water bath, read the fluorescence intensity, and obtain the sample concentration from a calibration curve obtained under the same conditions.

Results and discussion

The fluorescence spectra for D-glucose show maxima at 328 (excitation)/382 (emission) nm and 383 (excitation)/425 (emission) nm (Fig. 1). The fluorescence at the higher wavelength is the more intense. Other reducing carbohydrates gave similar spectra.

Optimization of the reaction conditions. The optimum conditions for the determination were investigated with 10^{-4} M D-glucose. Acetate, phosphate,

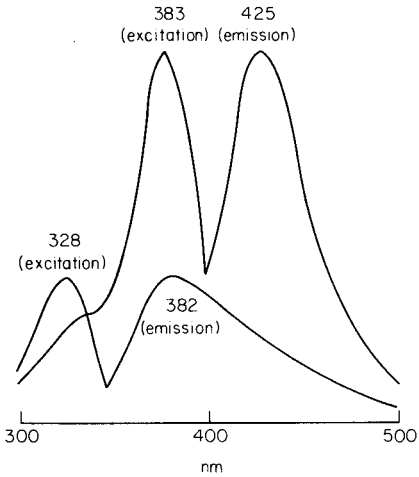


Fig. 1. Fluorescence spectra for D-glucose.

borate, and carbonate buffers were examined; 1 M carbonate buffer, pH 9.2 (±0.1), gave the most intense fluorescence at both emission wavelengths. The fluorescence intensity of both sample and blank solutions increased with increasing malonamide concentration. At the optimum concentration, 0.5 M, the intensity of the reagent blank was ca. 3% of that for the sample solution.

The intensity of the fluorescence at the higher wavelength increased rapidly at the initial stage of reaction, and reached a plateau in 90 min. This period is shorter than that for the ethylenediamine [1] procedure (3 h), but longer than that with taurine (30 min).

Calibration graphs. The calibration graph for standard D-glucose solutions was linear in the range 10^{-6}—10^{-3} M (in the original sample solution), for the fluorescence at 425 nm. The fluorescence at 382 nm gave a gentle sigmoidal curve. Similar results were obtained for other hexoses and pentoses. This concentration range is similar to that for the ethylenediamine [1] and taurine [2] methods. Table 1 gives reproducibility data for the determination of D-glucose. Similar results were obtained for other reducing carbohydrates.

TABLE 1

Precision of the determination of D-glucose

D-glucose (mol)	Coefficient of variation (%)[a]	
	328 nm (ex)/382 nm (em)	383 nm (ex)/425 nm (em)
5×10^{-9}	1.3	3.1
5×10^{-8}	0.9	1.8
5×10^{-7}	3.0	3.3

[a] $n = 8$.

TABLE 2

Relative fluorescence intensities from various carbohydrates

Carbohydrate	Relative fluorescence intensity		Carbohydrates	Relative fluorescence intensity	
	382 nm (em)	425 nm (em)		382 nm (em)	425 nm (em)
DL-Glyceraldehyde	0.28	1.30	Glycolic acid	0.01	0.01
L-Arabinose	0.29	0.59	D-Gluconic acid	0.00	0.00
D-Lyxose	0.30	0.58	Erythritol	0.00	0.00
D-Ribose	0.29	0.56	D-Glucitol	0.00	0.01
D-Xylose	0.30	0.60	Inositol	0.00	0.00
D-Galactose	0.32	0.72	Methyl α-D-glucoside	0.00	0.00
D-Glucose	0.33	1	Trehalose	0.00	0.00
D-Mannose	0.35	1.07	Sucrose	0.00	0.00
L-Fucose	0.29	0.61	Raffinose	0.00	0.01
L-Rhamnose	0.33	1.01	Maltose	0.44	1.10
D-Fructose	0.35	1.04	Cellobiose	0.42	1.08
L-Sorbose	0.35	0.82	Lactose	0.44	1.06
D-Galactosamine HCl	0.32	0.38	Gentiobiose	0.52	1.60
D-Glucosamine HCl	0.32	0.38	Melibiose	0.77	1.67
N-Acetyl-D-glucosamine	0.43 (0.45[a])	0.38 (0.41[b])	Starch	0.02	0.02
D-Galacturonic acid	0.33	0.51	Glycogen	0.01	0.00
D-Glucuronic acid	0.40	0.71	Dextran	0.01	0.00
2-Deoxy-D-glucose	0.13[c]		Pullulan	0.01	0.03

[a]328 nm (ex)/394 nm (em). [b]375 nm (ex)/423 nm (em). [c]328 nm (ex)/406 nm (em).

Fluorescence intensities for different carbohydrates. Table 2 summarizes the intensities of the fluorescences given by various carbohydrates. Generally, the intensity of the fluorescence at 382 nm does not change greatly for different reducing carbohydrates, though exceptions are observed for reducing disaccharides, *N*-acetyl-D-glucosamine, and D-glucuronic acid. The intensity of the fluorescence at 425 nm is strongly dependent on structure; the intensities for four pentoses were similar but those for hexoses varied significantly. D-Galactose, with an axial C-4 hydroxyl group, gave a lower value than D-glucose and D-mannose, which have an equatorial C-4 hydroxyl group. A similar effect was observed for methylpentoses and uronic acids. The wavelengths for maximal intensity shifted slightly for *N*-acetyl-D-glucosamine; 2-deoxy-D-glucose gave only one weak fluorescence with excitation and emission maxima at 328 and 406 nm, respectively. Reducing disaccharides with a 1→6 linkage (gentiobiose and melibiose) gave extraordinarily high molar intensities. The aldonic acids, alditols, glycosides, non-reducing oligosaccharides, and polysaccharides tested did not fluoresce under the reaction conditions described.

REFERENCES

1 S. Honda, K. Kakimoto, K. Sudo, K. Kakehi and K. Takiura, Anal. Chim. Acta, 70 (1974) 133.
2 T. Kato and T. Kinoshita, Chem. Pharm. Bull., 26 (1978) 1291.

Analytica Chimica Acta, 108 (1979) 425—427
© Elsevier Scientific Publishing Company, Amsterdam — Printed in The Netherlands

Short Communication

DIRECT FLUORIMETRIC DETERMINATION OF CARBARYL INSECTICIDE AND ITS HYDROLYSIS PRODUCT 1-NAPHTHOL

M. J. LARKIN* and M. J. DAY

Department of Applied Biology, UWIST, Cardiff (Gt. Britain)

(Received 1st November 1978)

Summary. Direct fluorimetric determinations are described for Carbaryl (1-naphthyl-*N*-methylcarbamate) and 1-naphthol in the range 0—1 μg ml^{-1} in the same solution. Spectra, quantum efficiencies and relative sensitivities are reported.

Carbaryl (1-naphthyl-*N*-methylcarbamate) is the active ingredient [1] of the widely applicable insecticide Sevin (Union Carbide Corporation) [2]. At alkaline pH values, Carbaryl hydrolyses to 1-naphthol and *N*-methylcarbamic acid, which then decomposes spontaneously to methylamine and carbon dioxide [2]. Although numerous methods have been employed in the detection and determination of Carbaryl and 1-naphthol [2], there is only one report of their simultaneous determination by means of their native fluorescence [3]. Spectra, quantum efficiencies and relative sensitivities have not been reported previously for Carbaryl. This communication describes the simultaneous determination of both compounds in dilute aqueous methanol solution.

Experimental

Reagents. Reagents of the purest grade obtainable were used without further purification. An aqueous solution (10%, v/v) of "Aristar" methanol (BDH) was used as the solvent for Carbaryl and 1-naphthol.

Instrumentation. Fluorescence spectra were obtained with a Baird-Atomic SFR 100 ratio-recording spectrofluorimeter which incorporates a rhodamine B reference cell and produces corrected emission spectra. Spectra were recorded with a Servoscribe RE541.20 recorder; peak areas were determined by weight (Oertling R51 balance). Molar absorptivities (ϵ) were determined with a Pye-Unicam SP 1800 spectrophotometer. The slit sizes of both instruments were adjusted to give an incident bandwidth of 1.0 nm; the emission slits of the spectrofluorimeter gave a bandwidth of 10.0 nm.

Quantum efficiencies and relative sensitivities. Quantum efficiencies (ϕ) were determined with quinine hydrogensulphate as reference standard (for a 5×10^{-3} M solution in 2 M H_2SO_4 at 25°C, $\phi = 0.51$ [4]). All measurements were made at 25°C and the following equation [5] was employed:

(corrected emission peak area 1)/(corrected emission peak area 2)
$= \phi_1 \epsilon_1 C_1 l / \phi_2 \epsilon_2 C_2 l$

where C is the molar concentration (4.95×10^{-6} M for Carbaryl, 6.94×10^{-6} M for 1-naphthol) and l is the pathlength (10 mm throughout). If all peak areas, molar absorptivities, molar concentrations and one standard quantum efficiency (ϕ_2) are known, then ϕ_1 can be calculated. All the determinations were the means of four separate measurements obtained in duplicate.

The relative sensitivities for Carbaryl and 1-naphthol were calculated [5] from the expression $\phi\epsilon/H$, where H, the half bandwidth of the fluorescence emission spectrum, was calculated as the bandwidth at half the peak height.

Oxygen quenching and solvent effects. When 1.0 μg ml^{-1} solutions of Carbaryl and 1-naphthol in 10% (v/v) methanol were flushed with nitrogen for 10 min, the fluorescence intensities increased by 5.2 and 2.2%, respectively (taking evaporation into account.) This indicated a low degree of oxygen quenching for both compounds. The fluorescence spectra and intensities for Carbaryl and 1-naphthol were unaltered in aqueous 0—30% (v/v) methanol solutions.

Results and discussion

The corrected excitation and emission spectra of Carbaryl and 1-naphthol in 10% (v/v) methanol are shown in Fig. 1 (note the higher gain setting for 1-naphthol and hence the expanded spectrum). The emission spectra overlap only slightly; it is possible to measure Carbaryl in the range 0—1 μg ml^{-1} in the presence of 1-naphthol up to 10 μg ml^{-1}. Above this concentration 1-naphthol quenched the Carbaryl fluorescence.

Table 1 shows the quantum efficiencies, molar absorptivities, half bandwidths and relative sensitivities. The direct method of measuring Carbaryl is

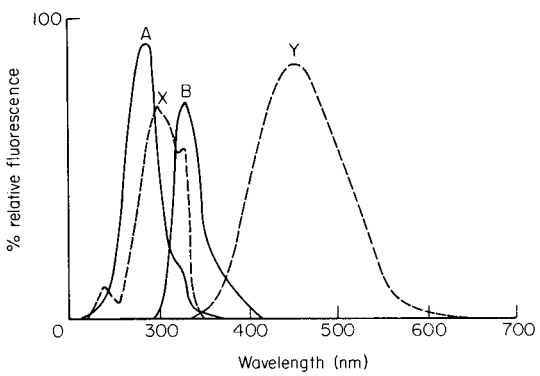


Fig. 1. The excitation and emission spectra of 1 μg ml^{-1} solutions of Carbaryl and 1-naphthol in 10% methanol. (A) Excitation spectrum of Carbaryl (gain setting × 30); (B) emission spectrum of Carbaryl (gain setting × 30); (X) excitation spectrum of 1-naphthol (gain setting × 100); (Y) emission spectrum of 1-naphthol (gain setting × 100).

TABLE 1

Calculation of relative fluorescence sensitivities

Compound	λ_{ex} (max.) (nm)	λ_{em} (max.) (nm)	ϕ	ϵ[a] (l mol^{-1} cm^{-1})	H (nm)	$\frac{\phi\epsilon}{H}$	Rel. sens. (%)
Quinine hydrogensulphate[b]	352	444	0.51[d]	5280	77	34.97	100
Carbaryl[c]	281	328	0.146	6170	39	23.10	66
1-Naphthol[c]	296	456	0.074	4890	85	4.26	12

[a]For maximum λ_{ex}. [b]In 2 M H_2SO_4. [c]In 10% (v/v) methanol. [d]Standard quantum efficiency of 5×10^{-3} M quinine hydrogensulphate in 2 M H_2SO_4 at 25°C [4].

only 34% less sensitive than the direct measurement of quinine hydrogensulphate in 2 M H_2SO_4. The measurement of 1-naphthol by the direct method was much less sensitive (12% that of quinine hydrogensulphate); measurement of 0—1 μg ml^{-1} was possible in the presence of Carbaryl up to 4 μg ml^{-1}. The low degree of overlap between the Carbaryl absorption and the 1-naphthol emission spectra, however, allows the determination of 1-naphthol without Carbaryl quenching its fluorescence. Some previous indirect fluorimetric methods for Carbaryl involved the determination of hydrolysed Carbaryl in 0.1 M NaOH and hence the measurement of the 1-naphthol fluorescence [3, 6]. Clearly, the direct measurement of Carbaryl in an aqueous solution is more desirable.

M. J. Larkin acknowledges support by the Science Research Council.

REFERENCES

1 Union Carbide Corporation, Technical Information Bulletin (1974).
2 R. J. Kuhr and H. Wyman Dorough, Carbamate Insecticides: Chemistry, Biochemistry and Toxicology, CRC Press, Cleveland, Ohio, 1976.
3 R. J. Argauer and W. Bontayan, J. Assoc. Off. Anal. Chem., 53 (1970) 1166.
4 W. H. Melhuish, J. Phys. Chem., 65 (1961) 229.
5 C. A. Parker and W. T. Rees, Analyst, 85 (1960) 587.
6 R. J. Argauer, H. Shimanuki and C. C. Alvarez, J. Agric. Food. Chem., 18 (1970) 688.

Analytica Chimica Acta, 108 (1979) 429—432
© Elsevier Scientific Publishing Company, Amsterdam — Printed in The Netherlands

Short Communication

SPECTROFLUORIMETRIC DETERMINATION OF EUROPIUM AND SAMARIUM WITH MIXTURES OF 2-THENOYLTRIFLUOROACETONE AND TRI-n-OCTYLPHOSPHINE OXIDE IN AQUEOUS SOLUTIONS CONTAINING TRITON X-100

TOMITSUGU TAKETATSU* and ATSUKO SATO

College of General Education, Kyushu University, Ropponmatsu Chuo-ku, Fukuoka 810 (Japan)

(Received 3rd January 1979)

Summary. The europium or samarium complex with thenoyltrifluoroacetone and tri-n-octylphosphine oxide in aqueous 0.2% Triton X-100 solution at pH 3.6 is used to determine europium (1.5—760 ng ml^{-1}) or samarium (15—1500 ng ml^{-1}). The excitation wavelength is 352 or 372 nm; the emission wavelength is 613 or 561 nm. The procedures give better sensitivity than the corresponding extraction methods. A standard addition method is used to overcome interferences.

Ternary complexes of europium, samarium or terbium with a β-diketone and a neutral donor extracted into organic solvents are useful for spectrofluorimetric determinations of these metals [1—3]. It is shown here that 2-thenoyltrifluoroacetone (TTA) and tri-n-octylphosphine oxide (TOPO) and the mixed complex with europium or samarium are readily soluble in aqueous solutions containing polyoxyethylene isooctylphenol (Triton X-100). The fluorescence intensities of these mixed complexes are considerably stronger than those of the corresponding mixed complexes extracted into several organic solvents. The spectrofluorimetric procedures based on these conditions are simple and rapid, and have the environmental advantage that organic solvents are unnecessary.

Experimental

Reagents and apparatus. Standard solutions of scandium and rare earths except cerium were prepared by dissolving the 99.9% pure oxides in dilute hydrochloric acid. Solutions of cerium(III) and thorium were prepared in dilute hydrochloric acid from reagent-grade cerium(III) chloride and thorium chloride. These solutions were standardized by titration with EDTA (xylenol orange indicator).

Separate standard 5×10^{-2} M TTA and 5×10^{-3} M TOPO solutions were prepared by dissolving the reagents (Dojin Co.) in an aqueous 10% (w/v) Triton X-100 (Wako Chemical Co.) solution. The mixed reagent solution used contained 5×10^{-3} M TTA, 5×10^{-4} M TOPO and 2% (w/v) Triton X-100.

Acetate buffer (pH 3.6) was prepared by adding 10 ml of 0.1 M sodium acetate to 160 ml of 0.1 M acetic acid. All other chemicals used were of analytical-reagent grade.

A Hitachi 204 spectrofluorimeter was used in combination with a high-pressure xenon tube.

Procedure. To a dilute hydrochloric acid solution containing 0.03—15 μg of europium or 0.3—30 μg of samarium were added 2 ml of the mixed TTA—TOPO reagent solution and 2 ml of the acetate buffer. After adjustment to about pH 3.5 with dilute hydrochloric acid and sodium hydroxide solutions, the solution was transferred to a 20-ml volumetric flask and made up to volume with water. The fluorescence was then measured in a 1-cm quartz cell at apparent excitation and emission wavelengths of 352 and 613 nm, respectively, for europium, or 372 and 561 nm for samarium. The spectrofluorimeter was standardized before use to a constant reading with a solution of rhodamine B.

Results and discussion

Fluorescence spectra. Figure 1 shows the apparent fluorescence spectra of aqueous 0.2% Triton X-100 solution (pH 3.4) containing the europium or samarium TTA—TOPO ternary complexes for excitation wavelengths of 352 and 372 nm, respectively. The apparent wavelengths of the prominent maxima of the fluorescence spectra are 613 nm for europium and 561, 597 and 641 nm for samarium; the emission at 561 nm was used to determine samarium to avoid overlap with the europium peak at 613 nm.

Effect of reaction variables. A study of the effect of pH showed that the fluorescence intensity at 613 nm for the europium—TTA—TOPO complex was constant over the pH range 3.0—4.0, decreasing quite rapidly on both sides of this range. Similar results were obtained for samarium. Optimum fluorescence intensities were obtained when the mole ratio of TTA to europium lay in the range 200—400, for a 9.8×10^{-7} M europium solution containing 5×10^{-5} M TOPO and 1% Triton X-100. At mole ratios above 400, the fluorescence decreased gradually. For the 9.8×10^{-7} M europium solution

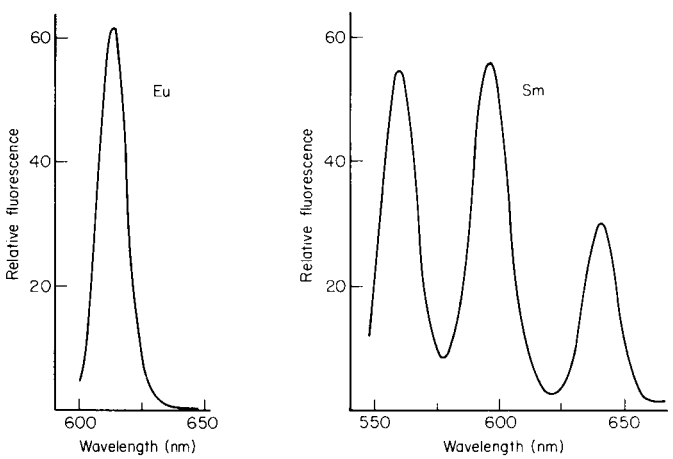


Fig. 1. Apparent fluorescence spectra of the europium and samarium TTA—TOPO complexes (i) Eu^{3+}, 9.8×10^{-7} M; (ii) Sm^{3+}, 1.0×10^{-6} M. TTA, 1×10^{-4} M; TOPO, 1×10^{-4} M; Triton X-100, 0.5%; pH 3.5.

with 5×10^{-4} M TTA present, mole ratios of TOPO to europium of 30—100 did not affect the fluorescence intensity. Changes in the concentration of Triton X-100 in the range 0.2—1.5% (w/v) also did not affect the intensity. With less than about 0.01%, the aqueous solution became turbid owing to the separation of TTA and TOPO. The fluorescence intensity remained constant for 24 h immediately after preparation of the complex. Similar results were obtained for samarium.

Calibration. The fluorescence intensity was a linear function of concentration in the range 1.5—760 ng ml^{-1} for europium and 15—1500 ng ml^{-1} for samarium.

Effects of diverse metals. The effects of scandium, rare earths and thorium on the fluorescence intensity of europium or samarium were investigated under the optimum conditions. Examination of the effects on europium (3.05 ng ml^{-1}) showed that 10-fold amounts of all these metals and 50-fold amounts of scandium, yttrium, lanthanum, neodymium, gadolinium, dysprosium, holmium, ytterbium, lutetium and thorium did not interfere. The fluorescence intensity of samarium (67.2 ng ml^{-1}) was not affected by the presence of equal amounts of these metals but europium interfered. However, large amounts of the diverse metals, especially rare earths absorbing in the ultraviolet and visible ranges, caused varying amounts of interference in the determinations of europium and samarium. Therefore, the standard addition method was applied for the determination of both the metals in such cases.

TABLE 1

Determination of europium and samarium by the standard addition method

Rare earth and thorium oxides (weight%)	Found (weight%)
Synthetic samples	
La_2O_3 7.19, CeO_2 32.8, Nd_2O_3 10.57, Sm_2O_3 2.27, Eu_2O_3 0.48, ThO_2 46.69	Eu_2O_3 0.49
Y_2O_3 26.82, Eu_2O_3 1.09, Dy_2O_3 5.54, Er_2O_3 6.17, Yb_2O_3 7.45, ThO_2 52.93	Eu_2O_3 1.16
Y_2O_3 63.32, Sm_2O_3 0.61, Gd_2O_3 22.17, Dy_2O_3 7.65, ThO_2 6.25	Sm_2O_3 0.63
CeO_2 99.92, Eu_2O_3 0.08	Eu_2O_3 0.09
Pr_6O_{11} 99.92, Eu_2O_3 0.08	Eu_2O_3 0.07
Tb_4O_7 99.91, Eu_2O_3 0.09	Eu_2O_3 0.09
Rare earth oxides (Xenotime)[a]	
Y_2O_3 64.3, La_2O_3 0.6, CeO_2 1.4, Pr_6O_{11} 0.2, Nd_2O_3 0.9, Sm_2O_3 1.1, Eu_2O_3 0.1, Gd_2O_3 3.3, Tb_4O_7 0.9, Dy_2O_3 7.8, Ho_2O_3 1.8, Er_2O_3 6.3, Tm_2O_3 0.9, Yb_2O_3 9.5, Lu_2O_3 0.9	Eu_2O_3 0.06 Sm_2O_3 1.27
Commercial oxides	
Gd_2O_3 99.9	Eu_2O_3 0.046
Gd_2O_3 99.9	Eu_2O_3 0.007

[a]Donated by Mr. M. Sato of the Shinetsu Chemical Co. Ltd. who also provided the x.r.f. results.

TABLE 2

Comparison between the fluorescence intensities obtained by the proposed and solvent extraction methods for 5×10^{-6} M solutions of europium and samarium

Method	Solutions	TTA (M)	TOPO (M)	pH	Relative fluorescence
Europium					
Recommended	Aq. 0.3% Triton X-100	5×10^{-4}	5×10^{-5}	3.5	100
Extraction	Benzene	5×10^{-4}	5×10^{-5}	4.5	0.96 (35%)[a]
	Carbon tetrachloride	5×10^{-4}	5×10^{-5}	4.5	1.42 (57%)
	1,2-dichloroethane	5×10^{-4}	5×10^{-5}	4.5	0.06 (7%)
	Benzene	5×10^{-3}	5×10^{-3}	4.1	0.06 (100%)
	Carbon tetrachloride	5×10^{-4}	1×10^{-2}	4.5	2.27 (100%)
	Carbon tetrachloride	5×10^{-3}	5×10^{-3}	4.1	0.07 (100%)
	Toluene	5×10^{-3}	5×10^{-3}	4.1	0.06 (100%)
	1,2-Dichloroethane	5×10^{-3}	5×10^{-3}	4.1	0.06 (100%)
	50% Ethanol	5×10^{-3}	5×10^{-3}	3.5	0.04
Samarium					
Recommended	Aq. 0.3% Triton X-100	5×10^{-4}	5×10^{-5}	3.5	10
Extraction	Carbon tetrachloride	5×10^{-4}	5×10^{-5}	4.0	0.16 (8%)
	Carbon tetrachloride	5×10^{-3}	5×10^{-3}	4.0	0.02 (100%)
	1,2-Dichloroethane	5×10^{-3}	5×10^{-3}	4.0	0.01 (100%)

[a] Values in parentheses show approximate percentage extraction.

The standard addition method was checked for the determination of europium in a mixed rare earth oxide obtained from Xenotime under the recommended conditions. The composition of the oxide estimated by x-ray fluorescence analysis is shown in Table 1. The results (Table 1) prove that the method is suitable for the determination of europium and samarium in the presence of large amounts of diverse metals.

Comparison between the proposed method and the solvent extraction method. Table 2 shows the difference between the fluorescence intensities obtained by the various methods. When the TTA and TOPO concentrations of the organic solutions are equal to those of the recommended method (5×10^{-4} M TTA and 5×10^{-5} M TOPO), europium and samarium are not completely extracted into the organic solutions and the fluorescence intensities are very weak even when extraction is complete. Though the percentage extractions increase as the concentrations of TTA and TOPO increase, the fluorescence intensities decrease. The intensity of the europium complex in a 50% ethanolic solution of 5×10^{-3} M TTA and 5×10^{-3} M TOPO is similar to that in the extraction method (Table 2). The differences in intensity seem to originate from the absorption spectra of TTA in the ultraviolet region.

It is concluded that the proposed method is superior to the solvent extraction method not only in simplicity and rapidity but also in sensitivity.

REFERENCES

1 R. P. Fisher and J. D. Winefordner, Anal. Chem., 43 (1971) 452.
2 T. Shigematsu, M. Matsui and R. Wake, Anal. Chim. Acta, 46 (1969) 101.
3 R. Belcher, R. Perry and W. I. Stephen, Analyst, 94 (1969) 26.

Analytica Chimica Acta, 108 (1979) 433—435
© Elsevier Scientific Publishing Company, Amsterdam — Printed in The Netherlands

Short Communication

INTERFERENCE OF TRACE AMOUNTS OF NITRILOTRIACETIC ACID IN ETHYLENEDIAMINETETRAACETIC ACID WITH THE SPECTROPHOTOMETRIC DETERMINATION OF NIOBIUM AS THE NIOBIUM—EDTA—PYROCATECHOL COMPLEX

J. P. J. VAN DALEN

Laboratory for Analytical Chemistry, Delft University of Technology, Jaffalaan 9, 2628BX Delft (The Netherlands)

(Received 18th January 1979)

Summary. The effects of 10^{-2}—10 mol-% NTA in the EDTA used in this determination are reported. Satisfactory results are possible only if the NTA contamination is less than 0.05% (w/w). Even analytical-grade EDTA from some sources may be grossly contaminated.

The photometric determination of niobium with pyrocatechol and EDTA as described by Patrovský [1] formed the basis of a Dutch draft national standard method for the determination of niobium in steel [2]. This draft has been withdrawn because of the inadequate limit of detection and because of the problems discussed below. In the draft standard, the steel is dissolved in a mixture of hydrochloric and nitric acids. The niobium is precipitated as niobium oxide with sulphurous acid, filtered off and fused with pyrosulphate; the melt is cooled and dissolved in a tartaric acid solution. After addition of pyrocatechol and disodium-EDTA, a red-brown colour develops and the absorbance of the solution is measured at 478 nm.

In applications of the draft standard, capricious results were obtained, and these were traced to the use of EDTA from different sources. With some samples of EDTA, the slope of the calibration plot was considerably reduced and the graph became slightly concave. Also, for a given concentration of niobium the absorbance was not independent of the concentration of EDTA, but decreased with the excess of EDTA added.

Results with EDTA from different sources

Analytical-grade EDTA from 17 different sources was tested. The reagents were obtained from different manufacturers and were dated over the period 1951 to 1975; they included mainly disodium salts, but also a few free acids or tetrasodium salts (with an equivalent quantity of sodium hydroxide or acetic acid added). The influence of the different EDTA samples on the measured absorbance will be discussed for a fixed concentration of niobium corresponding to the midpoint of the calibration curve in the draft standard.

Solutions containing 0.4 mg Nb, 1 g of pyrocatechol and 0.5 mmol of EDTA in 50 ml were made with all the different EDTA samples. The absorbance varied from 1.01 to 0.02; eight EDTA samples gave a value above 0.9 and three gave a value of 0.02 (see Fig. 1). Especially for those EDTA samples that gave absorbances between these extreme values, an increase of the EDTA concentration reduced the absorbance. Because the concentration of EDTA in the final solution was 50—1000 times higher than the niobium concentration, these results might be due to a contaminant in the EDTA with complexing properties for niobium. The influence of NTA, which is a known contaminant of EDTA (see, e.g. refs. [3—5]) was therefore analysed.

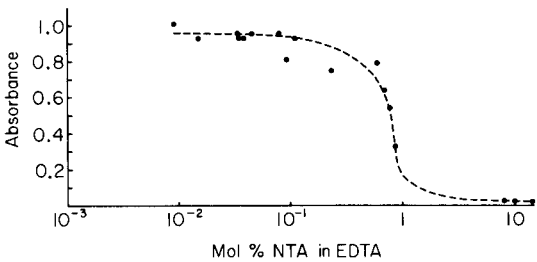
Effect of NTA

The addition of 1 mol-% NTA to several EDTA samples that had previously yielded high absorbances ($A > 0.9$) reduced the absorbances of the final solution to about 0.02; thus NTA could be the origin of the problems. To investigate the relation between the NTA concentration and the absorbance of the final solution, the NTA concentrations were determined by differential pulse polarography of the $Cd(NTA)_2$ complex as described by Farrow and Hill [5]. For each EDTA sample the standard addition technique was used with two additions. Unfortunately not all the standard addition plots obtained were strictly linear (in the concentration range where NTA added to a "pure EDTA" gave a straight calibration graph), but the precision of the measurements was still adequate.

In the polarographic analysis of some EDTA samples, an extra peak was observed, which could be attributed [4] to ethylenediaminediacetic acid (EDDA). The addition of pure EDDA to these EDTA samples confirmed this assumption. Because EDDA interferes with the NTA determination, the EDTA samples were treated with warm hydrochloric acid to convert the EDDA to the imide form which is stable on cooling and addition of sodium hydroxide to give pH 10—11. The EDDA-imide does not form a stable complex with cadmium, and so does not interfere with the NTA determination [4].

The concentration of NTA in the EDTA samples was found to vary from less than 0.01 mol-% to about 10 mol-%. No correlation was observed between the NTA concentration and the form (free acid, disodium or tetrasodium salt) or the year of purchase of the EDTA sample. The relation between the NTA content of the EDTA samples and the absorbance of the niobium solutions suggests an equivalence point from which the ratio of niobium and NTA in the Nb—NTA complex was calculated as about 1:1 (Fig. 1). This was verified by the addition of NTA to the EDTA with the lowest NTA content (<0.01 mol-%). The relation between the NTA concentration and the absorbance of the niobium—EDTA—pyrocatechol complex (Fig. 2) confirms the 1:1 ratio.

The possibility of a photometric determination of niobium through its NTA complex was briefly investigated. However, the absorption spectrum of a mixture of NTA, niobium and pyrocatechol showed no absorption peak above 300 nm; below 300 nm pyrocatechol itself absorbs strongly.



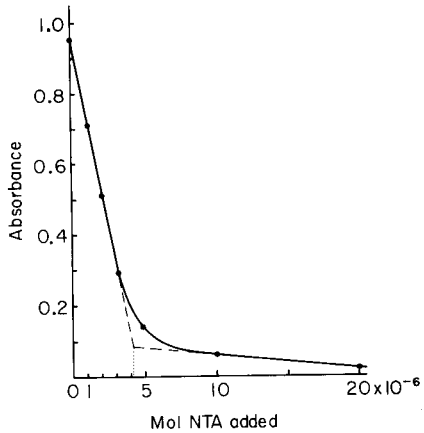


Fig. 1. Relation between the NTA concentration in EDTA and the absorbance found for 0.4 mg Nb, for 17 commercially obtained EDTA samples.

Fig. 2. Determination of the ratio of niobium and NTA in the NTA—Nb complex. Solutions of 50 ml containing 4.3×10^{-6} mol Nb (0.40 mg), 1 g of pyrocatechol, 0.5 mmol of high-purity EDTA and increasing amounts of NTA. The extrapolated equivalence point lies at 4.2×10^{-6} mol NTA, indicating a 1:1 NTA: Nb complex.

Finally EDTA with a very high NTA content of about 10 mol-% was purified by the elaborate procedure described by Barnard et al. [6]. The purification resulted in an NTA concentration below 0.01 mol-%. With 0.4 mg Nb, 1 g of pyrocatechol and 0.1 mmol of this purified EDTA in 50 ml of solution, the absorbance was 0.95, whereas before the purification the absorbance was 0.02.

In conclusion, it has been shown that impurities of NTA in EDTA interfere strongly with the photometric determination of niobium through its EDTA—pyrocatechol complex. Reliable results down to 0.025% Nb in steel (0.4 ppm Nb in the final solution) can be obtained only if the NTA content of EDTA is less than 0.05% (w/w) when the draft standard [2] is applied.

The contributions of L. de Galan, W. A. Maertens and J. F. Vandierendonck are gratefully acknowledged.

REFERENCES

1 V. Patrovský, Collect. Czech. Chem. Commun., 23 (1958) 1774.
2 Dutch Draft National Standard Method (Voornorm) NEN 1033-1, Nb. 1. (February, 1966).
3 R. L. Daniel and R. B. Le Blanc, Anal. Chem., 31 (1959) 1221.
4 R. L. Daniel and R. B. Le Blanc, Anal. Chem., 31 (1959) 1840.
5 P. Farrow and A. G. Hill, Analyst, 90 (1965) 210, 241.
6 A. J. Barnard, Jr., E. F. Joy, K. Little and J. D. Brooks, Talanta, 17 (1970) 785.

Analytica Chimica Acta, 108 (1979) 437—440
© Elsevier Scientific Publishing Company, Amsterdam — Printed in The Netherlands

Short Communication

THE DIRECT SPECTROPHOTOMETRIC DETERMINATION OF URANIUM(VI) IN TRIALKYLAMINE EXTRACTS WITH DIBENZOYLMETHANE

SAMUEL J. LYLE* and MASSOUD TAMIZI

The Chemical Laboratories, The University of Kent at Canterbury, Kent CT2 7NH (Gt. Britain)

(Received 23rd January 1979)

Summary. A spectrophotometric determination with dibenzoylmethane is described for uranium(VI) in trialkylamine sulphate extracts from sulphate leach liquors, without return of the uranium to an aqueous medium. The proposed method is less sensitive (apparent molar absorptivity, 3.8×10^4 l mol^{-1} cm^{-1}) than the Br—PADAP method but is more tolerant to sulphate and other ions found in leach liquor systems.

Uranium(VI) is extracted from acidified sodium sulphate leach liquors with trialkylamines in kerosene. Spectrophotometric methods for the determination of the uranium by direct colour formation in the diluted kerosene extract with 2-(5-bromo-2-pyridylazo)-5-diethylamino-phenol (Br—PADAP) have been described [1, 2]. These methods are satisfactory in many respects. In particular, with the method more recently advocated [2], good solvent compatibility on dilution and simplicity of operation are combined with improved sulphate tolerance. However, tolerance to sulphate and certain other ions in the amine extract is still somewhat restricted and interference from vanadium(V) can occur under conditions where it extracts appreciably with the uranium. Accordingly, dibenzoylmethane, long used for the determination in aqueous solution [3], was examined. When an ethanol-based non-aqueous medium is used for colour development, as described here, the final method has features superior to those found with the Br—PADAP method.

Experimental

Reagents and apparatus. Dibenzoylmethane (puriss grade; Koch-Light Ltd., Colnbrook) was recrystallized from methanol (m.p. 76.5—78°C). Other chemical substances and apparatus were described earlier [2]. Silica matched optical cells were used instead of glass.

Solutions. A 0.020% (w/v) solution of dibenzoylmethane was prepared by dissolving 200 mg in 700 ml of industrial methylated spirit (IMS), adding 20 ml of tri-n-octylamine (TOA) and diluting to 1 l with IMS.

The other solutions, including the uranium-free solvent and the uranium-containing solvent, were prepared as described previously [2].

Recommended procedure. Transfer 1—3 ml of the uranium extract containing up to 800 μg of uranium, and preferably not more than 21 mg of sulphate, to a 50-ml volumetric flask. Adjust the volume to 50 ml with dibenzoylmethane solution, mix well and measure the absorbance at 400 nm, using the dibenzoylmethane solution as reference.

Colour development is almost instantaneous and the colour remains stable for at least 12 h. Within the limits of measurement the absorbance remained constant from 20°C to 35°C. If 4 ml of uranium extract containing 28 mg of sulphate is taken, a 7% error occurs in the determination of 387 μg of uranium (VI).

Interference study. The methods of investigation were adopted, with small modifications, from the study of Br—PADAP [2]. Method 1 was used as previously described [2] except that after the initial 50-fold dilution of the extract with IMS, instead of 1 ml, 3 ml of the diluted solution was taken and treated as described in the recommended procedure.

To apply Method 2, some tolerance to water in the mixed uranium extract—dibenzoylmethane solution is required. Tests indicated that up to at least 6% (v/v) water in the colour-forming medium did not affect the absorbance of the final coloured product. Potentially interfering ions in aqueous solution were introduced into the medium in which the colour was developed in such a way that the latter contained not more than 4% (v/v) of water. The uranium-containing solvent was diluted with IMS made 2% (v/v) in TOA so that 2 ml contained 280 μg of uranium.

Results and discussion

Tests done to assist in selection of the optimum conditions for development of the uranium—dibenzoylmethane colour are summarized in Fig. 1. Curves 1—3, obtained by using different ratios of dibenzoylmethane to uranium, demonstrate the sensitivity of absorbance to change in the sulphate content of the medium and show that, although some improvement is obtained as the ratio increases, the dependence remains too great to be of much practical value. Addition of 2% TOA to the dibenzoylmethane reagent solution produces the improvement observed in curve 4; up to 21 mg of sulphate in the final measured solution does not reduce absorbance.

The optimum wavelength for measurement of absorbance was 400 nm. This was selected from spectra for 0.020% (w/v) dibenzoylmethane in IMS made 2% (v/v) in TOA and for a similar solution containing about 300 μg of uranium in 50 ml of the final solution. A mole ratio study indicated that the dibenzoylmethane-to-uranium ratio should be at least 15. With the 0.020% dibenzoylmethane solution, Beer's law was obeyed over the range 0—800 μg of uranium in the final 50 ml of solution. Mole ratio and continuous variations (Job) studies suggested that the ratio of dibenzoylmethane to uranium is 3:2 in the complex measured; this contrasts with the more readily explicable ratio of 2:1 for the colour in an aqueous 66% (v/v) ethanolic medium [3]. Assuming 2 moles of uranium in the complex measured here, the apparent molar absorp-

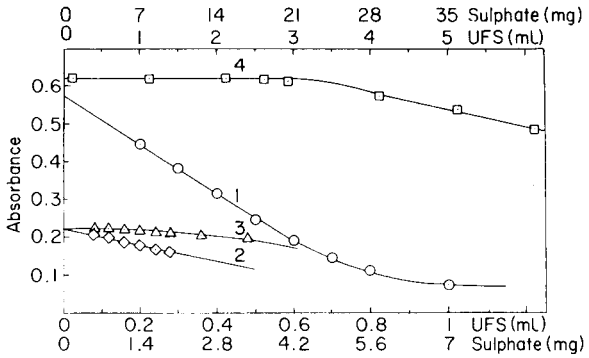


Fig. 1. Absorbance at 400 nm plotted against amount of uranium-free solvent and sulphate ion in 50 ml of colour-forming medium. The appropriate dibenzoyl methane concentration and colour-forming medium were used as reference solutions in these measurements. For curves 1—4, the solutions were, respectively, 2.98×10^{-5}, 1.19×10^{-5}, 1.19×10^{-5} and 3.25×10^{-5} M in uranium(VI) and 6.42×10^{-4}, 8.56×10^{-4}, 4.28×10^{-3} and $(7.49—8.56) \times 10^{-4}$ M in dibenzoyl methane, i.e., 21, 72, 360 and 23—26-fold excess over uranium. Curves 1—3 (lower scale) refer to IMS and curve 4 (upper scale) to 2% (v/v) TOA in IMS as colour-forming media.

tivity is 3.8×10^4 l mol^{-1} cm^{-1}. The sensitivity of the dibenzoylmethane method under the reaction conditions recommended is, therefore, only about 0.28 of that exhibited by Br—PADAP in the previous study.

Interference data (Fig. 2) obtained by introduction of the ion to be tested into the aqueous phase before extraction of the uranium, are very similar to those observed in the Br—PADAP work. This reinforces the earlier conclusion that the interferences are due largely to inhibition of uranium extraction rather than of colour development. Direct introduction of potentially interfering ions into the colour-forming medium (Fig. 3) shows that tolerances to vanadium(V), molybdenum(VI), nitrate and thiocyanate are improved. It can be concluded that iron(II), aluminium and phosphate ions do not interfere at their maximum concentrations reported in leach liquors. Dibenzoylmethane reacts with iron(III) to produce a yellow-orange colour and iron(III) at levels above 1.5 mg l^{-1} in the colour-forming medium would interfere. However, the poor extraction of iron(III) into the amine phase should prevent its interference in analysis of leach liquor extracts for uranium. Coloured products are not produced by vanadium(V) or molybdenum(VI).

In the search for a suitable colour reaction, 1-(2-pyridylazo)- 2-naphthol (PAN), (1,8-dihydroxy-3,6-disulpho-2-naphthylazo) benzene arsonic acid, disodium salt (arsenazo-I) and *N*-benzoyl-*N*-phenylhydroxylamine (BPHA) reacted with uranium(VI) in amine extract—IMS media. However, PAN exhibits a relatively poor tolerance to sulphate and the colour stability is not great, fading becoming evident visually within 2—3 h; addition of 2% TOA to the PAN in IMS induces formation of a red precipitate. Arsenazo-I and uranium(VI) give a blue solution (λ_{max} 590 nm) in IMS, and addition of 2% TOA increases

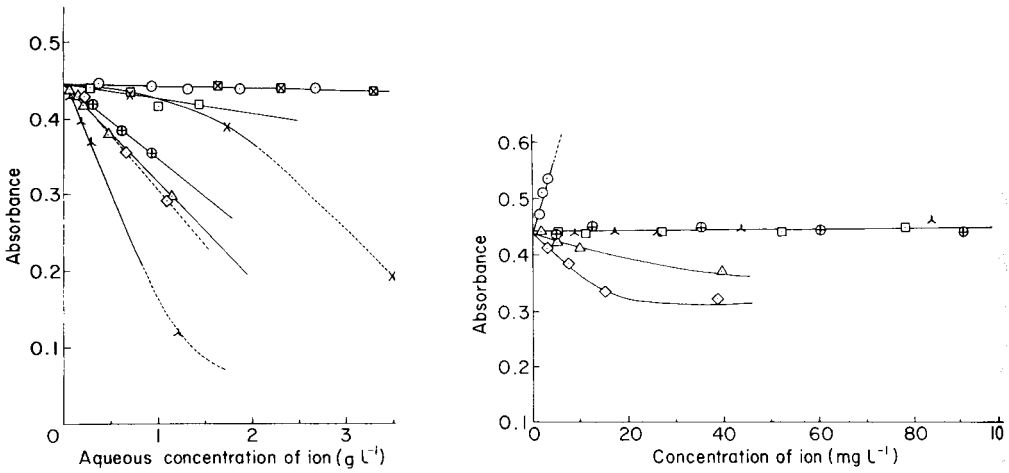


Fig. 2. Absorbance at 400 nm plotted against the aqueous concentrations of "interfering" ion (see Method 1, under *Experimental*). The reference solution was 0.020% (w/v) dibenzoylmethane in IMS containing 2% (v/v) TOA. (⊠) Al(III) added as $AlK(SO_4)_2 \cdot 12H_2O$; (○) Fe(II) as $FeSO_4 \cdot 7H_2O$; (□) PO_4^{3-} as $K_3PO_4 \cdot H_2O$; (×) V(V) as NH_4VO_3; (⊕) NO_3^- as $NaNO_3$; (△) F^- as KF; (◇) Mo(VI) as $(NH_4)_6 \cdot Mo_7O_{24} \cdot 4H_2O$; (⅄) SCN^- as KSCN. A broken line indicates a region of third phase formation.

Fig. 3. Absorbance for 2.35×10^{-5} M uranium at 400 nm plotted against concentration of "interfering" ion in the colour-forming medium (see Method 2, under *Experimental*). The reference was as described under Fig. 2. (○) Fe(III) added as $NH_4Fe(SO_4)_2 \cdot 12H_2O$; (□) Mo(VI) as $(NH_4)_6 \cdot Mo_7O_{24} \cdot 4H_2O$; (⊕) F^- as NaF; (⅄) V(V) as NH_4VO_3; (△) NO_3^- as $NaNO_3$; (◇) SCN^- as KSCN. Turbidity was observed with Fe(III) (broken line) and with F^- above 35 mg l^{-1} (not shown).

sulphate tolerance to 14 mg in 50 ml of reaction mixture. Unfortunately, water is necessary to keep the arsenazo in solution and this encourages phase splitting in the reaction mixture. BPHA gives a yellow colour with uranium in IMS only when free TOA is present, but there would be serious interferences from vanadium(V) and iron. Thus, in an IMS-based solvent, these three reagents are inferior to dibenzoylmethane or Br—PADAP.

Compared to the Br—PADAP method [2], the dibenzoylmethane method is superior with regard to tolerance to sulphate and to all ions likely to be encountered in leach liquor work except iron(III). The method is less sensitive but that is not a disadvantage when, as for typical leach liquor extracts, dilutions are necessary.

REFERENCES

1 P. Pakalns and B. R. McAllister, Anal. Chim. Acta, 62 (1972) 207.
2 S. J. Lyle and M. Tamizi, Anal. Chim. Acta, 108 (1979) 267.
3 J. H. Yoe, F. Will III and R. A. Black, Anal. Chem., 25 (1953) 1200.

Analytica Chimica Acta, 108 (1979) 441—443
© Elsevier Scientific Publishing Company, Amsterdam — Printed in The Netherlands

Short Communication

SIMULTANEOUS KINETIC DETERMINATION OF URIC ACID—ASCORBIC ACID MIXTURES

EZIO PELIZZETTI* and EDOARDO MENTASTI

Istituto di Chimica Analitica, Universitá di Torino, Via Giuria 5, 10125 Torino (Italy)

(Received 2nd January 1979)

Summary. A kinetic stopped-flow method is described for the simultaneous determination of uric acid and ascorbic acid with tris (2,2'-bipyridine)iron(III). For the least favourable ratios of uric to ascorbic acid, in a total concentration of 10^{-5} M, the error in the determination of uric acid is estimated at ±10%.

For many years, uric acid has been determined by techniques based either on reducing properties (tungstophosphoric acid reduction) [1] or on enzymatic degradation (uricase) [2]. Recently, a colorimetric technique based on the reduction of tris(1, 10-phenanthroline)iron(III) was described [3]. The interference from ascorbic acid was eliminated by adding an alkaline copper(II) solution.

Kinetic-based analytical methods have been extensively used in clinical applications [4, 5]; their inherent possibilities and advantages have been pointed out, particularly for the in situ analysis of complex systems [5—7].

This communication describes a kinetic stopped-flow technique for the simultaneous evaluation of uric and ascorbic acids.

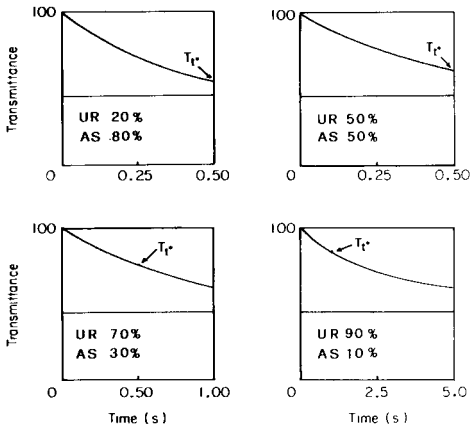
Experimental

Reagents. Uric and ascorbic acids (Merck) were recrystallized from water. Tris (2,2'-bipyridine)iron(II) (FeL_3^{2+}) was synthesized as described earlier [8]; solutions of tris(2,2'-bipyridine)iron(III) (FeL_3^{3+}) were obtained by oxidation with lead dioxide in sulphuric acid [8].

Procedure. The progress of the reaction was followed with a Durrum—Gibson stopped-flow spectrophotometer (cell path 2.00 cm) at 522 nm, the absorbance maximum for FeL_3^{2+} [8]. The runs were done at 25.0°C with 2.0 M sulphuric acid and with a total concentration of 1.00×10^{-5} M (uric + ascorbic acids); the concentration of FeL_3^{3+} was 8.8×10^{-5} M.

Results

The runs done with different ratios of uric acid to ascorbic acid at a constant total concentration, showed the same final transmittance (within experimental error) corresponding to a stoichiometric factor of 1.94 ± 0.08 (i.e., 2 $[FeL_3^{3+}]$/[uric + absorbic acids]); some examples are shown in Fig. 1.



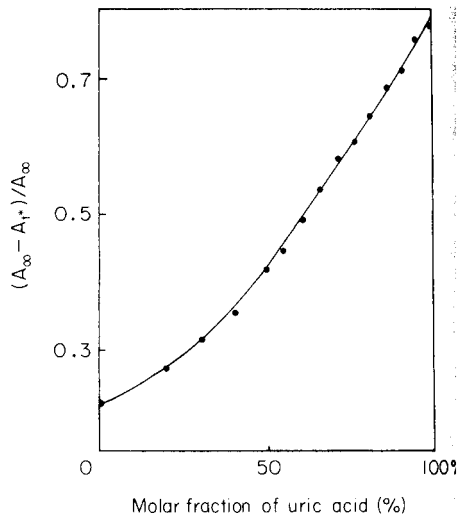


Fig. 1. Oscilloscopic traces (at 522 nm) of different mixtures of uric acid (UR) and ascorbic acid (AS). Conditions as in Procedure.

Fig. 2. Calibration curve for uric acid—ascorbic acid mixtures. The line has been interpolated for the experimental points shown. Conditions as in Procedure (t^* = 0.50 s).

Whereas the kinetics and mechanism of oxidation of ascorbic acid with FeL_3^{3+} and related complexes have been widely investigated [9], showing a first-order dependence on both reagents, information is not available for the analogous oxidation of uric acid. Measurements done with uric acid alone, in excess with respect to FeL_3^{3+}, showed however that the dependence of the reaction rate on FeL_3^{3+} (followed by monitoring FeL_3^{2+} formation) is not linear; the usual plots of ln $(A_\infty - A_t)$ (where A_∞ and A_t represent the absorbance at equilibrium and at time t, respectively) versus time are not linear for the entire course of the reaction. In consequence, the single-point method developed by Lee and Kolthoff [10] for binary mixtures undergoing simple first-order or pseudo-first order reactions is not applicable. For the present system, a plot of $(A_\infty - A_{t*})/A_\infty$ (where A_∞ and A_{t*} represent the absorbance at equilibrium and at a fixed time, t*, respectively) as a function of the molar fraction of uric acid, is not linear (Fig. 2) but gives a calibration curve which is analytically useful. The deviation is only a few percent units for uric acid with respect to ascorbic acid (or vice versa), and an error of ± 10% for the uric acid concentration is estimated for the most unfavorable case (2.0×10^{-6} M uric acid in the presence of 8.0×10^{-6} M ascorbic acid). Obviously the error decreases with increasing uric acid percentage. For the total concentration, previous conclusions apply [3].

The method is rapid and inexpensive; the aqueous reagents are simple to

prepare and are stable if stored at low temperature. Prior oxidation of the ascorbic acid is not needed for evaluation of the uric acid, and the high acidity reduces other interferences observed at higher pH. The optimum conditions for a stopped-flow kinetic method have already been described [6].

REFERENCES

1 R. J. Henry, Clinical Chemistry: Principles and Techniques, Hoeber, New York, 1964, p. 276.
2 E. Praetorius, Scand. J. Clin. Lab. Invest., 1 (1949) 222; K. Lorentz and W. Berndt, Anal. Biochem., 18 (1967) 58; N. Kageyama, Clin. Chim. Acta, 31 (1971) 429; N. Gochman and J. M. Schmitz, Clin. Chem., 17 (1971) 1154.
3 J. W. Nelson and K. K. Batra, Clin. Chem., 21 (1975) 125.
4 G. G. Guilbault, Enzymatic Methods of Analysis, Pergamon, Oxford, 1970.
5 H. B. Mark and G. A. Rechnitz, Kinetics in Analytical Chemistry, Interscience, New York, 1968.
6 E. Pelizzetti, E. Mentasti, E. Pramauro and G. Giraudi, Anal. Chim. Acta, 85 (1976) 161.
7 G. M. Ridder and D. W. Margerum, Anal. Chem., 49 (1977) 2090.
8 M. H. Ford-Smith and N. Sutin, J. Am. Chem. Soc., 83 (1961) 1830.
9 E. Pelizzetti, E. Mentasti and E. Pramauro, Inorg. Chem., 15 (1976) 2898; E. Mentasti, E. Pelizzetti and E. Pramauro, Ann. Chim. (Rome), 66 (1976) 575.
10 T. S. Lee and I. M. Kolthoff, Ann. N.Y. Acad Sci., 53 (1951) 1093.

Analytica Chimica Acta, 108 (1979) 445—452
© Elsevier Scientific Publishing Company, Amsterdam — Printed in The Netherlands

Book reviews

C. S. Barrett, D. E. Leyden, J. B. Newkirk and C. O. Ruud (Eds.), *Advances in X-ray Analysis, Vol. 21*, Plenum Press, New York, 1978, xvi + 325 pp., price $47.40.

The Denver Conferences on applications of x-ray analysis are yearly manifestations—the 28th Conference will be held in August 1979—which attract large numbers of participants, thus proving very directly that the conferences respond to a real need. A second tradition, which has become impressive with time, is the publication of the proceedings of the conferences as successive volumes of the series Advances in X-ray Analysis. The present volume contains 33 of the ca. 60 papers presented at the 1977 Conference. They deal mostly with x-ray fluorescence, as there is an annual alternation between fluorescence and diffraction spectrometry as the main topic. The book has been produced by direct reproduction of the typed manuscripts but there is no inacceptable disparity in printing and presentation from one paper to the other.

The overall value of this volume should be judged within the framework of the entire series, which aims at the publication of the plenary lectures at the conference and a number of papers on recent research and innovations. The standard of the contributed research papers is generally very good. Papers are presented in sections dealing with applications in metal analysis and mining, calculation methods and parameters of importance in x-ray spectrometry, instrumentation, proton-induced x-ray fluorescence, and x-ray powder diffraction. Compared with previous volumes of the series, the scant impact of the review papers is surprising. There is one on x-ray laser research which amounts to little more than an extended abstract followed by 20 literature references; a second, on x-ray excited optical luminescence and phosphorescence, is mentioned on the dust cover but does not appear in the book; only the third—on the interdependence of x-ray diffraction and x-ray fluorescence data—is of normal importance as a keynote article. The text is unlikely to be useful for those seeking an introduction to x-ray fluorescence; those working in the field may find various items of interest.

F. Adams

A. Strasheim and T. W. Steele (Eds.), *Analytical Chemistry in the Exploration, Mining and Processing of Materials*, Pergamon Press, Oxford 1978, 180 pp., price £18.00.

The plenary lectures of this International Symposium on Analytical Chemistry in the Exploration, Mining and Processing of Materials (Johannesburg, 1976), which was sponsored by the Analytical Chemistry and Applied Chemistry Divisions of I.U.P.A.C. in conjunction with the Council for Scientific

and Industrial Research, have previously appeared in Pure and Applied Chemistry. There are fifteen papers, seven of which deal with analytical requirements and the rest with analytical methods. This division and the subdivisions into, for example, Primary coal — Analytical needs, Analysis of Nonferrous Metals, and Analytical Requirements in Exploration Geochemistry — alongside reviews of the application of methods as apparently diverse as "classical" methods and applications of atomic absorption spectrometry — have served to give a collection of interest.

Listening to plenary lectures given by experts selected for their wide knowledge of their area of specialization is always a pleasant method of finding out how far a subject has developed; reading the lectures, at leisure, enables one to have the opportunity to go back and forth in order to savour some points of especial interest or value, and there are many here, for this is a good collection. For many teachers, it could prove to be a useful source or starting point for extended lectures on any part of the methods; for students it could serve as useful starting material for dissertations; for many working analysts, a pleasant way of catching up with current developments in someone else's field of work.

L. S. Bark

A. Pacault et G. Pannetier, (Eds.), *Compléments au Nouveau Traité de Chimie Minérale de P. Pascal Tome 11, Thallium*, par W. Freundlich, Masson SA, Paris, 1978.

Cet ouvrage s'inscrit, après les monographies déjà publiées, parmi les publications destinées à actualiser le Nouveau Traité de Chimie Minérale dont l'achèvement est intervenu en 1968. La chimie du thallium s'étant considérablement développée ces dernières années, il est apparu nécessaire aux auteurs du traité de compléter les données déjà publiées sur cet élément. L'ouvrage ainsi réalisé résulte de la compilation des nombreux travaux consacrés ces dernières années au thallium (928 références). Ceux-ci sont présentés de façon rationnelle par familles de combinaisons chimiques. Après un bref rappel des propriétés physiques du thallium, l'auteur passe en revue les combinaisons chimiques que cet élément donne avec les halogènes (dérivés halogénés et oxyhalogénés), l'oxygène et le soufre, l'azote, le phosphore et l'arsenic, le carbone, l'azote et l'oxygène, le silicium et le germanium, le bore, l'hydrogène. L'auteur cite également des exemples de composés intermétalliques et de dérivés organométalliques du thallium. Cet ouvrage qui contient une foule de données numériques (56 tableaux) et 46 figures (dont 18 diagrammes de phase et de nombreux exemples de structures) permettra au chimiste minéraliste de faire le point de nos connaissances sur le thallium.

G. Durand

A. J. Melveger (Ed.), *Resonance Raman Spectroscopy as an Analytical Tool*, Franklin Institute Press, Philadelphia, 1978, vii + 84 pp., price $10.50.

This is one of a series based on the symposia presented at the 17th Eastern Analytical Symposium in December 1977, and contains the contributions from four leading laboratories engaged in active development of resonance Raman techniques. The major part of each section is devoted to quite detailed descriptions of the equipment and the art of using it adopted in the laboratory concerned with, some examples of the spectra obtained. One section treats the problems associated with the use of laser sources that are strongly absorbed by the sample (sample heating, fluorescence and photodecomposition); another discusses the study of photodecomposition by laser Raman techniques. Some emphasis is put on the analytical potential of the methods described, but it seems clear that this potential is likely to be realised only after considerable effort has been applied to the individual problem; there are so far no prospects of standard operating systems applicable to a range of situations. Anyone contemplating entry to the field (the starting fee is about $100,000) could do worse than read this book! The book is well produced and seems to have been well proof-read.

S. Cradock

F. Cattabeni, A. Cavallaro and G. Gali (Eds.), *Dioxin—Toxicological and Chemical Aspects*, S. P. Medical and Scientific Books (Distributed by Halsted Press, J. Wiley), 1978, viii + 222 pp., price £14.50.

From the very title and the front cover, one is left in no doubt as to why this book is necessary. It is the first volume of a projected series from the Giovanni Lorenzini Foundation, the material arising from a 'workshop' attended by many experts which was organized by various Italian institutes. The object was to describe and collect the necessary information on the properties of the highly toxic 2,3,7,8-tetrachlorodibenzo-*p*-dioxin (TCDD) so as to advise and help the political and health authorities of the Lombardy region following the Seveso incident. Chapter 1 describes in some detail the incidents which are purported to have taken place at Seveso, as well as the events which took place immediately afterwards. The style of the report is mild, in marked contrast to what appeared in the popular media, but nevertheless the gravity of the situation comes through. Thus according to Table III (up to 10.10.76), with 1732 patients visiting the outpatient dermatological clinic, 500 lesions were of suspected toxic origin (the cloud also contained ethylene glycol, sodium hydroxide and trichlorophenol), but only 16 lesions were attributed to TCDD; whilst there were 183 deliveries at the obstetric-gynecological clinic, there were also 51 spontaneous abortions, plus 28 therapeutic abortions for women living in zones A and B. One shortcoming is that although zone A (highly contaminated) and zone B (lower pollution) are mentioned, a map depicting the geographical connotations of these zones is not provided.

The book is subsequently divided into three major sections, entitled Chemistry and Analysis, Toxicology, and Decontamination, respectively, containing some 20 papers-cum-contributions. As would be expected, the general standard of the papers is high, but for the analytical chemist the first four papers are worth special mention. In the paper by Holmstedt, we are instructed in the intricacies of mass fragmentography and chromatography, Buser describes the analysis for TCDD in grass and soil taken from Seveso after the incident. The procedure is completed by the use of a g.c.—m.s. system employing glass capillary columns, where particularly impressive separations of nine of the many possible isomers of TCDD are depicted, using the intensity of the m/e 320 peak. The complexity of the problem of determining a few parts per trillion (1 in 10^{12}) of TCDD is vividly seen in the large number of peaks in the final g.l.c. traces even with the most selective of detectors. The paper by O'Keefe is a fully detailed procedure which is necessary for the clean-up of TCDD from environmental samples. It shows how pedantic and exacting these procedures have to be in order to obtain satisfactory results. Here the analytical chemist took beef fat, doped it with TCDD and had to employ three columns (MgO/Celite 545, alumina and Florisil) in sequence followed by direct-probe, high-resolution mass spectrometry. The final paper in this section deals not with TCDD but with analyses for closely related and similarly acting chlorinated dibenzofurans which were responsible for Yusho disease (in 1000 people) following the ingestion of rice oil contaminated with polychlorinated biphenyls. Although the latter compounds were not responsible for the problem, they probably contained the chlorinated dibenzofurans as impurities, so that the level of these toxic agents was of the order of $\mu g\ g^{-1}$ of rice oil. The significance of these findings is fully discussed. In this section we can see the armament of the fully equipped analytical scientist at its pinnacle; indeed it is so specialized that to the uninitiated it must seem like a cabal full of esoteric mystery or art. A fascinating section from which to draw examples for the teaching of instrumental analytical chemistry. Frankly the reviewer can think of no better justification for the training of students in analytical chemistry.

The reviewer is not competent to judge the toxicology section but it makes good reading. The final section on decontamination is a very important section and here we are led through the procedures and research background in a clear and logical manner. The consensus of opinion appears to be that an essentially chemical approach to the elimination of TCDD from the environment might be possible; the basis of such opinion rests heavily on Crosby's work on the ultraviolet degradation of TCDD in the presence of hydrogen donors.

The book is fairly well produced; there are many small typographical errors and the diagrams are uneven in size, but that should not detract from this account of the Seveso incident and the background research which has been carried out on the most noxious of compounds, TCDD. The book should be standard reading for environmental chemists and on the shelves of most libraries which profess to concern themselves with the subject.

G. Nickless

L. Sachs, *Angewandte Statistik — Statistische Methoden und ihre Anwendungen* 5. Aufl., Springer-Verlag, Berlin, 1978, xxiv + 552 pp., price DM 59.80, US $29.90.

The 5th edition of the well-known book of Sachs contains a wealth of information on classical statistical techniques. Since the book is meant as a textbook as well as a reference work, this is hardly a disadvantage. A (loose) manual is provided for all who want to use the book as a textbook; the sequence of chapters to be read by beginners or advanced readers is clearly indicated. As a reference work it supplies the reader with a wealth of tables, comprehensive indexes on topics, names and tables, and comprehensive and up-to-date literature references. A drawback is that the book bears the mark of its first date of publication (1967). Newer techniques are mentioned, but their treatment is very meagre compared with the treatment of older techniques. Game theory is dealt with in one page, Monte Carlo and other simulation techniques in 3 pages and time series analysis in 1/3 page. Three pages are devoted to the estimation of roots; the use of electronic pocket calculators is hardly mentioned.

An appendix of 60 pages contains lists of books and periodicals on statistics, systematic literature references and a list of suppliers of statistical aids (e.g. probability paper and control charts). Although most examples are medical, analytical chemists will find the book adequate for their profession.

G. Kateman

S. W. Shalaby (Ed.), *Thermal Methods in Polymer Analysis* (selected papers from EAS 1977), The Franklin Institute Press, Philadelphia, U.S.A., 1978, 204 pp., $18.95.

There is a certain sanity in breaking down the proceedings of a major meeting such as the Eastern Analytical Symposium into a series of short subject-dedicated volumes. Moreover the practice has much to commend it when the result is an interesting, readable and well-indexed book.

Thermal methods of analysis are playing an ever-increasing role in the context of the definition of high polymers and the scope of some of the most important of these techniques is well-illustrated in this book. Characterization of the amorphous phase, the study of the more unusual properties of, e.g., polyamides, control of fibre morphology, performance prediction with respect to elastomers, and life prediction of a range of polymers under normal conditions are examples of some of the subjects presented. Invidious as it may be to make special mention of a particular contribution in a brief review, there is good reason to draw attention to the kinetic studies reported by Flynn; patient, precise experimentation and cogent argument combine to give a fascinating paper. Dare one ask the editor what happened to the work of Edward M. Barrall II? Although he appears in the list of contributors, his contribution has been omitted.

C. E. Roland Jones

R. Epton (Ed.). *Chromatography of Synthetic and Biological Polymers, Volume 2—Hydrophobic, Ion-exchange and Affinity Methods*, Ellis Horwood (for The Chemical Society Macromolecular Group).

This is the second of two volumes containing lectures given at an International Symposium held in Birmingham in 1976. The five papers devoted to hydrophobic chromatography demonstrate that hydrophobic interactions can be important in other forms of chromatography. Alternative mechanisms of binding are discussed, together with accounts of investigations with totally non-ionic matrices and materials containing imphilytes.

The section on biopolymer ion-exchange chromatography is concerned with aspects of protein separation on heat-stable (cross-linked), agarose-based, ion-exchange matrices, and in contrast composite DEAE-dextran—porous silica matrices and cellulose-based materials. Industrial applications are particularly discussed.

The largest section of this volume deals with various aspects of biospecific sorption chromatography. After an initial review of the theoretical and practical developments, design factors for successful operation of this technique are considered. Critical appraisal of the specificity of early examples in this field are interestingly presented together with a discussion of the efficacy of bio-elution as an additional and complementary technique. Further papers describe small-ligand affinity chromatography, with examples of binding techniques and specific applications. Finally a selection of work with macromolecular ligands is presented.

Although in a book of this type with multiple contributors, some overlap is inevitable, this has been kept to a minimum. This book is clearly of principal use to research workers, but the presentation is clear and the compilation such that it does provide a readable account of recent trends in the relatively new area of biopolymer fractionation. The volume is stimulating and informative.

P. J. Somers

National Institute of Occupational Safety and Health, *NIOSH Manual of Analytical Methods, Vols. 1—3;* and *NIOSH Documentation of the Validation Tests*, 2nd edn., U.S. Department of Health, Education and Welfare, (NIOSH Publication No. 77.157.A,B,C), Public Health Service, Center for Disease Control, Cincinnati, Ohio, 1977, total price $43.00 ($53.75 outside U.S.A.).

When occupational safety and health standards for nearly 400 chemical substances were adopted by the U.S. Department of Labor in 1971, few reliable analytical procedures were available to monitor accurately the exposure of workers to possible toxic substances. In 1974, NIOSH published the first edition of this Manual, which contained methods for 130 toxic substances. This second edition, which runs to the size of four large telephone directories, contains 337 sampling and analytical methods for use in industrial hygiene monitoring. Some of the procedures are useful for measuring toxic constit-

uents in blood, urine or body tissues, but most are intended for monitoring personal exposure to air. Volume 1 contains 110 methods developed by NIOSH, while Volumes 2 and 3 contain 227 methods validated under a joint NIOSH/OSHA Standards Completion Program. Volume 4 contains the documentation for the validation tests.

There is, of course, room for improvement of many of the procedures, and some eyebrows may be raised at the choice of some methods. However, this is an extremely valuable publication which should be on the bookshelf of every laboratory concerned with environmental analysis in work areas and industrial hygiene. Thanks to the U.S. taxpayer, these volumes not only should be but very realistically can be available everywhere.

Rolf K. Freier, *Wäßrige Lösungen - Daten für Anorganische und Organische Verbindungen*, W. de Gruyter, Berlin; Band 1: Daten, xxvii + 440 S., 1976, gebd. DM 185,00. Band 2: Ergänzungen, lxv + 477 S., 1978, gebd. DM 220,00.

Volume 1 of this compilation of data on aqueous solutions of inorganic and organic compounds is straightforward. After the introductory pages, which helpfully include a German—English vocabulary, the remainder of the text consists entirely of tabulated data for over 6000 compounds. The information given is listed under the headings: formula, name, colour, state (solid, liquid, gas), molecular weight, density, chemical standard potential, solubility in water at five temperatures (where available), dissociation constant or solubility product, electrochemical reaction or hydrolytic reaction, and the E_0 value or the hydrolytic equilibrium equation. As normally happens in such compilations, there are many empty spaces in many of the columns.

Volume 2 contains assorted supplementary information, which is more difficult to summarize. For example, the dissociation pressure of copper sulfate hydrate appears beside the physical properties of hydrogen isotopes; the use of β-benzoinoxime for the detection of copper follows data on benzene as a carcinogen. A large proportion of the text (over 160 pp.) is devoted to the properties of water itself. In some respects, this volume is rather a rag-bag of information; fortunately, the contents list is very clear so that it is not difficult to discover quickly if the information sought is actually there. Given the cheapness and ubiquity of the "Rubber Book", a wide readership cannot be foreseen for these expensive volumes despite the more detailed information that they contain in certain respects.

T. Braun, E. Bujdoso, R. Henkelmann, J. I. Kim, F. Lux, H. Stark and R. Zeisler (Eds.), *Proceedings of the 1976 International Conference on Modern Trends in Activation Analysis*, Akademiai Kiado, Budapest, 1977, Vol. I, 955 pp.; Vol. II, 1008 pp., price U.S. $175.00.

These two large volumes contain the entire proceedings of the conference held in Munich in September, 1976. After the Plenary Lectures, the contents

are distributed into the categories: Fundamental Developments and Technical Development; Biological and Biomedical Applications; Environmental Applications; Materials Science and Industrial Applications; Application in Geo- and Cosmo-Sciences; Applications in Archaeology, Art and Forensic Sciences; Accuracy and Precision; Sampling and Homogeneity Control; Standard Materials; Comparison with other Analytical Methods. There is a good author index but no subject index, something which could beneficially have replaced the list of participants and their addresses. There are many interesting papers in these volumes, which will be valuable to those interested in this field who do not have access to the Journal of Radioanalytical Chemistry. Given that this is a direct reprint of the journal, it is surprising that these Proceedings could not have been made available at a rather more sensible cost.

John G. Stevens and Virginia E. Stevens (Eds.), *Mössbauer Effect Data Index, covering the 1976 Literature*, IFI/Plenum Data Company, New York, 1978, x + 357 pp., price $114.00.

This compilation, like its predecessors in this series, lists sources of equipment and suppliers, tables for Mössbauer spectroscopy, the 1976 data index, 1976 topical reference lists, addendum reference lists for 1971—1975, a 1976 master reference list and the 1976 alphabetical author list. The entire collection should save many tedious hours of library searches for those interested in Mössbauer spectroscopy.

Z. Deyl and J. Kopecky (Eds.), *Bibliography of Liquid Column Chromatography, 1971—1973, and Survey of Applications*, Elsevier, Amsterdam, 1977, xix + 1135 pp., price Dfl. 259.00.

This supplementary volume, No. 6 of the Journal of Chromatography, further extends the coverage of the literature offered by earlier volumes. The editors, with their 8 collaborators, have served chromatographers well. There are 9976 individual entries: each of these is listed under the appropriate subject area; to find all the publications relating to proteins, for example, consultation of the comprehensive table of contents shows the pages on which they are to be found. Equally useful are the Author Index (65 pp.), and list of compounds chromatographed (200 pp.). With these aids it is very easy to find out whether a particular compound was investigated in the period involved. Volumes such as these should be on the shelves of every major reference library: in terms of the time that will be saved by so many people on so many occasions, the cost is easily justified. Perhaps the only snag is that the paper covers of this heavy book will not stand up to the handling they will receive, and re-binding at the outset would seem to be sensible.

ANALYTICA CHIMICA ACTA, Vol. 108 (1979)

AUTHOR INDEX

Adams, F., see de Jonghe, W. 21
Agterdenbos, J.
Calibration in quantitative analysis. Part 1. General considerations 315
Ariel, M., see Efron, C. 395

Beisel, N. F., see Yudelevich, I. G. 45
Beneyto, J. E., see Fabregas, J. L. 411
Bernal-Melchor, A., see Hernández-Méndez, J. 39
Boer, H. S. de, see de Boer, H. S. 389
Bos, M.
—, Lely, J. A. and Lengton, W.
Titration of binary mixtures of rare earth metals based on magnetic susceptibility measurements 309
Bower, J. N., see Tuell, T. M. 351
Bradshaw, J. D., see Tuell, T. M. 351
Bureau International Technique du Chlore Working Party
Standardization of methods for the determination of traces of mercury. Part 4. Determination of total mercury in gases by atomic absorption spectrometry 1
Burgess, C., see Fogg, A. G. 205
Butler, L. R. P., see Radziuk, B. 31

Chanysheva, T. A., see Yudelevich, I. G. 45
Chao, T. T., see Sanzolone, R. F. 357
Chau, Y. K., see Radziuk, B. 31
Chouaib, F.
—et Poitrenaud, C.
Etude des complexes sulfosalicylate de cuivre(II), nickel(II), cobalt(II) et uranyle(II) à l'aide d'une résine échangeuse de cations 333
Christian, G. D.
—, Vandenbalck, J. L. and Patriarche, G.J.
Cathode ray polarography and differential pulse polarography of the catalytic molybdenum(VI) wave 149
Collard, R. S.
—and Pryor, W. A.
A specific spectrophotometric determination of ozone in air in the presence of sulfur dioxide and nitrogen oxides 255
Costa Dantas, C., see van Grieken, R. 93
Covington, A. K., see Pierre Bütikofer, H. 179
Curran, D. J., see Strohl, A. N. 379

Dack, L. van't, see van Grieken, R. 93
Dalen, J. P. J. van, see van Dalen, J. P. J. 433
Dal Pont, G., see Gardner, D. 13
Da Silveira Dantas, H., see van Grieken, R. 93
Day, M. J., see Larkin, M. J. 425
de Boer, H. S.
—, Lansaat, P. H. and van Oort, W. J.
Polarographic analysis for corticosteroids. Part 2. Determination of corticosteroids in single-component solutions, suspensions, ointments and creams 389
de Jonghe, W.
—and Adams, F.
The determination of organic and inorganic lead compounds in urban air by atomic absorption spectrometry with electrothermal atomization 21
Deming, S. N., see Price, W. P., Jr. 227
Dryhurst, G., see Karber, L. G. 193

Eckert, J. M., see Rama Bhat, S. 293
Edmonds, T. E.
A microcomputer-based data acquisition and processing system for electrochemical analysis 155
Efron, C.
—and Ariel, M.
Lead dioxide-coated carbon paste electrodes 395
Eklund, R. H.
—and Holcombe, J. A.
Signal enhancement in carbon-filament atomic absorption spectrometry by metal—oxygen reactions 53
Elton-Bott, R. R.
A re-investigation of phenol as a spectrophotometric reagent for the determination of nitrate-nitrogen 285
Espersen, D.
—and Jensen, A.
Differential kinetic analysis and flow

injection analysis. Part 2. The (2.2.1) cryptates of magnesium and calcium 241

Fabregas, J. L.
—and Beneyto, J. E.
Determination of lysine in its cephalexin salt 411
Fayad, N. M., see Fogg, A. G. 205
Feldman, C., see Horton, A. D. 221
Fisk, M. B., see Korkisch, J. 63
Fogg, A. G.
—, Fayad, N. M., Burgess, C. and McGlynn, A.
Differential pulse polarographic determination of cephalosporins and their degradation products 205
Frech, W., see Lundberg, E. 75

Gardner, D.
—and Dal Pont, G.
A rapid, simple method for the determination of total mercury in fish and hair by cold-vapour atomic absorption spectrometry 13
Gether, J.
—, Lunde, G. and Steinnes, E.
Determination of the total amount of organically bound chlorine, bromine and iodine in environmental samples by instrumental neutron activation analysis 137
Geyer, R., see Rama Bhat, S. 293
Gibson, N. A., see Rama Bhat, S. 293
Goethals, P.
—, Vandecasteele, C. and Hoste, J.
The determination of carbon in aluminium by deuteron activation analysis 367
Gopala Rao, G.
—, Viswanath, S. G. and Somidevamma, G.
Spectrophotometric determination of trace amounts of antimony(V) after selective precipitation with ferroin and dissolution in nitrobenzene 417
Gough, B. S.
—and Sullivan, J. V.
Controlled temperature-gradient atomic spectral lamp 347
Gowda, H. S.
—, Ramappa, P. G. and Nayak, A. N.
Rapid spectrophotometric determination of phenothiazines with molybdophosphoric acid 277
Grieken, R. van, see van Grieken, R. 93
Grime, J. K.
The determination of iodide in the presence of other halides by enzymatic enthalpimetry 363

Hadjiioannou, T. P., see Lazarou, L. A. 375
Hernández-Méndez, J.
—, Polo-Diez, L. and Bernal-Melchor, A.
Analytical applications of emulsions. Determination of lead in lubricating oils by atomic absorption spectrometry 39
Hill, C. J., see Lash, R. P. 405
Hishiya, Y., see Imai, S. 103
Holcombe, J. A., see Eklund, R. H. 53
Honda, S.
—, Matsuda, Y., Terao, M. and Kakehi, K.
Fluorimetric determination of reducing carbohydrates with malonamide 421
Horton, A. D.
—, Jenkins, R. A. and Feldman, C.
Application of a glow discharge detector to the determination of trimethylsilyl-derivatized complex organic mixtures 221
Hoste, J., see Goethals, P. 367
Hoste, J., see Vandecasteele, C. 127

Iida, C., see Uchida, H. 87
Imai, S.
—, Kusaka, Y., Tsuji, H. and Hishiya, Y.
Emission spectrographic determination of trace elements in atmospheric particulate matter 103

Janata, J., see Shiramizu, B. 161
Jenkins, R. A., see Horton, A. D. 221
Jensen, A., see Espersen, D. 241
Jonghe, W. de, see de Jonghe, W. 21

Kakehi, K., see Honda, S. 421
Kamata, S.
—, Moody, G. J. and Thomas, J. D. R.
A PVC matrix membrane calcium-selective electrode based on calcium bis-4-(1,1,3,3-tetramethylbutyl)-2,6-dinitrophenoxide 385
Karber, L. G.
—and Dryhurst, G.
Differential pulse voltammetric oxidation of polyinosinic acid and its components 193
Kohashi, K., see Yamaguchi, M. 297
Korkisch, J.
—, Steffan, I. and Fisk, M. B.
Chemical analysis of manganese nodules. Part IV. Determination of nickel after anion-exchange separation 63
Kowalczyk, E., see Marczenko, Z. 261

Kuleff, I.
Determination of uranium by neutron activation and radiochemical separation of the tellurium fission product 371
Kusaka, Y., see Imai, S. 103

Laitinen, H. A., see Rosenfarb, J. 119
Lansaat, P. H., see de Boer, H. S. 389
Larkin, M. J.
—and Day. M. J.
Direct fluorimetric determination of carbaryl insecticide and its hydrolysis product 1-naphthol 425
Lash, R. P.
—and Hill, C. J.
Evaluation of ion chromatography for determination of selected ions in geothermal well water 405
Lazarou, L. A.
—and Hadjiioannou, T. P.
Kinetic potentiometric determination of citric acid with a perbromate-selective electrode 375
Lely, J. A., see Bos, M. 309
Lengton, W., see Bos, M. 309
Linden, W. E. van der, see van der Linden, W. E. 169
Loon, J. C. van, see Radziuk, B. 31
Lundberg, E.
—and Frech, W.
Direct determination of trace metals in solid samples by atomic absorption spectrometry with electrothermal atomizers. Part 3. Application of an autosampler to the determination of silver, bismuth, cadmium and zinc in steels 75
Lunde, G., see Gether, J. 137
Lyle, S. J.
—and Tamizi, M.
A study of the direct spectrophotometric determination of uranium(VI) in trialkylamine extracts with 2-(5-bromo-2-pyridylazo)-5-diethylaminophenol 267
Lyle, S. J.
—and Tamizi, M.
The direct spectrophotometric determination of uranium(VI) in trialkylamine extracts with dibenzoylmethane 437

Marczenko, Z.
—and Kowalczyk, E.
Sensitive flotation—spectrophotometric determination of rhodium with malachite green 261
Massoumi, A., see Tuell, T. M. 351
Matsuda, Y., see Honda, S. 421
McGlynn, A., see Fogg, A. G. 205
Mentasti, E., see Pelizzetti, E. 441
Michailidis, M. S., see Wu, C. Y. 233
Moody, G. J., see Kamata, S., 385
Mori, S.
Contamination of water and organic solvents stored in plastic bottles with phthalate ester plasticizers 325
Moss, S. D., see Shiramizu, B. 161

Nayak, A. N., see Gowda, H. S. 277

Ohkura, Y., see Yamaguchi, M. 297
Ohta, K.
—and Suzuki, M.
Atomic absorption spectrometry of vanadium with a tungsten electrothermal atomizer 69
Oort, W. J. van, see de Boer, H. S. 389
Oostervink, R., see van der Linden, W. E. 169

Patriarche, G. J., see Christian, G. D. 149
Pelizzetti, E.
—and Mentasti, E.
Simultaneous kinetic determination of uric acid—ascorbic acid mixtures 441
Pierre Bütikofer, H.
—and Covington, A. K.
Redetermination of the standard pH values for potassium hydrogenphthalate reference buffer solution from 0 to 85°C 179
Poitrenaud, C., see Chouaib, F. 333
Pollard, B. D., see Tuell, T. M. 351
Polo-Diez, L., see Hernández-Méndez, J. 39
Price, W. P., Jr.
—and Deming, S. N.
Optimized separation of scopoletin and umbelliferone and *cis—trans* isomers of ferulic and *p*-coumaric acids by reverse-phase high-performance liquid chromatography 227
Pryor, W. A., see Collard, R. S. 255

Radziuk, B.
—,Thomassen, Y., Butler, L. R. P., van Loon, J. C. and Chau, Y. K.
A study of atomic absorption and atomic fluorescence atomization systems as detectors in the gas chromatographic determination of lead 31

Rama Bhat, S.
—, Eckert, J. M., Geyer, R. and Gibson, N. A.
Extraction-spectrophotometric determination of sulphide and sulphite in waters based on formation of the bis(2,9-dimethyl-1,10-phenanthroline)copper(I) ion 293
Ramappa, P. G., see Gowda, H. S. 277
Rinsvelt, H. A. van, see Rosenfarb, J. 119
Roseboom, H.
— and Wiese, G.
Gas chromatographic determination of xanthinol in plasma 401
Rosenfarb, J.
—, Laitinen, H. A., Sanders, J. T. and van Rinsvelt, H. A.
Rapid non-destructive determination of thin films of platinum by particle backscattering 119

Samuelsson, R.
Pulse polarographic determination of nitrosamines. Part 2. Methods for the determination of *N*-nitrosodiphenylamine and *N*-nitrosodibutylamine 213
Sanders, J. T., see Rosenfarb, J. 119
Sanzolone, R. F.
—, Chao, T. T. and Welsch, E. P.
Determination of arsenic in geological materials by electrothermal atomic absorption spectrometry after hydride generation 357
Sato, A., see Taketatsu, T. 429
Schulman, S. G.
— and Underberg, W. J. M.
Fluorimetric determination of dissociation constants of aryl-substituted alkylammonium ions 249
Shiramizu, B.
—, Janata, J. and Moss, S. D.
Ion-selective field effect transistors with heterogeneous membranes 161
Somidevamma, G., see Gopala Rao, G. 417
Steffan, I., see Korkisch, J. 63
Steinnes, E., see Gether, J. 137
Strijckmans, K., see Vandecasteele, C. 127
Strohl, A. N.
— and Curran, D. J.
The pH response to the reticulated vitreous carbon electrode 379
Sullivan, J. V., see Gough, B. S. 347
Suzuki, M., see Ohta, K. 69

Taketatsu, T.
— and Sato, A.
Spectrofluorimetric determination of europium and samarium with mixtures of 2-thenoyltrifluoroacetone and tri-n-octylphosphine oxide in aqueous solutions containing Triton X-100 429
Tamizi, M., see Lyle, S. J. 267
Tamizi, M., see Lyle, S. J. 437
Terao, M., see Honda, S. 421
Terashima, S.
A direct method for the determination of carbonate and non-carbonate carbon in geological materials by infrared spectrometry 113
Thomas, J. D. R., see Kamata, S. 385
Thomassen, Y., see Radziuk, B. 31
Tsuji, H., see Imai, S. 103
Tuell, T. M.
—, Ullmann, A. H., Pollard, B. D., Massoumi, A., Bradshaw, J. D., Bower, J. N. and Winefordner, J. D.
A comparative study of standards for determinations of trace wear metals in jet engine oils 351

Uchida, H.
—, Uchida, T. and Iida, C.
Determination of major and minor elements in silicates by inductively coupled plasma emission spectrometry 87
Uchida, T., see Uchida, H. 87
Ullman, A. H., see Tuell, T. M. 351
Underberg, W. J. M., see Schulman, S. G. 249

van Dalen, J. P. J.
Interference of trace amounts of nitrilotriacetic acid in ethylenediaminetetraaceti acid with the spectrophotometric determination of niobium as the niobium—EDTA—pyrocatechol complex 433
Vandecasteele, C.
—, Strijckmans, K. and Hoste, J.
The determination of carbon in the refractory metals zirconium, niobium, tantalum and tungsten by instrumental deuteron activation analysis 127
Vandecasteele, C., see Goethals, P. 367
Vandenbalck, J. L., see Christian, G. D. 149

van Grieken, R.
—, van't Dack, L., Costa Dantas, C. and Da Silveira Dantas, H.
Soil analysis by thin-film energy-dispersive x-ray fluorescence 93
van der Linden, W. E.
—and Oostervink, R.
The formation of properties of mixed cadmium sulfide—silver sulfide, and mixed mercury sulfide—silver sulfide membranes for electrodes selective to cadmium(II) and mercury(II) 169
van Loon, J. C., see Radziuk, B. 31
van Oort, W. J., see de Boer, H. S. 389
van Rinsvelt, H. A., see Rosenfarb, J. 119
van't Dack, L., see van Grieken, R. 93
Vechernish, L., see Yudelevich, I. G. 45
Viswanath, S. G., see Gopala Rao, G., 417

Welsch, E. P., see Sanzolone, R. F. 357
Wiese, G., see Roseboom, H. 401
Winefordner, J. D., see Tuell, T. M. 351
Wittick, J. J., see Wu, C. Y. 233
Wu, C. Y.
—, Michailidis, M. S. and Wittick, J. J.
Determination of morphine in poppy straw by high-performance liquid chromatography 233

Yamaguchi, M.
—,Yutani, Y., Kohashi, K. and Ohkura, Y.
Analysis for catecholamines and related compounds based on luminescence at room temperature and at 77 K 297
Yudelevich, I. G.
—, Zelentsova, L. V., Chanysheva, T. A., Vechernish, L. and Beisel, N. F.
Atomic absorption spectrometric methods for analysis of high-purity gallium and rhenium and layers of doped silicon 45
Yutani, Y., see Yamaguchi, M. 297

Zelentsova, L. V., see Yudelevich, I. G. 45

(continued from following page)

A PVC matrix membrane calcium-selective electrode based on calcium bis-4-(1,1,3,3-tetramethylbutyl)-2,6-dinitrophenoxide
S. Kamata, G. J. Moody and J. D. R. Thomas (Cardiff, Gt. Britain) 385
Polarographic analysis for corticosteroids. Part 2. Determination of corticosteroids in single-component solutions, suspensions, ointments and creams
H. S. de Boer, P. H. Lansaat and W. J. van Oort (Utrecht, The Netherlands) 389
Lead dioxide-coated carbon paste electrodes
C. Efron and M. Ariel (Haifa, Israel) 395
Gas chromatographic determination of xanthinol in plasma
H. Roseboom and G. Wiese (Utrecht, The Netherlands) 401
Evaluation of ion chromatography for determination of selected ions in geothermal well water
R. P. Lash and C. J. Hill (Idaho Falls, ID, U.S.A.) 405
Determination of lysine in its cephalexin salt
J. L. Fabregas and J. E. Beneyto (Barcelona, Spain) 411
Spectrophotometric determination of trace amounts of antimony(V) after selective precipitation with ferroin and dissolution in nitrobenzene
G. Gopala Rao, S. G. Viswanath and G. Somidevamma (Waltair, India) 417
Fluorimetric determination of reducing carbohydrates with malonamide
S. Honda, Y. Matsuda, M. Terao and K. Kakehi (Higashi-Osaka, Japan) 421
Direct fluorimetric determination of carbaryl insecticide and its hydrolysis product 1-naphthol
M. J. Larkin and M. J. Day (Cardiff, Gt. Britain) 425
Spectrofluorimetric determination of europium and samarium with mixtures of 2-thenoyltrifluoroacetone and tri-n-octylphosphine oxide in aqueous solutions containing Triton X-100
T. Taketatsu and A. Sato (Fukuoka, Japan) 429
Interference of trace amounts of nitrilotriacetic acid in ethylenediaminetetraacetic acid with the spectrophotometric determination of niobium as the niobium–EDTA–pyrocatechol complex
J. P. J. van Dalen (Delft, The Netherlands) 433
The direct spectrophotometric determination of uranium(VI) in trialkylamine extracts with dibenzoylmethane
S. J. Lyle and M. Tamizi (Canterbury, Gt. Britain) 437
Simultaneous kinetic determination of uric acid–ascorbic acid mixtures
E. Pelizzetti and E. Mentasti (Torino, Italy) 441

Book Reviews 445

Author Index 453

(continued from page opposite)

S. G. Schulman and W. J. M. Underberg (Gainesville, FL, U.S.A.) 249
A specific spectrophotometric determination of ozone in air in the presence of sulfur dioxide and nitrogen oxides
R. S. Collard and W. A. Pryor (Baton Rouge, LA, U.S.A.) 255
Sensitive flotation–spectrophotometric determination of rhodium with malachite green
Z. Marczenko and E. Kowalczyk (Warsaw, Poland) 261
A study of the direct spectrophotometric determination of uranium(VI) in trialkylamine extracts with 2-(5-bromo-2-pyridylazo)-5-diethylaminophenol
S. J. Lyle and M. Tamizi (Canterbury Gt. Britain) 267
Rapid spectrophotometric determination of phenothiazines with molybdophosphoric acid
H. S. Gowda, P. G. Ramappa and A. N. Nayak (Mysore, India) 277
A re-investigation of phenol as a spectrophotometric reagent for the determination of nitrate-nitrogen
R. R. Elton-Bott (Thornlie, W. A., Australia) 285
Extraction-spectrophotometric determination of sulphide and sulphite in waters based on formation of the bis(2,9-dimethyl-1,10-phenanthroline)copper(I) ion
S. Rama Bhat, J. M. Eckert, R. Geyer and N. A. Gibson (Sydney, N.S.W., Australia) 293
Analysis for catecholamines and related compounds based on luminescence at room temperature and at 77 K
M. Yamaguchi, Y. Yutani, K. Kohashi and Y. Ohkura (Fukuoka, Japan) 297
Titration of binary mixtures of rare earth metals based on magnetic susceptibility measurements
M. Bos, J. A. Lely and W. Lengton (Enschede, The Netherlands) 309
Calibration in quantitative analysis. Part 1. General considerations
J. Agterdenbos (Utrecht, The Netherlands) 315
Contamination of water and organic solvents stored in plastic bottles with phthalate ester plasticizers
S. Mori (Tsu, Japan) 325
Etude des complexes sulfosalicylate de cuivre(II), nickel(II), cobalt(II) et uranyle(II) à l'aide d'une résine échangeuse de cations
F. Chouaib et C. Poitrenaud (Gif-sur-Yvette, France) 333

Short Communications

Controlled temperature-gradient atomic spectral lamp
B. S. Gough and J. V. Sullivan (Clayton, Victoria, Australia) 347
A comparative study of standards for determinations of trace wear metals in jet engine oils
T. M. Tuell, A. H. Ullman, B. D. Pollard, A. Massoumi, J. D. Bradshaw, J. N. Bower and J. D. Winefordner (Gainesville, FL, U.S.A.) 351
Determination of arsenic in geological materials by electrothermal atomic absorption spectrometry after hydride generation
R. F. Sanzolone, T. T. Chao and E. P. Welsch (Denver, CO, U.S.A.) 357
The determination of iodide in the presence of other halides by enzymatic enthalpimetry
J. K. Grime (Denver, CO, U.S.A.) 363
The determination of carbon in aluminium by deuteron activation analysis
P. Goethals, C. Vandecasteele and J. Hoste (Gent, Belgium) 367
Determination of uranium by neutron activation and radiochemical separation of the tellurium fission product
I. Kuleff (Sofia, Bulgaria) 371
Kinetic potentiometric determination of citric acid with a perbromate-selective electrode
L. A. Lazarou and T. P. Hadjiioannou (Athens, Greece) 375
The pH response to the reticulated vitreous carbon electrode
A. N. Strohl and D. J. Curran (Amherst, MA, U.S.A.) 379

(continued on previous page)

(continued from outside of cover)

Direct determination of trace metals in solid samples by atomic absorption spectrometry with electrothermal atomizers. Part 3. Application of an autosampler to the determination of silver, bismuth, cadmium and zinc in steels
E. Lundberg and W. French (Umeå, Sweden) 75
Determination of major and minor elements in silicates by inductively coupled plasma emission spectrometry
H. Uchida (Yokohama, Japan), T. Uchida and C. Iida (Nagoya, Japan) 87
Soil analysis by thin-film energy-dispersive x-ray fluorescence
R. van Grieken, L. van't Dack (Wilrijk, Belgium), C. Costa Dantas and H. Da Silveira Dantas (Recife, Brasil) 93
Emission spectrographic determination of trace elements in atmospheric particulate matter
S. Imai, Y. Kusaka, H. Tsuji and Y. Hishiya (Hyogo, Japan) 103
A direct method for the determination of carbonate and non-carbonate carbon in geological materials by infrared spectrometry
S. Terashima (Kawasaki, Japan) 113
Rapid non-destructive determination of thin films of platinum by particle back-scattering
J. Rosenfarb, H. A. Laitinen, J. T. Sanders and H. A. van Rinsvelt (Gainesville, FL, U.S.A.). . 119
The determination of carbon in the refractory metals zirconium, niobium, tantalum and tungsten by instrumental deuteron activation analysis
C. Vandecasteele, K. Strijckmans and J. Hoste (Gent, Belgium) 127
Determination of the total amount of organically bound chlorine, bromine and iodine in environmental samples by instrumental neutron activation analysis
J. Gether, G. Lunde (Oslo, Norway) and E. Steinnes (Kjeller, Norway) 137
Cathode ray polarography and differential pulse polarography of the catalytic molybdenum(VI) wave
G. D. Christian, J. L. Vandenbalck and G. J. Patriarche (Bruxelles, Belgium) 149
A microcomputer-based data acquisition and processing system for electrochemical analysis
T. E. Edmonds (Craigiebuckler, Gt. Britain) 155
Ion-selective field effect transistors with heterogeneous membranes
B. Shiramizu, J. Janata and S. D. Moss (Salt Lake City, UT, U.S.A.) 161
The formation and properties of mixed cadmium sulfide–silver sulfide, and mixed mercury sulfide–silver sulfide membranes for electrodes selective to cadmium(II) and mercury(II)
W. E. van der Linden and R. Oostervink (Amsterdam, The Netherlands) 169
Redetermination of the standard pH values for potassium hydrogenphthalate reference buffer solution from 0 to 85°C
H. Pierre Bütikofer and A. K. Covington (Newcastle upon Tyne, Gt. Britain) 179
Differential pulse voltammetric oxidation of polyinosinic acid and its components
L. G. Karber and G. Dryhurst (Norman, OK, U.S.A.) 193
Differential pulse polarographic determination of cephalosporins and their degradation products
A. G. Fogg, N. M. Fayad (Loughborough, Gt. Britain), C. Burgess and A. McGlynn (Durham, Gt. Britain) 205
Pulse polarographic determination of nitrosamines. Part 2. Methods for the determination of *N*-nitrosodiphenylamine and *N*-nitrosodibutylamine
R. Samuelsson (Umeå, Sweden) 213
Application of a glow discharge detector to the determination of trimethylsilyl-derivatized complex organic mixtures
A. D. Horton, R. A. Jenkins and C. Feldman (Oak Ridge, TN, U.S.A.) 221
Optimized separation of scopoletin and umbelliferone and *cis–trans* isomers of ferulic and *p*-coumaric acids by reverse-phase high-performance liquid chromatography
W. P. Price, Jr. and S. N. Deming (Houston, TX, U.S.A.) 227
Determination of morphine in poppy straw by high-performance liquid chromatography
C. Y. Wu, M. S. Michailidis and J. J. Wittick (Rahway, NJ, U.S.A.) 233
Differential kinetic analysis and flow injection analysis. Part 2. The (2.2.1) cryptates of magnesium and calcium
D. Espersen and A. Jensen (Copenhagen, Denmark) 241
Fluorimetric determination of dissociation constants of aryl-substituted alkylammonium ions

(continued on page opposite)

CONTENTS

Standardization of methods for the determination of traces of mercury. Part 4. Determination of total mercury in gases by atomic absorption spectrometry
Mercury Analysis Working Party of the Bureau International Technique du Chlore (Bruxelles, Belgium) 1
A rapid, simple method for the determination of total mercury in fish and hair by cold-vapour atomic absorption spectrometry
D. Gardner and G. Dal Pont (Cronulla, Australia) 13
The determination of organic and inorganic lead compounds in urban air by atomic absorption spectrometry with electrothermal atomization
W. de Jonghe and F. Adams (Wilrijk, Belgium) 21
A study of atomic absorption and atomic fluorescence atomization systems as detectors in the gas chromatographic determination of lead
B. Radziuk, Y. Thomassen, L. R. P. Butler, J. C. van Loon (Toronto, Canada) and Y. K. Chau (Burlington, Ontario, Canada) 31
Analytical applications of emulsions. Determination of lead in lubricating oils by atomic absorption spectrometry
J. Hernández-Méndez, L. Polo-Diez and A. Bernal-Melchor (Salamanca, Spain) 39
Atomic absorption spectrometric methods for analysis of high-purity gallium and rhenium and layers of doped silicon
I. G. Yudelevich, L. V. Zelenstova, T. A. Chanysheva, L. Vechernish (Novosibirsk, U.S.S.R.) and N. F. Beisel (Budapest, Hungary) 45
Signal enhancement in carbon-filament atomic absorption spectrometry by metal–oxygen reactions
R. H. Eklund and J. A. Holcombe (Austin, TX, U.S.A.) 53
Chemical analysis of manganese nodules. Part IV. Determination of nickel after anion-exchange separation
J. Korkisch, I. Steffan (Vienna, Austria) and M. B. Fisk (La Jolla, CA, U.S.A.) 63
Atomic absorption spectrometry of vanadium with a tungsten electrothermal atomizer
K. Ohta and M. Suzuki (Tsu, Japan) 69

(continued on inside page of the cover)

© Elsevier Scientific Publishing Company, 1979.
All rights reserved. No part of this publication may be reproduced, stored in a retrieval system or transmitted in any form or by any means, electronic, mechanical, photocopying, recording or otherwise, without the prior written permission of the publisher, Elsevier Scientific Publishing Company, P.O. Box 330, 1000 AH Amsterdam, The Netherlands.

Submission of a paper to this journal entails the author's irrevocable and exclusive authorization of the publisher to collect any sums or considerations for copying or reproduction payable by third parties (as mentioned in article 17 paragraph 2 of the Dutch Copyright Act of 1912 and in the Royal Decree of June 20, 1974 (S. 351) pursuant to article 16 b of the Dutch Copyright Act of 1912) and/or to act in or out of Court in connection therewith.

Submission of an article for publication implies the transfer of the copyright from the author to the publisher and is also understood to imply that the article is not being considered for publication elsewhere.

Printed in The Netherlands